2001-2002
Technical Progress Reports

University of California

Salinity/Drainage Research Program and Prosser Trust

Division of Agriculture and Natural Resources, University of California

October 2002

TABLE OF CONTENTS

FOREWORD

The UC Salinity/Drainage Program was initiated in 1985 to develop, interpret and disseminate research knowledge addressing critical agricultural and environmental problems of salinity, drainage and toxic trace elements in the West Side of the San Joaquin Valley in California.

The Water Resources Center and the Salinity/Drainage Program were administratively combined with the UC Center for Water Resources in 1993. John Letey serves as Director of the Center for Water Resources and is the coordinator of the Salinity/Drainage Program. He also has administrative responsibility for the Prosser Trust Fund. This report documents the 2001-2002 accomplishments of the Salinity/Drainage Program and Prosser Trust Fund.

A major function of the UC Salinity/Drainage Program is to support research and extension activities that will contribute to developing optimal management strategies to cope with salinity/drainage/toxics problems in the western San Joaquin Valley. Funded research projects must be both relevant and scientifically sound. The relevancy of proposals is evaluated by an external advisory committee consisting of individuals listed on page v. Appreciation is expressed to all the individuals that devoted time and made valuable contributions to the selection of the research to be supported.

The annual Salinity/Drainage Program meeting was held March 26, 2002, in Sacramento. Part of the day was devoted to oral 5-minute synopses of research projects and posters displaying the research findings in detail. The full research reports on each project are contained in this report. Presentations on other topics of interest were also presented at the annual meeting. See pages vi and vii for the complete program.

SALINITY/DRAINAGE PROGRAM
2002 ADVISORY COUNCIL

Manucher Alemi
Department of Water Resources
1020 Ninth Street
Sacramento, CA 95814

Tad Bell
Department of Food and Agriculture
1220 N Street
Sacramento, CA 95814

Thad Bettner
Westlands Water District
P. O. Box 6056
Fresno, CA 93702

Andrew Chang
UC Riverside
Dept. of Environmental Science
Riverside, CA 92521-0436

Doug Davis
Tulare Lake Drainage District
P. O. Box 985
Corcoran, CA 93212

Mike Delamore
U.S. Bureau of Reclamation
2666 North Grove Industrial Drive
#3106
Fresno, CA 93727-1551

Neil Dubrovsky
U.S. Geological Survey
6000 J Street
Sacramento, CA 95825-1898

Jose Faria
Deaprtment of Water Resources
3374 East Shields Avenue
Fresno, CA 93726

Sarge Green
Tranquility Irrigation District
P. O. Box 487
Tranquility, CA 93668

Dan Johnson
U.S. Department of Agriculture–NRCS
2121-C Second Street
Davis, CA 95616

Walt Shannon
State Water Res. Control Board–DWQ
P. O. Box 944213
Sacramento, CA 94244-2130

Joseph Skorupa
U.S. Fish and Wildlife Service
3310 El Camino Avenue
Suite 130
Sacramento, CA 95821-6340

SALINITY/DRAINAGE ANNUAL MEETING

March 26, 2002

8:10 **Welcome, John Letey**, Director, UC Center for Water Resources

8:15 Synopsis of Major Funding by PIs of Sponsored Research Projects
(See opposite page for presenters.)

10:00 Break

10:30 **Jason Phillips**, US Bureau of Reclamation
Update of San Luis Drainage Features Reevaluation

11:00 **Bill Jury**, UC Riverside
Travel Time Affects Long-term Consequences of Drain Water Reuse

11:20 **John Letey**, UC Riverside
An Example of Travel Time Long-term Effects

11:40 **Keith Knapp**, UC Riverside
Economics of Integrated Drain Water Management

12:00 Hosted Lunch and Posters

2:00 **Joe Skorupa**, US Fish and Wildlife Service, Department of the Interior
Evaporation Ponds: A fish and Wildlife Service Perspective

2:30 **Corey Yep**, Department of Toxic Substance Control
Selenium Hazardous Waste Regulation – Toxic Pits Act

3:00 Break

3:30 **Charles H. Hanson**, Hanson Environmental Incorporated
Evaporation Pond On-site Mitigation and Off-site Compensation for Wildlife Impact

4:00 **Teresa Fan and Rick Higashi**, UC Davis
Foodchain Disruption as a Management Practice for Selenium Ecotoxic Risk Reduction in Evaporation Basins

4:30 **Ken Tanji**, UC Davis
Selenium in Water, Sediments, and Evaporites in Evaporation Ponds

SYNOPSIS OF MAJOR FUNDING BY PIs OF SPONSORED RESEARCH PROJECTS

Prosser Funded

Louise Ferguson, Kearney Ag. Center, Potential for Using Blended Drainage Water for Irrigating West Side, San Joaquin Valley Pistachios

Allan Fulton, UC Coop. Ext. Tehama Co., Using EM and VERIS Technology to Assess Land Suitability for Orchard and Vineyard Development in Non-saline Environments

David Goldhamer, Kearney Ag. Center, Validation of Protocols for Using Trunk Diameter and Tree Water Potential Measurements in Orchard Irrigation Scheduling

Blaine Hanson, UC Davis, Response of Crop Yield and Water Table to Subsurface Drip Irrigation of Processing Tomato Under Saline, Shallow Groundwater Conditions

Daniel Munk, UC Coop. Ext. Fresno Co., Contrasting Irrigation Application Methods for Drainage Reduction and Soil Salinity Management

Larry Schwankl, UC Davis, Improving Water and Nutrient Management Practices on Dairies in the Southern San Joaquin Valley

Salinity/Drainage Funded

William Frankenberger, UC Riverside, (Carla Scheidlinger presenting), Removal of Selenium from Drainage Water in Lined Reduction, Attachment, and Open Oxidation Channels: A Field Study

Michael Fry, UC Davis, An Investigation into the Ecotoxicology of Selenium Bioaccumulation in Birds

Suduan Gao, UC Davis, Management Effects on Selenium Fractionation, Speciation and Bioavailability in Sediments from Evaporation Basins

Steve Grattan, UC Davis, Evaluation of Salt-Tolerant Forages for Sequential Reuse Systems

Thomas Harter, UC Davis, Salinization of Deep Production Wells in the Western San Joaquin Valley: Risk Analysis, Uncertainty, and Data Needs

Stephen Kaffka, UC Davis, Using Forages and Livestock to Manage Drainage Water in the San Joaquin Valley

Keith Knapp, UC Riverside, Economics of Integrated Drainwater Management

Eliska Rejmankova, UC Davis, (Rick Higashi presenting) Algal Community Assessment Under Different Nutrient and Grazing Intensity Regimes: Selenium Volatilization and Ecotoxic Risk

Ken Tanji, UC Davis, Mass Balance of Water and Se in the TLDD Flow-through Wetland Cells

Norman Terry, UC Berkeley, Selenium Volatilization in Rabbitfoot Grass Wetland Microcosms

Wes Wallender, UC Davis, Water and Land Management in Irrigated Ecosystems

Assessing the Efficacy of Macroinvertebrate Harvest and Algal Se Volatilization for Mitigating Se Ecotoxic Risk in Agricultural Drainage Systems and Biochemical Characterization of Microphyte Composition in Relation to Se Biogeochemistry and Bioavailability

(PART OF A TEAM PROJECT ENTITLED "MITIGATING SELENIUM ECOTOXIC RISK BY COMBINING FOODCHAIN BREAKAGE WITH NATURAL REMEDIATION")

Project Investigators:

Teresa W-M. Fan
Office: (530) 752-1450, E-mail: twfan@ucdavis.edu
Dept. of Land, Air & Water Resources, UC Davis

Jack Meeks
Office: (530) 752-3346, E-mail: jcmeeks@ucdavis.edu
Microbiology-Division of Biological Sciences, UC Davis

Richard Higashi
Office: (530) 752-1450, E-mail: rmhigashi@ucdavis.edu
Crocker Nuclear Lab., Univ. of Calif. Davis

Collaborators*:*

Drs. Eliska Rejmankova, Environmental Science & Policy, University of California, Davis
Sudan Gao & Randy Dahlgren, Dept. of Land, Air & Water Resources, Univ. of California, Davis
Dr. Jarka Komarkova, Hydrobiological Institute AS CR, Czech Republic
Dr. Robert Rofen, Novalek, Inc.
Julie Vance, California Dept. of Water Resources

Research Staff:

2 PGR (Jee Liu and Chris Coehlo)
1 SRA (Teresa Cassel)

ABSTRACT

As in the previous two years, we measured *in situ* Se volatilization from hypersaline and saline drainage evaporation basin cells of the Tulare Lake Drainage District (TLDD). We also investigated the monthly trend in water quality parameters and Se status of the biota in the TLDD basin cells from 2001 thru 2002. These included salinity, pH, waterborne Se concentration, algal Se burden, and brine shrimp Se burden.

Se volatilization continued to be active in TLDD basins cells, and was much more active in the hypersaline cells where brine shrimp harvest is ongoing but not where the harvest is absent. The higher Se volatilization from hypersaline basin cells is consistent with our previous observation. Diurnal variation in Se volatilization from the hypersaline cells was also noted and this variation was less prominent in the less saline cells or in the hypersaline cell with no brine shrimp harvest activity. Moreover, where brine shrimp harvest and hypersalinity coexist in the TLDD basin cells, waterborne Se concentration was lower while Se volatilization was higher than hypersaline cells with no brine shrimp harvest. This suggests that the combination of hypersalinity and brine shrimp harvest enhance Se volatilization, which in turn reduces Se load in the water.

The salinity of the hypersaline cells fluctuated monthly to a greater extent than that of the less saline cells, while the pH of both hypersaline and less saline cells remained in the range of 8.5-9.0, except for the hypersaline, unharvested cell. The simultaneous and rapid drop of salinity and pH in the hypersaline, unharvested cell could be a result of the carbonate precipitation, since carbonate is expected to be the main alkalinity factor in these cells. The microalgae in the hypersaline, unharvested cell also had a generally higher Se body burden than microalgae in the hypersaline, harvested cells. Up to 78% of the waterborne Se was present as microalgal Se in the former whereas the highest fraction of waterborne Se present as microalgal Se in the latter was only 35%. It was also noted that the Se bioconcentration factor (BCF) for microalgae was generally lower in hypersaline cells, as was observed in previous years. This could suggest that hypersalinity helps limit Se assimilation into microalgal biomass. For the hypersaline, harvested cells, lower Se burden of microalgae was associated with that of brine shrimp. However, this was not the case with the hypersaline, unharvested cell where the Se burden of brine shrimp was comparable or lower than those of other cells but its microalgae Se burden was by far the highest. This could suggest that the microalgal Se in the hypersaline, unharvested cells is less bioavailable, or these microalgae are less favored food source for the brine shrimp, or both. This raises the issue of the type of algal composition that can transfer Se to brine shrimp and/or sustain brine shrimp production.

To address the question, we conducted laboratory beaker experiment where a mixture of TLDD basin cell waters was grazed by brine shrimp adults. The daily time course change in the algal composition was examined by microscopy, which shows that *Synechocystis salina* appeared to be consumed the most while *Oocystis* was the least consumed. In addition, heterotrophic bacteria did not appear to be grazed. 16S DNA analysis of cyanophytes from several basin cells revealed both seasonal and cell-to-cell variations in the composition, with a single species dominated at times in the hypersaline cells, regardless of the brine shrimp harvest status. This dominance is most likely attributed to the influence of hypersalinity. By sequencing the 16S DNA separated by denaturing gradient gel electrophoresis and matching the sequence against the bacterial database, one of the hypersaline, harvested cells was found to be abundant in *Synechococcus*. This is consistent with the morphological assessment.

KEYWORDS

Tulare lake drainage district (TLDD), evaporation basins, se bioconcentration factor, 16S RNA typing, brine shrimp grazing, *Synechococcus*, *Synecosystis*,

BACKGROUND & OBJECTIVES

We have been investigating the potential of utilizing Se volatilization by microalgae to reduce Se ecotoxic risk in San Joaquin Valley's evaporation basins. We have observed the following phenomena that support the notion that microalgae are active players in Se volatilization, and that this process contributes to Se dissipation from drainage waters stored in the evaporation basins.

- Microalgae isolated from TLDD evaporation basins (cyanophytes in particular) are very active in volatilizing Se from waters and this activity leads to the depletion of a sizeable

fraction of waterborne Se (Fan and Higashi, 1998; Fan and Higashi, 1999; Fan et al., 1998; Fan et al., 1997).

- High activities of Se volatilization were observed *in situ* from TLDD basins where waterborne Se concentrations did not increase with evaporation (Fan and Higashi, 1999), as predicted by evaporite chemistry.
- Se volatilization is an order of magnitude more active in hypersaline TLDD basin waters than less saline TLDD basin and demonstration Flow-Through wetland waters (Higashi, 2001). This is consistent with the contribution of Se volatilization to the depletion of Se from hypersaline waters.

Thus, it is clear that some Se can be removed from evaporation basin waters by biological volatilization under existing basin operating conditions. It is also reasonable to assume that TLDD basins are not optimized for Se volatilization by microalgae and that there may be means by which this activity can be enhanced. However, removing Se by volatilization alone does not ensure reduction of Se ecotoxic risk, since the process of biological volatilization requires that microalgae (and vascular plants) first bioaccumulate Se into their biomass, which can then be transferred up the foodchain to pose risk to top predators.

To minimize this foodchain transfer process, we are also adopting the concept of foodchain disruption via exhaustive harvest of macroinvertebrates such as brine shrimp (*Artemia franciscana franciscana*). This concept not only may help reduce Se ecotoxic risk but also has good economic efficacy since there is a market demand for brine shrimp. Moreover, the requirement of hypersaline waters for brine shrimp production makes it compatible with coupling to other drainage mitigation plans such as IFDM (in-farm drainage management) and reverse osmosis (the end product of both is hypersaline waters).

Commercial brine shrimp harvest has been in operation at TLDD since 1998 through a cooperation between TLDD management and Novalek, Inc. (Hayward, CA). In coordination with this effort, we initiated in 2001 a monthly monitoring of Se status in the hypersaline ponds of TLDD where brine shrimp have been harvested. Our preliminary results indicate that Se status in these ponds appeared to be attenuated, in terms of waterborne Se concentration, algal Se burden, and brine shrimp/corixid Se burden, during peak harvest months. In addition, the hypersaline pond waters exhibited a substantially higher Se volatilization activity than the less saline pond waters, as observed in Year 2000 (Higashi, 2001). Interestingly, fertilizers administered by Novalek, Inc. in the hypersaline ponds have had an apparent positive effect on algal and brine shrimp productions. These results suggest that it may be practical to couple Se volatilization with foodchain disruption to remediate Se risk in evaporation basins, and that this coupled process may be sustained or enhanced by manipulating the water chemistry.

Our overall objective is to understand the effect of fertilization and brine shrimp harvest on Se biogeochemistry, and to uncover conditions that simultaneously favor Se volatilization by microalgae and brine shrimp production, while minimizing the accumulation of Se ecotoxic indicators. The study on the full-scale pond systems (project "Assessing the Efficacy of Macroinvertebrate Harvest and Algal Se Volatilization for Mitigating Se Ecotoxic Risk in Agricultural Drainage Systems") is coupled with the small-scale but better controlled trials conducted under the team project of Higashi et al initiated in 2001 (project "Biochemical Characterization of Microphyte Composition in Relation to Se Biogeochemistry and Bioavailability"). Together, a mechanistic insight can be acquired for enhancing *in situ* Se bioremediation via Se volatilization and foodchain disruption. We will achieve this by investigating the following:

- Change in Se status in TLDD hypersaline ponds (Hacienda A4 in particular since we have data on its Se status before harvest began) elicited by brine shrimp harvest;
- Changes in water chemistry associated with fertilizer input
- Effects of fertilizer input on nutrient status of microalgae and brine shirmp, microalgal community, as well as Se status in TLDD hypersaline ponds so that these effects may be related to changes in water chemistry, thereby guiding additional nutrient supplementation.
- Changes in algal composition as a function of brine shrimp grazing and fertilizer input in cotrolled mesocosm setup

SUMMARY OF PROGRESS FROM 2001-2002

ASSESSING THE EFFICACY OF MACROINVERTEBRATE HARVEST AND ALGAL SE VOLATILIZATION FOR MITIGATING SE ECOTOXIC RISK IN AGRICULTURAL DRAINAGE SYSTEMS

Se Volatilization at TLDD Evaporation Basins

We conducted *in situ* measurement of Se volatiles present in TLDD evaporation basin cell series varying in salinity and brine shrimp harvest. Namely, the South evaporation basin series S-S8-S9-S10, and two Hacienda evaporation basin series A2-A4 and C2-C4. The Se volatilization measurements were performed in the morning (am) and afternoon (pm) to see the extent of diurnal fluctuations. Figure 1 shows the amount of Se in ng purgeable from 800 ml of waters (gray and hashed bars) of S1, S9, and 10 as well as from A2, A4, C2, and C4. Also shown is the salinity or conductivity of the water (filled circles). It is clear that for S8, S9, S10, and A4 cells, the amount of Se volatiles was much higher than the less saline cells of the same series. This trend has been consistently observed for the last four years at TLDD basins (Higashi, 2001) In addition, a sizable difference in the amount of Se volatiles was observed between the am and pm measurements and there was no consistent trend whether Se volatilization was higher in a given time of the day. It should be further noted that these 4 cells have active brine shrimp harvest. In contrast, the less saline cells (S1, A2, and C2) did not exhibit as strong a diurnal variation in Se volatilization as the more saline cells, however neither did the hypersaline C4 cell. The C4 cell also had a lower extent of Se volatilization than the other hypersaline cells (A4 and S9). No viable amount of brime shrimp is present in S1, A2, and C2 to support harvest while C4 is too shallow to harvest despite its abundance in brine shrimp.

The different behavior in Se volatilization between the two Hacienda cell series (A and C) is interesting. These two cell series receive the same subsurface drain water but they are managed quite differently. As indicated above, the terminal A4 cell has been maintained with an adequate level of water to support brine shrimp harvest while the terminal C4 cell was not harvested and at times let dry. It is possible that the management practice associated with brine shrimp harvest supports a higher extent of Se volatilization. This practice may also be related to the higher extent of Se volatilization in the harvested S8, S9 (terminal), and S10 cells than in the untouched S1 cell.

Since brine shrimp harvest is necessarily associated with hypersalinity, hypersalinity may be one important factor regulating Se volatilization and waterbone Se concentration. Figure 2 plots the relationship of waterborne Se concentration (water [Se]) to the amount of Se volatiles for the 5 saline cells S8, S9, S10, A4, and C4. It is interesting to note that for the hypersaline and harvested cells S9 and A4, a higher Se volatilization (filled circles) was seen with a lower water [Se] (filled squares). An opposite relationship was observed for the hypersaline but unharvested C4 cell. This result could have the following implications. Hypersalinity and brine shrimp harvest together may be important for high Se volatilization. It is likely that the higher Se volatilization is a key to dissipating waterborne Se that would have accumulated in hypersaline cells.

Water Quality and Se Status in Biota at TLDD Evaporation Basins

Water Quality

In addition to Se volatilization measurement, we have followed the water quality and Se status in major categories of biota present in TLDD basins. Figure 3-7 illustrates the monthly trend of salinity, pH, waterborne Se concentration, algal Se burden, and brine shrimp Se burden, respectively, for South evaporation basin (SEB) cells 8, 9, and 10 as well as Hacienda evaporation basin (HEB) cells A4 and C4. As expected, the salinity of the terminal S9, A4 and C4 cells remained higher than that of S8, S10 throughout the period of Feb., 01 thru Jan., 02 (Figure 3). In addition, the salinity in the S9, A4, and C4 fluctuated much more than the less saline cells S8 and S10. This large fluctuation is presumably the consequence of evaporation and management practice. It is unclear on how such fluctuation can affect algal community, which can in turn influence Se volatilization and/or brine shrimp production.

Despite the large change in salinity, the pH of all of cell water had a relatively narrow range of 8.5-9.0 except for the C4 cell which dropped below 7.5 in Jan., 2002 (Figure 4). This constant pH trend could suggest that carbonate (the main alkalinity factor) may be precipitating out of solution presumably as $CaCO_3$ as salinity increases. The buildup of salinity to 150- 200 ppth in the months prior to the large pH and salinity drop in C4 is consistent with this explanation. However, the hypersalinity in S9 of Nov., 2000 (225 ppth, open circle) did not lead to a drop in pH although the salinity did decline in subsequent months. It is possible that the drop in salinity of S9 is due to dilution by inflow of less saline water, rather than salt precipitation.

Relative to the salinity, the amplitude of change in waterborne Se concentrations was much smaller for S9 and A4 but not for C4 (Figure 5). Despite the increase in salinity, the waterborne [Se] of S9 and A4 was comparable to that of the less saline S8 and S10, particularly during the summer months when evaporation is most active. Another notable trend is that the waterborne [Se] remained much higher in C4 with no harvest activity than other cells where brine shrimp harvest occurred. In view of the higher extent of Se volatilization observed for the harvested S9 and A4 (Figure 1), the waterborne [Se] data is consistent with the contribution of both Se volatilization and brine shrimp harvest to the lack of Se buildup in hypersaline S9 and A4 cells.

Se Status in Biota

Another striking influence of brine shrimp harvest is expressed on the Se body burden of microalgae (Figure 6). Throughout the one-year period, the Se load in microalgae (collected on 0.45 µm filters) was comparable among S8, S9, S10, and A4 but much higher in C4 starting from July, 2001 thru Jan., 2002. These amounts of Se load in microalgae constituted at times a major fraction of the Se present in the water (up to 78% of Oct, 2002). This is in contrast to S9 and A4 where the highest fraction observed was only 18% and 35%, respectively. This difference in algal contribution of waterborne Se could be related to both brine shrimp harvest and Se volatilization. It is reasonable to expect that shrimp harvest reduced algal biomass while increased Se volatilization helped dissipate Se accumulated in algal biomass in S9 and A4.

In comparison, the monthly trend in the Se body burden of brine shrimp was less discernable (Figure 7). However, the Se load of brine shrimp in S9 (open circles) remained lower from June to Nov., 2001 than the other hypersaline, harvested cell A4 (filled squares). This difference could reflect the lower Se burden of microalgae in S9 than in A4 (cf. Figure 6). However, the Se burden in microalgae does not explain the lower Se burden of brine shrimp in C4 than in A4. It is possible that the Se accumulated in the microalgae of C4 was less available to brine shrimp and/or the microalgal populations of C4 were a less favored food source for brine shrimp.

By normalizing algal Se burden against Se concentration in 0.45 µm filtered water (which removed contribution from particulate Se and approximated dissolved Se concentration), the algal bioconcentration factor (BCF) for Se was calculated and shown in Figure 8. It should be noted that these BCFs are based on algal dry weight, which should be distinguished from those based on wet weight. The algal BCF fluctuated widely, particularly for S10, which ranged from 160 to 8700. There appeared to be a tendency of higher algal Se BCF in the less saline S8 and S10 than the hypersaline S9, A4, and C4. However, no clear trend was evident in BCF change that could be related to shrimp harvest, or time of year, except that the algal Se BCF in the unharvested C4 cell (filled circle) remained the lowest despite its higher waterborne [Se] (cf. Figure 5). An inverse relationship between algal BCF and waterborne [Se] has also been noted by us previously (Fan et al., 2002). It is plausible that hypersalinity helps limit Se assimilation into algal biomass.

The Se BCF for brine shrimp was calculated similarly as the algal Se BCF and shown in Figure 9. Relatively speaking, Se bioconcentration from water into brine shrimp was less variant and lower in extent than that into microalgae, ranging from 650 to 2900, except for the BCF of S8 from Jan. 2002 that reached about 5400. Therefore, there was generally no further Se bioconcentration from microalge to brine shrimp and that brine shrimp may have an efficient meahnism for regulating Se uptake, assimilation, or depuration from the food source.

In addition to monthly brine shrimp monitoring, major water-column and benthic macroinvertebrates of the TLDD basins were collected on the same day in May, 2001, and analyzed for Se body burden as shown in Table 1. There are several notable points illustrated in Table 1. First, brine shrimp (Artemia) and corixid/nononactid were the main water-column macroinvertebrates while brine fly larvae/pupae and midge/mosquito larvae were the main benthic macroinvertebrates. Second, brine fly larvae/pupae exhibited the lowest range of Se body burden while corixid egg mass had the highest Se body burden. The high Se content of the corixid egg mass is consistent with our previous observation that Se tended to bioaccumulate in fish ovaries (Fan et al., 2002). Third, the Se burden of the macroinvertebrates in the more saline cells (e.g. A4, C4, and S9) was among the lowest, which has been consistently noted in the monthly brine shrimp data (Figures 7) and macroinvertebrate data from previous years (Fan and Higashi, 2000; Fan and Higashi, 2001).

In summary, the coupling of hypersalinity with brine shrimp harvest appeared to enhance Se volatilization that, together with the removal of brine shrimp and indirectly microalgae biomass, should help dissipate Se in TLDD evaporation basins. The fraction of the Se removed should also represent that most directly available to the bird species foraging in these basins. These processes may underlie the lack of Se buildup in waterbonre Se concentrations as well as Se body burden in the biota of the TLDD basins. The ability to sustain and optimize these processes should prove to be an effective and economical means for *in situ* Se remediation of contaminated drainage systems.

BIOCHEMICAL CHARACTERIZATION OF MICROPHYTE COMPOSITION IN RELATION TO SE BIOGEOCHEMISTRY AND BIOAVAILABILITY

Changes in Microalgal Composition under Brine Shrimp Grazing

In collaboration with Dr. Jarka Kormarkova, we performed laboratory beaker experiments where a mixture of cell waters from the South and Hacienda evaporation basins was incubated with 0, 6, or 12 brine shrimp adults for a week. The salinity of the combined water was 45 ppth. Water samples were collected daily for microscopic analysis of microalgal composition. Figure 10 illustrates the fluorescent micrographs of TLDD basin cell waters after grazing with 12 brine shrimp adults or none (control). The right two micrographs were based on Chl *a* red fluorescence, which indicated photosynthetic microalgae while the left two micrographs were based on the general DNA stain DAPI which revealed both microalgae and heterotrophic bacteria. Several microalgal species were found abundant in the combined water, including *Synechocystis salina*, *Synechococcus sp.* *Cyanodictyon planktonicum*, *Oocystis cf. parva*, and *Aphanocapsa salina*. It is clear from comparing DAPI and Chl a-based images that heterotrophic bacteria were also present. The disappearance of *Synechocystis* and *Cyanodictyon* from the brime shrimp-incubated water presumably indicates that these two microalgae were grazed by brine shrimp. In contrast, brine shrimp did not appear to consume the picoplankton *Synechococcus*, *Aphanocapsa*, *Oocystis*, and bacteria which remained abundant in the DAPI and/or Chl *a*-based micrographs after grazing activity.

Time course changes in four types of microalgae were also plotted to illustrate the kinetics of population change under the influence of brine shrimp grazing (Figure 11). It is clear that the fraction of total fresh matter (% FM) present as *Oocystis cf. Marssonii* changes little in the absence of brine shrimp but increased with time with 6 or 12 brine shrimp adults. This is consistent with *Oocystis* not being consumed by brine shrimp. In contrast, the % FM present as *Synechocystis salina* decreased substantially in the presence of brine shrimp even though *Synechocystis* population actually increased when brine shrimp was absent. This suggests that *Synechocystis* was grazed by brine shrimp. Similarly, although the populations of filamentous cyanophyte and *Cyanodictyon planktonicum* (CPP) declined under control conditions, this decline was further enhanced by the presence of brine shrimp. Thus, it is plausible that these two cyanophytes were also grazed by brine shrimp. It should be pointed out that grazed algae are not necessarily digested to support brine shrimp growth. However, such grazing analysis provides a list of algae indigenous in TLDD basin waters that are candidates for sustaining brine shrimp populations. Such information would be valuable for designing strategy for manipulating algal composition to optimize brine shrimp harvest.

Variations In Microalgal Composition In Tldd Basins

In addition to morphology-based identification, we initiated biochemical characterization of microalgal community using the 16S RNA typing approach (Ferris et al., 1996). Total DNA was isolated from the microalgal biomass collected monthly and the 16S cDNA was amplified from the DNA template using a pair of cyanophyte-selective primers and polymerase chain reaction (PCR). We choose to first focus on cyanophytes due to their abundance in the TLDD basins and their ability to volatilize Se (Fan and Higashi, 1998; Fan et al., 1998). The PCR-amplified cDNA was then separated by denaturing gradient gel electrophoresis (DGGE), which is capable of distinguishing DNA differing by one base pair. Figure 12 illustrates the DGGE profile of 16S cDNA prepared from microalgal collections at different dates from the four TLDD basin cells where brine shrimp harvest is ongoing. The DGGE profiles varied from different dates for all four basin cells, and for a given date they were also distinct among the four cells. This variance reflects the dynamic nature of the cyanophyte community in

these basin cells. It is interesting to note that the DGGE profile of the hypersaline S9, A4, and C4 cells was at times dominated by a single band (denoted by arrow) with a similar electrophoretic mobility. This phenomenon could be related to both hypersalinity and brine shrimp harvest. It is possible that the dominant species was well adpated to hypersalinity and was not consumed readily by brine shrimp.

To further explore the identity of the cyanophyte species separated by DGGE, a few of the DGGE gel bands were excised, from which DNA was eluated, reamplified, and sequenced, which yielded nucleotides of 341-360 base pairs (Figure 13). We tested this procedure with a laboratory *Synechococcus* monoculture maintained in Co-PI Meeks's laboratory. When search against the bacterial data base of Entrez, the *Synechococcus* 16S DNA had a nearly 100% match with Synechococcus PCC7943 (accession number AF216949) with an E value of e-171 (from forward NCBI BLAST search). When we applied this approach to two of the TLDD A4 bands (Figure 13), one band (band 2) had a 91% match (E value of e-117 and e-122 from forward and reverse NCBI BLAST searches, respectively) with a *Synechococcus* sp. (accession number AF330247). The other band (band 3) had a good match (E value of e-103 and e-102 from forward and reverse NCBI BLAST searches, respectively) with an uncultured bacterium (accession number AF428957). The abundance of *Synechococcus* as revealed by the 16S RNA typing approach is consistent with the morphological examination.

REFERENCES

Fan, T.W.-M. and Higashi, R.M. (1998) *Biochemical Fate of Selenium in Microphytes: Natural Bioremediation by Volatilization and Sedimentation in Aquatic Environments. In: Environmental Chemistry of Selenium, W.T. Frankenberger and R.A. Engberg, eds., pp. 545-563*. Marcel Dekker, Inc., New York.

Fan, T.W.M. and Higashi, R.M. (1999) In Situ Se Volatilization and Form Measurements at San Joaquin Valley Evaporation Basins. Univ. of California, Davis report to California Dept. of Water Resources, Davis, CA, p. 17.

Fan, T.W.M. and Higashi, R.M. (2000) Microphyte-mediated Se biogeochemistry and its role in bioremediation of Se ecotoxic consequences. University of Calif., Salinity/Drainage Program, Davis, p. 12.

Fan, T.W.M. and Higashi, R.M. (2001) Mitigating Selenium Ecotoxic Risk by Combining

Foodchain Breakage with Natural Remediation. Univ. of California, Salinity/Drainage Program, Davis, p. 12.

Fan, T.W.M., Higashi, R.M. and Lane, A.N. (1998) Biotransformations of Selenium Oxyanion by Filamentous Cyanophyte-Dominated Mat Cultured from Agricultural Drainage Waters. *Environ. Sci. Technol.*, **32**, 3185-3193.

Fan, T.W.M., Lane, A.N. and Higashi, R.M. (1997) Selenium biotransformations by a euryhaline microalga isolated from a saline evaporation pond. *Environmental Science & Technology*, **31**, 569-576.

Fan, T.W.M., Teh, S.J., Hinton, D.E. and Higashi, R.M. (2002) Selenium biotransformations into proteinaceous forms by foodweb organisms of selenium-laden drainage waters in California. *Aquatic Toxicology (Amsterdam)*, **57**, 65-84.

Ferris, M.J., Muyzer, G. and Ward, D.M. (1996) Denaturing gradient gel electrophoresis profiles of 16S rRNA-defined populations inhabiting a hot spring microbial mat community. *Applied and Environmental Microbiology*, **62**, 340-346.

Higashi, R.M. (2001) Chemical Nature of Selenium in Agricultural Drainage Sediments and its Implications for Bioavailability. Uinv. of California, Davis report to Univ. of California Salinity/Drainage Program, Davis, California, p. 14.

Table 1. Se body burden in various macroinvertebrate types collected from TLDD basins

InvertebrateType	TLDD Basin cell	Se µg/g dry wt
Artemia	HEB A4	6.87
	HEB C4	11.87
	SEB 10	10.66
Artemia with gonad	SEB 9	5.84
corixid	HEB C2	11.66
	HEB C4	4.95
	SEB 8	7.45
	SEB 10	8.11
corixid with egg	SEB 1	7.86
corixid egg mass	HEB C2	26.93
	HEB C4	12.03
nononactid + corixid	HEB A2	14.79
	SEB 1	10.50
brine fly larvae	HEB A4	4.89
	HEB C4	3.11
	SEB 10	4.23
	SEB 8	2.89
brine fly pupae	HEB A4	3.17
	HEB C4	2.66
	SEB 8	4.66
	SEB 9	1.60
benthic midge larvae	SEB 1	12.17
midge + mosquito larvae	HEB A2	9.72

Figure 1

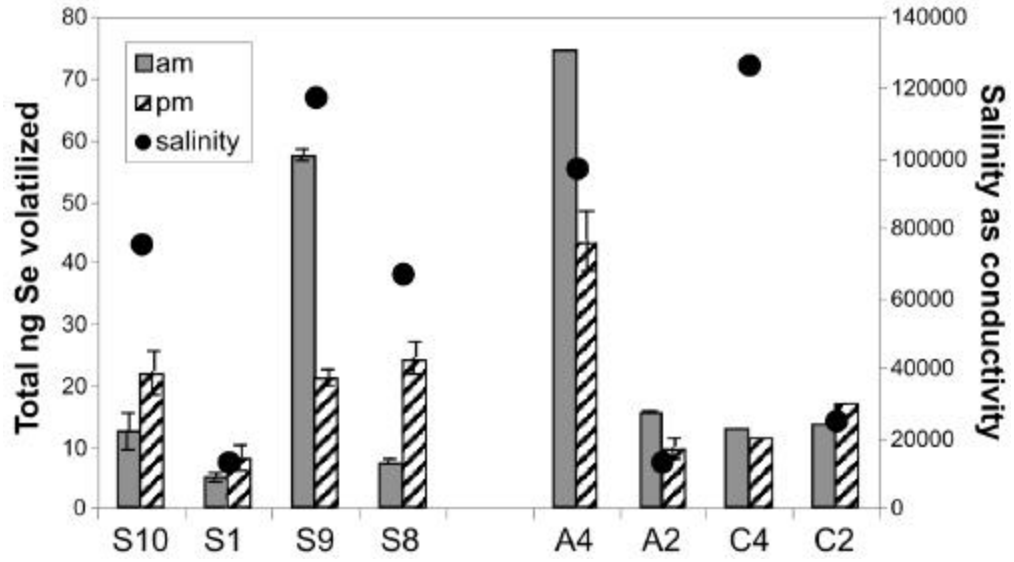

Figure 1. Diurnal variation in Se volatilization of TLDD basin cells varying in salinity and brine shrimp harvest activity.

Figure 2

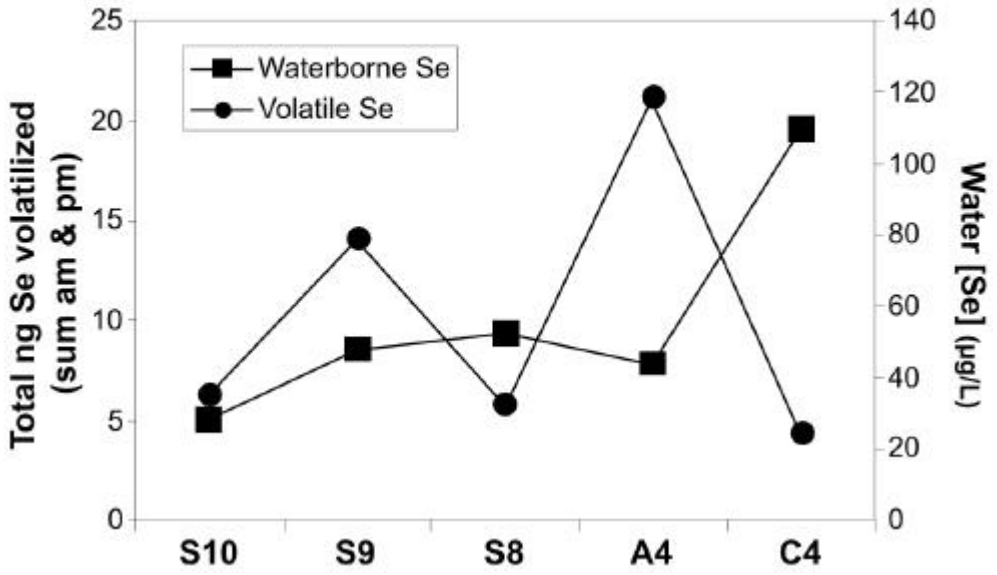

Figure 2. Se volatilization versus waterborne Se concentration for brine shrimp-harvested TLDD basin cells. Waterborne [Se] is defined as Se concentration in whole water with macroinvertebrate removed but microalgae retained.

Figure 3

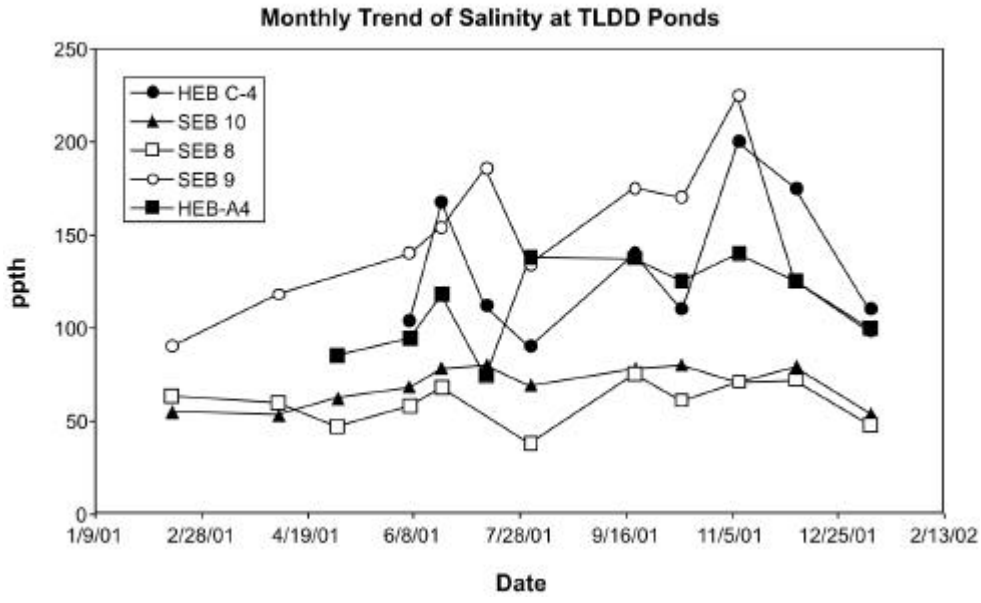

Figure 3. Monthly trend of salinity in brine shrimp-harvested TLDD basin cells. Salinity is expressed as part per thousand (ppth).

Figure 4

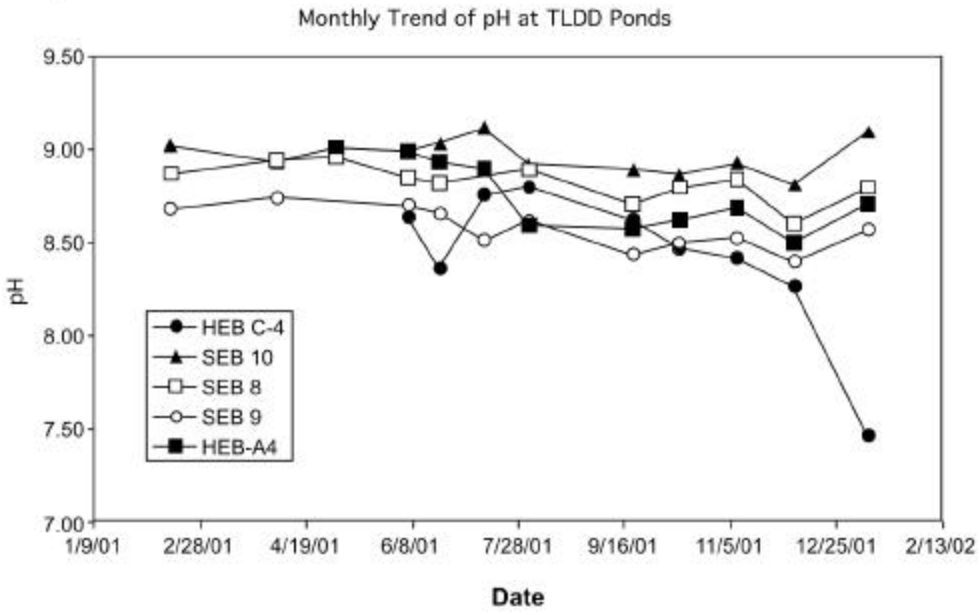

Figure 4. Monthly trend of pH in brine shrimp-harvested TLDD basin cells.

Figure 5

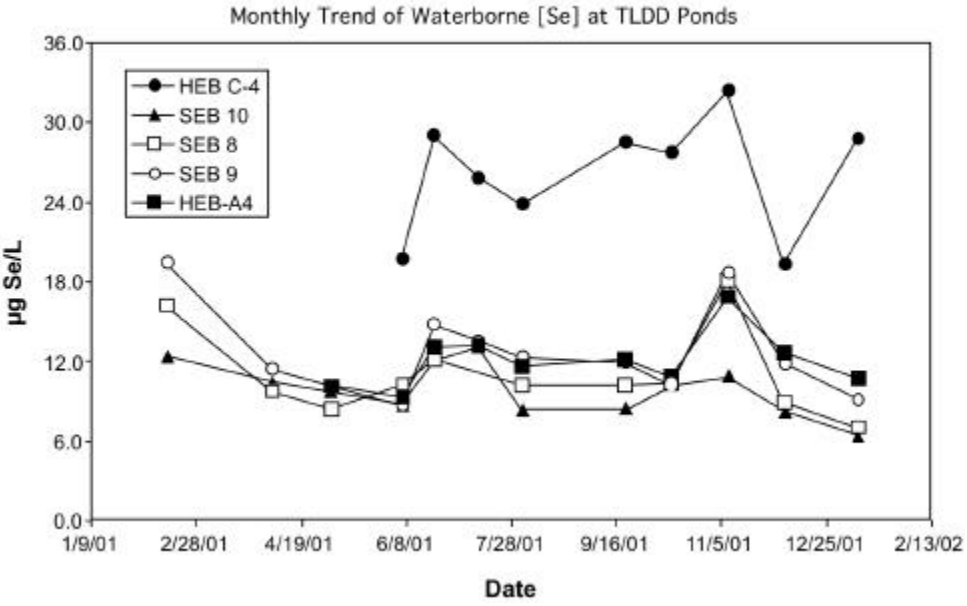

Figure 5. Monthly trend of waterborne Se concentration in brine shrimp-harvested TLDD basin cells. Waterborne Se was measured as total Se in whole water.

Figure 6

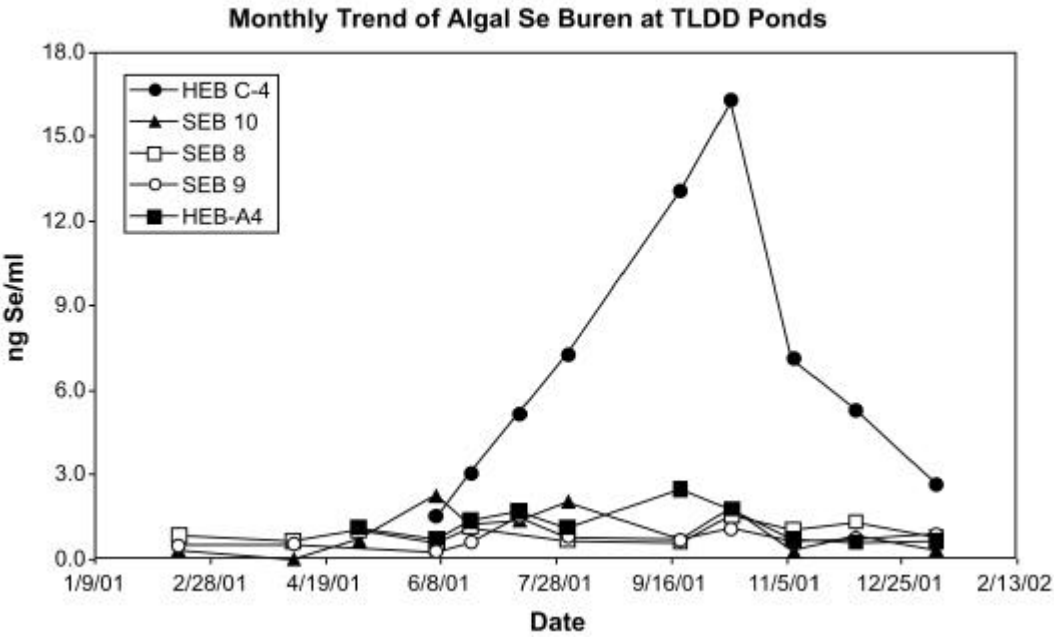

Figure 6. Monthly trend of algal Se body burden in brine shrimp-harvested TLDD basin cells.

Figure 7

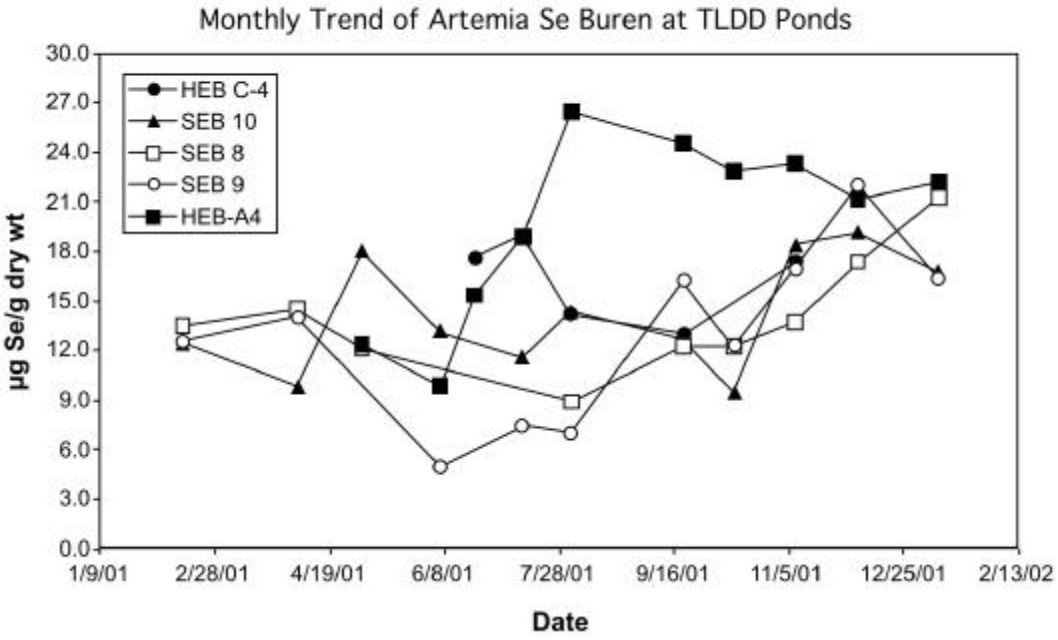

Figure 7. Monthly trend of brine shrimp Se body burden in brine shrimp-harvested TLDD basin cells.

Figure 8

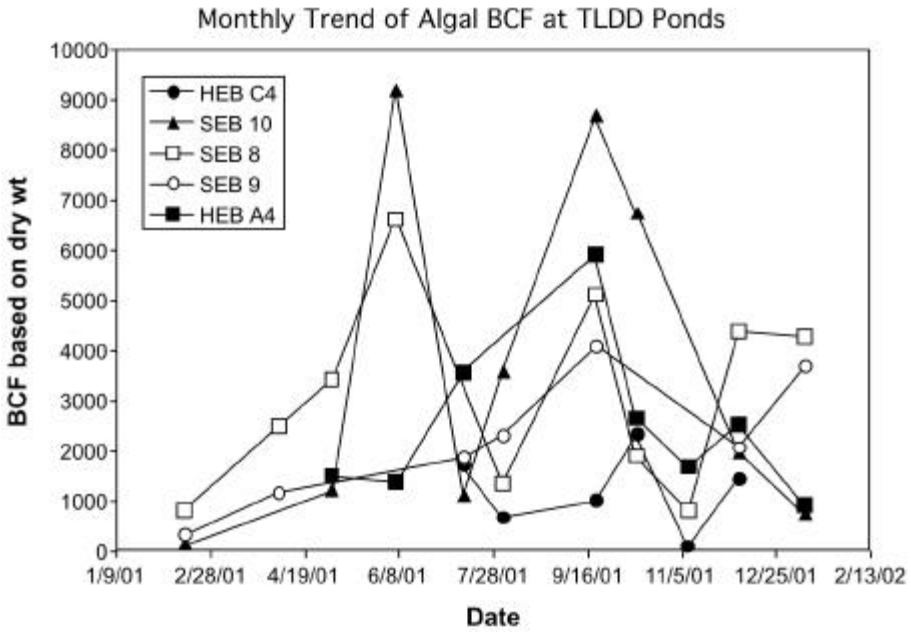

Figure 8. Monthly trend in bioconcentration factor (BCF) for Se in microalgae at brine shrimp harvested TLDD basin cells. BCF was calculated by dividing algal Se burden on dry wt basis with Se concentration of 0.45 µm filter-treated water. The latter approximates dissolved Se concentration in the water.

Figure 9

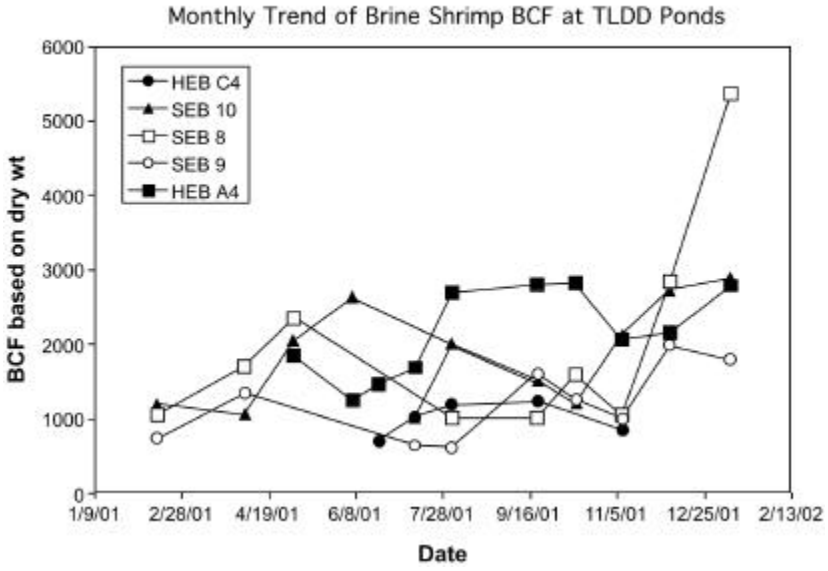

Figure 9. Monthly trend in bioconcentration factor (BCF) for Se in brine shrimp at brine-shrimp harvested TLDD basin cells. BCF was calculated by dividing brine shrimp Se burden on dry wt basis with Se concentration of 0.45 µm filter-treated water. The latter approximates dissolved Se concentration in the water.

Figure 10

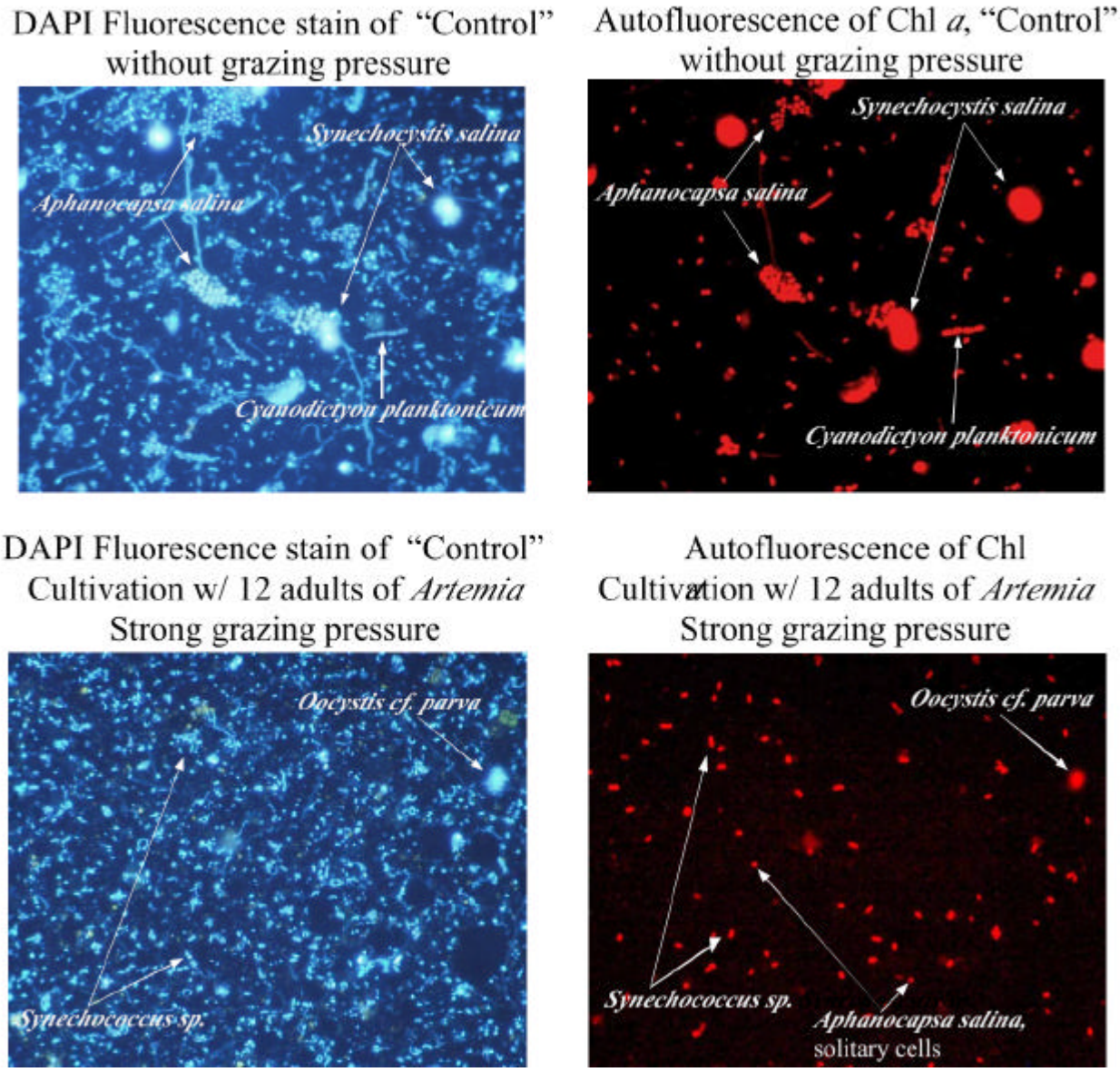

Figure 10. Chl *a* and DAPI-based fluorescence micrographs of TLDD basin waters in the absence or presence of brine shrimp grazing. DAPI is a general stain for DNA which allows both microalgae and heterotrophic bacteria to be visualized while only microalgae are visible with red Chl *a* fluorescence.

Figure 11

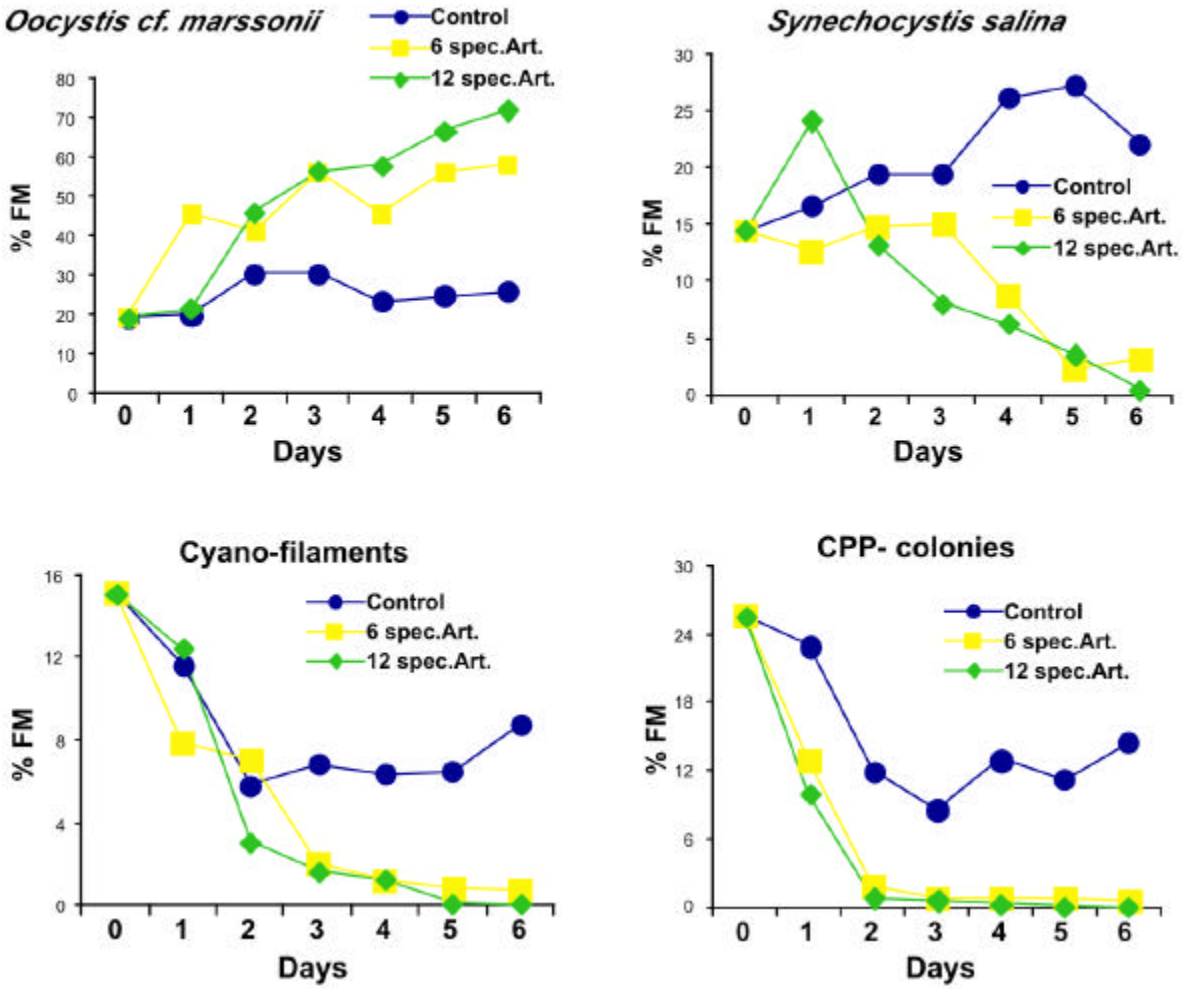

Figure 11. Time course changes in the abundant microalgae in the absence and presence of brine shrimp grazing.

Figure 12

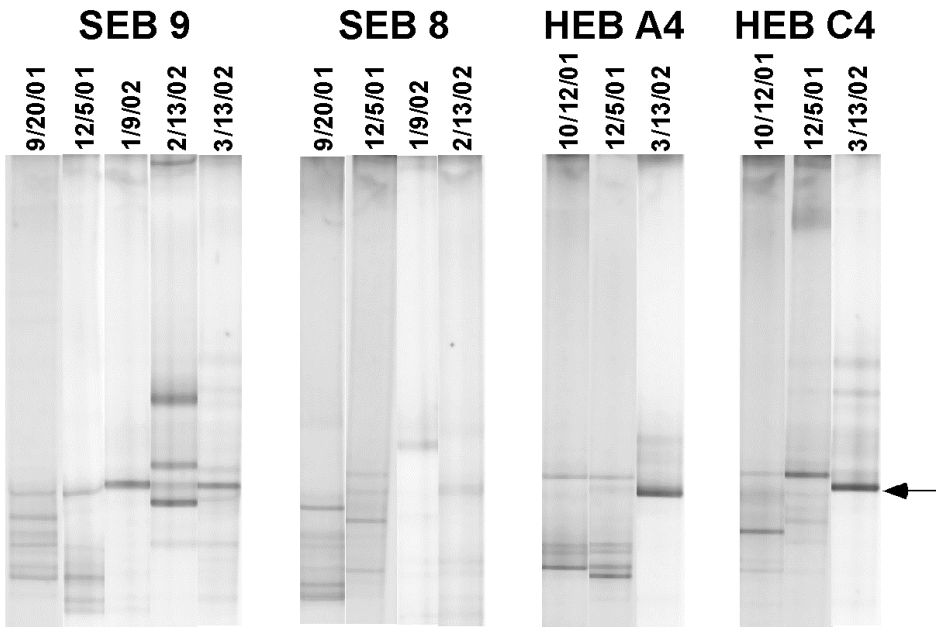

Figure 12. DGGE separation of 16S DNA amplified from the microalgae collected from saline TLDD basin cells at different dates. Brine shrimp harvest occurs at SEB 8, SEB 9, and HEB A4 but not at HEB C4. The band indicated by arrow was found to dominate at times in the hypersaline S9, A4, and C4.

Figure 13

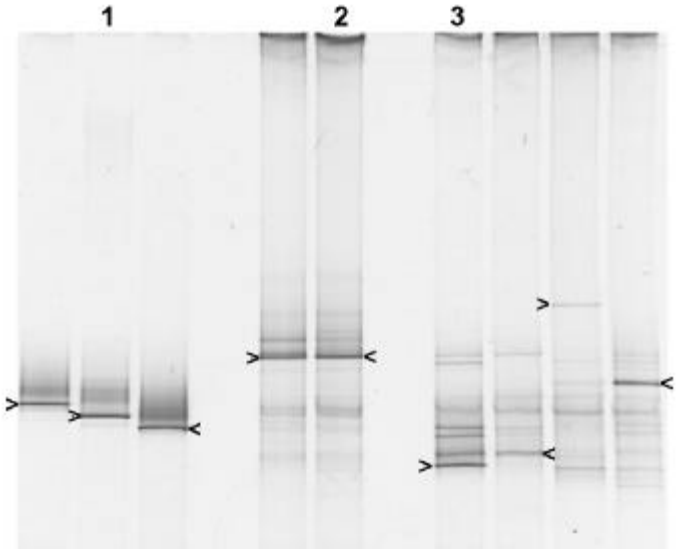

Figure 13. DGGE separation of 16S DNA amplified from the microalgae of HEB A4 cell and isolated cyanophytes. DGGE gel bands indicated by arrows were excised and DNA of bands 1-3 were reamplified and sequenced. Bands 1-3 are *Synechococcus* culture maintained in Co-PI Meeks's laboratory and microalga of A4 collected on 1/9/02 and 11/8/01, respectively.

Potential for Using Drainage Water for Irrigating Westside San Joaquin Valley Pistachios

Project Investigators:

Louise Ferguson
Office: (209) 646-6541, E-mail: louise@uckac.edu
Department of Pomology
University of California, Davis

Blake Sanden
Office: (661) 868-6218, E-mail: blsanden@ucdavis.edu
UC Cooperative Extension, Kern County

Steve Grattan
Office: (530) 752-1130, E-mail: srgrattan@ucdavis.edu
Department of Land, Air and Water Resources
University of California, Davis

Research Staff:

Heraclio C. Reyes, Laboratory Assistant III

ABSTRACT

A 1999 greenhouse rootstock salinity tolerance trial by our research group (Ferguson et al., 2002) and trials by others established salinity tolerances of, and the relative rankings among, various pistachio rootstocks. These greenhouse studies generally used unbudded, or in our 1999 study, budded seedlings, and measured growth in response to soil salinity. This long-term field trial was designed based upon the results of these earlier greenhouse studies. The major difference is that in this field trial individual tree marketable yield, the final product of growth, is used as the indicator of salinity tolerance. Growth by trunk circumference, tree nutrient status by leaf analysis, and tree water status by both pressure bomb and photosynthesis are also being measured. Water applied and water remaining in the soil are being monitored directly by flow-meter and neutron probe respectively. Ground evaporation and tree transpiration, tree water use, is calculated using the pistachio tree crop coefficient and local CIMIS station data. Pre and post season soil samples are analyzed to monitor soil salinity levels.

This trial was planted in 1989 and trees achieved full bearing in 1997. The four rootstocks being evaluated in this trial are *Pistacia integerrima*, Pioneer Gold I (PGI), *P. atlantica,* Atlantica*,* and two hybrids of these two species, *P. atlantica* X *P. integerrima,* known as Pioneer Gold II (PGII), and University of California Berkeley 1 (UCB1). The saline irrigation treatments began in 1994 and by 1997 produced salinity levels in the soil approaching or surpassing that of the respective irrigation water treatments. The yield data discussed in this report will focus on 1997 through 2001. The tree and soil water status data will focus on 1999 – 2001.

Yield results from 1997 through 2001 demonstrated that eight sequential seasons, 1994 through 2001, of irrigation with 8 dS/m (5,920 TDS) water produced no significant effect on the marketable yield of trees grown on all four rootstocks. Above 8 dS/m, at 12 dS/m (11,040 TDS) trees on all four rootstocks displayed consistent, but not always significant, decreases in yield, particularly in 2000 and 2001. Trees on UCB1 rootstocks had the most marked decreases annually averaging 35% less marketable crop than control trees when irrigated with 12 dS/m water. Trees on PGII and Atlantica rootstocks both had 12% annual average decreases in yield. Trees on PGI rootstocks had a 9% decrease in yield. These rankings differ with our earlier greenhouse study in that trees on PGI rootstocks demonstrated decreased growth when irrigation water salinity was above 8 dS/m and had significantly less growth than trees on UCB1 or Atlantica rootstocks when irrigation water was 16 dS/m.

As would be expected with the lack of effect on yield reported above, none of the trees, on any or rootstocks at any treatment level, were measurably stressed. Leaf water potentials, photosynthetic rate and stomatal conductance measurements were all within normal ranges for trees on all rootstocks at all treatment levels. Leaf nutrient levels are all within normal ranges with few exceptions.

Since 1999, despite the lack of statistically significant yield decreases or differences in plant stress indictors, all irrigation salinity treatments have shown significantly less water use that the control (0.75 dS/m). This is consistent with our earlier greenhouse trial that demonstrated vegetative growth decreases in trees on all rootstocks when soil salinity levels were greater than 8 dS/m. Further, when annual circumference measurements are graphed it appears the highest salinity treatment is beginning to impact tree growth. All the above evidence indicates the salinity tolerance threshold of the pistachio rootstocks in this trial is about 8 dS/m.

KEYWORDS

Pistacia vera, cv. 'Kerman', P. integerrima, P. atlantica, P. atlantica X P. integerrima, rootstocks.

■ ■ ■ ■ ■

INTRODUCTION

Pistachios can be grown in microclimates with combinations of heat, and poor soil and water quality, not favorable to other tree crops. The lower West Side of the San Joaquin Valley, where surface irrigation water is expensive or poor quality if it is ground or reclaimed drainage water, is an example. If irrigation in this microclimate could be supplemented by using poor quality ground or drainage water, profitable production would be more possible. Or more importantly, as water supplies become less available to agriculture, reclaimed drainage water or poor quality ground water could be a regular source of irrigation water. Currently, unused ground water supplies in

the Shafter area are reporting salinities of 5-6 dS/m. The decreased water allocations of the early 1990s are sure to be repeated as competition for California's better quality water supplies become more acute in future droughts. Some West Side districts are slated to receive 47% of their allocation in 2001. If the salinity tolerance of our current commercial pistachio rootstocks are known poor quality water can be used with confidence that growth and productivity will not be harmed.

Our 1999 greenhouse trial demonstrated pistachios are potentially among the most salt tolerant of the tree nut crops (Ferguson et al, 2002). However, measuring scion growth of two year old nonbearing, budded, seedling rootstocks for ten months and monitoring yield of mature bearing trees in a production orchard for nine years are completely different situations. This long-term field trial, with mature bearing trees, is an attempt to corroborate the salinity potential demonstrated in our earlier greenhouse trial. A long term field trial with bearing trees is particularly important as the effects of sustained salinity are slow to develop and subtle. Field trials like this one should be conducted until soil salinities cause statistically significant declines in growth and yield.

There are two ways saline irrigation can harm a plant. The first is by osmotic influences. The second is by specific – ion toxicities. Osmotic pressures manifest in slowed plant growth and productivity over a number of years. Specific ion toxicities manifest within a season. The former is more difficult to detect than the latter.

Osmotic effects are the more common way salts in irrigation water reduce plant growth and yield. Normally the concentration of solutes in root cells is higher than that in soil water. This allows water to move freely into the plant root. But, as the salinity of soil water increases, this difference in concentration between constituents in the soil water and those in the root lessens, initially making the soil water less available to the plant. To prevent salts in the soil from reducing the soil water available to the plant the plant cells must adjust osmotically. They must either accumulate salts, or synthesize organic compounds, generally sugars or organic acids, that raise the osmotic level of the plant root cells. This osmotic adjustment through the acquisition or synthesis of new cellular constituents allows the plant roots to compete more effectively for the available soil water. However, this synthesis process uses energy that would otherwise be used for plant growth and yield. The net result is a smaller plant that appears otherwise healthy. Some plants are more efficient at osmotic adjustment and are therefore more salinity tolerant. However, there are limits to a plant's ability to osmotically adjust.

The second way salts harm plants is specific ion toxicity. Specific-ion toxicities occur when chloride, boron or sodium ions in the soil water are absorbed by, and accumulate within, the plant, generally in stems or leaves. The most common manifestation of specific ion toxicity is marginal and tip leaf burn. Boron toxicity is an example of this. However, visible leaf symptoms do not necessarily result in compromised tree performance. Our 1999 greenhouse rootstock salinity trial demonstrated boron did not harm pistachio growth until it was above 1500 ppm in dried leaf tissue. However, boron commonly produces marginal leaf burn at much lower levels. This study also demonstrated sodium and chloride do not produce specific ion toxicity in 'Kerman' on any the rootstocks used in this field trial.

Our 1999 greenhouse trial demonstrated trees on PGI, Atlantica, and UCB-1 rootstocks tolerated irrigation with water up to 8dS/m. This trial also demonstrated Atlantica and UCB-1 rootstocks were equally tolerant, and significantly more tolerant, than the PGI rootstocks (Ferguson et al, 2002).

The objectives of this trial are:

1. Demonstrate at what soil salinity levels pistachio production declines.
2. Rank the relative salinity tolerance levels of the four pistachio rootstocks in this trial.
3. Determine if salts harm pistachio productivity through osmotic effects, by preventing water extraction from the soil or through specific ion damage.
4. To determine if greenhouse trials are an accurate predictor of field performance.

PROCEDURES

EXPERIMENTAL PLOT

This trial is located within a larger rootstock trial established by our research group in 1989 and maintained by Paramount Farms in Kern County, CA. Female trees were established with buds from one female tree, thus differences among trees

should be the result of rootstock influence as all the scions are genetically identical. All female trees were the same distance from a male pollinator tree.

The soil type at this field site, located approximately 15 miles southwest of Kettleman City, CA, has been classified as a silty clay loam, mixed, thermic Typic Haplargid. Good commercial fertilization, pest, disease, pruning and harvest practices have been performed by ranch personnel since planting.

SALINE IRRIGATION

The unit, decisiemen per meter, dS/m, is a measure of the electrical conductivity, EC, of a solution. The units dS/m and milliho per centimeter, mmho/cm, are equal. EC in dS/m X (640-840) = TDS ppm. The range of salinities used in this experiment ranged from 0.75 to 12 dS/m, or 480 to 11,040 ppm TDS.

Four saline irrigation treatments with ECw values of 0.75, 4.0, 8.0 and 12.0 dS/m were randomly replicated four times across 20 rows within a 400 tree pistachio rootstock trial established at Paramount Farms, in Kern County, in 1989. The experiment was conducted on 64 female 'Kerman' trees. There were four replications of four salinity treatment levels applied to sets of four trees budded onto four different rootstocks: *P. atlantica* (Atl), *P. integerrima* (PGI), and *P. atlantica* X *P. integerrima* (PGII and UCB1); 4 X 4 X. 4 = 64 trees. Two high salt concentration nurse tanks, one at 0.27 lbs / gal sodium sulfate and the other at 0.13 lbs/gal calcium chloride, 0.33 lb/gal NaCl and 0.006 lb/gal Solubor (20.5% B) were used as salt water sources for creating saline treatments with a Na:Ca ratio of 5:1 and increasing B concentration of 1 ppm for each 1 dS/m increase in salinity. These ratios are representative of Westside drain waters. Salt treatments were injected from each high salt concentration nurse tank using an impeller pump into a manifold equipped with flowmeters and then at differential rates into four sets of irrigation lines pressurized at 22 psi with canal water to produce the desired salinity treatment levels as measured with a portable EC meter. One irrigation line, the control treatment which was California Aqueduct canal water, received no salt injection. Each of the four irrigation lines was equipped with water meters to measure seasonal irrigation delivery. Each of the four irrigation lines appeared as headers at each of the twenty rows of trees to provide source outlets for drip irrigation lines to achieve the appropriate salinity treatment replication. Existing irrigation lines were plugged and new 360º micro sprinklers, (14.4 gph) were installed four feet from trunks of treatment trees with the water outlet pattern being directed back towards the trunk. Irrigations were scheduled using normal year evapotranspiration data. Excessive saturation has been a problem on the 8 and 12 dS/m treatments so reduced flow microsprinklers (12.0 gph) were installed on these trees in 2001. This still provides a 20 – 40% leaching fraction.

WATER AND SOIL SALINITY MEASUREMENTS

Field samples of irrigation water were collected in 400 ml containers over the course of each irrigation in order to determine water quality. Individual tree soil samples were collected before the irrigation season in April and after the irrigation season in November of each growing season. Water and soil analysis were conducted using established laboratory procedures at the Division of Agriculture and Natural Resources Laboratory in Davis, CA.

HORTICULTURAL MEASUREMENTS

Individual annual trunk growth and yield were determined on all trees. Individual tree yield samples were commercially graded at the Paramount Farming Processing Facility. Annual individual tree leaf samples were collected for nutritional analysis at the same lab as above.

TREE WATER STATUS MEASUREMENT

Tree water status by midday, bagged leaf water potential was measured before each irrigation, when trees should be most stressed, and within 24 hours after irrigation. Tree water status was measured by bagging one leaf from the lower internal part of the canopy from each tree of four replications of each rootstock-saline irrigation treatment combination. Bags were constructed from black polyethylene and aluminum foil with the intent of excluding measured leaves from light and micrometeorological environments. Leaves were bagged at 0900 Pacific Standard Time, then removed three hours later for water potential determination using a Scholander type pressure vessel. All leaves were selected based upon similar age and canopy position.

PHOTOSYNTHETIC GAS EXCHANGE MEASUREMENTS

A Licor LI-6400 portable photosynthesis system was used to measure gas exchange of individual tree leaves annually in August. The reference CO2 was set at 400 ppm. The PAR (photosynthetically active radiation) level was 1500 microeinsteins. Sample relative humidity was maintained at 55% =/- 5%. The flow rate was maintained at 500 micromoles and adjusted as required. Sample leaves were mature, fully expanded, and selected for maximum sun exposure and height. The same sample leaves were used each time and measured at the end of the irrigation cycle, immediately prior to the next irrigation. Measurements were made between 0900 and 1500 hours. Photosynthesis measurements were initiated in 2000 and 2001 as a more discrimination indicator of tree water stress in addition to bagged leaf water potentials.

SITING OF NEUTRON PROBE ACCESS TUBES, REPLICATION AND MEASUREMENT OF SOIL WATER CONTENT

Using a measurement of the backscatter of thermalized (slowed) neutrons, the neutron probe determines soil water content of a volume of soil the size of a basketball. For this study, 2 inch PVC Class 125 pipe access tubes have been installed to allow for repeated measurements of soil water content from 0.5 to 5 feet in one-foot increments. As demonstrated in figure 1, from 1994 through the 2000 season, one neutron probe access tube per tree was installed to a depth of 5.5 feet on every tree in the trial in approximately the same location relative to the trunk and the opposing fanjet; about 4 feet east of the trunk, 4.5 feet west of the fanjet and 1.5 feet south of the hose. This placed the access tube in an area that represented average to slightly better than average application of irrigation water. This wetted area, and the subsurface redistribution of water, gave the tree an active root volume of about 50% of the entire orchard floor. This meant that a 1-inch irrigation over the whole orchard equaled about 2 inch around the site of the neutron probe tube. Likewise, neutron probe readings that show a 2-inch extraction of water between irrigations represented about 1 inch of tree water use as transpiration over the whole orchard.

However, the variability in spatial distribution of tree roots and the precipitation pattern of the fanjets can result in different rates of water application and subsequent tree uptake throughout the root zone of a given tree. For this study, to get the most comparative information possible across all treatments, we measured soil water content to maximize replication across the most trees instead of opting for complete ET estimates using many tubes on only a few trees. The assumption was that the location of the neutron probe tube represented an equal water application and extraction opportunity for each tree and provided a relative comparison suitable for statistical analysis. Therefore results reported through 2000 were generated from neutron probe data taken from 4 replications times 4 rootstocks times 4 levels of salinity; a total of 64 tubes as demonstrated in figure 1.

However, water extraction figures from 1999 through 2000 suggested we were not obtaining an accurate picture of water extraction from the soil. Consequently, for the 2001 season the number of neutron probe tubes was increased to four per tree and sited as demonstrated in figure 2. As previous years showed very little difference in water extraction among trees on the different rootstocks we dropped neutron probe monitoring on trees on the Atlantica and PGII rootstocks. The result was a doubled number of access tubes, 128, that concentrated our ET estimates on trees on PGI and UCB-1 rootstocks. Tubes were also installed to a depth of 6.33 feet to allow for water content measurements to 6 feet. This new tube placement was designed to monitor the locations that receive the most water, tube 1, T1. The areas that receive somewhat less, T2. The areas adjacent to the fanjet, a little bit of surface wetting and at the edge and the substantial subbing of water to the 1-3 foot depths, T3. And areas that receive no surface wetting and minimal subbing in the middle of the drive row, T4. This tube arrangement effectively monitored a much larger area of the root system laterally and vertically. This siting of neutron probe tubes compensated for both the irregular fanjet irrigation pattern and the highly variable subsurface water redistribution during and after irrigation. It also compensated for the irregular root distribution. The net result was a better estimate of soil water content.

A further field site modification was done in 2001. Direct soil water status measurements by neutron probe and tree transpiration calculations from 1997 through 2000 suggested trees at the 8 and 12 dS/m irrigation salinity levels were extracting and transpiring only a fraction of the

applied water. Roots were proliferating outside the wetted zone, obtaining fresh water outside the saline irrigation zone. To prevent this 0.006 inch thick plastic barriers were installed around all treatments to a depth of 1.5 m, fig.3. Trenching to sink the barriers cut many small roots in the top three feet of the profile, but this did not appear to adversely affect tree vigor during the 2001 season.

RESULTS AND DISCUSSION

The larger rootstock trial that contains this salinity trial was planted in 1989 and reached full bearing in 1998. The salinity treatments commenced in 1994. By 1998, when the trees were full bearing, the soil salinity levels, as measured by soil saturation extract, were reflective of the irrigation water salinity. As the tables 1, 2, and 3 below demonstrate, eight sequential seasons of irrigation with 0.75 through 8.0 dS/m water had no consistent significant effect on mature tree marketable yield. As Table 4 shows irrigation water at 12 dS/m produced decreases, generally insignificant, in marketable yield of trees on all four rootstocks. However, trees on UCB-1 rootstocks appeared to be most adversely affected. This contradicts our greenhouse trial in which Atlantica was the most saline tolerant rootstock followed by an almost equally tolerant UCB-1. PGI was the most saline sensitive rootstock.

Figure 4 graphically synthesizes the data given in the four tables above. This figure demonstrates the effect of salinity on average annual yield, 1997-2001, of individual trees, on all four rootstocks. This graph corroborates our greenhouse study demonstrating irrigation water up to 8 dS/m, which produces an average root zone salinity of 7.7 dS/m, has no effect on marketable yield of trees on any rootstock. However, and again consistent with our 1999 greenhouse trial, all four rootstocks produced statistically insignificant yields when irrigation water salinity was 12 dS/m and soil salinity averaged 9.8 dS/m.

EFFECT OF SALINE IRRIGATION ON GROWTH

Figures 5, 6, 7 and 8 graph the annual increase in rootstock growth of 'Kerman' trees on the four different rootstocks. Among the trees on PGII, Atlantica and UCB-1 rootstocks the trees irrigated with 12 dS/m water are displaying slightly slower growth, though not significant decreases in annual growth. As stated earlier, the effects of salinity are slow to develop. However, these small decreases in the rate of trunk growth suggest the sustained salinity in the root zone may be beginning to affect growth. If so, yield will eventually be impacted.

EFFECT OF SALINE IRRIGATION ON TREE NUTRIENT STATUS AND SPECIFIC ION TOXICITY

No differences in tree macronutrient or micronutrient status, including sodium, boron or chloride, have been observed. All leaf nutrient levels have remained within normal ranges throughout this trial. This is consistent with the results of our earlier greenhouse trial. The single exception is trees on PGI rootstocks have had consistently high levels of sodium when irrigated with 8 dS/m water.

No consistent, visible, specific ion tonicities have been observed. Our 1999 greenhouse trial demonstrated that if they did manifest they were a result of boron accumulation.

EFFECT OF SALINE IRRIGATION TREATMENTS ON SOIL WATER CONTENT, PLANT STRESS AND TREE WATER USE

The following discussions address the impact of salinity averaged over all rootstocks for 1999 through 2001. This provides 12 replicates of data for each salinity level for the factors being discussed: irrigation water applied, leaf water status, available amount of soil moisture, transpiration and rates of photosynthesis and stomatal conductance.

IRRIGATION APPLICATION; CIMIS ET AND APPLIED IRRIGATION

Irrigations during the season were scheduled using normal year CIMIS potential evapotranspiration (ET_0) multiplied by pistachio crop coefficients determined in a previous study by Goldhamer (1985). When the orchard was young and coverage of the orchard floor was about 50%, crop ET was further discounted to 95% of a mature orchard depending on age (Snyder, 1989). As the orchard matured this was adjusted upward. Irrigation was timed to match this demand with the same depth applied to all salinity treatments. Separate flowmeters record the application depth for each treatment. Figures 9a, b, and c show pistachio ET for the 1999 through 2001 seasons calculated using the real time CIMIS ET_0 at the Shafter Field Station multiplied by the appropriate crop coefficient for that time of year along with individual treatment irrigation depths. CIMIS ET_0 from the Shafter Field Station was used

instead of Lost Hills or Dudley Ridge due to the quality of data and weather station siting. In general, application depths matched calculated ET fairly well. Total water application in the higher salinity treatments was less than the 0.75 dS/m control treatment; probably due to some precipitation of calcite around fanjet nozzles and declines in meter accuracy due to some marginal calcite precipitation in the meters. In 2001 water application in the 8 and 12 dS/m treatments were decreased to avoid soil saturation.

LEAF WATER STATUS MEASUREMENTS

Bagged leaf water potential is an indicator of overall trunk water potential. Midday bagged leaf water potentials for 1999 and 2001, leaf water potential were not done in 2000, indicated the trees were not under water stress as shown in figures 10 a and b. Figures 10 c and b, demonstrating percentage differences from the control among treatments and cumulative leaf water potentials through the season demonstrate increasing differences between the control and 12 dS/m irrigation treatments. This suggests tree water stress is developing at the 12 dS/m irrigation treatment level.

However, it is clear that leaf water potential measurements appear inadequate for estimating the very large differences that were found this season in actual tree transpiration (Figures 12 a, b and c).

It is also possible that the more negative soil water matric potential, the ability of the soil to hold water more tightly, caused by lower available soil water in the 0.75 dS/m treatment could cause a similar bagged leaf water potential resulting from the osmotic stress caused by the salt in the 8 and 12 dS/m treatments. But it is clear this method of measurement is inadequate for estimating the very large differences that were found in actual tree transpiration (Fig 13 a, b and c.).

EFFECT OF SALINE IRRIGATION TREATMENT ON PHOTOSYNTHETIC EFFICIENCY AND STOMATAL CONDUCTANCE

Because midday bagged leaf water potentials did not demonstrate any significant difference in tree water status, photosynthetic rate and gas exchange measurements, generally more accurate indicators of tree stress, were attempted. As with bagged midday leaf water potentials there were no significant differences within each rootstock or among the four salinity treatments. By these measurements in 2000 and 2001 the trees were not stressed. This is consistent with the appearance of leaves of trees on all four rootstocks at all four salinity levels, and with the results of bagged midday leaf water potential measurements.

SOIL WATER STATUS MEASUREMENTS

Figures 12a, b and c for 1999 through 2001 demonstrate major differences in root zone soil water content. Initially, in 1999, beginning in July the 12 dS/m treatment remained at or above field capacity for the entire season while the fresh water control treatment, 0.75 dS/m, declined to 40% after harvest. This pattern of soil water content was much more obvious in 2000 and 2001 with the 12 and 8 dS/m treatments beginning the season with strikingly higher soil water contents and maintaining this pattern throughout the season. This indicates that the depth of irrigation in the low salinity treatment was insufficient to meet all the ET demand for these trees; causing excessive extraction of available soil water. The maintenance of near 100% field capacity in the higher salinity treatments indicates the trees are extracting less water, and that leaching is occurring in these treatments.

TREE WATER USE

For the 1999 and 2000 seasons actual comparative treatment transpiration was calculated by measuring the soil water depletion in between irrigations. Since the wetted volume from the fanjets is only 50% of the entire orchard floor, net depletion of soil water in the area of the neutron probe tubes is then multiplied by 0.5 to estimate transpiration over the whole orchard floor. Thus, a 3 inch average depletion would mean 1.5 inches of transpiration. Water consumption in Figure 12 a and b is reported as transpiration and not evapotranspiration (ET) because the neutron probe is incapable of accurately measuring water content changes in the top three inches of soil; the zone from which most evaporative water loss will occur. This means that the depletion measured between irrigations is either extraction by the tree (transpiration), or leaching. Nearly all measurements of depletion for 1999 and 2000 seasons consisted solely of transpiration as we waited two to five days after irrigation before making the initial soil water content measurement, with the subsequent

measurement immediately before the next irrigation. This technique woefully underrated the Actual ET. With the addition of plastic barriers and now four access tubes per tree to provide average water content for the whole orchard floor occupied by a given treatment, the 2001 measured ET is virtually the same as the calculated CIMIS ET.

This depletion measured by the neutron probe is multiplied by 0.5 and then divided by the actual CIMIS ET_0 for that same period. This calculated crop coefficient value (K_c) for each treatment is then multiplied by the CIMIS ET_0 during the following irrigation interval to estimate the treatment transpiration during that period. This provides a continuous cumulative estimate of crop transpiration over the season.

For the 2001 season the additional three additional probe tubes per tree gave a much better estimate of tree water extraction as well as the ability to estimate leaching. The data collected in 2001 demonstrated trees receiving the 0.75 control and 4 dS/m treatments transpired almost equal amounts of water. Trees receiving the 8 and 12 dS/m irrigation water transpired less water. This is a function of 20% less water being applied when 12 gph emitters were substituted for the 15 gph emitters in mid July to avoid marked soil saturation. Thus the two higher salinity treatments are producing an osmotic effect that is decreasing the water extraction ability of the trees on all rootstocks.

CONCLUSIONS

In summary, from 1994 through 2001 results indicate irrigation water salinity above 8 dS/m can, though not consistently or significantly, decrease yield of pistachios grown on all four rootstocks tested. Using marketable yield as an indicator of salinity tolerance, the rootstocks ranked as follows, from least to most saline tolerant; UCB-1, Atlantica, PGII and PGI. Trees on UCB-1 rootstocks were also the trees beginning to demonstrate a slightly decreased growth rate. Leaf macronutrient and micronutrient levels; including chloride, sodium and boron have remained, with few exceptions, within normal ranges. No consistent specific ion tonicities have been observed.

Not surprisingly, considering the lack of significant effects on tree growth, nutritional status or yield, the trees on all rootstocks also have normal leaf water status, photosynthetic rate and stomatal conductance. However, measurements of tree water application, extraction and use indicate salinities above 8 dS/m are deleteriously affecting the trees' ability to extract water at soil water salinities above 8 dS/m.

The results from this trial thus far strongly suggest osmotic pressure, and not specific ion toxicity, is the mechanism by which salinity harms pistachios.

All the results above, with the exception of rootstock salinity tolerance rankings, are consistent with our 1999 greenhouse rootstock salinity trial and those of others.

While the trees have demonstrated great tolerance through the eight years of this trial, these decreases must eventually manifest in decreased growth, and therefore yield. It is these limits that must be definitively known if drainage water is to be successfully integrated into future irrigation programs.

ACKNOWLEDGEMENTS

The authors wish to thank 'Goyo' Jacobo, Rick Cole, Kiko Garza, Joe Gonzales, Dennis Elam and Brenda Hansen of Paramount Farming Company for the generous contribution in time and service to this trial. We also gratefully acknowledge the support of California Pistachio Commission and the UC Westside Salinity/Drainage Task Force.

■ ■ ■ ■ ■

LITERATURE CITED

Ferguson, L., P.A. Poss, S.R. Grattan, C.M. Grieve, D. Want, C. Wilson, T.J. Donovan, and C. T. Chao. 2002. Pistachio rootstocks influence scion growth and ion relations under salinity and boron stress. J. Amer. Soc. Hort. Sci. 127(2): in press.

Goldhamer, D.A., R.K. Kjelgren, and R. Beede. 1985. Water use requirements of pistachio trees and response to water stress. Annual report, CA Pistachio Commission. Pp. 85-92.

Picchioni, G. A., A. Miyamoto, and J. B. Storey. 1999. Salt effects on growth and ion uptake of pistachio rootstock seedlings. J. Am Soc. Hort. Sci. 115:647-653.

Snyder, R.L., B.J. Lanini, D.A. Shaw, and W.O. Pruitt. 1989. Using reference evapotranspiration (ET_o) and crop coefficients to estimate crop evapotranspiration (ET_c) for trees and vines. Univ. CA Coop. Ext. Leaflet 21428.

Walker, R. R., E. Torokfalvy, and M. H. Behouboudian. 1987. Uptake and distribution of chloride, sodium and potassium ions and growth of salt treated pistachio plant. Austral. J. Agr. Res. 38:383-394.

■ ■ ■ ■ ■

Table 1. Individual tree yields, Kg of dry, inshell splits per tree, for trees receiving 0.75 dS/m irrigation water.

	Mean Root Zone Salinity as ECe (dS/m) for 0.75 dS/m irrigation water				
	2.1	1.8	1.2	2.3	**
Rootstock	Yield (kg/tree)*				
	1997	1998	1999	2000	2001
Atlantica	6.0 a	8.4 a	0.2 a	13.6 a	7.0 a
PGI	7.6 a	11.9 a	1.7 a	14.8 a	9.9 a
PGII	6.5 b	10.8 a	0.3 a	14.0 a	8.7 a
UCB1	6.3 b	11.9 a	0.5 a	14.8 a	8.8 a

*Values for a specific rootstock for a given year followed by the same letter are not significantly different from the same rootstock at a different salinity level within that same year.
+12 dS/m irrigation was only applied for 1997 through 2000 seasons.
**Soil samples not yet analyzed.

Table 2. Effect of irrigation water salinity (dS/m)* and average root zone soil water extract. Water averaged over 1-4 ft depth (dS/m) on yield of trees on four pistachio rootstocks. The top line of the table is the irrigation water salinity. The line below is the salinity of the soil water extract that year.

	Salinity of Irrigation Water (ECw) 4.0 dS/m				
	Salinity of Soil (ECe) in dS/m				
	2.1	5.3	5.4	6.2	**
Rootstock	Yield (kg/tree)*				
	1997	1998	1999	2000	2001
Atlantica	6.1 a	7.6 ab	0.5 a	13.3 a	7.6 a
PGI	8.6 a	9.0 b	3.4 a	12.4 a	10.1 a
PGII	7.8 a	10.9 a	0.4 a	13.1 a	9.5 a
UCB1	8.2 a	12.3 a	0.8 a	16.1 a	10.7 a

*Values for a specific rootstock for a given year followed by the same letter are not significantly different from the same rootstock at a different salinity level within that same year.
+12 dS/m irrigation was only applied for 1997 through 2000 seasons.
**Soil samples not yet analyzed.

Table 3. Effect of irrigation water salinity (dS/m)* and average root zone soil water extract. Water averaged over 1-4 ft depth (dS/m) on yield of trees on four pistachio rootstocks. The top line of the table is the salinity of the irrigation water. The next line is the salinity of the soil water extract that year.

	Salinity of Irrigation Water (ECw) 8.0 dS/m				
	Salinity of Soil (ECe) in dS/m				
	6.0	6.9	8.5	9.5	**
Rootstock	Yield (kg/tree)*				
	1997	1998	1999	2000	2001
Atlantica	6.5 a	8.3 a	0.7 a	11.3 a	8.5 a
PGI	8.1 a	10.8 b	2.3 a	10.6 a	8.5 a
PGII	8.1 a	10.8 a	1.2 a	15.3 a	10.1 a
UCB1	8.8 a	10.9 a	0.4 a	13.3 a	10.2 a

*Values for a specific rootstock for a given year followed by the same letter are not significantly different from the same rootstock at a different salinity level within that same year.
+12 dS/m irrigation was only applied for 1997 through 2000 seasons.
**Soil samples not yet analyzed.

Table 4. Effect of irrigation water salinity (dS/m)* and average root zone soil water extract. Water averaged over 1-4 ft depth (dS/m) on yield of trees on four pistachio rootstocks. The top line of the table is the salinity of the irrigation water. The next line is the salinity of the soil water extract that year.

	Salinity of Irrigation Water (ECw) 12.0+ dS/m				
	Salinity of Soil (ECe) dS/m				
	7.5	10.3	11.5	10.0	**
Rootstock	Yield (kg/tree)*				
	1997	1998	1999	2000	2001
Atlantica	5.2 b	6.9 b	0.7 a	10.5 a	7.51 a
PGI	7.7 a	10.3 b	0.7 a	13.0 a	10.1 a
PGII	6.7 b	9.0 b	1.2 a	11.4 a	7.2 a
UCB1	5.1 c	6.1 b	0.3 a	9.3 a	6.5 a

*Values for a specific rootstock for a given year followed by the same letter are not significantly different from the same rootstock at a different salinity level within that same year
+12 dS/m irrigation was only applied for 1997 through 2000 seasons.
**Soil samples not yet analyzed.

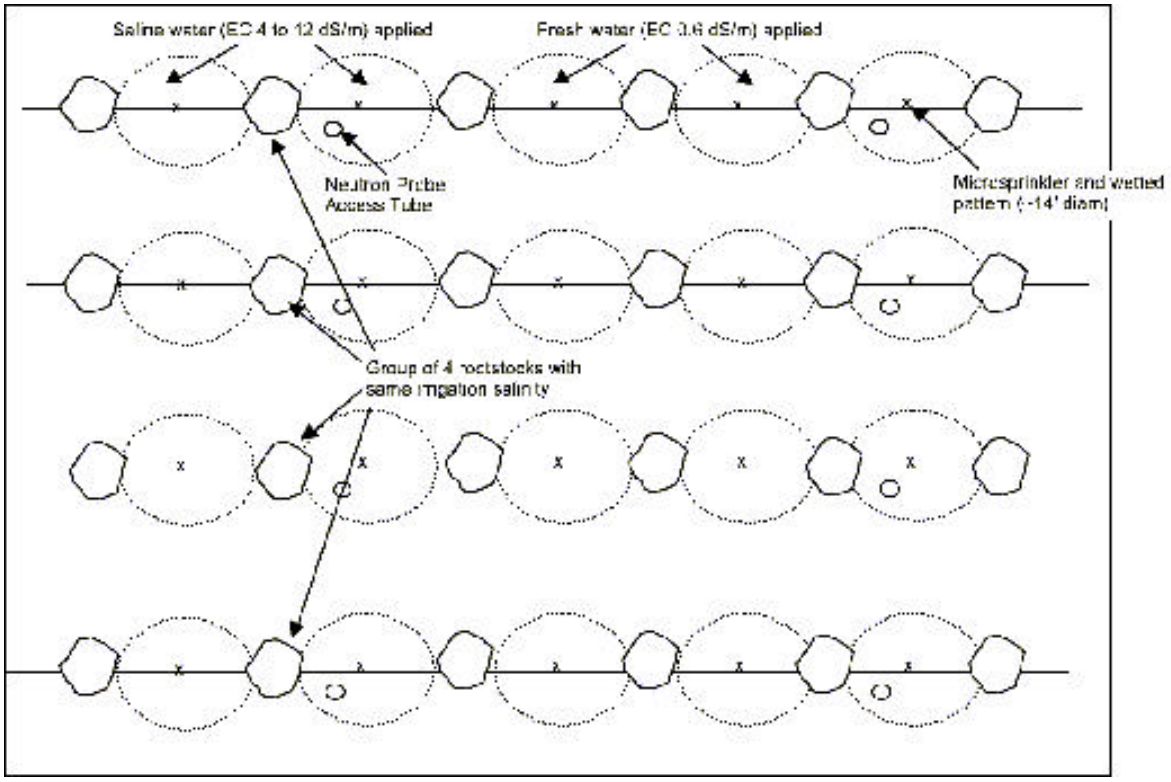

Figure 1. Neutron probe tube placement 1994 through 2000.

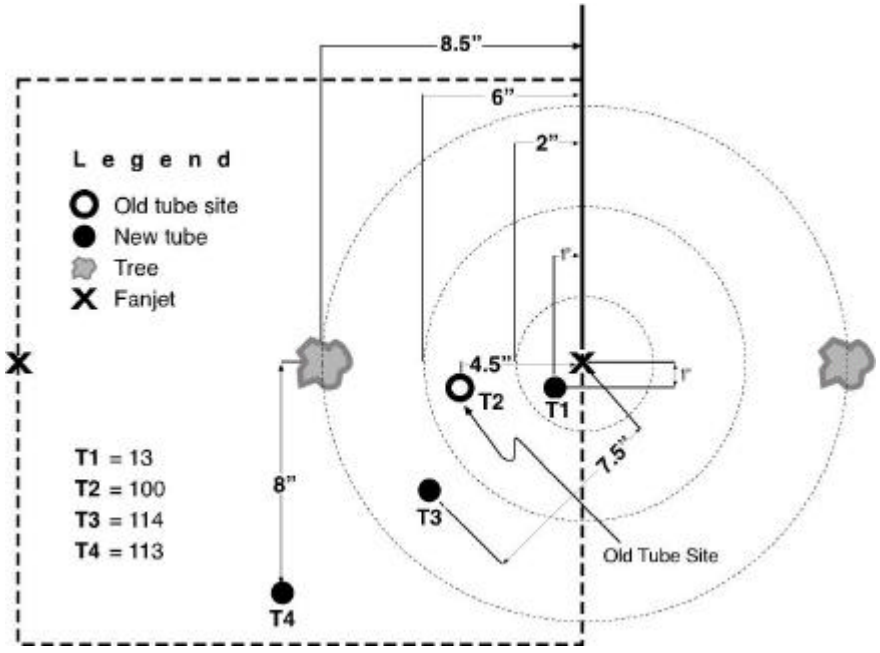

Figure 2. Neutron tube placement in 2001. Note that the number of tubes was increased to four per tree.

Figure 3. Barriers of 0.006 inch plastic were sunk to 1.5m depth around each irrigation treatment replication in March, 2001.

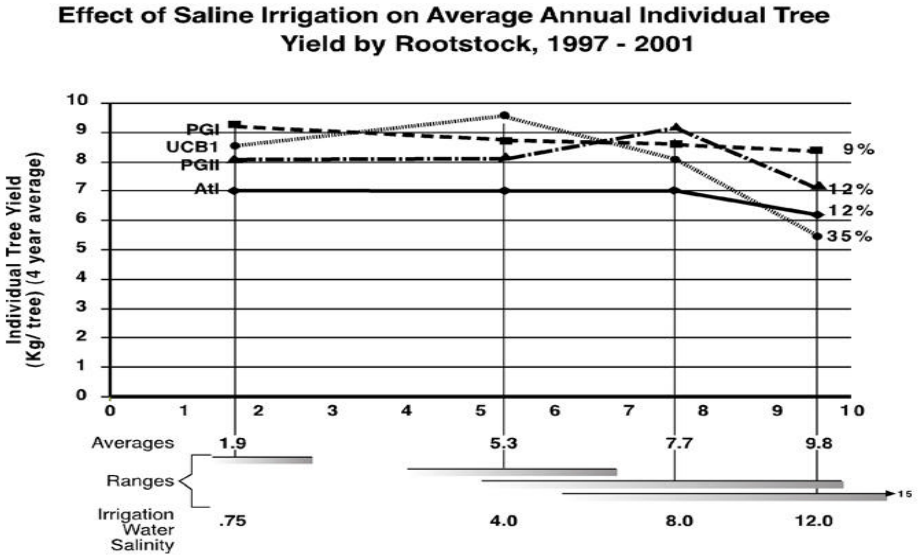

Figure 4. Effect of saline irrigation on per tree yield averaged over 5 seasons, 1997 through 2001. The horizontal axis, bottom, indicates irrigation water salinity, middle, the range of soil salinities produced in the soil, and, top, the root zone salinity averaged over five feet and five years, 1997 – 2001. Average individual tree yields did not decrease until irrigation water salinity was 12 dS/m and produced a root zone salinity of 9.8 dS/m. However, these percentage tree yield decreases versos the control treatment were not statistically significant, as they are an average calculated value.

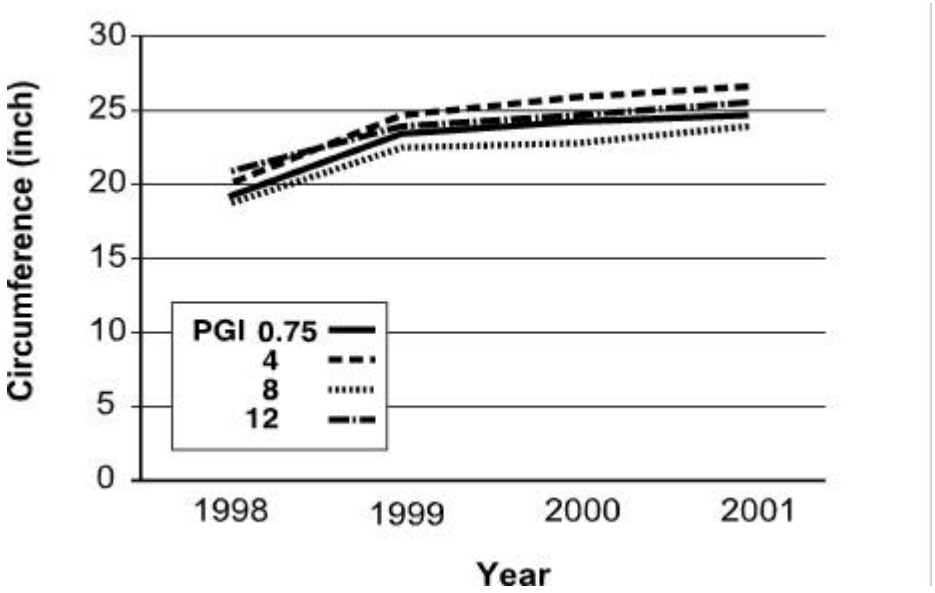

Figure 5. Effect salinity on annual trunk growth of trees on PGI rootstocks. There are no significant differences among treatments or rootstocks.

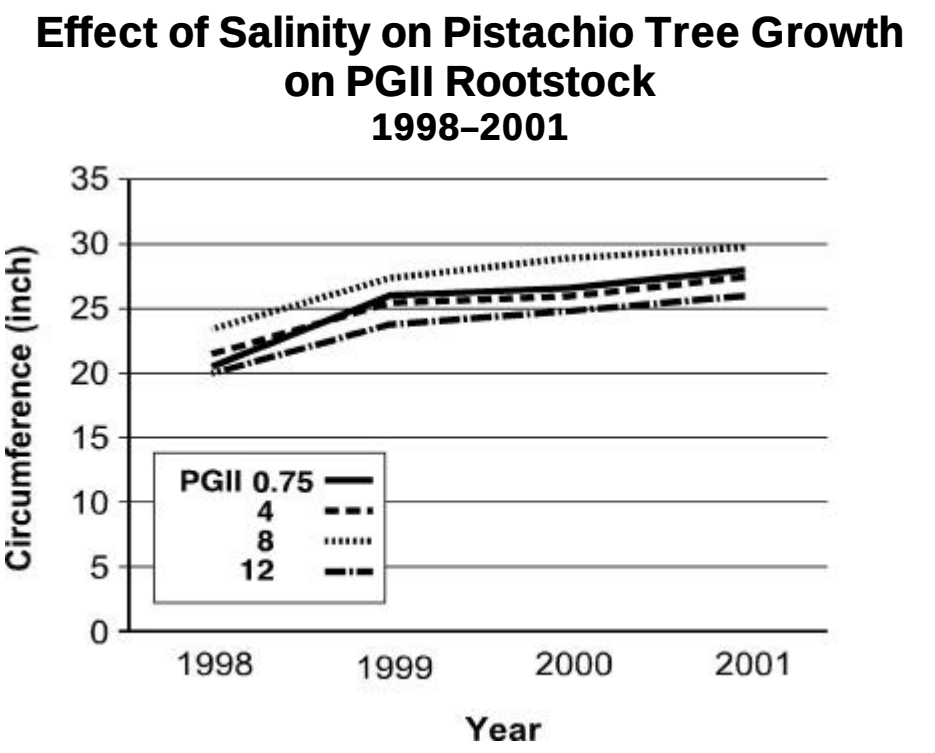

Figure 6. Effects of sustained salinity on trunk growth of trees on PGII rootstocks. There are no significant differences among treatments but the growth rate of trees receiving the 12 dS/m treatment is decreasing

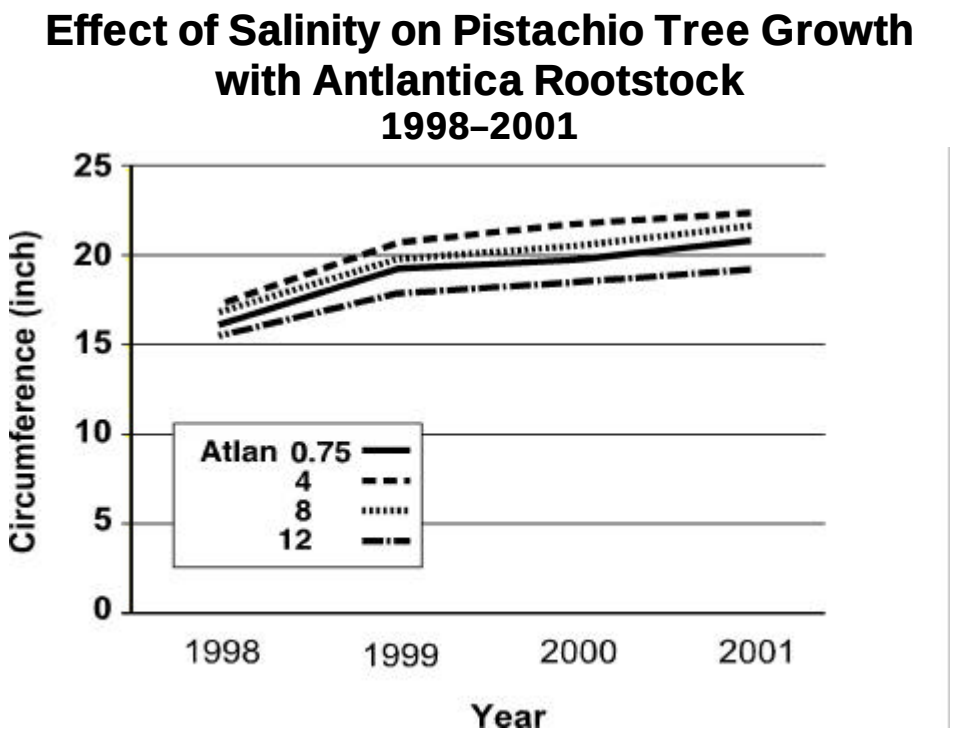

Figure 7. Effects of sustained salinity on trunk growth of trees on Atlantica rootstocks. There are no significant differences but the growth rate of trees receiving 12 dS/m water is decreasing.

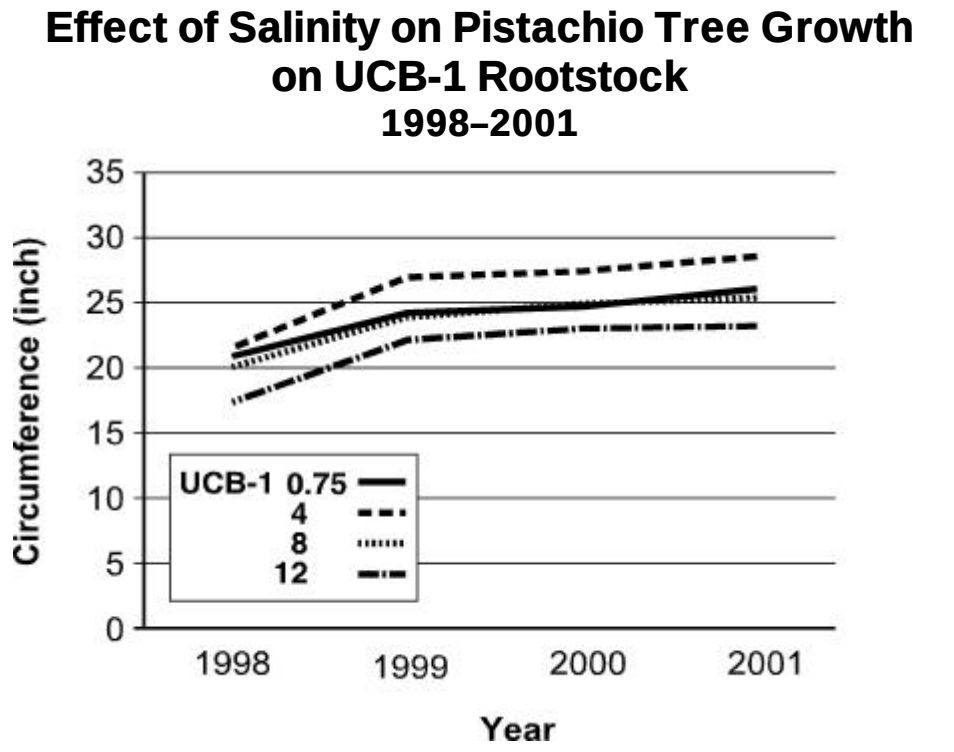

Figure 8. Effect of salinity on growth rate of trees on UCB1 rootstocks. There are no significant differences but the growth rate of trees receiving 12 dS/m water is decreasing.

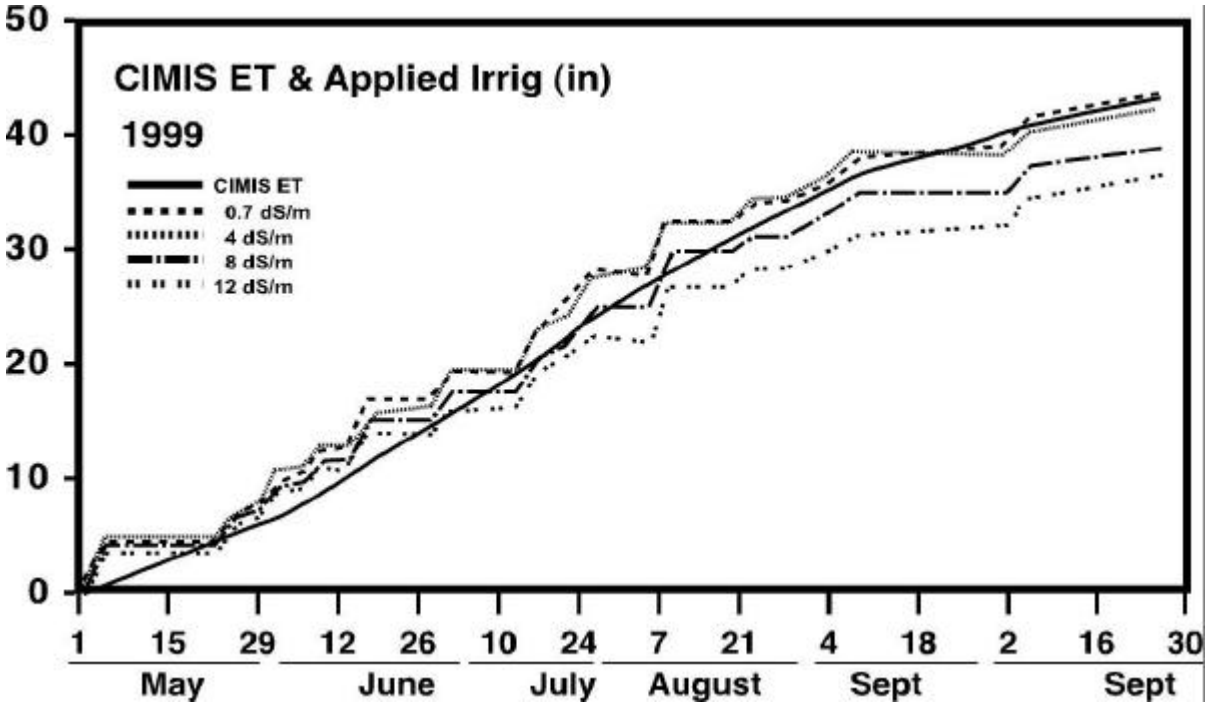

Figure 9a. Cumulative seasonal applied irrigation water to all treatments and calculated pistachio ET using 1999 CIMIS ET_0 as measured at the Shafter Field Station multiplied by crop coefficients described by Goldhamer (1987).

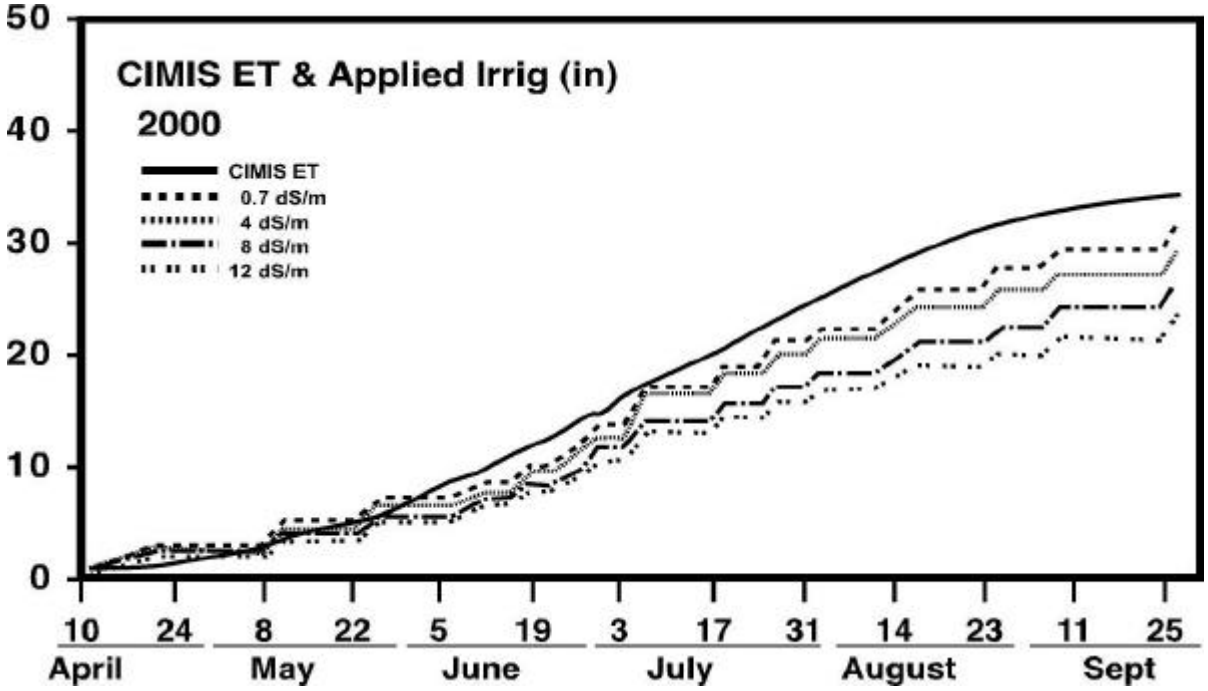

Figure 9b. Cumulative seasonal applied irrigation water to all treatments and calculated pistachio ET using 2000 CIMIS ET_0 as measured at the Shafter Field Station multiplied by crop coefficients described by Goldhamer (1987).

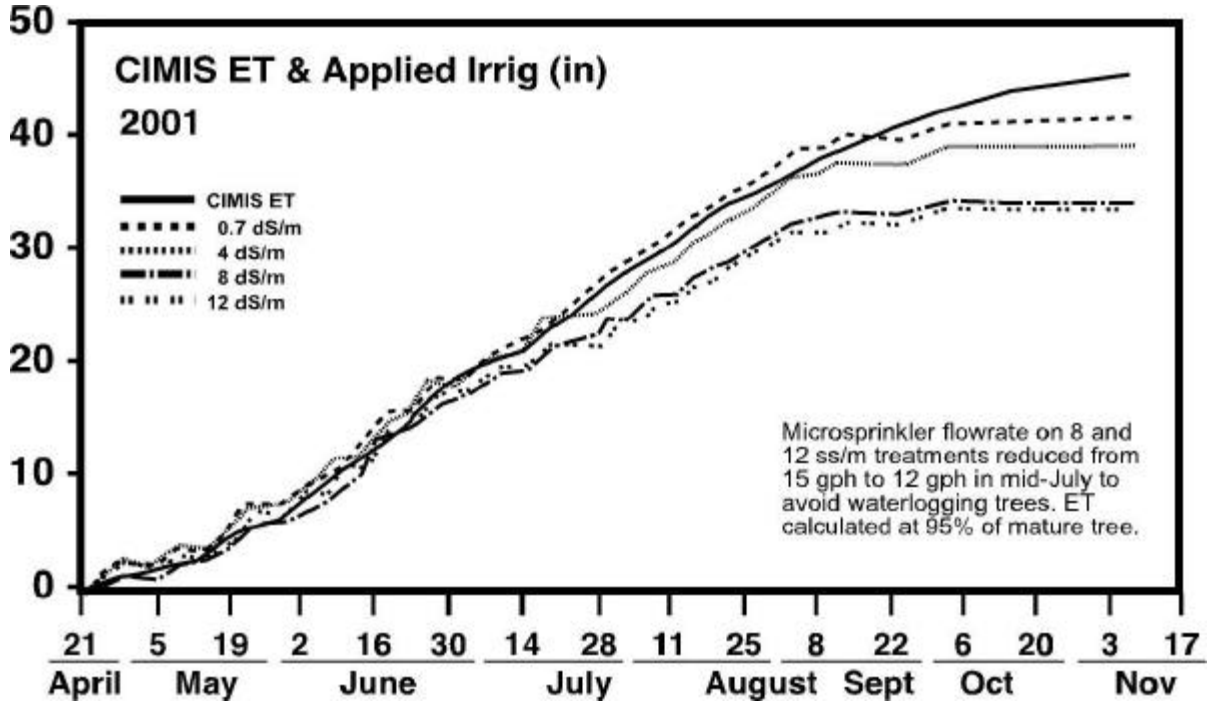

Figure 9c. Cumulative seasonal applied irrigation water to all treatments and calculated pistachio ET using 2001 CIMIS ET_0 as measured at the Shafter Field Station multiplied by crop coefficients described by Goldhamer (1987).

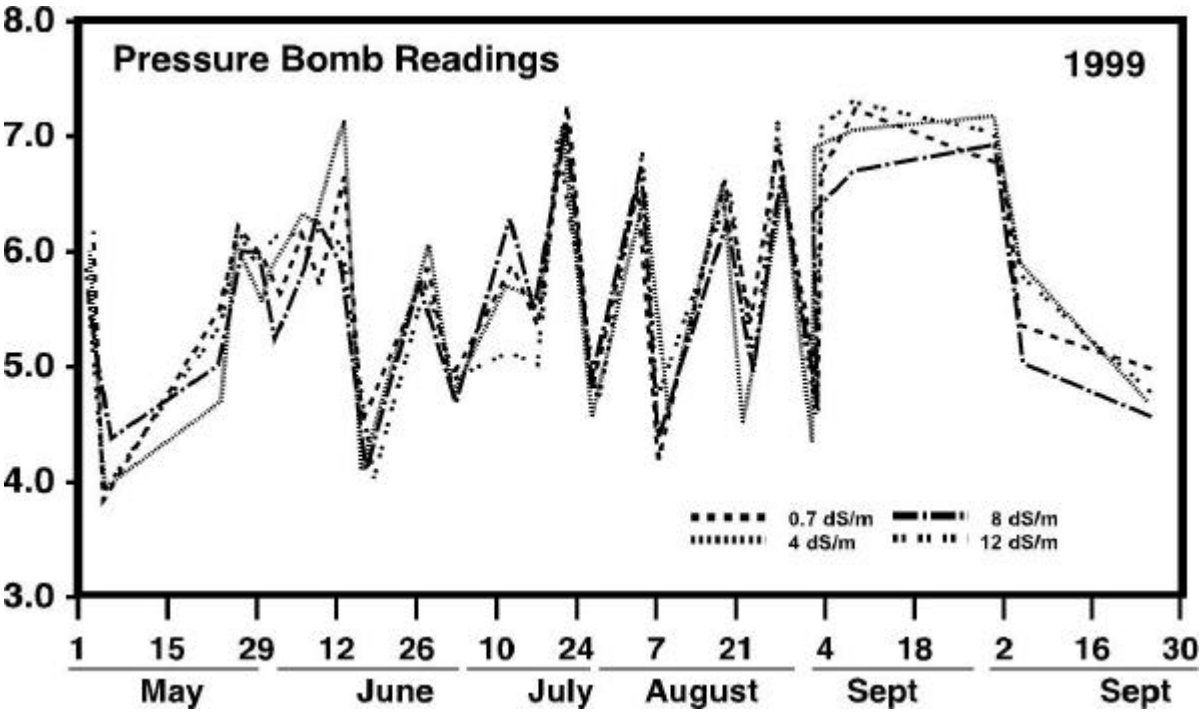

Figure 10a. Midday bagged leaf water potentials over season, 1999. No measurements were done in 2000.

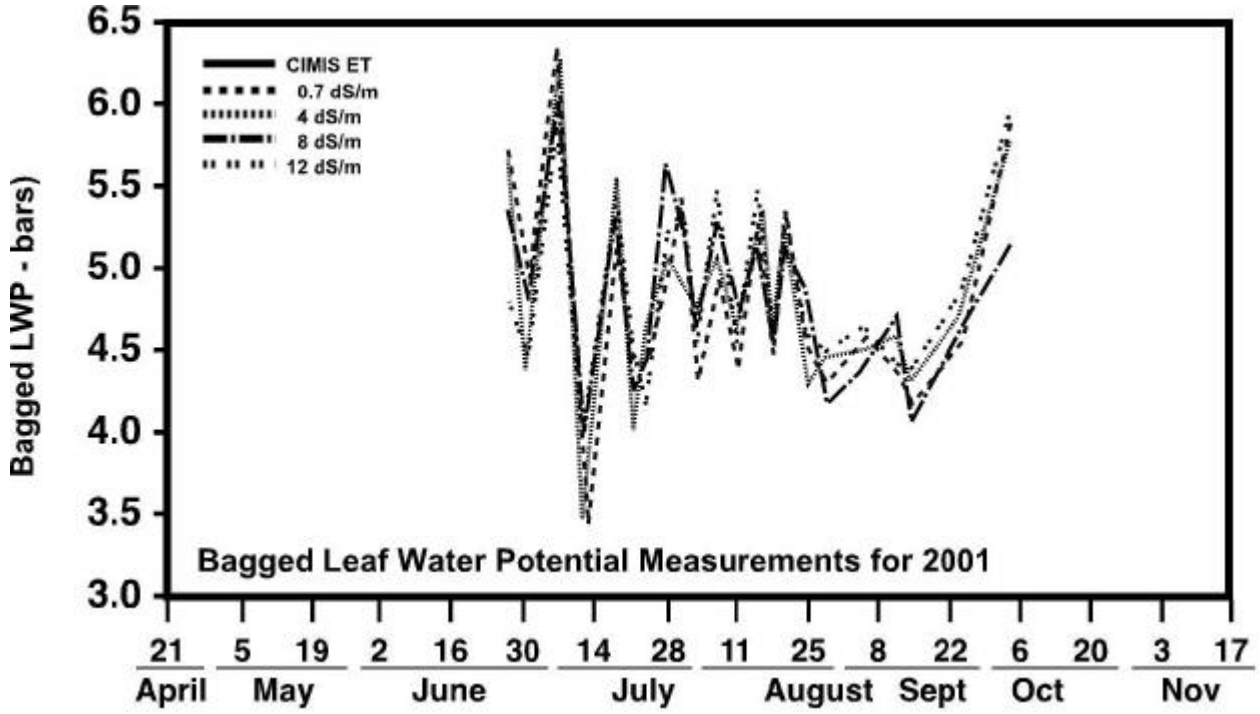

Figure 10b. Bagged midday leaf water potentials for 2001.

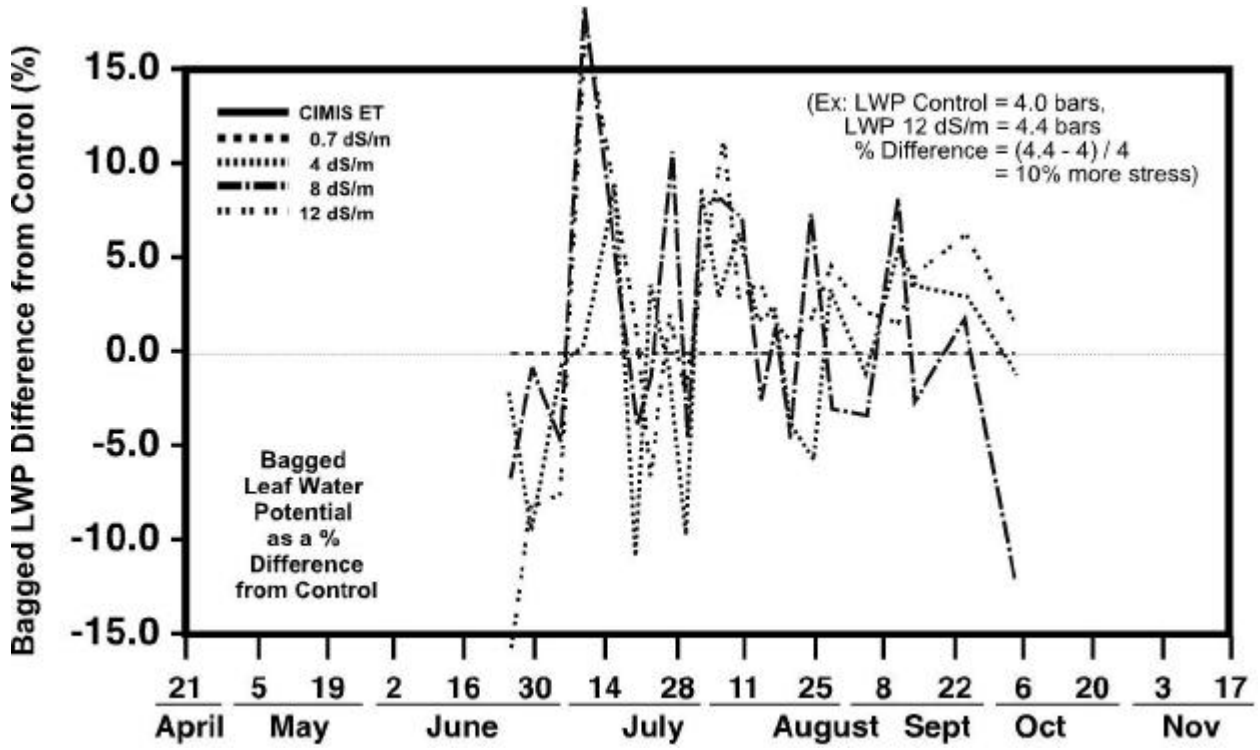

Figure 10c. Bagged midday leaf water potentials demonstrating percentage difference from the control among treatments.

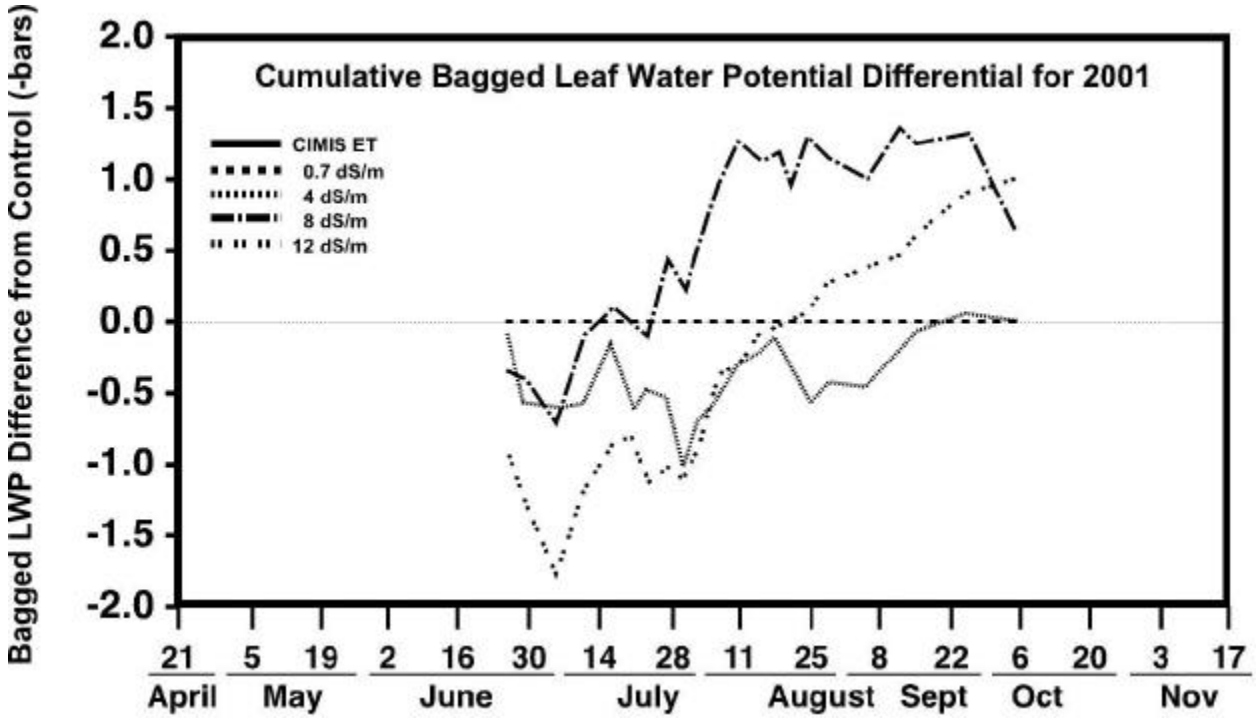

Figure 10d. Cumulative bagged midday leaf water potentials showing cumulative differential from control treatment.

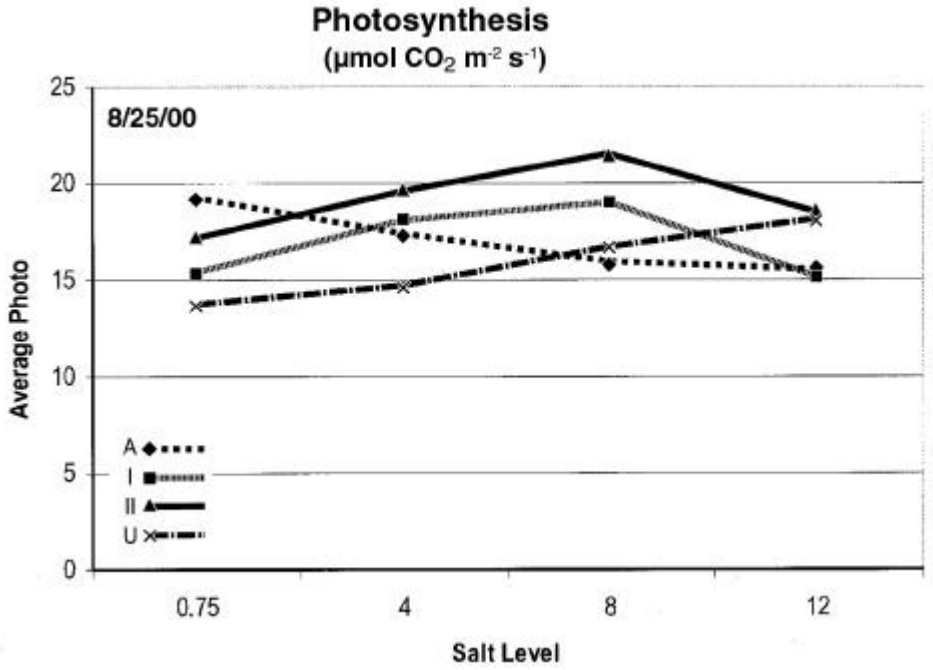

Figure 11a. Photosynthetic rate in August 2000, ten days before harvest.

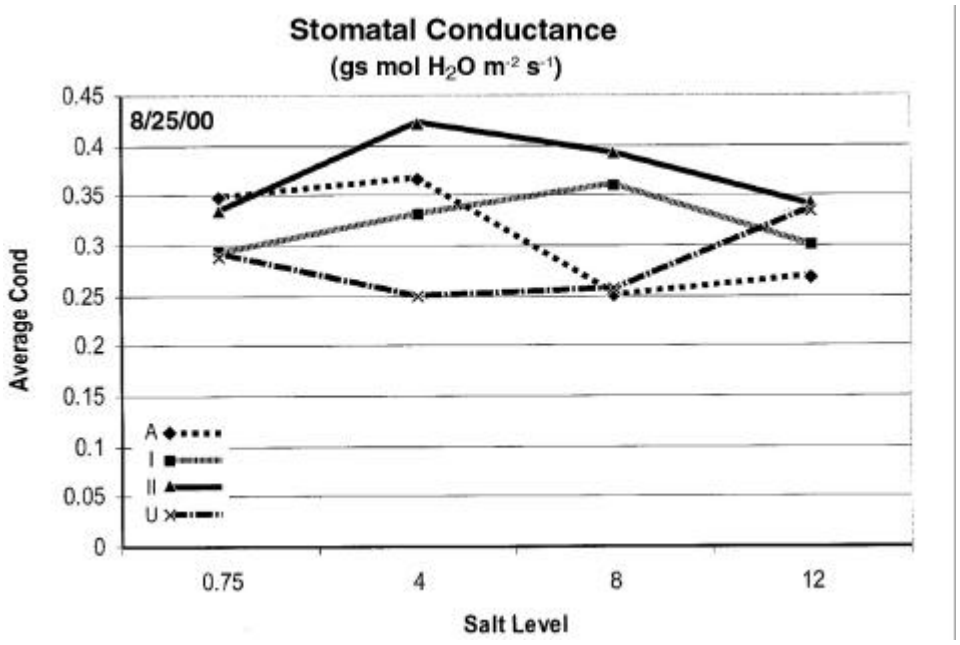

Figure 11b. Stomatal conductance rate in August 2000, ten days before harvest.

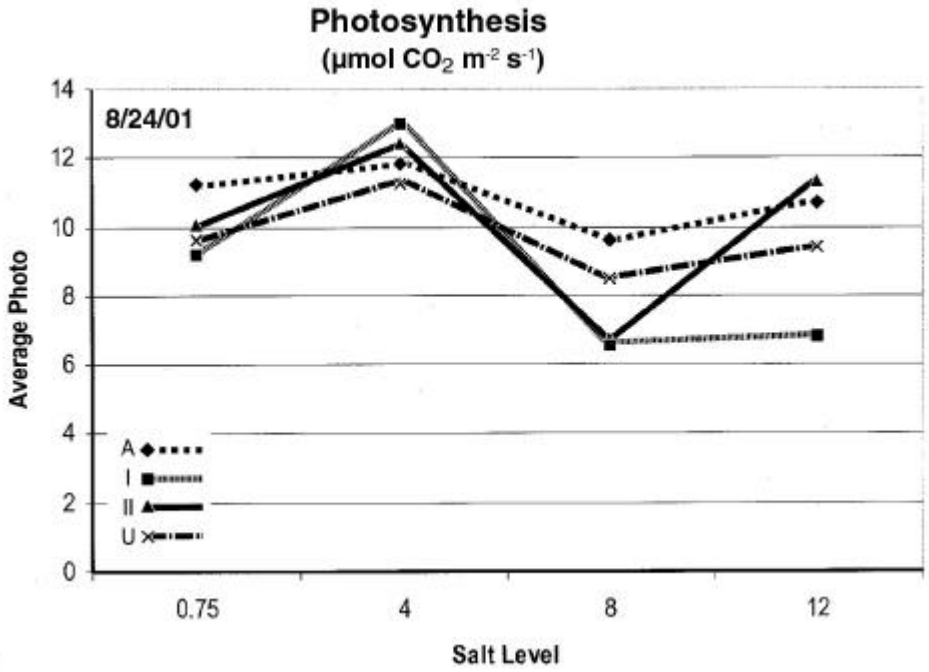

Figure 11c. Photosynthetic rate 2 weeks before harvest in August, 2001.

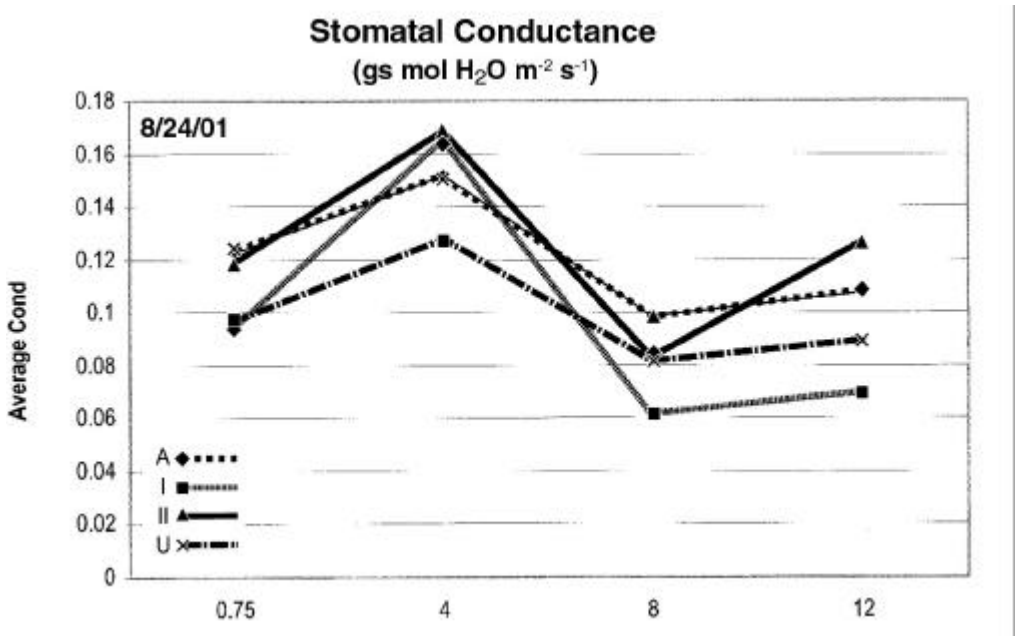

Figure 11d. Stomatal conductance rate measured 2 weeks before harvest in August, 2001.

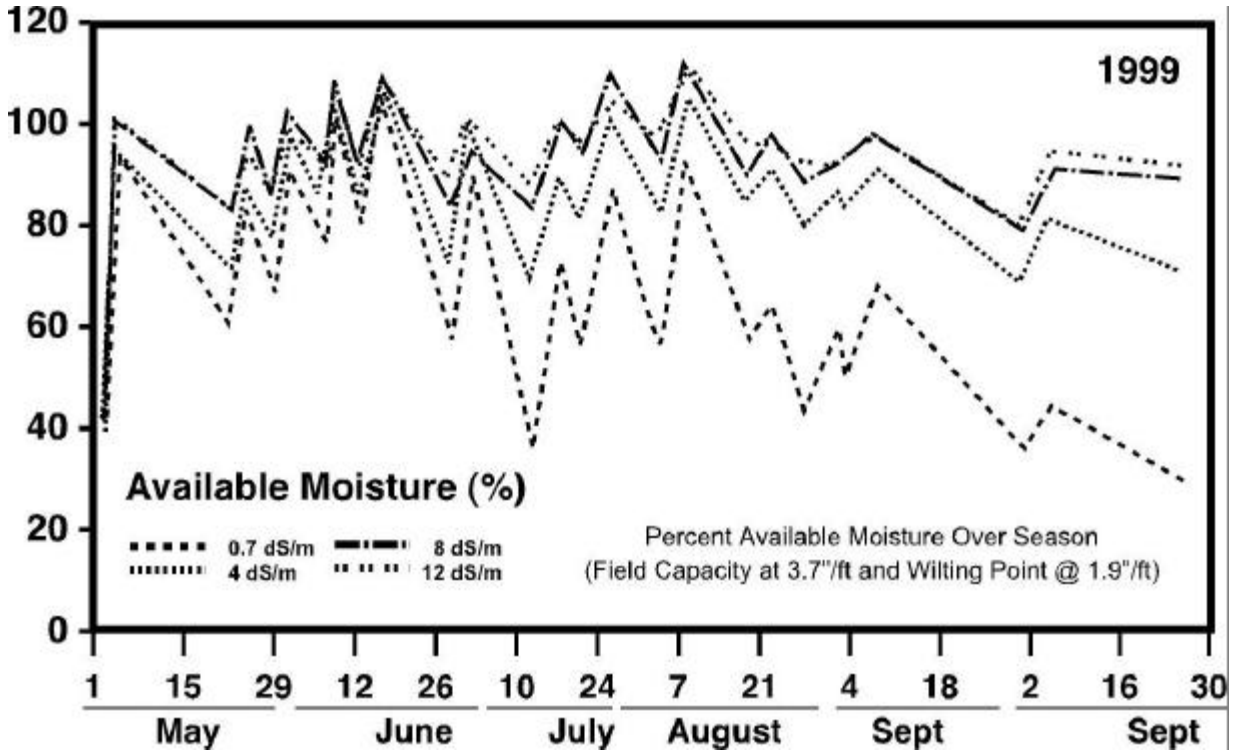

Figure 12a. Percent available water for all treatments from 0.2 to 5.2 foot depth. Calculated using field capacity at 3.7 in/ft, 18.5 inches total over 5 feet, and wilting point of 1.9 in/ft, 9.5 inches total over 5 feet. Total available water at 100% = 9.0 inches.

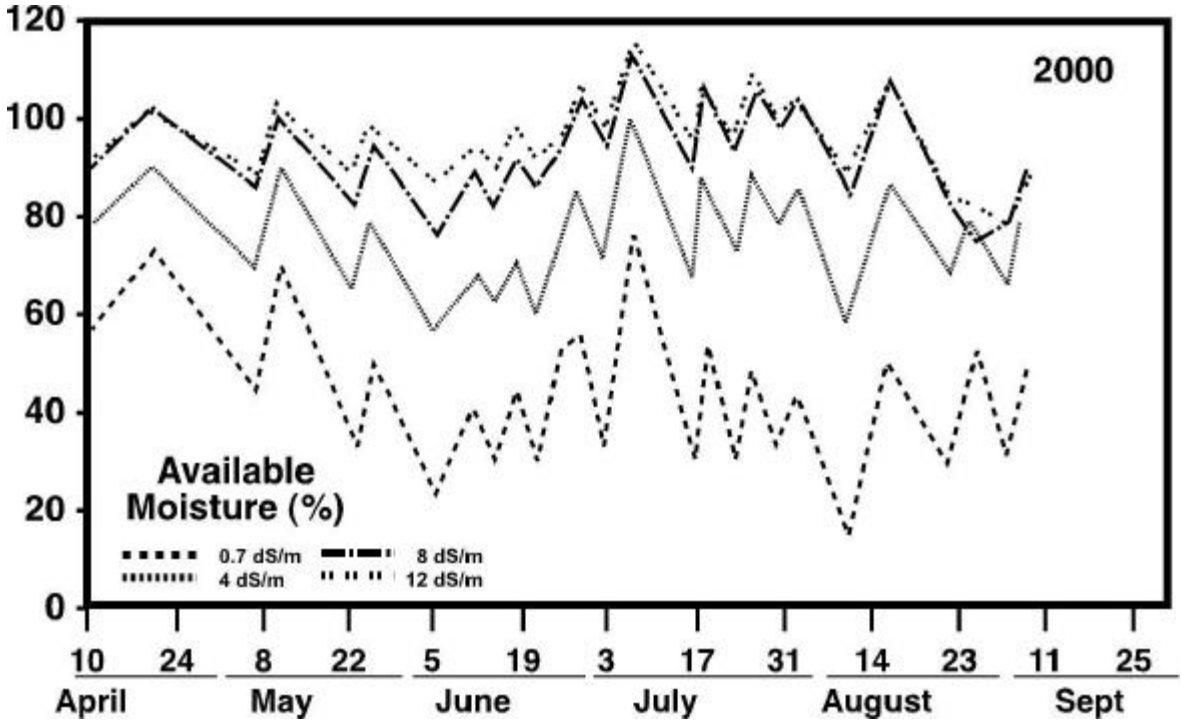

Figure 12b. Percent available water for all treatments from 0.2 to 5.2 foot depth. Calculated using field capacity at 3.7 in/ft, 18.5 inches total over 5 feet, and wilting point of 1.9 in/ft, 9.5 inches total over 5 feet. Total available water at 100% = 9.0 inches.

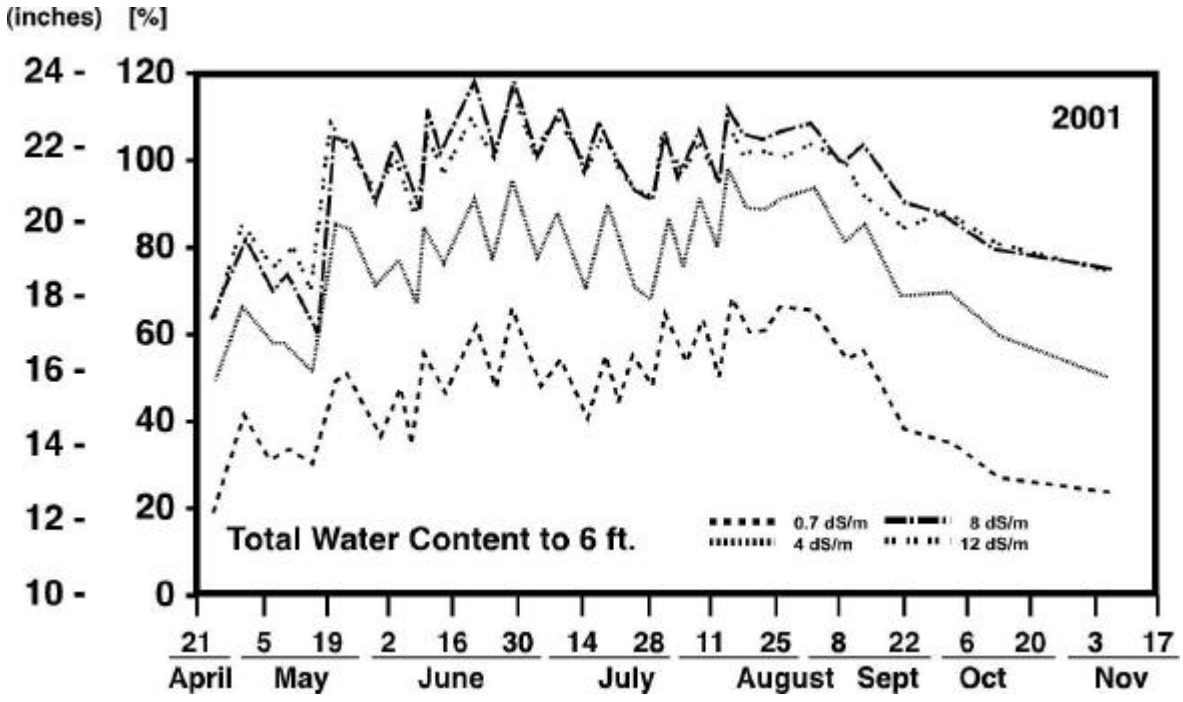

Figure 12c. Percent available water and total water content in inches for all treatments from 0.2 to 5.2 foot depth. Calculated using field capacity at 3.7in/ft, 18.5 inches total over 5 feet, and wilting point of 1.9 in/ft, 9.5 inches total over 5 feet. Total water available at 100% = 9.0 inches.

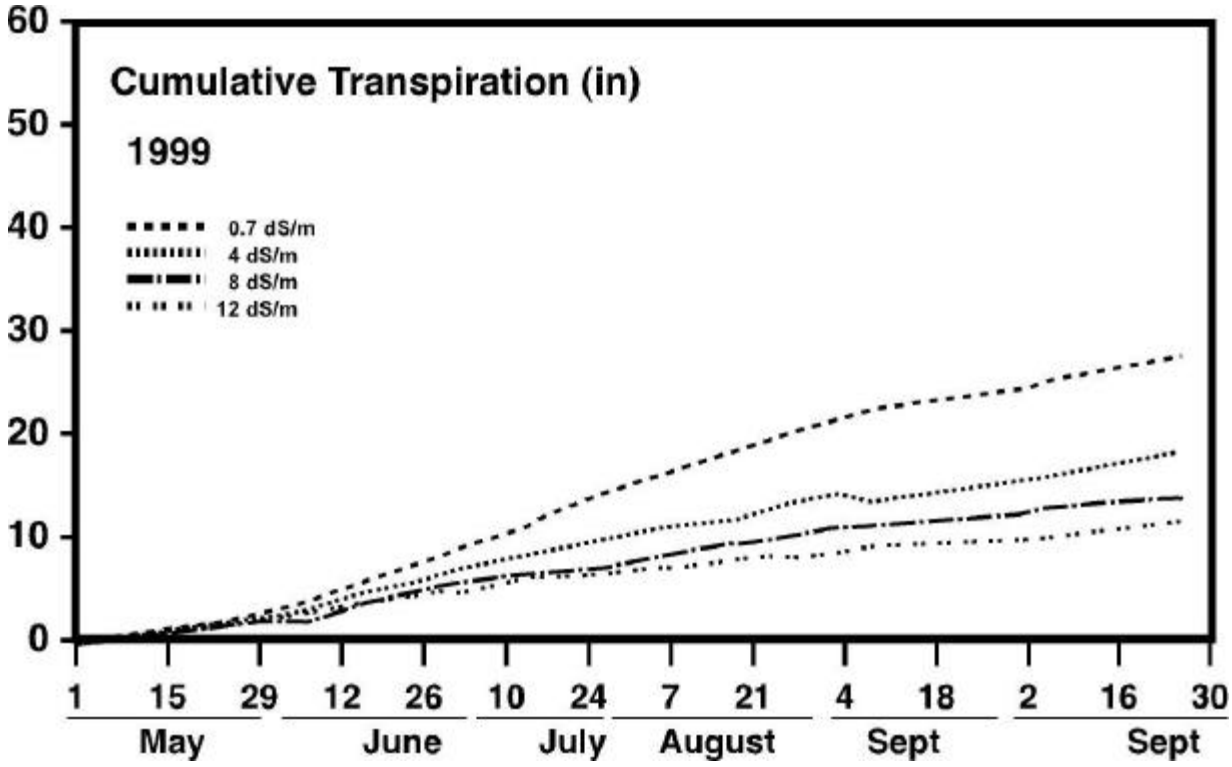

Figure 13a. Comparative seasonal transpiration for all treatments as determined by soil water content depletion between irrigations.

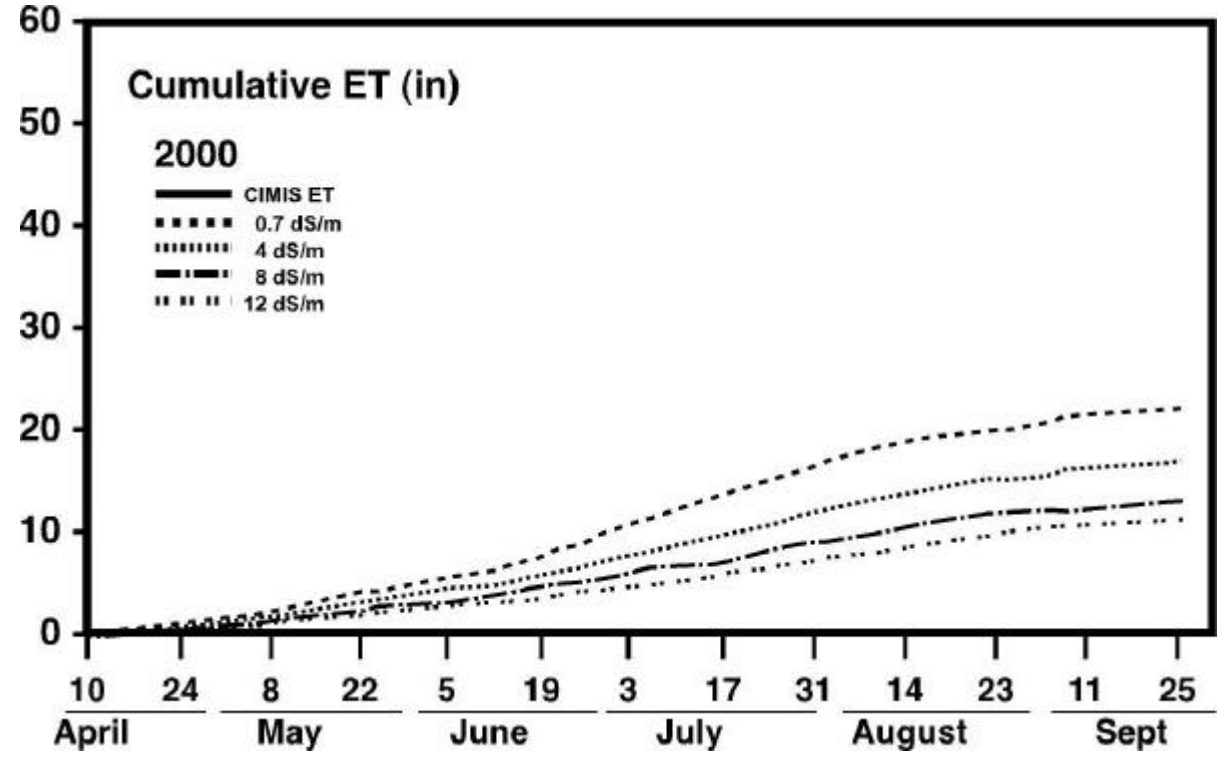

Figure 13b. Comparative seasonal evapotranspiration for all treatments as determined by soil water content depletion between irrigations.

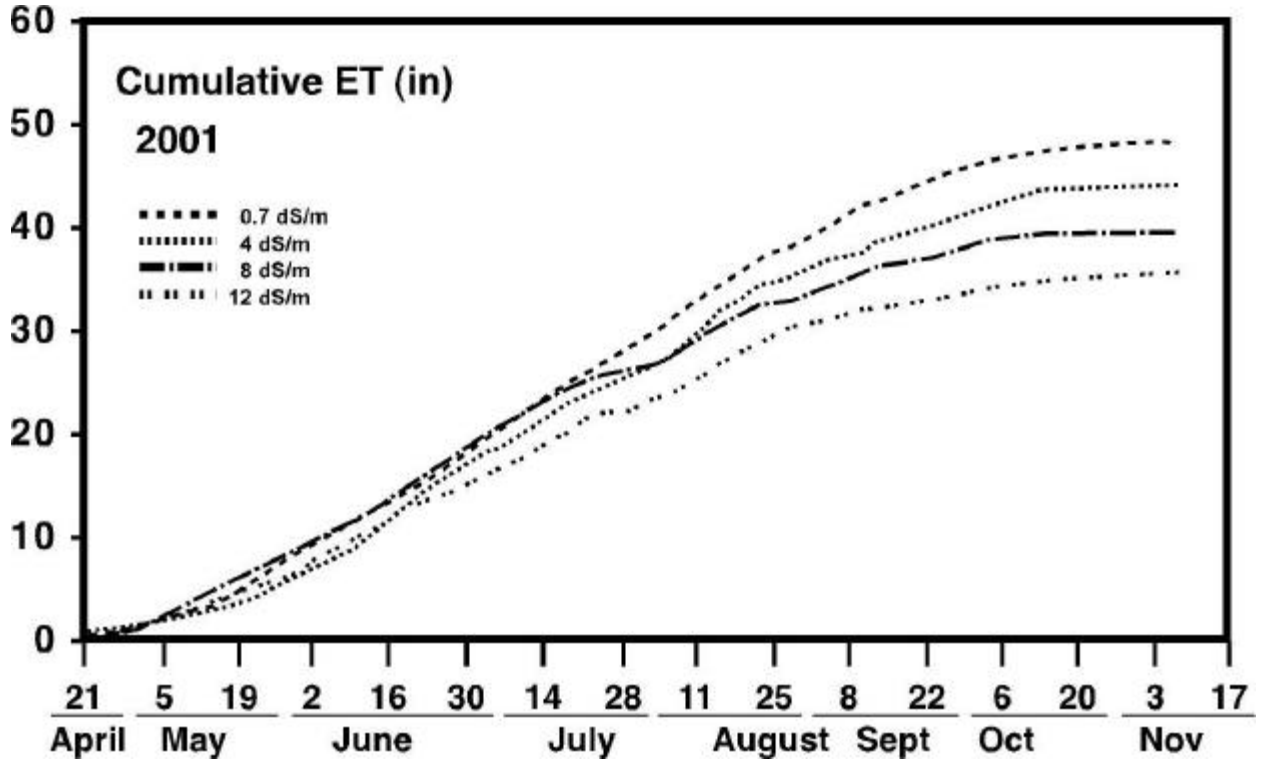

Figure 13c. Comparative seasonal evapotranspiration for all treatments as determined by soil water content depletion between irrigations and local CIMIC station evaporation.

Removal of Selenium from Drainage Water in Lined Reduction, Attachment and Open Oxidation Channels (Factors Affecting Removal of Selenate in Agricultural Drainage Water Utilizing Rice Straw)

Project Investigators:

William T. Frankenberger, Jr.
Office: (909) 787-3405, E-mail: williamf@orange.ucr.edu
Department of Environmental Sciences
University of California, Riverside

Yiqiang Zhang
Office: (909) 787-5218, E-mail: yqzhang@orange.ucr.edu
Department of Environmental Sciences
University of California, Riverside

ABSTRACT

Microbial reduction of selenate [Se(VI)] to elemental selenium [Se(0)] is a useful technique for removing Se from agricultural drainage water. A series of batch experiments were conducted in the laboratory to determine the effects of pH (5 to 10), NO_3^- (100 to 500 mg/L), and SO_4^{2-} (0 to 5,000 mg/L) on the removal of Se(VI) from drainage water with 1000 µg/L of Se(VI) and different amounts (1 to 4 g) of rice straw. Results showed that rice straw was very effective in creating a reducing environment (Eh = -205 to -355 mV) in the first 3 days of the pH–effect experiments. The optimum conditions for rapid Se(VI) removal from drainage water were a pH range of 6 to 9, high amounts of SO_4^{2-} (1,000 to 5,000 mg/L), low amounts of NO_3^- (100 mg/L) and high amounts of rice straw (3 to 4 g). Under these conditions, it took 5 to 7 days to reduce 93 to 95% of the added Se(VI) to Se(0). This study indicates that rice straw may be an inexpensive reducing agent to remediate Se(VI)–dominant San Joaquin Valley drainage water in the field.

KEYWORDS

Rice straw, Selenium speciation, Selenate reduction, Nitrate, Sulfate, pH.

■ ■ ■ ■ ■

INTRODUCTION

California's San Joaquin Valley is one of the world's most productive agricultural regions, supplying more than 70% of the United States' fruits and vegetables. Irrigation in the western part of the valley has produced high–salt drainage water containing selenium (Se) at levels that have ranged from 140 to 1400 µg/L (Sylvester, 1990). Introduction of the high–Se (mostly as selenate [Se(VI)]) drainage water into nearby wetlands has created serious hazards to wetland waterfowl (Presser and Ohlendorf, 1987; Ohlendorf, 1989). Removal of Se from agricultural drainage water before it reaches the wetlands is very important for protecting wetland wildlife.

Several strategies have been proposed for removing Se from drainage water. One strategy is the adsorption of Se by mineral adsorbents. Oxides such as Fe–, Mn– and Al–oxyhydroxides have been tested to adsorb soluble Se from water (Balistrieri and Chao, 1987; 1990; Glasauer et al., 1995; Kuan et al., 1998). The adsorption behavior of Se relies on its oxidation states (Neal et al., 1987a; 1987b). Because of the much lower adsorption character of Se(VI) than Se(IV), this technique has not been directly used to treat Se(VI)-dominant drainage water in the field.

The second strategy is Se methylation/ volatilization to the atmosphere. Bacteria, fungi and algae are capable of methylating Se in aquatic systems. The rates of Se volatilization are dependent on the Se species present, microbial activity and various environmental conditions (Karlson and Frankenberger, 1988; 1989; Thompson-Eagle and Frankenberger, 1992; Zhang and Moore, 1997). The methylation rates of Se have been enhanced in several laboratory studies when specific microorganisms and algae are used to methylate Se in drainage water (Thompson-Eagle et al., 1989; Thompson-Eagle and Frankenberger, 1990; Fan et al., 1998). However, these microorganisms and algae have not directly been used in the field for removal of Se from drainage water.

The third strategy is microbial reduction of Se(VI) to Se(0). In aquatic systems, Se(VI) can serve as an electron acceptor for microbial respiration. Many bacteria have been found to be capable of reducing Se(VI) to Se(0) (Francisco et al., 1992; Lortie et al., 1992; Cantafio et al., 1996; Losi and Frankenberger, 1997; Oremland et al., 1999). The reduction rates of Se(VI) are related to microbial activity, competitive electrons and various environmental conditions (Francisco et al., 1992; Lortie et al., 1992; Cantafio et al., 1996; Losi and Frankenberger, 1997; Oremland et al., 1999). Because of the insolubility character of Se(0) in aquatic systems, reduction of Se(VI) to Se(0) is considered to be a useful technique for bioremediation.

In a pilot scale Se bioremediation system in the San Joaquin Valley, Cantafio et al. (1996) used a Se(VI)-respiring bacterium (*Thauera selenatis*) to reduce Se(VI) to Se(0). Using acetate as the electron donor, Se(0) reduction proceeded rapidly in a series of four columns. About 98% of Se(VI) and Se(IV) in the seleniferous agricultural drainage water was reduced to Se(0). However, high costs make it less feasible to use acetate as an electron donor and carbon source for bacteria to reduce Se(VI) to Se(0) during full-scale operation in field conditions. Therefore, alternative economical organic sources are needed, not only to provide electron donors and carbon sources for bacteria to reduce Se(VI) to Se(0), but

also to serve as attachment sites for bacteria and formed red Se(0).

The purpose of this study was to test inexpensive rice straw in the removal of Se(VI) from drainage water and to determine the effects of pH, nitrate (NO_3^-), sulfate (SO_4^{2-}) and the amounts of rice straw on Se(VI) removal in a series of batch experiments.

MATERIALS AND METHODS

MATERIALS

Sodium selenate (Na_2SeO_4) was purchased from Sigma (St. Louis, MO). Sodium nitrate ($NaNO_3$), sodium bicarbonate ($NaHCO_3$), sodium sulfate (Na_2SO_4), sodium chloride (NaCl), calcium chloride ($CaCl_2$), magnesium sulfate ($MgSO_4$), magnesium chloride ($MaCl_2{\cdot}6H_2O$) and other chemicals were purchased from Fisher Scientific (Pittsburgh, PA).

The air-dried rice straw was obtained from the Broadview Water District (Firebaugh, CA) and was used without any post-treatments. The rice straw contained 0.412 µg/g of total Se and 0.346 µg/g of soluble Se. In order to keep the same salt concentrations in each series of batch experiments, artificial drainage water was prepared containing the major elements present in agricultural drainage water. In the experiments with different pH and different amounts of NO_3^- and rice straw, the artificial drainage water contained SO_4^{2-} (5,000 mg/L), Cl^- (1,500 mg/L), HCO_3^- (300 mg/L), Ca^{2+} (550 mg/L), Mg^{2+} (300 mg/L) and various concentrations of Na^+ (2,320 to 2470 mg/L) and NO_3^- (100 to 500 mg/L). In the experiments with different amounts of SO_4^{2-}, the artificial drainage water contained Cl^- (2,500 mg/L), HCO_3^- (300 mg/L), Ca^{2+} (550 mg/L), Mg^{2+} (300 mg/L) and various amounts of Na^+ (536 to 2,930 mg/L) and SO_4^{2-} (0 to 5,000 mg/L). Before mixing all chemical solutions, each chemical was separately dissolved in deionized water and autoclaved (18 psi at 121 °C) for 20 minutes. Se(VI) standard solution [10,000 mg/L] was passed through a sterile 0.2 µm membrane prior to its addition to the drainage water.

BATCH EXPERIMENTS

A series of batch experiments were conducted in the laboratory to determine the effects of pH, NO_3^-, SO_4^{2-} and amounts of rice straw on Se(VI) removal from drainage water through Se[VI] reduction to Se[0]. The terms "pH–effect", "NO_3^-–effect", "SO_4^{2-}–effect" and "straw–effect" represent four batches of experiments. In the pH–effect experiments, 4 g of rice straw were placed in each 500–ml flask, followed by 450 ml of drainage water containing 1,000 µg/L of Se(VI) ranging in pH from 5 to 10. In the NO_3^-–effect experiments, 4 g of rice straw were placed in each 500–ml flask, followed by 450 ml of drainage water (pH 8) containing 1,000 µg/L of Se(VI) with NO_3^- ranging from 100 to 500 mg/L. In the SO_4^{2-}–effect experiments, 4 g of rice straw were placed in each 500–ml flask, followed by 450 ml of drainage water (pH 8) containing 1,000 µg/L of Se(VI) with SO_4^{2-} varying from 0 to 5,000 mg/L. In the straw–effect experiments, 1, 2, 3 or 4 g of rice straw were placed in each 500–ml flask, followed by 450 ml of the drainage water (pH 8) containing 1,000 µg/L of Se(VI). Each flask was capped with a plastic foam plug in order to avoid build-up of gases produced in the flasks. The experiments were run in triplicates at room temperature (21±1 °C). Water samples were collected daily for total soluble Se analysis until soluble Se concentration had little change with time. On the final day (day 14) of the experiments, water samples were collected for Se species analysis, which included total solution Se [(total soluble Se plus unprecipitated Se(0)], total soluble Se, Se(VI), Se(IV), unprecipitated Se(0) and organic Se(-II) (Fig. 1).

ANALYSIS

Redox potential and pH were measured daily in the pH 5, 8 and 10 experiments, and at the final day in the pH–, NO_3^-– and SO_4^{2-}–effect experiments. A 720A pH/ISE meter (Thermo Orion, Beverly, MA) was used to monitor the pH and redox potential (Eh) in the experimental flasks. pH was measured using an Accumet pH combination electrode. The redox potential was measured with an Accumet combination platinum electrode (Ag/AgCl). The measured potential ($Eh_{measured}$) was converted to potential in the rice straw solution (Eh_{actual}) relative to a standard H electrode as $Eh_{actual} = Eh_{measured} + 224.4$ mV (Jayaweera and Biggar, 1996). The Eh electrode was tested by immersing in pH 4 and 7 buffer solutions saturated with quinhydrone (Q_2H_2) prior to each day's measurement.

Fig. 1 shows the procedure for determination of Se species in the water samples. Water soluble Se speciation was determined using a method developed by Zhang and Frankenberger (2002)

after removing unprecipitated Se(0) by centrifugation at 12,000 rpm for 10 minutes. In brief, soluble Se speciation was carried out as follows: Se(IV) in the water samples was determined in a pH 7 buffer solution. The sum of Se(IV) and organic Se(-II) was determined when the organic Se in the water samples was oxidized to Se(IV) by $K_2S_2O_8$, which was indicated by precipitation of Mn oxides. The organic Se(-II) concentration was calculated as the difference between Se in this water sample and Se(IV) concentration determined in another subsample. Total soluble Se in the water samples was determined by oxidizing all Se to Se(VI) by $K_2S_2O_8$, followed by reduction to Se(IV) in 6 N HCl. Se(VI) concentration was calculated as the difference between total soluble Se concentration and Se(IV) and organic Se(-II) concentration determined in another subsample. Total solution Se [sum of total soluble Se and unprecipitated Se(0)] in the water samples was determined using the same procedure as total soluble Se (Zhang and Frankenberger, 2002). Se concentrations in all prepared solutions were analyzed by hydride generation atomic absorption spectrometry (HGAAS) (Zhang et al., 1999a; 1999b). NO_3^- in the water samples was determined using a steam distillation method (Keeney and Nelson, 1982).

RESULTS

EFFECT OF PH ON SE(VI) REMOVAL

The removal of Se from drainage water in the pH–effect experiments is presented in Fig. 2. Total soluble Se in the rice straw solution decreased with time. However, the time needed for the total soluble Se to decrease from 1,000 to about 70 µg/L differed in the pH–effect experiments, which took 5, 7 and 9 days in the pH 7 to 9, pH 6 and pH 10 experiments, respectively. In the pH 5 experiments, total soluble Se decreased slowly from 1,000 to 341 µg/L at day 14. In the final day of the experiments (Table 1), unprecipitated Se(0) and organic Se(-II) were the major forms of Se in the rice straw solution ranging from 101 to 159 and 53.9 to78.2 µg/L in the pH 6 to 10 experiments, respectively. Se(VI) plus Se(IV) was about 10 µg/L. In the pH 5 experiment, the concentrations of Se[VI], Se(IV), unprecipitated Se[0] and organic Se(-II) were 277, 13.2, 208 and 50.4 µg/L, respectively.

In the pH 5, 8 and 10 experiments (Fig. 3), redox potential in the rice straw solution decreased rapidly from 275 to 362 to -203 to -355 mV in the first 3 days. It increased to -8 to -124 mV from day 4 to day 6, and then stabilized with time at -100 to -130 mV. The change in pH differed among the experiments. pH decreased with time from an initial pH of 10 to 7.5 in the pH 10 experiment, with an increase from an initial 5 to 6.8 in the pH 5 experiment. In the pH 8 experiment, pH changed slightly with a range of 7.3 to 8.

EFFECT OF NO_3 ON SE(VI) REMOVAL

The removal of Se from drainage water in the experiments with different NO_3^- concentrations (100 to 500 mg/L) is presented in Fig. 4. In the 100 and 250 mg/L NO_3^- experiments, the drop in total soluble Se from 1,000 to 66 µg/L in the rice straw solution took 7 and 12 days, respectively. In contrast, total soluble Se decreased very slowly in the high NO_3^- (500 mg/L) experiment, and only one of the triplicates showed a rapid decrease in concentration of total soluble Se at days 13 and 14. In the final day of the experiments, unprecipitated Se(0) and organic Se(-II) were the major forms of Se in the rice straw solution, ranging from 144 to 319 and 46.7 to 84.3 µg/L in the 100 and 250 mg/L NO_3^- experiments, respectively. Se(VI) and Se(IV) were low, ranging from 0.78 to 7.49 and 6.23 to 13.7 µg/L, respectively. Redox potential in these experiments (100 and 250 mg/L NO_3^-) ranged from -109 to -117 mV with a pH of 7.6.

In contrast, Se(VI) was the dominant Se form (621 µg/L) in the high NO_3^- experiment (500 mg/L), with 3.48 µg/L of Se(IV), 136 µg/L of unprecipitated Se(0) and 65.6 µg/L of organic Se(-II). With the addition of 500 mg/L NO_3^-, redox potential was higher at 33 mV with a pH of 7.6.

EFFECT OF SO_4^{2-} ON SE(VI) REMOVAL

The removal of Se from drainage water in the experiments with different SO_4^{2-} concentrations (0 to 5,000 µg/L) is presented in Fig. 5. In the high SO_4^{2-} (1,000 to 5,000 mg/L) experiments, the concentration of total soluble Se remained relatively stable during the first 3 days at about 960 to 1,000 µg/L, and then decreased rapidly to approximately 50 µg/L from day 4 to day 6. In the low SO_4^{2-} experiments (0 to 100 mg/L), it took about 10 days to decrease total soluble Se from 1000 to 80 µg/L in the rice straw solution. In the final day of the experiments, unprecipitated Se(0) and organic Se(-II) were the major forms of Se in

the rice straw solution ranging from 104 to 200 and 59.8 to 68.5 µg/L, respectively. Se(VI) and Se(IV) were low, ranging from 0.48 to 3.71 and 10.4 to 18.9 µg/L, respectively. Redox potentials in all the SO_4^{2-} effect experiments were -79.9 to -102 mV with a range of pH from 7.1 to 7.5.

EFFECT OF AMOUNTS OF STRAW ON SE(VI) REMOVAL

The removal of Se from drainage water in the experiments with different amounts (1 to 4 g) of rice straw added is presented in Fig. 6. Total soluble Se decreased with time. However, the amount of time needed for the decrease of total soluble Se from 1,000 to approximately 65 µg/L in the rice straw solution was 5 and 7 to 9 days for the 4 g and 2 to 3 g experiments, respectively. In the 1 g experiment, total soluble Se decreased slowly with a mean of 805 µg/L at day 14. In the final day of the experiments, unprecipitated Se(0) and organic Se(-II) were the major forms of Se in the rice straw solution ranging from 106 to 144 and 39.7 to 58.8 µg/L in the 2 to 4 g experiments, respectively. Se(VI) plus Se(IV) was 0.583 to 17.3 µg/L. In the 1 g experiment, Se[VI] was the dominant Se form with an average concentration of 720 µg/L. Se(IV), unprecipitated Se[0], and organic Se(-II) were 67.6, 13.5 and 16.9 µg/L, respectively.

DISCUSSION

The bacterial reduction of Se(VI) to Se(0) is a useful technique for removing Se from agricultural drainage water. Zhang and Frankenberger (2002) used air–dried rice straw as an economical organic source and a Se(VI)–reducing bacterial carrier to remove Se(VI) from drainage water and characterized the removal process of Se(VI) by bacterial reduction of Se(VI) to Se(0), followed by flocculation/precipitation of Se(0) or attachment of Se(0) on the surface of rice straw. This study showed that the efficiency of Se(VI) reduction to Se(0) in the presence of rice straw is related to pH, NO_3^- and SO_4^{2-} concentrations and the amount of rice straw added to the drainage water.

Water pH is an important parameter in drainage water. Changes in pH affect the reduction of Se(VI) to Se(0). In a study on the effect of pH on the reduction of Se(VI) to Se(0) by a *Pseudomonas stutzeri* isolate, Lortie et al. (1992) found that pH 7 to 9 was the optimum range for rapid reduction of Se(VI) to Se(0). Se(VI) reduction was limited when pH was below 6.5 or above 9.5. In this study, efficiency of Se(VI) reduction was different in each medium, although pH in the different pH experiments shifted to a neutral pH of 6.5 to 7.5 during the first several days. An optimum range of pH for rapid reduction of Se(VI) in drainage water in the presence of rice straw was 7 to 9. It took only 5 days to reduce 93% of the added Se(VI) to Se(0), whereas in the pH 5 experiment, about 72% of the added Se(VI) was reduced to Se(0) at day 14. In the San Joaquin Valley, the pH of drainage water ranges from 7 to 8 (Oswald et al., 1989), which is in the optimum range of pH for rapid reduction of Se(VI) to Se(0) in the rice straw solution.

Nitrate is one of the most common anions found in agricultural drainage water, due to the application of fertilizers in the San Joaquin Valley. The redox potential of NO_3^-/N_2 in an aquatic system is very similar to that of Se [VI]/Se [IV] and much higher than Se(IV)/Se(0) (Masscheleyn and Patrick, 1993), thus the presence of dissolved NO_3^- can serve as a competitive electron acceptor affecting Se[VI] reduction to Se(IV) and inhibiting Se(VI) reduction to Se(0) (Steinberg and Oremland, 1990; Weres et al., 1990; Lortie et al., 1992; Masscheleyn and Patrick, 1993; Wright, 1999). This study reveals that the presence of NO_3^- in a rice straw solution can retard Se(VI) reduction to Se(0). In the 500 mg/L NO_3^- experiment, Se(VI) was not reduced in the rice straw solution until day 14 was approached, when almost all the NO_3^- was removed from solution (Table 1). However, inhibition of NO_3^- on Se(VI) reduction is also related to the composition of the rice straw. Organic materials released from rice straw can promote bacterial immobilization of NO_3^-, which led to a 93% reduction of the added Se(VI) to Se(0) in the rice straw solution at day 7 in the 100 mg/L NO_3^- experiment, and promoted a similar reduction of Se(VI) to Se(0) at day 12 in the 250 mg/L NO_3^- experiment. This indicates that rice straw is a very strong natural reducing agent that can be used not only to reduce Se(VI) to Se(0), but also to remove NO_3^- from drainage water. In the San Joaquin Valley, agricultural drainage water typically contains 3 to 234 mg/L of NO_3^- with an average of 97 mg/L (Oswald et al., 1989). Therefore, NO_3^- in the San Joaquin Valley drainage water can be simultaneously removed during the reduction of Se(VI) to Se(0) using rice straw.

Sulfate is an important anion found in drainage water (Oswald et al., 1989). SO_4^{2-} redox

potential is much lower than Se[VI] and thus, it does not serve as a competitive electron acceptor for Se[VI] reduction (Masscheleyn and Patrick, 1993). However, SO_4^{2-} can serve as an electron acceptor for microbial oxidation of organic materials, and its reducing product, sulfide (S^{2-}) can serve as an electron donor for microbial respiration (Murase and Kimura, 1997). In this study, we found that a relatively high level of SO_4^{2-} did promote the reduction of Se(VI) to Se(0) in the rice straw solution. It only took 6 days to reduce 95% of the added Se(VI) to Se(0) in the high SO_4^{2-} (1,000 to 5,000 mg/L) drainage water, while it took 10 days to reach a similar reduction level in the low SO_4^{2-} (0 to 100 mg/L) drainage water. In the San Joaquin Valley drainage water, SO_4^{2-} ranges from 607 to 10,100 mg/L with an average of 2,282 mg/L (Oswald et al., 1989). Therefore, the relatively high amount of SO_4^{2-} in the San Joaquin Valley water may promote Se(VI) reduction to Se(0) during treatment in the field using rice straw.

Organic materials play a very important role in Se(VI) reduction to Se(0) in aquatic systems (Stolz and Oremland, 1999). Organic matter can serve as electron donors and carbon sources for bacterial respiration. Therefore, the efficiency of Se(VI) reduction to Se(0) in drainage water is related to the amount of organic materials present in drainage water. This was confirmed in our study, in which it took 5 days to reduce about 94% of the added Se(VI) to Se(0) in the 4 g straw experiment. In the 1 g straw experiment, only 20% of the added Se(VI) was reduced to Se(0) in 14 days. In the field, it is important to determine the optimum amount of rice straw to be used to rapidly reduce Se(VI) to Se(0) in the drainage water.

Organic Se(-II) is an important form of Se in aquatic systems. This study showed that about 5% of the added Se(VI) was reduced to organic Se(-II) in the final day of the experiments. Although organic Se(-II) can be transformed to volatile organic Se compounds or be mineralized to inorganic Se species, its fate in the rice straw solution was not determined in this study.

CONCLUSIONS

This study revealed that pH of 7 to 9 and high SO_4^{2-} levels in the San Joaquin Valley drainage water supports the reduction of Se(VI) to Se(0) in the presence of rice straw. Although NO_3^- is a competing electron acceptor to Se(VI), the range (<250 mg/L) of its concentration typically in the San Joaquin Valley drainage water will not significantly affect Se(VI) reduction. Therefore, rice straw may be an ideal reducing agent to remediate Se(VI) in the high–SO_4^{2-} drainage water. There are several advantages in using rice straw to remediate the San Joaquin Valley drainage water. The first is that rice straw is available at a much lower cost in the San Joaquin Valley than any other agricultural organic sources. There is such an abundance of rice straw in the valley, that often it has to be burned for disposal. The second is that rice straw often carries Se(VI)-reducing bacteria. There is no need to bioaugument with Se(VI)-reducing bacteria into the drainage water. The third advantage is that it not only promotes rapid reduction of Se(VI) to Se(0), but also NO_3^- to N_2O or N_2 in removing excess NO_3^- in the drainage water. In order to examine whether rice straw can directly be used economically in the field to treat seleniferious drainage water, a flow-through system will need to be built to monitor the feasibility of this technology.

■ ■ ■ ■ ■

REFERENCES CITED

Balistrieri LS, Chao TT. Adsorption of selenium by amorphous iron oxyhydroxides and manganese dioxide. Geochim. Cosmochim. Acta 1990;54:739-751.

Balistrieri LS, Chao TT. Selenium adsorption by geothite. Soil Sci. Soc. Am. J. 1987;51:1145-1151.

Cantafio AW, Hagen KD, Lewis GE, Bledsoe TL, Nunan KM, Macy JM. Pilot-scale selenium bioremediation of San Joaquin drainage water with Thauera selenatis. Appl. Environ. Microbiol. 1996;62:3298-3303.

Fan TW-M, Higashi RM, Lane AN. Biotransformation of selenium oxyanion by filamentous cyanophyte-dominated mat cultured from agricultural drainage waters. Environ. Sci. Technol. 1998;32:3185-3193.

Francisco AT, Barton LL, Lemanski CL, Zocco, TG. Reduction of selenate and selenite to elemental selenium by *Wolinella succinogenes*. Can. J. Microbiol. 1992;38:1328-1333.

Glasauer S, Doner HE, Gehring AU. Adsorption of selenite to goethite in a flow-through reaction chamber. Europ. J. Soil Sci. 1995;46:47-52.

Karlson U, Frankenberger Jr., WT. Accelerated rates of selenium volatilization from California soils. Soil Sci. Soc. Am. J. 1989;53:749-753.

Karlson U, Frankenberger Jr., WT. Effects of carbon and trace element addition on alkylselenide production by soil. Soil Sci. Soc. Am. J. 1988;52:1640-1644.

Keeney DR, Nelson DW. Nitrogen-inorganic forms. In: Page AL, Miller RH, Keeney DR, editors. Methods of soil analysis. Madison, WI: ASA and SSSA, 1982:649-658.

Kuan WH, Lo SL, Wang MK, Lin CF. Removal of Se(IV) and Se(VI) from water by aluminum-oxide coated sand. Wat. Res. 1998;32:915-923.

Lortie L, Gould WD, Rajan S, Mccready RGL, Cheng KJ. Reduction of selenate and selenite to elemental selenium by a *Pseudomonas stutzeri* Isolate. Appl. Environ. Microbiol. 1992;58:4042-4044.

Losi ME, Frankenberger Jr., WT. Reduction of selenium oxyanions by Enterbaxter cloacae strain SLDaa-1: Isolation and growth of the bacterium and its expulsion of selenium particles. Appl. Environ. Microbiol. 1997;63:3079-3084.

Masscheleyn PH, Patrick WHJ. Biogeochemical processes affecting selenium cycling in wetlands. Environ. Toxicol. Chem. 1993;12:2235-2243.

Murase J, Kimura M. Anaerobic reoxidation of Mn^{2+}, Fe^{2+}, S^{0} and S^{2-} in submerged paddy soils. Biol. Fertil. Soils 1997;25:302-306.

Neal RH, Sposito G, Holtzclaw KM, Traina SJ. Selenite adsorption on alluvial soils: I. Soil composition and pH effects. Soil Sci. Soc. Am. J. 1987a;51:1161-1165.

Neal RH, Sposito G, Holtzclaw KM, Traina SJ. Selenite adsorption on alluvial soils: II. Solution composition effects. Soil Sci. Soc. Am. J. 1987b;51:1165-1169.

Ohlendorf HM . Bioaccumulation and effects of selenium in wildlife. In: Jacobs LW, editor. Selenium in agriculture and the environment. Madison, WI: ASA and SSSA, 1989:133-177.

Oremland RS, Blum JS, Bindi AB, Dowdle PR, Herbel M, Stolz JF. Simultaneous reduction of nitrate and selenate by cell suspensions of selenium-respiring bacteria. Appl. Environ. Microbiol. 1999;65:4385-4392.

Oswald WJ, Chen PH, Gerhardt MB, Green BF, Nurdogan Y, Von Hippel DF, Newman RD, Chown L, Tam CS. The role of microalgae in removal of selenate from subsurface tile drainage. In: Huntley ME, editor. Biotreatment of agricultural wastewater. Boca Raton, FL: CRC Press, 1989:131-141.

Presser TS, Ohlendorf HM. Biogeochemical cycling of selenium in the San Joaquin Valley, California, USA. Environ. Manage. 1987;11:805-821.

Steinberg NA, Oremland RS. Dissimilatory selenate reduction potentials in a diversity of sediment types. Appl. Environ. Microbiol. 1990;56:3550-3557.

Stolz JF, Oremland RS. Bacterial respiration of arsenic and selenium. FEMS Microbiol. Rev. 1999;23:615-627.

Sylvester MA. Overview of the salt and agricultural drainage problem in the western San Joaquin Valley, California. US Geological Survey Circular, No. 1033c 1990;pp119-124.

Thompson-Eagle ET, Frankenberger Jr., WT. Biomethylation of soils contaminated with selenium. Adv. Soil Sci. 1992;17:261-310.

Thompson-Eagle ET, Frankenberger Jr., WT. Volatilization of selenium from agricultural evaporation pond water. J. Environ. Qual. 1990;19:125-131.

Thompson-Eagle ET, Frankenberger Jr., WT, Karlson U. Volatilization of selenium by *Alternaria alternata*. Appl. Environ. Microbiol. 1989;55:1406-1413.

Weres O, Bowman HR, Goldstein A, Smith EC, Tsao L. The effect of nitrate and organic matter upon mobility of selenium in groundwater and in a water treatment process. Water Air Soil Pollut. 1990;49:251-272.

Wright WG. Oxidation and Mobilization of selenium by nitrate in irrigation drainage. J. Environ. Qual. 1999;28:1182-1187.

Zhang YQ, Frankenberger Jr., WT. Characterization of Senate removal from drainage water utilizing rice straw. J. Environ. Qual. (Submitted for publication)

Zhang YQ, Moore JN. Environmental conditions controlling selenium volatilization from a wetland system. Environ. Sci. Technol. 1997;31:511-517.

Zhang YQ, Frankenberger Jr., WT. Moore JN. Measurement of selenite in sediment extracts by using hydride generation atomic absorption spectrometry. Sci. Total Environ. 1999a;229:183-193.

Zhang YQ, Moore JN, Frankenberger Jr., WT. Speciation of soluble selenium in agricultural drainage waters and aqueous soil-sediment extracts using hydride generation atomic absorption spectrometry. Environ. Sci. Technol. 1999b;33:1652-1656.

PUBLICATIONS AND REPORTS

Zhang YQ, Frankenberger Jr., WT. Characterization of Senate removal from drainage water utilizing rice straw. J. Environ. Qual. (Submitted for publication)

Table 1. Se species (µg/L), pH, redox potential (Eh) and NO_3^- (mg/L) in the rice straw solution at experimental day 14

Experiments	Se(VI)	Se(IV)	Se(0)	Org Se (-II)[a]	pH	Eh(mV)	NO_3^-
pH–effect							
pH 10	4.53±1.08	5.87±0.95	107±33.7	53.9±4.56	7.6±0.1	-79.9±17.2	ND[b]
pH 9	4.74±3.28	5.26±1.02	125±32.2	78.2±8.06	7.5±0.1	-93.6±38.4	ND
pH 8	4.42±0.21	12.84±8.99	144±56.6	58.8±4.18	7.4±0.1	-109±19.9	ND
pH 7	4.13±2.59	5.87±0.05	101±8.66	73.9±12.3	7.4±0.1	-107±7.8	ND
pH 6	4.80±2.25	3.64±2.17	159±60.1	69.8±17.6	7.0±0	-108±7.2	ND
pH 5	277±305	13.2±10.3	208±185	50.4±5.69	6.8±0.2	-85.9±33.5	ND
SO_4^{2-}							
0 mg/L	0.97±3.39	18.9±7.90	200±79.3	66.71±3.37	7.2±0.1	-102±41.1	ND
100 mg/L	0.48±4.56	12.7±8.32	129±79.5	59.75±3.76	7.1±0.3	-79.9±56.1	ND
1000 mg/L	3.71±1.21	18.1±3.75	104±51.2	62.69±7.73	7.3±0.1	-97.9±27.6	ND
5000 mg/L	1.33±3.20	10.4±0.19	157±29.9	68.55±5.71	7.5±0	-88.3±6.66	ND
NO_3^-–effect							
100 mg/L	0.78±0.30	6.23±1.75	144±33.3	84.25±5.98	7.6±0.1	-109±12.7	2.33±0.48
250 mg/L	7.49±6.04	13.7±10.6	319±151	46.73±23.6	7.6±0.1	-117±106	1.69±0.82
500 mg/L	621±471	3.48±3.30	136±234	65.62±54.7	7.6±0.1	33.1±3.79	3.66±0.50

[a] Organic Se(-II).

[b] Not determined.

Table 2. Se species (µg/L) in the rice straw solution at experimental day 14

Rice straw	Se(VI)	Se(IV)	Se(0)	Org Se (-II)[a]
1 g	720±246	67.6±94.8	13.5±9.67	16.93±6.85
2 g	5.22±1.39	4.76±1.39	122±22.1	41.36±6.15
3 g	0.583±1.08	BDL[b]	106±28.7	39.69±5.29
4 g	4.42±0.21	12.84±8.99	144±56.6	58.84±4.18

[a] Organic Se(-II).

[b] Below detection limit (3 µg/L).

An Investigation into the Ecotoxicology of Selenium Bioaccumulation in Birds

Project Investigators:

D. Michael Fry
Office: (530) 754-8562, E-mail: dmfry@ucdavis.edu
Department of Animal Science
University of California, Davis

Research Staff:

RA: Steven Detwiler (50%)

Lab Assistants: Uland Wong (10%), Janice Rahman (10%)

ABSTRACT

Marked variation between wild bird species exists in sensitivity to the teratogenic effects of selenium. Our working hypothesis has been that more tolerant species have the ability to distinguish between methionine and selenomethionine during protein synthesis, and as a result, the embryos of resistant species incorporate less Se into proteins, and are thus protected from the teratogenic effects of Se. As one measure of evaluation, both wild bird eggs and chicken eggs have been separated into yolk, albumin, and embryo fractions and analyzed for Se to evaluate the ability of different species to avoid toxic effects of Se during embryo development.

Work to this point has included the examination of 231 eggs from 9 species of wild birds nesting in selenium-contaminated environments. The wild species have been compared to chickens and to mallards in laboratory feeding trials, in which eggs from dosed birds have been set and evaluated to compare with the developmental studies of wild Se exposed birds.

The egg contents of all birds were fractionated into embryonic, yolk, and albumin compartments and extracted for determination of total selenium and protein associated selenium, to quantify the differences between species with respect to the ability of embryos to partition selenium into protein fractions during development. The Se compartmentalization and chemical form in fresh eggs was followed as embryos grew, synthesized new protein, and incorporated Se into protein. Our hypothesis has been that more tolerant avian species (American avocet) could effectively exclude selenium from embryonic tissues relative to the more sensitive species with similar dietary ecology.

The laboratory feeding trial with chickens was completed in 2001. Birds were fed diet containing SelenoMax™ selenized yeast, containing about 70% of selenium as selenomethionine.

Hen weights during the feeding trial were monitored before and after each dose administration. Dose-dependent cachexia (wasting syndrome) was observed in the study hens. Measurements of chicken embryonic masses at defined incubation periods were also collected to detect dose-dependent retardation of embryogenesis. A decrease in embryo weight was detected in eggs from the 4 ppm selenium diet, without detected teratogenesis. At dietary levels of 8 ppm. selenium, embryo weights were severely reduced and 17% of embryos were abnormal. At 12 ppm. selenium in the diet, 97% of the embryos were deformed, and live embryos averaged only 37% of control weights.

A feeding trial with Mallards duplicating the chicken feeding was conducted during 2001, with 2 elevated SelenoMax™ selenized yeast dose groups. Eggs were collected and incubated to ¾ term, and broken out exactly as in the chicken experiment. 390 eggs were collected for analysis, including at least 55 eggs per treatment group. The comparative data for chickens and mallards will provide the links for interpreting the dose response, protein bound Se, and terata observed in the more resistant wild species.

A model to analyze [Se] within each compartment of eggs was developed to test the hypothesis that embryos of tolerant species area able to exclude Se from synthesized proteins.

Analysis of the model indicates that sensitive species have the potential to remove significant amounts of egg-borne Se from the embryonic compartment, so this ability in itself is insufficient to explain differences between species in Se tolerance. Further, while this process seems more pronounced in the more tolerant species up to teratogenic doses, at this threshold surviving embryos in the sensitive species nevertheless express significant depuration potential. Indications are that other factors are involved allowing tolerant species to withstand higher realized [Se] *in-vivo* before expressing toxic effects.

KEYWORDS

Selenium, Birds, Ecotoxicology, Bioaccumulation, Development

■ ■ ■ ■ ■

INTRODUCTION

In 1983, scientists discovered significant reproductive impairment and avian mortality at Kesterson Reservoir--a waterfowl enhancement area operated by the U.S. Bureau of Reclamation as a unit of the Federal National Wildlife Refuge System in the San Joaquin Valley of California (Ohlendorf et al., 1986a). Embryo toxicosis (embryo deaths and deformities) and/or reduced

hatchling survival were observed in American coots (*Fulica americana*), eared grebes (*Podiceps nigricollis*), black-necked stilts (*Himantopus mexicanus*), and several dabbling duck species (mallard [*Anas platyrhynchos*], gadwall [*Anas strepera*], cinnamon teal [*Anas cyanoptera*], and northern pintail [*Anas acuta*]) nesting at the reservoir (Ohlendorf et al., 1986b; Ohlendorf, 1989). In subsequent years, similar observations were reported in embryos of killdeer (*Charadrius vociferus*) and American avocets (*Recurvirostra americana)* (Ohlendorf et al., 1986b; Ohlendorf et al., 1989). Researchers attributed the observed reproductive impairment and adult mortality to the effects of elevated concentrations of selenium in the subsurface agricultural drainwater, which supplied the reservoir (Hoffman et al., 1988; Ohlendorf, 1989; Ohlendorf and Skorupa, 1989; Ohlendorf et al., 1988; Ohlendorf et al., 1986a; Ohlendorf et al., 1986b).

Beginning in 1987, similar ecotoxicological results to those documented at Kesterson Reservoir have been reported at several subsurface agricultural evaporation ponds further south in California's Tulare Lake Basin (Moore et al., 1990; Skorupa and Ohlendorf, 1991).

BIOLOGICAL EFFECTS IN BIRDS

In birds, reproductive impairment is manifested as reduced hatchability due to increased embryo mortality, induced deformities, and/or embryo malpositioning. All of these are fatal and result in failure to hatch. Typical deformities include exencephaly, beak malformations, and reduced or absent eyes and limbs. Classic selenium deformities are generally overt, and include some or all of the aforementioned conditions concurrently. A relatively good degree of information has been generated regarding feed supplementation, tissue distributions, and toxicity due, in large part, to the observations of selenium's toxicological and teratogenic properties in poultry fed seleniferous grain.

INTERSPECIFIC VARIABILITY IN SELENIUM TOLERANCE

The US Fish and Wildlife Service has monitored breeding populations of birds throughout the San Joaquin Valley during the past 15 years. An extensive database has been generated, including observations from nest monitoring and quantitative analyses of wild bird eggs.

The results, presented in our previous annual reports, demonstrate that selenium dose-response curves for avian populations in contaminated environments vary by species. Ducks are the most sensitive in this dataset, with an EC50 (effective concentration to cause 50 % deformities) of about 30 ppm Se egg concentration (dry weight basis), compared to an EC50 for stilts of 57ppm, and for avocets of about 109ppm. (Skorupa, 1998). In addition, monitoring of western snowy plover (*Charadrius alexandrinus nivosus*), revealed no deformities despite exposures as high as 100ppm. Published laboratory studies have demonstrated that chickens (EC50 of 10ppm) are more sensitive to selenium exposure than mallards (EC50 of 30ppm), screech owls and black-crowned night herons (Heinz, 1989; Smith et al., 1988). In his Ph.D. thesis, however, Detwiler has provided data that shows greater tolerance of some chickens, and his data indicate an EC50 of 42.9ppm. The fourfold difference in tolerance of chicken strains, and a great variability between individuals may inhibit our ability to identify the factors responsible for tolerance in some avian species. The composite data from the most recent analysis of wild bird species and chickens is given in Figure 1.

CHEMICAL FORM DETERMINES TOXICITY

The chemical form of selenium determines its metabolism and toxicity. In aquatic systems, it has been shown that selenomethionine is preferentially taken up as compared to inorganic selenite and selenate (Besser et al, 1989). Smith et al (1938) observed this same pattern in lab animals. Heinz et al (1987) confirmed that dietary selenium as selenomethionine was much more readily taken up by mallard hens and passed into the egg. Selenomethionine is also the most teratogenic chemical form (Heinz et al, 1989; Heinz et al, 1987; Hoffman and Heinz, 1988; Palmer et al, 1973; Martin, 1988), and apppears to produce qualitatively different deformities than other forms. In mallards, dietary selenite generally caused edema and stunted growth, whereas selenomethionine resulted in overt, multiple malformations including micropthalmia, hydrocephaly, bill, foot, and leg deformaties

(Hoffman and Heinz, 1988). The mechanism for differences in teratogenesis of different chemical forms is as yet not understood. The detailed study of Se biochemistry in bird egg tissues, along with the understanding of the bioaccumulation of different chemical forms is a critical part of defining this relationship.

STUDY OBJECTIVES

Our working hypothesis has been that species resistant to the teratogenic effects of Se have a better ability to distinguish between methionine and selenomethionine during protein synthesis, and as a result, the embryos of resistant species incorporate less Se into proteins, and are thus protected from the teratogenic effects of Se. This year we have data to exclude this hypothesis as the major protective factor that prevents malformations in tolerant species of birds exposed to high concentrations of selenium. We now believe that the correlation of protein bound Se with toxicosis does not explain species differences in toxicological risk, but the identification of specific Se modified proteins critical for normal development may be more important than exclusion of Se from generalized protein synthesis in embryos. The speciation of Se in other organisms within the food web may also provide a better understanding of the bioaccumulation and toxicity of Se to both plants and animals.

The four-fold difference between wild species' tolerance to selenium toxicosis (that observed between duck species versus avocets) should be detectable in wild collected eggs as differences in protein bound Se in embryos. Chickens are even more sensitive, and the measurement of Se transfer from diet into eggs and incorporation of Se into chicken embryos should provide a comparison for other species.

In 2001, we began a dietary study with mallard ducks that may provide a bridge between laboratory studies with chickens and the studies of field collected eggs of wild species.

SPECIFIC EXPERIMENTAL OBJECTIVES OF THIS STUDY

1. To determine the protein-bound fraction (and specific forms) of selenium in bird eggs.
2. To determine if eggs and tissues of species exhibiting greater and lesser tolerance to selenium poisoning contain variable concentrations of specific selenium metabolites.
3. To determine whether the incorporation of Se into protein correlates with teratogenicity, and whether Se tolerant species have the ability to reduce the incorporation of Se into protein.
4. To investigate the metabolism and toxicokinetics of selenium through inferred metabolic and ecological pathways using tissues and proteins from field-collected eggs.
5. To provide laboratory confirmation of 3) and 4) by conducting similar analyses on eggs from domestic chickens fed diets comprised with natural-source Se in known doses under controlled conditions.
6. To bridge the laboratory data set and the field data by conducting a feeding trial with mallard ducks using a similar protocol as for chickens.
7. To determine if a particular form of selenium (e.g., selenomethionine) is a better measure of ecotoxic risk across species and between systems (i.e., a more universal regulatory standard than total recoverable selenium).

During the past two years we have addressed Objectives 1-3, and have completed Objective 5. We have completed the feeding trial portion of Objective 6, and are in the process of processing and analyzing the mallard duck eggs and embryos. In 2001 as part of his Ph.D. thesis, Steve Detwiler analyzed the data for wild shorebirds and chickens to critically evaluate the ability of embryos of tolerant species to detect and exclude Se from proteins as the primary explanation for tolerance to Se exposure and avoidance of embryo malformations. Detwiler's thesis clearly demonstrates that chickens have an ability to depurate Se that is nearly as efficient as the more tolerant shorebird species, and the ability to exclude Se from protein synthesis during embryogenesis is not the explanation for increased tolerance of avocets and other shorebird species.

PROGRESS

CHICKEN LABORATORY FEEDING TRIALS

A feeding trial has been conducted with domestic (white leghorn) chickens for a focused study under controlled conditions. Since no firmly established dose response data were available for selenized yeast fed to chickens, the experiment was conducted in a paired block design—where all six-treatment birds were placed on control,

followed by treatment diets. This particular experimental design allowed for the use of fewer eggs and hens through increased statistical power by removing inter-individual variability. When dietary Se was changed, hens were fed the new diet for a minimum of two weeks prior to insemination and egg collections to allow egg [Se] to normalize. Previous investigators (Arnold et. al, 1971; Latshaw and Osman, 1975) observed that egg [Se] plateaus within a period of 2 weeks or less on an amended diet. The initial dietary [Se] was 4 ppm, followed by 12 ppm. The very high toxicity of the nominal 12 ppm diet prompted us to test an intermediate diet of 8 ppm. Se. Hens were placed on control diet for approximately 2.5 weeks before beginning the final 8 ppm dietary interval.

The nominal Se levels in the diets were 0.5ppm in the reference diet, and 4, 8 and 12 ppm in the treatment diets. The actual measured concentrations of Se in the diets were 0.53, 4.87, 9.43, and 13.2 mg Se/kg diet, respectively.

Eggs were collected during each of the treatment periods, and were incubated artificially to 16 days of incubation, at which time eggs were broken out to examine embryo development, and to collect embryo, yolk sac, and albumin contents, as in the field collection experiments. All fractions were saved for Se analysis, to determine partitioning and Se uptake by embryos. Chemical analyses for total Se were contracted to the California Animal Health and Food Safety Laboratory (CAHFS) (formerly the California State Veterinary Diagnostic Laboratory) at UC Davis. Duplicate samples were analyzed in the laboratory of Teresa Fan at UCD using the microdigestion and fluorescence-based microanalysis (Fan et. al, 1997) previously used for field collected eggs to compare the variation between the two laboratories. Results of the Se analysis have not yet been compiled and reviewed.

Hen weights during the feeding trial were monitored before and after each dose administration. Dose-dependent cachexia (wasting syndrome) was observed in the study hens. Measurements of chicken embryonic masses at defined incubation period were also collected to detect dose-dependent retardation of embryogenesis (as suggested in the literature).

The feeding trial successfully produced eggs from the range of dietary exposures. At 4 ppm (4.87ppm wet weight in the diet), embryos demonstrated decreased weight relative to eggs from the reference diet, and at higher selenium levels embryo weights were very significantly reduced. (FIGURE 2) No malformations or terata were observed in embryos from the control or 4 ppm diets, but terata were increased and viability of embryos was markedly reduced for the higher selenium levels (17% at 9.43ppm, and 97% in the 13.2ppm diet). A statistically significant decrease in embryo weight at the 4 ppm dietary level is the most sensitive parameter for detecting an effect of selenium in chickens.

MALLARD DUCK FEEDING TRIAL

In early 2001 a selenium feeding trial was initiated with Mallard ducks to essentially duplicate the chicken feeding trial in an effort to determine the species differences in Se incorporation into eggs and into embryonic tissues. Because individual housing of ducks is not practical, groups of 5-6 female and two male ducks were housed together in floor pens using the same procedures as for toxicity testing conducted by the US EPA. Pens of ducks were randomly assigned to three groups: reference controls, 4 ppm. Se, and 8 ppm. Se as nominal treatments. Eggs were collected from each group prior to introduction of treatment feed as pre-treatment controls, and the groups were fed control or treatment diets for 2 months, with eggs collected on a daily basis. Eggs were collected and stored at 12°C for up to one week, and artificially incubated to 21 days of the normal 28-day incubation period, to produce embryos ¾ through the normal incubation period. This embryo age duplicates our studies with chickens and wild bird species.

148 eggs were collected from ducks in the 4 ppm diet treatment group, 95 from the 8 ppm treatment, and 103 from the pretreatment and reference diet. Eggs were weighed, broken out, and contents separated into embryo, yolk, and albumin fractions, exactly as in the chicken study. We are currently in the process of preparing the samples for Se analysis at CAHFS. Selenium partitioning results will be compared to the chicken and wild bird studies, to evaluate the ability of each species to prevent incorporation of selenium into proteins that result in terata.

DEVELOPMENT OF A MODEL TO EVALUATE SE EXCLUSION HYPOTHESIS

Data on [Se] in the embryos, albumin, and yolk were used to determine whether embryos exposed to specific concentrations of Se during development are able to prevent incorporation of the Se into tissues to prevent malformations and growth depression. The analysis of each compartment revealed important parameters to use in the subsequent model and analysis. Albumen is enriched with Se, increasingly so with dose. Albumen is synthesized in the oviduct, but it is unexplained why albumen [Se] appears increased relative to dose fed to the hen. An additional factor for Se exposure to the embryo is that yolk is initially taken up by the embryo as a source of nutrients, and albumen is only utilized later in embryogenesis. Since the embryo growth and malformations are consequences of early developmental exposure, the yolk [Se] may be more important than that from albumen. Measuring the contribution of each compartment is complicated, however, because the yolk swells during incubation, and albumen is constantly entering the yolk as nutrients are consumed. The last complicating factor in this analysis is that embryo excretion or urinary waste products are sequestered in the allantois, a membrane compartment that we were unable to separate from the albumen compartment during processing. The albumen compartment, therefore, contains both the hen synthesized albumen, as well as an increasing amount of embryonic waste products.

Detwiler developed a model to assess the changes in embryonic Se during incubation, in order to determine the ability of species to avoid Se toxicosis. The object was to model the "expected" embryo [Se] from measured variables of albumen [Se], yolk [Se], embryo [Se] and the dry masses of all compartments at the time of processing. The observed deviation from expected and observed embryo [Se] was then calculated. This parameter is termed "depuration efficiency," and represents the best available measure of a given egg's ability to discriminate and exclude eggborne Se from embryonic tissue. Analyses of covariance can be fit to the model output, and differences between species with respect to total Se partitioning compared. In essence, if embryos of one species have a greater ability to exclude Se from the embryo than other species, that species would be more able to avoid the toxic consequences of Se exposure.

The model calculations are given below:

For 13+ day old eggs:

$$DE = (Y_c * Yolk[Se]_i + A_c * Extracorp[Se]_i - EmbSe_i) * (Emb\ mass)^{-1} * (Emb\ age)^{-1}$$

For eggs <13 days old:

$$DE = ({}^aY_c * Yolk[Se]_0 + 0.267A_c * Extracorp[Se]_I - EmbSe_i) * (Emb\ mass)^{-1} * (Emb\ age)^{-1}$$

Where:

DE = *Modeled* Depuration Efficiency

E_i = g embryo tissue (d.w.)/total g whole egg contents (d.w.) (embryo stage at process)

$Y_c = |m|_y * E_i$ (yolk consumption)

$A_c = |m|_a * E_i$ (albumen consumption)

$Yolk[Se]_i$ = Measured yolk [Se] (mg/kg, d.w. basis)

$Extracorp[Se]_i$ = Measured extracorpus [Se] (mg/kg, d.w. basis)

$EmbSe_i$ = Measured embryo Se load (total ug Se in tissue)

Emb mass = Measured (dry weight) embryo mass at time of process

Emb age = embryo age (in days) at time of process

${}^aY_c$ = predicted yolk consumption in <13d egg = $Y_c + 0.733(A_c)$

$Yolk[Se]_0 = (Yolk[Se]_i * YolkMass_i - 0.733A_c * Extracorp[Se]_i) * (YolkMass_i - 0.733A_c)^{-1}$

The predicted embryo Se loading function is split into two discrete phases to reflect actual albumen transport. The expected embryo Se load in <13d embryos is calculated differently to reflect the minimal albumen consumption prior to this developmental stage.

The model was applied to measured parameters of [Se] in each compartment for 4 species of birds. The data for each of the species is given in Figures 3-6. The most robust dataset is for American Avocets, with analysis of 97 eggs; for Black-necked Stilts, 37 eggs; and for Killdeers, 39 eggs. For the analysis in chickens, only fresh eggs and eggs with 16-day embryos were available, and 44 eggs were analyzed.

The model output for each species is presented in Figure 7, which presents the outputs from the model. In all cases, model fit is fairly tight–as evidenced by the high correlation coefficients. In all but one case, statistical comparisons were not possible due to violation of the parallel slopes assumption (significant interaction terms).

In the one case where species comparisons were practical, there was a significant difference between the model outputs for the black-necked stilt and American avocet ($p = 0.0125$). Review of the model regressions indicates that the function defining the stilt depuration efficiency was actually *steeper*, and included a *higher* y-intercept. Superficially, the suggestion is that the stilt is more adept at partitioning Se away from embryonic tissues towards the albumen compartment. The species with the greatest tolerance to Se is the American avocet, which has a depuration efficiency in the model very close to that of the chickens. The greatest depuration efficiency was exhibited by Killdeer, which are the least tolerant of the shorebird species.

DISCUSSION

In important respects, the final model outputs ran counter to initial expectations. At least the derived functions do not provide easily defensible, statistically significant support for the hypothesis that tolerant species are more adept at partitioning eggborne Se away from the developing embryo.

The data indicate that sensitive species have the potential to remove significant amounts of egg-borne Se from the embryonic compartment, so this ability in itself is insufficient to explain differences between species in Se tolerance. Further, while this process seems more pronounced in the more tolerant species up to teratogenic doses, at this threshold surviving embryos in the sensitive species nevertheless express significant depuration potential. Indications are that other factors are involved allowing tolerant species to withstand higher realized [Se] *in-vivo* before expressing toxic effects.

Analysis of the mallard eggs will provide more data to evaluate the depuration model. We will continue to evaluate the data within the constraints of our analytical techniques to better understand the dynamics of the toxicity of selenium.

■ ■ ■ ■ ■

LITERATURE CITED

Besser, J.M., J.N. Huckins, E.E. Little, and T.W. La Point. 1989. Distribution and bioaccumulation of selenium in aquatic microcosms. Env. Pollut. 62:1-12.

Detwiler, S. J. toxicokinetics of Selenium in the Avian Egg: Comparisons Between Species Differing in Embryonic Tolerance. Ph. D. Thesis, University of California Davis, 2002

Heinz, G.H., D.J. Hoffman, A.J. Krynitsky, and D.M. Weller. 1987. Reproduction in mallards fed selenium. Env. Toxic. Chem. 6:423-33.

Heinz, G.H. 1989. Selenium poisoning in birds--Information from laboratory studies. USFWS Res. Inf. Bull. No. 89-98. USFWS-PWRC, Laurel MD.

Heinz, G.H., D.J. Hoffman, and L.G. Gold. 1989. Impaired reproduction of mallards fed an organic form of selenium. J. Wildl. Manage. 53(2):418-28.

Hoffman, D.J., and G.H. Heinz. 1988. Embryotoxic and teratogenic effects of selenium in the diet of mallards. J. Toxic. Env. Health. 24:477-90.

Hoffman, D.J., H.M. Ohlendorf, and T.W. Aldrich. 1988. Selenium teratogenesis in natural populations of aquatic birds in Central California. Arch. Env. Cont. Toxic. 17:519-25.

Martin, P.F. 1988. The toxic and teratogenic effects of selenium and boron on avian reproduction. Master of Science thesis. U.C. Davis. Davis, CA.

Moore, S.B., J. Winckel, S.J. Detwiler, S.A. Klasing, P.A. Gaul, N.R. Kanim, B.E. Kesser, A.B. DeBevec, K. Beardsley, and L.K. Puckett. Fish and Wildlife Resources and Agricultural Drainage in the San Joaquin Valley, California. Sects. 3-4, San Joaquin Valley Drainage Program, Sacramento CA.

Ogle, R.S., K.J. Maier, P. Kiffney, M.J. Williams, A. Brasher, L.A. Melton, and A.W. Knight. 1988. Bioaccumulation of selenium in aquatic ecosystems. Lake Reserv. Manage. 4(2):165-73.

Ohlendorf, H.M., D.J. Hoffman, M.K. Saiki, and T.W. Aldrich. 1986a. Embryonic mortality and abnormalities of aquatic birds: Apparent impacts of selenium from irrigation drainwater. Sci. Tot. Env. 52:49-63.

Ohlendorf, H.M., R.L. Hothem, C.M. Bunck, T.W. Aldrich, and J.F. Moore. 1986b. Relationships between selenium concentrations and avian reproduction. Trans. N. Am. Wildl. Nat. Res. Conf. 51:330-42.

Ohlendorf, H.M., A.W. Kilness, J.L. Simmons, R.K. Stroud, D.J. Hoffman, and J.F. Moore. 1988. Selenium toxicosis in wild aquatic birds. J. Tox. Env. Health 24:67-92.

Ohlendorf, H.M. 1989. Bioaccumulation and effects of selenium in wildlife. Pages 133-177 *in* Selenium in Agriculture and the Environment (L.W. Jacobs, Ed.). Am. Soc. Agr. Soil Sci. Soc. Am. Publication 23, Madison WI.

Ohlendorf, H.M., and J.P. Skorupa. 1989. Selenium in relation to wildlife and agricultural drainage water. Pages 314-338 *in* Proceedings of the Fourth International Symposium on Uses of Selenium and Tellurium. May 7-10, 1989, Banff, Alberta (S.C. Carapella, Jr., Ed.). Selenium-Tellurium Development Association, Inc., Darien CT.

Palmer, I.S., R.L. Arnold, and C.W. Carlson. 1973. Toxicity of various selenium derivatives to chick embryos. Poult. Sci. 52:1841-46.

Presser, T.S. 1994. The Kesterson effect. Env. Manage. 18(3):437-54.

Rosenfeld, I., and O.A. Beath. 1964. Selenium: geobotany, biochemistry, toxicity, and nutrition. Academic Press, New York NY.

Skorupa J.P. 1998. Selenium poisoning of fish and wildlife in nature: lessons from twelve real-world examples *In* Environmental Chemistry of Selenium (W.T. Frankenberger and R.A. Engberg, Eds.). Marcel Dekker, Inc. New York NY.

Skorupa J.P., and H.M. Ohlendorf. 1991. Contaminants in water and avian risk thresholds. Pages 345-368 *in* The Economics and management of Water and Drainage in Agriculture (A. Dinar and D. Zilberman, Eds.). Kluwer Academic Publishers, New York, NY.

Smith, M.I., B.B. Westfall, and E.F, Stohlman. 1938. Studies on the fate of selenium in the organism. U.S. Publ. Health Rept. 53:1199-1216.

Smith G.J., G.H. Heinz, D.J. Hoffman, J.W. Spann, and A.J. Krynitsky. 1988. Reproduction in black-crowned night herons fed selenium. Lake Reserv. Manage. 4:175-80.

Spallholz, J. E. 1994. On the nature of selenium toxicity and carcinostatic activity. Free Rad. Biol. Med. 17(1):45-64.

■ ■ ■ ■ ■

Figure 1: Dose Response Curves in Three Wild Species and Domestic Chickens

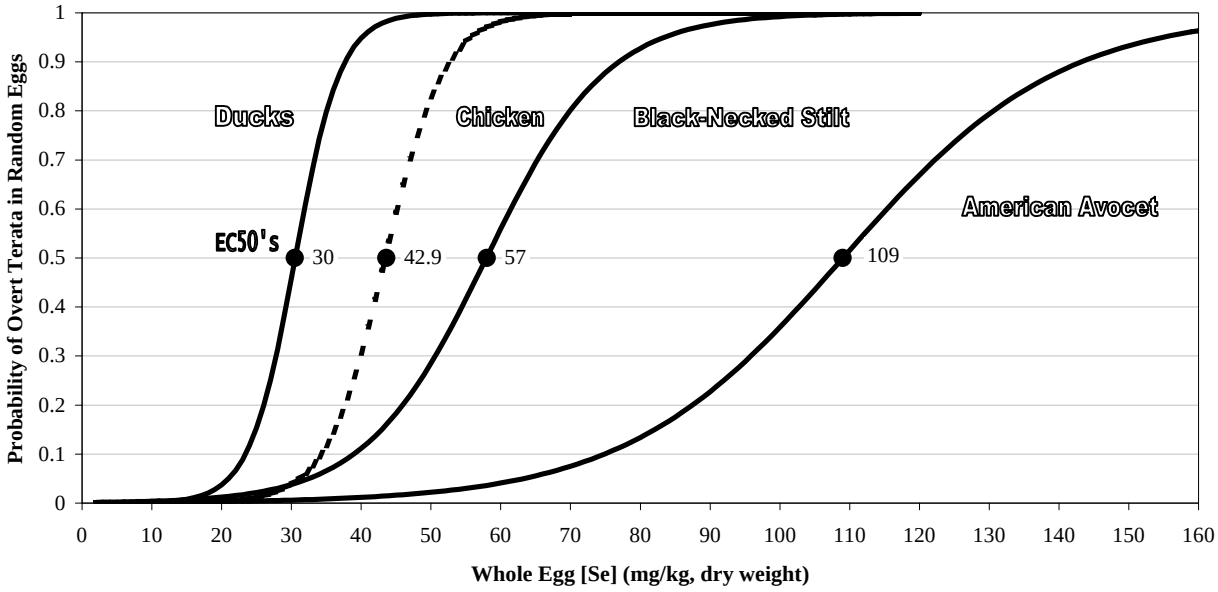

Figure 2: Embryo Mass as a Function of Whole Egg Selenium

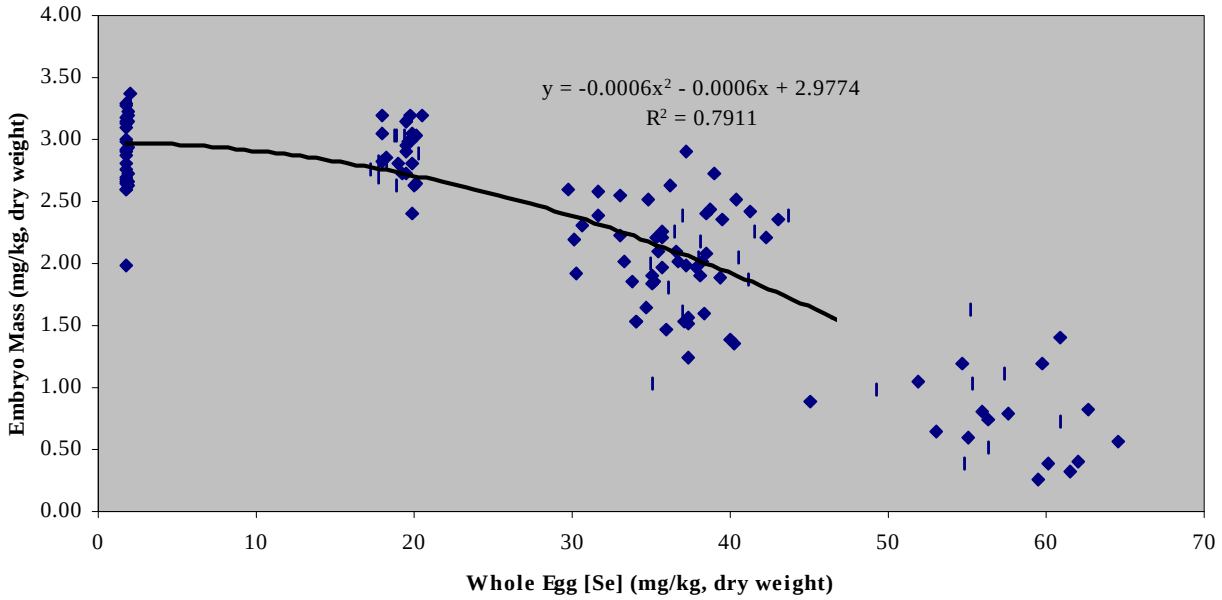

Figure 3: Avocet Dry Mass Tissue Consumption by Embryo Stage

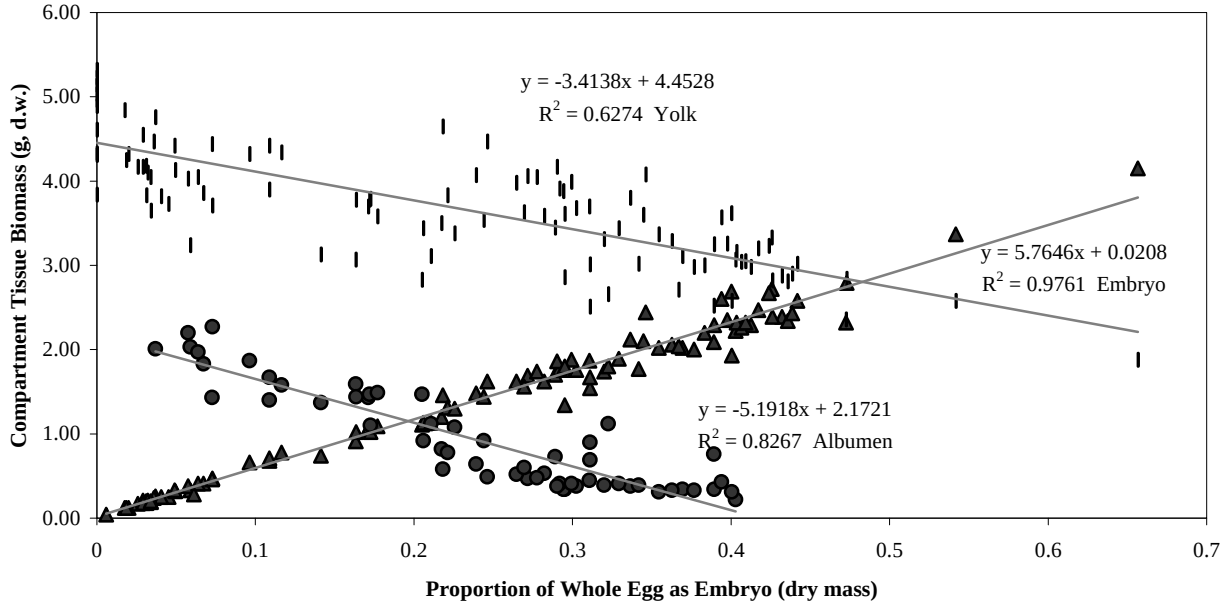

Figure 4: Stilt Dry Mass Tissue Consumption by Embryo Stage

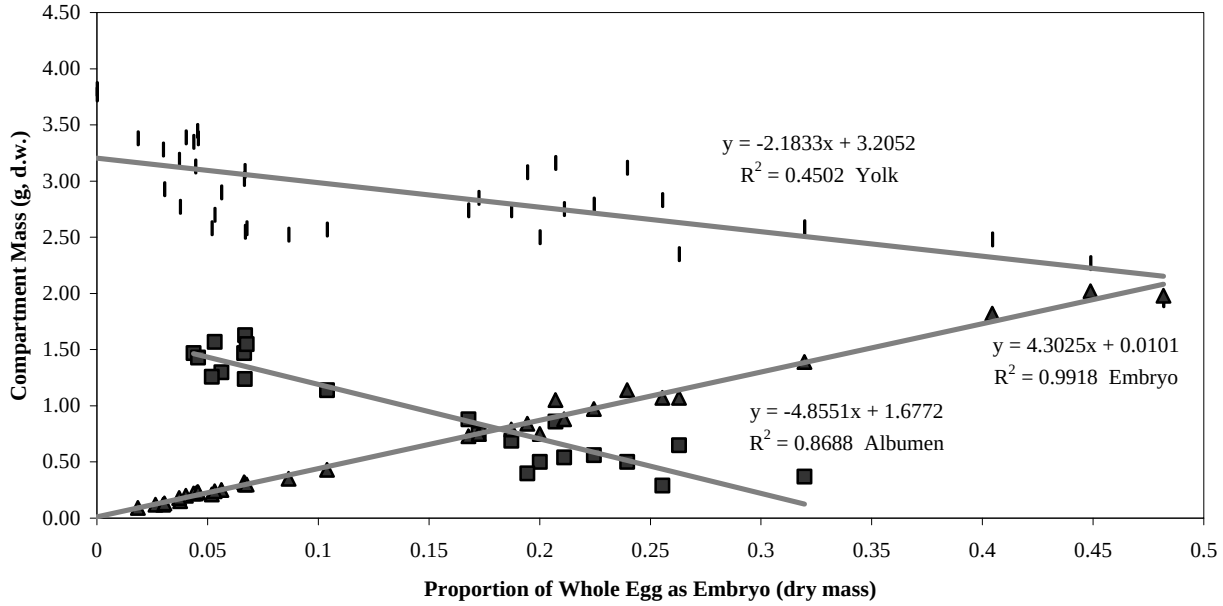

Figure 5: Killdeer Dry Mass Tissue Consumption by Embryo Stage

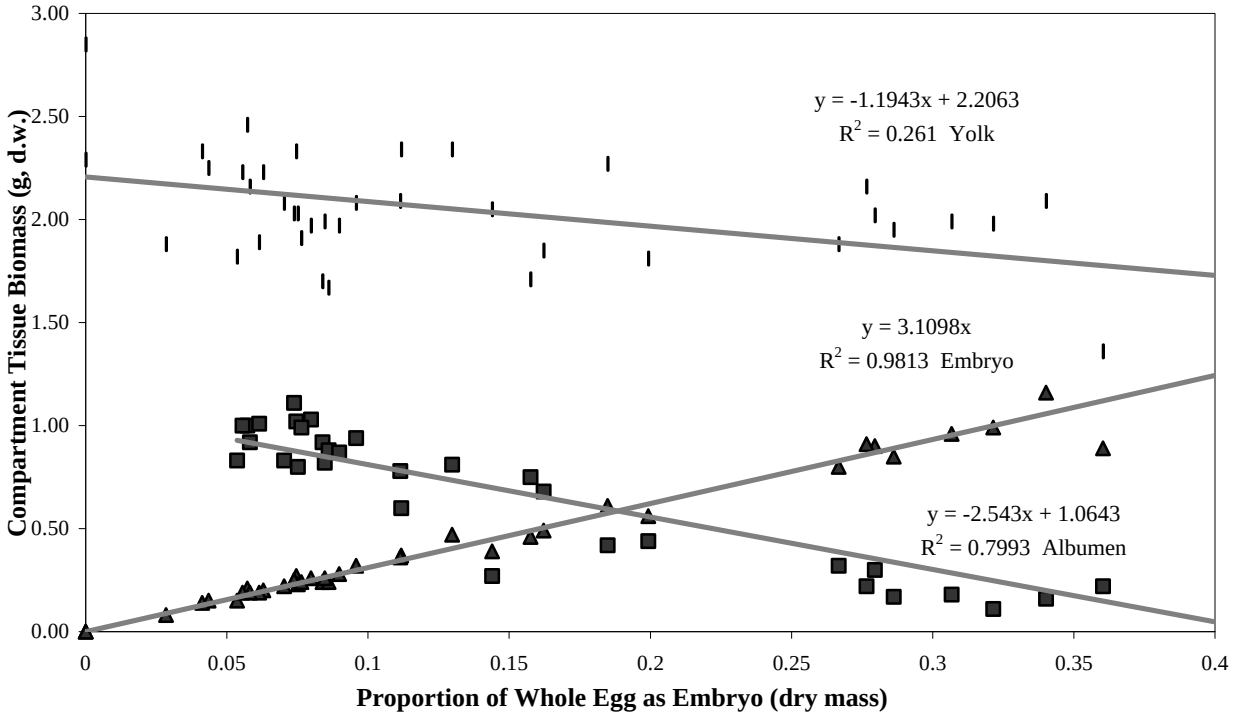

Figure 6: Mean Egg Mass by Compartment Versus Incubation Stage in Chickens (Control Treatment)

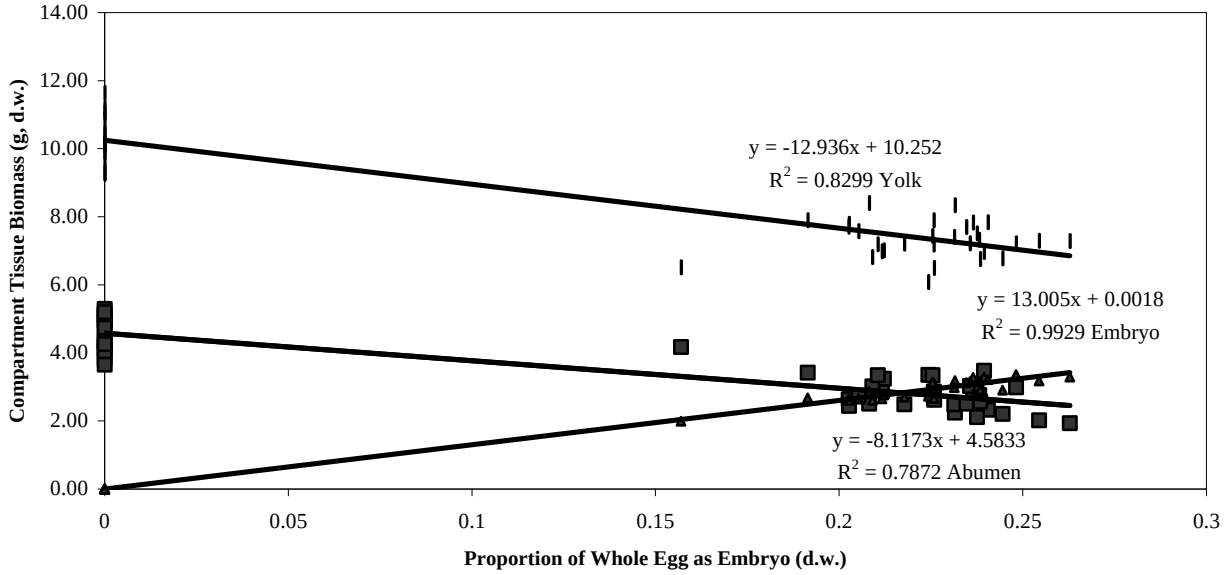

Figure 7: Calculated Depuration Efficiency in Embryos

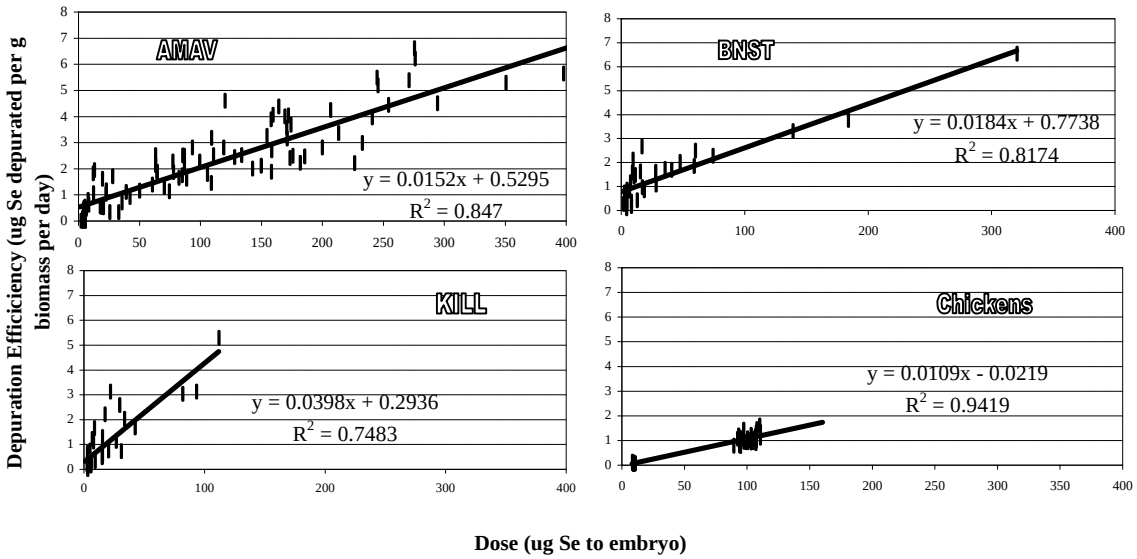

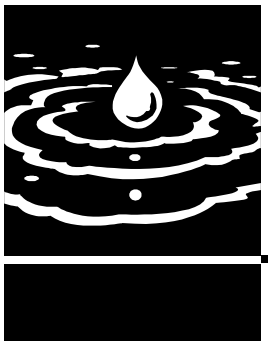

Using EM and VERIS Technology to Assess Land Suitability for Orchard and Vineyard Development in Non-saline Environments–Interim Report

Project Investigators:

Allan Fulton
Office: (530) 527-3101, E-mail: aefulton@ucdavis.edu
UC Cooperative Extension
Tehama County

Larry Schwankl
Office: (530) 752-1130, E-mail: ljschwankl@ucdavis.edu
Department of Land, Air, and Water Resources
University of California, Davis

Terry Prichard
Office: (209) 462-2085, E-mail: tlprichard@ucdavis.edu
Department of Land, Air, and Water Resources
University of California, Davis

Bruce Lampinen
Office: (530) 752-2588, E-mail: bdlampinen@ucdavis.edu
Department of Pomology
University of California, Davis

Research Staff:

Dan Rivers, SRA, Dept. of LAWR, UC Davis, 0.15 FTE
Kris Lynn. Kearney Agricultural Center, 0.05 FTE

ABSTRACT

Preplant orchard or vineyard development is expensive. Producers can easily invest $200 to $500 per acre for deep tillage such as slip plowing, moldboard plowing, or excavating planting sites with a backhoe. Orchard and vineyard producers generally give serious consideration to preplant site evaluations, land preparation, and irrigation system choices to avoid planting permanent tree and vine crops into soil conditions that cannot be managed and where the crop will not perform to its highest level or attain its full life expectancy.

Because of this risk and expense producers are interested in Electromagnetic Induction (EM 38) and Four-probe soil resistance sensors (VERIS) that can be used in combination with global positioning systems (GPS) to map spatial variability of in-situ soil electrical conductivity (ECa). The hypothesis under evaluation in this study is that rapid, continuous, low cost methods of measuring ECa (EM 38 and VERIS) can effectively identify and map soil variability in non-saline environments. The supposition is that ECa levels will relate well to soil texture and water holding capacity and can be used to guide preplant tillage decisions, irrigation system choices and water management strategies, and other orchard or vineyard design considerations.

Three orchard sites in the Sacramento Valley have been mapped each with EM 38 and VERIS methods. Soil samples have been collected from each site to ground truth the ECa maps. Results are pending completion of laboratory and statistical analyses. In general, the ECa maps appear to identify more soil variability than soils maps from published soil surveys. If results from the soil sampling and laboratory analysis of soil properties verify the in-situ measurements of ECa, EM 38 and VERIS technologies may offer improved information at reasonable cost (about $10/acre) to guide orchard or vineyard development decisions.

KEYWORDS

Electrical Conductivity, Electromagnetic Induction, EM 38, Land Suitability, Orchards, Soil Mapping, Soil Resistance, Spatial Soil Variability, Soil Texture, VERIS, Vineyards

■ ■ ■ ■ ■

BACKGROUND

Use of rapid, in-situ measurement of electrical conductivity (ECa) combined with use of global positioning systems (GPS) and geographical information systems (GIS) to map soil variability may improve land suitability assessments before establishing permanent orchards or vineyards. More precise soils information may improve decisions concerning appropriate deep tillage and influence the choice of irrigation system design and approach to water management. Improved soils information may also influence orchard or vineyard design choices such as rootstock and planting density. Water and soil resources may be utilized more productively and efficiently, by minimizing chronic orchard problems associated with unsuitable soil conditions and declining root health.

In-situ measurement of electrical conductivity (ECa) can be measured with electromagnetic induction (EM 38). An EM 38 instrument consists of two electronic coils, a primary and secondary coil, inside a plastic casing. When energized, the primary coil radiates an electromagnetic (EM) field into the soil and creates a secondary field. The strength of the secondary EM field is measured by the secondary coil and is an indicator of the electrical conductivity of the soil. The higher the secondary EM-field the higher the electrical conductivity of the soil. In commercial applications of high frequency EM 38 measurement used in combination with GPS, two instruments are used together to detect bulk electrical conductivity within two soil zones, one placed in horizontal mode (shallow, 0 to 1 foot) and one in vertical mode (deep, 0 to 3 feet). In one commercial application of EM 38, both instruments are placed inside a protective, PVC housing and towed along the soil surface using an all terrain vehicle (ATV). Global positioning equipment is also used. Refer to photos 1 and 2 for illustrations.

As an alternative to the EM 38, bulk, in-situ electrical conductivity (ECa) of soil can be determined by directly measuring the soil resistance with a VERIS implement. Like the EM 38, the VERIS implement can be use in combination with GPS and GIS. The VERIS implement is patterned after earlier four-probe devices. It consists of pairs of coulters mounted to a tool bar

for towing. One pair of coulter electrodes penetrates a few inches of the soil surface and injects an electrical current. Another pair of coulters penetrates the soil and receives the electrical signal. The measure of voltage drop due to the resistance of the soil is measured. A lower level of resistance indicates a higher level of soil electrical conductivity. Distance between pairs of coulters determines depth of measurement. Commercial applications of VERIS typically consist of four pairs of coulters, two pair more closely spaced measure the bulk ECa in a shallow soil zone (0 to 1 foot) and two pair more widely spaced measure the bulk ECa in a deeper soil zone (0 to 3 feet). Refer to photo 3 for an illustration.

Research has shown that ECa measurements determined with either EM 38 or VERIS technologies can be highly correlated with conventional measurements of ECe (electrical conductivity of the saturated soil extract), especially when calibrated for different soil textures. Other research has demonstrated that ECa measurements can be used to accurately detect temporal changes in soil water content, especially, when calibrated for salinity. Today, commercial services are adapting EM 38 and VERIS technologies to a third application by providing a one-time, rapid, reasonable cost ($10/acre) assessment of spatial soil conditions under non-saline conditions. The hypothesis is, that in non-saline soils, in-situ measurements of EC (ECa) will correlate well with soil-water content and accurately indicate differences in soil texture and soil water holding capacity.

OBJECTIVES

Orchard and vineyard producers are interested in soil mapping with EM 38 and VERIS techniques if they lead to improved orchard or vineyard preparation decisions but they are unsure of the accuracy of the information and how it should be incorporated into their decision-making.

Our goal is to address a number of questions related to these orchard and vineyard assessment services.

1. Are EM and VERIS methods effective in identifying important differences in physical soil properties in non-saline environments and/or is there an advantage of one technology over the other?
2. Does equipment operation, calibration, methods of data interpolation, and interpretation affect success and usefulness?
3. Can orchard production and decline in tree health in an existing orchard be correlated with adverse physical soil properties identified with these technologies?
4. Can improved knowledge of spatial soil variability before establishment of a permanent crop lead to practical solutions? Can the assessment results suggest ways to retrofit an existing irrigation system in an established orchard to more appropriately manage areas where trees are in declining health?

Project objectives are:

1. Survey field-wide soil variability in three non-saline, orchard sites with both EM and VERIS techniques. A commercially operated provider of EM 38 services and another provider of VERIS services will conduct independent surveys and soil mapping.
2. Confirm the commercial results with third-party (UC personnel) soil sampling and laboratory analysis for selected physical and chemical soil properties (both spatially and with vertical depth).
3. Assess whether seven years of almond production data from an orchard with areas of declining tree health can be associated with adverse physical or chemical soil properties detected with EM and VERIS techniques.

METHODS

STUDY SITES

Three locations in the Sacramento Valley have been involved in this project. Site #1, "Cottonwood" is a 57-acre parcel of undeveloped land designated for walnut establishment in 2003. The entire parcel is mapped as the Maywood loam soil series in the 1967 Tehama County Soil Survey. It is located east of Cottonwood, CA (15 miles north of Red Bluff, CA). Site #2, "Evergreen" is a 20 acre undeveloped parcel located west of Cottonwood, CA (15 miles north of Red Bluff, CA). The Tehama County Soil Survey describes this parcel of land as two soil series, Perkins gravelly loam and Arbuckle gravelly loam. Site #3 is a 22 acre established almond orchard located at the Nickel's Soils Lab about 4 miles southwest of Arbuckle, CA. This site was an experimental

orchard with seven years of intensive yield measurement. In this report, it is referred to as "Nickels". According to the Colusa County soil survey, three predominant soil series are evident at this site: 1) the Arbuckle gravelly loam; 2) Arbuckle gravelly loam over clay stratum; and 3) the Kimball series, a shallow alluvial layer, over an old clay deposit.

The Cottonwood site had been planted to sudangrass the previous season, so the soils had been tilled in the fall prior to soil mapping. The Evergreen site had been in permanent pasture with no recent history of tillage. Likewise, the Nickels site was planted to almonds, irrigated with microirrigation, and had no recent history of tillage.

The primary rainfall season is from November through March at these sites. Average annual rainfall ranged from 14 inches at the Nickels site to 22 inches at the Cottonwood and Evergreen sites.

EM AND VERIS MEASUREMENTS

Two independent, commercial operators, one EM practitioner and a VERIS user, surveyed each of the sites. They developed maps of the ECa patterns and defined zones with different spatial and vertical soil patterns for each site. The operation of the EM and VERIS equipment was performed mid to late winter (February) after significant cumulative rainfall to assure as uniform of soil moisture as possible to at least a depth of three feet. Each EM or VERIS survey was performed within 5 to 10 days after recent and significant rains to assure soil-water contents near field capacity, and to enable passage of the equipment. It was not possible to arrange EM and VERIS measurements on the same day at each site. In general, the EM and VERIS measurements were taken with 7 to 10 days of each other at each study site. Winter EM 38 and VERIS measurements were preferred to summer or fall measurements to avoid collecting data that was confounded by spatially variable degrees of soil water depletion. This requirement delayed initiation of the project well into the funding year. Each site was mapped by pulling the EM or VERIS equipment in a serpentine pattern across the entire site and taking continuous measurements in transects spaced 60 feet apart (Figure 3 (VERIS) illustrates this travel pattern). Development of the ECa maps required converting the measures of the electromagnetic field (EM 38) or soil resistance (VERIS) to electrical conductivity and required Interpolation of data between the measured transects. Each provider used proprietary calibration and interpolation methods to designate different soil zones.

Each commercial service provided a final report for each site and recommendations of locations for soil sampling. The reports were representative of what would be provided to agricultural customers.

SOIL CORE AND BACKHOE SITE SAMPLING:

Following the EM and VERIS operations, UC personnel used the EM and VERIS results to develop a soil-sampling grid to confirm the findings of these in-situ soil-mapping techniques. At the Cottonwood site 57 backhoe sites were dug for observation and to collect soil samples. This sampling represented an average of about 1 backhoe pit per acre. The locations of the backhoe pits were selected based upon the soil zones defined by the EM and VERIS mapping. Refer to Figure 1 for illustration. Maps of the shallow (0 to 1 foot) ECa soil zones were superimposed over the maps of the deep (0 to 3 feet) soil zones to assist with positioning the backhoe sites. One or more backhoe sites, depending upon the area within a soil zone, were located within a defined zone where both the shallow and deep measurements of ECa were consistent. Some backhoe sites were purposely located in areas where the shallow and deep ECa measurements were different. The supposition was that these areas represented transitions zones from one soil zone to another.

Backhoe locations were geo-referenced using satellite differential global positioning equipment with accuracy within 10 feet. Since the EM and VERIS operators provided ECa results for the 0 to 1 foot soil depth and for the 0 to 3 foot depth, soil samples were collected in one-foot increments to a depth of three feet. In total, 171 soil samples were collected at this site for laboratory analysis.

At the Evergreen site, soil samples were collected with a hand auger from 23 auger holes, again averaging about 1 sample point per acre. Similarly to the Cottonwood site, the auger hole locations were selected based upon the soil zones defined by the shallow and deep ECa maps. Soil samples were collected in one-foot increments to a depth of three feet. The auger hole locations were geo-referenced using satellite differential GPS equipment with accuracy within 10 feet.

At the Nickels site, soil samples were collected with a hand auger from 72 auger holes. Like the other sites, soil samples were collected in one-foot increments to a depth of three feet. In total, 216 soil samples were collected. Locations of the auger holes were also geo-referenced using the same GPS equipment.

Locations of the auger holes were determined largely by the existing randomized experimental plot design so that soil samples were collected to correspond with each plot of Non Pareil almond variety with a known production history. The 72 auger holes represent more intensive soil sampling than the other two sites, averaging about one auger hole per 0.3 acres. The more intense sampling assured a soil sample from each plot with yield history and adequate samples from within each soil zone as defined by the ECa mapping.

SOIL SAMPLE PREPARATION AND LAB ANALYSIS:

After the field collection of soil samples was completed, the soil samples were oven dried for 48 hours at 105 degrees Celsius and total sample weight was recorded. Samples were manually ground, the gravel fraction was sieved, weighed, and recorded. The remaining sample was collected and analyzed at the Division of Agriculture and Natural Resources Analytical Laboratory at University of California, Davis. Percent sand, silt, and clay using the hydrometer method, pH of the saturated paste, Ece of the saturated paste extract, and the saturation percentage of the saturated paste were or are in the process of being determined for each soil sample.

DATA ANALYSIS

The laboratory analytical results of selected physical and chemical soil properties have been completed for the Cottonwood and Evergreen sites. Results are pending for the Nickels site. Data analysis is just underway. A discussion of analytical methods will be presented in a final report when all results are available for presentation.

PRELIMINARY RESULTS AND DISCUSSION

Since the initiation of the project was delayed until mid winter to achieve the desired field conditions for operating the EM 38 and VERIS equipment, only preliminary results comparing the ECa maps from EM 38 and VERIS technique are presented in this report.

Figures 2 through 4 displays the ECa maps based upon the EM 38 and VERIS measurements taken from 0 to 3 feet for the Cottonwood, Evergreen, and Nickels site, respectively. Visually comparing the spatial pattern of the ECa maps is difficult especially since each map has not yet been ground-truth to any physical or chemical soil properties and they each have different scales and map colors defined for the legend. Presentation of these maps in black and white rather than in color also complicates the discussion as well. More discussion will be provided in the final report when the ground-truth and analysis of data has been completed. In general, the VERIS maps tend to indicate more explicit soil zones and a more refined break down of the ECa patterns.

At the Cottonwood site, Figure 2 shows some commonalities in ECa patterns are apparent between the maps. Both maps denote a zone of low ECa levels in the north central and west central portion of the field, indicated by the black pixels on the EM 38 map and the white or light gray pixels on the VERIS map. The spatial pattern of this low ECa zone appears different in size and shape between these two maps. The VERIS map does illustrate another low ECa zone located in the eastern one-third of the field, whereas, the EM 38 does not as definitively. Both maps show the predominantly, widespread ECa values to be mid range levels as indicated by the white or light gray pixels on the EM 38 map and the medium gray pixels on the VERIS map. The VERIS map designates a significant area of high ECa zone on the eastern edge of the field (indicated by the dark gray or black pixels), whereas, the EM 38 shows this zone to be much smaller (also denoted by the dark gray pixels along the very east edge). Possibly the most the significant commonality among these two maps is that they each denotes three different ECa zones and corresponding zones of different soils in the parcel, whereas, the 1967 Tehama County soil survey have described this field as one soil series, the Maywood loam soil series.

Figure 3 displays the spatial ECa zones for the Evergreen site based upon the EM 38 and VERIS measurements. Both maps suggest significant spatial soil variability at this site, whereas, this parcel of land has been mapped in the 1967 Tehama County Soil Survey as two soil series. The soil survey maps the northern two-thirds of this parcel as the Perkins gravelly loam series and the

southern one-third as the Arbuckle gravelly loam series. The spatial ECa patterns mapped with EM 38 and VERIS clearly meander in random patterns across both soil series. Due to the black and white presentation of the EM 38 and VERIS maps in Figure 3 of this report, it is difficult to discuss the two maps in much detail or with much accuracy. With the exception of the dark and medium gray in northeast corner of the EM 38 map, most of the dark gray and medium gray pixels in the EM 38 map represent low ECa values (less than 5.2 ms/m^2). In general, these low ECa levels in the EM 38 map correspond to low ECa levels represented by the white pixels (denoted by the zone #4, #5, and #6) on the VERIS map. The dark and medium gray shaded regions in the northeast corner of the EM 38 map represent a zone of high ECa levels (12 to 13.5 ms/m^2). This zone of high ECa levels partially corresponds with zone of dark gray pixels designated in the VERIS map has high ECa zones.

Figure 4 illustrates the ECa maps based on EM 38 and VERIS measurements at the Nickels site. Both the EM 38 and VERIS suggest at least two, possibly three distinctly different soil zones which agrees with detailed soils mapping described by Harradine in 1948 and Andreu et. al. in 1997. Both the EM 38 and VERIS mapped a high ECa zone in the southeast corner of the orchard, as indicated by the gray and medium gray shaded zones (48 to 89 ms/m^2 – EM 38 and 18.8 to 70.9 ms/m^2 – VERIS). Both maps indicate a predominant and widespread low ECa zone in the orchard that transcends from the northeast corner of the orchard towards the southeast corner of the orchard (the very dark gray or black pixels located in the center of the EM 38 map represent low ECa level of 12 to 24 ms/m^2). One notable difference existed in the mapping. The VERIS map suggests a sizeable area of medium levels in the northwest corner of the orchard, whereas, the EM 38 map does not identify this zone nearly to the extent of that indicated by the VERIS.

CONCLUSIONS

No firm conclusions can be made at this point in the study pending analysis of the soils data. Generally, it has been observed that ECa mapping with both the EM 38 and VERIS suggest more spatial soil variability than indicated by soil survey maps and could possibly provide improved information to producers for orchard planning. Differences in the spatial patterns of ECa zones were evident in the maps developed from the EM 38 and VERIS measurements taken at each site but their importance and significance is unknown at this time.

■ ■ ■ ■ ■

REFERENCES CITED

Andreu, L., J.W. Hopmans, and L.J. Schwankl. Spatial and temporal distribution of soil water balance for a drip irrigated almond tree–The soils on the Nickels property. Agricultural Water Management. 35 (1997) 123-146

Canon, M.E., R.C. McKenzie, and G. Lachapelle. Soil salinity mapping with electromagnetic induction and satellite-based navigation methods. March 1994. Canadian Journal of Soil Science. pp. 335 – 343.

Carter, Lyle M., J.D. Rhoades and J. H. Chesson. Mechanization of soil salinity assessment for mapping. December 1993. Paper presented at Water Meeting of American Society of Agricultural Engineering, Chicago, IL.

Hanson, Blaine, Douglas Peters, and Steve Orloff. Effectiveness of tensiometers and electrical resistance sensors varies with conditions. May-June 2000. California Agriculture. Vol. 54. No. 3. pp. 47-50.

Harradine, F.F. Soils of Colusa County California. 1948. University of California, College of Agriculture, Agricultural Experiment Station, Berkeley 4, California.

McNeill, J. Duncan. Rapid Accurate Mapping of Soil Salinity by Electromagenetic Ground Conductivity Meters. Advances of measurement in soil physical properties: Bringing theory into practice. 1992. Special Publication no. 30. Soil Science Society of America.

Rhoades, J. D. 1994. Soil salinity assessment: Recent advances and findings. July 1994. Proceedings: ISSS Sub-commission Salt-Affected Soils Conference. Acapulco, Mexico.Sheets, Keith R and Jan M. Hendrickx. Noninvasive soil water content measurement using electromagnetic induction. October 1995. Water Resources Research. Vol. 31. No. 10. pp. 2401-2409.

Soil Survey, Tehama County California. May 1967. United States Department of Agriculture Soil Conservation Service and Forest Service, University of California Agricultural Experiment Station.

PUBLICATION AND REPORTS

None at this time.

Photo 1. Two EM 38 units. One unit is laying horizontal to the soil surface to measure ECa of the shallow soil (0 to 1 foot). The second unit oriented vertically to the soil surface to measure bulk ECa to a soil depth of 3 feet.

Photo 2. The two EM 38 devices as shown in photo 1 have been placed inside a PVC housing and are towed along the soil surface behind an ATV. The global positioning system (GPS) receiver is housed in the box at the front of the ATV along with a palm computer to log the continuous EM 38 measurements. The GPS antenna is visible at the back of the ATV.

Photo 3. A VERIS implement is being towed behind a pickup. Two pair of coulters are visible near the center of the toolbar. These coulters measure the ECa of the shallow (0 to 1 foot) soil. Two more pairs of coulters are located outside the wheels. These coulters measure the bulk ECa of the soil 0 to 3 feet deep. The GPS antenna is visible on the pickup cab. A GPS receiver is located inside the cab along with a palm or lap top computer to log the continuous ECa data.

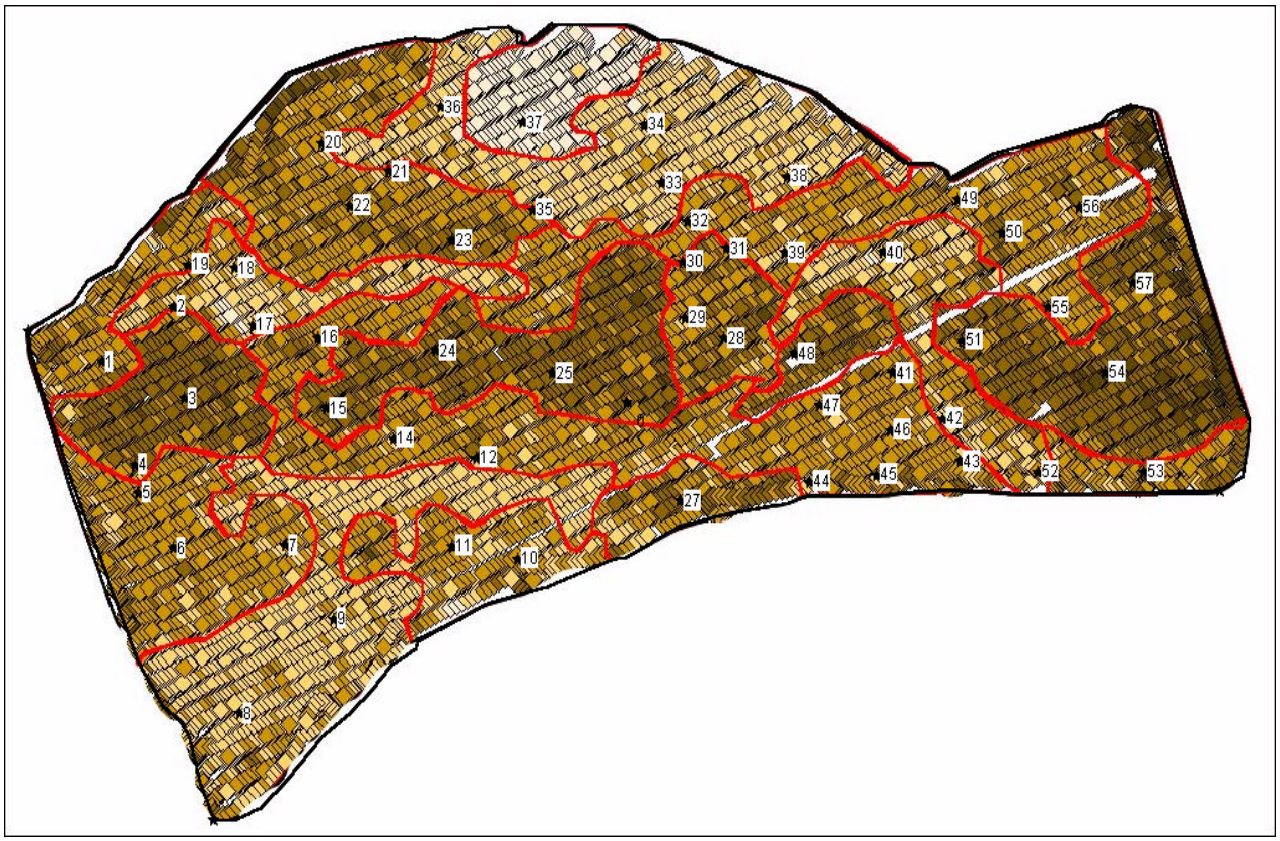

Figure 1. The map above illustrates the soil sampling methodology used at the Cottonwood site. The numeric markers designate the location of each backhoe site. Some backhoe sites were located in the center of prescribed soil zones based upon the VERIS and EM mapping. Other backhoe sites were located near or on the boundaries between prescribed zones to evaluate transitions from one zone to another. Each backhoe site was geo-referenced.

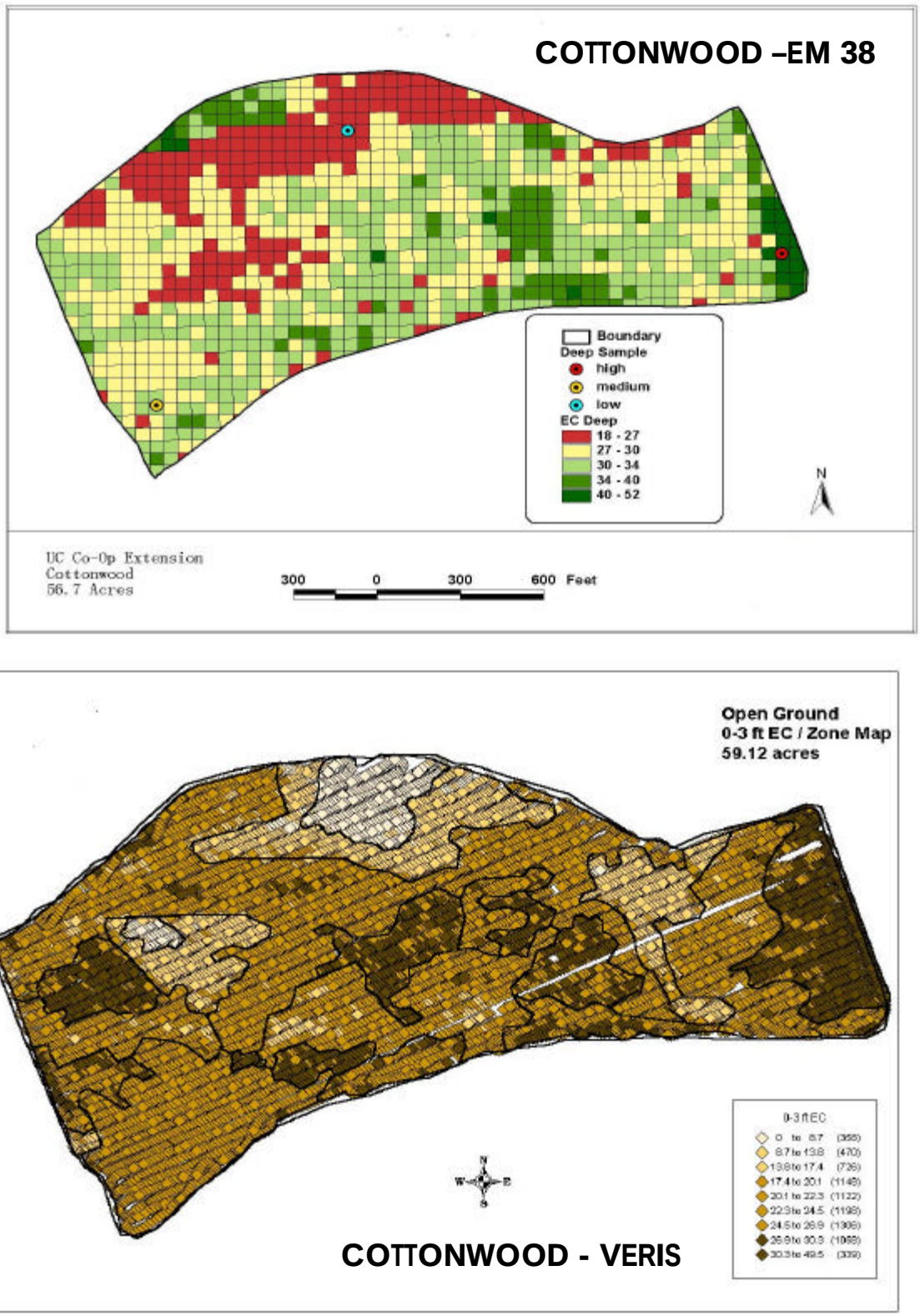

Figure 2. Illustration of the spatial ECa maps developed using EM 38 (top) and VERIS (bottom) methods at the Cottonwood site.

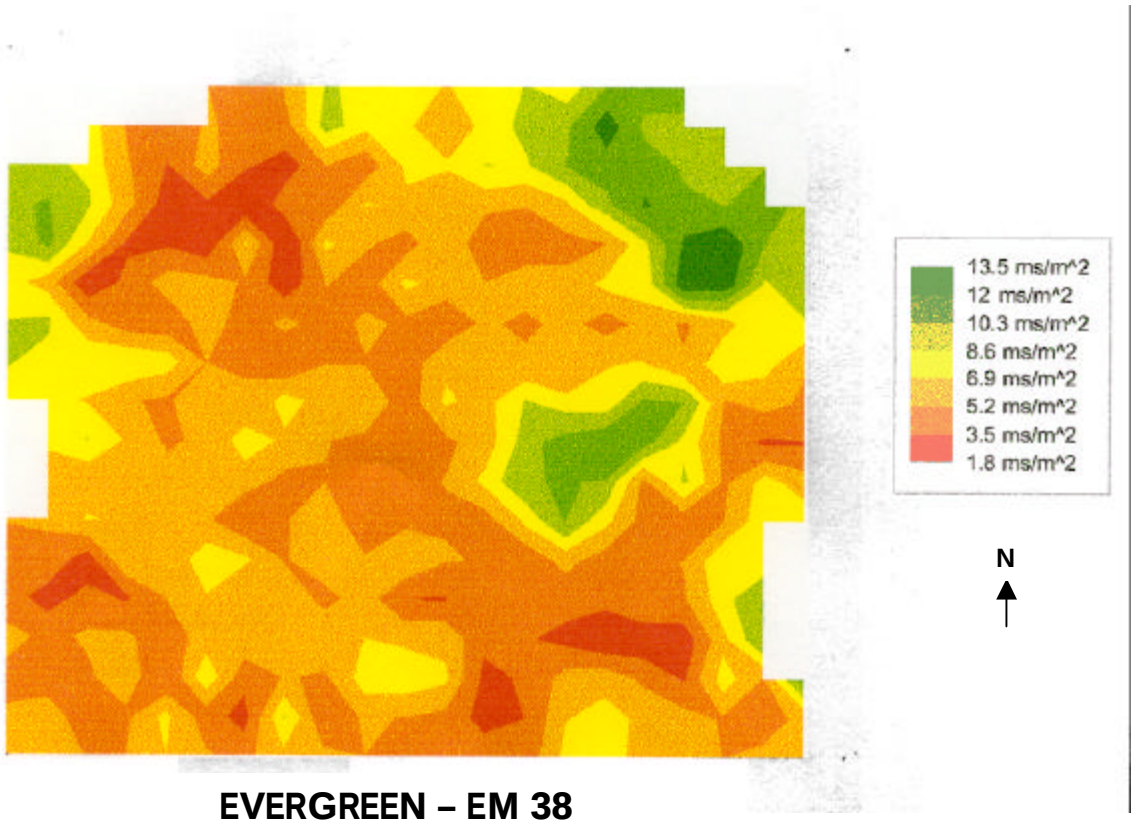

Figure 3. Illustration of the spatial ECa maps developed using EM 38 (top) and VERIS (bottom) methods at the Evergreen site. The VERIS map also illustrates the serpentine travel pattern used when operating the EM 38 or VERIS equipment.

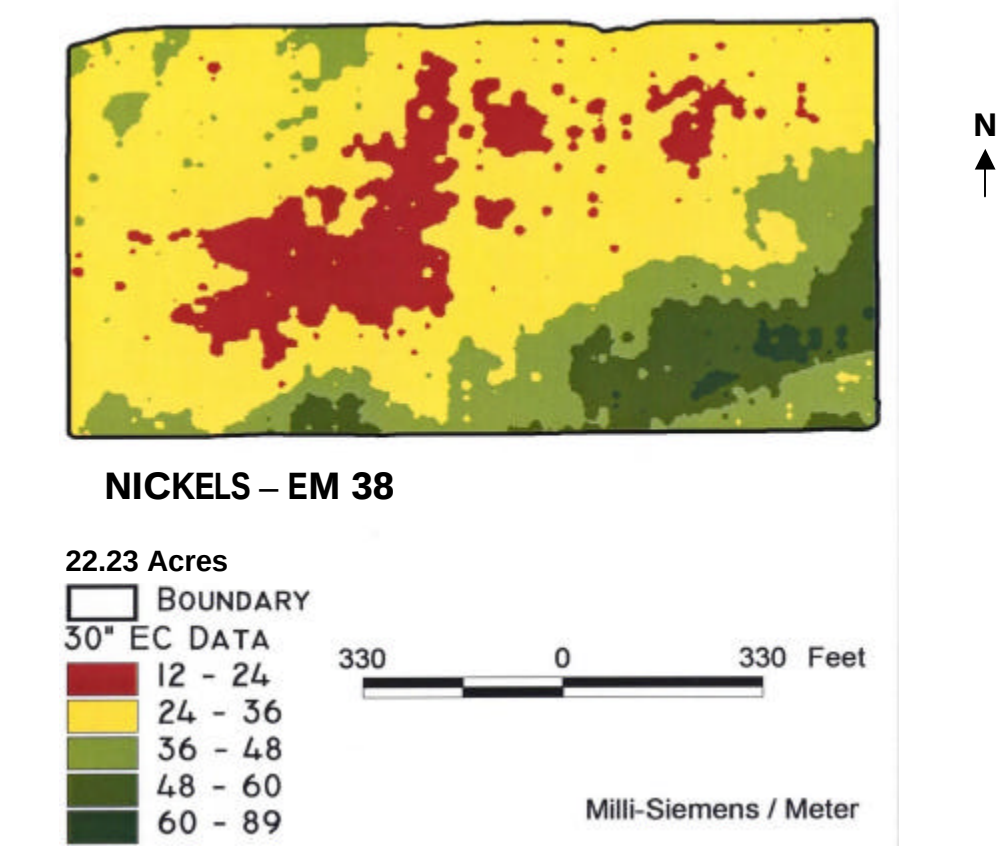

Figure 4. Illustration of the spatial ECa maps developed using EM 38 (top) and VERIS (bottom) methods at the Arbuckle site.

Management Effects on Selenium Fractionation, Speciation and Bioavailability in Sediments from Evaporation Basins

Project Investigators:

Suduan Gao
Office: (530) 752-5105, E-mail: sugao@ucdavis.edu
Dept. of Land, Air & Water Resources
University of California Davis

Randy A. Dahlgren
Office: (530) 752-2814, E-mail: radahlgren@ucdavis.edu
Dept. of Land, Air & Water Resources
University of California Davis

Research Staff:

1 Assistant Researcher: 40%
1 lab assistant (10%)

Coordinating Project Investigators:

Richard M. Higashi, and Robert G. Flocchini
Crocker Nuclear Laboratory, University of California, Davis

Teresa W-M. Fan
Dept. of Land, Air & Water Resources, University of California, Davis

Eliska Rejmankova
Dept. Environmental Science & Policy, University of California, Davis

ABSTRACT

Research was initiated to improve our understanding of selenium fractionation, speciation and bioavailability within the Joint Research Project "Mitigating Selenium Ecotoxic Risk by Combining Foodchain Breakage with Natural Remediation." The joint research project involves a team of multidisciplinary investigators and cooperators joining forces to conduct a comprehensive investigation of Se biogeochemistry and ecotoxicity associated with disposal of agricultural drainage waters in evaporation basins within the San Joaquin Valley. Evaporation basins are a proven economic means for disposing of agricultural drainage waters, but there is much concern with potential Se toxicity to migratory waterfowl. The primary objective of the joint project is to minimize environmental hazards associated with using evaporation basins for removal of Se from agricultural drainage waters. The method involves breaking the food chain by harvesting invertebrates and volatilization of selenium by aquatic microorganisms. Additional scientific data are required to validate the effectiveness of such a management system in reducing Se ecotoxicity.

This research component provides important information concerning the relationship between the chemical forms of selenium in the water column and sediments and Se bioavailability in evaporation basins. The specific objectives of this research were to:

1. determine patterns of selenium speciation in the water column and fractionation of solid-phase selenium in sediments from evaporation basins under contrasting management practices, and
2. evaluate the bioavailability of Se in sediments using Se speciation and bioavailability indicators.

The investigation was conducted at Hacienda Evaporation Basin [HEB] in Tulare Lake Drainage District (TLDD). Pond water, sediment core and detrital material samples were taken from ponds with and without invertebrate harvesting. Aqueous selenium was speciated into inorganic (selenate [Se VI] and selenite [Se IV]) and organic forms (Org-Se). Selenium in detrital materials and surface sediment were fractionated by selective-extraction methods into soluble (water), ligand-exchangeable or adsorbed (0.1 *M* PO_4, pH 8.0), organic matter-associated (OM-associated) (0.1 M NaOH), and an insoluble fraction consisting of elemental Se and residual resistant forms of Se. Selenium speciation was also performed on 0.1 M NaOH extracts. Proteinaceous Se (peptidic constituents), a potential site-specific Se risk indicator, was determined for both detrital material and sediment extracts. Results showed that Se undergoes significant biochemical transformations both in the water column and sediments. We also find that there is large spatial variability in Se concentrations and speciation between sites in a given evaporation basin. The interface between pond water and sediment offers important links to bioavailable Se. Selenium associated with the organic matter in the detrital material is a very important source of bioavailable Se because it contains the most proteinaceous Se. Continued studies will verify our research findings at other ponds, as well as in other projects proposed by the joint research team. The integrated research will provide essential scientific understanding of Se biogeochemistry in the foodchain and this knowledge will greatly assist in managing evaporation basins to minimize Se ecotoxic risk in the San Joaquin Valley.

KEYWORDS

Evaporation basin, Se speciation, selenate, selenite, organic Se, Se fractionation, organic matter associated Se, elemental Se, proteinaceous Se.

■ ■ ■ ■ ■

INTRODUCTION

Evaporation basins are a proven economic means for disposing of agricultural drainage water in the San Joaquin Valley, however, there remains great concern about potential Se toxicity to migratory waterfowl. The top predators in the food chain receive Se primarily through their diet of aquatic invertebrates and fish. Thus, Se ecotoxicity risk largely depends on the transfer of Se into the food chain. Recent research by Fan and Higashi demonstrates the potential for managing evaporation basins to break the food chain (harvesting invertebrates) and volatilize Se with aquatic microorganisms. Higashi and Fan have demonstrated that breaking the foodchain by harvesting brine shrimp resulted in reduced organic carbon in the sediment and no accumulation of Se in the sediment as compared to management with no harvesting. To better

understand these management effects, there is a critical need to study selenium biogeochemistry associated with these selenium remediation efforts.

This research is part of a Joint Research Project "*Mitigating Selenium Ecotoxic Risk by Combining Foodchain Breakage with Natural Remediation*", proposed by a team of multidisciplinary investigators and cooperators for selenium (Se) ecotoxicity remediation in evaporation basins in the San Joaquin Valley. The ***overarching*** objectives of the joint project are focused on Se in the foodchain of evaporation ponds and include:

- evaluating the efficacy of reducing Se risk by intensive commercial harvest of brine shrimp (*Artemia franciscana*) and other macroinvertebrates,
- assessing effects of fertilizer inputs on algal dynamics for optimizing the harvest of brine shrimp and other macroinvertebrates as well as Se volatilization so that total and bioavailable Se are reduced, and
- evaluating the ecotoxicological status in different evaporation basins of widely varying salinity and physio-chemical conditions so that general factors leading to reduced ecotoxic risk can be discerned.

Research examining flow-through wetlands to remove Se from agricultural drainage water shows that selenate (Se VI), the dominant form of Se in the drainage water, undergoes reduction to selenite (Se IV) and organic Se (org-Se) as water flows through the wetland (Gao et al., 2000; Tanji, 2000). The major mechanism removing Se in flow-through wetlands is reduction to Se (0) and immobilization in the organic phase of the sediments. Vegetation plays an important role in Se reduction and immobilization in the wetland cells by providing a carbon source for aquatic microorganisms. Similar processes are expected to occur in agricultural evaporation basins mainly due to microphyte and microbial activity, although vascular plants are not present in the evaporation basins. The extent of these transformations will largely depend on the management of the system, such as invertebrate harvesting versus no harvesting.

There is scientific consensus that sediments harbor important pools of selenium having potential ecotoxic effects (EPA Office of Water, 1998). The surface sediment is a zone of high microbial activity and has been shown to accumulate Se in the fine organic detrital layer and top mineral sediments (<20 cm). Thus, the surface sediment serves as an important source of potentially bioavailable Se. To evaluate the solid-phase associations of Se as related to its bioavailability, sequential selective-extractions methods are used (Chao and Sanzolone, 1989; Lipton, 1991) as summarized in Huang and Fujii (1996). The soluble and ligand-exchangeable Se are considered to be readily bioavailable. A large amount of Se was transformed and incorporated into organic matter-associated Se (OM-Se) in wetlands (Gao et al., 2000). Insoluble elemental Se [Se (0)] is another major product in Se reduction processes and it is immobilized in sediments which may be subject to reoxidation once exposed to the atmosphere (Zhang and Moore, 1996; Zawislanski and Zavarin, 1996; Tokunaga et al., 1996).

Selenium speciation is a key factor in determining Se bioavailability. Major aqueous species of Se are inorganic (Se(VI) and Se(IV)) and organic forms of Se. Organic Se is generally considered more toxic and bioavailable than inorganic Se to fish and wildlife, both in waterborne and dietary exposure (Fan and Higashi, 2000). An example of relative toxicity of various Se species follows: selenomethionine (Se-Met) 100-1,000X > selenite 10X > selenate 1 (Lemly et al., 1993). Organic Se as Se-Met is much more available to algae and invertebrates than the typical inorganic Se(VI) and Se(IV) forms (Rosetta and Knight, 1995; Maier and Knight, 1994). Aquatic hazard assessment of Se is characterized in terms of the potential for food-chain bioaccumulation and reproductive impairment in fish and aquatic birds (Lemly, 1995). Recent discussions, however, indicate that *waterborne exposure* to Se in all its various forms is much less important than *dietary exposure* in determining the potential for chronic effects in aquatic organisms in general and for fish in particular.

Proteinaceous (peptide- and protein-bound) Se in the diet of aquatic organisms is emerging as a critical factor for assessing the potential for chronic effects in aquatic organisms (USEPA, 1998). It was stated previously that proteinaceous Se may be the most bioavailable form of Se in the foodchain (Fan, 2001; Fan et al., 2002). Fan (2001) pointed out that since Se is expected to be transformed into proteins by primary producers and considering that proteins are highly available to consumers and preditors, that proteinaceous Se

should be biomagnified through the food chain. Research results (Fan et al., 2002) indicate that proteinaceous Se appears to be biomagnefied up the food chain and is better correlated with symptoms observed in fish reproductive systems compared to total biomass or waterborne Se concentrations. It is possible that similar Se forms in detritus and sediment are also highly available to benthic organisms. Thus, proteinaceous Se may serve as a site-specific indicator of Se risk. In this study, we quantified proteinaceous Se in evaporation basin sediments to determine its efficacy as a Se ecotoxicity indicator and its role in Se biogeochemistry.

The specific objectives of this research are to:

1. determine patterns of selenium speciation in the water column and fractionation of solid-phase selenium in sediments from evaporation basins under contrasting management practices, and
2. evaluate the bioavailability of Se in sediments using Se speciation and bioavailability indicators.

STUDY METHODS

FIELD SAMPLING AND ANALYSIS

In Fall 2001, pond water, sediment core (~ 25 cm depth) and detrital material samples were taken from Hacienda Evaporation Basins (HEB) in Tulare Lake Drainage District (TLDD) (Figure 1). Two ponds (A4 with brine shrimp harvesting and C4 with no harvesting) were chosen. Two sites were selected in each pond and are identified as northwest (NW) and southeast (SE). Three replicates were taken for each sample type. In addition to the detrital materials above the mineral sediment at each sampling site, a visible layer of detrital materials buried a few cm below the surface of the sediment in C4-NW was collected.

Water samples were stored on ice during transfer to the lab and stored in a refrigerator (3 ^{o}C) through completion of analyses. Solutions were analyzed for pH, electrical conductivity (EC), total Se concentration and Se speciation (selenate (Se VI), selenite (Se IV), and organic Se (org-Se)) as described below.

Sediment cores were taken using 5-cm diameter acrylic tubes. The cores were sealed immediately with a plastic cap and duct-tape and stored on ice. After transferring to the lab, the core samples were frozen until ready for analysis. Organic detrital materials were sectioned from the mineral sediment cores. The mineral cores were then sectioned into the 0-5, 5-10, 10-15 and 15-20 cm segments. Both detrital and mineral sediments were determined for total Se and fractionation. Subamples of each sample were used for selective sequential extractions, determination of moisture content, total Se by chemical digestion.

Sequential selective dissolution procedures were developed based on research by Chao and Sanzolone (1989), Lipton (1991), and Velinsky and Cutter (1990). The detailed procedures are described in Gao et al. (2000). In this study, Se in the sediments was fractionated into soluble, ligand-exchangeable, and organic matter-associated using (1:10 soilid:water ratio) of water, 0.1 *M* K_2HPO_4 (PO_4, pH 8.0), and 0.1 *M* NaOH, respectively. The unextractable fraction, i.e., the difference between the total and the extracted, was comprised primarily of elemental Se and a very small amount of residual (most-resistant) Se based on previous findings by Gao et al. (2000).

As a potential bioavailability indicator, proteinaceous Se was determined in collaboration with other project investigators. The peptidic Se constituents in detrital materials and sediment extracts were determined by pyrolysis-GCMS and performed by Higashi. This methodology can detect and structurally identify most of the hypothesized bound selenoamino acids in a single analysis, including Se-Met, Se-Cys, and methyl-Se-Cys (Fan et al., 1998).

In addition, sediments from a microcosm experiment carried out by Rejmankova were fractionated by sequential extractions as well as for proteinaceous Se. The microcosm experiment tested the effect of nutrient treatments on productivity and Se concentrations and the details were described in the reports by Rejmankova (2002) and Higashi and Flocchini (2002).

SELENIUM ANALYSIS

Selenium speciation (Se VI, Se IV, and org-Se) for water and 0.1 M NaOH extracts was determined based on the methods developed by Zhang et al. (1999). Three determinations were performed: direct measurement of Se(IV) using phosphate pH 7 buffer (for NaOH extracts, solution pH was adjusted to pH 7 with HCl prior to the analysis), Se(IV) + org-Se using persulfate to selectively oxidize organic-Se(-II) to Se(IV) using manganese

oxide as an indicator for completion of oxidation, and total Se. Total Se concentration in water samples was determined using persulfate digestion followed by reduction to Se (IV) (Cutter, 1982, Yoshimoto, 1992). The Se(IV) in solution was analyzed using HGAAS (hydride generation atomic absorption spectroscopy). Organic-Se(-II)) is obtained as the difference between Se(IV)+org-Se and Se(IV) and Se(VI) is obtained by the difference between total Se and Se(IV)+org-Se analysis.

Total Se in the detrital materials and sediments was determined using a modified $HClO_4$-HNO_3 digestion (Zasoski and Burau, 1977), followed by a reduction of Se(VI) to Se(IV) for HGAAS (hydride generation atomic absorption spectroscopy) analysis.

RESULTS AND DISCUSSION

TOTAL SE CONCENTRATION AND SPECIATION IN EVAPORATION BASIN WATERS

Pond waters in HEB are hypersaline with EC values of 95.0, 89.5, 118.7, and 95.5 dS/m for A4-NW, A4-SE, C4-NW and C4-SE, respectively. The pH values were 8.7, 8.7, 8.5 and 7.5 for A4-NW, A4-SE, C4-NW and C4-SE, respectively. Total Se concentrations ranged from 9.4 to 28.5 ppb and demonstrated some spatially variability between samples (Figure 2). Selenium speciation results showed that pond waters were dominated by inorganic Se species (about 60% selenate and 40% selenite) with very low concentrations of organic Se (<2%). Since agricultural drainage water input to TLDD are dominated by selenate (>90%) (Gao et al., 2000; Tanji and Gao, 2001), the results of this study indicate that there is significant Se reduction occurring within the evaporation pond waters.

SELENIUM IN SEDIMENTS AND DETRITAL MATERIALS

Total Se concentrations in the sediment profile (Fig. 3) varied with depth in the sediment core and spatially within the evaporation basin. First of all, detrital material samples (depth 0) showed concentrations either higher (A4-NW and C4-SE) or lower (A4-SE and C4-NW) than the underlying mineral sediment. This may directly link to the age of the deposited materials, which varies spatially. The same reasoning may be used for explaining the mixed pattern of A4-NW and C4-SE sediment Se profiles. For A4-SE and C4-NW, Se concentration decreased with increasing depth, similar to what was observed in a newly constructed wetland for Se removal in the TLDD (Gao et al., 2000). The deep detrial materials buried several cm below the sediment surface at C4-SE showed extremely high Se concentration of 4.1 and 3.8 mg/kg (data not shown). This shows that biological activity has an important role in Se transformation and accumulation. The distribution pattern seems related to the redox status as judged by their colors. The profiles in which Se concentrations decreased with depth were those cores that showed black color at the top and lighter color at the bottom. If the color was black throughout, Se concentration was mixed. The large variation observed in Se concentration in the sediment appears to be related to sediment deposition dynamics, which shows great spatial variability. Regardless, the top few cm of sediment is the most important in Se accumulation as the majority of the benthic invertebrates reside there.

SELENIUM FRACTIONATION AND SE BIOAVAILABILITY INDICATOR

Selenium fractionation results for detrital materials (DM) and surface sediment (0-5 cm) are shown in Figure 4. It includes four detrital material samples collected above the mineral sediment at each sampling location and one buried detrital material collected a few cm below the surface in C4-NW. Generally speaking, the 0.1 M NaOH extractable fraction (representing organic matter-associated Se) and the unextractable fraction (mainly elemental Se) were the largest fractions, ranging from 33-56% and 36-48% of total Se, respectively. Soluble and adsorbed Se comprise only a small fraction. However, it was noticed that detrital materials contained a significantly higher fraction of soluble and adsorbed Se compared to the mineral sediment except for the buried detrial materials in C4-NW. Soluble and adsorbed Se fractions for detrial materials at the mineral surface ranged from 10-11 and 5 to14%, respectively. For 0-5 cm sediment, soluble and adsorbed Se fractions ranged from 3-5 and 4-7%, respectively. These results indicate that more available Se is residing in the surface of mineral sediment.

The organic-Se phase is of particular interest because we assume this phase is related to Se biomagnification in the food chain. Thus 0.1 M NaOH extracts containing the organic-Se fraction were speciated to determine the form of Se contained in this fraction (Figure 5). Although large variation was observed, there were differences between detrital materials and mineral sediment.

Detrital materials contained a relatively higher percentage of Se (VI) (22-37%) compared to the mineral surface sediment (10-22%), and a relatively lower percentage of Se (IV) (25-38%) than sediment extracts (45-58%). Organic Se was identified as 30-49% for detrital materials and 20-40% of total extracted Se in the surface mineral sediment. Although it is not certain if the extraction procedure altered Se speciation, the large proportion of total extracted Se was directly bound with organic carbon. If means of 35% for detrital materials and 40% for mineral sediments are used for organic-Se, at least 16% of the total Se in the detrital materials and surface sediments was present in organic forms. Small amounts of organic Se may be extracted in the previous extractions for soluble and adsorbed.

Peptidic Se constituents in the detrital materials and surface sediments were determined by Higashi for the various fractions (Figure 6). The majority of the peptidic constituents were found in the adsorbed and OM-associated fractions. Detrital material contained significantly higher peptidic Se than the 0-5 cm mineral sediment. In conjunction with the data in Figure 4, it is concluded that the OM-associated detrital material may harbor the most proteinaceous Se.

Detrital materials and surface sediment from Rejmankova's microcosm study for testing nutrient treatments on productivity and Se concentration were also taken for Se fractionation and peptidic constituents. Selenium fractionation data were analgous to those reported above. A small difference was that the adsorbed fraction had more peptidic materials than the 0.1 M NaOH extracts. The presence of brine shrimp always reduced the peptidic materials and the addition of N+P generally increased it. Thus treatment effects were demonstrated for the short period of the experiment (7 days). For details, refer to the reports by Rejmankova, and Higash and Flocchini.

In terms of the management effects of the ponds with brine shrimp harvesting and without harvesting activities, there were no differences in the patterns of Se speciation and fractionation. The major difference resides in the smaller amount of detrital materials accumulated in surface sediments in the ponds with invertebrate harvesting. Thus, the total mass of Se in detrital materials and protanecous Se would be less compared to the ponds with no harvesting activities. This difference could not be detected in terms of Se concentration (Figures 2 and 6).

SUMMARY

Selenium concentration and speciation in pond water samples, detrital materials, and surface mineral sediments show that Se has undergone significant biochemical transformations and that Se biogeochemistry is spatially complex. The interface between pond water and sediment offers important links to bioavailable Se. The most important organic-Se phase can be extracted with 0.1 *M* NaOH and OM-associated detrital material may harbor the most proteinaceous Se. Continued studies will attempt to verify these findings in other ponds, as well as in other projects proposed by the joint research team. The integrated research will provide essential scientific understanding of Se biogeochemistry in the foodchain and this knowledge will greatly assist in managing evaporation basins to minimize exposure to Se ecotoxic risk in the San Joaquin Valley.

■ ■ ■ ■ ■

REFERENCES CITED

Chao, T.T., and R.F. Sanzolone. 1989. Fractionation of soil selenium by sequential partial dissolution. *Soil Sci. Soc. Am. J.* 53:385-392.

Cutter, G.A. 1982. Selenium in reducing waters. *Science* 217:829-831.

EPA Office of Water. 1998. Report on the Peer Consultation Workshop on Selenium Aquatic Toxicity and Bioaccumulation, EPA-822-R-98-007, September 1998. Available at the website http://www.epa.gov/ost/selenium/report.html

Fan, T. 2001. Proteinaceous Selenium: A More Reliable Indicator of Se Ecotoxic Risk. Currents. A Newsletter of the UC Center for Water Resources. Vol. 2, Issue 2. Winter 2001.

Fan, T. W.-M, and R. M. Higashi. 2000. Microphite-Mediated Se Biogeochemistry and Its Role in Bioremediation of Se Ecotoxic Consequences. Annual Report. Salinity/Drainage Program, University of California.

Fan, T.W.-M, A.N. Lane, D. Martens, and R.M. Higashi. 1998. Synthesis and structure chractarization of selenium metabolites. *Analyst* 123(5), 875-884.

Fan, T. W-M., S.J. Teh, D.E. Hinton, and R.M. Higashi. 2002. Selenium biotransformations into proteinaceous forms by foodweb organisms of selenium-laden drainage waters in California. Aquatic Toxicology (In press).

Gao. S., K.K. Tanji, D.W. Peters, and M.J. Herbel. 2000. Water selenium speciation and sediment Se fractionation in TLDD flow-through wetland system. *J. Environ. Qual.* 29:1275-1283.

Huang, P.M., and R. Fujii. 1996. Selenium and arsenic. p. 793-831. *In* D.L. Sparks (ed.) Methods of Soil Analysis. Part 3. Chemical Methods. SSSA Book Series No. 5. Soil Science Society of America, Inc., Madison, WI.

Lemly, A.D. 1995, A protocol for aquatic hazard assessment of selenium. *Ecotox. Environ. Saf*. 32:280-288.

Lemly, A.D., S.E. Finger, and M.K. Nelson. 1993. Sources and impacts of irrigation drainage contaminants in arid wetlands. *Environ. Toxicol. Chem*. 12:2265-2279

Lipton, D.S. 1991. Associations of Selenium with Inorganic and Organic Constituents in Soils of a Semi-Arid Region. Ph.D. Dissertation, UC Berkeley.

Maier, S.B., and A.W. Knight. 1994. Ecotoxicology of selenium in freshwater systems. *Environ. Contam. Toxicol.* 134:31-48.

Rosetta, T.N. and A.W. Knight. 1995. Bioaccumulation of selenate, selenite, and seleno-DL-methionine by the brine fly larvae *Ephydra cinerea* Jones. Arch. *Environ. Contam. Toxicol*. 29:351-357.

Tanji, K.K. 2000. TLDD Flow-Through Wetland System: Inflows and Outflows of Water and Total Se as well as Water Se Speciation and Sediment Se Fractionation. Annual Report 1999-2000. Salinity/Drainage Program, University of California, Davis.

Tanji, K.K. and S. Gao. 2001. Selenium Removal and Mass Balance Balance in a Constructed Flow-through Wetland System. Annual Report 2000-2001. Salinity/Drainage Program, University of California, Davis.

Tokunaga, T.K., I.J. Pickering, and G.E. Brown, Jr. 1996. Selenium transformations in ponded sediments. *Soil Sci. Soc. Am. J*. 60:781-790.

U.S. Environmental Protection Agency (USEPA). 1998. Report on the Peer Consultation Workshop on Selenium Aquatic Toxicity and Bioaccumulation. Publication EPA-822-R-98-007. USEPA. Office of Water. Washington, DC.

Velinsky, D..J., and G.A. Cutter. 1990. Determination of elemental selenium and pyrite-selenium in sediment. *Analytica Chimica Acta,* 235:419-425.

White, A.F., S.M. Benson, A.W. Yee, H.A. Wollenberg, Jr, and S. Flexer. 1991. Groundwater contamination at the Kesterson Reservoir California. 2. Geochemical parameters influencing selenium mobility. *Wat. Resour. Res.* 27:1085-1098.

Yoshimoto, J.T. 1992. Potential Mechanisms Controlling Soluble Selenite in Sierran Sands. Master's Thesis. University of California, Davis.

Zasoski, R.J. and R.G. Burau. 1977. A rapid nitric-perchloric acid digestion procedure for multi-element tissue analysis. *Commun. Soil Sci. Plant Anal.* 8:425-436.

Zawislanski, P.T. and M. Zavarin. 1996. Nature and rates of selenium transformations: a laboratory study of Kesterson Reservoir soils. *Soil Sci. Soc. Am. J.* 60:791-800.

Zhang, Y.Q. and J.N. Moore. 1996. Selenium fractionation and speciation in a wetland system. *Environ. Sci. Technol*. 30:2613-2619.

Zhang, Y.Q., J. Moore and W.T. Frankenberger, Jr. 1999. Speciation of soluble selenium in agricultural drainage waters and aqueous soil-sediment extracts using hydride generation atomic absorption spectrometry. *Environ. Sci. & Technol*. 33:1652-1656.

PUBLICATION AND REPORTS

MANUSCRIPTS SUBMITTED

Gao, S., K.K. Tanji, D.W. Peters, Z.Q. Lin, and N. Terry. Selenium removal from irrigation drainage water flowing through constructed wetland cells with special attention to accumulation in sediments. Submitted to Water, Air, and Soil Pollution.

Gao, S., K.K. Tanji, Z.Q. Lin, N. Terry, and D.W. Peters. Selenium removal and mass balance in a constructed flow-through wetland system. Submitted to Journal of Environmental Quality.

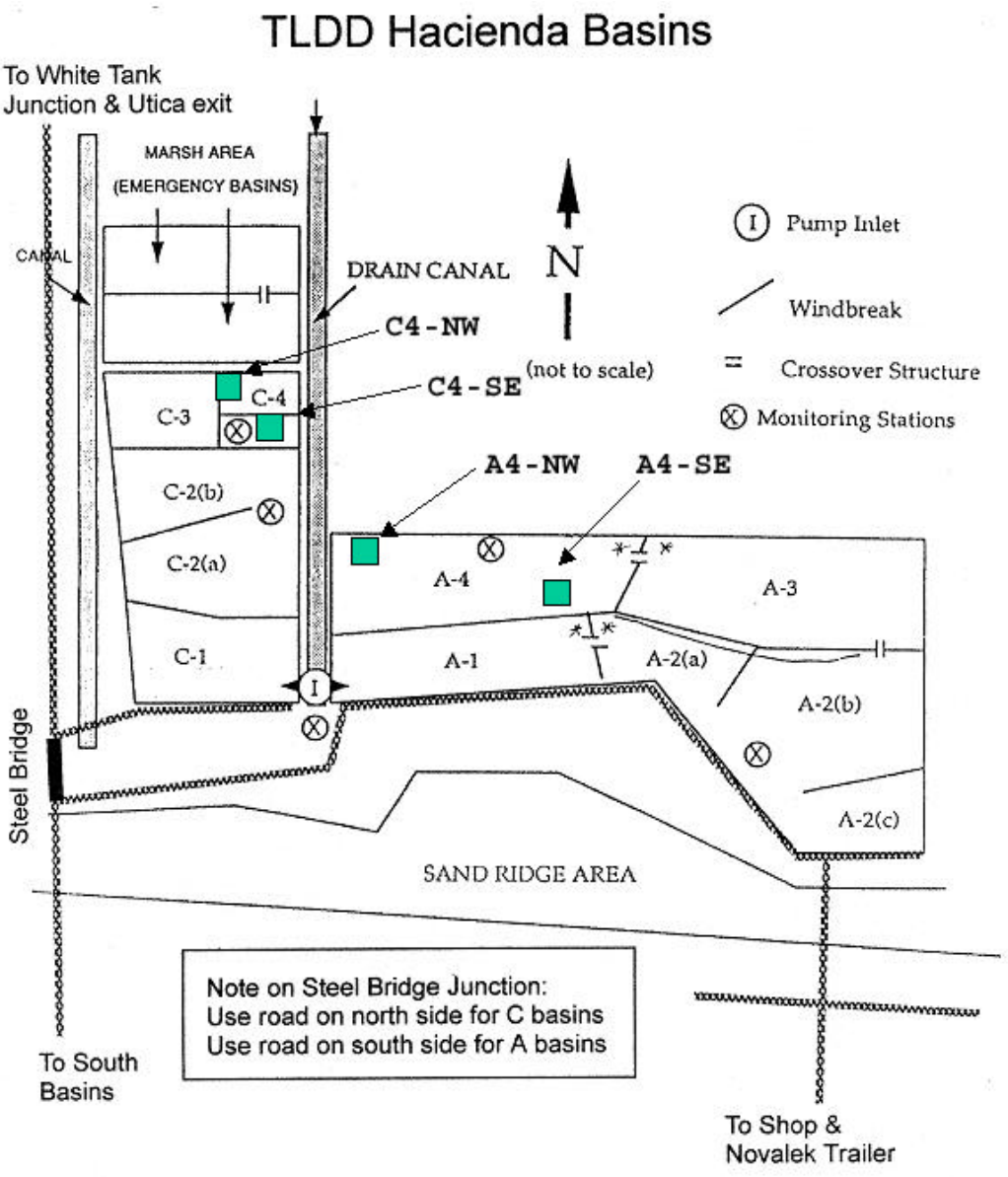

Figure 1. Sampling locations in Hacienda Evaporation Basin (HEB) in Tulare Lake Drainage District (TLDD)

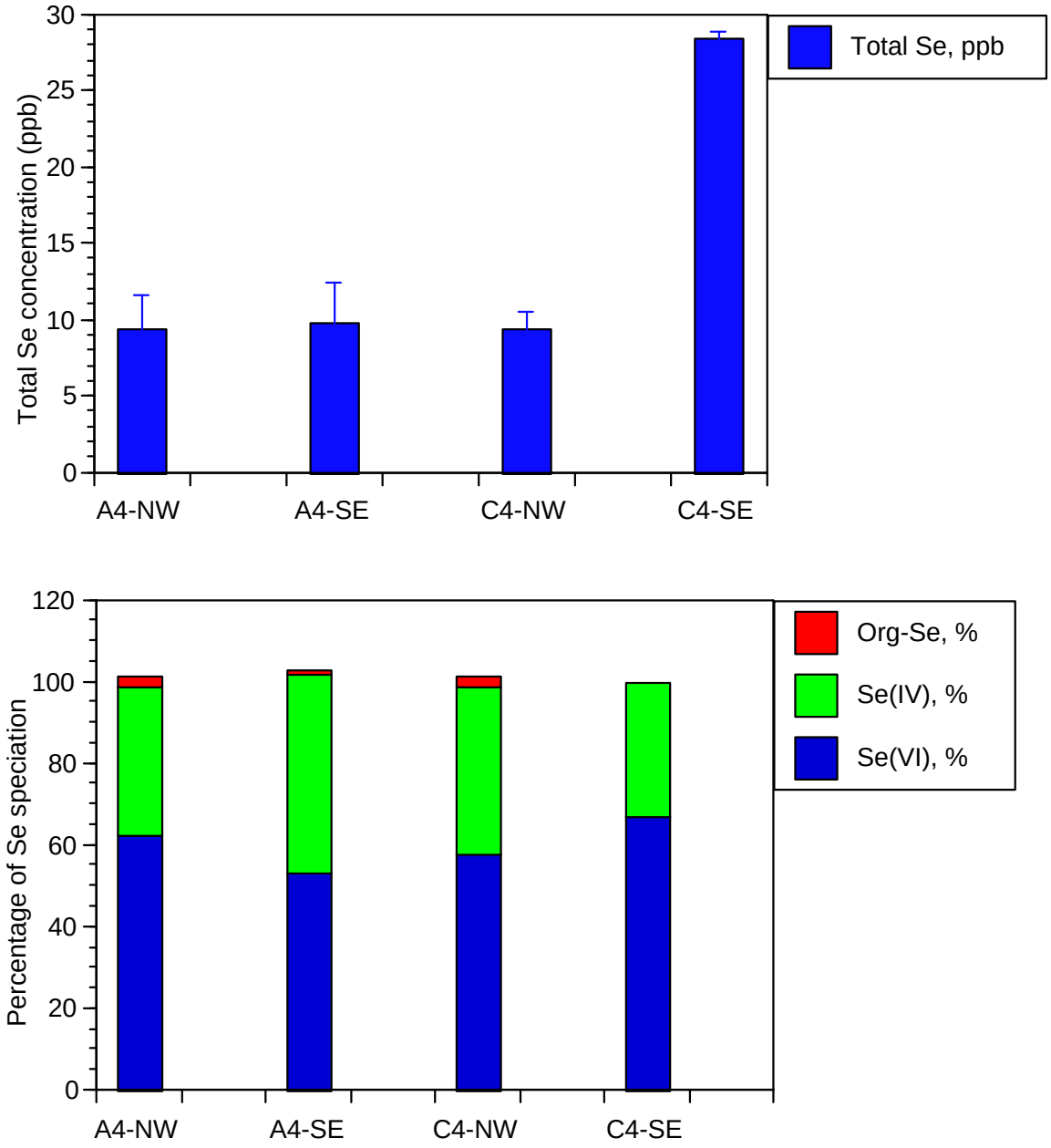

Figure 2. Se concentration and speciation in Hacienda Evaporation Pond waters.

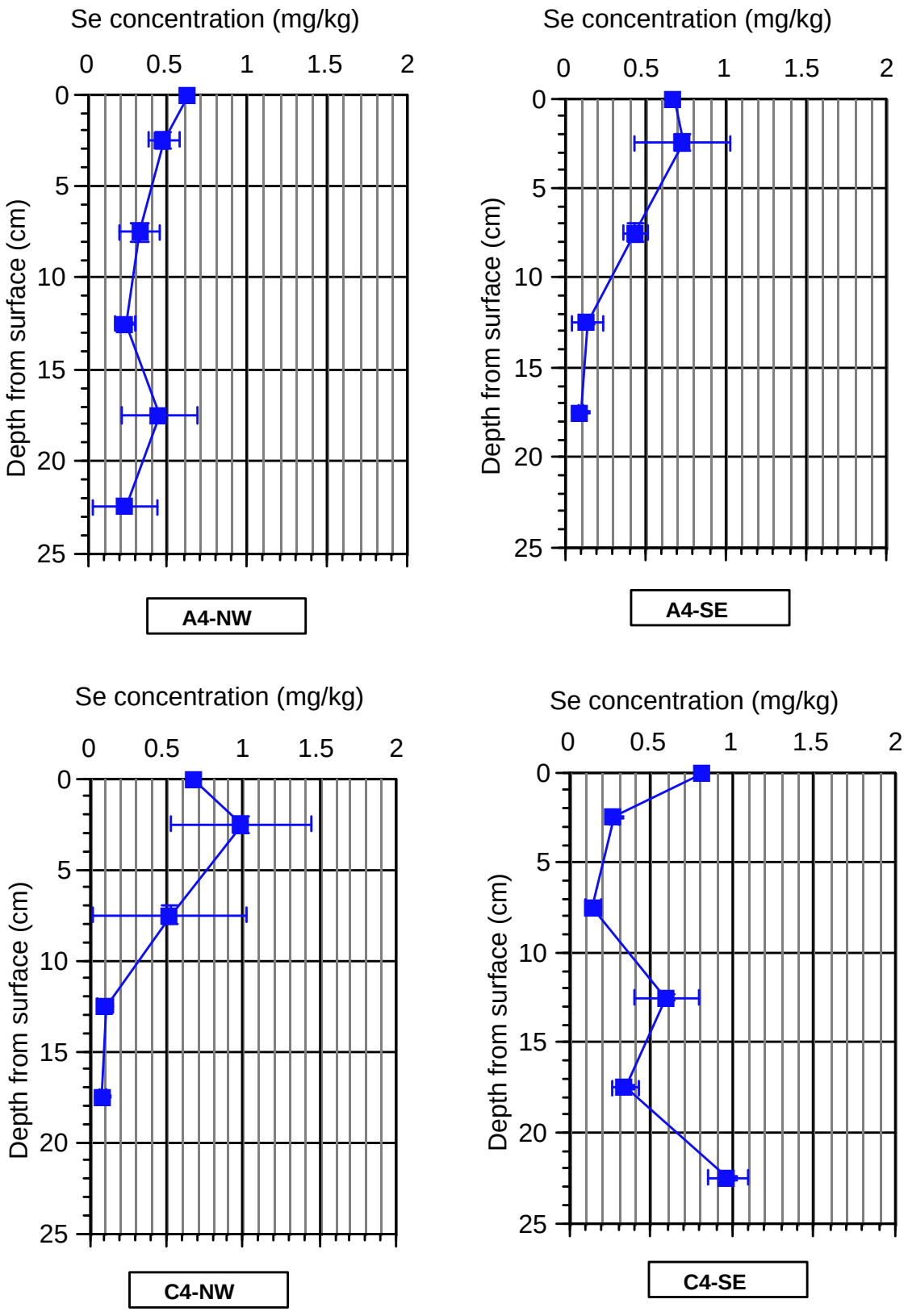

Figure 3. Total Se concentration profile in Hacienda Evaporation Pond sediments.

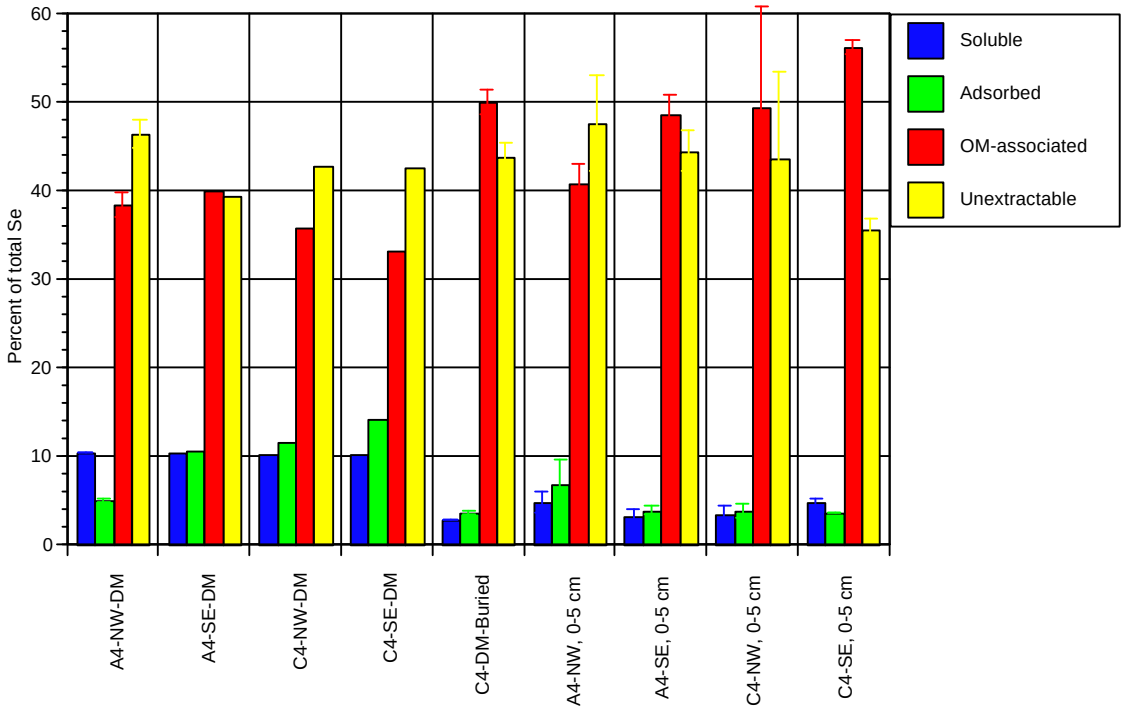

Figure 4. Sediment Se fractionation in Hacienda Evaporation Ponds.

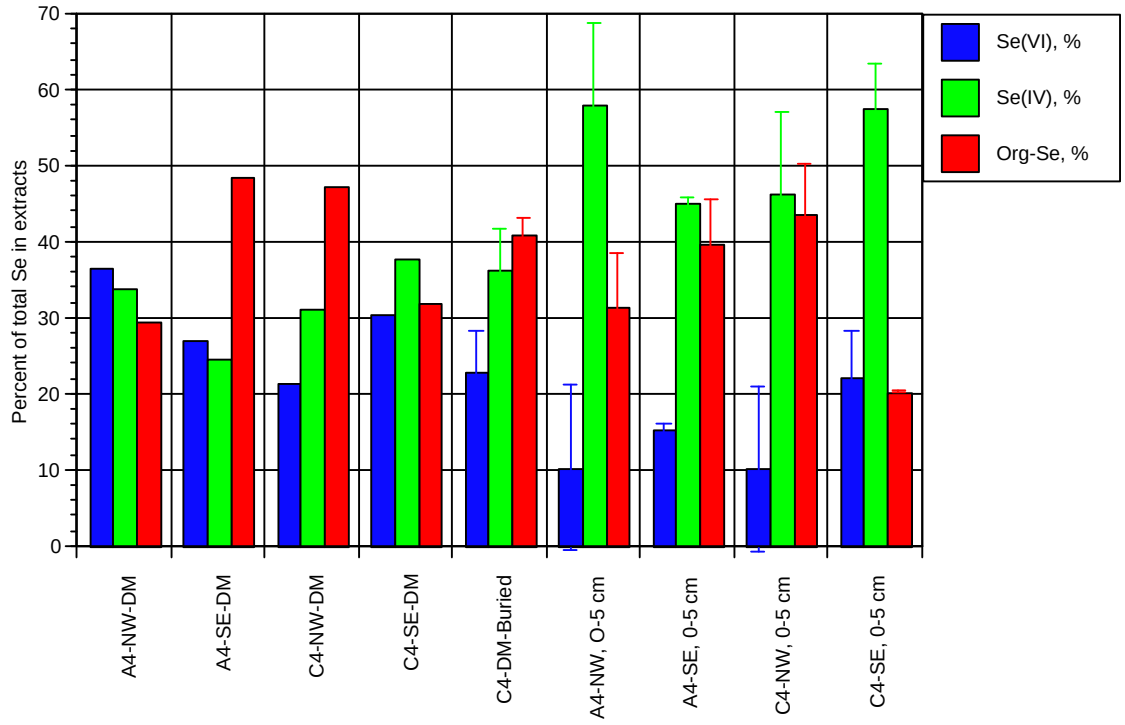

Figure 5. Se speciation in 0.1 N NaOH extracts from Hacienda Evaporation Pond sediments

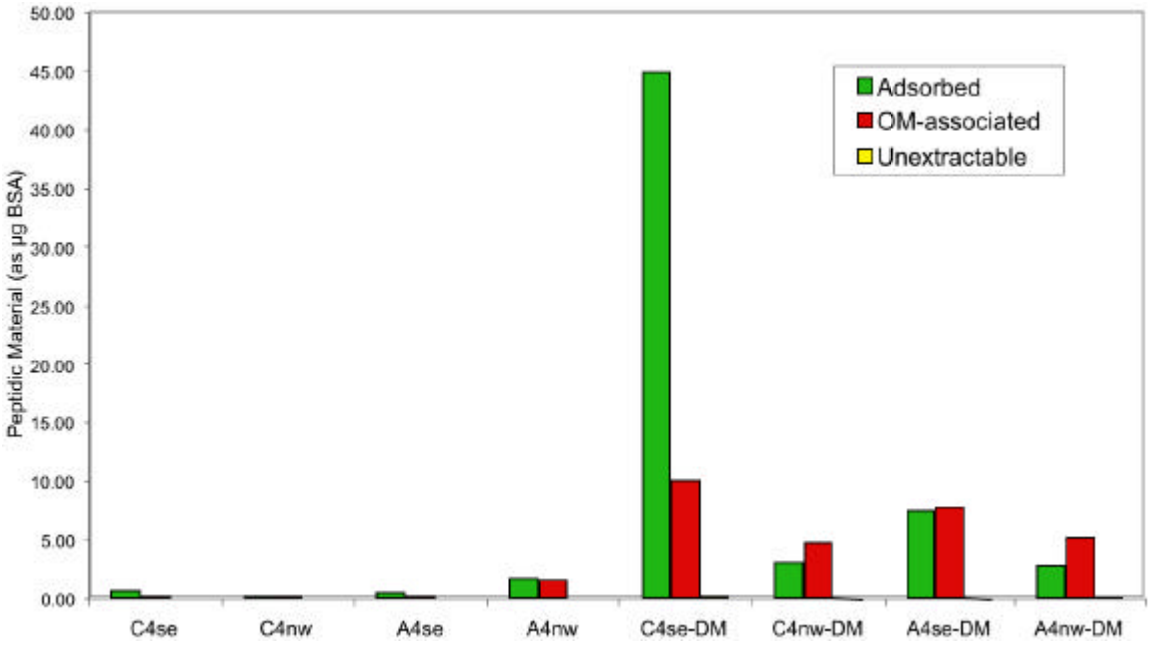

Figure 6. Peptidic constituents in sediment and detrital material fractions (analysis performed by Higashi)

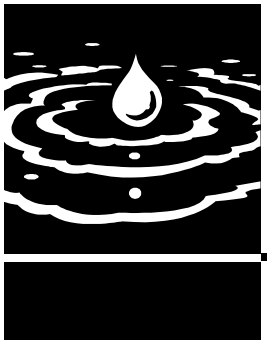

Validation of Protocols for Using Trunk Diameter and Tree Water Potential Measurements in Orchard Irrigation Scheduling

Project Investigators:

David A. Goldhamer
Office: (559) 646-6500, E-mail: Dagoldhamer@ucdavis.edu
Kearney Ag. Center/Dept. of LAWR
University of California, Davis

R. Scott Johnson
E-mail: SJohnson@uckac.edu
Kearney Ag. Center/Dept. of Pomology
University of California, Davis

Ken Shackel
E-mail: kashackel@ucdavis.edu
Dept. of Pomology
University of California, Davis

Research Staff (RAs)

Mario Salinas - 0.50 FTE
Jesus Salinas - 0.50 FTE
Miguel Marquez - 0.50 FTE

ABSTRACT

Irrigation scheduling using Maximum daily trunk shrinkage (MDS) gleaned from trunk diameter fluctuations measured with linear variable displacement transducers (LVDTs) was evaluated in a commercial almond orchard in the southern San Joaquin Valley. The scheduling protocol was based on calculated Signals; the MDS measurement on the trees to be scheduled divided by a reference (baseline) MDS value representing behavior on fully irrigated trees. Reference MDS values were determined using a relationship between MDS and mean daily vapor pressure deficit (VPD) developed using previously measured data. The scheduling protocols called for a 10% decrease in the rate of applied water when the signal exceeded a threshold value (either 1.75 or 2.75) for 3 consecutive days. Conversely, there was a 10% increase in the rate of applied water when the signal was less than 1.75 or 2.75 for 3 consecutive days.

Using a signal threshold of 1.75 resulted in slightly more applied water than estimated ETc while T2.75 applied 32.6% less than estimated ETc. Both of these MDS-based scheduled regimes had significantly better hull split at harvest than the ranch practice, which applied a similar seasonal amount of applied water as T1.75 but at different rates over the season. Kernel size measured in 3 dimensions was not significantly different between treatments although they trended lower for the T2.75 regime. However, both dry kernel and nut unit weights were lower for T2.75. On the other hand, fresh and dry kernel percentage was higher for T2.75. There were no statistically significant differences in gross or fresh yields. T1.75 and the Ranch yields were nearly equivalent.

This work demonstrates that a continuously recorded plant-based indicator of tree water status can be successfully used as a stand alone measurement for irrigation management of almonds. By selecting a relatively modest MDS signal threshold, equivalent kernel yields and enhanced fruit quality can be achieved while using about the same amount of water as more traditional scheduling techniques. Using a higher threshold may reduce kernel size (10% or less) but save significantly (greater than 30%) amounts of water. We believe this technique offers the potential to use deficit irrigation to achieve large water savings by coupling continuously recorded tree stress with automated irrigation system controllers.

KEYWORDS

Irrigation scheduling, plant sensors, linear variable displacement transducer, LVDT, stem diameter fluctuations

■ ■ ■ ■ ■

BACKGROUND AND JUSTIFICATION

The most popular methods of irrigation scheduling in orchard crops are based on soil and atmospheric parameters even though these measured parameters are only indirectly related to the well-being of the tree. It has long been recognized that the plant is the best indicator of its water status but until recently, plant-based monitoring involved discrete measurements in both space and time. Assessing plant water status requires that a technician travel to the field with a rather cumbersome pressure chamber. The timely detection of critical plant water stress depends on the monitoring frequency and how much labor is allocated for this approach.

The current state of the art in plant water status monitoring is measuring stem water potential. This technique requires that a small, foil covered polyethylene bag be placed on the leaf for a given amount of time prior to the leaf being excised and placed in the pressure chamber (Shackel et al., 1997). In our previous work, we found that interior, shaded leaf water potential (SLWP) was highly related to stem water potential in almond trees. Thus, using SLWP saves time compared with measuring stem water potential.

Another problem in using plant water status measurements as indicators for water management is that they are very dynamic, reflecting the balance between soil water supply and atmospheric demand. Thus, a single measurement may not be very informative as the value is influenced by both soil water level and weather conditions. What's needed are instruments that continuously record plant water status or a plant feature that is related to water status. The development of instruments of this type and associated protocols for their use can result in the automation of irrigation scheduling (coupling of plant-based indicator to computer/electronic irrigation controller), as suggested by Huck and Klepper (1976) and Huguet et al., (1992).

Our work during the past three years shows that changes in trunk diameter correlate with tree water status (Goldhamer et al., 1999; Goldhamer et al., 2000; Goldhamer et al., 2001). We use linear variable displacement transducers (LVDTs) to continuously record trunk diameter at the micron level. Trunk diameters have diurnal oscillations; maximum and minimum sizes occur in the early morning and late afternoon, respectively. While there are various parameters that can be gleaned from the trunk diameter oscillations, we have found that maximum daily trunk shrinkage (MDS), defined as the difference between daily maximum and minimum values, is related to plant water status in mature trees.

Last season, we developed and tested an MDS-based irrigation scheduling protocol for the first time in a daily irrigated, mature, commercial almond orchard. This was compared with a regime that received in excess of potential ETc and the ranch practice irrigation strategy. The performance of each irrigation treatment was assessed based on applied water, plant water status during the season, and yield component results. For the MDS treatment, we calculated a signal as the actual measurement divided by reference values taken on trees that received in excess of full evapotranspiration (ETc). This protocol resulted in applied water for the MDS regime greatly exceeding ETc. We believe this was due to high variability in the fully irrigated MDS values and a signal threshold value that was too low. Our work in 2002 used a different approach to determine reference MDS and tested signal thresholds of 1.75 and 2.75.

OBJECTIVE

To refine operational parameters in an MDS-based irrigation scheduling protocol and to evaluate its performance in a mature, commercial almond orchard.

METHODS

This work was conducted in cooperation with Paramount Farming Co., West Valley Ranch, located near Lost Hills. The experi-mental orchard is irrigated with a buried drip system that contains multiple irrigation sets (blocks), applies water 2-3 times/day, and can be irrigated independently. Sites were established in three adjacent blocks. The 3 sites will be referred to as: (1) T1.75, (2) T2.75, and (3) Ranch.

Each site contained 4 trees instrumented with LVDT's (Model 2.5 DF Solartron Metrology, Bagnor Regis, U.K.). The LVDTs were installed on primary scaffolds on the north side of each tree. They were mounted on holders built of aluminum and INVAR--an alloy comprised of 64% Fe and 35% Ni that has minimal thermal expansion (Li et al, 1989)-and covered with silver foil to provide constant shade. Measurements were taken every 30 secs and the datalogger (Model CR 10, Campbell Scientific, Logan, Utah, US) was programmed to report 20 min means. Data were downloaded to a laptop computer every 3-4 days and taken for analysis to the Kearney Ag. Center.

Our development of protocols for using MDS for irrigation scheduling is predicated on the assumption these measurements can be used to indicate the presence of very mild water stress. Moreover, that almond trees tolerate this mild stress without negative impacts on production. We used the following MDS protocol (Goldhamer and Fereres, 2001) in this study:

1) The irrigation starting date is selected and a fixed amount (irrigation duration) is applied.
2) Reference MDS is calculated based on a previously determined relationship between MDS and mean daily atmospheric pressure deficit (VPD) for fully irrigated trees.
3) The LVDT indicator signals are calculated as the actual MDS of the test trees divided by the calculated reference MDS values.
4) When the Indicator signals exceeds either 1.75 or 2.75 for 3 consecutive days (depending on which plot is being scheduled), the daily irrigation rate is raised by 10%. Similarly, if the MDS indicator signals do not reach either1.75 or 2.75for 3 consecutive days, the irrigation rate is decreased by 10%.

Interior SLWP was measured using a pressure chamber each weekday on each of the 12 LVDT-instrumented trees. The SLWP procedure involves covering leaves with a damp cloth prior to excision. The cloth is removed just prior to placing the leaf in the pressure chamber. These measurements were made between 12:30 and 1:30 pm. Precautions recommended by Hsiao (1990) were taken to prevent leaf water loss during the measurement.

Water meters were used to measure applied water. At the end of the season, 10 randomly

selected trees of similar size were individually harvested in late Sept. and 2 kg nut samples collected and dissected. To remove the impact of variable nut load, which was not a result of this season's treatments, on nut component weight/size, 5 trees per treatment with nearly equivalent fruit loads were used in the statistical analysis (Duncan's New Multiple Range Test).

RESULTS

The relationship between MDS and mean daily VPD developed from last year's data for fully irrigated trees is shown in Figure 1. We used this relationship and real-time daily mean CIMIS vapor pressure and relative humidity data to calculate the MDS reference (baseline) values for the signal calculations.

The MDS values generally mirrored SLWP values over the season for the different irrigation regimes (Figs. 2a, 2b). Signal values for the T2.75 regimes were generally greater through the season than those of T1.75 or the Ranch (Fig. 3). There was greater signal oscillation around the desired threshold than desired, suggesting that computer control of scheduling adjustments would be superior than the manual adjustments we used in our protocol.

The higher signal thresholds this season resulted in much less applied water than in 2000. The T1.75 regime and the Ranch practice applied slightly more than estimated ETc while T2.75 applied 32.6% less than estimated ETc (Fig. 4a). While total amounts of applied water were similar with T1.75 and the Ranch, there were differences in the rates of applied water over the season (Fig. 4b).

Both LVDT-scheduled regimes had significantly better hull split at harvest than the ranch (Table 1). Kernel size measured in 3 dimensions was not significantly different between treatments although they trended lower for the T2.75 regime. However, both dry kernel and nut unit weights were lower for T2.75 (Table 1). On the other hand, fresh and dry kernel percentage was higher for T2.75. There were no statistically significant differences in gross or fresh yields. T1.75 and the Ranch yields were nearly equivalent.

CONCLUSIONS

We have demonstrated, we believe for the first time, that a continuously recorded plant-based indicator of tree water status can be successfully used as a stand alone measurement for irrigation management of almonds. By selecting a relatively modest MDS signal threshold, equivalent kernel yields and enhanced fruit quality can be achieved while using about the same amount of water as more traditional scheduling techniques. Using a higher threshold may reduce kernel size (10% or less) but save significantly (greater than 30%) amounts of water. We believe this technique offers the potential to use deficit irrigation to achieve large water savings by coupling continuously recorded tree stress with automated irrigation system controllers.

■ ■ ■ ■ ■

REFERENCES

Goldhamer, D. A., E. Fereres, M. Mata, J. Girona, and M. Cohen. 1999. Sensitivity of Continuous and Discrete Plant and Soil Water Status Monitoring in Peach Trees Subjected to Deficit Irrigation. J. of Hort. Sci. 124(4):437-444.

Goldhamer, D. A., E. Fereres, M. Soler, M. Salinas, M. Mata, J. Girona, and M. Cohen. 2000. Comparison of continuous and discrete plant-based monitoring for detecting tree water deficits and barriers to grower adoption for irrigation management. Acta Horticulturae 537(1):431-445.

Goldhamer, D. A. and E. Fereres. 2001. Irrigation scheduling protocols using continuously recorded trunk diameter measurements. Irrig. Sci. 20:115-125.

Hsiao, T.C., 1990. Measurements of plant water status. In: Irrigation of Agricultural Crops. (Stewt, B.A. and D.R. Nielsen, ed) American Society of Agronomy, Madison, Wisconsis, USA. (30) p. 243-279.

Huck, M. G. and B. Klepper. 1976. Water relation of cotton. II. Continuous estimates of plant water potential from stem diameter measurements. Agron. J. 69:593-597.

Huguet, J. G, S. H. Li, J. Y. Lorendeau, and G. Pellous. 1992. Specific micromorphometric reactions of fruit trees to water stress and irrigation scheduling automation. J. of Hort. Sci., 67(5):631-640.

Li, S. H., J. G. Huguet, and C. Bussi. 1989. Irrigation scheduling in mature peach orchard using tensiometers and dendrometers. Irrigation and Drainage Systems, 3, 1-12.

Shackel, K. A., H. Ahmadi, W. Biasi, R. Buchner, D. Goldhamer, S. Gurusinghe,J. Hasey, D. Kester, B. Krueger, B. Lampinen, G. McGourty, W. Micke, E. Mitcham, B. Olson, K. Pelletrau, H. Philips, D. Ramos, L. Schwankl, S. Sibbett, R. Snyder, S. Southwick, M. Stevenson, M. Thorpe, S. Weinbaum, J. Yeager. 1997. Plant water status as an index of irrigation need in deciduous fruit trees. HortTechnology 7(1):23-29.

PUBLICATIONS AND REPORTS

Goldhamer, D. A., and E. Fereres. 2001. Simplified tree water status measurements can aid almond irrigation. California Agriculture. 55(3):32-37.

Goldhamer, D. A. and E. Fereres. 2001. Irrigation scheduling protocols using continuously recorded trunk diameter measurements. Irrig. Sci. 20:115-125.

Fereres, E. and D. A. Goldhamer. 2002. Suitability of stem diameter variations and water potential as indicators for irrigation scheduling of almond trees. J. Hort. Sci. and Biotech (In Press)

Table 1. Almond yield and yield component values for the 2001 season.

Irrigation Regime	Applied Water Thru Harvest (inches)	Full Hull Split Nuts (%)	Full Hull Split Kernel Length (mm)	Full Hull Split Kernel Width (mm)	Full Hull Split Kernel Girth (mm)	Dry Kernel Weight (gm)	Dry Nut Unit Weight (gm)	Fresh Kernel/ Nut Unit (%)	Dry Kernel/ Nut Unit (%)	Fruit Load (#/tree)	Gross Nut Yield (lbs/acre)	Fresh Kernel Yield (lbs/acre)
T1.75	35.4	89.8 b*	21.8	12.2	9.32	1.04 b	3.35 b	29.8 b	31.1 b	9183	7558	2257
T2.75	21.9	95.2 c	21.1	11.9	9.03	0.92 a	2.99 a	29.5 b	30.8 b	9311	6720	1982
Ranch	36.8	82.2 a	21.8	12.0	9.15	1.02 b	3.47 b	28.1 a	29.5 a	9304	7718	2176
			NSD**	NSD	NSD					NSD	NSD	NSD

*Values in each column not followed by the same letter are significantly different according the Duncan's New Multiple Range Test at the 5% confidence level.

**NSD indicates no significant difference.

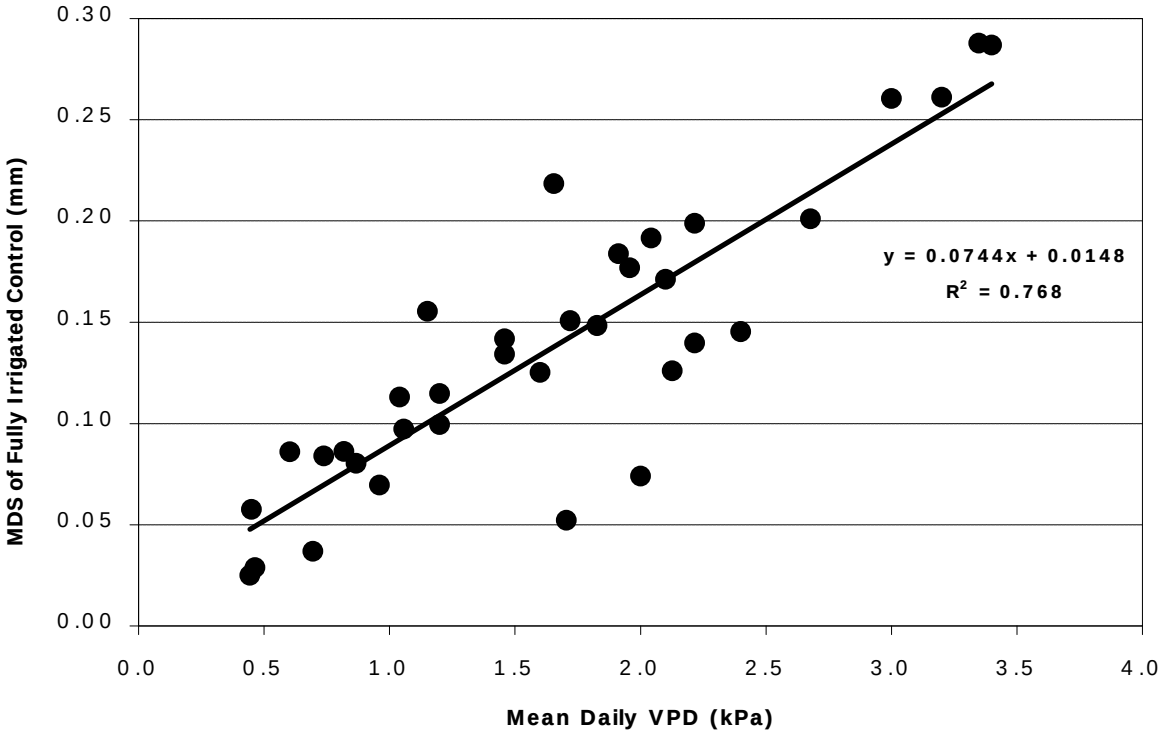

Figure 1. Maximum daily trunk shrinkage (MDS) for fully irrigation trees versus mean daily vapor pressure deficit (VPD). Data is from 2000 and was used to calculate reference (baseline) MDS based on real-time VPD in 2001.

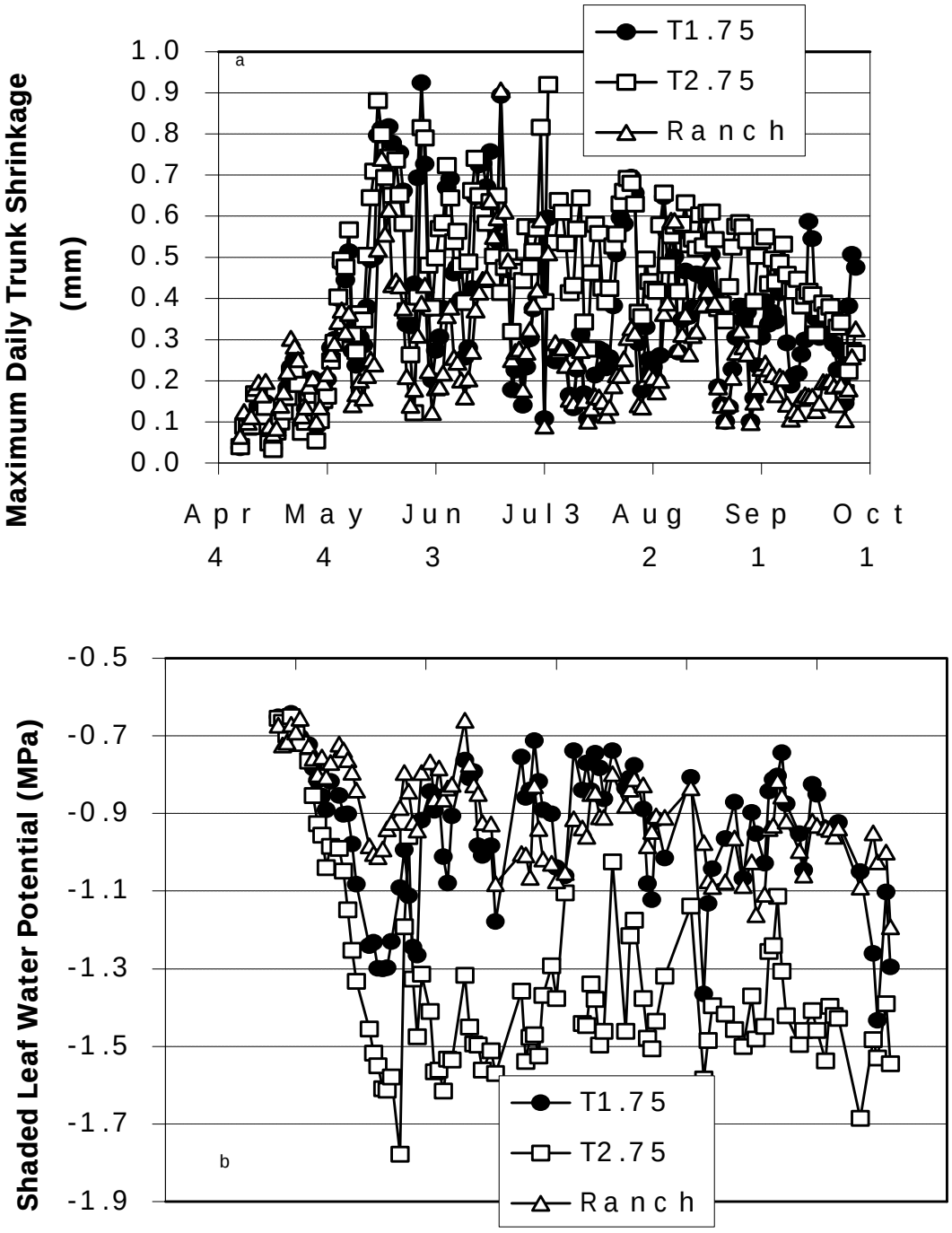

Figure 2. Irrigation treatment influences on a) maximum daily trunk shrinkage (MDS), and b) shaded midday leaf waterpotential (SLWP).

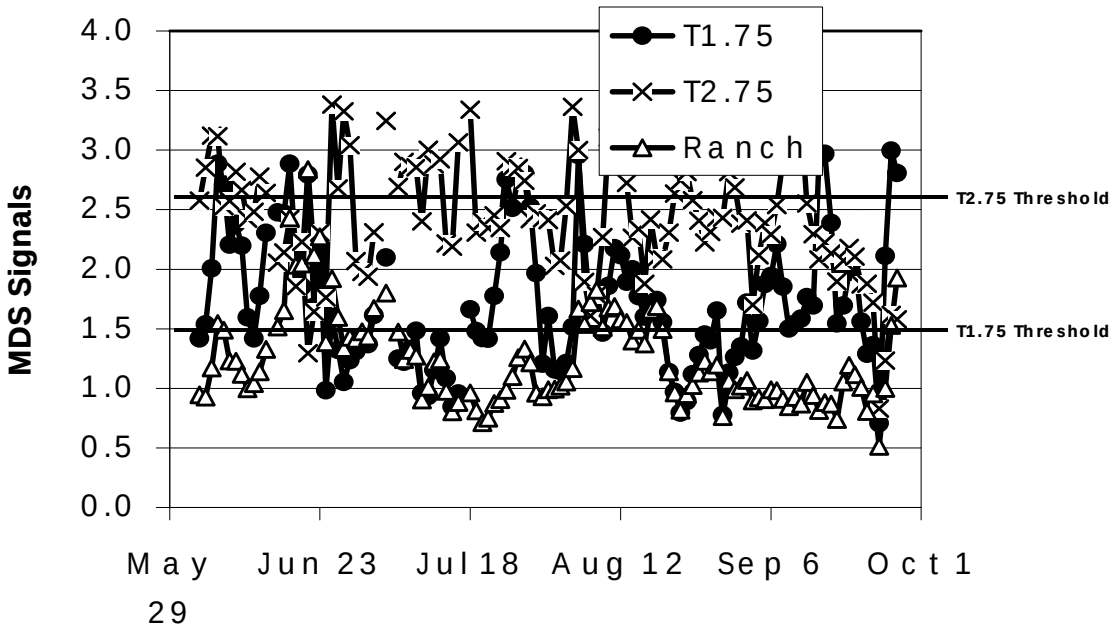

Figure 3. Maximum daily trunk shrinkage (MDS) signals (actual MDS/reference MDS) in 2001.

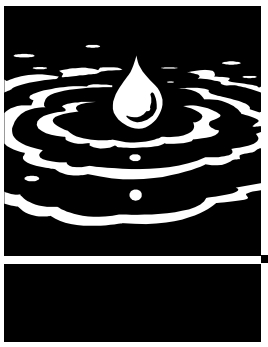

Evaluation of Salt-tolerant Forages for Sequential Reuse Systems

Project Investigators:

Steve Grattan, Team Leader
Office: (530) 752-1130, E-mail: srgrattan@ucdavis.edu,
Department of Land, Air, and Water Resources
University of California, Davis

Catherine Grieve, E-mail: cgrieve@ussl.ars.usda.gov
USDA-ARS Salinity Laboratory
UC Riverside campus

Jim Poss, E-mail: jposs@ussl.ars.usda.gov,
USDA-ARS Salinity Laboratory
UC Riverside campus

Peter Robinson, E-mail: phrobinson@ucdavis.edu,
Department of Animal Science
UC Davis campus

Don Suarez, E-mail: dsuarez@ussl.ars.usda.gov,
USDA-ARS Salinity Laboratory
UC Riverside campus

Sharon Benes, E-mail: sbenes@csufresno.edu,
Department of Plant Science
Cal State University –Fresno campus

Research Staff:

Four UCR students, casual labor (1.5 FTE)

ABSTRACT

Reuse of saline drainage water is a management option on the west side of the San Joaquin Valley (SJV) that is necessary for reducing the volume of drainage water. There are a number of salt-tolerant forages that may play an important role in reducing drainage water volumes in the San Joaquin Valley while at the same time producing a food source for sheep and dairy cattle. Their actual suitability for sequential reuse systems, however, will depend upon their production potential under saline-sodic conditions and their resulting forage quality.

A controlled study using an elaborate sand-tank system was conducted at the US Salinity Laboratory to evaluate a number of promising forage crops including Bermuda grass, 'Salado' and 'SW9720' alfalfa, 'Duncan' and 'Polo' paspalum, Big and Narrow leaf trefoil, Kikuyu grass, 'Jose' Tall wheatgrass, and Alkali sacaton. Forages were irrigated frequently with synthetic drainage waters with an EC of either 15 or 25 dS/m each containing 500 µg/L Se and Mo. Forages were cut periodically to determine cumulative biomass, mineral content, trace elements, and the standard forage quality parameters.

The forage species tested performed differently in terms of biomass accumulation, trace element concentration and ion ratios, and various forage quality parameters, which also varied from cutting to cutting.

Cumulative biomass varied among cultivars as did their relative response to increased salinity. At 15 dS/m, the cumulative biomass for both alfalfa cultivars at 275 days after salinization was substantially higher than the other forages. However as salinity increased to 25 dS/m, 'Jose' tall wheatgrass (JTWG) and Kikuyu grass edged out the alfalfa cultivars after this same 275 day duration due to their higher tolerance to salinity. Increased salinity reduced cumulative biomass of the alfalfa cultivars by nearly half whereas JTWG and Kikuyu grass were only reduced by about 15%.

Forage quality was evaluated based on the forage's potential energy value (i.e. metabolizable energy, ME) using a number of parameters including *in vitro* gas evolution, organic matter content, *in vitro* true degradability, *in vitro* neutral detergent fiber degradability, crude protein and fat content. Increased salinity influenced various forage quality parameters including NDF, OM, gas production and crude protein (CP) but their significance varied among species and cuttings. In nearly all cases when salinity significantly influenced these quality parameters, it did so in a positive manner such that it improved the overall forage quality. At the first cutting, the ME was highest for the alfalfa cultivars and 'Duncan' paspalum. The ME of Narrow leaf trefoil, JTWG, Bermuda grass and 'Polo' paspalum was only slightly lower. By the fifth cutting, the ME value of 'Duncan' declined while that of JTWG increased, equaling that of the alfalfa cultivars. Kikuyu remained as the forage with the least energy value.

Our synthetic saline drainage water containing 0.50 mg/L of both Se and Mo affected the trace element and S concentration in the forages. Although forage tissues were elevated in Se compared to the national average content in forages, concentrations were maintained below the maximum tolerable concentration (MTC) set at 2 mg/kg dw.

Copper nutrition of ruminants is affected not only by the concentration of Cu in the forage material, but the accompanying concentrations of Mo and S as well. The available Cu in the forage is reduced as both the Mo and S increase.

In our forages, the S concentration was either close to or exceeded the MTC set at 0.4% (125 mmol/kg dw). Increased salinity (i.e. increased sulfate), increased S in the alfalfa cultivars. Therefore forages and in particular alfalfa grown in the SJV with high saline-sulfate waters should be evaluated carefully for S effects on animal nutrition.

The concentration of Mo in forage tissue varied dramatically among forage types as did salinity's effect on tissue Mo. The legumes (alfalfa and trefoil species) demonstrated the ability to accumulate the most Mo and accumulated it to concentrations exceeding the MTC which is set at 5 mg/kg dw. The concentration of Mo in the grasses fell into the marginal range (1-3 mg/kg dw) that would induce antagonism with Cu.

Despite alfalfa's high biomass accumulation and energetic forage quality, its niche in saline reuse systems may be limited to very low saline drainage water due to its moderate sensitivity to salinity. Moreover the inorganic forage quality is adversely affected due to combined high S, high

Mo, and moderate concentrations of Cu. It is possible that Cu deficiency or S toxicity could arise in ruminants feeding on alfalfa or any other forage that we tested if irrigated with saline drainage water.

'Jose' tall wheat grass, on the other hand, emerged as a forage with considerable potential. The cumulative biomass was only slightly affected when salinity increased from 15 to 25 dS/m demonstrating salt tolerance. Its forage quality was very good with its ME equivalent to that of alfalfa by the 5th harvest. JTWG also accumulated modest amounts of Mo and maintained S levels below the MTC.

KEYWORDS

Biomass, Drainage reuse, forage quality, molybdenum, salinity, selenium

■ ■ ■ ■ ■

INTRODUCTION

Reuse of saline drainage water is a management option on the west side of the San Joaquin Valley (SJV) that is necessary for reducing the volume of drainage water (San Joaquin Valley Drainage Implementation Program, 2000). Several methods of utilizing saline water (i.e. sequential, cyclic and blending) have been tested experimentally or are being demonstrated under field conditions. Under 'sequential reuse', part of the farm or sub-region is designated as the reuse area. It consists of a sequence of fields, within the boundaries of a farm or an irrigation district that are irrigated with saline drainage water of increasingly higher concentrations. The main purpose is to manage the salt and drainage water on the farm, reduce the area affected by shallow water tables and reduce the volume of drainage water requiring disposal without sacrificing the potential productivity of these lands.

High quality forages for dairy cattle, beef cattle, and sheep are in short supply in the Central Valley. Identifying salt-tolerant forage crops that could grow well under irrigation with saline drainage water would not only increase forage supplies, but could play a key role in drainage water management. Their actual suitability for reuse systems, however, will depend upon their production potential under saline-sodic conditions and their resulting forage quality.

Currently, field studies and field demonstrations are underway to test the feasibility of a few salt-tolerant forages and forage cropping strategies (S. Benes, S. Kaffka, and J.Oster, personal communication) for irrigation with saline-sodic water. Nevertheless a considerable amount of additional research in this area is needed to identify other suitable forages and crops (Oster et al., 1999; San Joaquin Valley Drainage Implementation Program, 2000).

Naturally occurring trace elements in soils in the SJV and in the underlying shallow-groundwater adds a new dimension to the management of saline drainage waters (van Schilfgaarde, 1990). Selenium (Se) and molybdenum (Mo) are trace elements of particular interest. They occur in relatively high concentrations (<1.0 to 5,000 µg/L for Mo and <1.0 to 3,800 µg/L for Se) at many locations in the geochemically mobile and biologically available forms i.e. selenate and molybdate (Deverel et al., 1984).

Due to the presence of these trace elements, there are potential toxicological and nutritional concerns regarding livestock whose diet may rely almost entirely on forage grown with drainage water that contains appreciable levels of these constituents. Selenium and molybdenum are essential nutrient elements for animals; however, the concentration range in forage that would result in deficiency or toxicity to livestock is rather narrow. Selenium toxicity can occur in livestock that graze on forage containing high levels of Se (Rosenfeld and Beath, 1964). Alkali disease is one form of selenosis that can result from ingestion of forage containing as low as 35 mg/kg Se (Klasing and Schenker, 1988). Molybdenosis is a nutritional disorder that ruminant animals, particularly sheep and dairy cows, may develop if the animals feed on forage containing high levels of molybdenum (Barshad, 1948; Ward, 1978). Molybdenosis results from a molybdenum-induced Cu deficiency and is often called a molybdenum-induced hypocuprosis (Mason, 1990). Molybdenum, sulfur and copper have a complex interrelationship (Suttle, 1991). Molybdenum and sulfur combine to form insoluble complexes in the rumen such as thiomolybdates, which effectively reduce that amount of Cu absorbed by the animal (Mortimer et al., 1999).

A number of investigations funded by the UC Salinity/Drainage Task Force showed that sulfate

had a profound influence on reducing selenate and molybdate accumulation in alfalfa and other plants. Therefore, the presence of sulfate in the drainage water may in fact maintain forage quality by preventing excessive accumulation of these potentially toxic elements. Furthermore, saline drainage water applications could increase total digestible nutrients and protein within the forage (Rhoades et al., 1988). On the other hand, high sulfate in the water may increase the sulfur content in the forages to undesirable levels resulting in sulfur toxicity and/or reduced Cu availability. Although forage productivity may be reduced when irrigated with drainage water, we hypothesize that if managed appropriately, the quality and production of forage in well-grazed pastures can be sufficiently maintained to support acceptable rates of livestock growth.

Therefore an interdisciplinary research project was developed involving scientists from the University of California, USDA-ARS, and Cal State University Fresno. The team members have expertise in soils and irrigation management, plant physiology, salinity and plant nutrition, and ruminant nutrition. We conducted a controlled study to evaluate a number of promising forage crops as suitable candidates for drainage water reuse systems.

RESEARCH OBJECTIVES

The overall objective of this study was to evaluate a number of promising forage crops in terms of their production potential and forage quality when irrigated with saline-sodic drainage water, containing selenate and molybdate.

SPECIFIC OBJECTIVES

1. To investigate the interactive effects of saline-sodic drainage water containing SeO_4^{2-} and MoO_4^{2-} on (a) forage production at different salinities and (b) the accumulation, distribution and selected ratios of Se, S, Mo, Cu and other inorganic elements in plant shoots.
2. To assess the effects of saline-sodic drainage water on forage quality (i.e. in-vitro gas evolution, Acid Detergent Fiber (ADF), Total Digestible Nutrients (TDN), Neutral Detergent Fiber (NDF), crude protein, and trace element concentration) in reference to ruminant nutrition. The influence of sequential harvests on forage quality will also be examined.

RESEARCH METHODS

The experiment was conducted in sand-tanks in a greenhouse at the USDA-ARS, George E. Brown, Jr. Salinity Laboratory located on the U. C. Riverside campus. The sand tank system creates a uniform and controlled rootzone such that actual production potentials among forages can be compared. There were 30 large tanks (1.2 m x 0.6 m x 0.5 m deep) filled with washed sand and that had an average bulk density of 1.4 Mg m^{-3}. At saturation, the sand had an average volumetric water content of 0.34 m^3 m^{-3}. Each tank was irrigated with a complete nutrient solution salinized to either 15 or 25 dS/m. The salt solutions were prepared to simulate the composition of typical drainage water in the San Joaquin Valley and from predictions based on appropriate simulations (Suarez and Simunek, 1997) (Table 1). Tanks were irrigated three times daily for a 15 min duration. These irrigations allowed the sand to become completely saturated, after which the solutions drained to 765 L reservoirs below the sand tanks for reuse in the next irrigation. Therefore the salinity of the irrigation water was more or less equivalent to that of the sand water. The irrigation waters were analyzed by inductively coupled plasma optical emission spectrometry (ICPOES) to confirm that target ion concentrations were maintained. Chloride in the solutions was determined by coulometric-amperometric titration.

Water lost by evapotranspiration was replenished automatically to maintain constant volumes and osmotic potentials in the irrigation-treatment waters. A Class I agrometerological station was situated immediately adjacent to the experimental site. Micrometeorological data, including sand and air temperature, pan evaporation, photosynthetically active radiation (PAR), relative humidity, and wind velocity were recorded.

Ten forages were grown in sand tanks at two salinity levels (15 or 25 dS/m) and each treatment was replicated three times. The forage species chosen for this study were: alfalfa (*Medicago sativa*) cvs. 'Salado' and 'SW 9720', narrow leaf trefoil (*Lotus glaber*), big trefoil (*L. ulginosus*), kikuyu grass (*Pennisetum clandestinum*) cv. Whittet, alkali sacaton (*Sporobolus airoides*), paspalum (*Paspalum vaginatum*) cvs. 'Polo' and 'Duncan', tall wheatgrass (*Agropyron elongatum*) cv. 'Jose', and bermuda grass (*Cynodon dactylon*) cv. 'Tifton'. The date of planting, the source of the

material and the date salinization began are provided in Table 2. In each tank, two different forages were planted in a 0.6 x 0.6 m area, separated by a plastic partition extending ~8" below and 4" above the surface of the sand. With the exception of bermuda grass, all species were well-established in the tanks by irrigation with complete nutrient solution (EC_w) prior to application of salinity.

Shoots were sampled periodically from Sept 2000 to Aug 2001. Harvest scheduling depended on growth pattern of the forage in question. For example, alfalfa cultivars were sampled at first flowering; alkali sacaton, kikuyu, tall wheatgrass, on plant height; the trefoils, paspalums, and bermudagrass on biomass production. At each harvest, herbage was cut 2 to 4" above the surface of the sand. Shoot material was weighed, washed in deionized water, dried in a forced-air oven at 70°C for 72 hr. Statistical analyses were performed by analysis of variance with mean comparisons at the 95% level based on Tukey's studentized range test.

Dry-ground forage material was analyzed for a number of inorganic constituents including Ca, Cu, Mg, Mo, Na, K, P, N, Cl, S, B, Se and Mo. Total-S, total P, Ca^{2+}, Mg^{2+}, Na^{+}, and K^{+} were determined on nitric-perchloric acid digests of the tissues by ICPOES. Chloride was determined on nitric-acetic acid extracts by coulometric-amperometric titration. For tissue Se analysis, the method described by Briggs and Crock (1986) was followed.

In vitro gas production was carried out using 30 ml of buffered rumen fluid according to the *in vitro* gas method of Menke et al. (1979). Approximately 200 mg sample was incubated in water bath at 39°C and gas production at 24 h was recorded and corrected for blank incubation (buffered rumen fluid with no sample). Organic matter (OM) was determined according to Association of Official Analytical Chemists (AOAC, 1990). *In vitro* true degradability (IVTD), neutral detergent fiber (NDF), and *in vitro* neutral detergent fiber degradability (dNDF) were determined by incubating the samples in multi-layer polyethylene polyester cloth bags (F57 filter bag; ANKOM, NY) as described by Robinson et al. (2000).

Forage quality determinations were statistically analyzed as a factorial experiment with salinity, forage, cut and the forage by harvest interaction as factors in the model. In a number of forage nutritive value descriptors, the cut by forage interaction was statistically significant (i.e., $P<0.05$). Therefore forages were statistically analyzed within cuts and data presented represent all forages that were cut once, thrice and five times.

RESULTS AND DISCUSSION

BIOMASS ACCUMULATION

Shoot biomass accumulation is shown in relation to days after salinization (Figures 1-10). There are a couple important features that can be derived from these graphs.

First, the biomass accumulation represents potential accumulation under field conditions if the average rootzone salinity of the soil water is either 15 or 25 dS/m. However under field conditions, the salinity of the soil is often expressed as the average rootzone salinity of the saturated soil extract (ECe). As a rule of thumb, the ECe is about half the ECsw (soil water EC). Moreover, there may be additional stresses under field conditions that could affect plant growth such as anoxia, increased soil strength or pathogenic pressures such as phytophthora.

We have ranked the forage production potential based on cumulative biomass production (kg/ha dw) at 275 days after salinization. At 15 dS/m, both alfalfa cultivars 'SW 9720' and 'Salado' were the greatest biomass producers (i.e. > 20,000 kg dw/ha). 'Duncan' paspalum, 'Jose' Tall wheatgrass, and Kikuyu grass fall into the next largest biomass class (i.e. 15,000-17,000 kg dw/ha). Bermuda grass, Narrow leaf trefoil and 'Polo' paspalum fall into the third largest group (i.e. 8,000-11,000 kg dw/ha) and Big trefoil was in a class by itself as the lowest biomass producer (i.e. < 2,000 kg dw/ha).

At 25 dS/m, the ranking differed slightly: JTWG = Kikuyu $\geq$ 'SW 9720' alfalfa $\geq$ 'Salado' alfalfa > Bermuda grass = 'Duncan' paspalum > 'Polo' paspalum = Narrow leaf trefoil. Big trefoil died at the 25 dS/m salinity level.

The second important feature in the figures is the relative difference in the slopes (cumulative biomass in relation to time) between the 15 and 25 dS/m treatments. The smaller the ratio of slope at 25 / slope at15 dS/m, the more sensitive the crop is to salinity between 15 to 25 dS/m. In this study, with the exception of Big trefoil that died at 25

dS/m shortly after salinization, both alfalfa cultivars are among the most salt-sensitive along with perhaps Narrowleaf trefoil (slopes 0.52-0.59). 'Duncan' paspalum also showed sensitivity to salinity (slope 0.64). The other forages show considerably more tolerance to this synthetic drainage water (slopes 0.85-0.90). This ranking is consistent with the ranking by Maas and Grattan (1999) for those forages whose tolerances have been documented (i.e. all but the paspalums and kikuyu grass). These differences in salt tolerance suggest that the performance rankings would differ from those given above should the salinity increase further. Therefore the alfalfa cultivars grew vigorously at these salinity levels (i.e. accumulated high biomass at both salinities) despite showing less overall tolerance to salinity.

It is also important to emphasize that these production functions reflect production potentials when the average root zone salinity of the soil water is 15 and 25 dS/m. If one assumes that the soil water salinity is about twice that of the saturated soil extract, corresponding average root zone salinities would be 7.5 and 12.5 dS/m. Since soil salinities in reuse systems in the SJV can readily exceed 12.5 dS/m, caution is advised is selecting cultivars whose biomass was reduced substantially as salinity increased (i.e. the legumes).

FORAGE QUALITY

The potential nutritive value of the forages was evaluated based on their content of organic matter (OM), neutral detergent fiber (NDF), *in vitro* (at 30 h) digestible NDF (dNDF), *in vitro* (at 30 h) true digestibility (IVTD) and *in vitro* (at 24 h) gas evolution. The NDF is an estimate of the cell wall minus pectin and the dNDF is a measure of the NDF that is digestible in vitro at 30 h. The gas evolution at 24 h *in vitro* estimates digestion when fed to cows at a high level of production and is used later is estimate energy value. In general the quality or energy value of the forage increases as: OM increases, NDF decreases, dNDF increases, IVTD increases and as Gas production increases.

All forage quality parameters at each of the three cuttings were significantly different among the species tested (P< 0.001). Salinity, on the other hand, had differential effects depending upon the species, forage quality parameter and harvest date.

At the first cutting, the OM content of Bermuda grass was higher at 25 dS/m than it was at 15 dS/m, but the reverse was true for Big trefoil (P<0.05) (Table 3). The NDF levels of 'Salado' alfalfa, Big trefoil and 'Jose' Tall Wheatgrass (JTWG) were lower (P<0.05) when grown at 25 dS/m vs. 15 dS/m, but the opposite was true for bermuda grass (P<0.05). The digestibility of NDF (i.e. dNDF) and the *in vitro* digestibility of DM (IVTD) were not influenced by salinity. However gas production, an indicator of the energy value, was higher (P<0.05) in JTWG and Kikuyu grass at 25 dS/m as compared to material from the 15 dS/m treatment. The overall metabolizable energy (ME) for the forages was not significantly influenced by salinity except JTWG where salinity increased energy value.

In the third cutting, increased salinity generally increased OM content (P<0.01) and reduced the NDF value (P<0.001) (Table 4). Increased salinity tended to decrease fat content (i.e. ether extract, EE) (P<0.05) but this effect was slight. Other nutritive descriptors were not influenced by the salinity of the applied water except in 'Salado' alfalfa where increased salinity increased the metabolizable energy (P<0.05).

At the fifth harvest, as salinity increased from 15 to 25 dS/m, the OM and CP content in the forages increased (P<0.05) (Table 5). The NDF content of 'SW 9720' alfalfa was lower (P<0.05), and the gas production was higher (P<0.05), for 25 dS/m vs. 15 dS/m material. This translated into a significantly higher metabolizable energy (P<0.05) in 'SW 9720' alfalfa grown at the higher salinity level. NDF digestibility and IVTD were not influenced by the salinity of the applied water.

Salinity therefore influenced various forage quality parameters including NDF, OM, gas production, ME and crude protein (CP) but their significance varied among species and cuttings. Whenever salinity significantly influenced these quality parameters, it did so in a positive manner such that it improved forage quality. The only exceptions were NDF for Bermuda and OM in Big trefoil during the first cutting.

The ability to compare forages per se is limited statistically and we did not test for significant differences among forages between quality descriptors. Nevertheless, based on our forage quality results for the first, third and fifth cuttings, the quality rankings based on overall metabolic energy values (i.e. ME) from highest to lowest as a first approximation are:

First Cut:

'Duncan' Paspalum = 'Salado' alfalfa = 'SW 9720' alfalfa ≥ Narrowleaf Trefoil ≥ JTWG = Bermuda grass = 'Polo' Paspalum = Alkali Sacaton > Big Trefoil > Kikuyu grass

Third Cut:

Narrow leaf Trefoil = 'Salado' alfalfa ≥ 'SW 9720' alfalfa = JTWG > Bermuda grass = Alkali Sacaton > 'Duncan' Paspalum ≥ Kikuyu grass = 'Polo' Paspalum = Big Trefoil

Fifth Cut:

JTWG = 'Salado' alfalfa = 'SW 9720'alfalfa >> 'Duncan' Paspalum = 'Polo' Paspalum = Bermuda grass > Alkali Sacaton > Kikuyu grass

ION RELATIONS

Plant performance may be adversely affected by salinity-induced nutrient imbalances that result from the effect of salinity on nutrient availability, competitive uptake, transport and partitioning within the plant (Grattan and Grieve, 1999a; 1999b). Most of these interactions are directly related to the concentration and ratios of ions in the rootzone. Ion compositions typically present in saline agricultural effluents in the SJV often result in extreme or unusual ratios of Na^+/Ca^{2+}, Na^+/K^+, Mg^{2+}/Ca^{2+}, Cl^-/NO_3^-, and SO_4^{2-}/Cl^-. The influence of these external ion ratios on ion accumulation by salt-stressed plants is complex.

As has been our experience with other crops irrigated with high sodium-high sulfate saline waters, none of the forages examined in this study showed symptoms associated with adverse ion interactions, deficiencies, or toxicities. However, the forages, in many cases, exhibited unique ion uptake patterns that were unexpected based on our previous studies, and these results will require further investigation. A manuscript is in preparation that discusses ion relations in these forages in much detail. With the exception of sulfur, relations of major ions will not discussed in this report.

SULFUR AND TRACE ELEMENT RELATIONS

Sulfur is an essential macronutrient for animals but too much can reduce feed intake and growth rate. The National Research Council set the maximum tolerable concentration (MTC) of sulfur in forage at 0.40 % dw (125 mmol/kg dw)(Mortimer et al., 1999). Animal diets that contain considerably higher concentrations than this can lead to restlessness, muscle twitching and diarrhea (Mortimer et al., 1999).

In all instances the S concentration in our forages either came close to or exceeded this MTC (Table 6). In many cases, S greatly exceeds the MTC, particularly Big Trefoil and the Paspalum species. Alfalfa was the next largest S accumulator.

The salt-stressed forages present several species-specific patterns regarding shoot-S accumulation. As salinity increased from 15 to 25 dS/m, sulfate in the treatment increased from 112 to 195 mmol/L, yet tissue S only increased significantly and consistently in the alfalfa cultivars. Although cattle can tolerate more S from natural feed ingredients than from supplemental sulfate (McDowell, 1985), alfalfa grown under irrigation with high-sulfate waters should be evaluated carefully for S effects on animal nutrition. Sulfur concentrations in the grasses, on the other hand, did not increase with increased salinity in nearly all cases.

In no cases was 0.50 mg/L Se in the substrate found to elevate forage Se concentrations above the maximum tolerable concentration of 2 mg/kg dw (Minson, 1990; Mortimer et al.,1999) (Table 6). It is very likely that the high levels of substrate sulfate, characteristic of SJV drainage waters, suppress the uptake selenate.

Increased salinity (i.e. increased sulfate), affected forage Se concentration differently (Table 6). In most cases (eg Bermuda grass, Kikuyu grass, 'salado' alfalfa, alkali sacaton and JTWG it reduced the Se content as would be expected. However increased salinity did not affect forage Se concentration in 'SW9720' alfalfa, 'Polo' paspalum and the trefoils while it increased tissue Se in 'Duncan' paspalum.

The concentration of Mo in forage tissue varied dramatically among forage types as did salinity's effect on tissue Mo. The legumes (alfalfa and trefoil species) accumulated the most Mo. In most cases they accumulated Mo to concentrations exceeding the MTC which is set at 5 mg/gk dw (Mortimer et al., 1999). The concentration of Mo in all the forages at least fell into the marginal range (1-3 mg/kg dw) that would induce antagonism with Cu. Equally interesting was salinity's effect on forage Mo concentration and how dramatically it varied from

harvest to harvest. For example, at the first harvest, increased salinity markedly reduced shoot Mo concentration in alfalfa from 137 and 42 mg/kg to 2 mg/kg for cultivars 'salado' and 'SW 9720', respectively. However for the 2nd and 3rd harvests, increased salinity had the opposite effect. Regarding the other forages, increased salinity either increased, decreased and had no effect on tissue Mo concentration.

High Mo concentration in forages is usually associated with molybdenum- induced Cu deficiency (i.e. hypocuprosis) but high Mo concentration in itself can be problematic (i.e. molybdenosis) (Suttle, 1991). Copper deficiency in ruminants can cause a number of disorders including depressed growth, temporary infertility, weak bones and even heart failure (McDowell, 1985; Suttle, 1991).

Copper nutrition of ruminants is complicated by a complex interaction with Mo and S (McDowell, 1985 and Suttle, 1991. As Mo and S increase in the forage, the percentage of Cu available to the animal is reduced substantially due to the formation of unabsorbable thiomolybdate complexes (Suttle, 1991).

The concentration of Cu in the forage tissue varied somewhat among species. Bermuda grass and the paspalum species accumulated the most Cu. The alfalfa species, on the other hand, accumulated the least and fell within the marginally deficient category (Mortimer et al., 1999). This marginal Cu concentration coupled with accompanying high concentrations of S and Mo would likely result in a copper deficiency within the animal, should dietary Cu supplements not be provided.

Increased salinity had very little impact on forage Cu concentration. In a few instances, increased salinity reduced Cu concentration where the most notable case was the first cutting of Bermuda grass.

The copper concentration in our forages (Table 6) is at least equal to or greater than average concentrations found in forages (Minson, 1990). Concentrations range from 4 to >20 mg/kg dw. Nevertheless due to the accompanying high concentrations of both Mo and S, it is likely that ruminants would suffer from Cu deficiency should they be dependent on only this diet without Cu supplementation oral Cu boluses or Cu injections (Suttle, 1991).

The Cu/Mo ratio in the forage is also an important indicator of the potential Cu-deficiency hazard of the forage. For example in the presence of adequate S, Cu/Mo ratios less than 2.8 in forages can result in Cu-deficiency (McDowell, 1985). The legumes in our study had ratios less than one in nearly all cases suggesting that Cu deficiency is likely if animals rely on such a diet and preventative measures are not taken.

Since antagonistic ions such as sulfur and molybdenum are found in our forage tissue in high concentrations, it is likely that the fraction of available Cu to the animal is reduced substantially. The alfalfa cultivars create perhaps the greatest potential of Cu-deficiency in animals due to the combined high Mo and S concentrations and relatively low Cu concentrations. It is suggested that when antagonistic ions are present at relatively high levels that the best way of monitoring animal Cu status is not through analysis of the forage sample but rather monitoring the animals themselves through tissue samples such as liver biopsies (Mortimer et al 1999).

CONCLUDING COMMENTS

Selecting forages that are suitable for SJV drainage water reuse systems is somewhat complicated by variable salinities, different drainage water compositions and different locations of intended reuse. Therefore some forages may be the more suitable in one case while others are most suitable in another.

Despite alfalfa's high biomass accumulation and energetic forage quality, its niche in saline reuse systems may be limited to very low saline drainage water due to its moderate sensitivity to salinity. Moreover the inorganic forage quality is adversely affected due to combined high S, high Mo, and moderate concentrations of Cu. It is possible that Cu deficiency or S toxicity could arise in ruminants feeding on alfalfa or any other forage that we tested if irrigated with saline drainage water.

'Jose' tall wheat grass, on the other hand, emerged as a forage with considerable potential. The cumulative biomass was only slightly affected when salinity increased from 15 to 25 dS/m demonstrating salt tolerance. Its forage quality was very good with its ME equivalent to that of alfalfa by the 5th harvest. JTWG also accumulated modest amounts of Mo and maintained S levels below the MTC.

CURRENT STUDY

An experiment is currently underway at the USDA-ARS, George E. Brown, Jr. Salinity Laboratory using outdoor sand tanks to examine the inter-relationships between osmotic (i.e. salt) and matric (i.e. water) stresses on forage growth, ET, leaching, and a number of other parameters. Two forages that performed well in the first experiment (i.e. 'Jose' Tall wheatgrass and "Salado' alfalfa) were selected. These forages will be grown at different salinities and fractions of ET measured directly in the low saline, well-watered treatment.

The sand-tank lysimeter system has been modified by P. Shouse, J. Poss, R. Austin, W. Russell (USSL) and is highly instrumented with tensiometers, neuron probe access tubes, salinity 4-probes, pressure transducers in the storge tanks and a data acquisition system. The system applies a very even "film" of irrigation water approximately 1 cm deep during a one-minute irrigation cycle (about 30 liters) that minimizes bypass and provides an even vertical wetting front.

The data acquisition system measures sensors ten times every hour. The pressure transducers on the reservoirs monitor irrigation solution dynamics including irrigation volumes, drainage volumes, refill estimates of evapotranspiration, and transducers instrumented into soil tensiometers to measure the soil water matric potential. The sensors download into a central datalogger that is equipped with a modem to transmit the data from external computers. Two central data loggers are used: the sensor system and the weather station to monitor input variables needed to calculated estimates of evapotranspiration calculated from a modified Penman equation.

■ ■ ■ ■ ■

REFERENCES

AOAC (Association of Official Analytical Chemists International. 1990. Official Methods of Analysis. 15th ed. AOAC, Arlington, VA.

Barshard, I. 1948. Molybdenum content of pasture plants in relation to toxicity to cattle. Soil Sci. 66: 187-195.

Briggs, P. H. and J. G. Crock. 1986. Automated determination of total selenium in rocks, soils, and plants. U. S. Department of Interior, Geological Survey. Report 86-40.

Deverel, S.J.,R.J. Gilliom, R. Fujii, J.A. Izbicki and J.C. Fields. 1984. Aereal distribution of selenium and other inorganic constituents in shallow groundwater of the San Luis Drain Service Area, San Joaquin Valley, California: a preliminary study. U.S. Geol. Surv. Water-Resour. Invest. Rep. 84, 4319.

Grattan, S. R. and C. M. Grieve. 1999a. Salinity-mineral nutrient relations in horticultural crops. Sci. Hort. 78:127-157.

Grattan, S. R. and C. M. Grieve. 1999b. Mineral nutrient acquisition and response by plants grown in saline environments. pp. 203-229. In: Handbook of Plant and Crop Stress. M. Pessarakli (ed.). Marcel Dekker, Inc. New York.

Klasing, S.A. and M.B. Schenker. 1988. Public health implications of elevated dietary selenium. In K.K. Tanji ed, Selenium contents in animal and human food crops grown in California. Division of Agriculture and Natural Resources. Publication # 3330 pp 3-10.

Maas, E. V. and S. R. Grattan. 1999. Crop yields as affected by salinity. In R. W. Skaggs and J. van Schilfgaarde (eds) Agricultural Drainage. Agron. Monograph 38. ASA, CSSA, SSA, Madison, WI pp. 55-108.

Mason, J. 1990. The biochemical pathogenesis of molybdenum-induced copper deficiency syndromes in ruminants: towards the final chapter. Irish Veterinary J. 43(1): 18-20.

McDowell, L. R. 1985. Nutrition of Grazing Ruminants in Warm Climates, Academic Press. New York.

Menke, K. H., Raab, L., Salewski, A., Steingass, H., Fritz, D., Schneider, W., 1979. The estimation of the digestibility and metabolizable energy content of ruminant feedingstuffs from the gas production when they are incubated with rumen liquor *in vitro*. J. Agric. Sci. Camb. 93, 217-222.

Minson, D. J. 1990. Forage in Ruminant Nutrition. Academic Press. New York

Mortimer, R.G., D.A. Dargatz and L.R. Corah. 1999. Forage analyses from Cow/Calf Herds in 23 states. USDA:APHIS:VS, Centers for Epidemiology and Animal Health. Fort Collins, CO #N303.499

Oster, J.D., S.R. Kaffka, M.C. Shannon and S.R. Grattan. 1999. Saline-sodic drainage water: A resource for forage production? Proceeding of 17th International Congress on Irrigation and Drainage. 11-19 Sept., Granada, Spain.

Rhoades, J.D., Bingham, F.T., Letey, J., Dedrick, A.R., Bean, M, and G.J Hoffman, Alves, W.J., Swain, R.V. Pacheco, P.G. and Lemert, R.D. (1988). Reuse of drainage water for irrigation: Results of Imperial valley study. *Hilgardia* 56:1-45.

Robinson, P.H. , Mathews, C and Fadel, J. G. 2000. Influence of storage time and temperature on *in vitro* digestion of neutral detergent fibre at 48 h, and comparison to 48 h in sacco neutral detergent fibre digestion. Animal Feed Sci, and Technology 80:257-266.

Rosenfeld, I. and O.A. Beath. 1964. Selenium: Geobotany, biochemistry, toxicity and nutrition. Academic Press, New York.

San Joaquin Valley Drainage Implementation Program. 2000. Evaluation of the 1990 Drainage Management Plan for the Westside San Joaquin Valley, California. Final Report submitted to the Management Group of the an Joaquin Valley Drainage Implementation Program (SJVDIP). January, 2000. SJVDIP and University of California Ad Hoc Coordination Committee 87pp

Suarez, D.L. and J. Simunek, 1997. UNSATCHEM: Unsaturated water and solute transport model with equilibrium and kinetic chemistry. Soil Sci. Soc. Am. J. 61:1633-1646.

Suttle, N.F. 1991. The interactions between copper, molybdenum and sulphur in ruminant nutrition. Annu. Rev. Nutr. 11:121-140

van Schilfgaarde, J. 1990. Irrigation agriculture: is it sustainable? In: K.K. Tanji, ed. Agricultural Salinity Assessment and Management ASCE Manu Rep Practices 71 pp 584-594.

Ward, G. M. 1978. Molybdenum toxicity and hypocuprosis in ruminants: A review. J. Animal Sci. 46: 1078-1085

PUBLICATIONS AND REPORTS

Grattan, S., C. Grieve, J. Poss, P. Robinson, D. Suarez and S. Benes. 2002. Reuse of saline-sodic drainage water for irrigation in California: Evaluation of potential forages. Proceedings of the 17th World Congress of Soil Science. 14-21 August 2002. Bangkok, Thailand

Table 1. Ionic composition of the simulated drainage water treatments. Both means and standard errors (se) are provided.

Salinity		Ca $mmol_c$ /L	Mg $mmol_c$ /L	Na $mmol_c$ /L	K $mmol_c$ /L	S $mmol_c$ /L	Cl $mmol_c$ /L	B mg/L	Se mg/L	Mo mg/L
15 dS/m										
		24.2	28.8	126	3.7	112	57.8	0.25	0.50	0.50
	se	0.3	0.2	1	0.3	0.6	0.6			
30 dS/m		23.8	55.3	246	4.7	195	106	0.25	0.50	0.50
	se	0.3	0.3	4	0.2	2	3			

Table 2. Schedule for planting and salinization, and number of harvests of forages grown in greenhouse sand cultures irrigated with saline waters.

Forage	Planting Date	Salinization Date	First Harvest	Number of Harvests
Alfalfa, 'Salado'	07-17-00*	08-14-00	09-11-00	12
Alfalfa 'SW 9720'	07-17-00*	08-14-00	09-11-00	12
Narrowleaf Trefoil	07-17-00*	08-25-00	09-20-00	7
Big Trefoil	07-17-00*	08-25-00	09-20-00	3
Tall Wheatgrass 'Jose'	07-28-00*	08-25-00	09-20-00	10
Kikuyu grass	08-03-00*	09-19-00	09-19-00	10
Alkali Sacaton	07-28-00*	08-25-00	09-20-00	8
Paspalum 'Polo'	08-31-00†	01-18-01	01-18-01	5
Paspalum 'Duncan'	08-31-00†	01-18-01	01-18-01	5
Bermuda grass 'Tifton'	01-22-01 †‡	01-22-01	01-18-01	6

*Seeded
†Sprigs
‡Planted in pre-salinized sand tanks

Table 3. Effect of salinity level on nutritive value of different species of forages at the first cut.

Forage species	Salinity	OM	CP	EE	NDF	IVTD	dNDF	Gas	ME
	(ds/m)	(% DM)					(% NDF)	(ml/200 mg DM)	(MJ/kg DM)
Alfalfa 'salado'	15	88.8	20.4	3.2	31.6a	84.3	50.4	47.7	9.9
	25	88.7	28.8	3.4	26.5b	86.7	49.8	45.8	10.1
Alfalfa 'SW 9720'	15	88.5	23.9	3.4	34.1	81.7	47.5	43.9	9.6
	25	88.5	30.2	3.3	25.1	87.2	49.6	46.6	10.3
Alkali sacton	15	86.6	25.9	4.4	55.8	75.3	55.6	41.7	9.4
	25	87.4	25.4	5.1	53.9	79.3	61.6	40.2	9.2
Bermuda grass	15	87.5b	23.2	2.8	55.9b	81.8	67.3	43.2	9.4
	25	89.3a	21.1	2.2	60.9a	78.3	64.4	44.1	9.4
'Big' trefoil	15	82.4a	23.2a	2.7	19.1a	92.3	59.8	36.0	8.5
	25	77.4b	18.5b	2.3	16.1b	93.7	61.0	34.9	8.0
'Duncan' paspalum	15	88.0	13.6	1.6	59.9	89.0	81.7	55.3	10.5
	25	86.0	12.9	1.7	59.7	87.9	79.9	53.3	10.2
'Jose' tall wheat grass	15	86.2	30.6b	6.6	46.2a	89.6	77.4	37.3b	9.1b
	25	87.1	33.4a	7.7	43.5b	89.9	76.9	41.0a	9.8a
Kikuyu grass	15	82.6	26.5	2.9	49.5	78.3	56.1	19.8	6.4
	25	84.0	27.9	2.8	43.9	80.2	55.2	17.7	6.2
'Narrow leaf' trefoil	15	87.5	26.3	2.9	25.1	88.9	55.8	44.1	9.7
	25	88.0	28.2	3.0	22.9	89.7	54.8	43.8	9.8
'Polo' paspalum	15	87.3	16.4	2.0	53.8	86.5	75.0	45.9	9.4
	25	86.5	18.4	2.5	51.8	85.9	72.8	42.8	9.1
SEM		0.27	0.52	0.10	0.53	0.59	1.20	0.95	0.13
Salinity		NS	*	NS	***	NS	NS	NS	NS
Species		***	***	***	***	***	***	***	***
Salinity X Species		**	**	NS	**	NS	NS	NS	NS

OM, organic matter; CP, crude protein; EE, ether extract; NDF, neutral detergent fiber; IVTD, in vitro true digestibility; dNDF, digestible fiber; ME, metabolizable energy

Different letters between salinity levels within species indicate significant difference ($P < 0.05$).
*, $P < 0.05$; **, $P < 0.01$; ***, $P < 0.001$; NS, not significant.

Table 4. Effect of salinity level on nutritive value of different species of forages at the third cut.

Forage species	Salinity	OM	CP	EE	NDF	IVTD	dNDF	Gas	ME
	ds/m	(% DM)					(% NDF)	(ml/200 mg DM)	(MJ/kg DM)
Alfalfa 'salado'	15	87.9	27.9	3.4	25.5	88.7b	55.4	42.3b	9.6b
	25	88.3	27.5	2.7	22.4	90.1a	55.9	46.7a	10.2a
Alfalfa 'SW 9720'	15	88.2	24.9	2.6	31.1	85.9	56.6	43.0	9.5
	25	88.2	22.3	2.4	24.3	89.3	56.3	46.3	9.8
Alkali sacton	15	87.9	16.4	3.0	59.8	67.8	46.0	40.6	8.7
	25	88.4	17.9	2.9	59.4	71.9	52.7	42.4	9.0
Bermuda grass	15	89.1b	25.8	2.0	57.4	82.2	69.1	38.8	9.0
	25	89.4a	24.1	1.7	57.7	79.1	64.1	37.5	8.7
'Big' trefoil	15	85.1	19.8	2.8	22.9	79.9	12.0	33.7	8.0
	25	-	-	-	-	-	-	-	-
'Duncan' paspalum	15	85.9	13.0	1.8	58.8	78.6	63.7	40.2a	8.4
	25	86.2	15.3	2.0	57.3	79.6	64.4	37.7b	8.2
'Jose' tall wheat grass	15	84.4b	20.3b	3.9	46.1a	88.8	75.7	45.5a	9.6
	25	86.5a	30.8a	3.2	40.2b	90.9	77.2	41.6b	9.6
Kikuyu grass	15	83.3b	22.5	2.5	48.0a	84.8	68.4	33.6	8.1
	25	84.4a	25.6	2.6	40.6b	88.0	70.4	29.5	7.7
'Narrow leaf' trefoil	15	85.3	27.3	3.7	22.6	92.1	65.1	49.0	10.5
	25	85.9	27.2	3.7	21.8	91.4	60.5	49.9	10.6
'Polo' paspalum	15	85.1	16.1	2.8	57.3	77.9	61.6	33.9	7.7
	25	84.8	17.4	2.6	55.5	81.3	66.3	36.0	8.1
SEM		0.12	0.66	0.08	0.56	0.75	1.40	0.75	0.09
Salinity		**	NS	*	***	NS	NS	NS	NS
Species		***	***	***	***	***	***	***	***
Salinity X Species		*	*	NS	*	NS	NS	NS	NS

OM, organic matter; CP, crude protein; EE, ether extract; NDF, neutral detergent fiber; IVTD, in vitro true digestibility; dNDF, digestible fiber; ME, metabolizable energy

Different letters between salinity levels within species indicate significant difference ($P < 0.05$).
*, $P < 0.05$; **, $P < 0.01$; ***, $P < 0.001$; NS, not significant.

Table 5. Effect of salinity level on nutritive value of different species of forages at the fifth cut.

Forage species	Salinity	OM	CP	EE	NDF	IVTD	dNDF	Gas	ME
	(ds/m)	(% DM)					(% NDF)	(ml/200 mg DM)	(MJ/kg DM)
Alfalfa 'salado'	15	87.5b	28.2	4.5	25.2	89.4	57.2	45.9	10.1
	25	88.6a	29.4	4.4	22.2	90.7	58.2	48.1	10.5
Alfalfa 'SW 9720'	15	87.8	27.0	4.2	27.6a	88.9	59.8	43.9b	9.8b
	25	88.4	27.6	4.0	24.3b	89.4	56.6	48.9a	10.5a
Alkali sacton	15	90.3	12.7b	2.4	64.0	69.6	52.5	35.8	7.8
	25	88.7	15.9a	2.7	62.0	71.1	53.3	35.7	8.0
Bermuda grass	15	89.1b	8.0b	1.7b	65.2	67.6	50.3	41.3	8.3
	25	90.6a	10.8a	2.2a	66.6	67.3	50.9	41.7	8.5
'Big' trefoil	15	-	-	-	-	-	-	-	-
	25	-	-	-	-	-	-	-	-
'Duncan' paspalum	15	86.8	11.4	2.3	57.4	76.8	59.6	41.6	8.5
	25	87.2	11.6	2.4	59.4	77.6	62.3	40.9	8.5
'Jose' tall wheat grass	15	86.3	33.2	5.2a	42.2	91.9	80.7	45.7	10.4
	25	87.3	31.3	4.3b	44.2	90.6	78.8	48.0	10.6
Kikuyu grass	15	82.6b	29.3	3.2	44.6	82.0	59.7	27.9	7.7
	25	83.8a	29.5	3.4	43.3	77.3	47.9	22.2	6.9
'Narrow leaf' trefoil	15	-	-	-	-	-	-	-	-
	25	-	-	-	-	-	-	-	-
'Polo' paspalum	15	86.6	13.2	2.6	59.0	79.8	65.8	39.2	8.3
	25	87.5	12.9	2.6	58.7	78.5	63.4	40.6	8.5
SEM		0.23	0.24	0.06	0.36	0.68	1.38	0.64	0.09
Salinity		*	*	NS	NS	NS	NS	NS	NS
Species		***	***	***	***	***	***	***	***
Salinity X Species		NS	**	**	*	NS	NS	NS	NS

Different letters between salinity levels within species indicate significant difference (P<0.05).
*, P < 0.05; **, P< 0.01; ***, P < 0.001; NS, not significant.

OM, organic matter; CP, crude protein; EE, ether extract; NDF, neutral detergent fiber; IVTD, in vitro true digestibility; dNDF, digestible fiber; ME, metabolizable energy

Table 6. Cu/Mo ratios, S and trace element concentrations in forages from the first three harvests.

Shoot Se Concentration (mg/kg dw)

Harvest 1

	Big Trefoil	Narrow Trefoil	Polo Paspalum	Duncan Paspalum	Jose Tall Wheatgrass	Sacaton	Salado Alfalfa	SW9720 Alfalfa	Kikuyu Grass	Bermuda Grass
EC 15	2.17a	0.71a	1.56a	0.60b	0.94a	1.73a	1.34a	0.98a	1.81a	0.65a
EC 25	1.45a	0.67a	1.50a	1.10a	0.19b	0.81b	0.89b	0.94a	0.86b	0.39b

Shoot Cu Concentration (mg/kg dw)

Harvest 1

	Big Trefoil	Narrow Trefoil	Polo Paspalum	Duncan Paspalum	Jose Tall Wheatgrass	Sacaton	Salado Alfalfa	SW972 0 Alfalfa	Kikuyu Grass	Bermuda Grass
EC 15	5.55a	5.81a	15.20a	31.80a	17.67a	15.70a	12.91a	10.73a	19.90a	66.50a
EC 25	4.47a	6.13a	13.33a	22.27 b	15.93a	11.43a	14.27a	9.58a	20.87a	16.97 b

Harvest 2

	Big Trefoil	Narrow Trefoil	Polo Paspalum	Duncan Paspalum	Jose Tall Wheatgrass	Sacaton	Salado Alfalfa	SW9720 Alfalfa	Kikuyu Grass	Bermuda Grass
EC 15	12.39	6.51a	16.70a	15.43a	10.63a	13.67a	7.12 b	7.58a	15.17a	18.87a
EC 25		6.82a	15.07a	23.00a	10.50a	14.57a	8.45a	8.41a	8.51a	25.10a

Harvest 3

	Narrow Trefoil	Polo Paspalum	Duncan Paspalum	Jose Tall Wheatgrass	Sacaton	Salado Alfalfa	SW9720 Alfalfa	Kikuyu Grass	Bermuda Grass
EC 15	12.40a	16.20a	19.87a	12.82a	13.93a	5.85a	5.63a	10.56a	20.60a
EC 25	7.97 b	18.37a	23.37a	13.49a	15.57a	6.60a	6.61a	12.20a	16.00a

Shoot Mo Concentration (mg/kg dw)

Harvest 1

	Big Trefoil	Narrow Trefoil	Polo Paspalum	Duncan Paspalum	Jose Tall Wheatgrass	Sacaton	Salado Alfalfa	SW9720 Alfalfa	Kikuyu Grass	Bermuda Grass
EC 15	128.67a	37.63a	2.99a	2.05a	2.98a	3.54 b	136.60a	42.40a	5.03a	4.41a
EC 25	144.00a	42.83a	3.12a	2.42a	3.17a	5.64a	2.45 b	1.87 b	3.84a	2.28 b

Harvest 2

	Big Trefoil	Narrow Trefoil	Polo Paspalum	Duncan Paspalum	Jose Tall Wheatgrass	Sacaton	Salado Alfalfa	SW9720 Alfalfa	Kikuyu Grass	Bermuda Grass
EC 15	128.37	49.40a	2.82a	1.67a	3.93 b	1.21a	13.20 b	14.13 b	3.38a	4.84a
EC 25		57.03a	3.00a	1.74a	5.53a	0.96a	23.93a	27.33a	2.57a	3.84a

Harvest 3

	Narrow Trefoil	Polo Paspalum	Duncan Paspalum	Jose Tall Wheatgrass	Sacaton	Salado Alfalfa	SW9720 Alfalfa	Kikuyu Grass	Bermuda Grass
EC 15	99.47a	2.87a	1.92a	2.77 b	1.88a	6.76 b	5.99 b	2.34a	6.80a
EC 25	49.80 b	3.22a	1.85a	4.49a	1.39 b	23.23a	30.27a	2.32a	3.56a

Shoot Cu/Mo Ratio

Harvest 1

	Big Trefoil	Narrow Trefoil	Polo Paspalum	Duncan Paspalum	Jose Tall Wheatgrass	Sacaton	Salado Alfalfa	SW9720 Alfalfa	Kikuyu Grass	Bermuda Grass
EC 15	.043a	.158a	5.16a	15.98a	6.00a	4.28a	.105 b	.259 b	4.02a	15.57a
EC 25	.031a	.143a	4.36a	9.22 b	5.03a	2.03a	5.86a	5.13a	5.28a	7.48 b

Harvest 2

	Big Trefoil	Narrow Trefoil	Polo Paspalum	Duncan Paspalum	Jose Tall Wheatgrass	Sacaton	Salado Alfalfa	SW9720 Alfalfa	Kikuyu Grass	Bermuda Grass
EC 15	.109	.133a	5.94a	9.56a	2.70a	11.19a	.543a	.536a	4.62a	4.00a
EC 25		.121a	5.02a	13.09a	1.91 b	15.77a	.354 b	.308 b	3.33a	6.41a

Harvest 3

	Narrow Trefoil	Polo Paspalum	Duncan Paspalum	Jose Tall Wheatgrass	Sacaton	Salado Alfalfa	SW9720 Alfalfa	Kikuyu Grass	Bermuda Grass
EC 15	.133a	5.66a	10.31a	4.64a	7.63a	.884a	.944a	4.56a	4.36a
EC 25	.166a	5.69a	12.82a	2.96a	11.04a	.292 b	.218 b	5.29a	4.65a

Shoot S Concentration (mmol/kg dw)

Harvest 1

	Big Trefoil	Narrow Trefoil	Polo Paspalum	Duncan Paspalum	Jose Tall Wheatgrass	Sacaton	Salado Alfalfa	SW9720 Alfalfa	Kikuyu Grass	Bermuda Grass
EC 15	394.33 b	105.03a	303.00a	251.33a	109.33a	212.00a	164.00 b	126.00 b	185.33a	140.33a
EC 25	732.33a	166.00a	397.33a	311.00a	115.00a	206.33a	213.33a	210.67a	155.67 b	122.33 b

Harvest 2

	Big Trefoil	Narrow Trefoil	Polo Paspalum	Duncan Paspalum	Jose Tall Wheatgrass	Sacaton	Salado Alfalfa	SW9720 Alfalfa	Kikuyu Grass	Bermuda Grass
EC 15	795.67	144.33 b	393.00a	227.67a	102.33a	194.00a	138.33 b	130.67 b	154.33a	150.33a
EC 25		224.33a	427.67a	256.00a	100.80a	204.00a	173.00a	180.33a	132.33 b	136.33a

Harvest 3

	Big Trefoil	Narrow Trefoil	Polo Paspalum	Duncan Paspalum	Jose Tall Wheatgrass	Sacaton	Salado Alfalfa	SW9720 Alfalfa	Kikuyu Grass	Bermuda Grass
EC 15	532.50	214.33a	384.00a	256.00a	103.70 b	198.00a	194.67 b	170.67 b	144.33a	143.33a
EC 25		217.33a	383.33a	267.67a	116.33a	204.67a	288.00a	288.67a	142.00a	131.00a

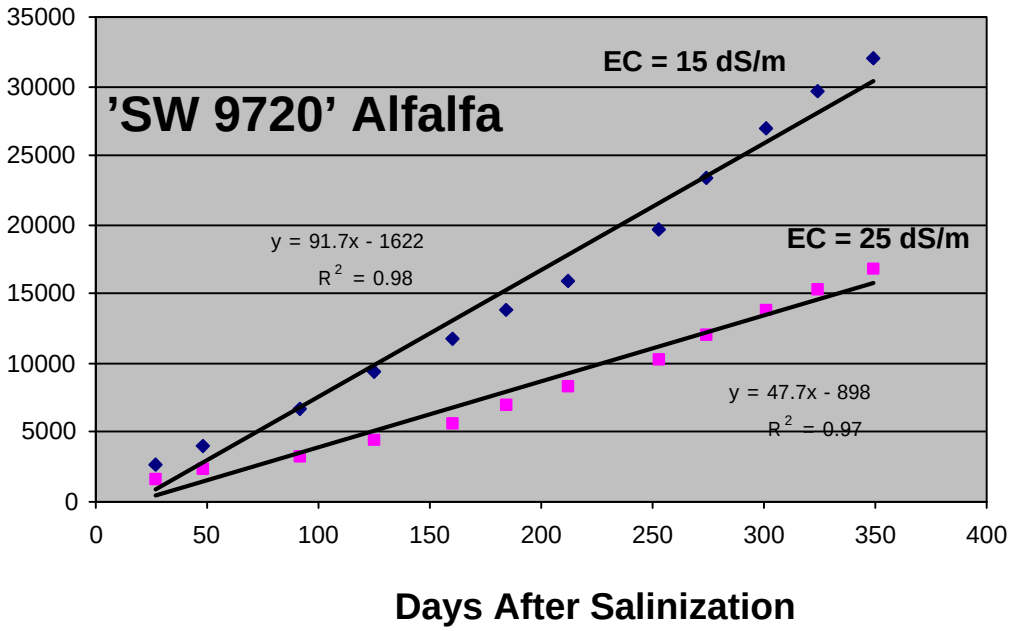

Figure 1. Cumulative biomass production of 'SW 9720' alfalfa (kg/ha dry wt.) at either 15 or 25 dS/m in relation to days after salinization.

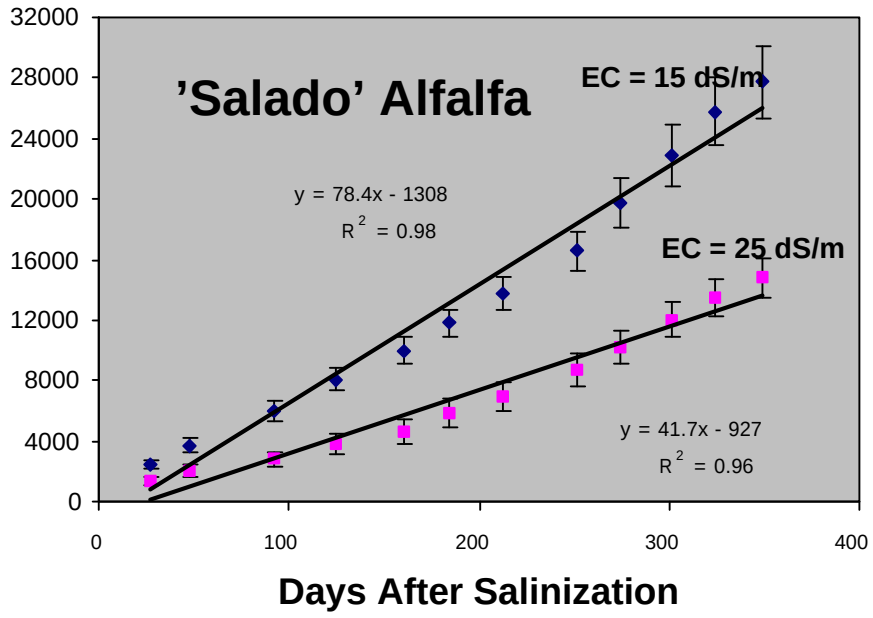

Figure 2. Cumulative biomass production of 'salado' alfalfa (kg/ha dry wt.) at either 15 or 25 dS/m in relation to days after salinization.

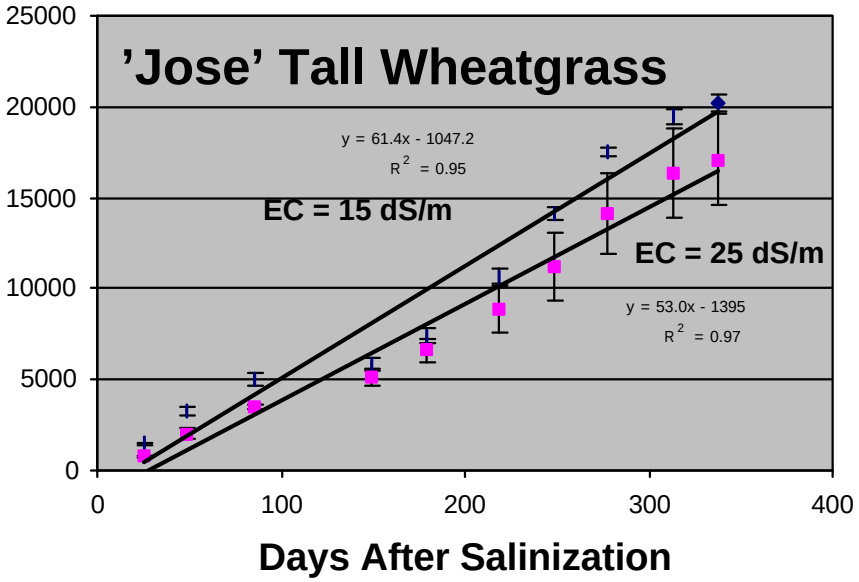

Figure 3. Cumulative biomass production of 'Jose' Tall wheatgrass (kg/ha dry wt.) at either 15 or 25 dS/m in relation to days after salinization.

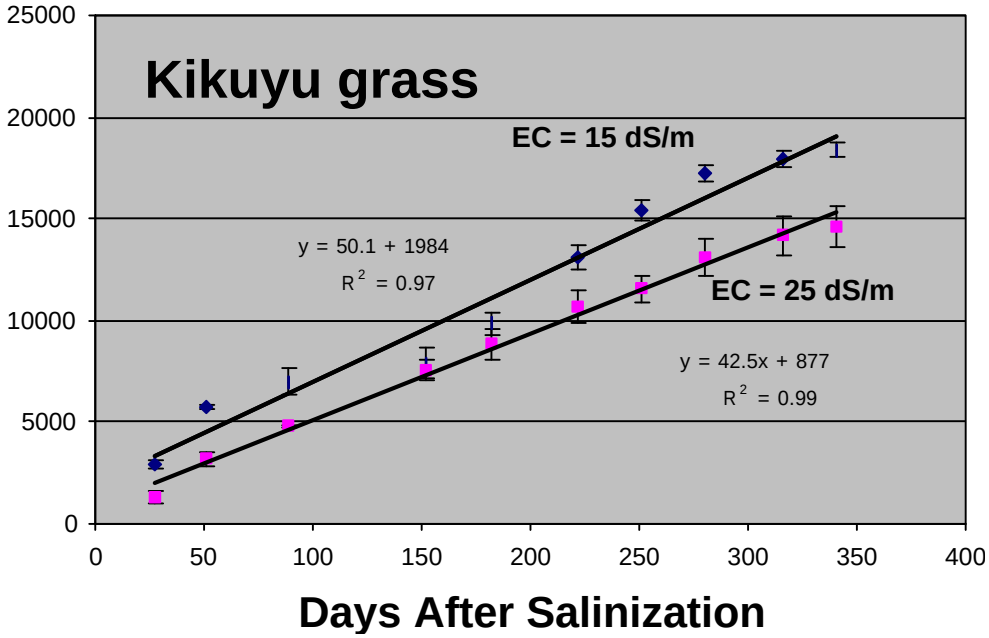

Figure 4. Cumulative biomass production of Kikuyu grass (kg/ha dry wt.) at either 15 or 25 dS/m in relation to days after salinization.

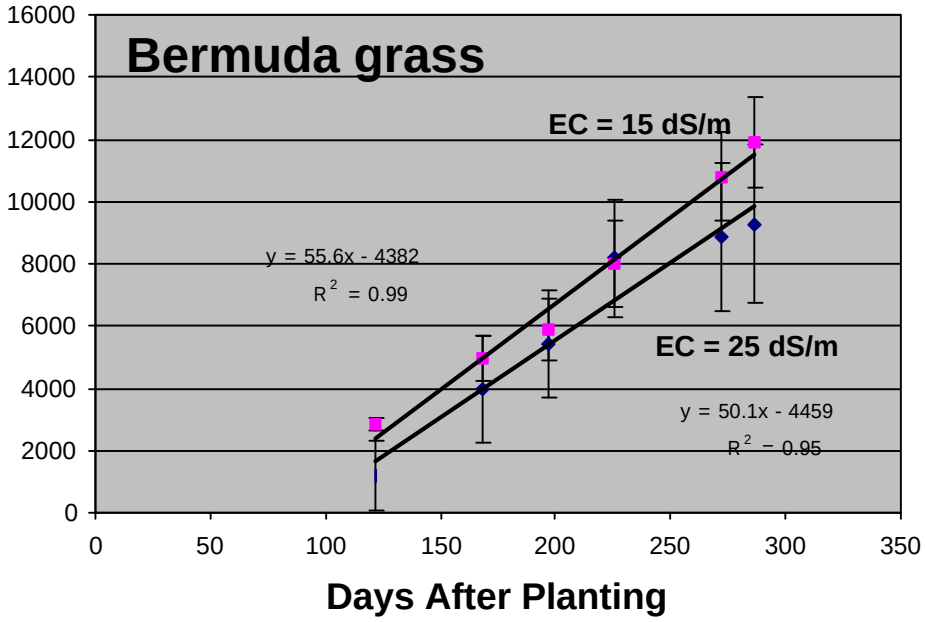

Figure 5. Cumulative biomass production of Bermuda grass (kg/ha dry wt.) at either 15 or 25 dS/m in relation to days after planting.

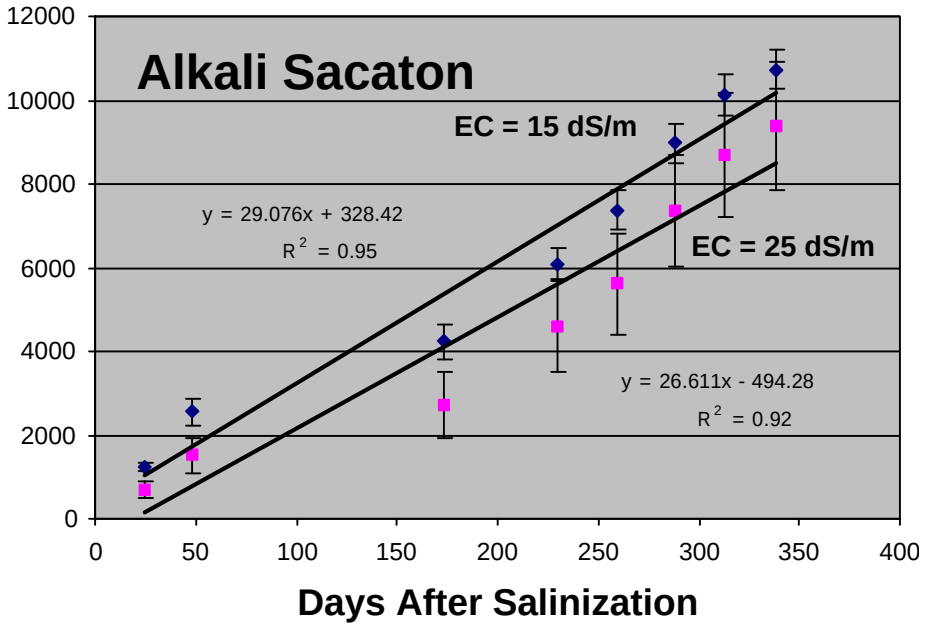

Figure 6. Cumulative biomass production of Alkali Sacaton (kg/ha dry wt.) at either 15 or 25 dS/m in relation to days after salinization.

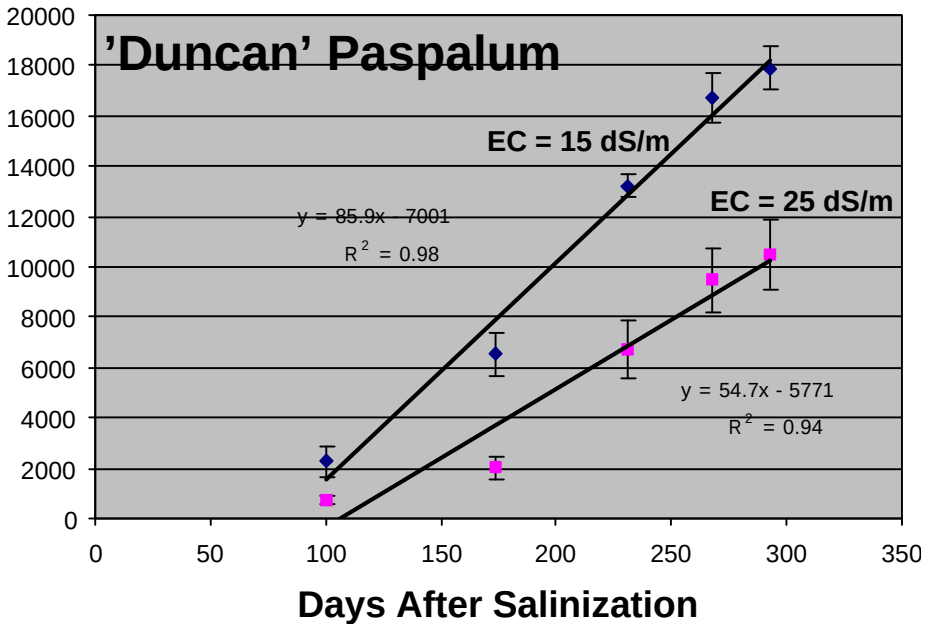

Figure 7. Cumulative biomass production of 'Duncan' Paspalum (kg/ha dry wt.) at either 15 or 25 dS/m in relation to days after salinization.

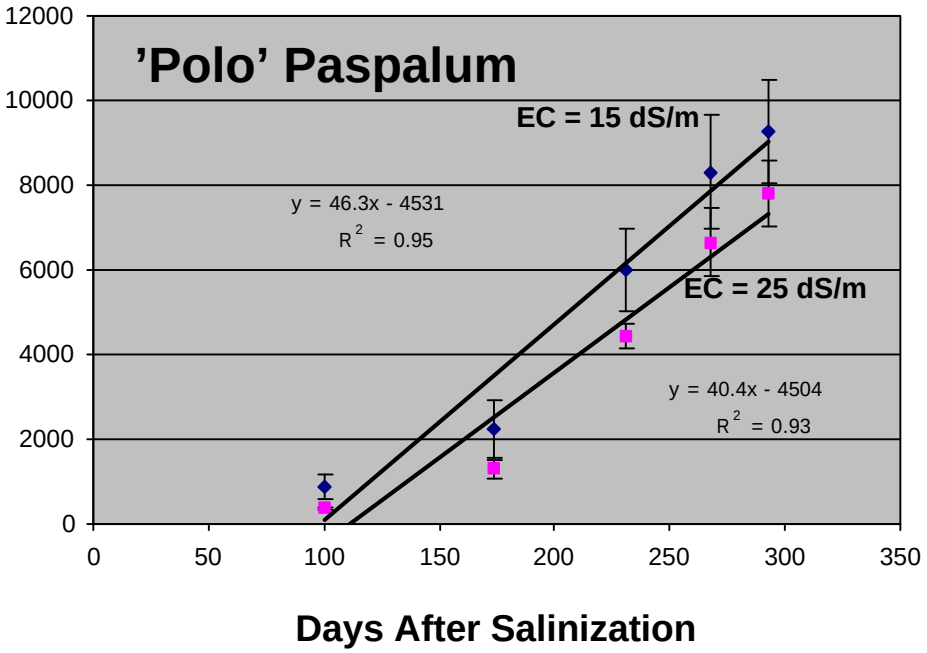

Figure 8. Cumulative biomass production of 'Polo' Pasplaum (kg/ha dry wt.) at either 15 or 25 dS/m in relation to days after salinization.

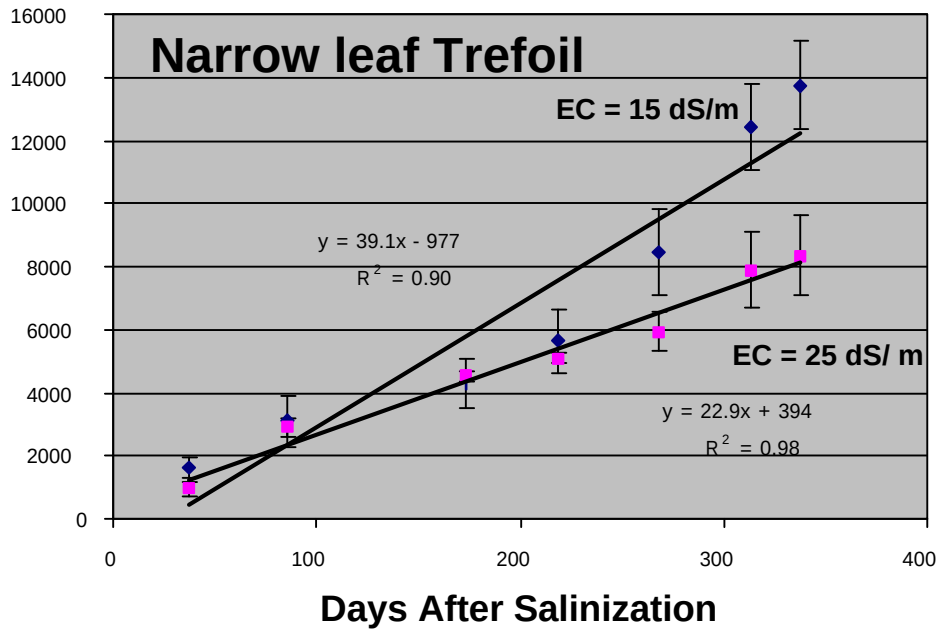

Figure 9. Cumulative biomass production of 'Narrow leaf' Trefoil (kg/ha dry wt.) at either 15 or 25 dS/m in relation to days after salinization.

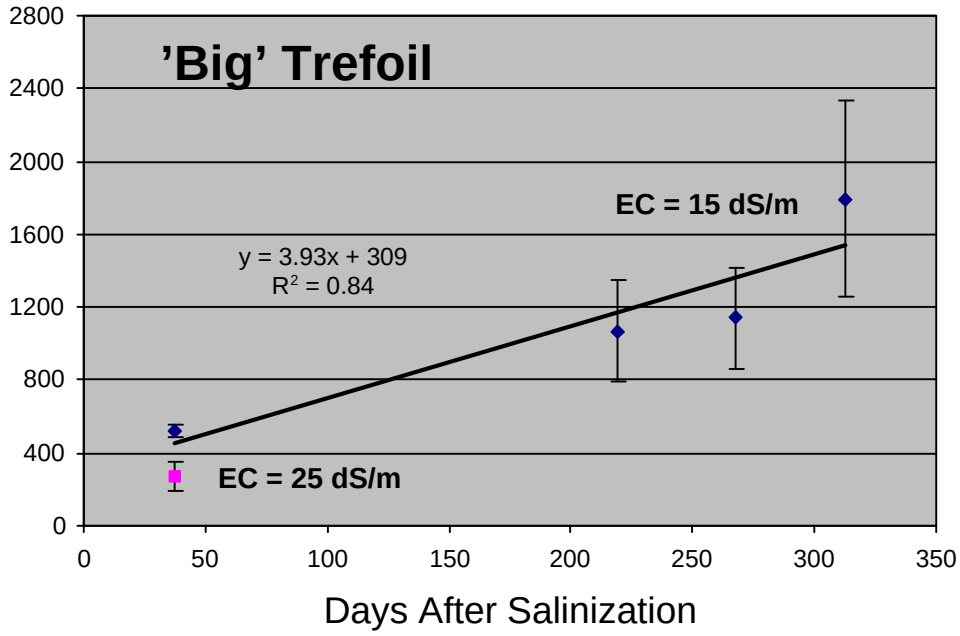

Figure 10. Cumulative biomass production of 'Big' Trefoil (kg/ha dry wt.) at either 15 or 25 dS/m in relation to days after salinization.

Response of Crop Yield and Water Table to Subsurface Drip Irrigation of Processing Tomato Under Saline, Shallow Groundwater Conditions

Project Investigators:

Blaine Hanson
Office: (530) 752-1130, E-mail: brhanson@ucdavis.edu
Department of Land, Air and Water Resources
University of California, Davis

Don May, Farm Advisor Emeritus
E-mail: dmay@ucdavis.edu
University of California Cooperative Extension
Fresno County

Research Staff:

1 SRA (0.3 FTE)
2 Field Assistants (0.6 FTE)

ABSTRACT

The objective of this study was to evaluate the potential for subsurface drip irrigation of processing tomato for reducing subsurface drainage and controlling soil salinity, and for increasing farm profits. Subsurface drip irrigation systems were installed in three fields with fine-textured, salt-affected soil. Sites were located along the west side of the San Joaquin Valley in an area with subsurface drainage problems. No subsurface drainage systems were installed in these fields. Yield and quality of processing tomato were of the drip systems were compared with sprinkler irrigation systems used in the remainder of the fields.

Results showed yield increases of 12 to 22 Mg/ha for the drip systems compared to the sprinkler systems with similar amounts of applied water. Solids content of the drip-irrigated processing tomato were generally acceptable. Response of water table levels during drip irrigation showed that properly managed drip systems could reduce percolation below the root zone. Results also showed that yields of the drip systems were not correlated to soil salinity even though soil salinity levels varied from levels less than the threshold value for tomato to values several times higher than the threshold value.

KEYWORDS

irrigation, processing tomato, salinity, shallow groundwater

ACKNOWLEDGEMENTS

We wish to acknowledge the contributions of the Bureau of Reclamation, Westlands Water District, Britz Farming Corp., Farming D. Inc., AgriValley Irrigation Company, T-Systems International, Netafim Irrigation Company, Roberts Irrigation Products, Rain Bird, Toro Ag, and the UC Salinity/Drainage Program.

■ ■ ■ ■ ■

INTRODUCTION

Subsurface drainage problems continue to afflict many areas along the west side of the San Joaquin Valley of California. Concurrent with the drainage problems are excessive levels of soil salinity, the result of upward flow of the shallow, saline groundwater and insufficient leaching. Subsurface drainage systems, normally installed to drain fields affected by shallow groundwater, cannot be used because no economically, technically, and environmentally feasible drain water disposal method exists for the San Joaquin Valley. Thus, the drainage problem must be addressed through options such as better management of irrigation water to reduce percolation below the root zone, increasing crop water use of the shallow groundwater without any yield reductions, and drainage water reuse for irrigation.

One option for improving irrigation water management is to convert from furrow or sprinkler irrigation to drip irrigation. Drip irrigation can apply water both precisely and uniformly compared with furrow and sprinkler irrigation. Drip irrigations can occur more frequently compared with furrow and sprinkler irrigation, thus better controlling soil salinity in the root zone. Drip irrigation systems can be managed to reduce subsurface drainage by decreasing percolation below the root.

The main disadvantage of drip irrigation is its cost, about $2,500/ha. For drip irrigation to be at least as profitable as the other irrigation methods, higher yields and reduced irrigation and cultural costs must occur. Yet, several large-scale comparisons of furrow and drip irrigation of cotton revealed much uncertainty in the economic benefits of drip irrigation (Hanson and Trout, 2000). Thus, growers converting to drip irrigation assume an economic risk.

During the past four years, a project has been conducted in the Westlands Water District to evaluate subsurface drip irrigation of processing tomato in fine-textured soil underlain by saline, shallow groundwater. The objective of this project is to determine the effect of drip irrigation on yield and yield quality, soil salinity, and depth to the water table. Because processing tomato is a high cash value crop, a better potential for increased profitability with drip irrigation exists compared to cotton. On the other hand, tomato is much more sensitive to soil salinity, which could result in reduced crop yields in the areas with the saline groundwater.

MATERIALS AND METHODS

Drip irrigation systems were installed in three fields located in the Westlands Water District. Sites DI (32 ha) and BR (16 ha) were installed in 1999, while DE (16 ha) was installed in 2000. The remainder of the each field was irrigated with sprinkler irrigation. Processing tomato was grown

at each site. Westlands irrigation water was used at DI and BR. Well water with an electrical conductivity nearly three times that of the Westlands water was used at Site DE. Measurements made at all sites were field-wide yield (machine harvested), yield quality, depth to the water table, irrigation water salinity, groundwater salinity, and applied water. The growers determined irrigation scheduling at each site. No subsurface drainage systems existed at the drip-irrigated sites. A drainage system was installed in the sprinkler-irrigated field of DE2000 (site/year), but the grower felt that its effectiveness was questionable because of the age of the system.

Each drip system consisted of 22-mm diameter low-flow drip tape buried about 200 mm deep. Emitter spacing ranged from 0.3 m to 0.45 m depending on the type of tape. Drip line lengths were about 400 m at all sites. At BR2001, the experimental site was changed to another part of the field where two drip lines per bed were installed. Spacing between the drip lines was about 0.6 m.

At each site, an experiment consisting of different irrigation amounts was conducted to determine the minimum amount of applied water needed to prevent yield reductions under these shallow groundwater conditions. Target amounts of applied water were 90, 75, 60, 45, and 30 percent of the potential crop evapotranspiration. At DI (1999) and DE (2000), three varieties were grown under the differential irrigation treatments. Measurements made during these experiments were yield, fruit quality, soil salinity, soil moisture content, applied water, and canopy growth.

The experimental design used in 1999 and 2000 for the differential irrigation treatments consisted of dividing the field length into five blocks, each block 15 beds wide. Width of each plot was three bed spacings. Block lengths were about 80 m. For a given treatment, the inflow rate of a plot in a given block was the outflow rate of that treatment from the previous block. The treatments were arranged in a Latin square design results (Ott and Longnecker, 2001) to minimize any bed effects on the treatment results. Cumulative applied water of a given treatment was measured at the inlet of the first block. Linear regression was used by regressing total yield along the field length against cumulative applied water for each treatment. Differential irrigation amounts were obtained by different irrigation set times for each treatment. This in turn required coordination with the irrigators, which proved to be difficult, and thus target amounts were not achieved.

A randomized block design was used in 2001 to overcome the coordination problems. This design used four irrigation treatments replicated five times. Each treatment consisted of one continuous bed along the field length. A manifold for each treatment was installed at the head of the field to supply water to each block. Differential irrigation amounts were obtained by using different manifold pressures. The flow rate was measured for each manifold. Linear regression was used to describe the relationship between yield and applied water.

All plots were machine harvested. Harvest data were total yield, solids content, percent red, green, and non-marketable fruit, and color. Soil moisture contents were measured throughout the irrigation crop season with a neutron moisture meter. Soil salinity was determined at the beginning and end of the crop season for three of the irrigation treatments. Canopy growth was measured with a digital infrared camera mounted on a pole about 2.4 m above the crop. The canopy coverage (fraction of the bed area shaded by the canopy at mid-day) was calculated from the camera images using software supplied by the manufacturer.

Crop evapotranspiration was estimated using a computer evapotranspiration model developed by Hsiao and Henderson (1985). This model uses canopy growth with time after planting and reference crop evapotranspiration to partition the solar radiation into that used for evaporation from the soil and that transpired by the plant.

RESULTS

FIELD-WIDE YIELD CHARACTERISTICS

Yields of the drip-irrigated fields were 12 to 22.5 Mg/ha more than those of the sprinkler irrigated fields (Table 1). Average yields were 93.6 and 74.8 for drip-and sprinkler-irrigation, respectively. Differences in yields were statistically significant (level of significance of 5%). Drip yields were considered to be high for these fine-textured, salt affected soils. Unfortunately, only one year of comparison was possible at each site. At BR and DE, after the first year, the rest of the fields were converted to drip irrigation. At DI, a different crop rotation was used for the sprinkler part of the field. After the first year, yields at DI and DE continued

to be high. Yields at BR for 2000 and 2001 were relatively low due to late plantings. For late plantings, however, the yields were higher than normally experienced.

Applied water at BR was similar for drip and sprinkler irrigation comparison in 1999. About 152 mm more water was applied to the drip field at DE compared with the sprinkler field because the drip field was irrigated about two weeks later than was the sprinkler field. Applied water data for the sprinkler field at DI were not available.

The solid contents of the drip-irrigated fields were acceptable for all years except 2001 for BR and DI. For the comparisons, the average Brix was 5.3 for sprinkler irrigation and 5.5 for drip irrigation. A trend of increasing Brix with increasing soil salinity was found with average Brix values of 4.9, 5.3, and 5.4 for DI (lowest salinity level), BR, and DE(highest salinity level), respectively. The average color was 24.3 and 22.5 for sprinkler and drip irrigation respectively. (The lower the color, the better the quality.) Differences in Brix and color between drip and sprinkler fields were not statistically significant (level of significance of 5%).

DIFFERENTIAL IRRIGATION EXPERIMENTS

Yield declined with decreasing irrigation water applications for all sites and all years (Figure 1). However, considerable differences in behavior occurred among the sites and years. In 1999, a 45% decrease in applied water caused a 37% decrease in yield at BR1999. However, at DI1999, a 36% decrease in applied water resulted in yield decreases ranging from 9%(H9557) to 17% (H8892). In 2000, a reduction of 13% in applied water caused yield reductions of 22% to 24% at DE2000. At BR2000, a 32% yield reduction occurred for an 18% decrease in applied water. The 2001 results showed a 33% applied water reduction to cause an 8% yield reduction at DI2001; a 45% applied water reduction to cause a 14% yield reduction at DE2001; and a 52% applied water reduction to cause an 11% yield reduction at BR2001. Regression equations relating yield and applied water were statistically significant (level of significance of 5%) for DI1999 (H9665), DE2000 (Halley 3155), DE2000 (H9665), BR2000, DI2001, and BR2001.

Brix percentage increased with decreasing applied water for all sites and all years (Figure 2). As with yield, considerable differences were found among sites and years. A 46% decrease in applied water increased the Brix by about 15% for BR1999, whereas, for DI1999, 36% decrease in applied water increased the Brix by 9% (H9665) to 14% (H8892). In 2000, a 13% decrease in applied water increased the Brix by 6% (Halley) to 17% (H9665, H8892) at DE2000, while an 18% decrease in applied water increased the Brix by 14%. The 2001 results showed a 2% increase in the Brix for a 57% decrease in applied water at BR2001; a 4% Brix increase for a 45% decrease in applied water at DE2001; and an 8% Brix increase for 33% decrease in applied water at DI2001. Regression equations relating Brix and applied water were statistically significant for DI1999 (H9557), DI1999 (H9665), BR2000, and BR2001.

There was little effect of decreasing applied water on color and percent red fruit (data not shown). Regression equations relating color and applied water were statistically insignificant for all sites except DI1999 (H9557). Relationships between red fruit and applied water were also statistically insignificant except at DI1999 (H8892) and BR2001.

WATER QUALITY

The electrical conductivity of irrigation and ground water showed the low-salinity irrigation water at Sites BR and DI to be about 0.34 dS/m (Table 2). The irrigation water at these sites was supplied by the Westlands Water District, which in turn receives northern California water from the California Aqueduct. At DI2001, higher ECs were found which might reflect fertigation occurring at the time of measurements. At DE, the electrical conductivity of the irrigation water supplied by a well was about 1.06 - 1.2 dS/m, about three times higher compared with the other sites. The EC of the shallow ground water ranged from 4.7 to 7.4 dS/m at BR for all three years (Table 2). At DI, the ground water EC ranged from7.9 to 11.1 for 1999 and 2000, but was 4.0 to 4.7 in 2001 even though sampling locations were within 50 m of each other. Reasons for the smaller values are unknown. EC values at DE were less in 2001 compared to 2000. Interestingly, there is little correlation between soil salinity and ground water quality. DI, which had the highest ground water salinity, had the lowest values of soil salinity (discussed later).

SOIL SALINITY

Soil salinity as measured with the electrical conductivity of the saturated extract (ECe) differed considerably among the three sites in 2000. At DI2000, ECe values were about 2.0 or less

for all depths and sampling dates for the wet treatment (Figure 3a). (The threshold value of ECe for tomato is 2.5 dS/m. This has been determined as the maximum level of salinity at which no yield reduction will occur.) ECe varied little with depth for both sampling times. Above about 0.6-m deep, salt levels increased slightly with time, while below that depth, they decreased with time. ECe values of the wet treatment ranged from about 2.5 dS/m near the surface to nearly 7.2 dS/m at about 7.2 dS/m at 1.37 m deep at BR2000 (Figure 3b). Salinity increased with time above about 0.3 m and decreased with time below that depth. At DE2000, ECe values of the wet treatment ranged between about 3.5 dS/m and 7 dS/m in May (Figure 3c). An increase in ECe about 0.5 m and a decrease below 0.5 m was found in August. For both BR and DE, soil salinity levels generally exceeded the threshold value. Little correlation was found between irrigation treatment and soil salinity.

In 2001, similar differences among the three sites were found. However, at DI2001, slightly higher ECe values were found for the wet irrigation treatment compared to the 2000 values with a maximum value of about 4 dS/m at 0.91 m deep (Figure 4a). At BR2001, May salinity levels were similar to those of 2000, but below about 0.4 m deep, more leaching occurred compared to 2000 (Figure 4b). These lower ECe values reflect the leaching that occurred under the dual drip lines installed in each bed in 2001. ECe values near the surface were similar to those in 2000 at DE (Figure 4c). However, much higher values were found at the deeper depths with a maximum value near 12 dS/m. Little correlation was found between irrigation treatment and soil salinity.

Patterns of soil salinity about the drip line reflected the differences in soil salinity levels among the three sites. At DI2000, low values of soil salinity occurred throughout the soil profile (Figure 5a). A slight increase in salinity occurred near the surface. At BR (2000), salinity was the least near the drip line with values less than about 1 dS/m (Figure 5b). Salinity increased with distance and depth from the drip line to values of about 7 dS/m. Salinity also increased near the soil surface. The area of relatively low soil salinity (less than the threshold value of 2.5 dS/m) extended to about 400 mm horizontally from the drip line and to about 560 mm deep below the drip line. This pattern shows that most of the root zone probably consisted of low salinity soil.

A much different pattern of soil salinity was found at DE (2000) (Figure 6a). Soil salinity was the highest near the drip line and decreased with horizontal distance. Values near the drip line were about 3 to 4 dS/m. At distances beyond about 200 to 400 mm, soil salinity was less than 2.5 dS/m. The high salinity near the drip line reflects the salinity of the irrigation water. The low levels of salinity near the edge of the pattern, however, suggest that for depths less than about 400 mm, considerable leaching of salt had occurred prior to irrigation, probably caused by ponding from a severe rainfall. In 2001, a different pattern was found (Figure 6b). Soil salinity levels near the surface were much higher than in 2000 with EC values ranging between 5 and 7 dS/m. In the immediate vicinity of the drip line, EC levels were between 3 and 4 dS/m. EC values rapidly increased with horizontal distance from the drip line over distances of 200 mm to 400 mm from the drip line.

SOIL MOISTURE CONTENT

The average soil moisture content of the top 0.61 m of the soil profile decreased with time during the irrigation season at all locations and for all years (Figure 7). Soil moisture values at the start of the measurement period were generally between 37% and 43% (except DI1999) and decreased to between 27% and 38% prior to harvest. Moisture contents of the wet irrigation treatments were slightly higher than those of the dry irrigation treatments. This behavior indicates that seasonal depletion of soil moisture occurred even for the wet irrigation treatments.

Measurements of the wetting patterns about the drip line showed lateral movement of water to about 400 mm from the drip line at DI (Figure 8) and BR (not shown). At about that distance, drier soil occurred compared to smaller and larger distances. Drying also occurred near the surface except just above the drip line. Beyond about 500 mm (in the furrow), soil moisture content increased slightly and then decreased for depths less than about 200 mm. More drying above about 200 mm deep occurred for the dry irrigation treatment (Figure 8b) than for the wet irrigation treatment (Figure 8a). Lateral movement at DE appeared to be between 200 mm and 400 mm based on the salinity patterns previously discussed. The wetting pattern at this location was not directly measured. At BR2001, where two drip lines per bed were used, wetting across the bed was more uniform

compared to the single drip line configuration (not shown).

WATER TABLE DEPTH

Water table depth at BR declined from about 0.6 m to about 1.3 m in 1999 (Figure 9a). No response of water table to drip irrigations was evident. At DI, the water table at the start of the measurements was at about 2.5 m deep. The depth decreased with time to about 1.5 m during the later part of July 1999 and then increased with time. This behavior is believed to be caused by regional flows into the drip-irrigated field. During the later part of July, a slight response to drip irrigation occurred with a rise in the water table of about 25-mm every 3 to 4 days.

In 2000, a substantial response of water table depth to drip irrigation occurred at BR before about July 15 (Figure 9b). After drip irrigation, the depth was nearly 0.5 m in some cases. After mid-July, the water table depth increased with time to a depth of about 1.7-m, the result of decreased applications of irrigation water. Prior to July 15, water applications were about 10% more that the estimated crop evapotranspiration. After July 15, the applications were reduced to about 80-90% of the estimated crop evapotranspiration. At DI, the water table depth remained between about 1.7 to 1.9 m deep during the measurement period. No response to drip irrigation was found. No water table data were collected at DE due to problems with the observation well filling with sediment.

Water table depth at DE in 2001 fluctuated between about 0.6 m and 1.2 m (Figure 9c). A definite water table response to drip irrigation was found. At BR and DI, water table depth increased with time with little or no response to drip irrigation. The gaps in the data were due to the water level in the observation well dropping below the sensors, thus requiring a deepened well.

IRRIGATION SYSTEM EVALUATION

One drawback to drip irrigation is the tendency for emitters to clog due to suspended material in water, chemical precipitation, biological growth, root intrusion, and soil ingestion. To assess any clogging problems, drip lines at DI2001 and DE2001 were evaluated by uncovering the drip line at about 100-ft intervals along its length and measuring the discharge rates of two emitters at each location. These data were used to calculate the emissions uniformity, defined as the ratio of the average discharge rate of the lowest one-fourth of the measurements to the average discharge rate of all of the measurements. The drip line at DI2001 had been used for three crop seasons, while that of DE2001 was used for two crops.

Little or no clogging was found along the drip line at DI2001 (Figure 10a). The variation in emitter discharge rates along the drip line would be expected due to variation in pressure caused by friction losses along the drip line length. The emissions uniformity was 88%, considered to be good. Considerable clogging was found at DE2001 (Figure 10b). Clogging was somewhat random along the upper half of the drip line, but a trend of gradually decreasing discharge rates occurred along the lower half with the discharge rate decreasing at an increasing rate with distance. The emissions uniformity was 69%.

The clogging at DE2001 was caused by root intrusion. The data behavior indicates more clogging in areas where water application rates were less (lower part of the drip line). Reasons for the clogging appear to be a lack of chemical treatment to reduce or prevent clogging and deficit irrigation. In contrast, a chemical treatment program to reduce clogging was used at DI2001 for the past years of operation.

CROP EVAPOTRANSPIRATION

Canopy growth curves relating canopy coverage with days after planting are needed for the computer evapotranspiration model developed by Hsiao and Henderson (1985). Canopy growth curves showed a rapid increase in canopy develop for DAPs less than about 60 to 80 (Figure 11a). Maximum canopy coverage generally occurred between 60 and 80 DAP. In some case, canopy coverage decreased after maximum coverage was reached due to pruning of vines by growers and canopy reduction during the later part of the late season stage.

Reasons for differences among canopy growth curves may include different cultural practices among the growers, different climate characteristics between years, and irrigation practices. For example, planting dates of DI2001 and BR2001 varied by a couple of days. However, at BR2001, stand establishment consisted of direct-seeded plants while at DI2001, transplants were used. As a result, canopy development of the transplants was about 20 days ahead of that of

the direct-seeded plants. At BR2000, replanting was necessary because of crop damage due to a storm. Canopy development of the late-planted crop was delayed and only reached a maximum coverage of about 80%.

Results of the evapotranspiration model for BR2001 and DI2001 show relatively high ET just after planting for BR2001 compared to DI2001 (Figure 11b). This difference is caused by sprinkler irrigation used to establish the direct-seeded crop, whereas drip irrigation only was used for the transplanted crop. The ET rate decreased rapidly with soil drying. ET rapidly increased with DAP during the rapid growth stage (between DAP 20-50 for DI2001 and DAP 50 to 65 for BR2001). The rapid growth stage of BR2001 lagged that of DI2001 because of the differences in canopy development. ET rates were similar during the mid-season growth stage, and then decreased during the late season stage. This decrease reflects the reduction in canopy coverage during that growth stage.

A summary of seasonal cumulative ET for all years of the project shows ET values to range from 424 mm to 615 mm (Table 3). Reasons for the behavior reflect the different rates of canopy development and size. The cumulative ET at BR2000 was 424 mm, reflecting the smaller canopy development, and thus, ET of the late-planted crop. Seasonal irrigation efficiency, defined as the ratio of cumulative crop ET to seasonal applied water, ranged from 82% to 114%. Values near or exceeding 100% indicate deficit irrigation throughout much of the field. Under these conditions, shallow ground water and seasonal soil moisture depletion must supply the additional water to meet the crop ET.

DISCUSSION AND CONCLUSIONS

The field-wide results shows that subsurface drip irrigation in these fine-textured salt-affected soils along the west side of the San Joaquin Valley increased yield of processing tomato by 12 to 22 Mg/ha with acceptable Brix levels compared to sprinkler irrigation, normally used in these areas for tomatoes. At the same time, subsurface drainage below the root zone can be controlled with properly managed drip systems. The field-wide results also showed no correlation between soil salinity and crop yield with salinity levels ranging from values less than the threshold soil salinity of tomato to several times higher than the threshold value. Brix levels increased with increasing soil salinity. Subsurface drip irrigation also allowed better late-season water management, a time when careful water management is needed to prevent excessive deficit irrigation or phytophthora from excessive wet soil.

Properly managing drip irrigation systems requires knowing the daily crop ET and the amount of applied water. Irrigation amounts should be about 90% of the potential crop ET as estimated from the product of reference crop ET and crop coefficients. Results of the differential irrigation treatments showed that applying less water could reduce crop yield. For crops planted in April to early May, the potential seasonal ET was between 550 and 600 mm. The ET of late crops (late May) may range from 400 to 450 mm. Proper management also requires monitoring soil moisture content and water table levels. At BR2000, the water table response during June showed excessive percolation. Adjustments made at that time subsequently greatly reduced percolation and as a result, the ground water level declined. Irrigation should occur two to three times per week.

High frequency drip irrigation can help control soil salinity. Where good quality irrigation water is available, drip irrigation can reduce salt levels in the root zone to levels conducive for high yields, as shown at BR2000, where upward flow of saline ground water had previously salinized the soil. The use of more saline irrigation water under drip irrigation still resulted in high yields, as occurred at DE.

Drip irrigation under these saline soils was found to be more profitable compared with sprinkler irrigation. A crop price of $112/Mg and a yield increase of 22 Mg/ha resulted in a revenue increase of $2460/ha. A rough estimate of the annualized amortized capital cost of a subsurface drip system is $370/ha to $490/ha. This results in a net increase of at least $1970/ha. Because of this economic advantage, the growers who provided their fields for this project converted most of their tomato acreage in the high-water table areas with fine-textured soil from sprinkler irrigation to subsurface drip irrigation. This conversion may be partly responsible for the relatively deep water table levels found at BR2001 and DI2001.

It should be noted that subsurface drip irrigation in these marginal soil conditions was found to be very profitable compared to other irrigation methods. However, under soil conditions where high tomato yields are obtained under

furrow and sprinkler irrigation, converting to drip irrigation may not be profitable. Under these conditions, the potential for large yield increases may not exist, and thus, any increase in revenue under drip irrigation may be insufficient to offset capital, energy, maintenance, and management costs of subsurface drip irrigation. Also, using drip irrigation on lower-valued crops may also be unprofitable even if yield increases occur. Hanson and Trout (2002) found that higher cotton yields were obtained with less water under drip irrigation compared with furrow irrigation, but furrow irrigation was more profitable.

■ ■ ■ ■ ■

REFERENCES

Hanson, B. R. and T. J. Trout. 2001. Irrigated agriculture and water quality impacts. In: Agriculture Nonpoint Source Pollution (Ed. W. F. Ritter and A Shirmohammadi). Lewis Publishers. 342 p.

Hsiao, T. C. and D.W. Henderson. 1985. Improvement of crop coefficients for evapotranspiration. In: California Irrigation Management Information System Final Report, June 1985.

Ott, R.L. and M. Longnecker. 2001. Statistical Methods and Data Analysis. Duxbury, Pacifc Grove, CA. 1152 p.

Table 1. Summary of field-wide applied water and yield characteristics for all sites and years.

Irrigation System	Variety	Applied Water (mm)	Yield (Mg/ha)	Soluble Solids (°Brix)	Color
		BR			
Sprinkler (1999)	H8892	427	81.69	5.3	24.2
Drip (1999)	H8892	406	103.62	6.0	21.1
Drip (2000)	Halley 3551	427	78.33	5.4	23.4
Drip (2001)	H9665	521	71.46	4.6	25.3
		DI			
Sprinkler (1999)	H9557	**	78.9	5.2	24.8
Drip (1999)	H9557	563	90.9	5.0	22.8
Drip (2000)	H9492	737	103.9	4.8	21.0
Drip (2001)	H9492	582	115.8	4.9	24.1
		DE			
Sprinkler (2000)	H9557	579	63.9	5.5	23.9
Drip (2000)	H9557	711	86.4	5.6	23.7
Drip (2001)	H8892	561	102.6	5.2	23.6

Table 2. Electrical conductivity (dS/m) of the irrigation water and groundwater for all sites.

Year	Irrigation Water	Ground Water
	BR	
1999	0.34-0.46	6.9
2000	0.34	4.7-7.4
2001	0.34	6.1
	DI	
1999	0.34-0.46	9.8-11.1
2000	0.34	7.9-10.8
2001	0.5-0.68	4.0-4.7
	DE	
2000	1.06	13.6-16.4
2001	1.06-1.2	9.0-9.5

Table 3. Total amount of applied water, cumulative crop ET, and irrigation efficiency (IE).

Year	Applied Water (mm)	Cumulative Crop ET (mm)	IE (%)
	BR		
1999	406	462	114
2000	427	424	99
2001	521	518	99
	DI		
1999	563	584	104
2000	737	605	82
2001	582	591	102
	DE		
2000	711	615	87
2001	561	557	99

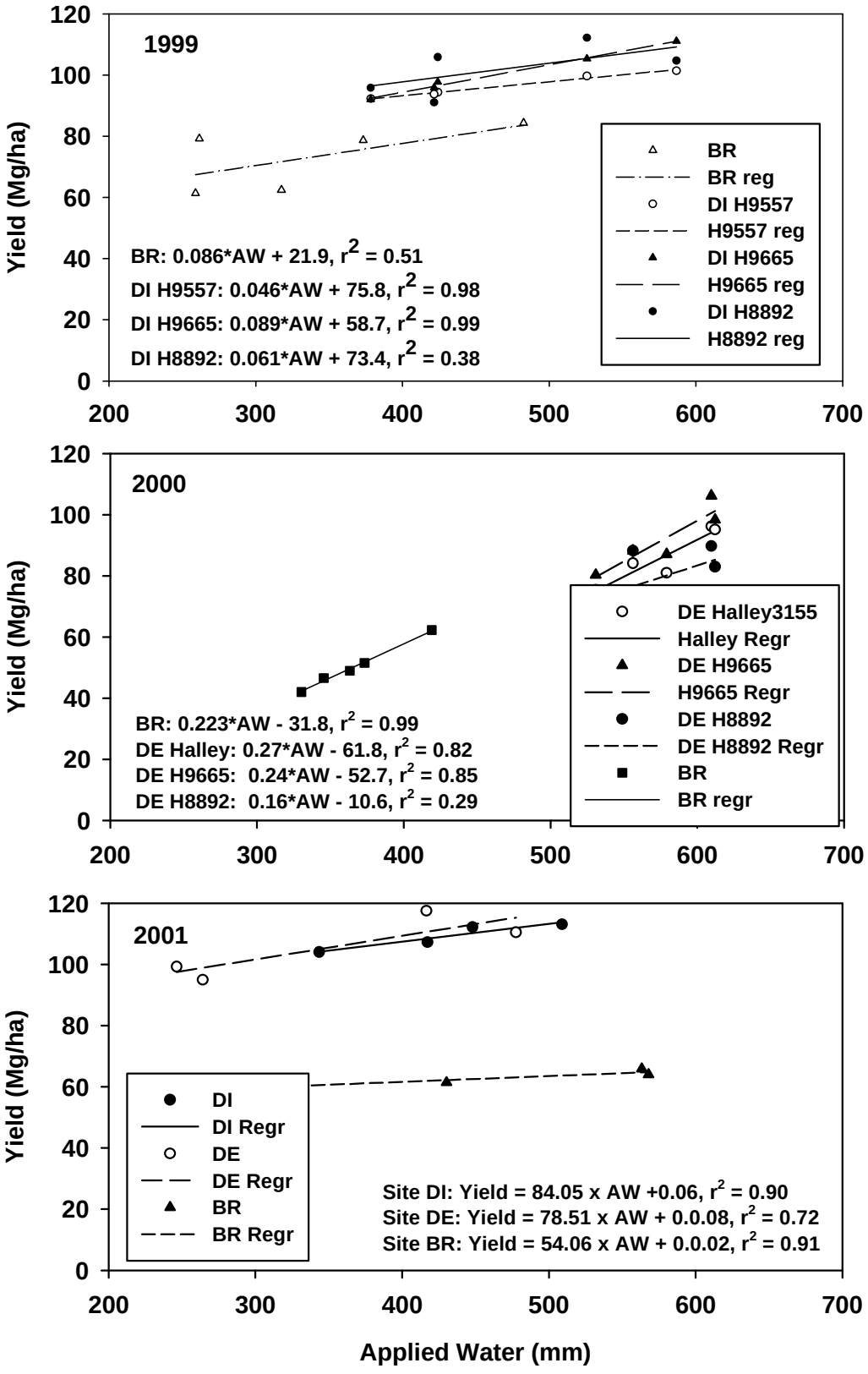

Figure 1. Yield versus applied water of the differential irrigation treatments.

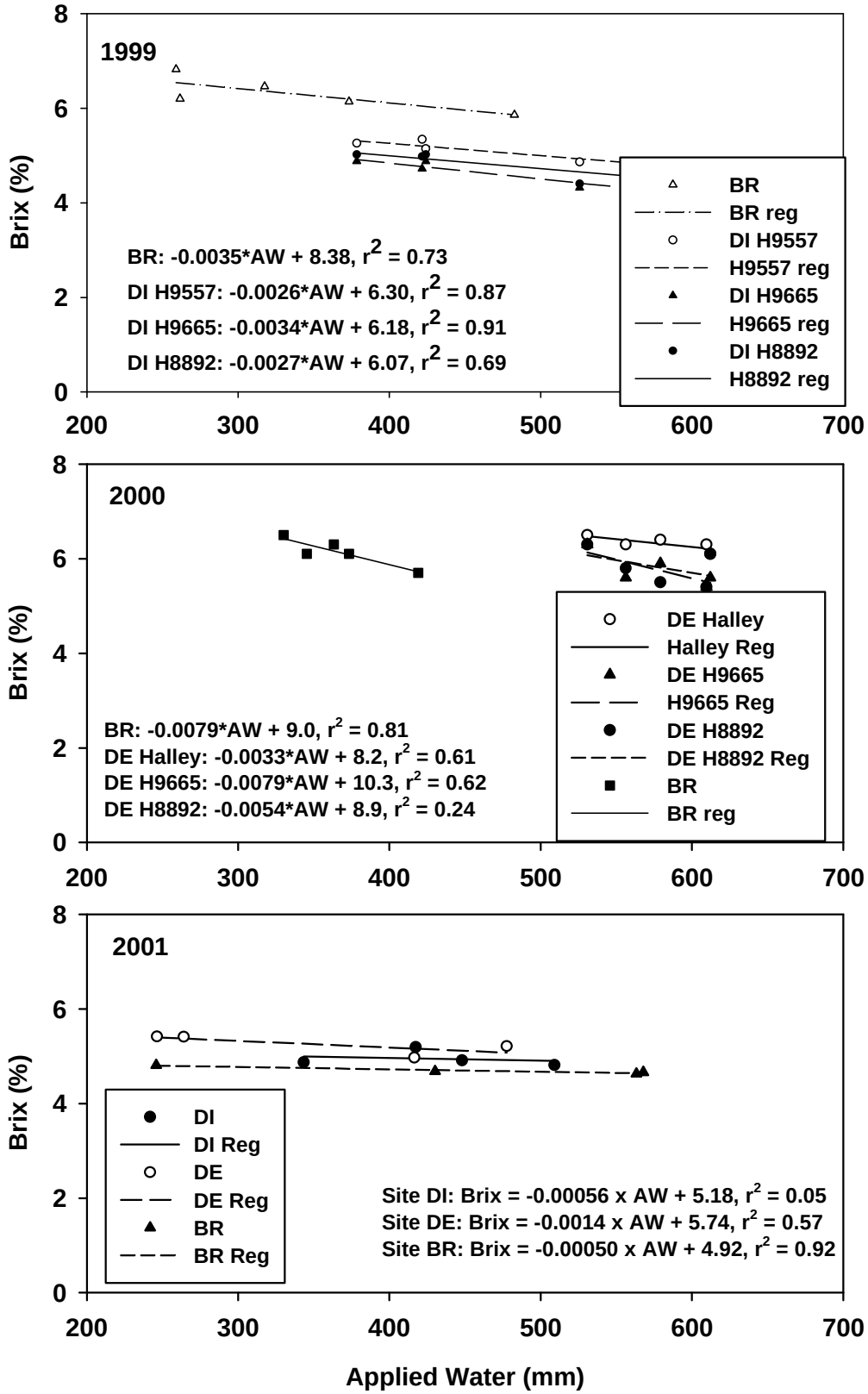

Figure 2. Soluble solids versus applied water of the differential irrigation treatments.

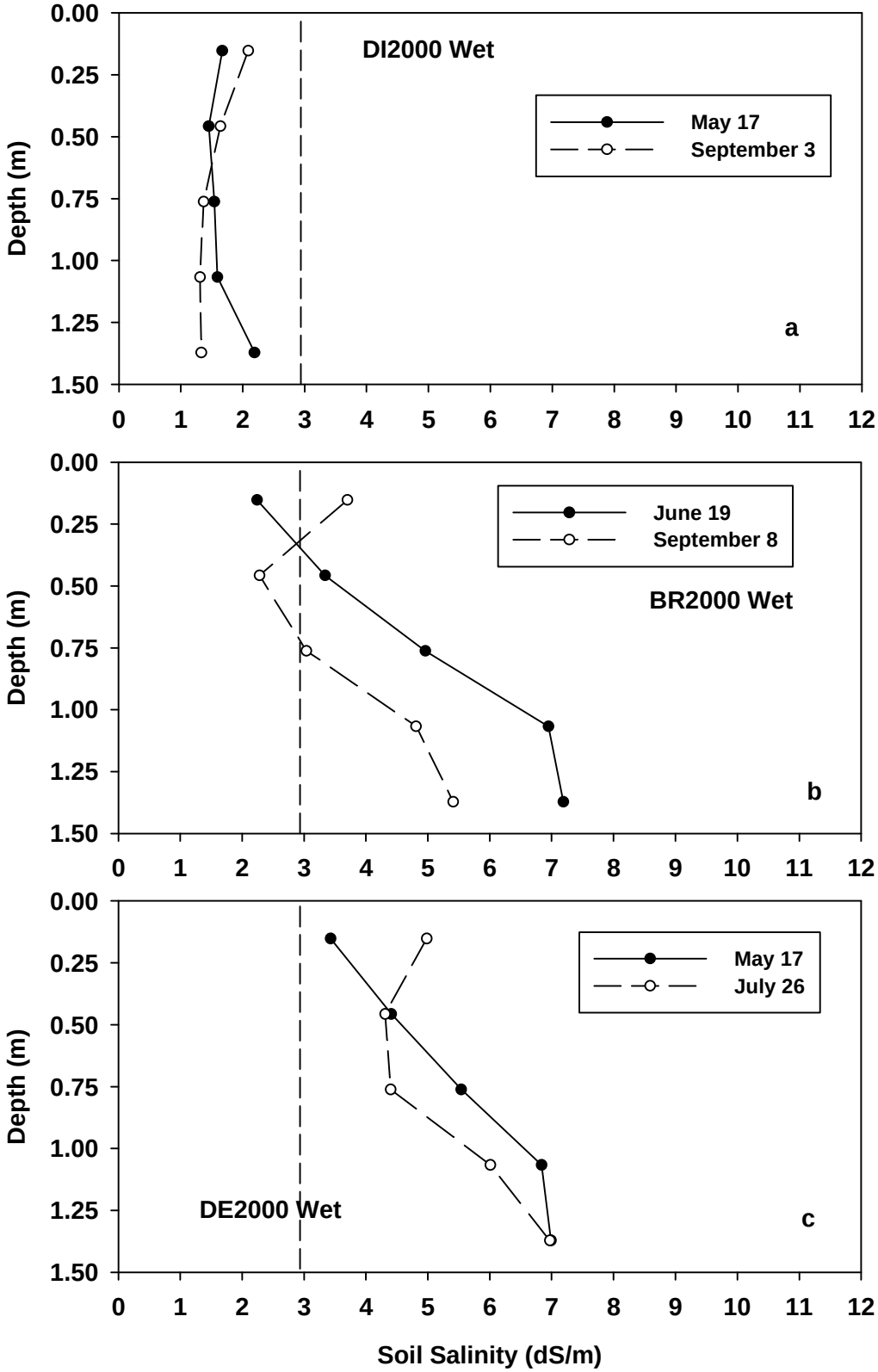

Figure 3. Soil salinity with depth for the wet irrigation treatment of the 2000 sites.

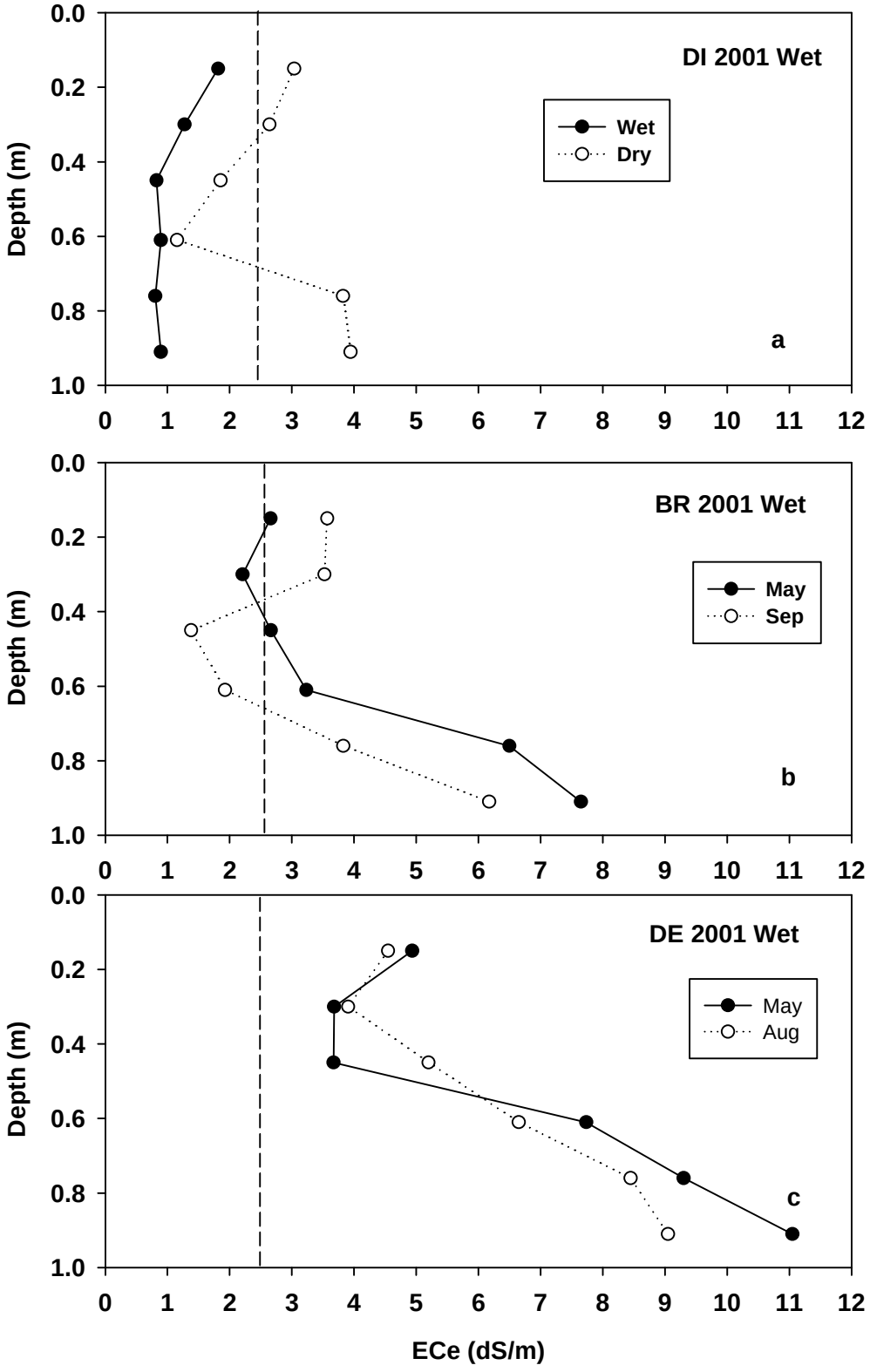

Figure 4. Soil salinity with depth for the wet irrigation treatment of the 2001 sites.

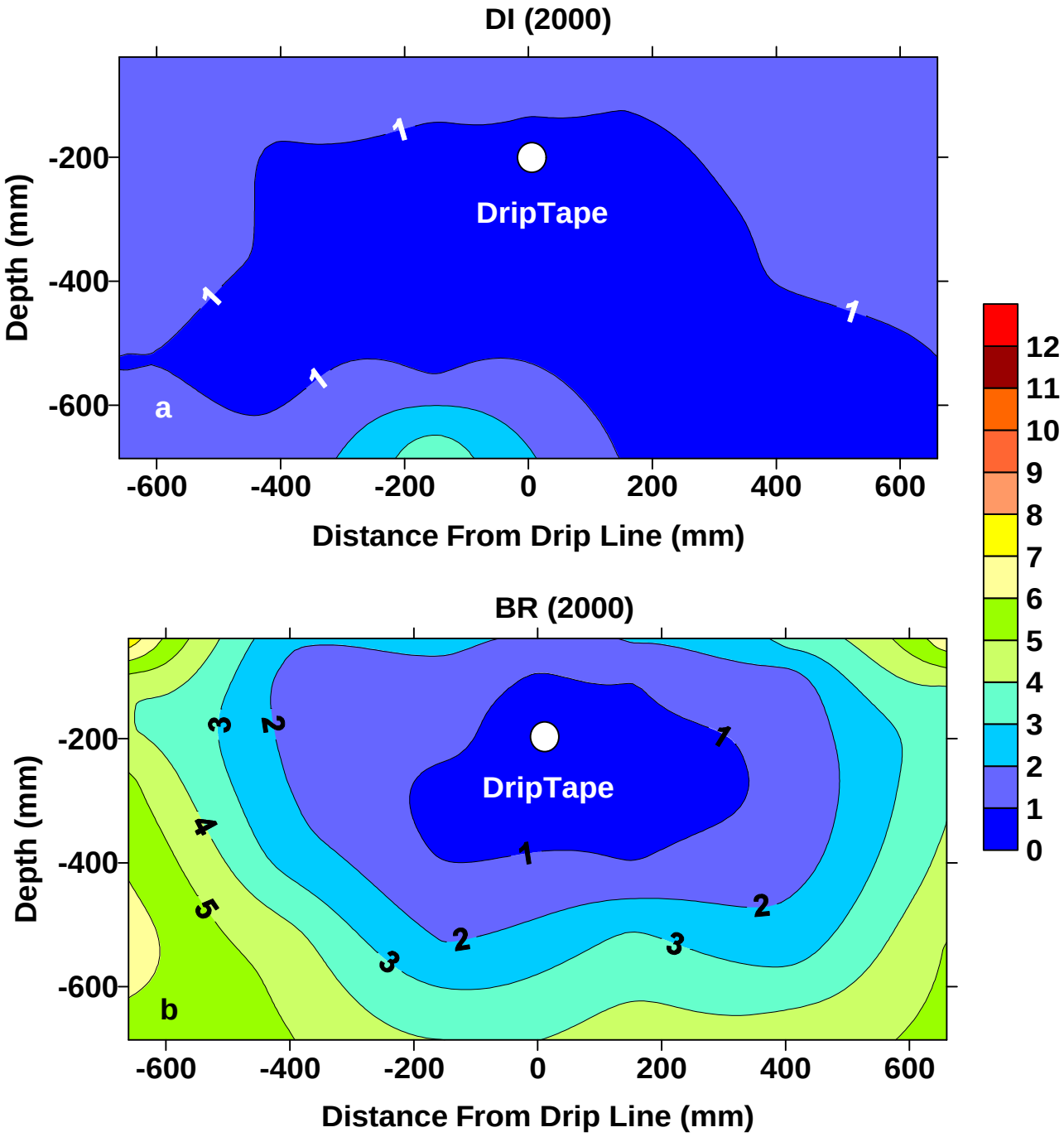

Figure 5. Patterns of soil salinity about the drip line for DI and BR in 2000.

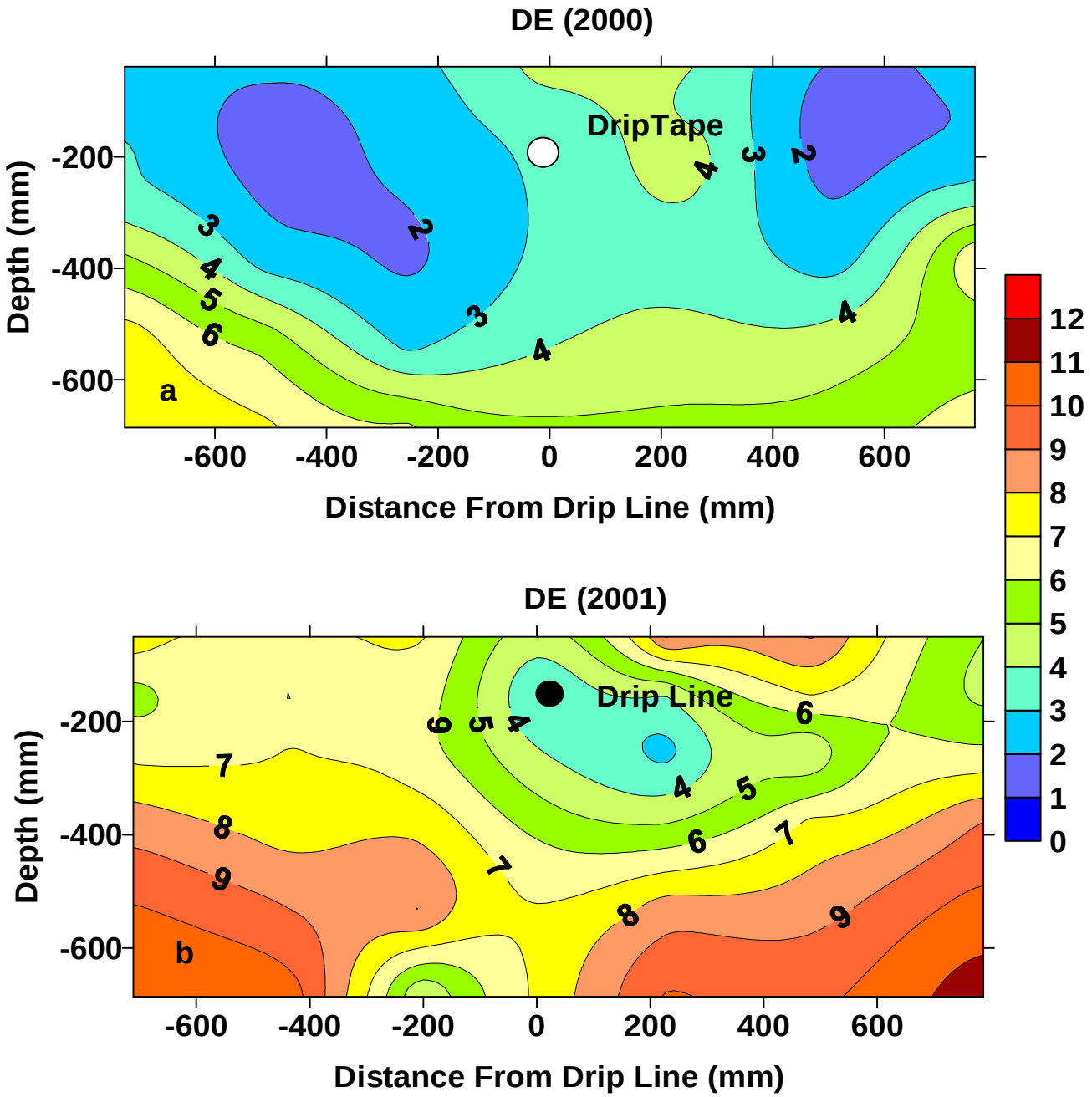

Figure 6. Patterns of soil salinity about the drip lline for DE2000 and DE2001.

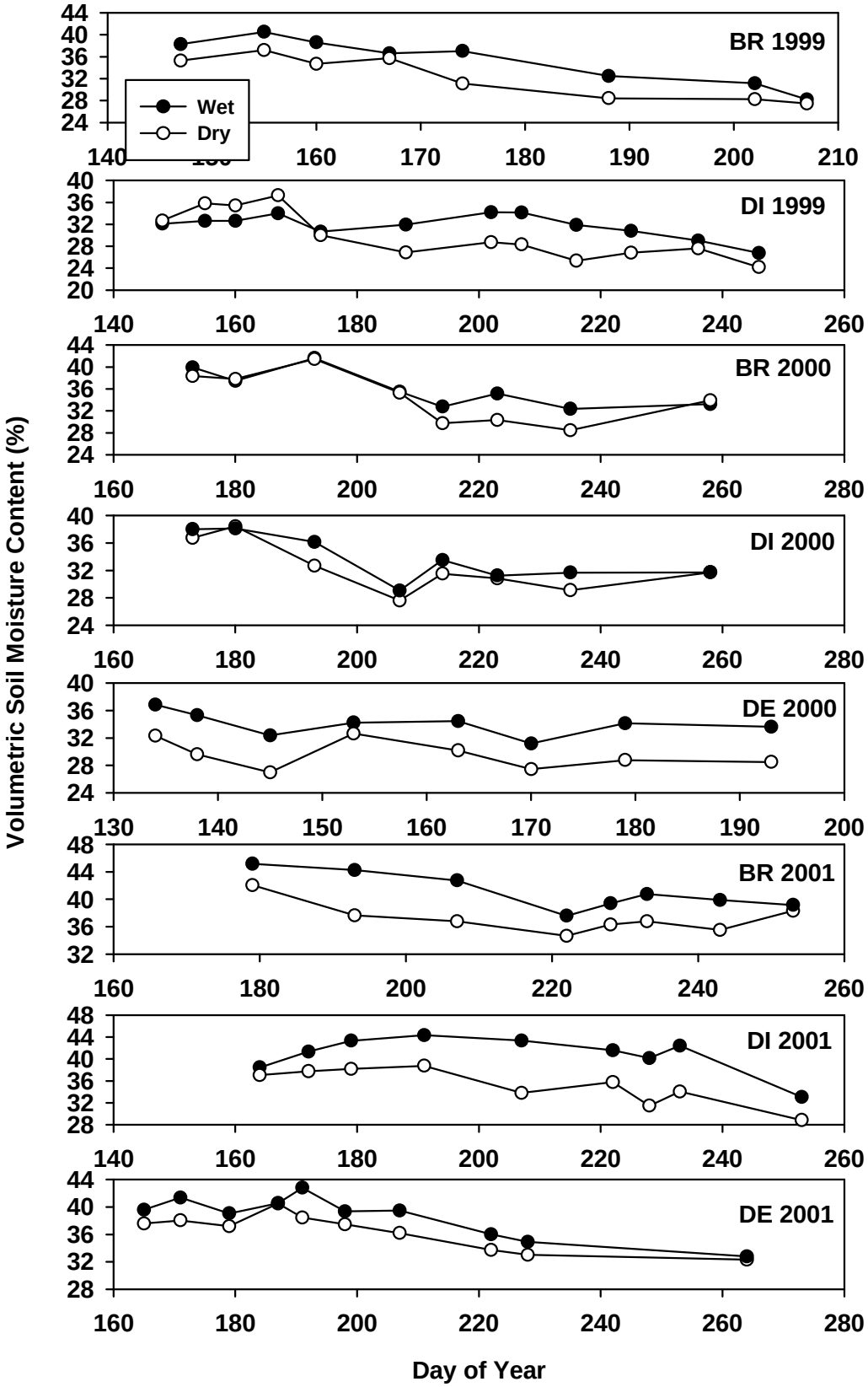

Figure 7. Soil water content with time for wet and dry irrigation treatments.

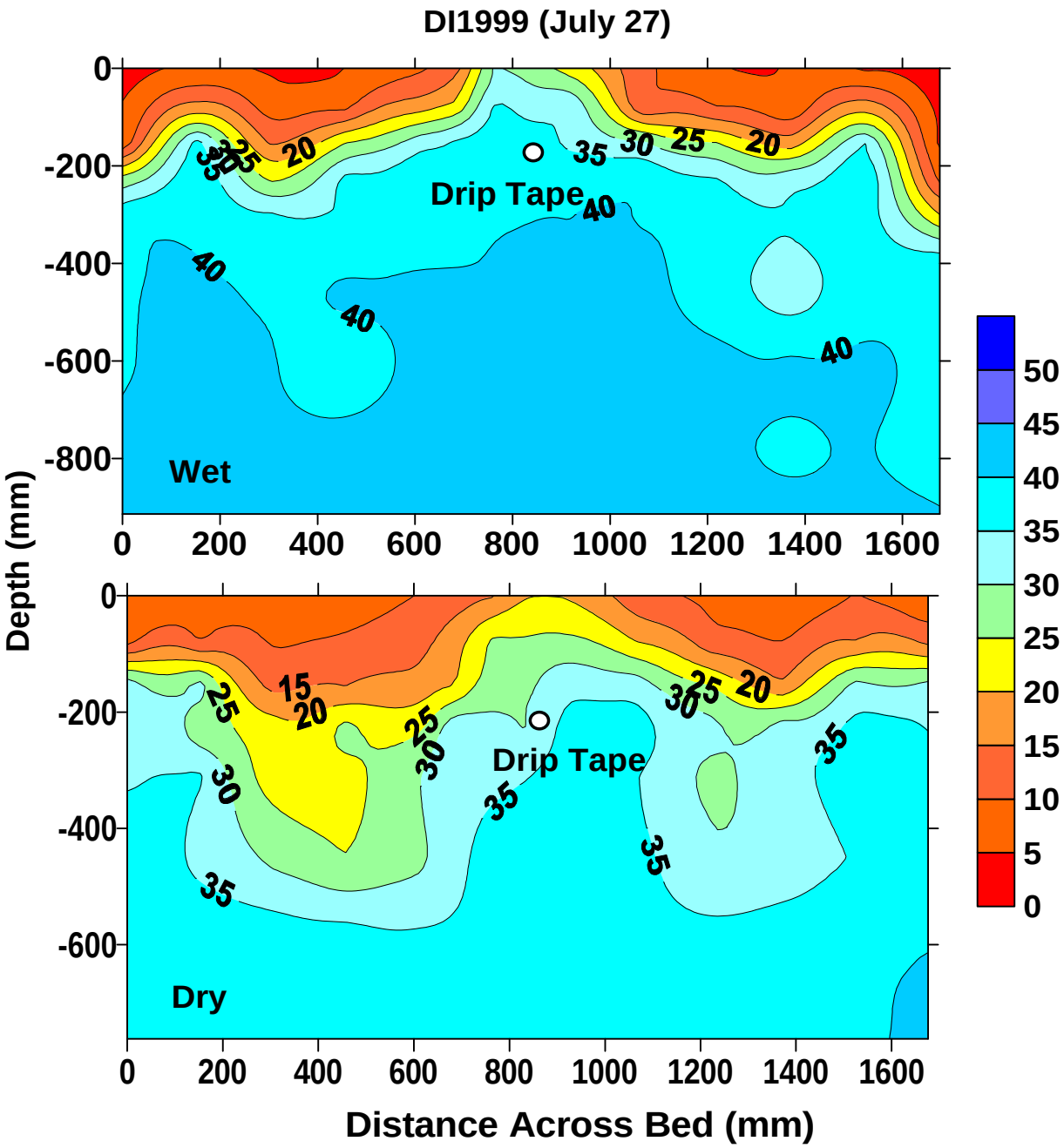

Figure 8. Patterns of soil water content about the drip line of the wet and dry irrigation treatments for DI1999.

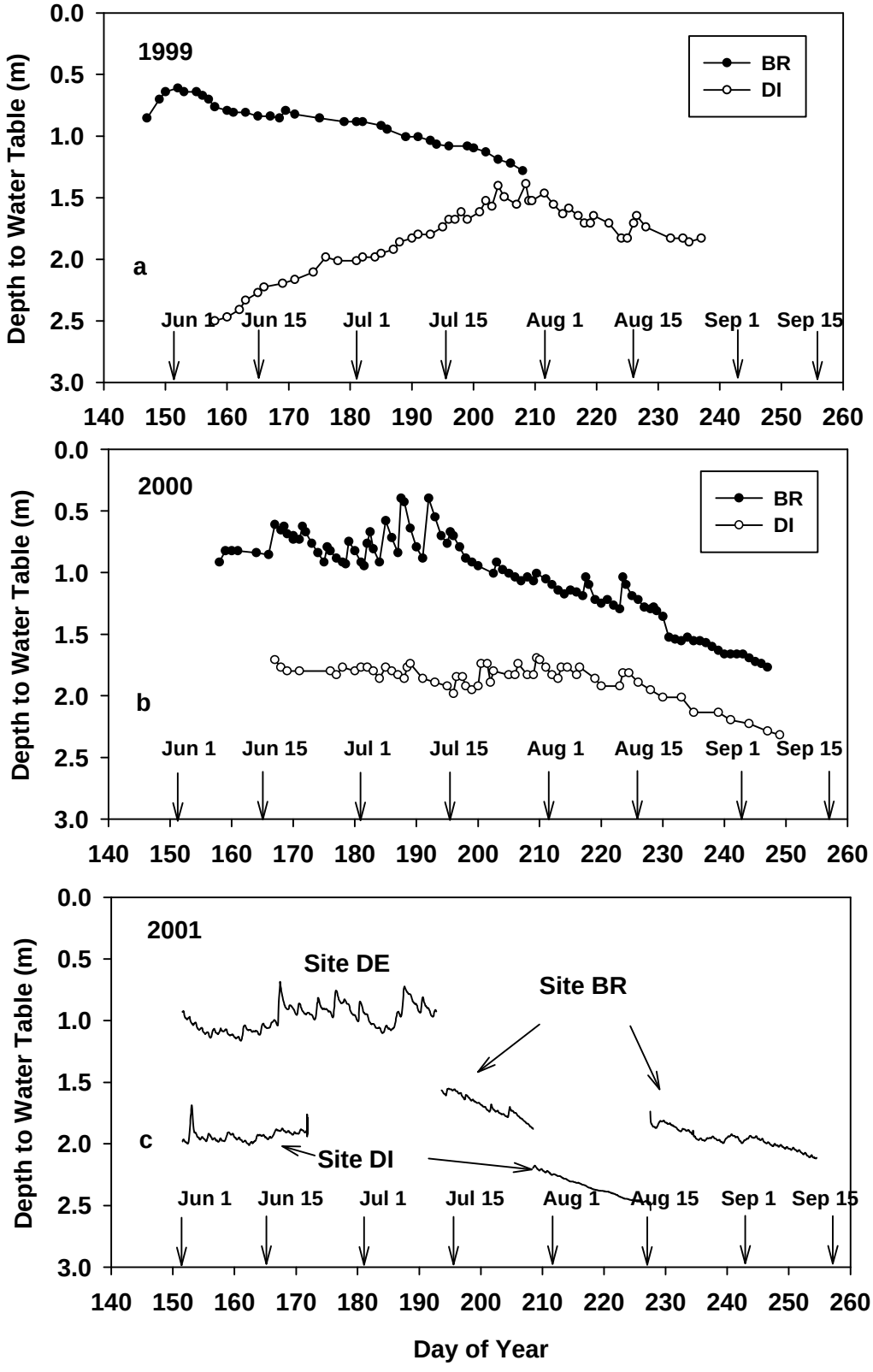

Figure 9. Water table depths for all years and sites.

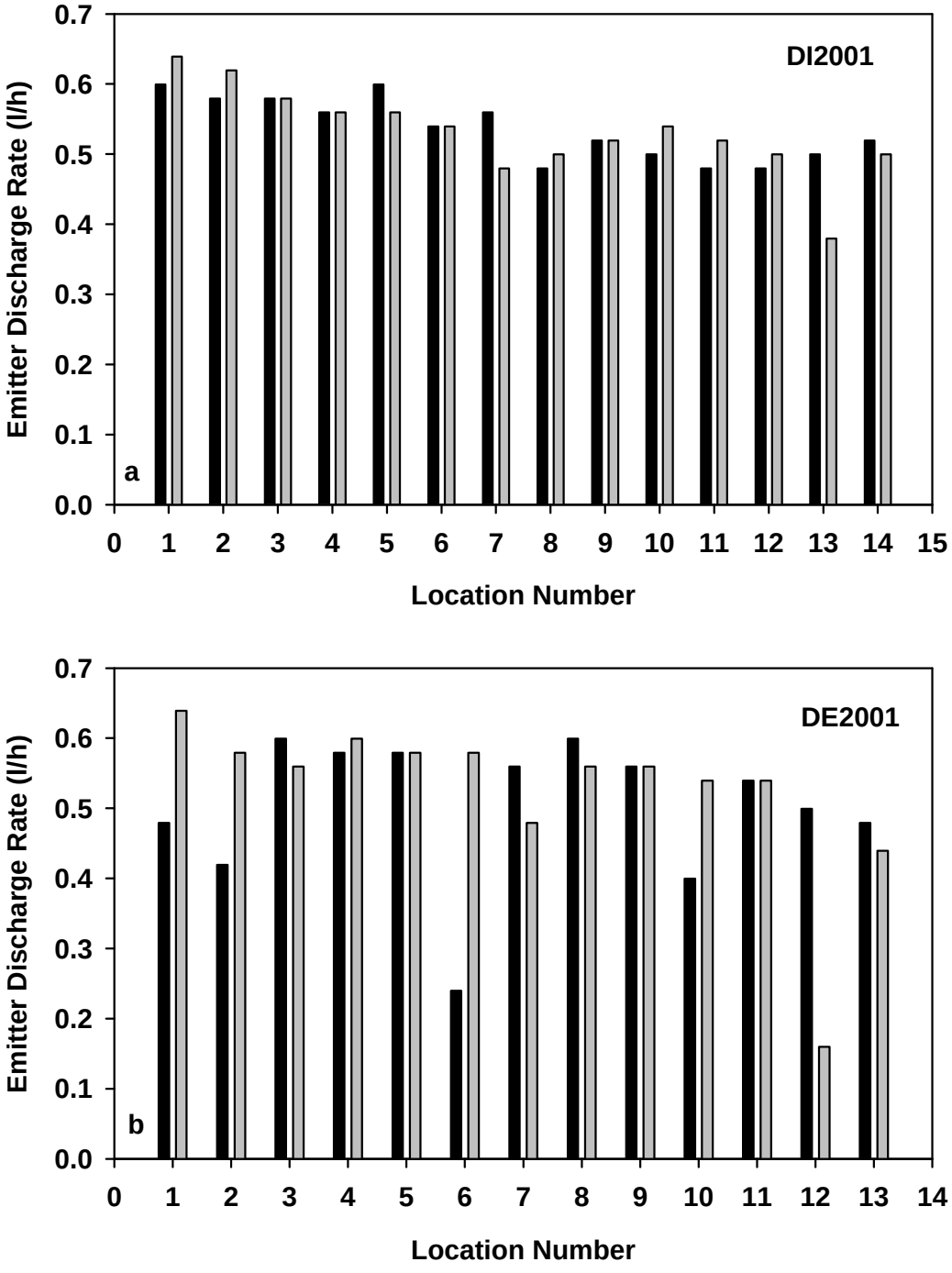

Figure 10. Emitter discharge rates along dripline at DI2001 and DE2001.

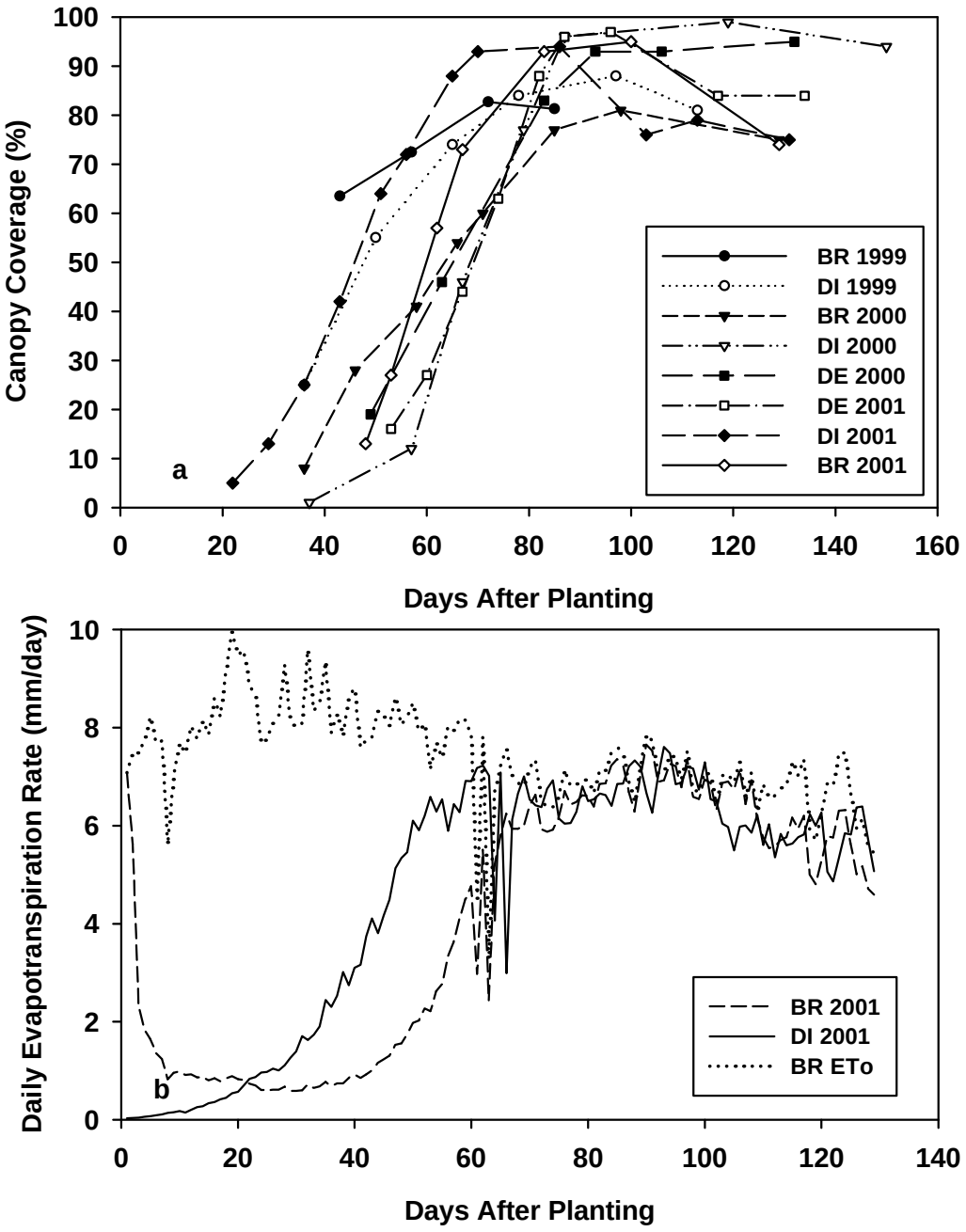

Figure 11. Canopy growth curves (a) and daily evapotranspiration of DI2001 and BR2001 (b).

Salinization of Deep Production Wells in the Western San Joaquin Valley: Risk Analysis, Uncertainty, and Data Needs

Project Investigators:

Thomas Harter
Office: (530) 752-2709, E-mail: thharter@ucdavis.edu,
Dept. of Land, Air, and Water Resources
University of California, Davis

Graham E. Fogg
Office: (530) 752-6810, E-mail: gefogg@ucdavis.edu
Dept. of Land, Air, and Water Resources
University of California, Davis

Research Staff:

Nels Ruud, Postdoctoral Researcher

Hua Zhang, Graduate Research Assistant

ABSTRACT

The alluvial aquifer system of the central part of western San Joaquin Valley, California consists of a highly heterogeneous semi- confined aquifer overlying a similarly complex confined aquifer. Groundwater in the shallow part of the semi-confined aquifer is highly saline. Based on regional groundwater models, the projected time of encroachment of the saline groundwater to the lower depths of the semi-confined aquifer and the confined aquifer is 200-600 years. The objective of our work is to quantify the risk of locally accelerated encroachment due to the presence of highly permeable pathways within the alluvial fan. Specifically, we are interested in the statistical properties of the arrival time of the salt front at deep production wells and its sensitivity to the hydrostratigraphic structure of the alluvial fan and interfan deposits in the region, which itself is subject to considerable uncertainty. Well drilling logs and soil survey map information are used in conjunction with a transition probability/Markov chain geostatistical methodology to quantify the spatial variability of the aquifer system hydrostratigraphy. In the current reporting year, a sensitivity analysis is being completed to determine the effect of uncertainty in the geostatistical parameters. Multiple realizations of the aquifer hydrostratigraphy are generated and Monte Carlo simulations of salt-transport are performed. Within this stochastic framework, risk is defined as the probability that individual wells become contaminated within a specified time horizon. Risk of water quality degradation in the lower semi-confined and confined aquifers will be quantified as a function of well placement, sub-regional area, and management practices. Preliminary results from the sensitivity study indicate that a meaningful risk analysis will depend to a large degree on the accurate characterization of: the number of hydrostratigraphic elements that make up the aquifer, the proportion of coarse grained sediments that may carry large amounts of salt to depth over relatively short periods of time, the mean lengths of important stratigraphic units, particularly the ratio of length and thickness of coarse materials, and the degree of entropy (sorting, juxtapositional preference) found among the hydrostratigraphic elements.

KEYWORDS

San Joaquin Valley, salinity, groundwater, salinization, risk analysis, hydrogeology, modeling

INTRODUCTION

BACKGROUND

The aquifer system in the salt-affected region of the western San Joaquin Valley (Figure 1) is conceptually divided into three major vertical zones: an upper semi-confined aquifer, a middle confining layer (known as the Corcoran Clay Member of the Tulare Formation or simply, the "Corcoran Clay"), and a lower confined aquifer. The geologic material in the semi-confined aquifer consists of Coast Range alluvium in the western part of the region, Sierran sand in the middle region near the Valley trough, and shallow flood-basin deposits in the eastern region in the vicinity of the San Joaquin River. Overall, the thickness of the semi-confined aquifer ranges from approximately 300 feet near the valley trough to over 600 feet at the base of the Coast Ranges. The Corcoran Clay is a laterally extensive lacustrine deposit ranging in thickness from approximately 20 to over 100 feet. It is often conceptualized as a single, continuous layer of very low hydraulic conductivity. However, a preliminary analysis of drilling logs indicates that the semi-confined aquifer consists of alternating layers of coarse and fine textured material and that the Corcoran clay is not homogeneous, but possesses inter-bedded bodies of coarse-textured material (Figure 2). The confined aquifer below the Corcoran Clay consists primarily of flood-basin, deltaic, alluvial-fan, and lacustrine deposits. Its thickness ranges from approximately 570 to 2460 feet.

The salinity of the groundwater in this region is quite high with dissolved-solids concentrations ranging from 983–35,000 mg/L (Dubrovsky et al., 1993). Although not well quantified, the vertical variability in salinity concentrations is known to be highest near the water table while decreasing with increased depth (Dubrovsky et al., 1993). Evaporation from an area with a highly saline shallow water table results in the detrimental accumulation of salts on the soil surface and in the crop root zone. The inability to lower the water table by exporting drainage water to off-farm sites has resulted in an effort to find alternative drainage management options to hydraulically control (lower) the water table to more acceptable levels.

The groundwater flow modeling study conducted by Belitz and Phillips (1995) numerically evaluated the effectiveness of four different alternative drainage management options to hydraulically control the highly saline shallow water table in the salt-affected region of the western San Joaquin Valley. These alternatives were 1) land retirement, 2) reduced aquifer recharge, 3) increased groundwater pumping, and 4) simultaneous reductions in aquifer recharge and increased groundwater pumping. They found that options 3) and 4) numerically produced the greatest reductions in areas subject to bare-soil evaporation–the indicator used to evaluate the extent of hydraulic control of the water table in their study.

Since the salinity is known to decrease with depth, any groundwater pumped for the purpose of re-application to the soil surface as irrigation water would have to be extracted from either deep within the semi-confined aquifer or within the confined aquifer to avoid applying highly saline groundwater to the crops. However, the Groundwater Management Final Report (Task 6), issued by the Groundwater Management Technical Committee (April 1999) to the San Joaquin Valley Drainage Implementation Program and the University of California Salinity/Drainage Program, identified several unresolved technical issues concerning the use of increased pumping as a means to hydraulically control the water table in this region. Two issues of relevance are: 1) what will the vertical rate of migration of highly saline shallow groundwater be if pumping rates are increased in deep production wells either above or below the Corcoran Clay, and how will it vary spatially?, and 2) how will the location of the well screen above or below the Corcoran Clay affect the rate of change of water quality? The Groundwater Management Final Report also identified the need for improved spatial resolution and characterization of the aquifer-system hydrostratigraphy in future groundwater flow and contaminant transport studies used to assess the impacts of increased pumping from wells on vertical migration rates and changes in deep aquifer water quality.

The Belitz and Phillips (1995) study estimated that although increased pumping would result in a downward migration of poor-quality groundwater from the shallow zone, it would take 200 to 400 years to reach pumping wells located in the lower semi-confined zone, and 250 to 600 years to reach the wells located in the confined aquifer. On a regional basis, the proposed management strategy increases specific discharge across the Corcoran clay from 0.27 ft/yr to 0.42 ft/yr. Belitz and Phillips (1995) emphasize, "that flow rates and TDS [total dissolved solids] concentrations vary spatially and that arrival times may vary from subarea to subarea". However, their study did not include an estimate of the distribution of these arrival times. Furthermore, their model did not account for the spatial variability of the aquifer-system hydrostratigraphy in the semi-confined zone and in the Corcoran Clay. The presence of interconnected coarse-textured bodies in the semi-confined aquifer and in the Corcoran Clay could significantly accelerate the migration of highly saline groundwater to the deep semi-confined and confined aquifer zones and lead to the degradation of water quality there.

CONTRIBUTION TO PROBLEM SOLUTION

In this study, we evaluate the long-term risk of groundwater degradation in the deep semi-confined and confined aquifers due to increased pumping in these zones. We have developed a toolbox that includes an "aquifer generator" to study various random arrangements of alluvial fan deposits, a groundwater flow model, and a transport model. We developed programs to bundle the third-party software elements into a tool specifically designed for this project to estimate the probability of early arrival of highly saline water in these zones due to the presence of vertically extensive interconnected coarse-textured bodies in the semi-confined aquifer and in the Corcoran Clay or to leakage inside wells and boreholes hydraulically connecting these zones. The risk analysis accounts for the sub-regional spatial variability of aquifer-system hydrostratigraphy, vertical and horizontal flow rates, and salinity concentrations. During this first funding year of the second project cycle (third year overall), a sensitivity analysis is being performed to assess the reliability of the risk analysis predictions in terms of data scarcity problems associated with the characterization of the spatial variability of aquifer-system hydrostratigraphy and water quality. Results will be used to implement the final risk analysis and to recommend additional data collection and groundwater quality monitoring efforts to improve the characterization of aquifer chemical and physical heterogeneity and ultimately the predictions of salt migration in the deep sub-surface by the transport model.

By employing a stochastic approach, we can estimate the percentage of wells likely to become unusable as a function of time. The results of the risk analysis could then be used in cost-benefit analyses of various groundwater management alternatives. It is also worth noting that historical pumping rates during the 1970s and 1980s were approximately 60% of those recommended by Belitz and Phillips (1995). However, potential reductions in surface water deliveries in this region due to the implementation of the Central Valley Project Improvement Act (CVPIA) may result in an increase in groundwater pumping to levels recommended by Belitz and Phillips (1995). Consequently, our risk analysis may also be used to assess the impacts of reduced surface water allocations on groundwater quality on a sub-regional basis.

OBJECTIVES

Current project work continues the research started during a previous 2-year project funded by the University of California Salinity/Drainage Program. The updated project objectives are 1) to continue to develop geostatistical models of the hydrostratigraphy and water quality for the semi-confined aquifer and the Corcoran clay layer; 2) to continue to develop the groundwater flow and salt transport model by incorporating the geostatistical models of the aquifer-system hydrostratigraphy and defining pumping and recharge inputs using data from previous modeling studies; 3) to assess the reliability of the risk predictions by performing a sensitivity analysis; 4) to determine the risk of well-water degradation in the deep semi-confined and confined aquifers for 25, 50, and 100 year forecast horizons for two different management scenarios evaluated by Belitz and Phillips (1995); and 5) to develop recommendations for future data needs that can improve the risk predictions. We are currently in the third project year.

METHODS

GEOSTATISTICAL MODELING

Data Collection

Data collection efforts for the characterization of the aquifer-system hydrostratigraphy include the ongoing gathering of drilling well logs, electrical well logs, and soil survey maps. These data are used to characterize and refine the hydrostratigraphy of the semi-confined aquifer and the Corcoran Clay through interpretation and development of geostatistical models of their spatial variability. The drilling logs provide a description (e.g. texture, color, hardness, etc.) of the sediment observed during drilling at different depth intervals down the borehole. The electrical well logs are used to validate the quality of the drilling well logs and provide additional lithology information. Together they are used to delineate the vertical locations and thicknesses of texture-based hydrostratigraphic units. The soil survey maps are used to locate texture-based units on the land surface and to estimate their mean lengths in the dip and strike directions. A listing of existing wells, including state well numbers and screen locations, is given in the geographic information system by Gronberg et al. (1990). Copies of drilling and electrical well logs, to be used for strictly academic purposes, are provided courtesy of the California Department of Water Resources.

Published data characterizing the aquifer-system water quality is very limited. However, estimates of the spatial distribution of shallow groundwater quality are given by Swain (1990). Sparse water quality measurements in the deeper subsurface can be found in Dubrovsky et al. (1993). Additional water quality measurements may be available from irrigation and water districts within the project area. The collection of additional water quality data will undoubtedly be a major recommendation of the sensitivity analysis performed in this study.

Products in Progress

A complete database of collected drilling and electrical well logs, a classification scheme used to assign texture descriptions to hydrostratigraphic categories, and the interpretation of each well log using the classification scheme will be provided. The well log analysis will include a map showing the spatial locations of each log and relevant well log statistics. A classification scheme used to interpret the soil survey map is also developed. The soil survey map and its associated interpretation will be presented in map and text formats. Water quality measurements and information collected from published reports, districts, or other sources will also be presented in map and text formats.

Geostatistical analysis

In this study, we employ a transition probability/Markov chain approach specifically

developed to analyze the hydrostratigraphy of alluvial and fluvial systems (Carle, 1996; Carle et al., 1998). The geostatistical analysis and "aquifer generator" software is called TSIM (Carle, 2001). Unlike other geostatistical methods, this approach defines the aquifer-system hydrogeology in terms of its major hydrostratigraphic units rather than by extensive knowledge of the aquifer hydraulic conductivity distribution. In this method, the number of major textural categories, their volume proportions, average thicknesses, dip and strike directions, and juxtapositional relationships defines the hydrostratigraphy. This information is readily obtained from well logs and soil survey maps (Weissmann et al., 1999).

An example of the application of the transition probability/Markov chain model is presented in Figure 3 (Ruud et al., 1999). Here we model the semi-confined aquifer located beneath townships T14S-R13E and T15S-R14E. For this case, we categorize the associated drilling well log descriptions and soil survey map unit descriptions into fine-textured and coarse-textured categories. Analysis of the associated drilling well logs in T15S-R14E indicates that approximately 20% of the volume consists of coarse-textured material and 80% is fine-textured. The analyses for T14S-R13E yield estimates of 41% coarse and 59% fine. The mean lengths of the fine and coarse material in the vertical direction for T15S-R14E are approximately 85 and 20 feet, respectively. The mean lengths of the fine and coarse material in T14S-R13E are 20 and 15 feet, respectively. The large percentage volume of observed coarse material in T14S-R13E reflects its location in the mid- to upper-fan area.

Using the soil survey maps, geologically plausible mean lengths of the coarse-textured units in the northwest-southeast and southwest-northeast directions were chosen as 2500 and 15000 feet, respectively, for both T14S-R13E and T15S-R14E. The mean lengths of the fine-textured units are computed from the ratio of the proportions and from consideration of marginal probabilities.

Similar geostatistical realizations can be simulated by defining any number of texture categories. In this study, we plan to generate geostatistical models for each sub-area using two-, three-, and four-category textural classification schemes. The number of texture categories necessary to adequately characterize the aquifer-system hydrostratigraphy will be assessed in the sensitivity analysis of the transport predictions. The sensitivity analysis will also assess the impact of using different mean length estimates for texture categories in the vertical, dip, and strike directions.

Products in Progress

A geostatistical model characterizing the hydrostratigraphy of the semi-confined aquifer, the Corcoran Clay, and the confined aquifer for each sub-area. Models are being developed for two-, three-, and four-texture category classifications.

GROUNDWATER FLOW AND SALT TRANSPORT MODELING

Model Development

A three-dimensional transient flow and salt transport model has been developed for the implementation of the risk analysis via Monte Carlo simulation. The groundwater flow model is developed using MODFLOW (McDonald and Harbaugh, 1988) and the salt transport model is developed using the particle-tracking program RWHET (LaBolle, 2002). The groundwater flow and particle-tracking models are defined and interact by use of the Groundwater Vistas graphical-user-interface software. This flow and transport model accounts for the spatial variability of the aquifer-system hydrostratigraphy at a sub-regional horizontal scale of a few hundred feet and a vertical scale of a few tens of feet at most. The size of the individually modeled sub-areas is approximately that of a township-range (i.e. ~36 square miles). The model horizontal scale is determined by the mean lengths in the dip and strike directions of the coarse-textured soil survey mapping units. Likewise, the vertical scale is determined by the mean length of the coarse-textured units in the vertical direction. The length of finite-difference grid spacings in the two principal horizontal directions are equal and equivalent to approximately one fifth of the mean length of the coarse-textured material in the strike direction. Similarly, the vertical grid spacing is equal to approximately one fifth of the mean length of the coarse-textured material in the vertical direction. For simplification, the resolution of the flow and transport model is identical to the geostatistical model.

The geostatistical model is used to generate a number equiprobable realizations of the aquifer hydrostratigraphy. The simulated hydrostratigraphic

units are assigned hydraulic conductivities representative of those reported by Belitz and Philips (1995). Groundwater flow and salt transport simulations are performed for each realization of the aquifer heterogeneity. Each flow and transport simulation is constrained such that the average regional groundwater levels and fluxes between the three main vertical units are identical to those reported by Belitz and Phillips (1995). The results of the Monte Carlo simulation are processed to calculate statistical moments and sampling distributions to be interpreted in the risk analysis.

For each aquifer realization, groundwater flow and salt transport will be simulated for 25, 50, and 100 year forecast horizons for two different management scenarios evaluated by Belitz and Phillips (1995): 1) continuation of current irrigation and groundwater management practices (i.e. no action) , and 2) a reduction in recharge and an increase in groundwater pumping (i.e. alternative management option 4).

The main effort during the first nine months of this first funding year was the development of a Fortran Code to automate the modeling setup including the generation of input files, and to couple the three software programs TSIM, MODFLOW, and RWHET into single super-program called SASHA-RB (Sensitivity Analysis of Stochastic Hydrostratigraphy in a Aquifer–Rectangular Box). Extensive testing was implemented to validate the new transport code RWHET against analytical solutions, and to ensure that SASHA-RB produces identical output to manual process of assembling input files, executing the three programs, and transferring data output and input between the three software components.

Products in Progress

A groundwater flow and salt transport model developed in TSIM, MODFLOW and RWHET, respectively, through the SASHRA super-code. The numerical grid of the flow and transport model is adjustable to adequately resolve the heterogeneity of the semi-confined aquifer, Corcoran Clay, and confined aquifer. We currently plan to follow up on SASHA-RB with SASHA-DP (Sensitivity Analysis of Stochastic Hydrostratigraphy in an Aquifer with Distributed Pumping) and SASHA-WI (Sensitivity Analysis of Stochastic Hydrostratigraphy in an Aquifer – Westside Implementation).

DETERMINE RELIABILITY OF RISK PREDICTIONS

Sensitivity analysis

The reliability of our risk analysis depends on the reliability of the underlying parameters. The proposed geostatistical-stochastic approach depends on several key parameters, including:

1. parameters characterizing the hydraulic properties of individual hydrostratigraphic units (permeability, storage coefficient, porosity, small-scale dispersion)
2. parameters characterizing the model domain boundary conditions
3. parameters characterizing the pumping and recharge stresses
4. the appropriate number of textural categories (from 2 to 4)
5. parameters describing the geostatistical models of spatial variability within the alluvial, fluvial, and lacustrine sediments that dominate the project area (mean lengths in dip, strike and vertical directions; juxtaposition patterns among hydrostratigraphic units; volume proportions)
6. parameters characterizing the numerical flow and transport solutions (numerical grid and time discretization)

Items 4 and 5, above, are unique to our approach and deserve careful evaluation. While we can define distinctly different geostatistical models for hydrogeologic sub-areas, such as the upper (proximal) and lower (distal) alluvial fan sediments, the geostatistical parameters of these are not precise. The database will constrain these parameters only to a certain range. Within that range, the sensitivity analysis will define a number of key model scenarios to specifically address the following questions:

1. Is the risk for early salinization of production wells dependent on the number of major textural categories? Our research hypothesis is that early salinization occurs only where significant vertical connectivity exists in the coarsest textural fraction (sands, gravels, sandy loams).
2. Is the risk of early salinization very sensitive to the volumetric fractions occupied by coarse material? Does a threshold volumetric fraction exist for the coarse-textured material,

below which vertical movement is dominated by flow through fine-textured material, and above which movement in coarse-textured material dominates it?

3. To which degree does early salinization depend on the mean lengths in the dip, strike, and vertical directions of individual alluvial strata? What is the role of horizontal and vertical anisotropy of these length scales?

4. Do juxtaposition tendencies (e.g. a preference for a loam to be located above a sand rather than a clay above a sand) influence the risk analysis?

To answer these questions, a factorial design simulation scheme is proposed that will systematically vary these parameters within the range defined by the database.

Products in Progress

As will be seen in the results section, connectivity of channel deposits plays an important role in determining the risk of early salinization. We have developed our own algorithm and Fortran Code ("FLOWPATH") to check for connectivity (percolation clusters in random media, see discussion below). We have also written Fortran programs to analyze the percolation properties of random hydrostratigraphic media generated with TSIM. This, together with SASHA applied to the above issues will provide the confidence intervals to be added to the probability plots/risk analysis.

LONG-TERM RISK ANALYSIS

Statistical Analysis

Based on the Monte Carlo simulations of the final stochastic hydrostratigraphic models (SASHA-WI) for the two study townships are completed, a statistical analysis will be applied to each to evaluate the effects of the two different management scenarios evaluated by Belitz and Phillips (1995). For each, we will compute:

1. the average groundwater level and fluxes in the semi-confined and confined aquifers to assure coherence with the regional analysis by Belitz and Phillips (1995).

2. for each group of wells within the study area, completed either above or below the Corcoran clay, the probability that salt concentration exceeds 1500 mg/l after 25, 50, and 100 years. Repeat the analysis for concentrations exceeding 3000 mg/l.

3. the mean percentage of wells with salt concentrations exceeding 1500 or 3000 mg/l after 25, 50, and 100 years. Also, compute the variance about the mean percentage of wells contaminated.

FUTURE WORK: RECOMMENDATIONS FOR FUTURE DATA COLLECTION

Evaluate Data Needs and Interpret Sensitivity Analysis

The sensitivity analysis will provide information about the need to provide accurate parameters as input to the risk analysis. If the risk prediction is insensitive to a parameter within the given range, then the data provided are adequate for risk analysis. On the other hand, if the risk prediction is very sensitive to a parameter, that is, if the results vary significantly depending on the value a parameter takes on within a realistic range, then more precise data are needed for risk analysis. Data should be collected such that the sub-range, within which the risk model is most sensitive, can be defined more accurately. This leads to recommendations of specific data collection needs.

Evaluation and Reporting

The statistical results represent a quantitative risk analysis of well water contamination from poor quality groundwater originating in the shallow aquifer zone. A discussion of the results will include an analysis of spatial distribution of risk within the study area to determine areas that are more prone to groundwater degradation than others, to determine the role of well leakage through the Corcoran Clay, to analyze to which degree spatial variability of hydrogeologic properties must be taken into account by future groundwater and irrigation management decisions, and to propose a future field monitoring program that can further reduce the uncertainty inherent in the proposed analysis.

Results will be shared with the irrigation and water districts on the west side of the San Joaquin Valley, with local and state water authorities, and with the University of California Salinity and Drainage Program.

Expected Products

Recommendations for future data needs to improve confidence in the risk analysis;

Presentation, discussion and conclusions regarding the overall scope of the study; final publications.

RESULTS AND DISCUSSION

We conceptualize the fluvially dominated alluvial aquifers on the Westside of the San Joaquin Valley to consist of individual hydrostratigraphic elements that belong into two or more stratigraphic categories (types) (Carle et al., 1998; Weissmann et al., 1999a,b). Examples of the types or categories of hydrostratigraphic elements to be considered are "channel deposits" (coarse grained deposits associated with stream channel deposition), "overbank deposits" (intermediate grained deposits associated with stream bank deposition), "flood plain deposits" (fine grained deposits associated with deposition of fines carried in floods that cover large areas of land), and others. We further define an "element" of a category (or type) as a localized occurrence of a specific deposition type. For example, the well logs in Figure 2 each contain a sequence of many stratigraphic elements belonging into two major stratigraphic categories: coarse grained sediments and fine grained sediments.

The geostatistical concept of transition probability describes the arrangement of individual elements in terms of their individual volume proportions, the mean (average) length in the dip, strike, and vertical directions, and their juxtaposition preference (for more detailed discussion, see below). For the sensitivity analysis, the four critical geostatistical parameters describing the only vaguely known hydrostratigraphy of the alluvial fans on the west side of the San Joaquin Valley are the connectivity of the coarser materials, the average length of the major hydrostratigraphic elements in the dip (slope), strike (cross-slope), and vertical directions, the role of the classification of hydrostratigraphic elements, and the amount of juxtapositional preference between some of the hydrostratigraphic elements (Weissmann et al., 1999b). We discuss the importance of each of those separately and present the preliminary results of the sensitivity analysis implemented with SASHA-RB.

CONNECTIVITY OF COARSE SEDIMENTS

Connectivity is the degree to which individual elements of a specific hydrostratigraphic category, e.g., "channel deposits", which are the coarsest type of deposits in the alluvial fans on the west side, are connected to each other throughout the aquifer. A single connected body of channel deposits, however strange its shape (Figure 4, typically something akin to a three-dimensional ganglion labyrinth made out of a sequence of interlaced channel beds as they evolved on the surface of a growing alluvial fan), is called a "cluster" (Stauffer and Aharony, 1991). An important measure of connectivity is the integral connectivity scale (Western et al., 2001), which is the average distance between two points in individual clusters, i.e., between points that belong to the same hydrostratigraphic category and are connected to each other (via the "ganglion"). The integral connectivity scale can be thought of as a mean (average) connectivity length, a term that we will apply in the remainder of this report in lieu of the term coined by Western et al. (2001).

Connectivity is important, because it may have a significant impact on the amount of salt transport from the surface to the deeper part of the aquifer: If the channel deposits (which have by far the highest hydraulic conductivity) are connected all the way from the land surface to, say, the Corcoran Clay aquitard, salts may have a "freeway"–even though crooked–to the deeper part of the aquifer by simply traveling through the channel deposits downward. The hydraulic gradient on the west side is largely a vertical gradient from the land surface, where water is recharged to the deeper parts of the alluvial fan, where the pumping occurs: towards the lower portion of the semi-confined upper aquifer and across the Corcoran Clay aquitard in the lower confined aquifer.

The crooked "freeway", if it indeed exists, is a single cluster (or what we here call a ganglion) of channel deposits that connects the land surface with the Corcoran Clay. We call such a ganglion that traverses the entire aquifer (in this case from top to bottom) a "percolating cluster" (Stauffer and Aharony, 1991).

The connectivity of the coarse sediments and whether or not a percolating cluster exists depends on the degree of order or structure that dominates in the alluvial fan. We call this the entropy in the hydrostratigraphic arrangement. We illustrate this by way of a simple sandbox example: Let's take a rectangular, empty sandbox (say with dimensions 12" wide, 12" deep, and 6" high, which is a volume of 0.5 cubic feet,

about 3.7 gallons, 15 quarts, or 60 cups). Let's say we have a small amount of medium sand (6 cups), and lots of silt available that we will use to build an aquifer inside this sandbox. Principally, we have two choices to build that sandbox: we can create an orderly, pre-meditated structure made of sand and surrounded by silt–something that we call "ordered media". Or we can randomly place alternate heaps of sand (as little as it is) and silt into the sandbox to create what we refer to as "random media". What can we say about the connectivity in either one of those two media?

In ordered media, we can create any degree of connectivity we desire: even with the smallest amount of sand, we can build a single string or plane or single arbitrary body (cluster) of sand such that all sands are completely connected to each other. The most compact cluster form that we can create is a sphere (ball) with a volume of 1.5 quarts (6 cups), surrounded by silt. While all sand is connected to itself, the integral connectivity length is the smallest of any cluster that we can create with that amount of sand. The sand cluster with the largest mean connectivity length would be a sand cluster that we create that connects two diagonally opposite corners of the box–one being at the top of the box and the other being at the bottom of the box (that's the largest distance anywhere inside the box). With the sand (after laying out an appropriate bed of silt), we could create a straight sand tube, with a volume of 1.5 quarts, connecting these two corners. If we wanted to create an aquifer that allows some water to go very fast from the top of the sandbox to the bottom of the sandbox (let's assume, the sandbox has a highly permeable mesh as a floor, is suspended on four legs and is continuously flooded with 0.25" of water at the top), we could create a vertical wall or a vertical cylinder of sand (again, with a volume of 1.5 quarts) surrounded by silts. That gives us the perfectly straight "freeway". On the other hand, if we were to create an aquifer that has the least flow from top to bottom, we could built a thin horizontal layer of sand somewhere in the box – now all water has to travel mostly through silt as it percolates through the aquifer top to bottom.

The example illustrates that order within geologic structures can create both extremes: highly permeable, preferential pathways, and highly impermeable aquitards. It is those highly ordered elements in the architecture of an alluvial basin that are recognized in the general geology and hydrogeology. On the west side, there is a strong order (although not perfect) of higher permeable material (the semi-confined aquifer) overlying a lower permeable stratum (the Corcoran Clay aquifer), which in turn sits on top of yet another higher permeable part of the alluvial fan (the confined aquifer). In their regional groundwater flow model, Belitz and Phillips (1995) have captured the structures of this order including some regionally averaged subfeatures within the upper, semi-confined aquifer (Figure 5).

Within each of these major systems, the exact order is not that simple to recognize. In fact, the arrangement of coarse material (channel deposits) and fine material (overbank and flood deposits) may be completely random. The Belitz and Phillips model (Figure 4) only captures sub-regional differences, but not actual hydrostratigraphic elements.

What about the connectivity in random media? What is the connectivity of the sand, if we randomly (but carefully) placed teaspoonfuls of sand and silt into the sandbox until it is full (again, we only have 1.5 quarts of sand)! What is the average size of sand clusters? Will there be a percolating cluster (a sand ganglion that connects the top and bottom of the sandbox, or any opposing sides)? These kinds of questions have been extensively studied in physics and applied to many different fields unrelated to hydrology. This field of research is called "percolation theory" (Stauffer and Aharony, 1991).

Percolation theory, much of which has been derived based on empirical (mostly numerical) work, was originally conceived not with aquifers in mind and most of its applications have been in physics and material sciences (Sahimi, 1994). But hydrogeologists have recently begun to apply its principles to groundwater flow and transport (Berkowitz and Balberg, 1993). Percolation theory is teaching us some fundamental and intriguing insights into the connectivity of sand ganglions (or sand clusters). Its applications in hydrogeology have been limited to dual media (sand/silt, sand/clay, sandstone/shale) or to Gaussian random fields (*cf.* Berkowitz and Balberg, 1993). Our work is the first to study the percolation properties of Markov chain random fields defined by transition probabilities.

Since Markov chain random fields with only two hydrostratigraphic elements (dual media) are

identical to Gaussian indicator random fields (Carle and Fogg, 1996), the percolation properties should be those derived for Gaussian random fields (e.g., Desbarats, 1987). Some general key findings that we have found reported in the literature (Berkowitz and Balberg, 1993; Sahimi, 1994; Renault, 1991; Sahimi and Mukhopadhyay, 1996; Mendelson, 1997), can be directly applied to our 60 cup (0.5 cubic feet) sandbox experiment with sand and silt. It is equally applicable to the alluvial fan hydrostratigraphy at the Westside. Interpreted to and illustrated with these cases, the following can be said:

1. If we randomly place little sugar cubes (.25" by .25" by .25" or similarly sized) in a regular, nonoverlapping, brick-pattern into our example sandbox, it is almost completely unlikely that, by chance, we create a sand ganglion that connects the top of the aquifer (where all the recharge occurs) with the bottom of the aquifer (where all the pumping occurs). In fact, percolation theory tells us that we would need about 18 cups (or 31% of the total sandbox volume) of sand, placed randomly in this regular grid of sugar cube sized cubes before we have a reasonable chance to have at least one sand ganglion that connects the top and the bottom of the aquifer. The sand ganglion or ganglion of channel deposits that connects two opposite sides of the aquifer (e.g., top and bottom) is called the "percolating cluster". The percentage above which a percolating cluster is likely to occur, 31% (18 cups), is the "percolation threshold". Below the percolation threshold (say with 17 cups of sand) it is highly unlikely that we create a percolating cluster by randomly placing sand and silt cubes into the sandbox.

2. Percolation theory, and our numerical experiments with TSIM and our percolation analysis of TSIM fields confirm that, also tells us that depending on the number of little sand or silt cubes that fit into the sandbox, there may be more or less variation from the percolation threshold. Let's say that we randomly place microcubes, sized 0.025"x0.025" x0.025", of sand and silt into the sandbox. That's a total of 480x480x240 (55.3 million) cubes that fit into the box. If we created many of these sandboxes, with varying amounts of sand, we would find that the chances to have a percolating cluster with any less than 30.5% sand are practically null. But with 31.5% (or anything more than that) sand we practically always have at least one percolating cluster, no matter how long we try! Now, as we increase the size of the cubes (relative to the size of the sandbox) to something much more than about 1/20th of the sandbox, it becomes more likely that we find a percolating cluster even with a much lower percentage sand than 31%. By the same token, it is also more likely that we don't have percolation at all even with a much higher percentage sand than 31%. That is because we create a certain degree of order by making the cubes larger (relative to the size of the sandbox). Think about the amount of order created with cubes that are 2" x 2" x 2" (6x6x3=108 cubes) relative to the tiny 55 million cubes with 0.025" length! Within each 2" x 2" x 2" cube, there is complete homogeneity (that is, order).

3. Numerical experiments (including our own with TSIM) and percolation theory show that the percolation threshold becomes lower, if we allow overlapping between the individual bodies of sand and silt as they are placed into the sandbox, or if the bodies have irregular shapes and, perhaps, even have a different mean size (as opposed to placing randomly selected silt and sand cubes of the same size into a regular, nonoverlapping grid pattern). In the geostatistical literature, such a pattern is referred to as a "correlated" random media. If we allow any kind of overlap (i.e., we create correlated random media), the percolation threshold has been shown in the literature (Renault, 1991; Sahimi and Mukhopadhyay, 1996; Mendelson, 1997) to drop to somewhere between 12% and 18% (Figure 6). We are currently implementing large Monte Carlo simulations to exactly determine the percolation threshold for three-dimensional, correlated media.

4. The percolation threshold has been found to be independent of the type of randomness (Gaussian, Markov chain, others) that characterizes the placement of sand and silt (or other material) in the sandbox (Sahimi and Mukhopadhyay, 1996). Our preliminary experiments confirm that the Markov chain random fields create the same percolation threshold as the Gaussian random fields, that is a percolation cluster or crooked "freeway" of sand that connects the land surface and

the wells just above the Corcoran Clay always exists if at least 12% to 18% of channel deposits are present within the upper aquifer.

5. At sand volume fractions that are within one to a few percent above the percolation threshold, the percolating cluster (sand ganglion) includes half or more of all the sand within the sandbox (aquifer, Figure 6). In other words, except near the percolation threshold, the majority of the sand is part of a single, giant ganglion that connects all sides of the aquifer.

We are currently further investigating the connectivity and percolation properties of Markov chain random fields. These findings are critical to understanding the salt transport at the west side of the San Joaquin Valley: it appears that if channel deposits make up at least 18% of the upper aquifer, no matter in which way they are arranged, there is a 100% chance that the crooked "freeway" for salts exists–unless of course, there is an extraordinary amount of order in that system, such as extensive horizontal clay layers. On the other hand, if the channel deposits made up less than 12% of the aquifer, there are many barriers for salt to go through. It is thoroughly unlikely that salt quickly drops from the land surface to the lower, pumped portion of the aquifer. The only exceptions are such highly ordered anthropogenic "aquifer elements" as the gravel pack of a pumping well. That is a perfectly straight freeway from the top to the bottom, but fortunately very small–whether it's small enough is one of the questions that we are investigating.

As a result of the connectivity (and sand volume) changes, the vertical flux is a function of the percent sand in the aquifer. Figure 9 demonstrates the dependence of the effective vertical hydraulic conductivity (the ratio of total vertical flux to mean vertical hydraulic gradient). For comparison, the graph also shows the harmonic mean vertical hydraulic conductivity (for a perfectly stratified aquifer with the indicated percent sand in an arbitrary number of layers) and the geometric mean vertical hydraulic conductivity. It can be seen that the effective hydraulic conductivity is lower than the geometric mean hydraulic conductivity, but larger than in a perfectly stratified aquifer. For this example, the dip to vertical mean length ratio is 300:1 (see below).

Figure 10 shows a comparison of the probability distribution function (pdf) of salt travel time from near the water table to near the Corcoran Clay. The x-axis of the curve shows the travel time (in years), while the y-axis gives the probability that salt needs that many years to travel from the water table to the deep portion of the semi-confined aquifer just above the Corcoran Clay. The travel time pdf is computed for three different mean length ratios. The mean length ratios were obtained based on a reasonable range obtained from our preliminary geostatistical analysis. The results shown here are for dual media (sand and clay) with hydraulic conductivities as determined by Belitz and Phillips (1995). The figure compares results for sand (channel deposits) proportion of 15% and 60% of the aquifer volume. It also shows the travel time pdf for various mean length ratios (see below). The upper panels show the travel time pdf of salt particles that will arrive at the bottom of the aquifer in clay material; the lower panels show the travel time pdf of salt particles that will arrive at the bottom of the aquifer in sand material. The latter is the likely location of production wells. Note that the two panels are only separated based on the arrival location (sand or clay), not based on where the salt traveled before arrival.

The vertical travel times for the idealized condition of perfectly horizontal multi layered sand–clay aquifer (with 15% or 60% sand, respectively) are indicated by the thick vertical line. For comparison, the vertical line is indicative of the travel time indicated by the more homogeneous, regional groundwater model of Belitz and Phillips (1995).

As indicated by Figure 10, the travel time pdf in the aquifer with 15% coarse grained (sand) material is much different from that in the aquifer 60% coarse-grained material. Besides a shift in travel time (with a corresponding shift in travel time for the harmonic mean aquifer), the shape of the travel time pdf is significantly different: with small amounts of coarse-grained material, the pdf's tail is to the left. In other words, some salt does arrive early (although not nearly as early as in the coarser grained aquifer), but the mode of the arrival time pdf is very late–at about the same time as in a perfectly layered aquifer. In the coarse grained aquifer, the pdf's tail is to the right. The travel time for most particles is very short (much shorter than in a stratified aquifer), but few "stragglers" will take a considerably longer travel

time. These results are quite different from those predicted in the stochastic subsurface transport literature, which often assumes that the tail of the travel time pdf is to the right.

These results lead us to the following preliminary conclusions: In the characterization of the connectivity of higher permeable material within the alluvial fan aquifer, the foremost factors to determine are:

- Any highly ordered elements in the aquifer stratigraphy–extensive clay layers, extensive sand layers (with mean lengths that are within an order of magnitude of the size of the aquifer of interest), vertical structures such as the gravel pack of large diameter wells, to name a few.
- The percent volume of the highly permeable hydrostratigraphic elements that are most likely to transport salts quickly from the shallow portions of the aquifer to the deeper production level of the aquifer.

AVERAGE DIMENSIONS OF INDIVIDUAL HYDROSTRATIGRAPHIC UNITS

Just because a crooked freeway exists between the top (recharge zone) and the bottom (production zone) of the aquifer, doesn't mean that the salts will necessarily arrive in short time at the bottom of the aquifer. The freeway is, after all, crooked: while there may be quite continuous and sleek ganglion of channel deposits along the dip direction of the alluvial fan (the direction of the stream depositing the coarser material), the downward way may be extremely tortuous (Figure 4). In other words, while two parts of the same channel deposit (or sand) ganglion may be only a few feet apart vertically, one may have to travel several tens or even hundreds of feet to find the shortest connected path within that ganglion between those two places. Hence, the slowdown in salt transport occurs not because water needs to slow down to make the turns. The crookedness means that while the water wants to travel from the top of the aquifer to the bottom, due to the regional hydraulic gradient, going the crooked freeway may force it to take very large (and given the slow groundwater velocity, very long) roundabout ways to get just a few feet deeper. If the energy required to go the long roundabout way is more than that required to go straight across through the low permeable material, the water will in fact *not* use the freeway.

We investigate this phenomenon by determining the sensitivity of salt transport to the ratios of mean length of channel deposits in the dip, strike, and vertical direction. The geostatistical parameter 'mean length' of the transition probability method is the average straight (!!) length (in each of these three directions) of a hydrostratigraphic element–it is not the same as the mean connectivity length. For example, we find that the mean length of the channel deposits in the analysis of the soils map (Figure 7) is a few hundred feet. Clearly, the connected length is much, much longer, since the channel traverses the entire study area.

What do mean length ratios have to do with crookedness or tortuosity of the sand ganglion? To explain that relationship, we again perform a thought experiment around the small tabletop sand box mentioned. Let's imagine a ganglion of sand within the sandbox, one that connects top and bottom of the box and takes up, say, 20% of the total volume of the box. We can measure the average thickness of the ganglion in the x, y, and z directions. Let's say the mean length, width, and depth of the ganglion is 1", 1", and 1". That means, that there are no ganglions that go straight for a long way in either the horizontal or the vertical direction.

Now, let's magically stretch the sandbox with everything in it–like rubber–and make it ten times as wide and ten times as deep (but not thicker, Figure 8). It is easy to see now, how the paths have become a lot more tortuous–to go down in the ganglion now means that one travels back and forth a lot. At the same time, the mean length of the ganglion has become 10" wide, 10" deep, but still 1" thick. Also, we have not changed the proportion of sand (Sand still takes up 20% of the sandbox)! One can now imagine, how it would take more work (more energy) to move down through the entire ganglion than before we stretched the box.

In an analogous fashion, we analyze the effect of mean length ratios–dip to strike mean length ratio and dip to vertical mean length ratio) on the effective transport of salt through an aquifer, where the average hydraulic gradient is downward. We generate a random Markov field consisting of 101 by 101 by 101 blocks, with given proportions of the individual hydrostratigraphic elements (sand and clay, or sand, loam, and clay) and a mean length of sand (or sand and loam)

equal to four blocks in each direction. The mean length of clay (the so-called "background material") is a function of its proportion and the mean length of the other materials (sand or sand and loam). In the numerical flow model, we can then arbitrarily stretch or condense the width, depth, or height of the finite difference blocks associated with each random field block and thus change the mean length ratios in a rigorously defined manner, without changing the arrangement, proportions, or hydraulic properties of materials within the random field.

As shown in Figure 10, at 15% and 60% sand, there is a small, but significant difference between the 2:1 and 5:1 dip to strike mean length ratio. In both cases, the breakthrough curve is similarly skewed, but at a 5:1 dip to strike mean length ratio, salt arrives earlier than at the 2:1 ratio. The reason for this behavior is that the dip to vertical mean length ratio is kept constant. Hence the strike to vertical mean length ratio is shorter in the "5:1" case than in the "2:1" case. And the travel time is very sensitive to the horizontal to vertical mean length ratio as indicated in the two right most panels of Figure 10. That last set of panels shows the travel time for a dip to vertical mean length ratio of 50:1 (all other panel pairs show results for a dip to vertical mean length ratio of 300:1). With the 50:1 ratio the peak of the travel time pdf is even earlier and a large amount of salt arrives within a relatively short period of time.

Note that the simulation would have given a single peak (or delta function), in lieu of a breakthrough curve, if we had simulated a perfectly layered aquifer (regardless of the distribution or number of layers), since our simulations do not account for the effects of pore scale dispersion. The spread of the breakthrough curve is entirely due to the randomness in the sand distribution. This results in a highly heterogeneous velocity field distribution. The earliest arrival times in the 15% sand aquifer are approximately half of the harmonic mean travel time. In the 60% sand aquifer, the fastest travel time is but a few years. The longest travel times are somewhat larger than that for a uniform clay aquifer, due to the fact that some salt may travel only through clay, but on a somewhat tortuous path due to the irregular shape of the hydraulic gradient field. In other words, some salt is pushed and pulled between various sand places, but never quite gets there before being pulled in another direction. That makes its travel time longer than if it had traveled straight down through clay. Figure 11 further illustrates the differences in arrival time for the different mean length ratios. Specifically it shows that travel time for the 1% fastest salt particles as a function of the volume coarse-grained material in the aquifer. Clearly, the shorter the horizontal to vertical mean length ratios, the faster the travel time. The differences are due to the corresponding decrease in travel path tortuosity.

INFLUENCE OF HYDROSTRATIGRAPHIC CLASSIFICATION

Driller's logs are not an exact measure of the subsurface lithology. In fact, many driller's logs are very poor reports of the subsurface lithology encountered and it is standard practice to pre-select drilling logs based on their overall quality and consistency, prior to any interpretation. We selected two townships (land area: 36 square miles), one representing an upper alluvial fan area (Panoche Creek) and one representing an interfan alluvial area (Tumey Gulch). From the existing well logs, several were selected to determine the stratigraphic structure and a geostatistical model of the hydrofacies distribution based on the transition probably theoryn (Ruud et al., 1999). Even in the selected logs, typical borehole log descriptions of individual facies are very general "clay", "sand", "sandy clay", "clayey sand", with few more specific textural qualifiers. Most logs also identify the blue color of the clay textures typically associate with the Corcoran Clay formation (Figure 12).

Belitz and Phillips (1995) chose to lump well records from pre-selected depth intervals. For each depth interval the fraction of coarse sediments and fine sediments reported for in the well log was computed. For each depth interval at each well, an effective horizontal hydraulic conductivity was calculated as the arithmetic mean of sand and clay hydraulic conductivity. The vertical hydraulic conductivity was computed as the harmonic mean hydraulic conductivity. Note that only two values of hydraulic conductivity were used: that for sand and that for clay. The resulting hydraulic conductivity data were kriged to obtain a spatially continuous map of hydraulic conductivity (Figure 5). Whereas the clay and sand K have a four order of magnitude difference, the resulting effective K varied by little more than one order of magnitude between regions. As discussed earlier, this approach neglects the effects of the heterogeneity

observed in the borehole logs on salt transport, while providing a regionally appropriate water budget and groundwater hydraulics.

Weissmann et al. (1999a,b) took a different approach. They created a new sedimentological model of alluvial fan stratigraphy, based on the ideas put fourth in sequence. Their theory is based on the classification of alluvial fan into five hydrostratigraphic categories: gravel, sand, muddy sand, mud, and paleosol. Geostatistical properties of these five categories were computed separately for three deposit types: open alluvial fan deposits (Pleistocene), incised valley fill deposits (Pleistocene), and Pliocene deposits.

While we anticipate a similar stratigraphic model for the alluvial fans on the west side, there is little *a priori* information available from which to draw a strong conclusion regarding the applicability of the stratigraphic units defined by Weissmann et al. (1999b) to the west side. That raises the question, how sensitive the risk analysis of salt transport to the deeper aquifer is to the particular stratigraphic model put forth, even within the framework of transition probability. For example, would we observe significant differences in the salinization risk between a model that is based on two major elements (coarse and fine grained) and a model that is based on three major elements (coarse, intermediate, and fine grained)?

We used the selected borehole logs from the two study townships and created a total of four different hydrostratigraphic models (Figure 13):

1. a model that distinguishes only coarse and fine grained sediments. Textural log identifiers that included descriptors "sand", "sandy", "gravel", "gravelly" were considered coarse grained sediments, while all others are considered fine grained sediments.
2. a model that distinguishes three types of sediments: coarse (all "sand", "gravel"), fines (all "clay", coarse and fines (all others).
3. a model that distinguished four hydrostratigraphic units based on driller's logs: textural identifiers "sand", "gravel" are considered coarse grained, textural identifiers "clay" are considered fine grained, textural identifiers "sandy clay", "gravelly clay" are considered coarse fines, whereas "clayey sand", "clayey gravel" are considered fine coarse material.
4. a model with six hydrostratigraphic units based on driller's logs: same as 3.), but with two additional classes: fine grained sediments described as "blue", and other sediments described as "blue" or containing "blue" sediments (predominantly clay).

For the sensitivity analysis, we modeled dual and triple media aquifers. We already discussed results for dual media aquifers (with "sand" and "clay" elements) above. When we introduced a third category ("loam"), with a hydraulic conductivity (0.04 ft/d) that is one order of magnitude larger than "clay" (0.004 ft/d), but three orders of magnitude smaller than "sand" (31 ft/d). The arrival time distribution of the salt shifts significantly when compared to a dual media with the same amount of sand (Figure 14). A significant amount of salt arrives much earlier (shorter travel time) than in the dual media aquifer. The travel time pdf in the triple-media aquifer is much broader than in the dual media aquifer indicating large effective field dispersion created by the internal heterogeneity of the aquifer. The effective field dispersion in the triple-media aquifer is much larger than in the dual media aquifer, and even the skewness of the travel time pdf shifts from left-skewed to right-skewed. The change in the travel time pdf indicates a significant dependence of the risk analysis on the specific hydrostratigraphic model chosen. We are currently analyzing these results and comparing them to existing stochastic theories of transport in heterogeneous aquifers.

JUXTAPOSITIONAL PREFERENCE

As mentioned earlier, the transition probability model requires essentially four parameters that can be derived in a number of ways to characterize the distribution of hydrofacies within an aquifer: the number of different hydrofacies, the proportion of each hydrofacies, the mean lengths (in dip, strike, and vertical directions) of all but one of the hydrofacies (the mean lengths of the so-called 'background' hydrofacies is calculated as a complementary to all other hydrofacies), and the juxtapositional preference in hydrofacies arrangements.

The juxtapositional preference is a quantitative parameter describing the degree of entropy in the arrangement of the individual

hydrostratigraphic elements: a large juxtapositional preference refers to a situation with relatively low entropy, that is, a situation with a significant amount of order or sorting in the arrangement of hydrostratigraphic facies. That means, certain elements have a preference to occur either next to or away from a specific second hydrostratigraphic element. For example, channel deposits generally occur adjacent to overbank deposits and have a tendency not to be adjacent to flood plain deposits. This behavior is referred to as juxtapositional preference. When no juxtapositional preference occurs, the entropy is large since no sorting or order occurs in the arrangement of individual elements.

Juxtapositional preference can be determined from borehole-logs by computing the intrinsic transition probability along the vertical borehole profile (Carle and Fogg, 1996, 1997). For the sensitivity analysis, we chose two cases, one with the entropy determined from borehole records and maximal entropy (no juxtapositional preference). Due to the theoretical model underlying the TSIM random field generator, it was difficult to generate highly ordered media with strong juxtapositional preference. Preliminary simulations did show small differences between two example simulations and we are currently further investigating this point.

ANTICIPATED WORK

1. Work will continue on the sensitivity analysis to include a broader spectrum of scenarios. The objective is to provide a rigorous analysis of the basis of our risk analysis so that we can better understand its strength and limitations
2. The current model is a simplified hydrologic scenario of the Westside aquifer. We will adjust this model to reflect more realistically the distribution of pumping wells (and ultimately other aquifer stresses, such as drains) within the aquifer. The objective is to gradually adjust the simplified model to the conceptual hydrologic stress model proposed by Belitz and Phillips (1995).
3. Upon completion, we will develop recommendations for future data collection.

CONCLUSIONS

The following are the major conclusions that we are drawing from the study to date:

The transition probability/Markov chain approach is well suited for simulating alluvial fan stratigraphy when data are sparse. It also provides extensive opportunities to test the degree of uncertainty that exists about the hydrostratigraphy in the west side aquifers given the limited reliability and/or interpretability of existing data, primarily driller's logs.

1. A significant risk for early salinization of deep wells potentially exists, given the range of input data that we determined to be reasonable. Ongoing work will further quantify the risk prediction and the confidence interval to be put on that risk prediction.
2. Early breakthrough of salts is very sensitive to facies categorization and the dip to vertical mean length ratios defined by various means (e.g., soils maps, outcrop analysis).
3. Early breakthrough of salts is most sensitive to the fraction of highly permeable hydrofacies fraction. Even if the highly permeable facies fraction is as little as 12%-18% of the total volume in the aquifer, a connected pathway can be found across the entire thickness of the aquifer.
4. The preliminary results of our work demonstrate the importance of aquifer heterogeneity within the alluvial fans of the west side, when computing the risk for early salinization of pumping wells currently used for agricultural irrigation. We are employing a stochastic approach for the statistical risk analysis. In contrast to other applications of the stochastic approach, we are performing an extensive sensitivity analysis to determine how strongly the results of the risk analysis depends on the stochastic, geostatistical, or hydrostratigraphic parameters chosen for the analysis. Such sensitivity analysis is common in deterministic groundwater models, including those generated for the west side. But sensitivity analysis has not been applied widely to stochastic models of subsurface transport.

■ ■ ■ ■ ■

REFERENCES

Belitz, K. and S. P. Phillips, Alternative to agricultural drains in California's San Joaquin Valley: Results of a regional-scale hydrogeologic approach, Water Resources Research, 31(8), 1845-1862, 1995.

Berkowitz, B. and I. Balberg, Percolation theory and its application to groundwater hydrology, Water Resources Research, 29(4), 775-794, 1993.

Carle, S. F., A transition probability-based approach to geostatistical characterization of hydrostratigraphic architecture, Report 100033, Reprint of Ph.D. dissertation, Hydrology Program, Department of Land, Air, and Water Resources, University of California, Davis, 1996

Carle, S. F. and G. E. Fogg, Transition probability-based indicator geostatistics, Mathematical Geology, 28(4), 453-475), 1996.

Carle, S. F. and G. E. Fogg, Modeling spatial variability with one and multi-dimensional continuous-lag Markov chains, Mathematical Geology 29(7), 891-918, 1997.

Carle, S. F., E. M. Labolle, G. S. Weissmann, D. Van Brocklin, G. E. Fogg, Conditional simulation of hydrofacie architecture: A transition probability/Markovapproach, *In*: Fraser, G. e., and J. M. Davis, Hydrogeologic Models of Sedimentary Aquifers, Concepts in Hydrogeology and Environmental Geology No. 1, SEPM Special Publication, p. 147-170, 1998.

Carle, S. F., T-PROGS: Transition Probability Geostatistical Software, Version 2.1, Department of Land, Air, and Water Resources, University of California Davis, 1999.

Desbarats, A. J., Numerical estimation of effective permeability in sand-shale formations, Water Resources Research 23(2), 273-286, 1987.

Dubrovsky, N. M., S. J. Deverel, and R. J. Gilliom, Multiscale approach to regional ground-water quality assessment: Selenium in the San Joaquin Valley, California, in W. M. Alley, ed., Regional Ground-Water Quality, Van Nostrand Reinhold, 537-562, 1993.

Gronberg, J. M., K. Belitz, and S. P. Phillips, Distribution of wells in the central part of the western San Joaquin Valley, California, USGS Water-Resources Investigations Report 89-4158, 1990.

LaBolle, E. M., RWHet: Random Walk Particle Model for Simulating Transport in Heterogeneous Permeable Media, Version 2.0, User's Manual and Program Documentation, Department of Land, Air, and Water Resources, University of California Davis, 2000.

McDonald, M.G. and A. H. Harbaugh, A modular three-dimensional finite-difference ground-water flow model, in Techniques of Water-Resources Investigations of the United States Geological Survey, Book 6, Chap. A1, USGS, Washington, D.C., 1988.

Mendelson, K. S., Percolation threshold of a class of correlated lattices, Physical Review E, Vol. 56(6), 6586-6588, 1997.

Pollack, D. W., User's Guide for MODPATH/MODPATH-PLOT, Version 3: A particle tracking post-processing package for MODFLOW, the U. S. Geological Survey finite-difference ground-water flow model, U. S. Geological Survey Open-File Report 94-464, 1994.

Renault, P., The effect of spatially correlated blocking-up of some bonds or nodes of a network on the percolation threshold, Transport in Porous Media, Vol. 6, p. 451-468, 1991.

Ruud, N. C., T. Harter, G. Weissmann, and G. E. Fogg, Conditional geostatistical model of alluvial hydrofacies for risk analysis of deep groundwater quality deterioration from shallow salinity, Proceedings, International Conference on Calibration and Reliability in Groundwater Modeling, Zuerich, Switzerland, 20-23 Sept. 1999, 443-448, 1999.

Sahimi, M., Applications of Percolation Theory, 258 pp., Bristol, PA, 1994.

Sahimi, M. and S. Mukhopdhyay, Scaling properties of a percolation model with long-range correlations, Physical Review E 54 (4), 3870-3880, 1996.

San Joaquin Valley Drainage Implementation Program, Groundwater Management Final Report, submitted by the Groundwater Management Technical Committee, April 1999.

Stauffer, D. and A. Aharony, Introduction to Percolation Theory, 191 pp., Philadelphia, PA, 1991.

Swain, W. C., Estimation of shallow ground-water quality in the western and southern San Joaquin Valley, California. Technical Information Record for the San Joaquin Valley Drainage Program, Sacramento, California, September, 1990.

Weissmann, G. S., S. F. Carle, and G. E. Fogg, Three dimensional hydrofacies modeling based on soil surveys and transition probability geostatistics, Water Resources Research, 35(6), 1761-1770, 1999a.

Weissmann, G. S., G. E. Fogg, Multi-scale alluvial fan heterogeneiety modeled with transition probability geostatistics in a sequence straigraphic framework, J. of Hydrology, Vol. 226, 48-65, 1999b.

Western, A. W., G. Bloeschl, R. B. Grayson, Toward capturing hydrologically significant connectivity in spatial patterns, Water Resources Research, 37(1), 83-97, 2001.

■ ■ ■ ■ ■

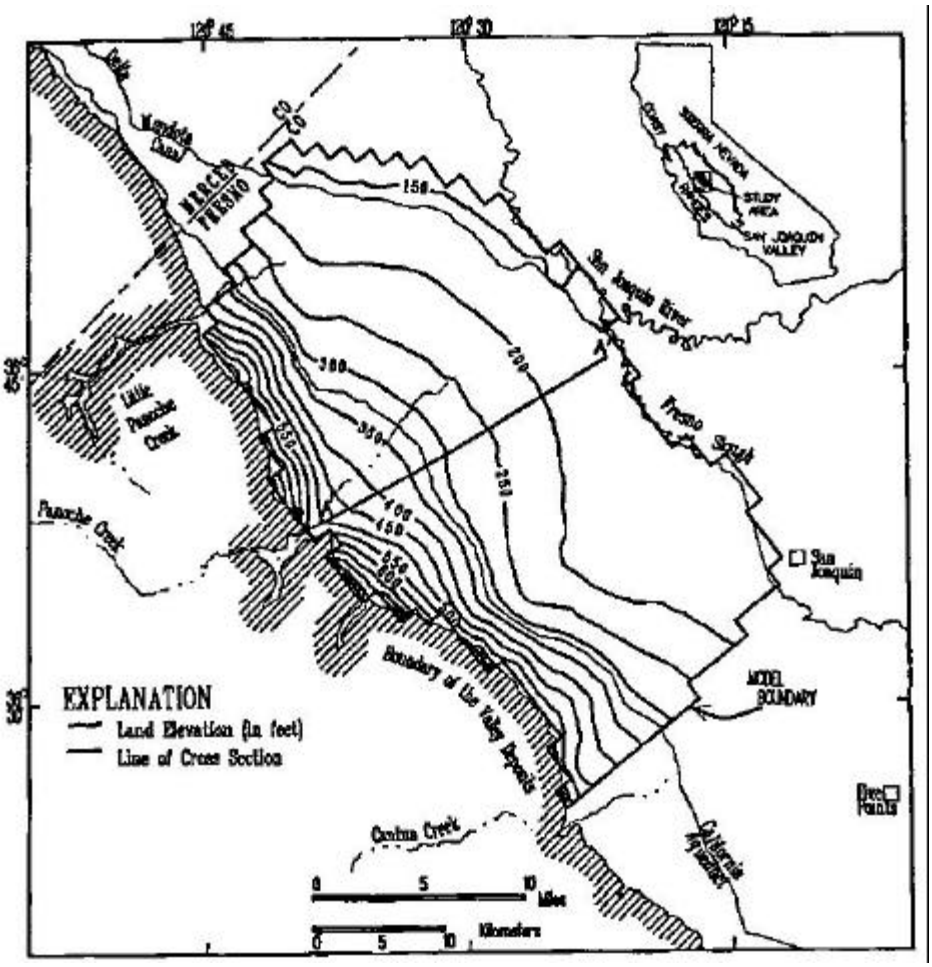

Figure 1: Topography and location of the proposed project area (Belitz and Phillips, 1995).

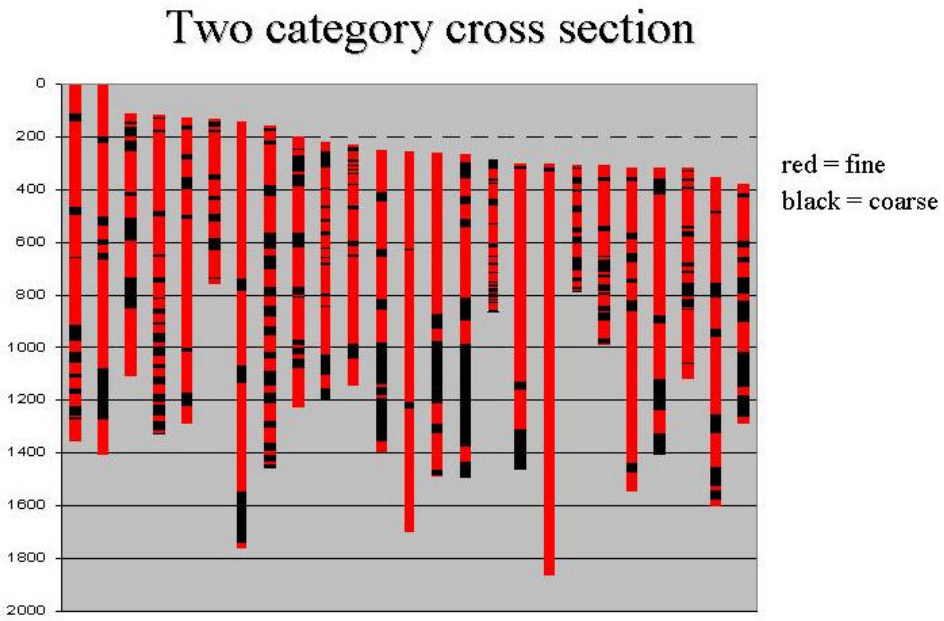

Figure 2: Southwest northeast cross section of driller's well logs for the lower section of the Panoche alluvial fan. The vertical axis is depth in feet (from an arbitrary datum). Black: coarse-textured. White: fine textured.

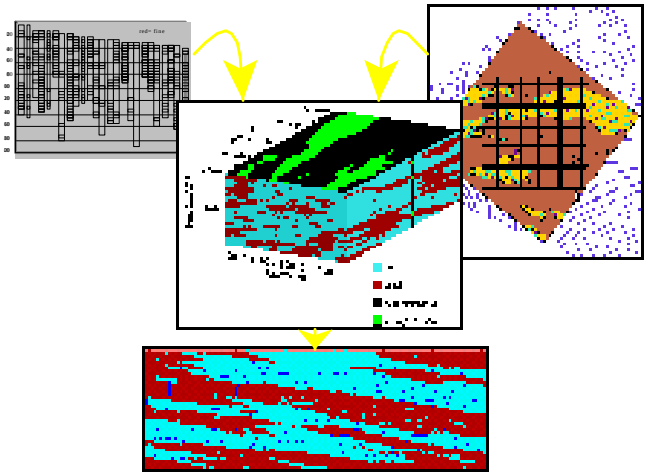

Figure 3: Simulation procedure for generating a random realization of the semi-confined aquifer hydrostratigraphy: from the analysis of well logs (top left) and soils maps (top right), we derive geostatistical models of heterogeneity (transition probabilities and Markov chain models), which form the basis for generating random aquifer hydrostratigraphy (center); these, in turn, are the basis for flow and transport modeling (bottom).

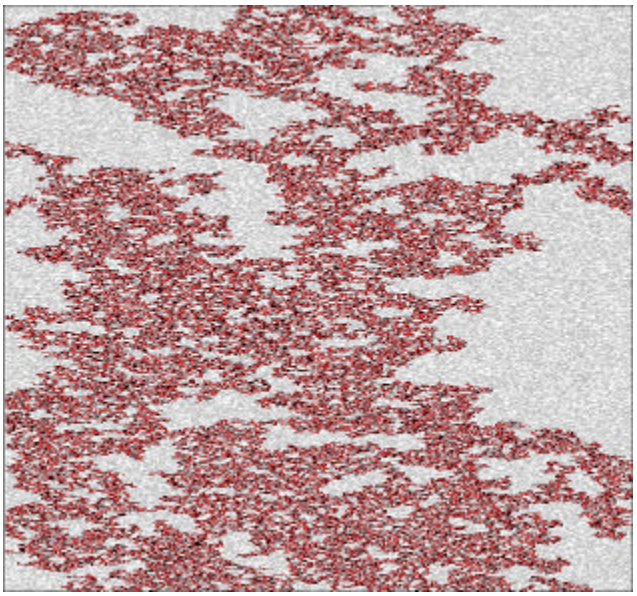

Figure 4: A single two-dimensional percolation cluster ("sand ganglion") of completely connected channel deposits (red). In this example, the channel deposits (grey) represent 55% of the aquifer (clay: white), half of which is contained in this single percolating cluster.

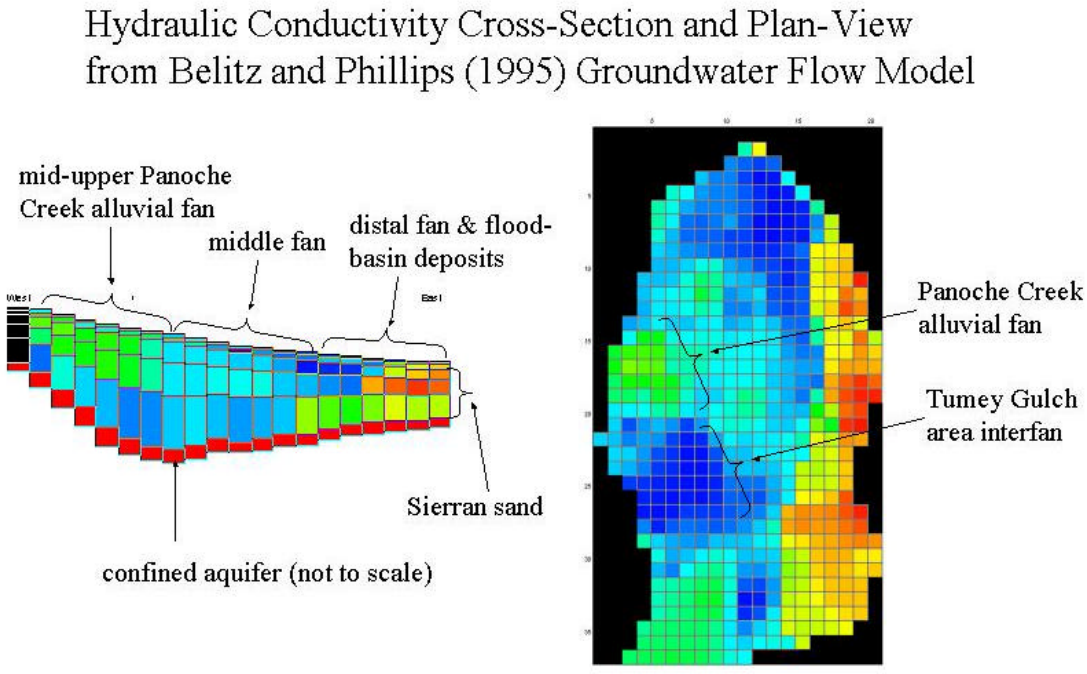

Figure 5: Calibrated hydraulic conductivity map and cross-section generated based on the regional groundwater model by Belitz and Phillips, 1995.

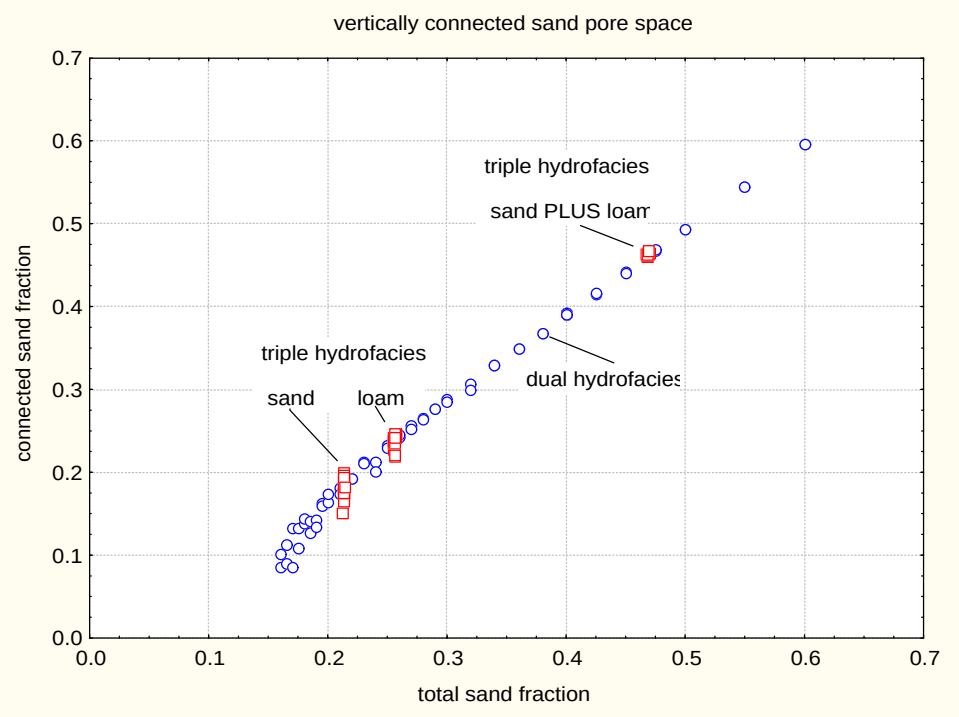

Figure 6: Connectivity of coarse material as a function of the percent coarse material.

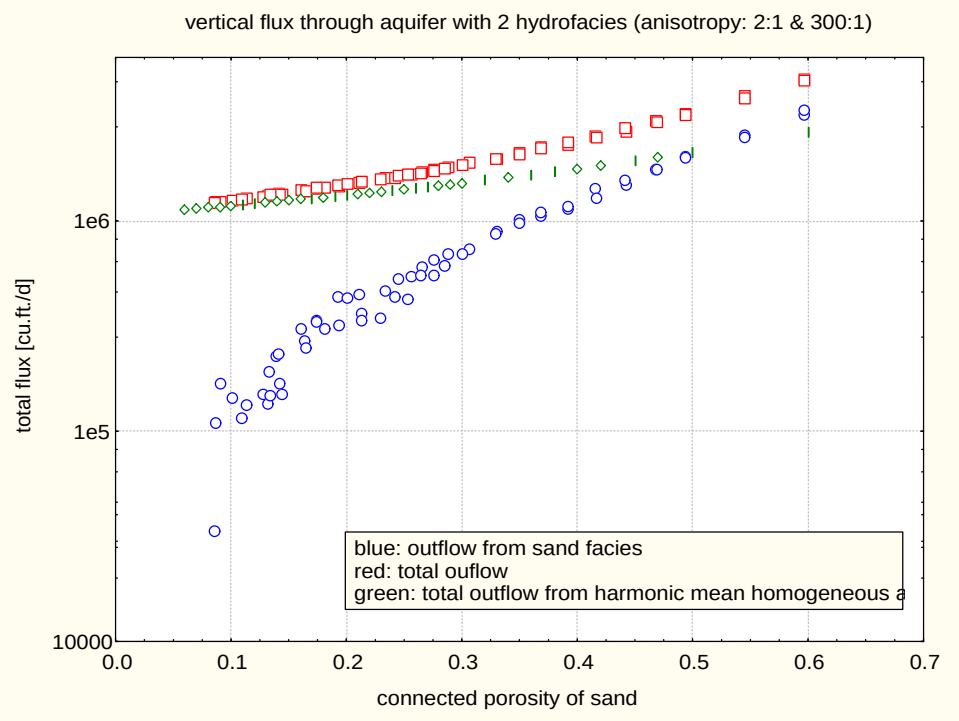

Figure 7: Total vertical flux rate in clay (squares) and sand (circle) at different volume percent sand, when compared to the harmonic mean hydraulic conductivity based flux rate (diamonds).

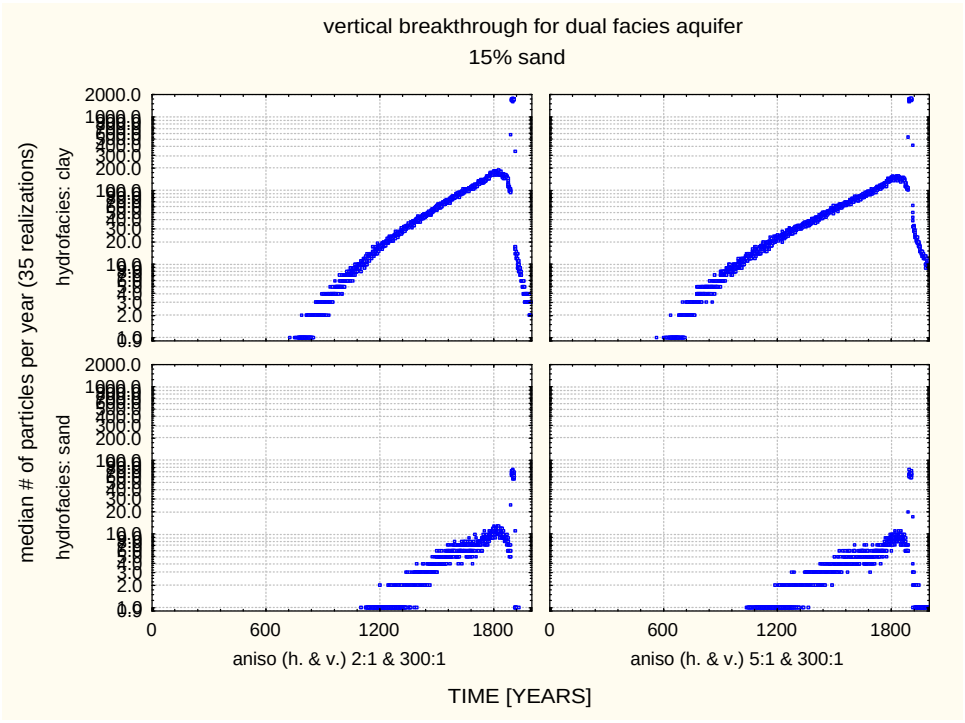

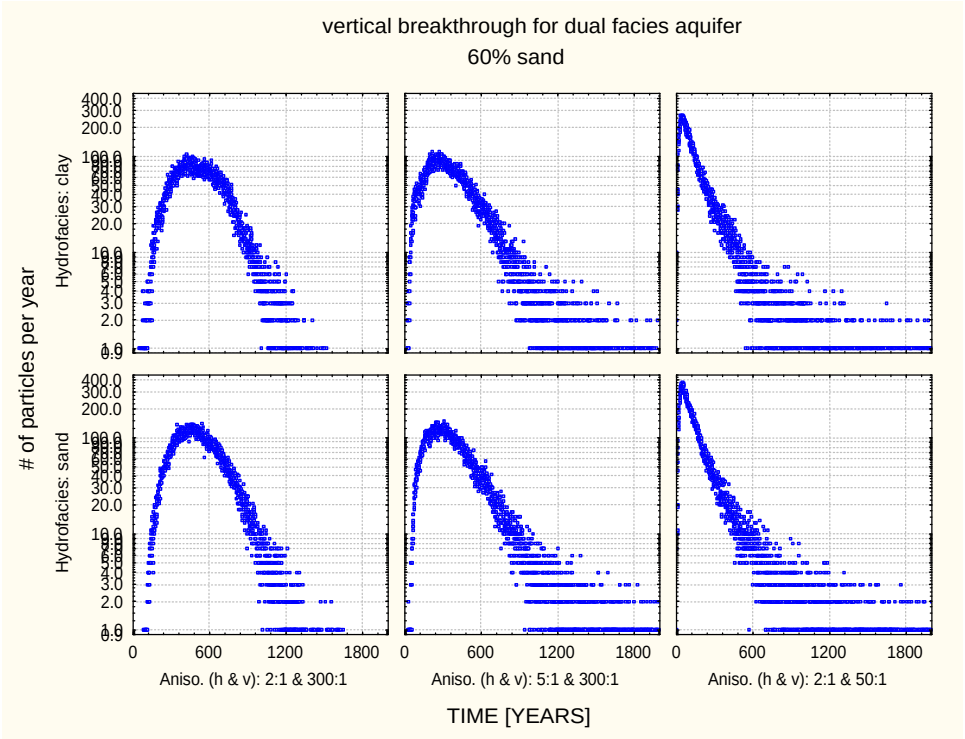

Figure 8: Arrival time distribution of salts for a dual media aquifer at various anisotropy ratios.

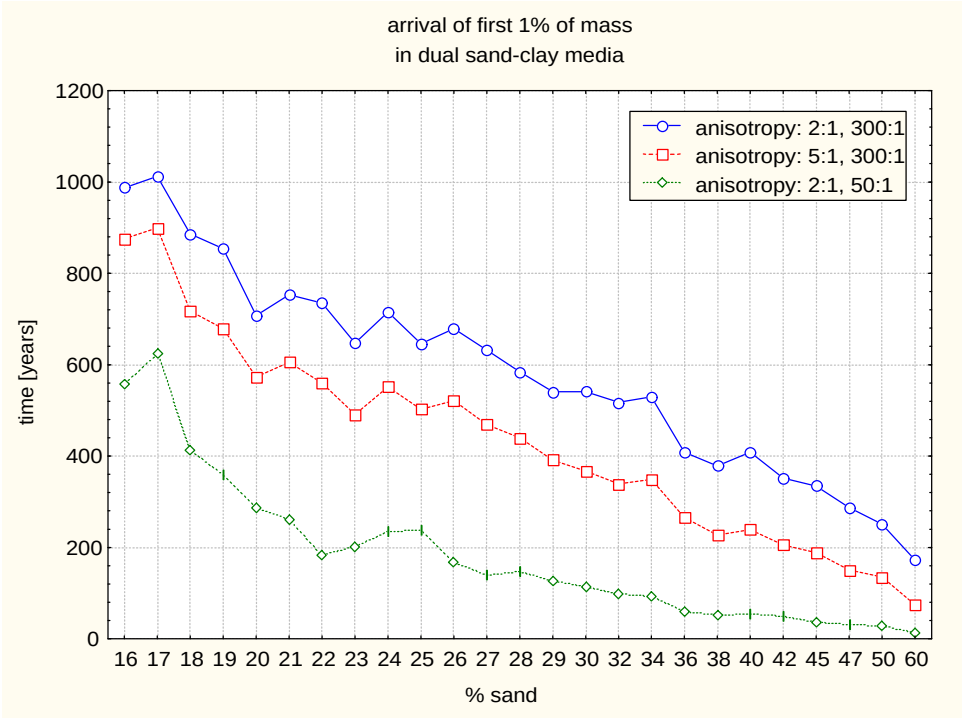

Figure 9: Sensitivity of the percentile mass arrival (risk analysis) to aquifer facies categorization, to fraction of coarse material, and to anisotropy ratios.

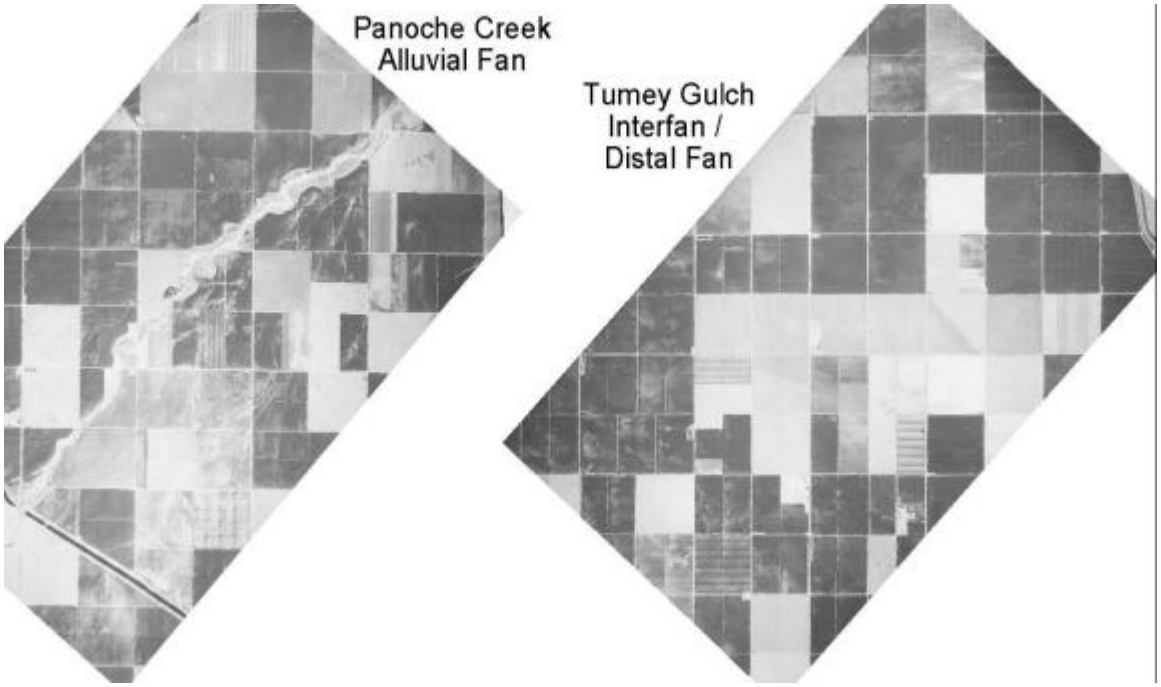

Figure 10: Aerial photos of two areas, one located on the mid-fan of Panoche Creek (left) and one located in the distal part of the Tumey Gulch interfan area south of Panoche Creek.

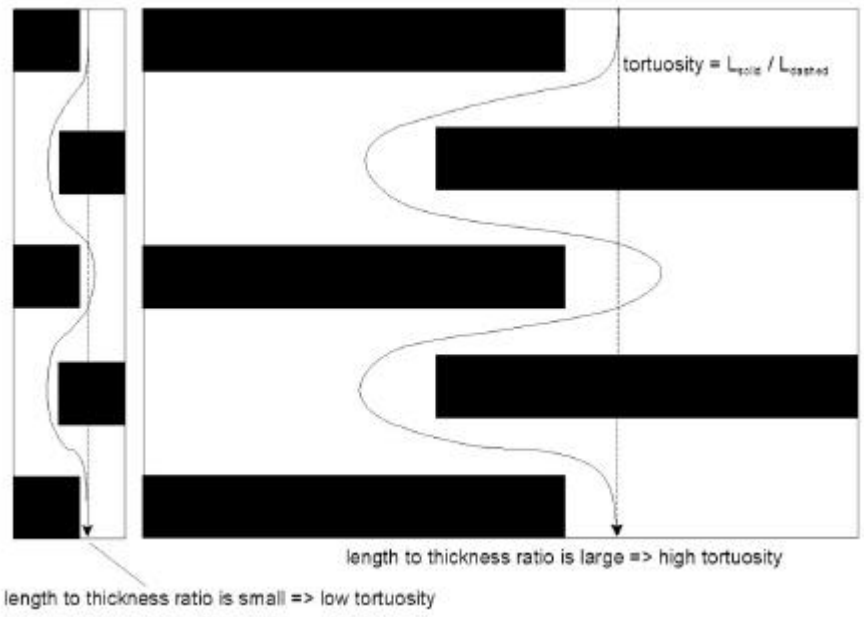

Figure 11: Illustration of the link between tortuosity and mean length ratios

Figure 12: Typical driller's log for a new well.

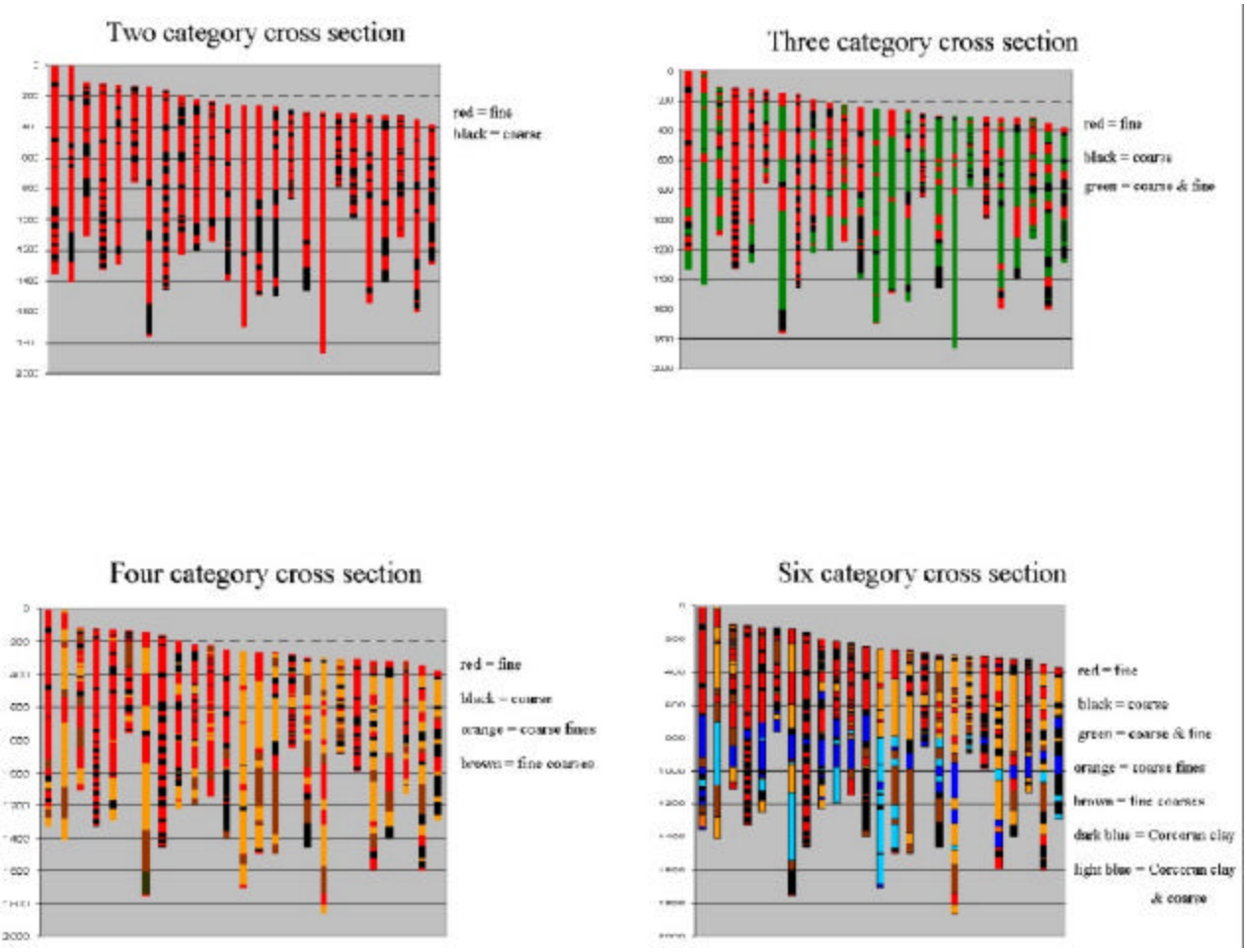

Figure 13: Alternative classification of the materials shown in Figure 2.

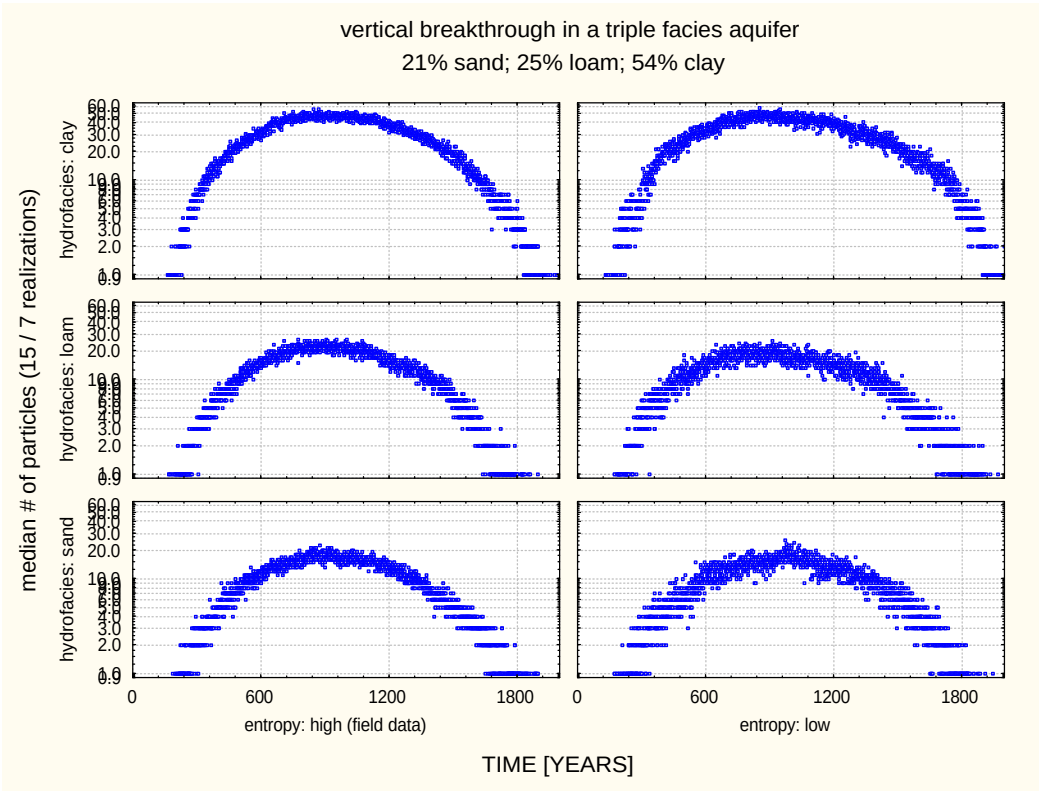

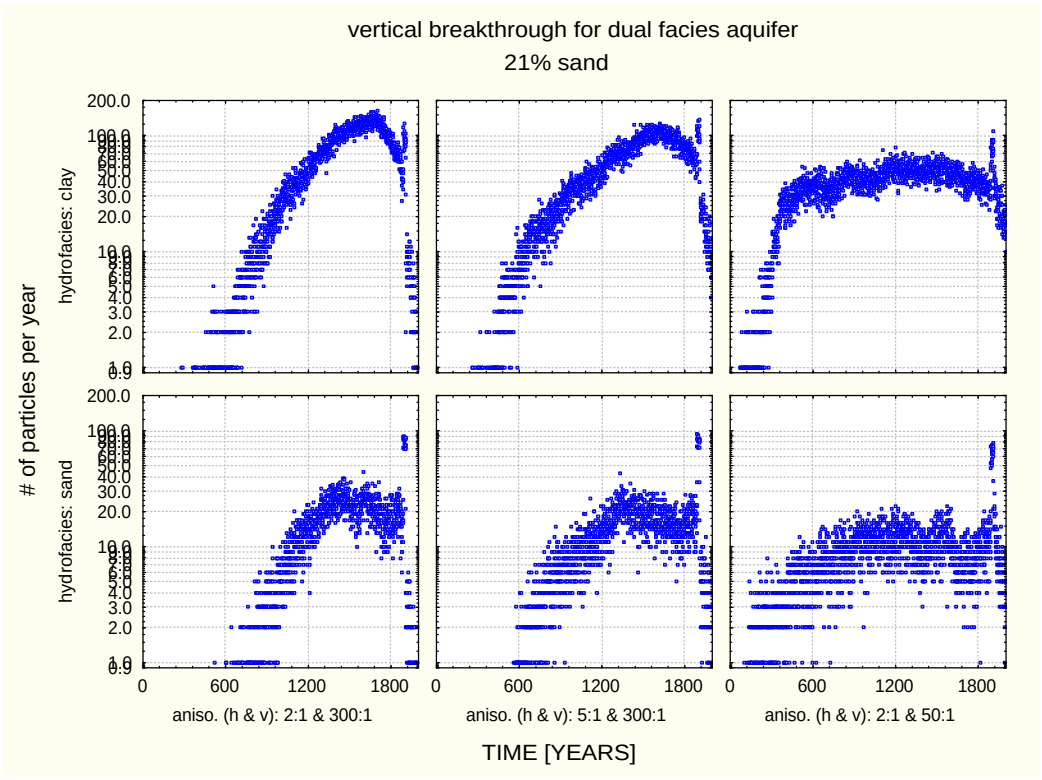

Figure 14: Arrival time distribution of salts for dual and triple media aquifers at various anisotropy ratios.

Physical-Chemical Nature of Sediment Selenium With Implications for Bioavailability

(**PART OF A TEAM PROJECT ENTITLED "MITIGATING SELENIUM ECOTOXIC RISK BY COMBINING FOODCHAIN BREAKAGE WITH NATURAL REMEDIATION**")

Project Investigators:

Richard Higashi
Office: (530) 752-1450, E-mail: rmhigashi@ucdavis.edu
Crocker Nuclear Lab., University of California, Davis

Robert G. Flocchini
E-mail: rgflocchini@ucdavis.edu
Crocker Nuclear Lab., University of California, Davis

Collaborators:

Drs. Eliska Rejmankova, Environmental Science & Policy, University of California, Davis
Teresa W-M. Fan, Dept. of Land, Air & Water Resources, University of California, Davis
Sudan Gao, Dept. of Land, Air & Water Resources, University of California, Davis
Randy Dahlgren, Dept. of Land, Air & Water Resources, University of California, Davis
Jack Meeks, Section of Microbiology, University of California, Davis
Dr. Jarka Komarkova, Hydrobiological Institute AS CR, Czech Republic
Dr. Robert Rofen, Novalek, Inc.
Julie Vance, California Department of Water Resources

Research Staff:

2 PGR (Jee Liu and Chris Coelho)
1 SRA (Teresa Cassel)

ABSTRACT

OVERVIEW OF THE JOINT PROJECT

The project proposed here is one part of a larger, Joint Research effort proposed for selenium (Se) ecotoxicity remediation in evaporation basins. Our focus on evaporation basins has several major endorsements: (a) it is a proven, economical means by which to dispose of waste agricultural water and contain the salt; (b) it is a "no discharge" technology for the disposal of water since it is terminal, thus capable of avoiding almost all aspects of the Total Maximum Daily Load (TMDL) regulations; (c) historically, its principal detracting feature has been Se toxicity to migratory waterfowl, yet in recent years, basin management schemes have significantly reduced this risk; (d) most recently, we have obtained field-scale evidence that remediation thru a combination of foodchain breakage with natural volatilization may be possible. This last is the topic of the Joint Research project.

In the San Joaquin Valley agricultural drainage waters, the only known issue with Se is toxicity to top predators such as aquatic birds, which receive Se primarily through their diet, such as aquatic invertebrates and fish. The research shows that waterborne Se concentration is not always a reliable predictor of Se content in aquatic organisms (Skorupa and Ohlendorf, 1991; Bowie et al., 1996) or observed toxicity (e.g. Reash et al., 1997). It is now clear that Se "biogeochemistry" - that is, how Se chemically transforms both inside and out of organisms - plays a pivotal role in determining the ecotoxic risk at particular sites (EPA Office of Water, 1998). Consequently, there has been scientific consensus that tissue or protein-bound Se concentrations are possibly better markers of ecotoxic risk (EPA Office of Water, 1998) than waterborne Se. There is additional scientific consensus that sediments harbor key pools of Se for ecotoxic effects (EPA Office of Water, 1998).

Thus, Se biogeochemistry is where the solution must be sought for the best chance at Se remediation. These processes must be evaluated for any remediation effort and may even be exploited to mitigate Se ecotoxic problems. These concepts form the foundation of the proposed projects at the Tulare Lake Drainage District (TLDD) evaporation basin site. This is in contrast to most projects in the San Joaquin Valley, which keyed on simple, but unfortunately unreliable, indicators such as Se water concentration.

The overarching objectives of the joint project, "Mitigating Selenium Ecotoxic Risk by Combining Foodchain Breakage with Natural Remediation", which involves the PIs listed above in separate but linked projects, plus cooperators at Novalek, DWR, and TLDD, are keyed around the foodchain system in TLDD evaporation basins, which include:

- Evaluating the efficacy of reducing Se risk resulting from intensive commercial harvest of brine shrimp (Artemia franciscana) and other macroinvertebrates in TLDD basins.
- Assessing effects of fertilizer inputs on algal dynamics for optimizing the harvest of brine shrimp and other macroinvertebrates as well as Se volatilization so that total and bioavailable Se are reduced in TLDD basins.
- Evaluating ecotoxic status in different basins of widely varying salinity and other conditions, so that general factors leading to reduced ecotoxic risk can be discerned.

OBJECTIVES AND APPROACH FOR THIS PROJECT BY HIGASHI AND FLOCCHINI

The biogeochemistry of Se must be at the core of design and implementation of remediation on Se ecotoxic impact. Part of the biogeochemistry is trophic transfer of Se, which is being examined by Salinity/Drainage investigators (Fan & Higashi, and Fry). However, the chemical basis of bioavailability - that is, the molecular mechanisms of lower trophic level entry of Se into the foodchain - remains largely unknown and unstudied. There is only a general consensus that organic forms are much more bioavailable than inorganic forms of Se (e.g. Rosetta and Knight, 1995), yet such impressions have already worked their way into the regulatory arena for water (EPA, 1996; EPA, 1997). Moreover, the sediment is the major Se sink, yet it is essentially uninvestigated (EPA Office of Water, 1998).

The specific objectives of this proposal key on newly deposited sediment (0-3 months old, using a sediment trap), from both *in situ* test enclosures (proposed by the Rejmankova and Fan & Meeks projects) and existing evaporation basins at TLDD. These represent basins that are both commercially harvested and non-harvested. The objectives are to probe the:

i) Microphysical basis for bioavailability of Se in sediments, by determining gaseous, “mobile” (waterborne), and “immobile” (solid) states of Se;

ii) Chemical basis for bioavailability, by analyzing mobile and immobile states for several known and hypothesized organo-Se structures, such as proteineceous Se;

iii) Physico-chemical basis of bioavailability, by extraction of the organic matter (“humic”) from the immobile Se state, and coarse size fractionation of the mobile Se into particulate-detrital and colloidal-soluble fractions, followed by (ii).

Approach for Objective (i). The physical state of organic Se forms defines the limits of exposure, and therefore the bioavailability. Three physical states will be separated from sediments: gaseous, mobile (e.g. waterborne), and immobile (e.g. solid-bound).

Approach for Objective (ii). In conjuction with physical state, the chemical form is a key factor in bioavailabilty of any element, including Se. The gaseous Se will be "extracted" by freeze-drying whole sediment. For the other fractions, we will probe for free and proteinaceous selenoamino acids as well as selenonium structures.

Approach for Objective (iii). The mobile state will be further separated on the basis of size (particulate/detrital vs. colloidal/soluble), while the immobile state will be extracted to yield the humic material. These will be subject to the battery of chemical analyses in (ii).

We will also study diagenesis of organic Se structures from (ii), by comparing recently-sedimented material with the more aged sediment cores that will be investiaged by the project of Drs. Gao and Dahlgren.

KEYWORDS

Tulare lake drainage district (TLDD), evaporation basins, Se speciation, selenate, selenite, organic Se, Se fractionation, organic matter associated Se, elemental Se, proteinaceous Se.

■ ■ ■ ■ ■

BACKGROUND & OBJECTIVES

BACKGROUND AND OBJECTIVES FOR THE JOINT PROJECT

The project proposed here is one part of a larger, Joint Research effort proposed for selenium (Se) ecotoxicity remediation in evaporation basins. Our focus on evaporation basins has several major endorsements: (a) it is a proven, economical means by which to dispose of waste agricultural water and contain the salt; (b) it is a "no discharge" technology for the disposal of water since it is terminal, thus capable of avoiding almost all aspects of the Total Maxiumum Daily Load (TMDL) regulations; (c) historically, its principal detracting feature has been Se toxicity to migratory waterfowl, yet in recent years, basin management schemes have significantly reduced this risk; (d) most recently, we have obtained field-scale evidence that remediation thru a combination of foodchain breakage with natural volatilization may be possible. This last is the topic of the Joint Research project.

In the San Joaquin Valley agricultural drainage waters, the utmost issue with selenium (Se) is toxicity to top predators such as aquatic birds, which receive their Se primarily through their diet, including aquatic invertebrates and fish. Past research has shown that waterborne Se concentration is not always a reliable predictor of Se content in aquatic organisms (Skorupa and Ohlendorf, 1991; Bowie et al., 1996). In turn, Se content is not always related to observed toxicity (e.g. Reash et al., 1997; Fan et al., 2002).

The worldwide research efforts on Se contamination in wastewaters, including research on the diet items, now indicates that Se "biogeochemistry" (biotransformations and foodchain transfer, in particular) plays a pivotal role in determining the ecotoxic risk of particular sites (EPA Office of Water, 1998; SJVDIP report, 2000). Consequently, protein-bound Se concentrations in food items and top predators may be more reliable markers of Se ecotoxic risk (EPA Office of Water, 1998; Fan et al., 2002).

Thus, the hard-learned lesson is that the complex "Se biogeochemistry" process lies at the heart of Se problems. Therefore, it is where the solution must be sought for the best chance at Se remediation. These concepts form the foundation of the proposed project at the Tulare Lake Drainage District (TLDD) evaporation basins. This is in contrast to most previous projects in the San Joaquin Valley, which depended on simple but unreliable indicators such as waterborne Se concentration.

The overarching objectives of the joint project, "Mitigating Selenium Ecotoxic Risk by Combining Foodchain Breakage with Natural Remediation", which involves the PIs listed above in separate but linked projects, plus cooperators at Novalek, DWR, and TLDD, are keyed around the foodchain system in TLDD evaporation basins, which include:

- Evaluating the efficacy of reducing Se risk resulting from intensive commercial harvest of brine shrimp (Artemia franciscana) and other macroinvertebrates in TLDD basins.
- Assessing effects of fertilizer inputs on algal dynamics for optimizing the harvest of brine shrimp and other macroinvertebrates as well as Se volatilization so that total and bioavailable Se are reduced in TLDD basins.
- Evaluating ecotoxic status in different basins of widely varying salinity and other conditions, so that general factors leading to reduced ecotoxic risk can be discerned.

The first two objectives will be fulfilled in cooperation with Dr. R. Rofen who has been conducting brine shrimp harvest at the TLDD South Evaporation Basin (SEB) and Hacienda Evaporation Basin (HEB) systems. These harvests have been sold as valued feedstock to aquarium and aquaculture industries. The HEB site, consisting of two sequential series "A" and "C", have been studied by Fan and Higashi for several years. These two series, despite receiving on average the same drainage water, have very different Se volatilization and algal communities (Fan and Higashi, 1997, 1998, 1999). Thus, the HEB site is a very interesting, and potentially a very important site to expand our work. The third objective will be a continuation of our previous effort (funded by this program and in collaboration with Julie Vance and John Shelton at DWR) to track foodweb Se for Se bioremediation.

Macronvertebrates are major food items (Cooper et al., 1997) - and constitute the major route (Skorupa, 1998, and references cited therein) - by which birds are exposed to Se. It therefore follows that reducing the abundance of food invertebrates (objective #1) as well as their Se concentration (objective #2) will lead to reduced risk. These concepts are illustrated by Figure 1 and its legend.

Our preliminary investigation at these basins indicates that both waterborne Se concentration and Se bioavailability from algae and brine shrimp appeared to be reduced by commercial harvest of macroinvertebrates. This reduction may be further enhanced by encouraging appropriate algal community that dissipate Se by volatilization, while sustaining brine shrimp production. Dr. Rofen has obtained permission for such manipulation at TLDD. To guide such effort, relationships among water chemistry, algal dynamics, and brine shrimp production must be understood. Understanding of these relationships will also avoid the situation whereby undesirable algal blooms may lead to an increase in bioavailable Se both in the water column and sediment.

RATIONALE FOR THIS PROJECT, "PHYSICAL-CHEMICAL NATURE OF SEDIMENT SELENIUM WITH IMPLICATIONS FOR BIOAVAILABILITY", HIGASHI & FLOCCHINI, PIS.

As stated above, it has been known that the major risk of Se toxicosis to aquatic top predators such as shorebirds occurs thru their diet, and therefore thru the foodchain (e.g. Skorupa, 1998 and references cited therein). Other routes of exposure, e.g. direct exposure to Se-contaminated water, is not considered to be significant. The chemical form(s) of Se that moves through the foodchain is not known, but a recent consensus (e.g. EPA Office of Water, 1998) proposes that protein-bound Se in food organisms may be the most available form to the next trophic level. Currently, UC Salinity/Drainage Program projects (those of Fan & Higashi, and Fry), as well as other agencies, are investigating these aspects.

On the other hand, little attention has been paid to the non-living forms of Se which enter the foodchain in the first place: that is, the bioavailability of Se to lower trophic levels. Organic forms appear to be important, as laboratory studies have shown that, directly from water, organic Se as selenomethionine (Se-Met) is much more available to algae and invertebrates than the typical inorganic forms, selenite (SeO_3) and selenate (SeO_4) (Rosetta and Knight, 1995; Maier and Knight, 1994 and references cited therein). However, commercially-available organic forms such as Se-Met occur only at very low concentrations in the water (Fan and Higashi, unpublished data), so they may not be relevant model compounds. Luoma et al. (1992) have shown that more complex, but unknown organic form(s) such as Se-enriched diatoms and

sediments have high bioavailability to clams. The sediment is often the largest pool of Se and considered to be an important source of foodchain Se (e.g., EPA Office of Water, 1998). In the sediment, Se is likely to be resident in all particle sizes, ranging from algal mats and detrital floc to colloidal and small-molecule sizes; but only the latter has been investigated. Thus, what is needed are studies of bioavailability of the various organic forms and sizes of Se – in water, food items, and particularly the sediment – to gain an understanding of how Se enters the foodchain.

Unfortunately, such studies are not feasible at the present stage of knowledge, because the relevant forms of Se in the sediment are simply not known. This is not a trivial list to compile, if we consider briefly the biogeochemical cycles of Se. Figure 1 illustrates a sort of biogeochemical "refluxing" of Se depiciting the relatively simple system of an evaporation basin, which is devoid of vascular plants and infaunal vertebrates. Waterborne and sediment Se as SeO_3 and SeO_4 are initially "fixed" into organic forms mostly by algae and microbes, some of which can head up the foodchain, or turn into organic material that is relatively unaltered - termed detritus - upon death. The detrital material can re-enter the foodchain immediately via microbes or invertebrates that are exposed (physically or thru ingestion) to the detritus. Other paths are for Se to re-enter the foodchain thru microbes or invertebrates after considerable chemical transformation has occurred to the detrital material - for the purposes of brevity, this aged material is lumped into the term humic material.

In any of the steps in Figure 1, multiple chemical forms of Se are involved, and for the most part these forms are unknown. In most cases, even the physical state (gaseous, soluble, insoluble) is unknown, which is also important to bioavailability. Furthermore, the size distribution of organic Se as it converts from detritus to humic material is likewise unknown. Size is of gross importance as it determines the target organism, exposure route, and chemistry of Se uptake, ranging from direct sorption or membrane transport for molecular-sizes, to ingestion and digestion for macroscopic particles and debris.

These considerations form the impetus for the proposed project. Evaporation basin systems (alkali ponds) in the southern San Joaquin Valley are a good place to conduct these studies, since the biogeochemistry and ecology are simpler relative to most other systems, and are already under study by the other PIs of the Joint Project.

The specific objectives of this proposal key on newly-deposited sediment (0-3 months old, using a sediment trap), from both *in situ* test enclosures (proposed by the Rejmankova and Fan projects) and existing evaporation basins at TLDD. These represent basins that are both commercially harvested and non-harvested. The objectives are to probe the:

i) Microphysical basis for bioavailability of Se in sediments, by determining gaseous, "mobile" (waterborne), and "immobile" (solid) states of Se;

ii) Chemical basis for bioavailability, by analyzing mobile and immobile states for several known and hypothesized organo-Se structures, such as proteineceous Se;

iii) Physico-chemical basis of bioavailability, by extraction of the organic matter ("humic") from the immobile Se state, and coarse size fractionation of the mobile Se into particulate-detrital and colloidal-soluble fractions, followed by (ii).

Approach for Objective (i). The physical state of organic Se forms defines the limits of exposure, and therefore the bioavailability. Three physical states will be separated from sediments: gaseous, mobile (e.g. waterborne), and immobile (e.g. solid-bound).

Approach for Objective (ii). In conjuction with physical state, the chemical form is a key factor in bioavailabilty of any element, including Se. The gaseous Se will be "extracted" by freeze-drying whole sediment. For the other fractions, we will probe for free and proteinaceous selenoamino acids as well as selenonium structures.

Approach for Objective (iii). The mobile state will be further separated on the basis of size (particulate/detrital vs. colloidal/soluble), while the immobile state will be extracted to yield the humic material. These will be subject to the battery of chemical analyses in (ii).

We will also study diagenesis of organic Se structures from (ii), by comparing recently-sedimented material with the more aged sediment cores that will be investiaged by the project of Drs. Gao and Dahlgren.

RATIONALE FOR APPROACH AND METHODS: PRIOR RESEARCH

In past UC Salinity/Drainage program research of Fan and Higashi, we have compared the Se concentrations in several evaporation basins at TLDD HEB basins, as well as several locations within these basins. Differences in Se concentration in sediment was found to be a function of the prevailing wind patterns, and irrespective of the inlet/outlet locations of each basin (Figure 2). This, in turn, was apparently due to the prevalence of floating cyanobacterial mats in these basins, a major reminder that biogeochemistry drives the Se, even the physical distribution, in these systems.

Once we established the wind-driven distribution phenomenon, we were able to design sediment sampling schemes with upwind and downwind locations at each basin, and we also installed sediment traps. Figure 3 shows the entire data set of the sediment and trap contents for 1997-2000. Note that the traps (dots) are generally higher in both OC and Se concentrations than the cores (squares). This is consistent and expected from trap contents, which contain primarily "new" (<3 months old) detrital material. In contrast, cores would be "diluted" with non-detrital as well as older Se-laden material. Thus, comparison of Se forms in cores vs traps would be important to interpretations of bioavailability.

Thus, Figure 2 (wind-driven deposition) and Figure 3 (positive OC-Se relation) comprise evidence for the probable strong coupling between the organic carbon (OC) and Se biogeochemical cycles, as alluded to back in Figure 1. At first, this appears to support contentions by some (most notably, Canton and Van Derveer, 1997) that sediment OC can be utilized for ecotoxic risk assessment.

However, Figure 4 shows that caution should be exercised, and that a more mechanistic approach is needed. These data from the TLDD south basins, which have a truncated biogeochemistry due to brine shrimp harvest (see Figure 1), show very little sediment relationship between OC and Se concentrations. Thus, when the biogeochemistry is disturbed - as will be the case for ecotoxic remediation schemes such as shrimp harvesting - potential indicators such as that in Figure 3 are no longer reliable. It follows that simple indicators such as OC is not valid for assessing the progress of biogeochemical-based remediation technologies. And, since ecotoxic risk is a function of the biogeochemistry, the latter cannot be readily dismissed in remediation efforts.

To improve the mechanistic understanding of bioavailability, our previously funded research (1999-2001) by the UC Salinity/Drainage program performed more detailed examination of the sediments. We have applied a physical-chemical fractionation approach to survey sediment trap contents. Figure 5 reveals clearly that "sediments" are not just a single compartment; the legend here explains the importance of distiguishing between the "mobile" and "immobile" fractions of the sediment. Recently, we have eschewed the traditional pore water approach in favor of the more bioavailability-oriented fractionation of Figure 6, that additionally account for the effect of fresher water flux events that occur in these basins. The legend for Figure 6 explains the concept of the bioavailability-based fractionation.

In summary, this project keys on both extant and newly-deposited sediment (0-3 months old, using sediment traps), expanding on the the scheme in Figure 6. The trap deployment and analyses will be coordinated with the project of Gao & Dahlgren, which will provide a comparison with Se speciation on flocculant and sediment core depth profiles. One type of sampling activity was at existing evaporation basins at TLDD at appropriate downwind locations. In addition, we examined the sediments within *in situ* test enclosures at TLDD that were conducted by the Rejmankova and Fan/Meeks projects. The Rejmankova project is conducting *in situ* enclosure experiments that tests three hypotheses regarding algal-nutrient-grazer (e.g. Brine shrimp) relationships, and provide morphological community structure analyses. The Fan/Meeks project will calibrate 16s RNA community typing (e.g. Ferris et al., 1996) and comprehensive pigment analyses (Fan and Higashi, 1998b) with the morphology-based community analyses, to be used as future high-throughput tools for assessment of lower foodchain Se biogeochemistry. Our contribution of conducting sediment traps within these multi-trophic level *in situ* enclosure experiments, will enable the joint research project to cover all the major components outlined in Figure 1.

SUMMARY OF PROGRESS FROM 2001-2002

SITES AND SAMPLING

As stated above, we have continued to focus on TLDD HEB and SEB evaporation basins because of the extensive algal environmental Se biochemistry work (e.g. Fan and Higashi, 1997; Fan et al., 1997; Fan and Higashi, 1998; Fan et al., 1998a; Fan et al., 1998b, Fan et al., 2002) as well as the existence of brine shrimp harvested and non-harvested basins.

Samples for water-column volatile Se survey were taken from HEB A4 (brine, harvested) and C4 (brine, not harvested), the non-harvested basins of medium salinity HEB A2 and C2, and from SEB 1 (low salinity, not harvested) and the high salinity harvested basins SEB 8, 9, 10. The methods were as described previously (Higashi and Flocchini, 2001)

Water and sediment core samples were taken from the same HEB basins, at upwind and downwind locations identified as NW (northwest) and SE (southeast), respectively. These covered a wide range of salinities and Se water concentrations, as well as both harvested and non-harvested basins. For volatilization, water samples were analyzed on site as reported previously, while those for other analyses were transported on ice and stored in a refrigerator (3°C) until use. Solutions were analyzed for pH, electrical conductivity (EC), total Se concentration and Se speciation (selenate (Se VI), selenite (Se IV), and organic Se (org-Se) as described below.

Sediment cores were taken using 5-cm diameter acrylic tubes. The cores were sealed immediately with a plastic cap and duct-tape and stored on ice. After transferring to the lab, the core samples were frozen until ready for analysis. Organic detrital materials were sectioned from the mineral sediment cores. The mineral cores were then sectioned into the 0-5, 5-10, 10-15 and 15-20 cm segments. Both detrital and mineral sediments were determined for total Se and fractionation. Subsamples of each sample were used for selective sequential extractions, determination of moisture content, total Se by chemical digestion.

In addition, we have sampled within the *in situ* enclosure experiments of the Rejmankova project. Lastly, sediment samplers were deployed at the HEB and SEB basins. All sediment sampling and analyses were coordinated with the project of Gao/Dahlgren.

SE CONCENTRATION AND SPECIATION IN WATERS

HEB basin waters were hypersaline with EC values of 95.0, 89.5, 118.7, and 95.5 dS/m for A4-NW, A4-SE, C4-NW and C4-SE, respectively. The pH values were 8.7, 8.7, 8.5 and 7.5 for A4-NW, A4-SE, C4-NW and C4-SE, respectively. As reported by the project of Gao and Dahlgren, total Se concentrations ranged from 9.4 to 28.5 ppb and demonstrated some spatial variability between samples (Figure 7). Basin waters were dominated by inorganic Se species (about 60% selenate and 40% selenite) with very low concentrations of organic Se (<2%). Since agricultural drainage water input to TLDD are dominated by selenate (>90%) (Gao et al., 2000; Tanji and Gao, 2001), the results of this study indicate that there is considerable Se reduction occurring in these sequential evaporation basins.

VOLATILE SE ANALYSIS

Analysis of total Se volatiles present in TLDD evaporation basin waters were conducted on cells varying in salinity and brine shrimp harvest/non-harvest. Methods used were described previously (Higashi and Fan, 1999; Higashi and Flocchini, 2001). The Se volatilization measurements were performed twice in each location, in the morning and afternoon. Figure 8 shows the ng of Se purgeable from 800 ml of waters of SEB basins S1, S9, and 10 as well as from HEB basins A2, A4, C2, and C4. Also shown is the salinity or conductivity of the water (triangles). It is clear that for S8, S9, S10, and A4 cells, the amount of Se volatiles was much higher than the less saline cells of the same series. This trend has been consistently observed for the last four years at TLDD basins (Higashi and Flocchini, 2001).

However, this time around, we determined that the Se volatile content varied with time of day, with no clear or consistent trend, reflecting the complex, multiple mechnisms at work. For example, the volatile Se in water is not simply a physical-chemical phenomenon (e.g. Henry's law relationship) due to temperature differences, since it is of very recent (e.g. seconds to minutes) biogenic origin that is likely dependent on - at the least - photon flux, nutrient status, and algal community composition.

The relationships of volatile Se to harvest practice, as well as brine shrimp and algal Se loads, are discussed in the Fan & Meeks project report.

SEDIMENT DISTRIBUTIONS OF TOTAL SE

As stated above, there are three gross physical states of importance to bioavailability: gaseous, mobile (e.g. waterborne), and immobile (e.g. solid), which are represented in Figure 6 as sub-samples II, V, and IV, respectively.

Our recent study (Higashi and Fan, 1999) shows that the gaseous compartment in field sediments appears to consist entirely of alkyl selenides, produced by microphytes (e.g., Fan, Higashi, and Lane, 1998; Fan, Lane, and Higashi, 1997) and microbes (e.g., Frankenberger and Karlson, 1994). Since they are very volatile with rapid diffusion from the sediment, they are likely to be only a minor source of bioavailable Se. However, all of the structures observed are very hydrophobic and reactive, which implies high intrinsic bioavailability; if concentrations are sufficiently high, there could be significant direct sorption of Se by organisms. The very same characteristics - extreme volatility and high reactivity - make them unreliable to quantify by conventional approaches such as difference total Se analysis, e.g., of whole vs. dried sediment.

Thus, we removed the gaseous chemical forms directly from sediment under inert conditions. This is accomplished by freeze-drying the frozen whole sediment (I, Figure 6) and trapping the high-vacuum extracted vapor at liquid N_2 temperature. This separates the gaseous Se compounds (II, Figure 6) from the continuously frozen sediment matrix in a high vacuum, minimizing decomposition while maximizing extraction of the volatiles. We have successfully used this technique to isolate reactive gaseous components such as dimethylsulfide from organic-rich matrices of wastewater and sediment (Higashi et al.,1992a; Higashi et al., 1992b).

Total Se in the detrital materials and sediments was determined using a modified $HClO_4$ –HNO_3 digestion (Zasoski and Burau, 1977), followed by a reduction of Se(VI) to Se(IV) for HGAAS (hydride generation atomic absorption spectroscopy) analysis. As reported by the project of Gao and Dahlgren, the depth profile of total Se concentration in the sediment showed variations with depth (Figure9). Further discussion of these profiles is found in the Gao & Dahlgren project report.

DETERMINATION OF SE CHEMICAL FORMS IN SEDIMENT

The freeze-drying process chemically stabilized the non-volatile portion of the sediment (III, Figure 6) for further processing. Of this portion, the mobile, or extractable, state is the Se that is potentially present in the sediment pore water, which can be in contact or ingested by organisms. This includes particulate matter (e.g. algae, detritus) that has neutral or positive buoyancy. The immobile, or solid state is operationally defined as negative buoyancy, particulate-bound Se that is transported only with substantial water current (generally not present at evaporation basins), and conceivably must be ingested to become bioavailable.

To obtain these states, sequential selective dissolution procedures were adopted from those previously used(Chao and Sanzolone 1989, Lipton, 1991, and Velinsky and Cutter 1990, Higashi and Flocchini, 2001, Gao et al. 2000). Non-volatile Se (III, Figure 6) in the sediments was fractionated into water-soluble, ligand-exchangeable, and organic matter-associated fractions using (1:10 soilid:water ratio) of water, 0.1 M K_2HPO_4 (PO_4, pH 8.0), and 0.1 M NaOH, respectively. The unextractable fraction, i.e., the difference between the total and the extracted, was comprised primarily of elemental Se and a very small amount of residual (most - resistant) Se based on previous findings by Gao et al. (2000).

Selenium speciation (Se VI, Se IV, and org-Se) for water and 0.1 M NaOH extracts was determined based on the methods developed by Zhang et al. (1999). Three determinations were performed: direct measurement of Se(IV) using phosphate pH 7 buffer (for NaOH extracts, solution pH was adjusted to pH 7 with HCl prior to the analysis), Se(IV) + org-Se using persulfate to selectively oxidize organic-Se(-II) to Se(IV) using manganese oxide as an indicator for completion of oxidation, and total Se. Total Se concentration in water samples was determined using persulfate digestion followed by reduction to Se (IV) (Cutter, 1982, Yoshimoto, 1992). The Se(IV) in solution was analyzed using HGAAS (hydride generation atomic absorption spectroscopy). Organic-Se(-II)) is defined as the difference between Se(IV)+org-Se and Se(IV) and Se(VI) is obtained by the

difference between total Se and Se(IV)+org-Se analysis.

Selenium fractionation results for detrital materials (DM) and surface sediment (0-5 cm) are shown in Figure 10. It includes detrital material samples collected above the mineral sediment at each sampling location and one buried detrital material collected a few cm below the surface on C4-NW. Generally speaking, the 0.1 M NaOH extractable fraction (representing organic matter-associated Se) and the unextractable fraction (mainly elemental Se) were the largest fractions, ranging from 33-56% and 36-48% of total Se, respectively. Soluble and adsorbed Se comprise only a small fraction. However, detrital materials contained a significantly higher fraction of soluble and adsorbed Se compared to the mineral sediment except for the buried detrital materials in C4-NW. Soluble and adsorbed Se fractions for detrial materials at the mineral surface ranged from 10-11 and 5 to14%, respectively. For 0-5 cm sediment, soluble and adsorbed Se fractions ranged from 3-5 and 4-7%, respectively. These results indicate that more available Se is residing in the surface of mineral sediment.

The organic-Se fraction is of particular interest because we assume this phase is related to Se accumulation in the food chain. Thus 0.1 M NaOH extracts (IVa & b, Figure 6) containing the organic-Se fraction were speciated to determine the form of Se contained in this fraction (Figure 11). Org-Se varied from 20-44% with basin and location within basins; in all cases, mor than half in these humic fractions was apparently SeO_3 and SeO_4 anions.

We also probed whether selected organic structures co-occurred with Se. For example, since detrital material is only slightly degraded, considerable proteinaceous material should be present. Even in many humics, which are highly degraded biogenic substances, there is thought to be substantial proteinaceous material still intact (Hayes, 1991 and references cited therein), as we have recently shown (Fan et al., 2000). Recall that protein-bound Se is hypothesized to be very bioavailable, as discussed above. Therefore, it is reasonable to place a priority on detecting proteinaceous Se forms in detritus and humic materials, and in fact the latter possibility has been demonstrated by Rael and Frankenberger (1995). For this past year's work, we concentrated on relating the speciation of Se with the presence of proteinaceous material to better characterize the physical-chemical fractions of Se in sediment. Total protein and protein remnants ("peptidic" material) was analyzed by pyrolysis-GC/MS (Figure 12); the rationale is explained in the legend.

Peptidic Se constituents in the detrital materials and surface sediments were determined inthe various fractions (Figure 13). The majority of the peptidic constituents were found in the adsorbed and OM-associated fractions. Detrital material contained substantially higher peptidic Se than the 0-5 cm mineral sediment. Taken together with the data in Figure 10, it can be surmised that the OM-associated detrital material may harbor the most proteinaceous Se.

Detrital materials and surface sediment from Rejmankova's microcosm study for testing nutrient treatments on productivity and Se concentration, were also taken for Se fractionation, and peptidic constituents, and volatile Se measured from their water columns. Figure 14 shows volatile Se from the microcosms. Interestingly, the volatile Se appeared to have a negative relationship with Chl***a*** - the opposite of open estuary relationships (Amouroux and Donnard, 1996) - possibly a reflection of the observation that pigment-depleted cyanophytes volatilize Se readily (Fan et al., 1998a). Figure 15 shows the peptidic constituents in the microcosm sediments. The adsorbed fraction had more peptidic materials than the 0.1 M NaOH extracts, in contrast with most of the trends in Figure 13. The presence of brine shrimp always reduced the peptidic materials and the addition of N+P generally increased it. Thus treatment effects were demonstrated despite the short period of the experiment (7 days). For details, refer to the reports by Rejmankova, and Fan & Meeks.

Analyses that are currently underway will further characterize the organic material in the non-volatile fractions: total organic carbon and nitrogen using a CN analyzer diffuse-reflectance infrared (DRIFT) spectroscopy, and UV-visible spectrophotometry, and conjugated organic structures using EEM fluorescence spectrometry. It is possible that some significant correlations of the chemical motifs will relate with the observed total Se or Se forms, or the foodchain Se relationships observed at the basins and *in situ* enclosure experiments.

■ ■ ■ ■ ■

REFERENCES

Amouroux, D. and Donard, O.F.X. 1996. Maritime emission of selenium to the atmosphere in eastern Mediterranean seas. Geophys. Res. Lett. 23, 1777-1780.

Bowie, G. L., Sanders, J. G., Riedel, G. F., Gilmour, C. C., Breitburg, D. L., Cutter, G. A., Porcella, D. B. 1996. Assessing selenium cycling and accumulation in aquatic ecosystems. Water, Air, and Soil Pollution 90: 93-104.

Canton, S.P. and Van Derveer, W.D. (1997) Selenium toxicity to aquatic life: An argument for sediment-based water quality criteria. Environ. Toxicol. Chem. 16: 1255-1259.

Chao, T.T., and R.F. Sanzolone. 1989. Fractionation of soil selenium by sequential partial dissolution. Soil Sci. Soc. Am. J. 53:385-392.

Cooper, R.J., C.S. McLailand, D.A. Barnum. 1997. Dietary ecology of shorebirds using evaporation ponds of the San Joaquin Valley, California, with implications for use of pesticides to limit toxic exposure. Report to California Dept. of Water Resources, Fresno, CA.

Cutter, G.A. 1982. Selenium in reducing waters. Science 217:829-831.

EPA 1996. Proposed Selenium Criterion Maximum Concentration for the Water Quality Guidance for the Great Lakes System, Federal Register 61/242: 66007-66008.

EPA 1997. Water Quality Standards; Establishment of Numeric Criteria for Priority Toxic Pollutants for the State of California Federal Register 62/150: 42159-42208.

EPA Office of Water. 1998. Report on the Peer Consultation Workshop on Selenium Aquatic Toxicity and Bioaccumulation, EPA-822-R-98-007, September 1998. Available at the website http://www.epa.gov/ost/selenium/report.html

Fan, T.W-M., A.N. Lane, and R.M. Higashi. 1997. Selenium biotransformations by a euryhaline microalga isolated from a saline evaporation pond. Environ. Sci. Technol. 31: 569-576.

Fan, T.W.-M., R.M. Higashi, and A.N. Lane. 1998a Biotransformations of Selenium Oxyanion by Filamentous Cyanophyte-Dominated Mat Cultured from Agricultural Drainage Waters", Environmental Science and Technology 32, 3185-3193

Fan, T.W.-M. and R.M. Higashi. 1998b Biochemical fate of selenium in microphytes: Natural bioremediation by volatilization and sedimentation in aquatic environments. In: Environmental Chemistry of Selenium, W.T. Frankenberger and R.A. Engberg, eds., Marcel Dekker, Inc., New York, pp. 545-563.

Fan, T.W.-M. and R.M. Higashi. 1998. *In situ* Se volatilization and form measurements at San Joaquin Valley evaporation basins. In: UC Salinity/Drainage program annual report, 1998-1999, p. 53-71.

Fan, T.W.-M. and R.M. Higashi. 1999. *In situ* Se volatilization and form measurements at San Joaquin Valley evaporation basins. In: UC Salinity/Drainage program annual report, 1998-1999, p. 53-71.

Fan, T.W.-M. and R.M. Higashi. 1997. UC Salinity/Drainage program annual report, 1996-1997, p. 53-71.

Fan, T.W-M., Higashi, R.M., Lane, A.N. 2000. Chemical characterization of a chelator-treated soil humate by solution-state multinuclear two-dimensional NMR with FTIR and pyrolysis-GCMS. Environmental Science and Technology, 34: 1636-1646.

Fan, T.W-M., Teh, S.J., Hinton, D.E., Higashi, R.M. 2002. Selenium biotransformations into proteinaceous forms by foodweb organisms of selenium-laden drainage waters in California. Aquatic Toxicology 57(1-2):65-84.

Ferris, M. J., G. Muyzer and D. M. Ward. 1996. Denaturing gradient gel electrophoresis profiles of 16S rRNA-defined populations inhabiting a hot spring microbial mat community. Applied and Environmental Microbiology 62: 340-346.

Frankenberger, W.T., U. Karlson 1994. Microbial volatilization of selenium from soils and sediments, In: Selenium in the Environment, Marcel Dekker, New York, pp. 369-387.

Gao. S., K.K. Tanji, D.W. Peters, and M.J. Herbel. 2000. Water selenium speciation and sediment Se fractionation in TLDD flow -through wetland system. J. Environ. Qual. 29:1275-1283.

Hayes, M.H.B. 1991. Concepts of the origins, composition, and structures of humic substances. In: Advances in Soil Organic Matter Research: The Impact on Agriculture and the Environment, W.S. Wilson, ed., The Royal Society of Chemistry, Cambridge, pp. 3-22.

Higashi, R.M., G.N. Cherr, J.M. Shenker, J.M. Macdonald, and D.G. Crosby. 1992a A polar high molecular mass constituent of bleached kraft mill effluent is toxic to marine organisms. Environmental Science and Technology, 26: 2413-2420.

Higashi, R.M., G.N. Cherr, C.A. Bergens, T.W-M. Fan, and D.G. Crosby. 1992b An approach to toxicant isolation from a produced water source in the Santa Barbara Channel, pp.223-233. In: Produced Water: Technological/ Environmental Issues and Solutions, J.P. Ray, ed., Plenum Publishing, New York.

Higashi, R.M., T. W-M. Fan, and A.N. Lane. 1998 Association of deferrioxamine with humic substances and their interaction with cadmium(II) as studied by pyrolysis-gas chromatography-mass spectrometry and nuclear magnetic resonance spectroscopy. The Analyst, 123: 911-918.

Higashi, R.M. and T.W-M. Fan. 1999. In Situ Se volatilization and form measurements at San Joaquin Valley evaporation basins, Final Report to the California Dept. of Water Resources, Contract B-80933.

Higashi, R.M. and R.G. Flocchini. 2001. Chemical nature of selenium in agricultural drainage sediments and its implications for bioavailability. In: UC Salinity/Drainage program annual report, 2000-01.

Lipton, D.S. 1991. Associations of Selenium with Inorganic and Organic Constituents in Soils of a Semi-Arid Region. Ph.D. Dissertation, UC Berkeley.

Luoma, S.N., C. Johns, N.S. Fischer, N.A. Steinberg, R.S. Oremland, J.R. Reinfelder. 1992. Environ. Sci. Technol 26: 485-491.

Maier, K.J. and Knight, A.W. 1994. Ecotoxicology of selenium in freshwater systems. Rev. Environ. Contam. Toxicol. 134: 31-48.

Rael, R. M. and W.T. Frankenberger. 1995. Detection of selenomethionine in the fulvic fraction of a seleniferous sediment, Soil Biol. Biochem. 27: 241-242.

Rosetta, T.N. and Knight, A.W. 1995. Bioaccumulation of selenate, selenite, and seleno-DL-methionine by the brine fly larvae Ephydra cinerea Jones. Arch. Environ. Contam. Toxicol. 29, 351-357.

Reash, R., T.W. Lohner, and K.V. Wood. 1997. Overview of selenium bioaccumulation studies near midwestern coal-fired power plants. Abstr & presentation at: Understanding Selenium in the Aquatic Environment, Organized by W. Adams, Kennecott Utah Copper Co., Salt Lake City, Utah, March 1997.

San Joaquin Valley Drainage Implementation Program report: Evaluation of the 1990 drainage management plan for the westside San Joaquin Valley, California, 2000.

Skorupa, J.P. 1998. Selenium poisoning of fish and wildlife in nature: lessons from twelve real-world examples. IN: Environmental Chemistry of Selenium, W.T. Frankenberger and R.A. Engberg, eds., Marcel Dekker, Inc., New York, pp. 315-354.

Skorupa, J.P., and H.M. Ohlendorf. 1991. Contaminants in drainage water and avian risk thresholds, p. 345. In : The Economy and Management of Water and Drainage in Agriculture, A. Dinar and D. Zilberman (eds), Kluwer Academic Publishers, Norwell, MA.

Tanji, K.K. and S. Gao. 2001. Selenium Removal and Mass Balance Balance in a Constructed Flowthrough Wetland System. Annual Report 2000-2001. Salinity/Drainage Program, University of California, Davis.

Velinsky, D..J., and G.A. Cutter. 1990. Determination of elemental selenium and pyrite-selenium in sediment. Analytica Chimica Acta, 235:419-425.

Yoshimoto, J.T. 1992. Potential Mechanisms Controlling Soluble Selenite in Sierran Sands. Master's Thesis. University of California, Davis.

Zasoski, R.J. and R.G. Burau. 1977. A rapid nitric-perchloric acid digestion procedure for multielement tissue analysis. Commun. Soil Sci. Plant Anal. 8:425-436.

Zhang, Y.Q., J. Moore and W.T. Frankenberger, Jr. 1999. Speciation of soluble selenium in agricultural drainage waters and aqueous soil-sediment extracts using hydride generation atomic absorption spectrometry. Environ. Sci. & Technol. 33:1652-1656.

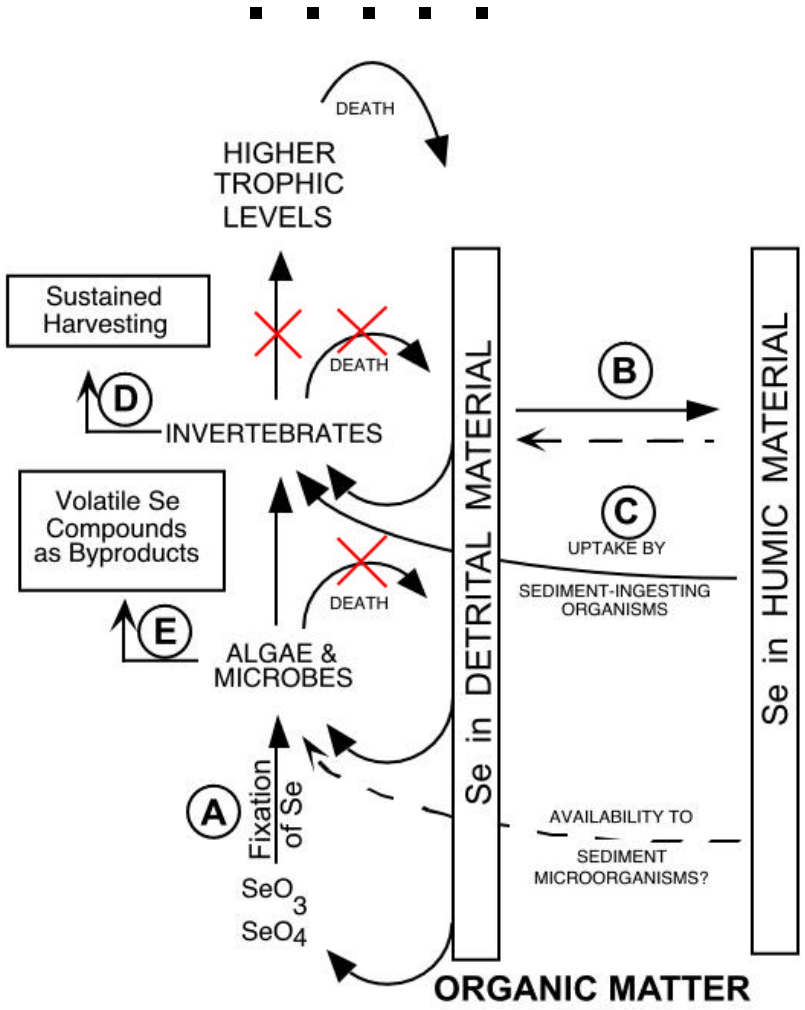

Figure 1. Reducing Se ecotoxic risk in drainage basins by invertebrate harvest and Se volatilization

In this "biogeochemical reflux" scheme, the drainage inorganic Se forms are initially biologically fixed by aquatic algae & microbes **(A)**. The fixed Se does not directly head up the foodchain in the water column, as is often portrayed. Instead, a major fraction enters into organic matter, taking a detour through detritus (recently dead organic matter) and sediment, then re-entering the foodchain at several trophic levels. Over longer periods, part of the detrital material is converted to recalcitrant humic material **(B)**, locking up the Se until sediment-ingesting organisms reintroduce them to the foodchain **(C)**. Through sustained harvesting **(D)** of water-column invertebrates that consume algae and microbes, the bioavailable Se is removed from water, plus detrital formation resulting from the death of water-column organisms is also blocked. Both types of blockages are shown by the three "X"s. In turn, this would help minimize the sediment-detritus foodchain pathway for Se. In the meanwhile, additional Se can be removed by manipulating the algae/microbe community for optimal Se volatilization **(E)**. This scheme would greatly improve the ecological “safety” margin of operating drainage basins. The economic efficacy of the approach is clear: (a) much of the scheme is water management; (b) costs of encouraging and managing brine shrimp growth is offset by marketing harvested materials.

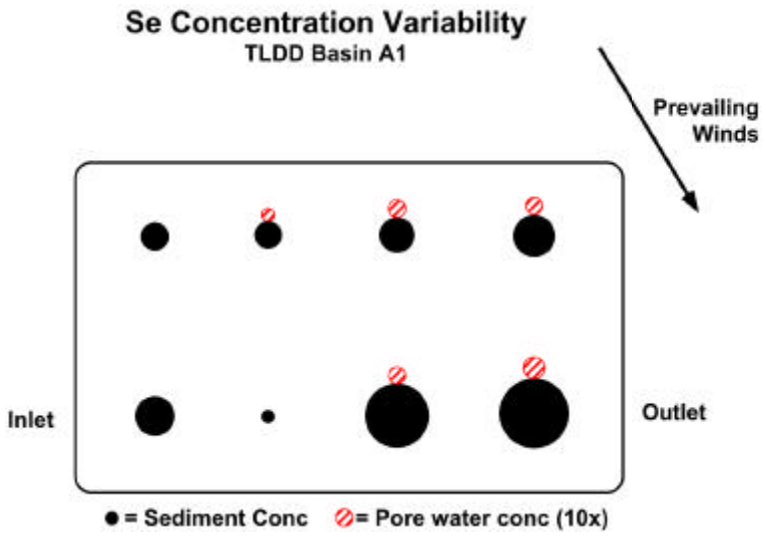

Figure 2. Heterogeniety of Se Distribution in a Basin.

Selenium concentrations in sediments—expressed here by dot size—are known to be highy variable. This diagram illustrates that, at TLDD, the distribution of Se was wind-driven, probably deposition via the floating cyanobacterial mats. This also affects the chemical form and compartment (see Figure 1). The uncovering of this phenomenon was the basis of our prior surveys of upwind and downwind locations for sediment sampling. (Fan& Higashi, 1997)

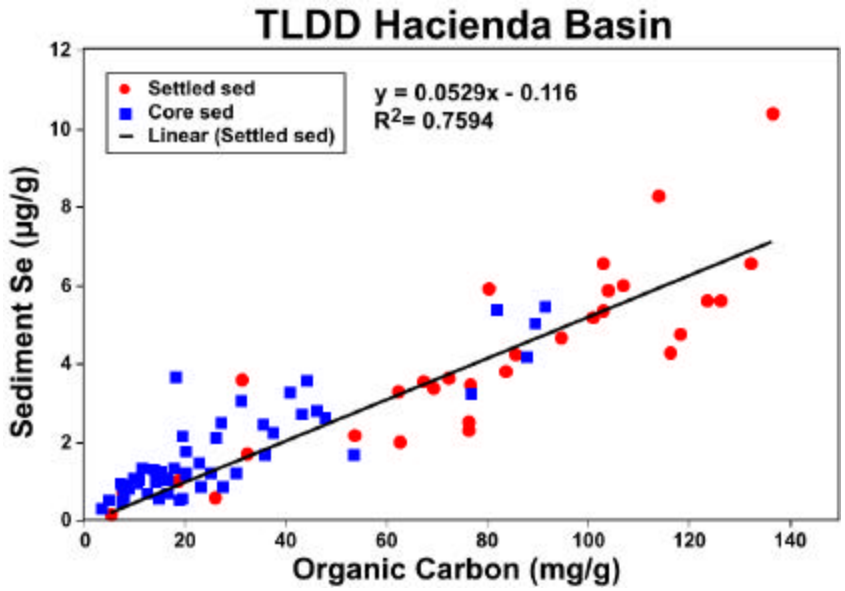

Figure 3. Global Data Set of Sediment Se vs. Organic Carbon (OC) for TLDD Hacienda Basins, 1997-2000 (Fan and Higashi, unpublished data).

Note the wide range of Se concentration and organic carbon among these basins, and sites within each basin. The sediment traps (round) generally contained both more Se and more OC than the cores, clearly indicating that the sources of both Se and OC are in the water column, e.g. algal detritus.

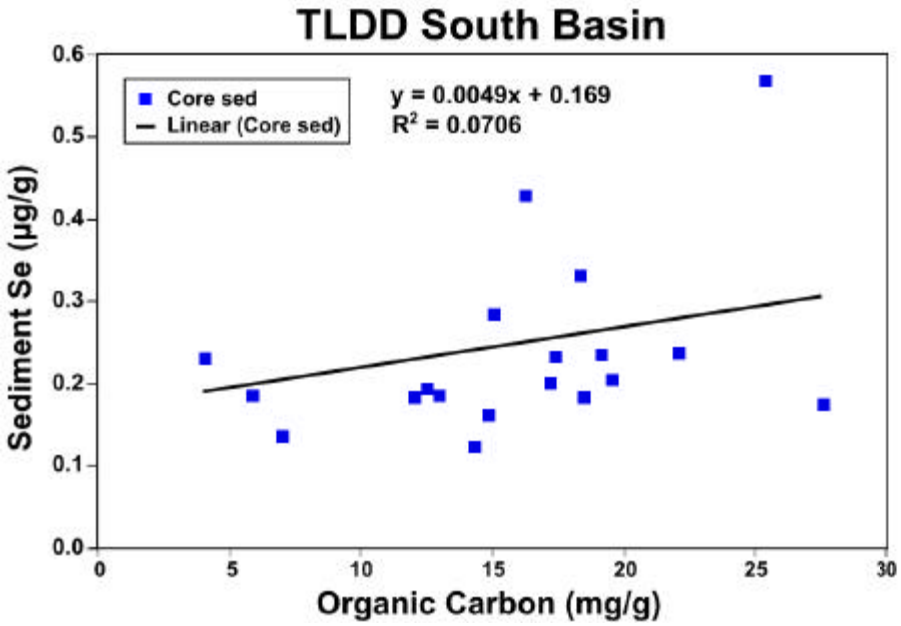

Figure 4. Global Data Set of Sediment Se vs. Organic Carbon (OC) for TLDD South Basins, 1999-2000 (Fan and Higashi, unpublished data).

Some of these basins are being harvested for brine shrimp, thereby truncating the food chain. There is no clear relationship present, in contrast with the non-harvested Hacienda basins.

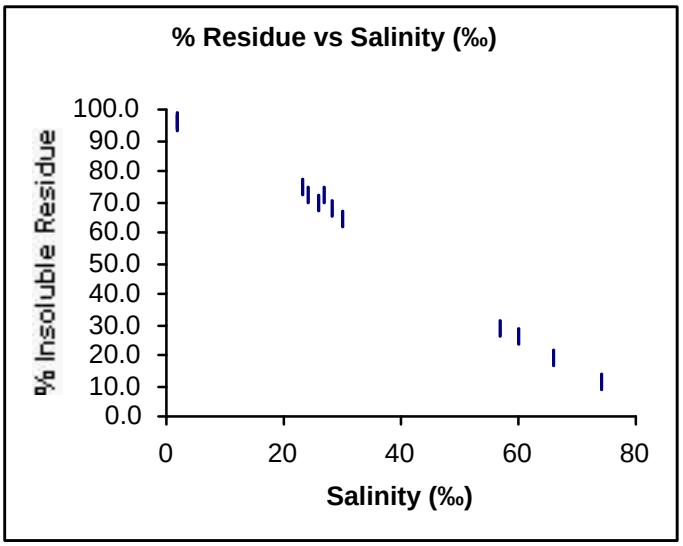

Figure 5. Non-soluble residue of sediment samples as a function of basin salinity.

These data from sediment traps deployed in TLDD basins (Apr –July, 2000) illustrates that "sediment" samples may consist of salts that can dissolve. These are very transient and are not a feature of the fixed sedimented material. Since evaporation basins routinely experience fluxes of fresher water, it is important to distinguish between such soluble ("mobile") and insoluble ("immobile") materials. Specifically, sediment and water-column algae and other organisms will be exposed differently to the mobile and immobile fractions of sediment and any associated Se.

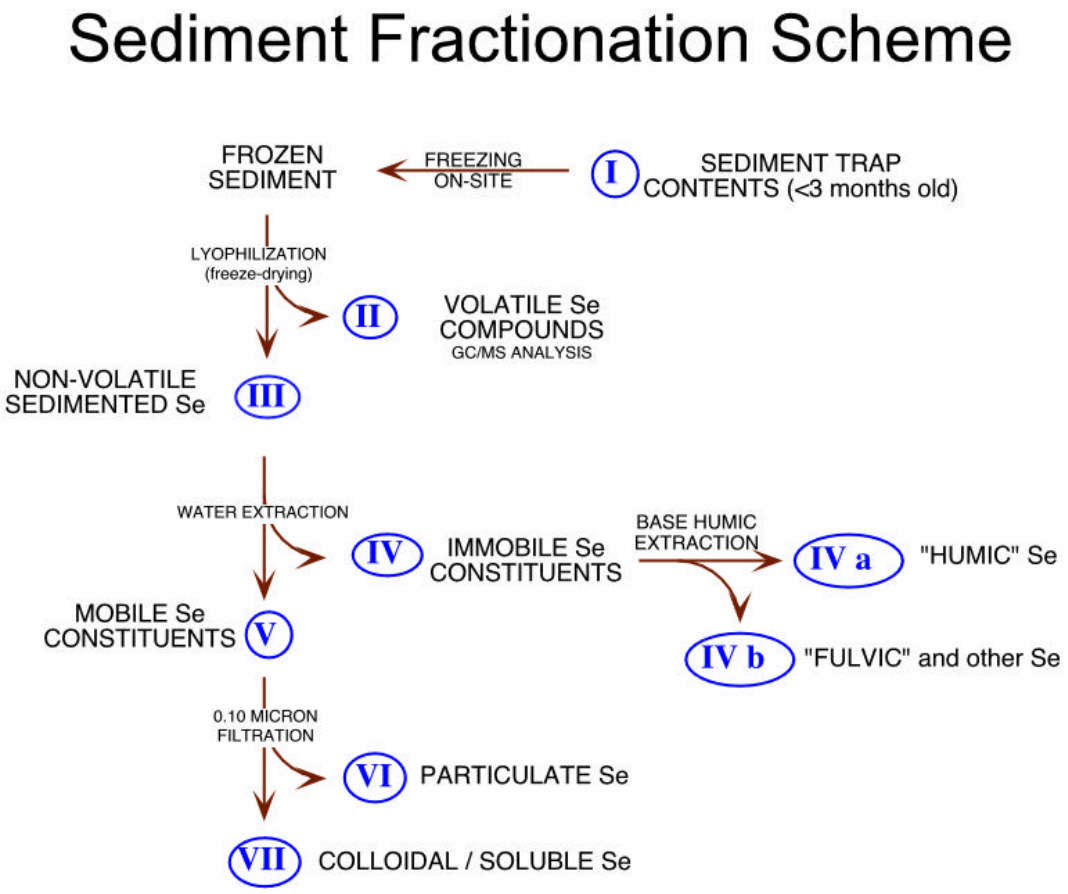

Figure 6. Chemical Fractionation Scheme Designed for Bioavailability Studies.

The general design follows the toxicity identification chemical fractionation approach we pioneered (Higashi et al., 1992). In the present case, the fractions are based on bioavailability considerations, not chemical classification. For example, both the volatile and humic forms may be "organic selenium", but are very unrelated in terms of exposure and bioavilability. An important consideration is that water-column organisms will be exposed to mobile, water-soluble S, but generally not to the immobile Se. The secondary consideration would then be the chemical form in each of these factions.

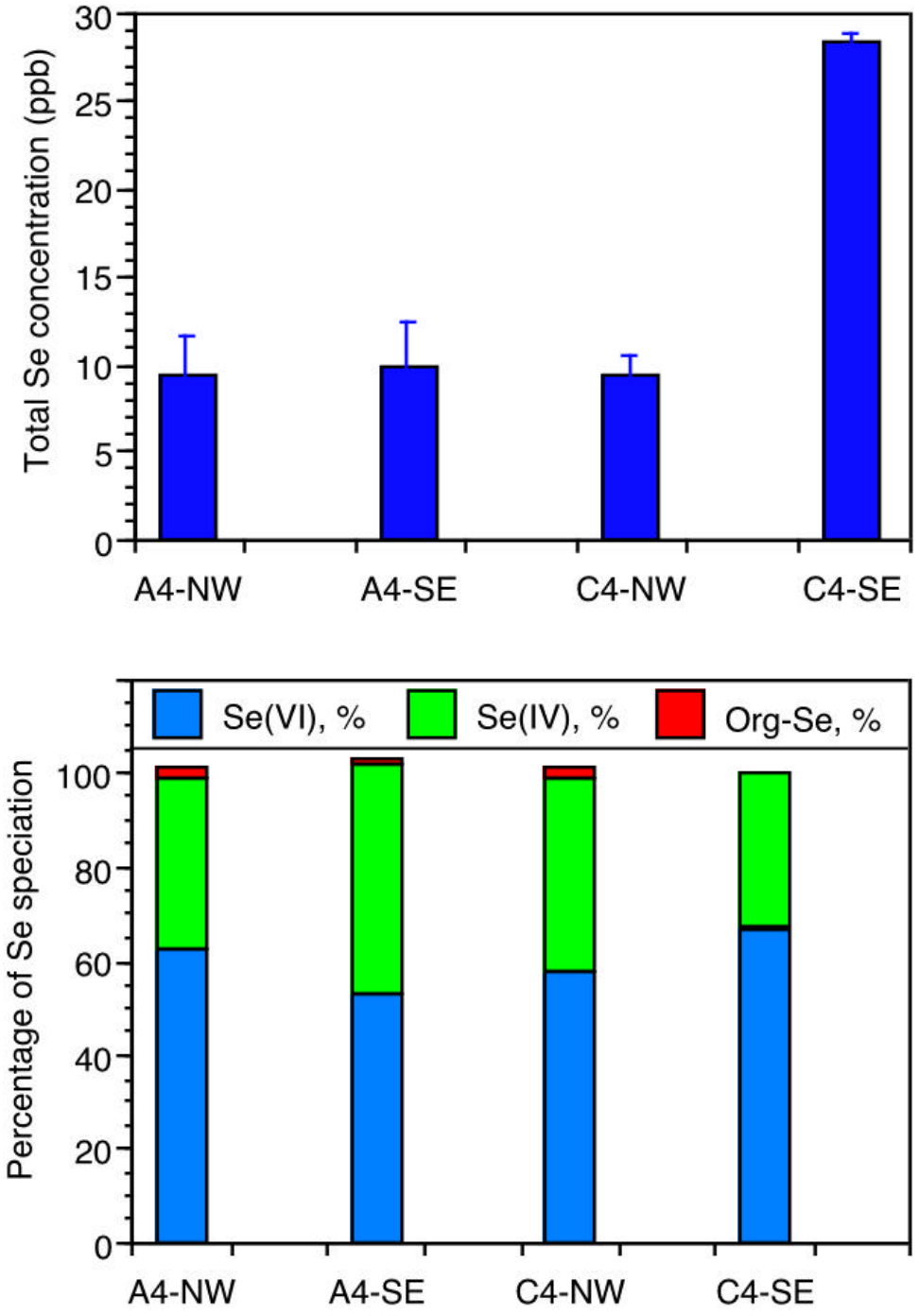

Figure 7. Se Concentrations and Speciation in TLDD Waters

Water Se speciation is thought to be important to "fixation" of Se into the foodchain (see Figure 1). Historically, total Se water concentrations in these basins have ranged from 5-30ppb; the left panel illustrates how that can differ at different locations within a basin (samples collected a few minutes apart). The right panel shows the speciation of Se in water in September, 2001. Although Se enters the basins mostly as Se(VI), the biogeochemistry converts ca. 40% to Se(IV), which is more bioavailable to some algae.

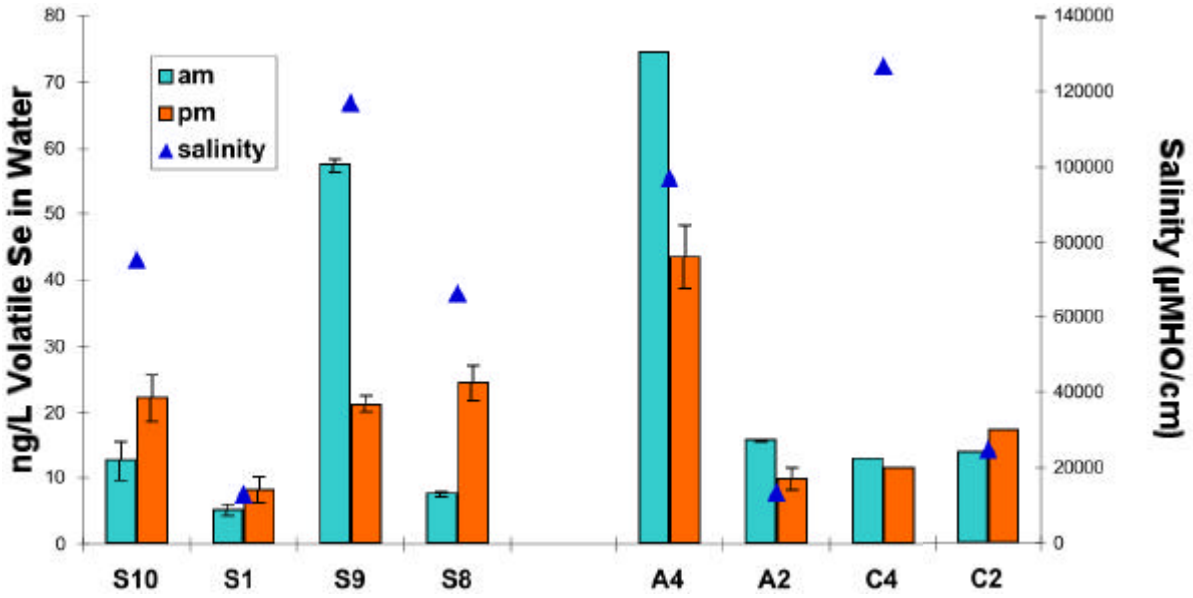

Figure 8. Volatile Se in TLDD Waters

Volatile Se was purged from 800mL water samples using helium gas over 1 hour periods both before and after noon on two consecutive days. Error bars represent standard deviations of simultaneous volatile collections. Basins with the highest levels of volatile Se (S9 and A4) also experienced the largest variation in volatile Se production, which were higher in the morning. Qualitatively, basins of higher salinity had higher volatile Se and diurnal fluctuations, though C4 is an exception. Volatile Se would be considered non-bioavailable and lost from the system.

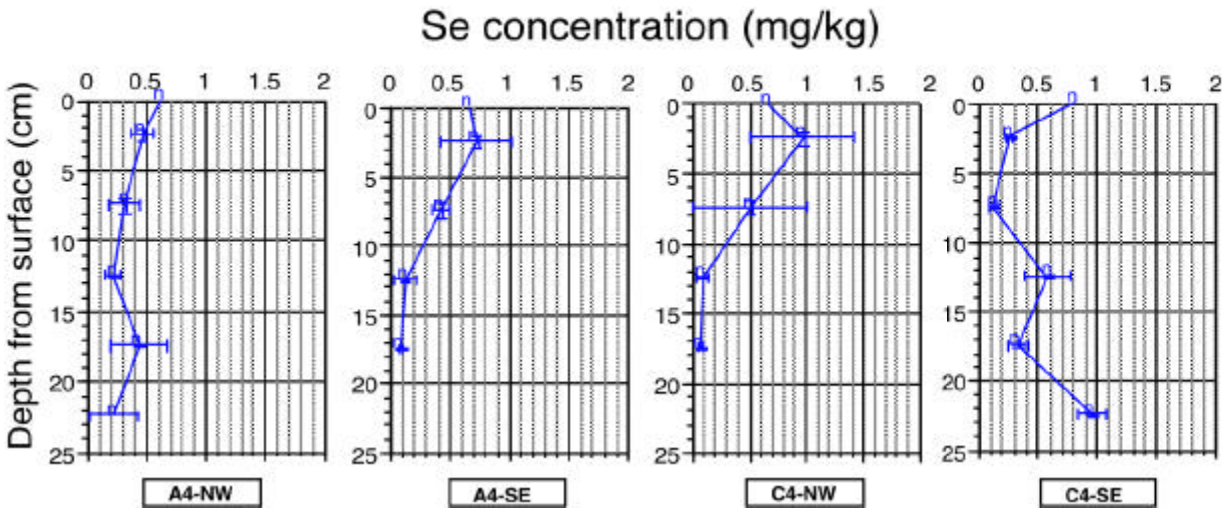

Figure 9. Total Se Concentration Profile in Hacienda Evaporation Pond Sediments

Total Se can not only vary spatially across a basin (as in Figure 2), but also with depth of the sediment. Shown above are depth-concentration profiles at opposite corners of A4 and C4 basins. It should be noted that density of the sediment varies widely; for example, there is deep muck at C4-SE, so the "age"-depth relationship is different at different sites. Regardless, the top few cm is the most important, as the majority of the benthic invertebrates reside there

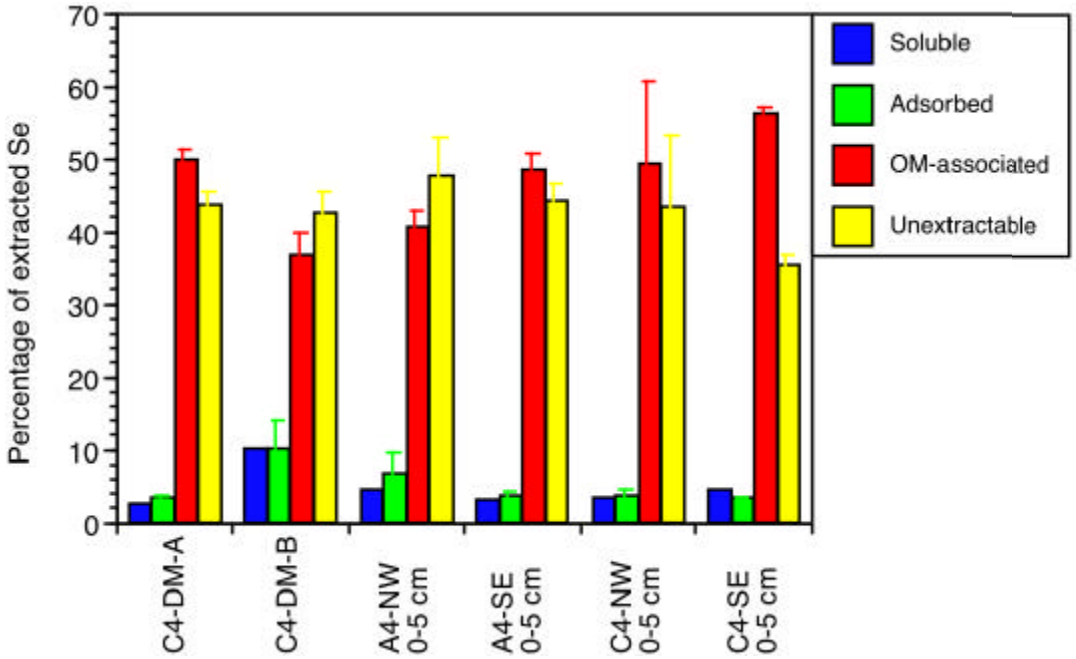

Figure 10. Total Se Distribution in Various Sediment Fractions

The total Se varied widely among the sediment fractions. The adsorbed is easily extracted and could include detrital material, while the OM-associated includes humified (aged organic) material.

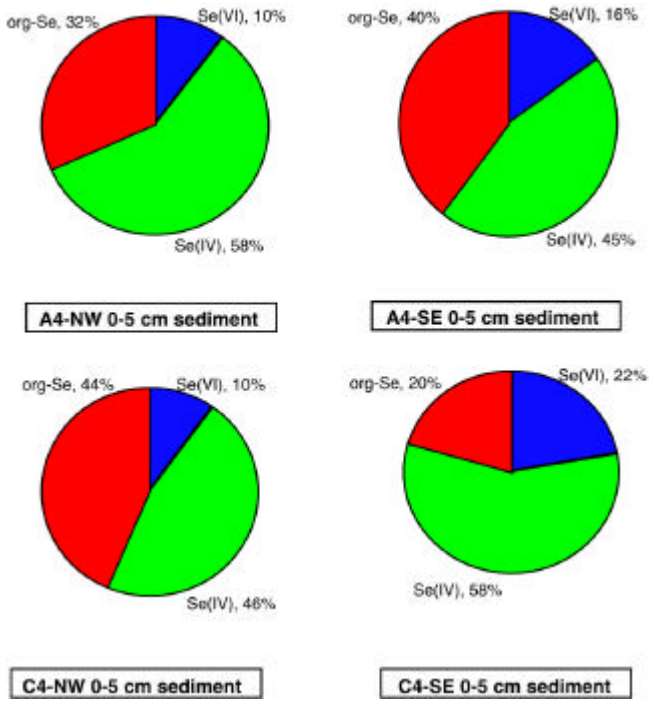

Figure 11. Se Speciation in OM-associated Fractions from Surface Sediments

The humified material from 0-5 cm depth sediments harbored varying amounts of organic Se. We made no distinction between detrital material and 0-5 cm sediments in this analysis. Note that less than half of the Se in these organic fractions was org-Se.

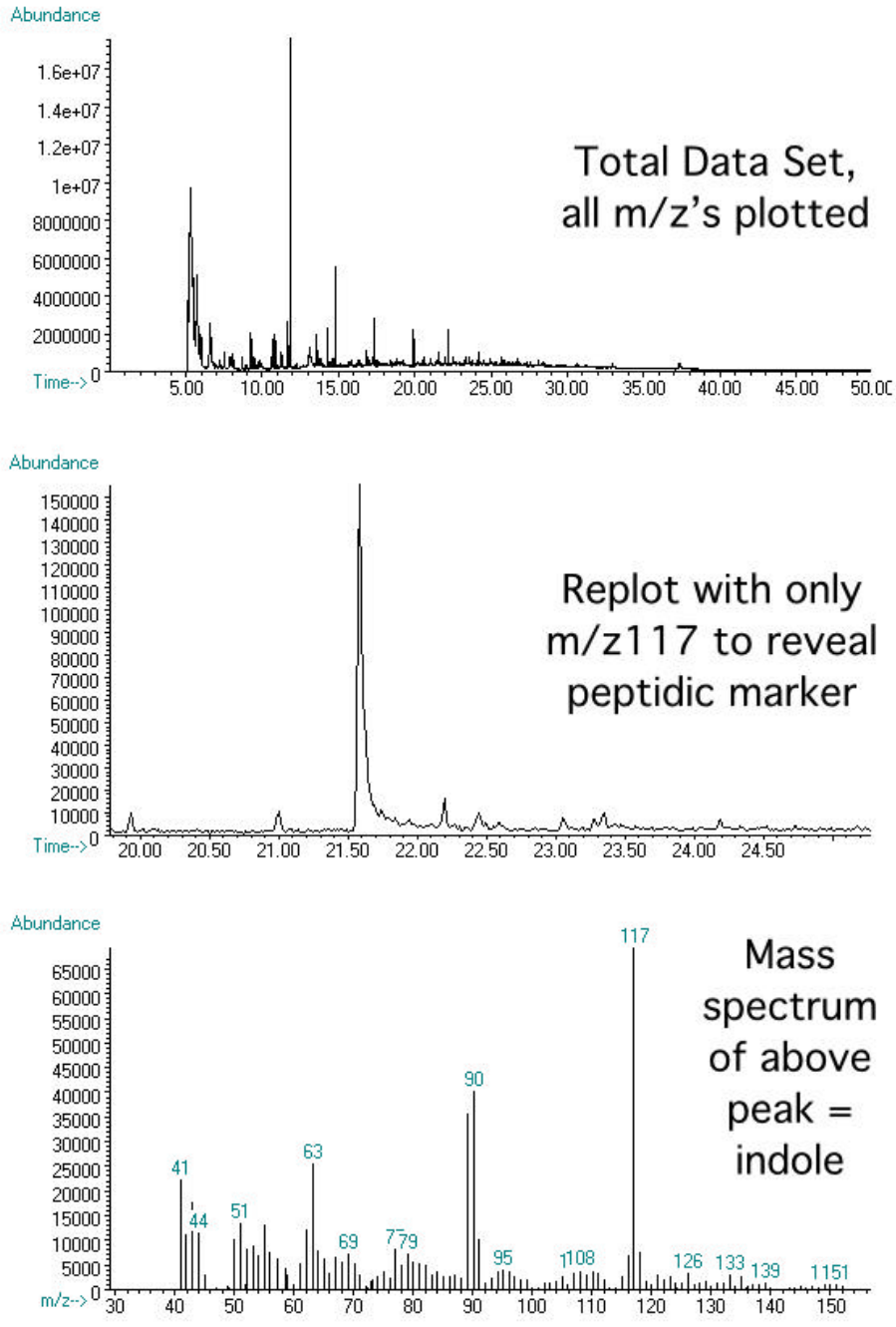

Figure 12. Pyrolysis-GCMS Obtains Peptidic Constituents from DM and Sediment

It was stated previously that proteinaceous Se may be the most bioavailable in the foochain (EPA, 1998; Fan et al., 2002). It is possible that similar Se forms in detritus and sediment are also highly available to benthic organisms.

Pyrolysis-GCMS was used to determine the abundance of peptidic constituents in DM and sediment fractions, following previous methods (Higashi et al., 1998; Fan et al., 2000). This panel describes our use of this unusual analysis. The full data set chromatogram for DM-adsorbed fraction from basin C4se is shown in the top panel. Pyro-GCMS causes the peptidic group to form indole, C_8NH_{10} with an ion at mass (m/z) 117. The middle panel shows this data subset. The bottom panel is the mass spectrum of the indole peak.

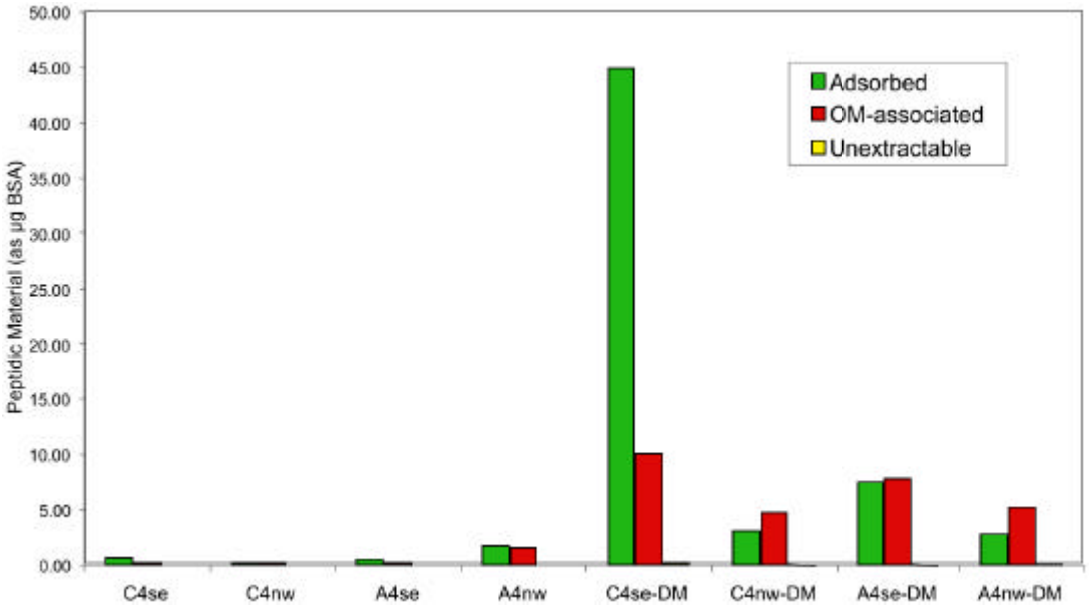

Figure 13. Peptidic Constituents in Sediment Fractions

The majority of the peptidic constituents was found in the adsorbed and OM-associated fractions. As expected, detrital material (DM) was always higher than the 0-5 cm sediment. Taken with the data in Figure 10, we conjecture that the OM-associated detrital material may harbor the most proteinaceous Se.

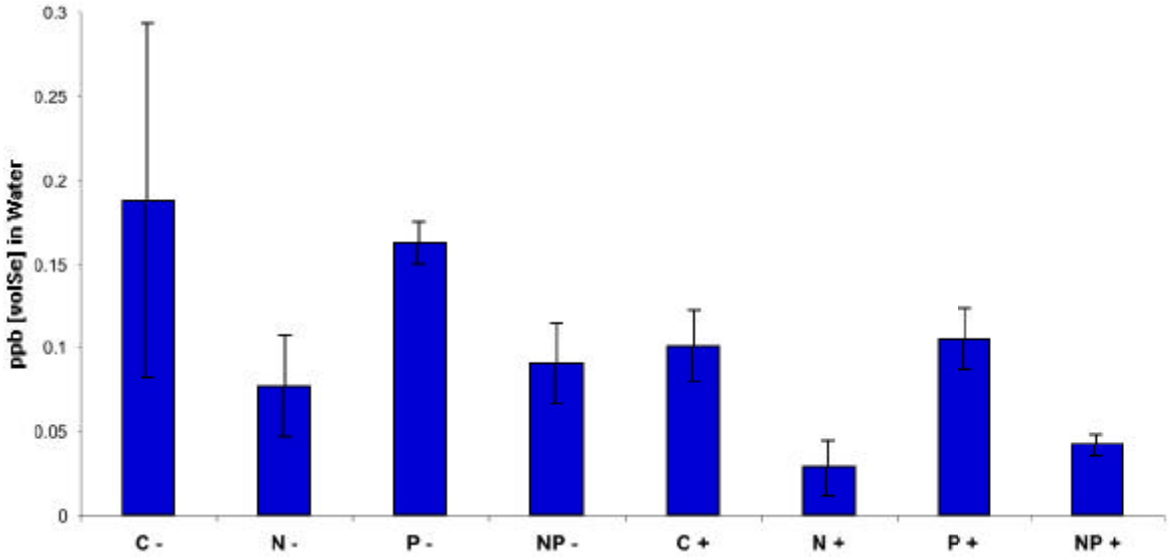

Figure 14. Volatile Se from Microcosm Experiment

The treatment designations are: C=control, N=nitrate amended, P=phosphate amended, NP=both N and P amended, +/- indicates brine shrimp added/none. The volatile Se in the water was roughly opposed in pattern to the Chl***a*** measurements (see Rejmankova project report), except that the presence of brine shrimp always reduced the volatile Se. We have previously reported (Fan et al., 1998) that pigment-depleted, senescent cyanophytes volatilize Se readily, which can help explain this dissociation of volatile Se with Chl***a***. In addition, the species distribution of algae is probably important to Se volatilization, a parameter that is being directly addressed in the Joint Project.

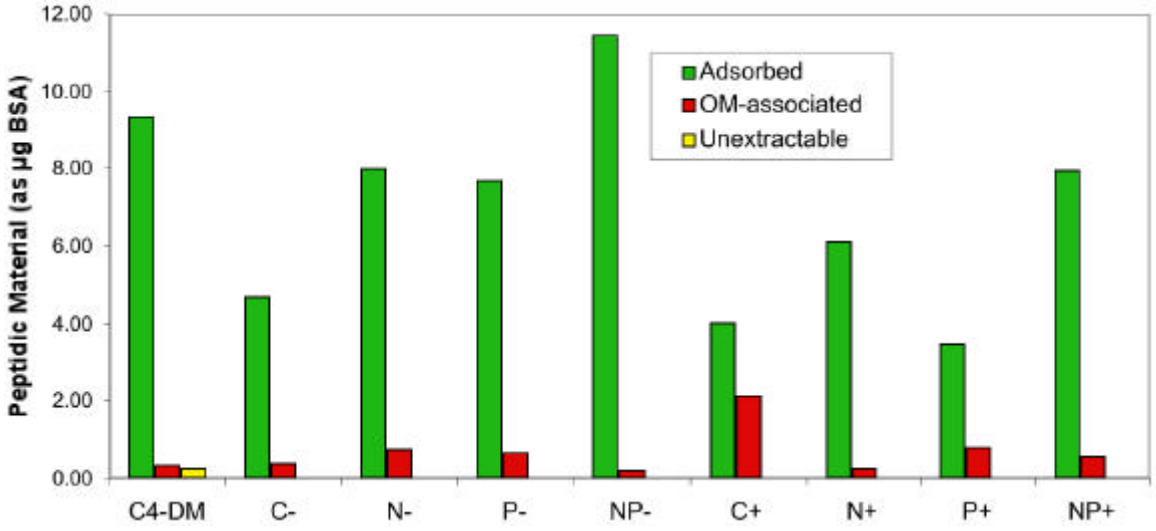

Figure 15. Peptidic Constituents in Sediment Fractions in Microcosm Experiment

[The treatment designations are: C=control, N=nitrate amended, P=phosphate amended, NP=both N and P amended, +/- indicates brine shrimp added/none. C4-DM is detrital material from outside the microcosms.] Clearly, the adsorbed fraction (green) had the most peptidic material; interestingly, this pattern tracked the Chl***a*** measurements from the same experiments (see the Rejmankova project report). Presence of brine shrimp always reduced the peptidic material, while addition of NP generally increased it. This effect is very strong: the experiment was only 7 days in duration. As expected, the longer time-integrated OM did not appear to have an interpretable pattern

Conceptual Modeling of Salt Management Problems in the Western San Joaquin Valley of California

Project Investigators:

William A. Jury
Office: (909) 787-51354, E-mail: wajury@mail.ucr.edu
Department of Environmental Sciences
University of California, Riverside

Laosheng Wu
Office: (909) 787-4664, E-mail: laowu@mail.ucr.edu,
Dept. of Environmental Sciences
University of California, Riverside, CA

Research Staff:

Dr. Atac Tuli, Postdoctoral Research Associate
Department of Environmental Sciences, UCR
0.5 FTE

ABSTRACT

Sequential reuse of agricultural drainage water recovered in tile lines has been proposed as a strategy for reducing drainage volume in the Western San Joaquin Valley of California. In this system, high-quality water is used to grow a salt-sensitive crop, and the drainage from this operation is collected by tile lines and subsequently used on a more salt-tolerant crop. This process is continued on progressively more salt-tolerant species until the final residual is collected and sent to evaporation ponds. In this paper we develop a transfer function model for simulating the drainage concentrations of each stage of a sequential reuse project. Transient salt concentrations are calculated for typical drain spacing and water management strategies, under the assumption that a subsurface barrier eventually restricts downward movement of water. Results of the calculations show that response times of fields managed in this way are extremely long, so that the drain lines primarily capture resident ground water for decades or more after the operation is started, especially if the barrier is assumed to be at a substantial depth below the surface. As a result, the system will never reach steady state in any practical period of time, and system design strategies based on steady state behavior will be flawed.

KEYWORDS

Tile drainage, chemical transport, sequential reuse, travel times

■ ■ ■ ■ ■

INTRODUCTION

California's Western San Joaquin Valley is experiencing a variety of irrigation-induced problems such as water scarcity, deteriorating water quality, and salinization of agricultural soils (Letey et al., 1986; San Joaquin Valley Drainage Program, 1990; Letey, 2000). A largely impermeable subsurface layer has caused drainage water to accumulate over many years, resulting in rising water tables and saline seepage into low-lying flood plains (San Joaquin Valley Drainage Program, 1990). As a consequence, agricultural fields in this region are commonly tile drained to keep the root zone aerated and free of salts. Earlier plans for surface detention and export of excess drainage water to the ocean through the San Francisco bay area were canceled because of high selenium levels in evaporation ponds, and concerns that export through the bay would have adverse environmental consequences for the local habitat (Letey, 2000). Since that plan was disrupted, efforts to control salinization have focused more on water reuse or various forms of land management (Letey and Oster, 1993; Belitz and Philips, 1995).

One strategy for salinity control consists of periodic leaching of the crop root zone to reduce the dissolved salt content to the tolerance limits of the crop to be grown (Biggar et al., 1984). Rhoades (1984) has proposed alternating saline and nonsaline irrigation waters together with crop rotation, including both salt-sensitive and salt tolerant crop species. Rhoades et al. (1988) tested this cyclic strategy in a field experiment with crops having different salt tolerance levels, and showed that high crop yield and quality could be achieved. Moreover, they concluded that the soil salinity level could be maintained within acceptable limits over time. Bradford and Letey (1992) used computer modeling to confirm the results of the Rhoades et al. (1988) experiments. They also showed that the soil salinity at the beginning of the cropping season was a significant factor influencing crop yield.

Another idea for drainage and salt control that is attracting considerable attention is a water-management program involving reuse of drainage water on successively more salt-tolerant crops, sometimes referred to as sequential reuse (Drainage Reuse Technical committee, 1999). In this system, high-quality water is used to grow a salt-sensitive crop, and the drainage from this operation is collected by tile lines and subsequently used on a more salt-tolerant crop. This process is continued on progressively more salt-tolerant species until the final residual is collected and sent to evaporation ponds. Since substantial water is evaporated at each stage, the drainage water volume available for irrigation is progressively reduced, while the salt concentration is correspondingly magnified.

Cervinka et al. (1999) presented results from a sequential reuse demonstration project conducted on irrigated farmland in the Western San Joaquin Valley. The crop areas, drainage volumes, anticipated dilution, and expected yields were all designed based on the steady-state assumption that the concentration of water

collected in the drainage system of each stage was the same as the concentration of water leaving the root zone. However, drain water concentrations during the years of operation of this project have differed significantly from their anticipated steady-state values, suggesting that the transition times to adjust to the new management may be considerable, and that correct design of a sequential reuse system will require knowledge of the response time of the soil to a change in surface management (Letey et al., 2001). Jury (1975a) calculated the response time of tile-drained fields as a function of their drainage rates, drain spacing, and depth to barriers reducing or preventing downward flow, and found that it may take years to leach existing salt out of fields of the type found in the San Joaquin Valley. This delay time might substantially affect the performance of a system designed for water reuse or remediation of saline soil (Jury, 1975b).

This report develops a conceptual-mathematical model of water and chemical movement through the soil and to the tile drain that is used to represent the sequential reuse system and calculate the buildup of salinity in the soil and drainage water over time.

METHODOLOGY

The purpose of this analysis is to construct a simple model of the tile-drain concentrations in a system where agricultural drainage water is sequentially pumped to fields containing increasingly more salt-tolerant crops. Tile drain concentrations are easily modeled as transfer functions, where the input concentration to the field C_{in} is converted to an output concentration C_{out} at the drain using the drainage probability density function (pdf) $f(Q)$, where Q is the amount of drainage required to move a mobile chemical from the surface to the drain (Jury and Roth, 1991). This pdf is assumed to be a unique function of the geometry and soil properties, so that a single pdf is all that is required to model the system. If portions of the system are draining at different rates, the cumulative drainage-time function $Q(t)$ may be used to convert the modeled concentration outflow to a time record. The following assumptions are used to construct the model:

- Each stage of the system has the same drain depth H, and drain spacing $2S$.
- The soil is homogeneous and bounded by a vertical flow barrier at a depth D below the drain
- The initial salinity level C_s in the soil and throughout the ground water is uniform.
- The first stage of the system using high quality irrigation water of concentration C_{irr} is leached at a low drainage rate R_1 and leaching fraction x_1.
- Subsequent stages are leached at a higher drainage rate R_2 and leaching fraction x_2.
- The water table is flat and the lateral ground water velocity is zero.

The travel time to the drain from any point of entry on the surface is the sum of two terms: i) the travel time t_u through the unsaturated zone (assumed to be constant); and ii) the variable travel time t_s from the point of entry at the water table to the tile drain. The saturated zone travel time t_s (and hence the pdf) is calculated by a model.

The two-dimensional calculation of the travel time t_s from the water table to the tile drain is described in detail in Jury (1975a). It begins with the Kirkham and Powers (1972) solution for the stream function $Y(x,z)$ through the saturated zone of a tile-drained system with drain spacing $2S$ and depth to barrier D. Lines of constant stream function represent water flow paths. First, the geometry of a given field is scaled by defining new variables $X=x/S$, $Z=z/S$. Then the streamlines of the scaled system are calculated as a Fourier series. This solution is given by (Jury, 1975a)

$$\Psi(x,z) = 1 - \frac{2}{p}\sum_{N=1}^{\infty}\frac{\sin[NpX]\sinh[Np(h-Z)}{\sinh[Nph]};$$

$$h = \frac{S}{D};\ X = \frac{x}{S};\ Z = \frac{z}{S} \qquad (1)$$

Streamlines are constructed for equally spaced points of entry into the saturated zone along X separated by DX. An illustrative set of streamlines for the particular geometry $h = S/D = 1$ is given in Figure 1.

The travel time from a point of entry at the water table to the drain is calculated from this information as follows. Since any water entering between two adjacent streamlines must remain between the lines all the way to the drain, the travel time of any mobile solute in the water is approximately equal to the amount of time required to replace the amount of water in storage (the area $a(x)$ times the saturated water content q_s) between the lines. Similarly, the

cumulative drainage flux $Q(x)$ arriving at the water table that is required to move solute from a point of entry a distance x laterally from the drain (multiplied by the area per width Dx between the lines) is equal to the water stored between the lines. If the system is draining at a steady flux rate R then $t_s(x)=Q(x)/R$. Thus, the travel time is equal to

$$t_s(x) = \frac{q_s a(x)}{R\Delta x} = (\frac{q_s S}{R})\frac{A(X)}{\Delta X} \qquad (2)$$

where $A(X)=a(x)/S^2$ is the dimensionless area between the two streamlines originating at the water table at X-DX and X. $A(X)$ is estimated by numerical integration.

Since after a given amount of drainage Q_1, a fraction $X_1=x_1/S$ of the chemical added to the field at $t=0$ has arrived at the drain, we may interpret $X(Q)=x(Rt)/S$ as the cumulative probability density function (cdf) $P_s(Q)=P_s(Rt)$ of the saturated zone travel time. Thus the pdf of the cumulative drainage through the saturated zone is given by $f_s(Q)=dP_s(Q)/dQ$.

Under these assumptions, the sequential outflow may be solved by the mathematics of transfer functions as follows. In general, a given tile drain outflow concentration $C_{out}(Q)$ is expressed as a function of its input concentration $C_{in}(Q)$ at the water table by (Jury and Roth,1991)

$$C_{out}(Q) = \qquad (3)$$
$$\int_0^Q C_{\text{int}}(Q-Q')f_s(Q')dQ' + C_s[1-P_s(Q)]$$

Note that Eq. [3] contains two terms, one representing the arrival of the drainage water that has reached the tile and a second describing the resident water in the saturated zone (assumed to be spatially uniform at $t=0$) being pushed out ahead of the incoming water. We may easily combine the saturated zone and unsaturated zone travel times (expressed as cumulative drainage), since the latter is assumed to be constant. The cdf of the total cumulative drainage is thus

$$P(Q) = 0 \qquad 0 < Q < Q_u \qquad (4)$$
$$P(Q) = P_s(Q-Q_u) \qquad Q > Q_u$$

where Q_u is the amount of drainage required to move solute from the soil surface to the water table at depth H.

We may now apply the model to the sequence of drains, noting that as the irrigation water passes through the unsaturated zone of a field with a leaching fraction x_i, it is concentrated by a factor $N_i=1/x_i$. Thus, if the irrigation water added to the first stage has a constant concentration C_{irr}, a drainage rate R_1, and a leaching fraction x_1, then the outflow concentration in the first drain is equal to

$$C_1(Q) = C_1(R_1t) = N_1C_{irr}P(R_1t) + C_s[1-P(R_1t)] \quad (5)$$

Similarly, since all other stages have drainage rates R_2 and leaching fractions x_2, the outflow in the Jth drain is equal to

$$C_J(Q) = C_J(R_2t) = \qquad (6)$$
$$N_2\int_0^{R_2t} C_{J-1}[R_2(t-t')]f_1(R_2t')R_2\,dt' + Cs[1-P(R_2t)]$$

These expressions become very simple after Laplace transformation (Jury and Roth, 1991)

$$\hat{C}_1(s) = N_1C_{in}\frac{\hat{f}}{s} + \frac{C_s}{s}(1-\frac{\hat{f}}{s}) \qquad (7)$$

$$\hat{C}_J(s) = N_2\hat{C}_{J-1}(s)\hat{f} + \frac{C_s}{s}(1-\frac{\hat{f}}{s}) \qquad (8)$$

where

$$\hat{f}(s) = \int_0^\infty \exp[-sQ']f(Q')dQ' \qquad (9)$$

is the Laplace transform of $f(Q)$. The recursive Eqs. (7)-(8) may be combined into a general expression for the solute concentration entering the Mth drain as follows.

$$\hat{C}_M = N_1(N_2)^{M-1}(\hat{f})^M\frac{C_{irr}}{s} + \frac{C_s}{s}(1-\frac{\hat{f}}{s})\sum_{J=0}^{M-1}(N_2\hat{f})^J \qquad (10)$$

Thus, if the Laplace transform of $f(Q)$ is known and Eq. (10) can be inverted, the tile drain concentration from each stage of the sequential reuse system may be calculated as a function of cumulative drainage and converted to time.

RESULTS AND DISCUSSION

Figure 2 shows the dimensionless cdf $P(T)$ as a function of the scaled travel time $T=Rt/q_sS=Q/q_sS$ for drain spacing to barrier depth ratios $h=S/D$ of 1, 5, and 20. In all calculations the dimensionless unsaturated zone travel time was set equal to 0.005. Each of these curves were parameterized approximately by fitting to the exponential model

$$P(T) = 1-\exp[-w(T-0.005)];\ T > 0.005 \qquad (11)$$

The representation in Eq. (11) becomes exact for shallow barriers (large h), but underestimates long times and overestimates short times when the barrier is deep (small h). With this parameterization, the solution to Eq. (10) may be obtained analytically or by numerical inversion of the Laplace transform. The solution may also be converted to actual time when the parameters of a particular system are known. We will illustrate the calculation using the data shown in Table 1 from the Red Rock Ranch sequential reuse demonstration facility (Cervinka et al. 1999). This facility overlies the Corcoran clay barrier at a substantial depth below the surface. However, it is possible that soil layering could distort the streamlines before they reach deep into the saturated zone. For this reason, we will conduct analyses for both a shallow barrier and a deep one. We will use the small drainage rate and leaching fraction in Table 1 for stage 1 and the larger leaching fraction and drainage rate for all subsequent stage calculations.

Figure 3 shows the response time and equilibration time of the first stage alone for the shallow and deep barrier cases. Even when only the first stage is considered, it is obvious that the system is inherently transient and does not reach steady state in any practical period of time. Moreover, the response time is lengthened considerably as the depth to barrier is increased. During the early stages, the drainage water concentration consists primarily of resident ground water that was removed by the tile lines.

Figure 4 shows the drain concentrations from all four stages of a system overlying a shallow barrier, using parameters from the Red Rock ranch in Table 1. Several features are noteworthy. First, each successive field requires longer to reach steady state than the previous one. Second, steady state concentrations (shown as dashed lines in the figure) can be exceeded during the transient stage, because the high concentration of the resident ground water can magnify as it passes through the system. Figure 5 is identical to Figure 4, except that the barrier now resides at great depth ($h=S/D=1$). The behavior of the field is qualitatively the same as the field with a shallow barrier, except the time scale for transition to the steady state is now expanded considerably because of the significantly greater volume of resident water that must be leached.

An approximate index of the response time of a field with a given geometry and flow rate may be estimated from Figure 2. Table 2 gives the time in years for 25%, 50%, and 75% of the solute added at t=0 to reach the drain for all of the cases studied. Median response times vary from a low of 2.1 years for the shallow system leached at 0.50 m/y to a high of 31.2 years for the deep barrier system leached at 0.225 m/y. The systems are also very asymmetric, requiring much longer to leach the remaining percentages of the field than early ones. What this implies is that during the first few years after initiation of the sequential reuse strategy, drain concentrations for systems with a large spacing between drains will consist mainly of water extracted from the ground water at or near the ground water concentration (Figure 5). Thus, the predominant early function of a sequential reuse operation would be ground water reclamation. This prediction is in qualitative agreement with the findings of Deverel and Fio (1991), who determined from oxygen 18 measurements that up to 60% of the water extracted by a drain tile in the San Joaquin Valley was from deep resident ground water. These authors also simulated water flow for the system they measured and calculated travel times of up to 34 years for arrival at the drain (Fio and Deveral, 1991).

The extremely long transition times to steady state for the tile geometries studied indicates that any management design for sequential reuse based on steady-state criteria will be flawed. For example, if crops are selected for the fields in succession based on their ability to tolerate the steady-state salinity coming from the previous drain, the irrigation water may have to be diluted for a substantial period of time to avoid damaging the crop. This transient effect persists for many years and must be part of any management design. The problems associated with a steady-state analysis are illustrated in Figure 6, which shows the percent dilution of the drainage water from stage 1 required to maintain the irrigation water to stage 2 at 5 dS/m or less (suitable for growing cotton at zero yield depression), using the Red Rock ranch parameters in Table 1. Since the steady state concentration coming from stage 1 is 4.2 dS/m, the steady-state design calls for zero dilution, whereas there is substantial dilution required for 20 years in the shallow barrier case, and indefinitely in the deep barrier case.

CONSLUDING REMARKS

Our analysis demonstrates the dominant effect of transient solute movement on the performance of a sequential reuse operation. For drain tile geometries of the type found in the San Joaquin Valley, steady state will never be reached, and initially saline ground water will significantly affect the concentration of irrigation water for stages beyond the first for the entire practical lifetime of the project. Because this resident ground water becomes concentrated after passage through a root zone, substantial dilution may be required to reduce the drainage water to levels suitable for irrigation of all but the most salt-tolerant of species.

The conceptual model used in this analysis was intended primarily to demonstrate the dominant effects of travel time on performance of a sequential reuse operation. A number of potentially important factors such as soil layering, ground water movement, or deep seepage unimpeded by a barrier were neglected in this study and will be examined by numerical methods in the coming year.

■ ■ ■ ■ ■

REFERENCES CITED

Belitz, K. and S. P. Philips. 1995. Alternative to agricultural drains in California's San Joaquin Valley: Results of a regional-scale hydrogeologic approach. Water Resour. Res. 31(8): 1845-1862.

Biggar, J.W., D.E. Rolston, D.R. Nielsen. 1984. Transport of salts by water. Cal. Agr. Cal. Agr. 38 (10): 10-11.

Bradford, S. and J. Letey. 1992. Cyclic and blending strategies for using nonsaline and saline waters for irrigation. Irrig. Sci. 13: 123-128.

Cervinka, V. J. Diener, J. Erickson, C. Finch, M. Martin, F. Menezes, D. Peters, and J. Shelton. 1999. Integrated system for agricultural drainage management on irrigated farmland. Report of Westside Resource Conservation District to US Bureau of Reclamation, Grant 3: 4-FG-20-11920.

Deverel, S. J. and J. L. Fio, 1991. Groundwater flow and solute movement to drain laterals, Western San Joaquin Valley, California. 1. Geochemical assessment. Water Resour. Res. 27: 2233-2246.

Drainage Reuse Technical Committee, 1999. Task 1. Drainage reuse. Final report of the technccal subcommittee of the University of California Salinity/Drainage Program to the The San Joaquin Valley Drainage Implementation Program. Calif. Dept. of Water Resources. 81 p.

Fio, J. L. and S. J. Deverel, 1991. Groundwater flow and solute movement to drain laterals, Western San Joaquin Valley, California. 2. Quantitative hydrologic assessment. Water Resour. Res. 27: 2247-2257.

Jury, W.A. 1975a. Solute travel-time estimates for tile-drained fields: I. Theory. Soil Sci. Am. Proc. 39: 1020-1024.

Jury, W.A. 1975b. Solute travel-time estimates for tile-drained fields: II. Application to experimental studies. Soil Sci. Am. Proc. 39: 1024-1028.

Jury, W. A. and K. Roth, 1990. *Transfer Functions and Solute Transport Through Soil: Theory and Applications.* Birkhaeuser Publ. Basel. 235 p.

Kirkham, D. and W. Powers, 1972. *Advanced soil Physics*, John Wiley & Sons, 534 p.

Letey, J., C. Roberts, M Penberth, and C. Vasek. 1986. An agricultural dilemma: Drainage water and toxics disposal in the San Joaquin Valley. University of California, Division of Agriculture and Natural Resources. Special Publication: 3319.

Letey, J. and J.D. Oster. 1993. Subterranean disposal of irrigation drainage waters in Western San Joaquin Valley. In Proc. on Management of irrigation and drainage systems: Integrated perspectives, Ed. R.G. Allen. ASCE National Conference on irrigation and Drainage Eng, Park City, Utah.

Letey, J. 2000. Soil salinity poses challenges for sustainable agriculture and wildlife. Cal. Agr. 54(2): 43-48.

Letey, J., S. Grattan, J.D. Oster, and D.E. Birkle. 2001. Findings and recommendations to develop the six-year activity plan for the Department's drainage reduction and reuse program. Final Report, Task Order No.5 Contract #: 98-7200-B80933.

Rhoades, J.D. 1984. Use of saline water for irrigation. Cal. Agr. 38 (10): 42-43.

Rhoades, J.D., F.T. Bingham, J. Letey, A.R. Dedrick, M. Bean, G.J. Hoffman, W.J. Alves, R.V. Swain, P.G. Pacheco, and R.D. Lemert. 1988. Reuse of drainage water for irrigation: Results of Imperial Valley study. I. Hypothesis, experimental procedures, and cropping results. Hilgardia 56(5): 1-16.

San Joaquin Valley Drainage Program. 1990. A management plan for agricultural subsurface drainage and related problems in the Westside San Joaquin Valley, final report, Sacramento, California

PUBLICATIONS AND REPORTS

William A. Jury*, Atac Tuli, and John Letey, Effect of Travel Time on Management of a Sequential Reuse Drainage Operation. Soil Sci. Soc. Amer. J. (in review).

Table 1. Tile drain and management parameters estimated for the Red Rock Ranch sequential reuse demonstration facility. (Cervinka et al. 1999)

Parameter	Symbol	Value	Units
Irrigation water concentration	*Cirr*	0.6	dS/m
Ground water concentration	C_s	12	dS/m
Tile drain half spacing	*S*	60	m
Depth to tile	*H*	2.4	m
Drainage rate (stage 1)	R_1	22	cm/y
Leaching fraction (stage 1)	x_1	0.14	-
Drainage rate (beyond stage 1)	R_2	50	cm/y
Leaching fraction (beyond stage 1)	x_2	0.33	-

Table 2. Time in years for *P(t)*=0.25,0.50, and 0.75 of the water added at the surface to arrive at the drain for a system with *S*=100m, q_s= 0.45, and *R*=0.22 or 0.5 m/yr.

P(t)	R (m/y)	*h = 1.0*	*h =2.0*	*h =5.0*	*h =10.0*	*h =20.0*
0.25	0.22	7.1	6.9	5.4	3.6	2.2
0.50	0.22	31.2	28.1	15.9	8.7	4.7
0.75	0.22	110.6	83.1	35.1	17.7	9.1
0.25	0.50	3.1	3.0	2.4	1.6	1.0
0.50	0.50	13.7	12.4	7.0	3.8	2.1
0.75	0.50	48.7	36.6	15.4	7.8	4.0

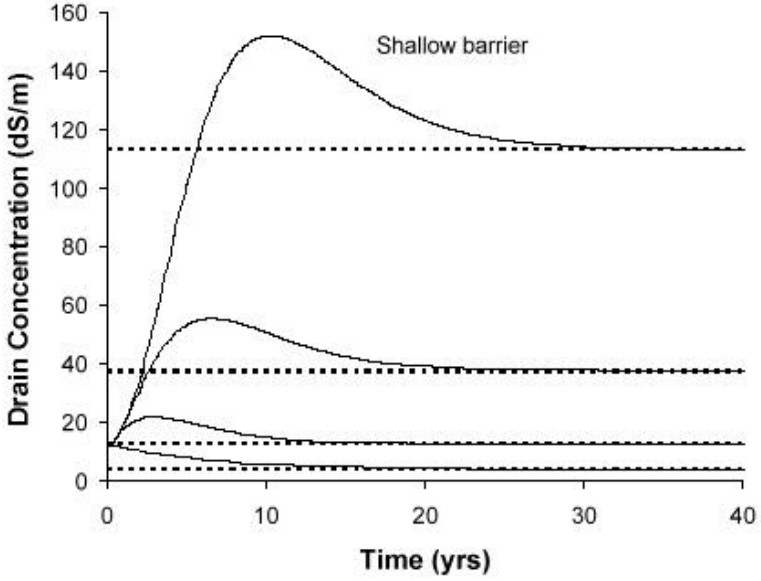

Figure 1. Water flow streamlines through the saturated zone of a tile line with η=S/D=1.

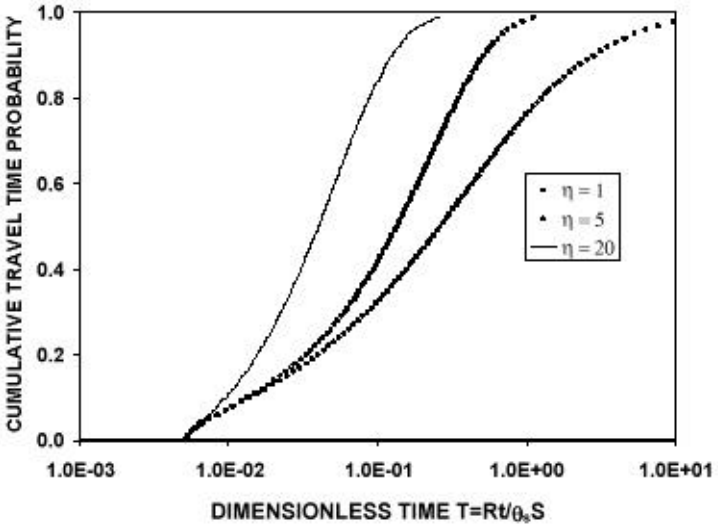

Figure 2. Dimensionless cumulative travel time probability density functions calculated for various ratios η = S/D.

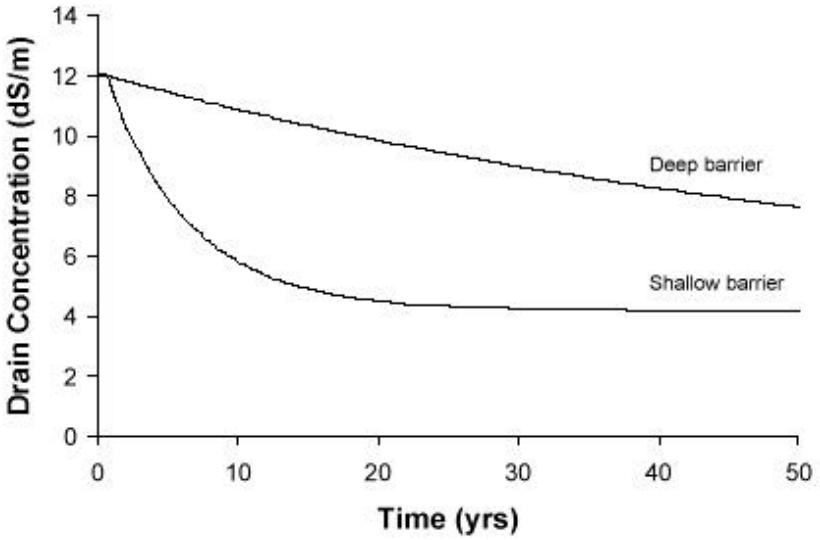

Figure 3. Response time and equilibration time of the first stage for the shallow and deep barrier cases.

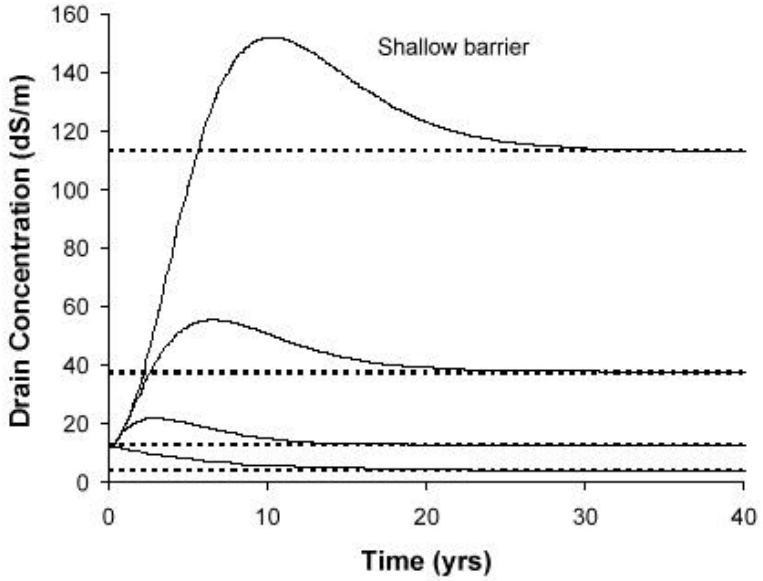

Figure 4. Drain concentrations from all four stages of a system overlying a shallow barrier, using parameters from the Red Rock ranch in Table 1. Dashed lines represent steady-state concentrations.

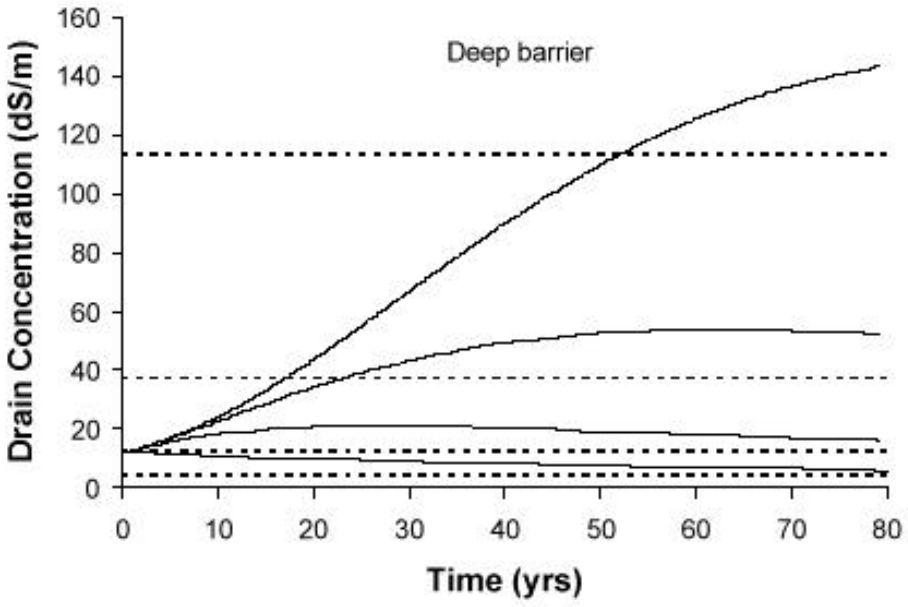

Figure 5. Drain concentrations from all four stages of a system overlying a deep barrier, using parameters from the Red Rock ranch in Table 1. Dashed lines represent steady-state concentrations.

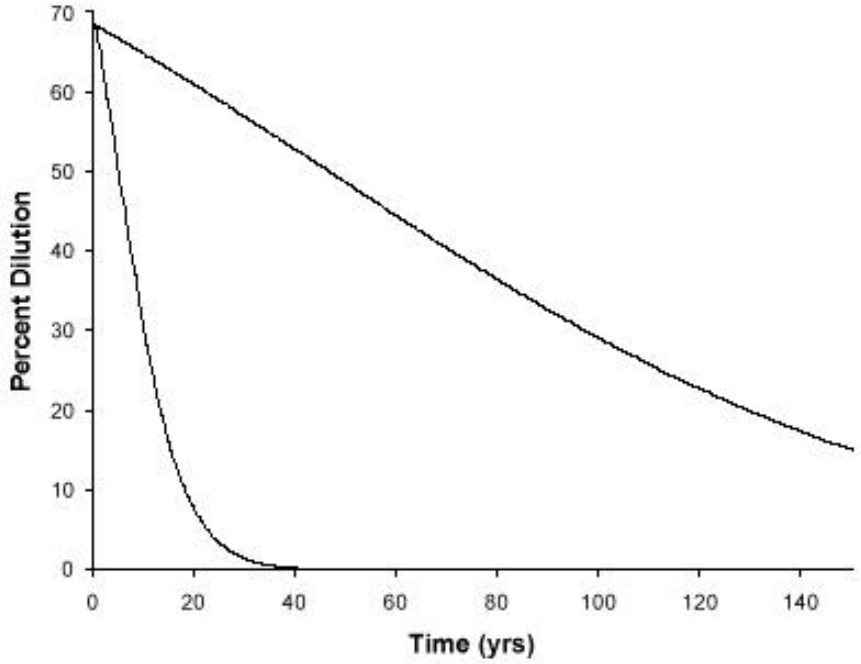

Figure 6. Percent dilution required to maintain the irrigation water of stage 2 at 5 dS/m or less, using parameters from the Red Rock ranch in Table 1. The predicted dilution using the steady-state model is zero.

Using Forages and Livestock to Manage Drainage Water in the San Joaquin Valley

Project Investigators:

S. R. Kaffka
Office: (530) 752-8108, E-mail: srkaffka@ucdavis.edu
Department of Agronomy and Range Science
University of California, Davis

J. D. Oster
E-mail: oster@mail.ucr.edu
Department of Environmental Science
University of California, Riverside

J. Maas
Office: (530) 752-3990, E-mail: jmaas@ucdavis.edu
School of Veterinary Medicine
University of California, Davis

D. L. Corwin
Office: (909) 369-4819, E-mail: dcorwin@ussl.ars.usda.gov
USDA-ARS George E. Brown, Jr. Salinity Lab
Riverside, California

ABSTRACT

Saline-sodic drainage water (4<EC(dS/m)<20; 10<SAR<40) is a potential resource for production of salt tolerant forages. Drainage water reuse also provides the means to concentrate salinity and reduce the volume of drainage water, the scale of effects on underlying soil strata and groundwater, and the direct disposal costs of the final effluent, whether in evaporation basins or by ocean disposal. To assess the productive potential and sustainability of using drainage water for forage production, Bermuda grass (*Cynodon dactylon* (L.) Pers.) was established in 2000 and 2001 on a salt-affected site (32.4-ha) with tile drainage in California's San Joaquin Valley. This site was characterized for initial soil quality and hydrologic properties. The salinity and volume of irrigation and drainage water, and forage biomass and quality have been monitored. Cattle were grazed in 2001 and rates of gain and trace element accumulation were monitored. Electromagnetic induction (EM) and Wenner Array techniques were used to characterize initial soil salinity. Using the EM data and a spatial statistics program (ESAP v2.0), forty sites were selected that encompassed the heterogeneity of the study area. At these sites, soil core samples were taken at 0.3-m intervals to a depth of 1.2 m for chemical and physical analysis. Variation in average soil chemical properties include: 12.8<EC_e < 36.6 dS m^{-1}; 28.8<SAR< 88.8, and 2.5< clay < 48.3%; 11.5< B<32.2 mg/L; 477<Mo<1960 ì g/LBased on the ratio of drainage volume to irrigation volume, the leaching fraction (LF) averaged 0.13 in late summer. Forage Mo contents determined from newly established Bermuda grass varied from 0.4 to 5.3 mg/kg DM and Cu: Mo ratios averaged 5.6. Forage yield declined with EC_e, and failed to grow above EC_e levels of 22 dS m^{-1}. Cattle gained approximately 0.5 kg d^{-1} and were Se and Cu deficient at the end of the grazing period.

KEYWORDS

Electrical conductivity, drainage water reuse, salinity, Mo, B, forage quality, Bermuda grass

■ ■ ■ ■ ■

INTRODUCTION

The productivity of an estimated 300,000 ha of land in the western San Joaquin Valley (WSJV) is adversely affected by the presence of shallow or perched water (0 to 1.5 m). Without a means of disposing of drainage water, increasing amounts of farmland in the WSJV will become salt impaired. If all lands with shallow water tables were drained, approximately 30,000 ha of land would be needed for evaporation ponds, an amount almost twenty times greater than that currently available. Regulations limit the expansion or development of new evaporation ponds. An alternative means of reducing drainage water volumes is reuse of drainage water on agricultural lands. Using drainage water to produce salt tolerant forages would reduce the volume of drainage water and the amount of land needed for its disposal by up to an order of magnitude (Oster, 1997), thereby lowering the cost of disposal and limiting the exposure of wildlife to potentially toxic waters in evaporation ponds. High quality forages for dairy cattle, beef cattle, and sheep are in short supply in the Central Valley of California. Salt-tolerant forages will increase forage supplies. Forage grasses like Bermuda grass will use more water than most tree species in the same locations because of greater salt tolerance, and have an obvious use for livestock. If the production of high quality forage using drainage water can be coupled economically to livestock enterprises, drainage water would become an asset rather than a problem. The use of forage-livestock systems, together with careful management of a small number of drainage ponds, will address the most serious problem affecting the long-term sustainability of farming in the WSJV, and provide additional benefits to areas throughout the world suffering similar problems. However, agricultural drainage water in the WSJV is sufficiently saline to be detrimental to most crops and often contains toxic trace elements, particularly Se, B, and Mo. Se is toxic to shore birds and migratory waterfowl when it concentrates in the food chain of evaporation ponds, which are productive artificial wetlands (Skorupa, 1998). B can reduce plant yields. Mo can cause harmful effects to ruminant animals. Barshad (1948) found that plants are able to absorb amounts of Mo harmful to cattle from soils that contain as little as 1.5-5.0 mg/kg total Mo. Accumulation of trace elements in soils and crops to toxic levels will result in failure of the system and the creation of a new pollution problem.

Maintenance of soil physical properties is another concern when reusing drainage water. As the level of sodicity increases, greater levels of salinity in irrigation water are required to prevent deterioration of water infiltration and redistribution,

and aeration. Irrigation with saline-sodic drainage water typically found in the WSJV (6<EC<20 dS m^{-1}; 5< SAR<35) will result in soil salinities ranging from 6 to 60 dS m^{-1} and SARs ranging from 5 to 60 if the leaching fraction (LF) is approximately 30%. Expected levels of salinity in the irrigation water should compensate for increased levels of exchangeable Na, which otherwise could impair infiltration rates, soil tilth, and reduce soil aeration (Oster and Jayawardane, 1998).

MATERIALS AND METHODS

SITE CHARACTERIZATION

Initial site characterization occurred in 1999. For this purpose, the site was irrigated in July and salinity mapping and soil sampling began in August. Electromagnetic induction (EM) and mobile fixed-arrays for measuring EC_a were used to characterize spatial distributions of soil salinity. EC_a was measured non-invasively with mobile EM equipment developed for this purpose and with a mobilized, tractor-mounted version of an invasive "fixed-array" unit (Rhoades et al., 1999). All measurements were geo-referenced with a global positioning system (GPS). Utilizing the EM data from the initial cursory survey and statistical software (ESAPv2.0) developed by Lesch et al. (1995), 5 sites within each paddock (40 total) were selected that characterize the spatial variability in EC_a across each paddock. At each of the 40 sites, two or more soil cores were taken at 0.3-m increments to a depth of 1.2 m. At each site, two sets of soil cores were taken. One set of soil cores was designated for soil chemical property analysis and the other set for soil physical property analysis. A total of 384 soil samples were taken. All spatial data was entered into a geographic information system (GIS). Maps of the soil physico-chemical properties were prepared by interpolating the measurements at the 40 sample sites using inverse-distance-weighting interpolation. Maps were prepared by interpolating the measurements at the 384 measurement sites.

DRAINAGE WATER VOLUME, COMPOSTION, AND LEACHING

A v-notch weir, instrumented with pressure transducers to measure the water elevation on the up-flow side of the weir, was installed on the center drains of paddocks 2, 3, 6, and 7. There are eight paddocks in all (Kaffka et al., 2001). This weir is installed in a 1.2-m diameter culvert located on the east end of the center drains. Details of the design, construction and calibration of the weirs can be found in Schoeneman and Ayars (1999) and in Kaffka et al. (2002). Data loggers (CR510, Campbell Scientific, Inc) were installed to record the height of water discharging over the weir and the electrical conductivity of the drainage water. The height of the water flowing across the v-notch is monitored with two calibrated pressure transducers (Honeywell Pressure Sensor, 162PC01D). The salinity of the drainage water was measured using a combined conductivity and temperature probe (CS547, Campbell Scientific, Inc) mounted about 15 cm above the bottom of the manhole on the up-flow side of the v-notch. Due to the limitations of the CR510 recorder, only conductivity was recorded. The temperature of the drainage water (22 $\pm$ 1ºC) was determined several times during the summer of 2000 during times when water was flowing across the v-notch. Recorded EC values were multiplied by 1.06 to adjust values to 25ºC (Table 15, U.S. Salinity Laboratory Staff, 1954). With the data obtained with these instruments it is possible to calculate the volume-weighted salt load in the drainage water. The amount of irrigation water applied was measured using a calibrated Sparling meter in 2000. In 2001 a digital flow meter with continuous recording capability for irrigation water volume was installed.

BERMUDA GRASS ESTABLISHMENT AND SAMPLING

Bermuda grass (*Cynodon dactylon (L>) Pers.*) was established after site assessment during late fall in 1999 and summer of 2000. Cultivar *Giant* was planted in plots 1 to 4 to allow both grazing and hay making, while cv. *Common* was planted in plots 5 to 8, for grazing purposes only. Systematic sampling of plots 1 to 4 began in late September of 2000, and of all eight plots in June 2001. Forage was sampled at locations selected initially for soil sampling. Subsequently, another 32 locations were chosen using ESAP software for a total of 72 sample locations. Plant material was collected from two 0.3 m by 1 m grids at each location, placed opposite each other approximately 1 m from the soil sample point. Soil sample points were located using a Trimble GPS system with an accuracy of less than 1 m. At each sampling, forage was collected at a new compass direction, to avoid re-sampling the same site. Sampling in this manner provides an estimate of standing biomass. While sampling, forage height before and after harvest was measured.

Additional samples were collected to study the relationship between soil Mo and forage Mo from locations outside the sampling grid used for the majority of samples collected. Soil samples to 25 cm were collected from within the forage sample area. Three soil samples were combined. Forage samples were dried in a forced air dryer at 35° C. After drying, forages were ground and sub-sampled for quality analysis. Forages were analyzed for total N, crude protein, ash, ADF and NDF, total P, K, S, Ca, Mg, Na, B, Zn, Mn, Fe, Cu, Mo, Se, and Cl.

LIVESTOCK PRODUCTION AND HEALTH

The cattle used were recently weaned Angus cross steers. The cattle were vaccinated with modified live vaccine for Interstitial Bovine Rhinotracheitis, bovine viral diarrhea, Parainfluenza Virus, and Respiratory Syncitial Virus. They were also vaccinated with an eight-way clostridial vaccine. Any animals observed with clinical signs of pneumonia were promptly treated, and any deceased animals were necropsied by the California Animal Health and Food Safety Laboratory System (CAHFS) – Tulare. The cattle were randomly assigned to control and test pasture groups. There were ten steers in the control group and twenty-two steers in the experimental pasture group. The control group was grazed on a Bermuda grass pasture irrigated with fresh water from the Kings River. The test pasture group was grazed at another location on a Bermuda grass pasture irrigated with saline drainage water. Baseline liver, serum, whole blood, and weight samples were taken on day 0 before the animals were allowed to graze on their respective pastures and on day 142 when the animals were removed from their pastures. The steers average daily gain (ADG), liver heavy metals, serum trace minerals, and selenium level changes from day 0 to day 142 were evaluated.

Liver Biopsy Procedure – On day 0 and day 142 blood and liver samples were taken for evaluation. Whole blood samples were analyzed for selenium levels, and serum samples were evaluated for trace minerals (calcium, copper, iron, magnesium, phosphorous, potassium, sodium, and zinc). All samples were analyzed by CAHFS – Davis. The liver samples were analyzed for heavy metals (arsenic, cadmium, iron, copper, mercury, manganese, molybdenum, lead, and zinc).

RESULTS AND DISCUSSION

SOIL SALINITY, OTHER PHYSICO-CHEMICAL PROPERTIES

The study area is a severely saline-sodic, gypsiferous soil that is heavy textured at the surface (0-0.3 m) and has low to very high levels of B and moderate to high levels of Mo (Table 1). In general soil salinity increases with depth with inverted conditions occurring only in two small areas (fig. 1). Water content (either PW or θ_v) also increases with depth (Table 1). Bulk density is the lowest in the top depth increment (0-0.3 m) with an average value of 1.29 Mg/m^3, and then becomes stable for the remaining depths reaching 1.51 Mg/m^3. pH_e typically averages around 7.5-7.6 for all depths and usually falls within the range of 7-8. Saturation percentage (SP) ranges from less than 40% to over 90% with the greatest range occurring at the bottom depth (0.9-1.2 m). The levels of Se and As are low with Se never exceeding 77 ìg/L and As never exceeding 116 ìg/L at any depth increment. SAR tends to be associated with EC_e and, like EC_e, tends to increase with depth (Table 1). The association between salinity (EC_e) and the soil chemical properties of Cl^-, SAR, and ESP is reflected by the Pearson correlation coefficients determined for EC_e and Cl^- ($r = 0.76$), EC_e and SAR ($r = 0.95$), and EC_e and ESP ($r = 0.54$) using values for composite soil cores over the depth of 0-1.2 m. CEC correlates well with SP ($r = 0.60$) indicating the influence that clay content has on the properties of CEC and SP. The Pearson correlation coefficient between Mo and B using values for composite soil cores over the depth of 0-1.2 m is $r = 0.59$. In the top depth increment (i.e., 0-0.3 m), Mo and B are positively correlated with salinity with r^2 values of 0.60 and 0.72, respectively. Consequently locations with high salinity may also be locations with forages high in these trace elements. In general the % clay tends to decrease with depth with an average value of 35.9 % in the 0-0.3 m depth increment decreasing to 23.3% in the 0.9-1.2 m depth increment. The higher clay content at the surface will enhance the formation of surface cracks, which will likely serve as conduits for water flow before the clay swells and closes the cracks. The averages of % sand, % silt, and % clay for the top 0-1.2 m are 38.6%, 32.4%, and 29.0%, respectively, making the soil a clay loam. The % sand tends to increase with depth with values of 31.3%, 38.5%, 42.5%, and 42.2% for the respective depths of 0-0.3, 0.3-0.6, 0.6-0.9, and 0.9-

1.2 m. The increase in the sand fraction with depth should be conducive to drainage.

DRAINAGE WATER VOLUME AND INITIAL WATER COMPOSITION

Crop water use will determine the land requirement and the economic feasibility of sequential reuse. When soil salinity exceeds the crop species' threshold salinity, as anticipated when irrigating with saline-sodic drainage waters, crop growth and water use will decline. This will directly affect the area of land and amount of water required for leaching. Leaching is important to the sustainable reuse of drainage water. Some leaching appears to have occurred at the site historically, since salinity, Cl, and SAR increase with depth (Table 1).

Table 2 summarizes irrigation and drainage water quality data obtained in 2001. The data in Table 2 were calculated from logged drainage volumes and electrical conductivities as well as logged irrigation volumes and electrical conductivities. The logged data consists of 5-minute averages measured every half-hour. The year 2001 was the second year of developing the site and learning how to obtain and manage saline-sodic drainage water. Because of a drastic reduction in cropped area in 2001, saline-sodic water in the nearest evaporation pond (20 <EC(dS/m) <30) had to be pumped back into the drainage canal system and mixed with non-saline Kings River water (EC = 0.5 dS/m) to obtain the EC_{iw} values given in Table 2. Consequently the salinity of the applied water was lower than the desired 5 – 9 dS/m, and varied between irrigations and among paddocks.

Both drainage volume and LF increased during the season (Table 2), particularly for Paddock 3. At the start of the irrigation season the water table was lower than the tile drains. It took several irrigations to establish a water table that was higher than the drains. Concurrent with the establishment of a higher water table, the EC of the drainage water increased, which is most evident in Paddocks 3 and 7; and LF also increased. The measured leaching fractions averaged 0.13 for Paddocks 6 and 7 during the last two irrigations that occurred during September. This number likely represents the leaching fraction that occurred during the establishment of the water table – the excess water passing through the root zone was the only source of water to raise the water table because there were no irrigated fields within about 1 km of the field.

BERMUDA GRASS ESTABLISHMENT AND YIELD

Bermuda grass is a halophytic, C4 species with a large degree of salt tolerance. Large amounts of forage biomass accumulated on the site because grazing pressure in the first year was very slight. Cattle were used in 2001 only for livestock health determinations. Figure 2 reports standing forage biomass on a dry matter basis for sampling events throughout the 2001 growing season. On most of the site, Bermuda grass tolerated soil and irrigation water conditions and grew vigorously, but above approximately 22 dS m^{-1}, little to no Bermuda grass was able to grow (Kaffka et al., 2002). This response matched estimates of salinity tolerance reported by Ayers and Westcott (1985).

Forage quality was analyzed for a subset of samples collected in 2000 and 2001, reflecting the range of growing conditions and times of year observed. Averages, standard deviations and other statistics for selected Bermuda grass samples collected in 2000 and 2001 are reported in Table 3. Mean forage quality values are similar to others commonly used for average estimates but the range in quality is large. Few data have been reported on trace element composition in Bermuda grass, so comparisons cannot be made with literature values.

Crude protein levels, ADF, K, P, Ca, and Mg levels all are close to standard values used in ratio formulation tables, in the absence of specific forage analyses (National Research Council, 1989). Ash contents are higher on average than those considered typical. At the highest ash levels found in these samples (>20%), some soil contamination likely occurred. Large amounts of soil Mo and B are found at this site. But average forage Mo levels were not particularly high, likely because Bermuda grass did not grow in locations with the largest amount of soil Mo (fig. 3). Reports of grass species Mo concentrations often cite 1 to 4 mg/kg as commonly observed values (Vlek and Lindsey, 1977; Albasel and Pratt, 1989; McBride et al., 2001; O'Connor et al., 2001). Mo may be toxic to cattle if consumed in large amounts, primarily by interfering with Cu metabolism (Suttle, 1991). Some samples were high in Mo, but on average, Mo concentrations reported are not excessive, especially in comparison to concentrations reported as typical for legumes like alfalfa and clover, which is usually 2 to 4 times as enriched as

grass species growing under similar conditions (O'Connor et al., 2001). The ratio of forage Cu to forage Mo (5.6:1) in these samples is above the ratio often cited for concern (2:1), but Suttle (1991) has proposed that the critical ratio declines as forage Mo increases. Cu levels of less than 5 mg/kg in the presence of soil Mo has been cited as of concern (Johansen, et al., 1997). Average Cu levels are approximately 8 mg/kg in these samples (Table 3). Most of the recent concern for Mo toxicosis is associated with Mo uptake by forages from soils amended with sewage sludge (O'Connor et al., 2001; McBride et al., 2001). There are fewer studies discussing the uptake of Mo by forages from soils naturally abundant in Mo (Vlek and Lindsey, 1977), so the ability to make comparisons is limited. In many instances, concern over the effects of Mo in forages is influenced by the concentrations of other elements like S (Suttle, 1991). Few feeding studies and fewer actual grazing studies under such conditions have been reported, so further work on livestock performance and health on these pastures will be of interest. Livestock are selective in their consumption of forages, so samples and analyses obtained in this way are only approximations of the forage actually consumed by cattle.

LIVESTOCK PERFORMANCE

Average Daily Gain

Average daily gain (ADG) was calculated for both the control and test group animals. The average daily gain of the control animals was 1.24 +/- 0.19 pounds per day, and the ADG of the test group was 1.11 +/- 0.23 pounds per day. There was no significant difference in weight gain between control and test group animals.

Liver Biopsy and Blood Sample Results

On day 143 steers in both groups were sampled and selenium, trace mineral, and heavy metal levels were compared. The blood selenium levels of both the control and pasture cattle significantly decreased from the beginning to the end of the trial period. There was no significant difference in selenium levels among control and experimental cattle at any testing date (fig. 4). Liver copper levels decreased from day 0 to day 143 in both the control and test pasture groups, but no significant difference between the tests groups existed (fig. 4). Both groups of cattle had liver copper levels in the deficient range by the end of the trial period. Liver zinc levels remained fairly constant and in the normal range in both groups throughout the experiment and there was no significant difference between the test and control group on any testing date. Liver manganese levels increased, but stayed within normal limits in both groups of steers. There was no significant difference between the test pasture and control animal manganese levels. Liver iron levels also increased in both the control and pasture groups during the trial period. However, iron levels for all animals remained within acceptable limits. There was also no significant difference between control and test group liver iron levels. Liver levels of arsenic, cadmium, lead, mercury, and molybdenum remained relatively constant or were slightly decreased during the experimental period, and were all within acceptable levels. There was no significant difference between the control and test groups in any of these trace minerals and heavy metals. The serum copper levels decreased during the experimental period in both the test and control pasture groups. Steers in both groups became very deficient in serum copper levels. There was no significant difference between the test and control group serum copper levels at either testing date. The serum zinc levels decreased in both pasture groups such that 11 of the animals had below normal serum zinc levels. There was no significant difference between the test and control group serum zinc levels. Changes in serum calcium, iron, magnesium, potassium, phosphorous, and sodium were unremarkable, and there was no significant difference in levels in control and test pasture levels.

SUMMARY AND CONCLUSIONS

Sustainability of a cropping system implies that, among other attributes, soil physical properties must be maintained or improved over time. The initial assessment of soil quality and future spatio-temporal changes in soil physico-chemical properties are the basis for evaluating the sustainability of drainage water reuse in the WSJV. At the research site, water flow and the influence of dispersion on infiltration due to Na^+ accumulation are the most crucial soil-related factors affecting the sustainability of drainage water reuse. Due to their elevated levels, temporal changes in salinity, SAR, B, and Mo levels are long-term chemical concerns. The sustainability of drainage water reuse depends on

maintaining a LF that prevents the accumulation of excessive salinity, B, and Mo to prevent the occurrence of toxic effects upon forage and grazing livestock, and yet low enough to meet the objective of minimizing drainage volumes and the dissolution of additional salts and minerals. Even though the soil at the research site has high SAR values with low measured saturated hydraulic conductivities, there are mitigating factors that make adequate leaching achievable: (1) the reused drainage water is high in salinity, (2) water flow through surface cracks is a common infiltration pathway of WSJV soils, (3) the presence of an efficient drainage system, and (4) a dense forage cover over most of the site. The establishment of a research site in the WSJV, coupled with forage and livestock management, provides an unusual opportunity to evaluate the sustainability of a drainage water reuse system at field scale, including its economic consequences for farms.

■ ■ ■ ■ ■

REFERENCES

Albasel, N., and P. F. Pratt. 1989. Guidelines for molybdenum in irrigation waters. J. Environ. Qual. 18:259-264.

Ayers, R. S., and D. W. Westcott. 1985. Water Quality for Agriculture. FAO Irrigation and Drainage Paper 29 Rev. 1. Food and Agriculture Organization of the United Nations. Rome.

Barshad, I. 1948. Molybdenum content of pasture plants: I. Nature of soil molybdenum, growth of plants, and soil pH. Soil Sci. 71:297-313.

Kaffka, S. R., D. L. Corwin, J. D. Oster, J. Hopmans, Y. Mori, C. van Kessel, and J. W. van Groenigen. (2001). Using forages and livestock to manage drainage water in the San Joaquin Valley: Initial site assessment. Kearney Foundation Report. Univ. of California, Berkely, CA.

Lesch, S. M., D. J. Strauss, and J. D. Rhoades. 1995. Spatial prediction of soil salinity using electromagnetic induction techniques: 2. An efficient spatial sampling algorithm suitable for multiple linear regression model identification and estimation. Water Resour. Res. 31:387-398.

McBride, M. B., B. K. Richards, T. Steenhuis, and G. Spiers. 2000. Molybdenum uptake by forage crops grown on sewage sludge-amended soils in the field and greenhouse. J. Environ. Qual. 29:848-854.

O'Connor, G.A., R. B. Brobst, R. L. Chaney, R. L. Kincaid, L. E. McDowell, G. Pierzynski, A. Rubin, and G. G. van Riper. 2001. A modified risk assessment to establish molybdenum standards for land application of biosolids. J. Environ. Qual. 30:1490-1507.

Oster, J. D. 1997. Impact of alternative crops on salt disposal strategies. *In* Proc. Calif. Plant and Soil Conference, Visalia, California.

Oster, J. D., and N. S. Jayawardane. 1998. Agricultural management of sodic soils, Ch. 8. *In* M.E. Sumner and R. Naidu (eds.). Sodic Soils: Distribution, Processes, Management and Environmental Consequences. Oxford University Press, New York.

Rhoades, J. D., D. L. Corwin, and S. M. Lesch. 1999. Geospatial measurements of soil electrical conductivity to assess soil salinity and diffuse salt loading from irrigation. p. 197-215. *In* D. L. Corwin, K. Loague, and T. R. Ellsworth (eds.) Assessment of Non-Point Source Pollution in the Vadose Zone, AGU Geophysical Monograph 108, American Geophysical Union, Washington, D.C.

Skorupa, J. P. 1998. Selenium poisoning of fish and wildlife in nature: lessons from twelve real-world experiences. p. 315-354. *In* W. T. Frankenberger and R. A. Engberg (eds.) Environmental Chemistry of Selenium. Marcel Dekker, Inc., New York.

Suttle, N. F. 1991. The interactions between copper, molybdenum, and sulphur in ruminant nutrition. Ann. Rev. Nutr. 4:121-140.

U.S.D.A. 1986. Soil Survey of Kings County, CA. Sheet No. 7. Page. 43.

Vlek, P. L. G., and W. E. Lindsey. 1977. Molybdenum contamination in Colorado soils. p 619-650. *In* W. R. Chappel and K. K. Peterson (eds.) Molybdenum in the Environment. Vol. 2. Marcel Dekker, New York.

Table 1: Mean and range statistics four depth intervals between 0 and 1.2 m.

Variable	Means				Coefficient of Variation			
	0.0-0.3 m	0.3 – 0.6 m	0.6 - 0.9 m	0.9 – 1.2 m	0.0-0.3 m	0.3 – 0.6 m	0.6 - 0.9 m	0.9 – 1.2 m
PW (%)	20.8	26.3	27.0	30.6	18	15	20	24
Vol. H_2O (cm^3/cm^3)	0.30	0.40	0.40	0.43	20	12	12	11
ρ_b (g/cm^3)	1.29	1.51	1.52	1.51	8	6	8	11
% Clay	35.9	30.4	26.2	23.3	19.1	16.0	25.9	26.9
EC_e (dS/m)	13.0	20.2	22.5	25.2	58	26	29	31
pH_e	7.61	7.58	7.63	7.57	3	3	2	3
SP (%)	58.8	63.0	59.1	58.7	13	16	19	22
Anions in saturation extract (mmolc/L):								
HCO_3^-	5.25	2.67	2.62	3.06	38	27	45	49
Cl^-	21.8	35.3	47.1	58.7	70	41	46	51
NO_3^{--}	0.70	0.89	0.65	0.32	195	165	125	63
SO_4^{--}	150	240	259	292	72	32	35	39
Cations in saturation extract (mmolc/L):								
Na^+	137	237	270	312	80	33	36	40
K^+	0.90	1.03	1.04	1.06	62	40	41	44
Ca^{++}	23.9	22.1	22.1	22.3	9	11	10	9
Mg^{++}	18.6	20.4	19.1	22.3	94	60	41	47
Exchangeable cations (mmolc/100 g):								
Na^+	5.88	7.90	7.88	8.77	47	25	30	36
K^+	1.09	0.67	0.47	0.41	21	32	48	52
Ca^{++}	8.58	5.96	4.55	4.25	51	70	81	83
Mg^{++}	6.27	4.94	4.32	4.64	20	19	26	32
SAR	28.2	51.4	59.0	64.9	59	25	28	30
ESP (%)	28.4	41.6	47.5	51.8	52	23	28	39
B (ppm)	17.0	19.0	17.5	17.9	48	30	27	35
Se (ppb)	8.75	14.04	12.90	14.15	145	61	72	99
As (ppb)	8.19	8.83	12.94	4.42	151	150	181	183
Mo (ppb)	862	750	781	947	62	57	43	48
CEC (mmolc/100 g)	21.7	19.5	17.0	17.5	18	26	29	27
$CaCO_3$ (%)	1.08	1.04	1.14	1.27	75	103	110	115
Gypsum (%)	3.41	5.37	6.63	6.41	51	60	60	72

Table 2. Irrigation and drainage water summary including leaching fraction (LF) for 2001. EC represents electrical conductivity, and the subscripts iw and dw represent irrigation water and drainage water, respectively.

Date	Irrigation	Drainage	EC iw	EC dw	LF
	mm		dS/m		
			Drain 6, Paddock 3		
18-Jul	158.0	0.013	0.39	8.7	< 0.001
2-Aug	98.8	0.960	3.11	14.4	0.010
24-Aug	142.0	0.610	3.45	11.5	0.004
14-Sep	129.8	2.057	1.69	16.2	0.016
28-Sep	77.0	4.877	3.39	31.3	0.063
			Drain 12, Paddock 6		
18-Jul	151.6	2.7	0.4	36.0	0.018
3-Aug	126.0	15.7	2.8	35.8	0.124
22-Aug	181.6	15.9	2.2	42.1	0.087
12-Sep	127.3	12.5	1.4	42.4	0.098
26-Sep	96.5	11.3	3.8	39.4	0.117
			Drain 14, Paddock 7		
19-Jul	177.0	1.5	0.6	22.6	0.008
2-Aug	132.1	13.7	4.0	31.6	0.104
21-Aug	181.6	23.8	4.1	37.1	0.131
12-Sep	120.1	15.3	1.3	35.6	0.127
26-Sep	95.8	16.0	3.3	37.2	0.167

Table 3. Forage quality and mineral contents from selected Bermuda grass harvests in 2000 and 2001.

Variable	Mean	Minimum	Maximum	Range	SD	Pr<W**
CP (%)*	13.4	6.2	22.1	16.0	4.12	0.0001
Ash (%)	13.4	8.3	24.1	15.8	2.98	0.0001
ADF (%)	29.8	22.1	40.8	18.7	3.11	0.2747
P (%)	0.195	0.115	0.34	0.225	0.042	0.0052
K (%)	1.83	0.99	3.41	2.42	0.44	0.0218
S (mg/kg)	6854	3780	9637	5857	1166	0.3707
Ca (%)	0.49	0.32	0.77	0.455	0.094	0.0013
Mg (%)	0.227	0.125	0.56	0.435	0.067	0.0001
Na (mg/kg)	6194	680	23920	23240	3418	0.0001
B (mg/kg)	217	73	1004	941	142	0.0001
Cl (%)	0.81	0.36	3.31	2.95	0.38	0.0001
Zn (mg/kg)	29.6	14	58	44	9.6	0.0006
Mn (mg/kg)	91.2	46	219	173	27.1	0.0001
Fe (mg/kg)	582.9	150	4714	4565	603	0.0001
Cu (mg/kg)	7.92	4.0	13.7	9.7	1.63	0.0148
Mo (mg/kg)	1.95	0.4	5.3	4.9	0.96	0.0001
Se (µg/kg)	84.9	16.0	328	312	47.3	0.0001

* % of dry matter. Shapiro-Wilk probability level for test for normality. Values < 0.05 indicate non-normality. N = 135 samples.

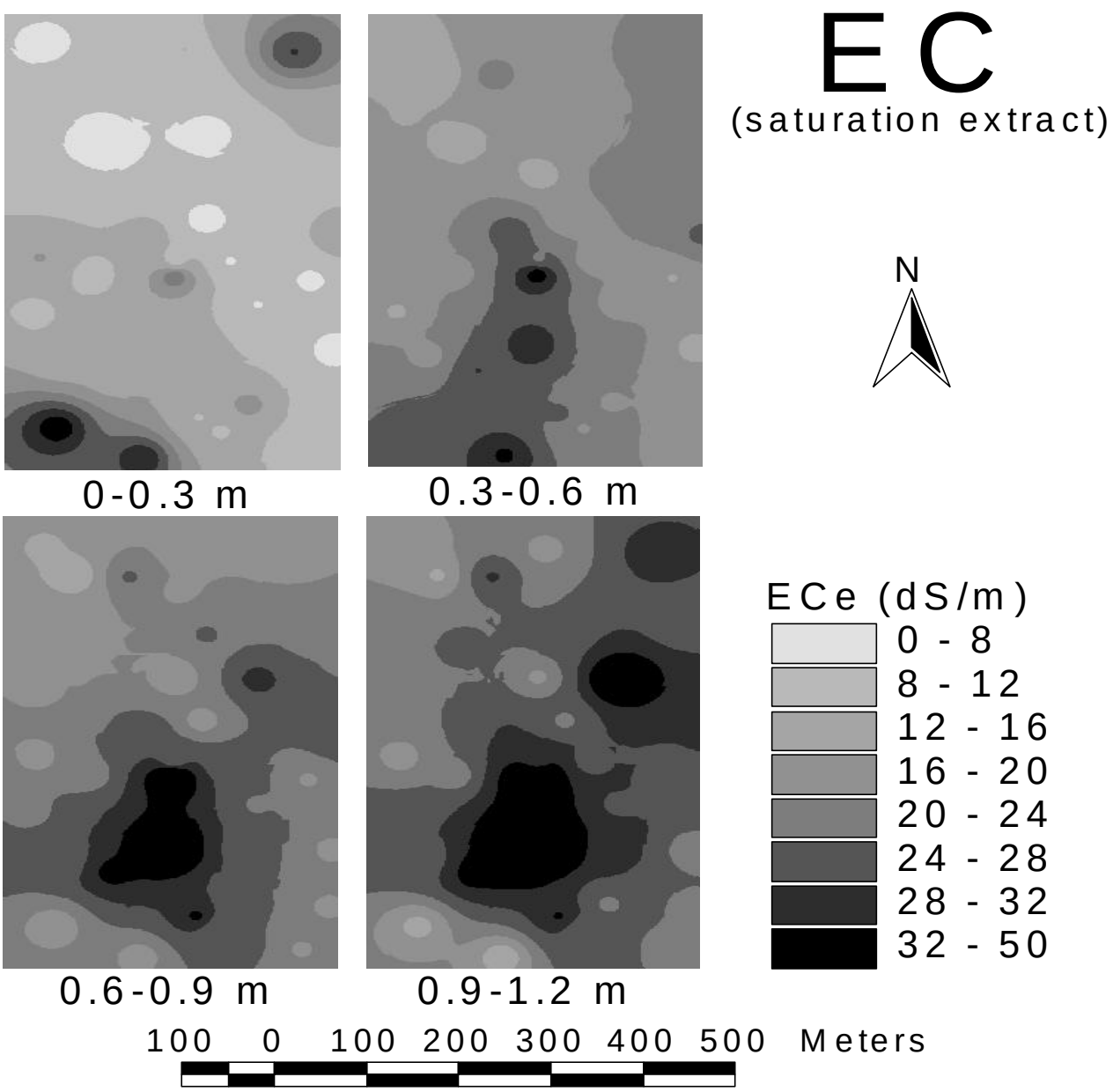

Figure 1. Maps of inverse-distance-weighting interpolations of ECe (dS/m).

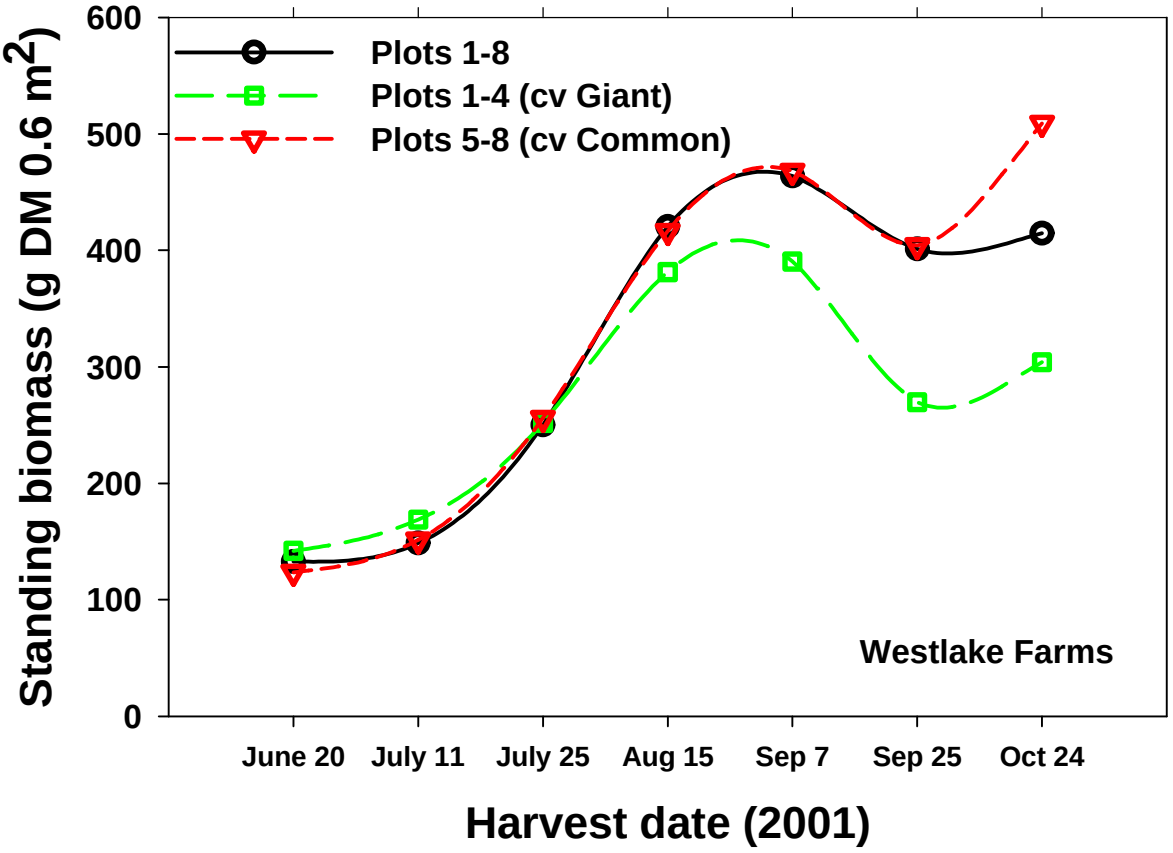

Figure 2. Standing forage biomass at successive harvests in 2001(g DM/0.6 m²).

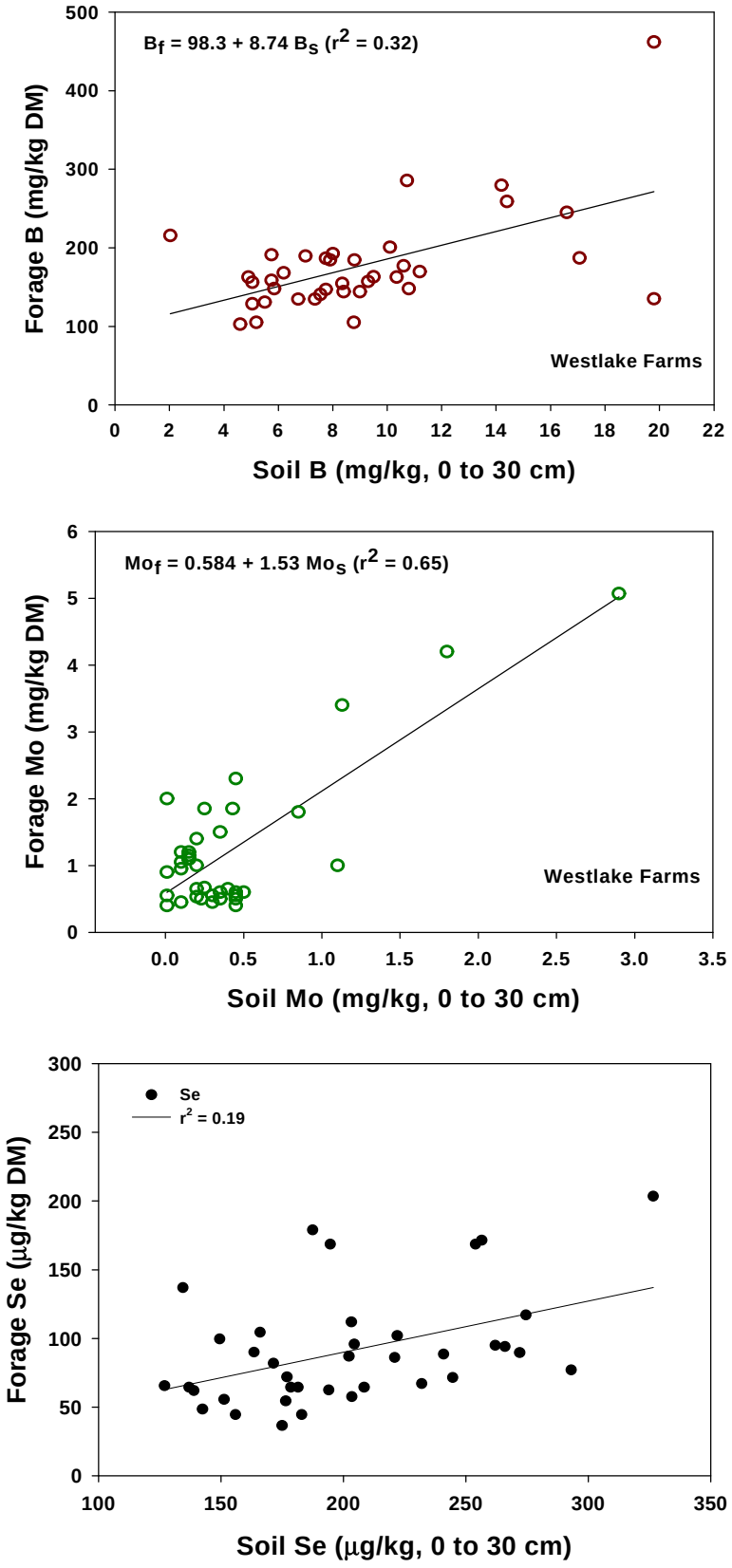

Figure 3. Correlations between forage and soil Mo, B, and Se

Liver Cu Levels

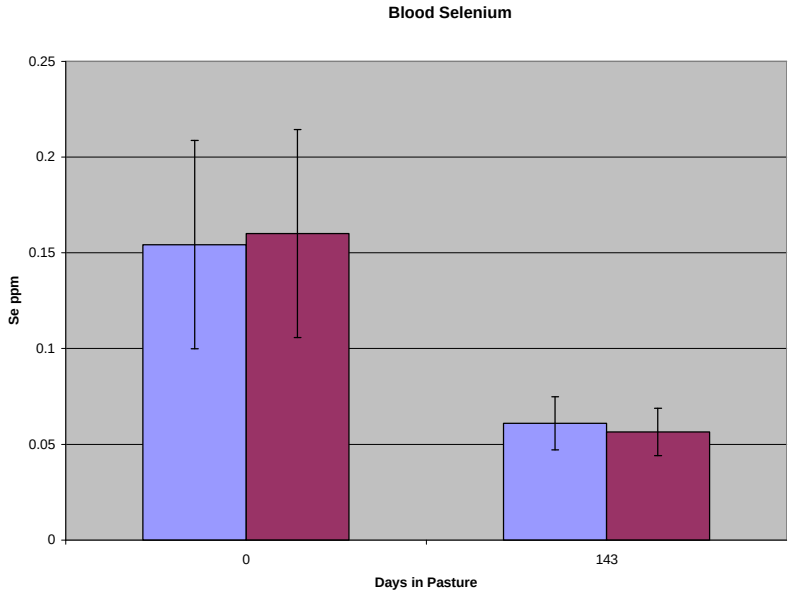

Days on Pasture

Blood Se

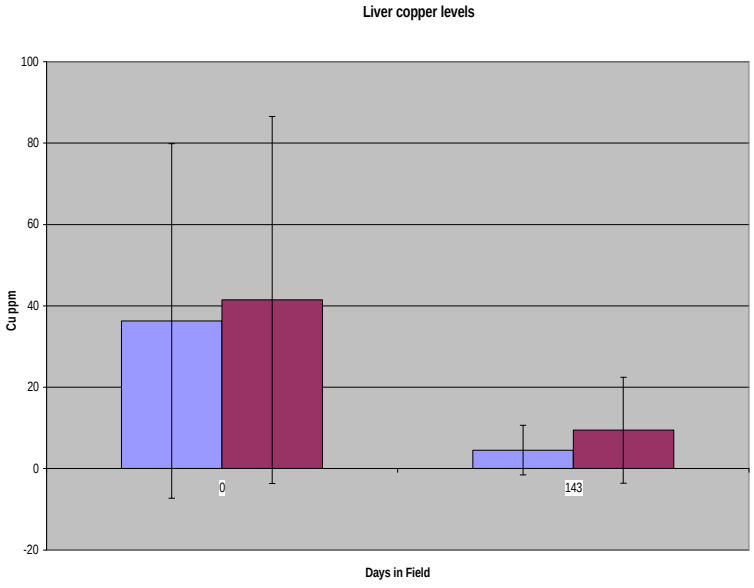

Days on Pasture

Figure 4. Cattle blood Se levels, Cattle liver Cu levels.

Contrasting Irrigation Application Methods for Drainage Reduction and Soil Salinity Management

Project Investigator:

Daniel Munk
Office: (559) 456-7561, E-mail: dsmunk@ucdavis.edu
UC Cooperative Extension–Fresno County

Project Cooperator:

John Diener, Red Rock Ranch, Five Points, CA

Research Staff:

0.20 FTE - Lab Assistant III

ABSTRACT

Sprinkler lines were used and contrasted with conventional furrow irrigation methods in ground having historically high surface salinity levels and relatively shallow groundwater levels. The objective in the first year of evaluation was to evaluate a single years activity in which an alternative irrigation practice might give rise to improved soil salinity levels and increase the likelihood that improved plant stands and plant growth would lead to improved crop performance and yield. The treatments included a single block of a large irrigated cotton field in western Fresno County where high quality sprinkler irrigation water was used in contrast to the tradition use of furrow irrigation. Late-season soil salinity levels were contrasted following the completion of the irrigation season and we found large differences in soil salinity levels of the two contrasting treatments. We also found large differences in soil salinity levels for areas of the field having vigorous versus low vigor growth in the furrow-irrigated system. Results of the first year of activity suggest that there were some yield improvements following a single season use of sprinklers with high quality water. We monitored plant growth and vigor as well as plant emergence difficulties resulting from poor soil quality and the direct result of high soluble salt levels in the top 30 cm of the soil surface. Following our end-of-season soil salinity monitoring, we concluded that it is highly probable that plant stands and plant vigor would be significantly improved during year two as pre-plant irrigation water might further improve surface soil quality and benefit crop performance. Large reductions in salinity for the soil surface can not only translate into improved plant stands during a very crucial period, but can also result in much higher yields as salt tolerance increases following the seedling stages.

KEYWORDS

Irrigation, sprinkler, furrow, drainwater reuse, cotton, shallow groundwater, soil salinity

■ ■ ■ ■ ■

INTRODUCTION

Drainage problems continue to afflict large areas of the most productive agricultural region worldwide resulting in billions of dollars worth of lost income annually. The lack of adequate drainage in this irrigated agricultural region has resulted in the accumulation of soil salts in or near the soil surface with few opportunities for soil amelioration. This situation produces management challenges to the producer that is trying to maintain profitability in a few select crops who have demonstrated good characteristics of salt tolerance or salt avoidance. Crops such as cotton and sugar beets are grown in large acreage in the area and are good examples of those crops exhibiting salt tolerance, while crops such as lettuce and onions can fit in these systems and avoid the salinity buildup using salt avoidance mechanisms. The shallow root systems of lettuce and tomatoes can sometimes be exploited and if surface salinity levels are maintained at low levels, high subsurface salinity may exist without detracting from yield.

Salt tolerant crops can also experience many of the same problems that salt sensitive crop do when salinity levels rise to relatively high levels. One of the first indicators that surface salinity problems are manifesting is in the erratic emergence of seedlings planted. The germinating seed and the seedling stage are the most sensitive time of a plant's development, and it is often this stage that struggles most as surface soil salt levels rise. Many times it can occur that when surface salinity levels can be managed, the yield reductions associated with soil salts can be minimized. It has been suggested, but seldom practiced, to improve the management of fields having poor drainage by modifying the timing, volume and approach of applied water during the season to improve the distribution of the large salt load present in or near the surface soil. Though the total salt load my change little, it is often considered helpful to reduce the incidence of poor early germination performance.

To accomplish this task we created a project that would help develop information related to the impact of in-season sprinkler irrigation on the distribution of soil surface salts and compare these patterns with those of the conventional practice of furrow irrigation in large-scale agricultural fields having poor drainage. The approach considered in this project was to make soil and plant observations in the field prior to and following the changes in irrigation practices that would ultimately lead to improved short and long term practices when compared with the existing irrigation systems management approach.

METHODS

A field site was selected in western Fresno County that contained significant drainage problems characteristic of many locations of the area. The production field evaluated had a shallow water table level that varied from 1.2 to 2.5 meters depending on the time of season and location in the field. The shallowest observations in the field came during the spring months from areas near the north end of the field that corresponded with the field's lowest point. Irrigation water in this field runs south to north and is located immediately adjacent (east) to a large study on integrated farm drainage management of the Red Rock Ranch, Five Points, California. Typical practices were used for the pre-irrigation activities that precede cotton planting in the area and the field was treated uniformly with respect to the pre-irrigation event.

Beginning in late May in-season irrigation events were varied in two areas of the field in which one block was irrigated using sprinklers of conventional spacing (40 feet) and the remainder of the field was irrigated using furrow methods. Irrigation water quality of the sprinkler-irrigated water was typical of the quality delivered by the CVP project and ranged from approximately 380 ppm to 450 ppm. Irrigation water quality of the furrow-irrigated system varied more widely between 400 and 1350 ppm. Irrigation water pH ranged from 7.5 for CVP project waters to 8.4 for the blended waters having both CVP and drainage water combined. The total application of sprinkler water during the production season was 13.0 acre-inches per acre for six application events while the furrow-irrigated areas received 27.5 acre-inches per acre of applied water with 7 events. Irrigation was initiated on May 19th and concluded on September 7th.

During the month of July, we established areas of the field that had significant problems with emergence and mapped the zones of poor plant stand in the field in an effort to identify areas that had difficulties with stand establishment. Plant growth and development data were collected at key developmental stages throughout the season in areas that represented the sprinkler irrigated block and compared with the high vigor furrow irrigated areas as well as the low vigor furrow irrigated areas. Each of the plant samples was obtained from five areas of the field from area determined to having representative growth.

The entire field was harvested with a spindle picker that had an attached yield monitor having known GPS coordinates throughout the harvest. The harvester was calibrated with weigh wagons equipped with pressure transducers to verify the accuracy of strips harvested at 25 locations throughout the field. Cotton was sub-sampled to establish the quality of the cotton fiber as well and determine if irrigation practices had any influence on the quality of cotton produced. An additional 12 sub-samples were ginned to determine the turnout and percent lint, which would allow an accurate determination of crop yield through out the field.

RESULTS

PLANT STAND EVALUATIONS

The monitoring of the plant stand present was basic to understanding the distribution and intensity of soluble salts in the soil surface. Plant stands were depressed for several reasons. There were numerous areas in which the plants germinated but did not emerge through the soil crust, and there were areas of unsuccessful stands that emerged but due to their weakened state in the seedling stage, experienced high losses to seedling diseases such as pythium and Rhizoctonia. We conducted a mapping activity that established the extent and severity of the plant stand problem and estimated its impact on yield (figures 1&2). From this activity it became very apparent that substantial reductions in crop yield were being experiences as a result of poor plant stand establishment. The plant stands ranged from areas having only a few plants per 20-foot section to the desirable 65 to 80 plants per 20 feet in the row.

SOIL SALINITY MEASUREMENTS

Observations of soil salinity were conducted in three primary areas of the field including low crop vigor/low plant density zones, high plant vigor/high plant density zones, and average vigor/average density zones for sprinkler irrigated areas. The evaluation of salt concentration with depth and location on the bed can be used to aid in the diagnosis and ameliorative capabilities of reclamation activities. In particular, these salinity profiles describe rather large differences in the three primary sampling zones identified above. The high vigor cotton areas depict a soil that has moderate accumulations of salt in the soil surface and subsurface. Salt concentrations of 6 to 11

dS/m dominated the upper 30-cm of the soil surface with a small pocket of subsoil measuring as high as 13.5 to 16 dS/m. Subsurface (30-60 cm) concentrations at large largely ranged from 8.5 to 13.5 dS/m (figure 3). Plant rows are at 38cm from center (0cm). At these salt concentrations, even the salt tolerant cotton can be impacted significantly. This type of salinity profile is consistent with salinity profiles in fields that have irrigation waters that leach soil salts to subsoil levels. Leaching is not complete as the flux of water from lower zone maintains some degree of salt load in the surface.

The low vigor areas of the cotton field showed a definite contrast in profile salinity intensity and, in most soil surface areas, were observed to be between 8.5 and 13.5 in the 0-30 cm sections of the bed (figure 4). Saturated paste concentrations below 8.5 dS/m were not observed in any part of this soil zone sampled. Subsoil concentrations above 13.5 dS/m were noted in the 30 to 60 cm depths, and salt loads at this level can result in severe reductions in cotton yield and plant performance.

Finally, the profile in which sprinkler irrigation was used can be seen and contrasts significantly with the two previous soil profiles (figure 5). Surface soil salinity levels sample late in the irrigation season showed salinity levels ranging from 1 to 8 dS/m with lowest salinity levels located near the bed center at the 0 to 15 cm depth with slight increased or salinity at the 45 to 30 cm depth. Soil salinity levels, though clearly measured in the subsurface, did not contain the high levels observed in either of the furrow-irrigated systems. From these samples, it is quite clear that using sprinklers with high-quality irrigation water had a substantially positive effect on improving the soil quality characteristics of this site. Moreover, since these samples were collected at the conclusion of the irrigation season, it is clear that the effects of sprinkler irrigation improved soil quality for the following crop (Canola) in the 2002 season.

These beneficial effects that resulted from the introduction of sprinklers were not only found in reducing total surface salt load. Individual constituent salts that can impact soil quality and crop performance were also seen. Chloride levels, for instance, were significantly lower where sprinklers were used and were typically less than half of the chloride levels measured in the high-vigor furrow irrigated areas (figures 6,7 & 8).

Surface soil sodium levels were also very high for the field location sampled, where cotton vigor was low. Soil sodium levels in the 0 to 30-cm depths were as high as 66 meg/L, while subsurface levels were found to be as high as 88 meg/L. The lowest sodium levels again were found in the sprinkler-irrigated samples with many samples coming in below half of the levels observed in either the high or low vigor areas irrigated using the furrow approaches (figures 9,10 & 11). Such a dramatic decline in sodium is not commonly associated with soil leaching, since it is a positively charged ion and influenced by the soil's cation exchange reactions. However, in this case, the chloride and other subsurface salts appear to be effective counter-ions that allow sodium to be a more mobile soil solution constituent. This seems to imply that effective reclamation may be possible without the use of large quantities of common reclamation amendments and water quality and balance alone may be most important. The quality, amount, and timing of water applied appears to be the major controlling factor that influences soil salt distribution in the short term, while also controlling the high salt buildup that often occurs as a consequence of restricted drainage condition.

YIELD RELATIONSHIPS

The patterns of yield harvested in salt affected fields having a shallow saline water table can be related to specific toxic ion concentration buildup in soils or related to basic salinity that builds in soils affecting water uptake by the plant as well as seed germination rate. The use of yield monitoring information can be useful in beginning to identify the regions of salt buildup in fields, better understand salt profile characteristics most detrimental to the crop type being studied, and begin to identify amelioration procedures that may improve yield.

Figure 12, is a graphic describing yield profile data from one of our study fields. The field has a long record of cotton, grain, and vegetable crop rotations and in recent years has grown increasingly saline in the soil surface as a result of the rise in the water table level. Field history also shows the field has a long history of surface irrigation, dominated by the use of furrow irrigation methods. The general pattern of salinity in many of these salt affected fields is that they have relatively high yields in the upper areas of the field, close to the head ditch with lowest yields found

near the tail-water ditch that carries excess irrigation waters from the field. This pattern is observed in the study field with poorest yields found in the north lowest lying area of the field.

To estimate the benefits of alternative irrigation strategies on cotton production, we used GPS geo-referencing to identify areas where sprinkler irrigation was introduced. These data were later used with the yield monitoring data to analyze and compare yield from two contrasting blocks. Both visually and numerically, few differences were found between sprinkler irrigated and furrow irrigated cotton, with the exception of the lower one fourth of the field. Sprinkler irrigation yields were numerically higher.

■ ■ ■ ■ ■

REFERENCES CITED

Ayars, J.E. and R.B. Hutmacher. 1994. Crop coefficients for irrigating cotton in the presence of groundwater. Irrig. Sci. 15:45-52.

Ayars, J., Hutmacher, R.B., Schoenman, R.B., Vail, S.S. and Pflaum, T. (1993). Long-term use of saline water for irrigation. Irrig. Sci. 14:27-34.

Maas, E.V. 1990. Crop Tolerance. In: Agricultural Salinity Assessment and Management, ASCE Manuals and Reports on Engineering Practice No. 71.

Plant, R.E. and D.S. Munk. 1999. Application of remote sensing to irrigation management in California cotton. In proceedings of the Fourth International Conference on Precision Agriculture pp.1511-1522. Madison, WI: Agronomy Society of America.

Figure 1. Number of feet of missing plants in -foot increments on sprinkler irrigated plots.

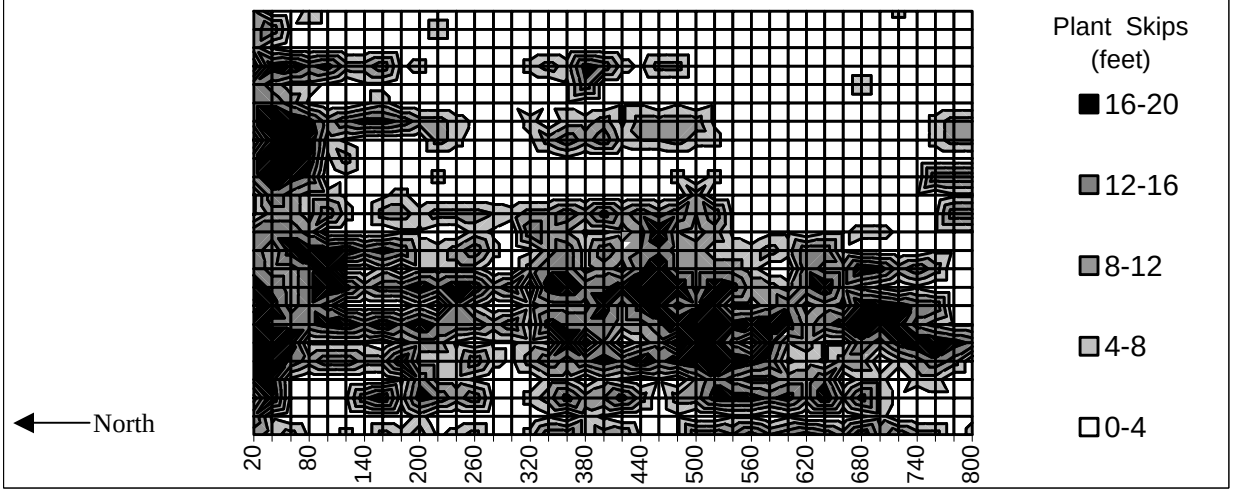

Figure 2. Number of feet of missing plants in -foot increments on furrow irrigated plots.

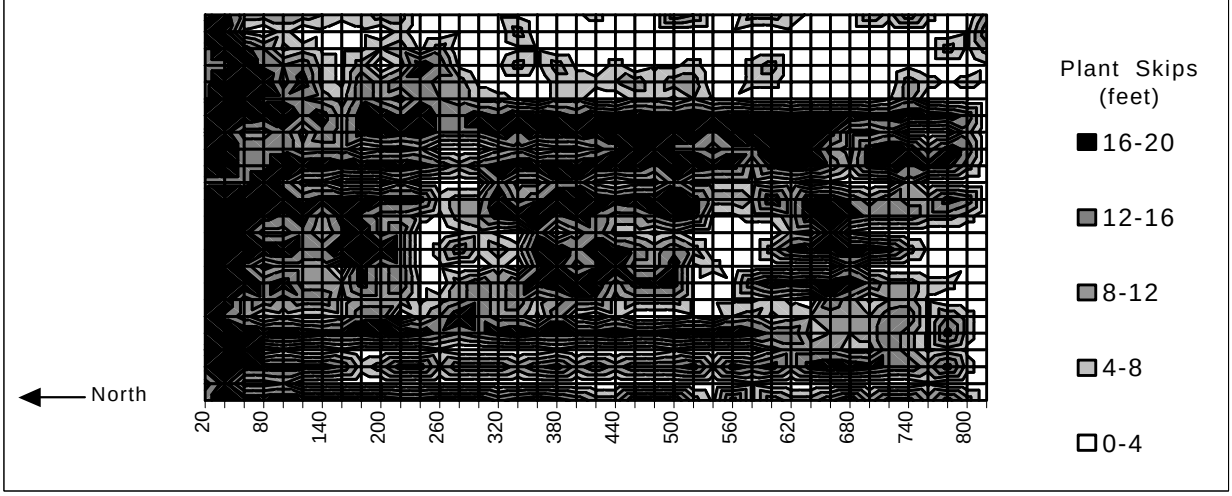

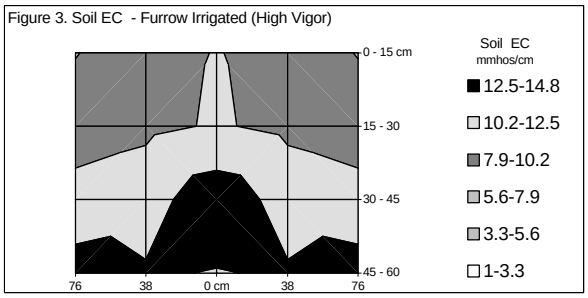
Figure 3. Soil EC - Furrow Irrigated (High Vigor)
Soil EC
mmhos/cm
12.5-14.8
10.2-12.5
7.9-10.2
5.6-7.9
3.3-5.6
1-3.3
0 - 15 cm
15 - 30
30 - 45
45 - 60
76
38
0 cm
38
76

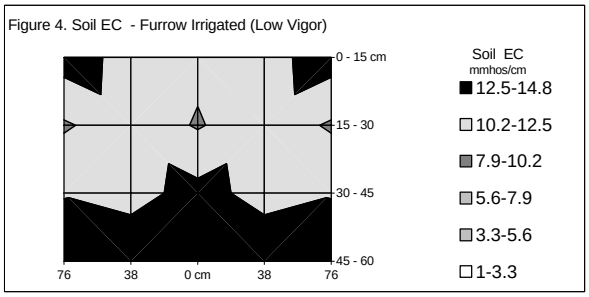
Figure 4. Soil EC - Furrow Irrigated (Low Vigor)
Soil EC
mmhos/cm
12.5-14.8
10.2-12.5
7.9-10.2
5.6-7.9
3.3-5.6
1-3.3
0 - 15 cm
15 - 30
30 - 45
45 - 60
76
38
0 cm
38
76

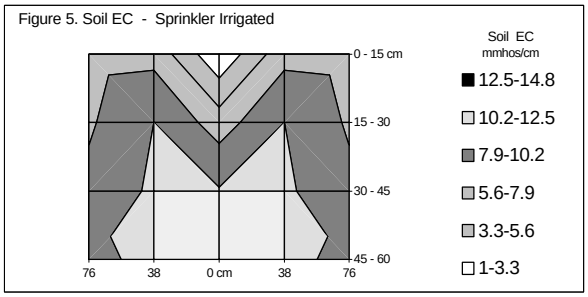
Figure 5. Soil EC - Sprinkler Irrigated
Soil EC
mmhos/cm
12.5-14.8
10.2-12.5
7.9-10.2
5.6-7.9
3.3-5.6
1-3.3
0 - 15 cm
15 - 30
30 - 45
45 - 60
76
38
0 cm
38
76

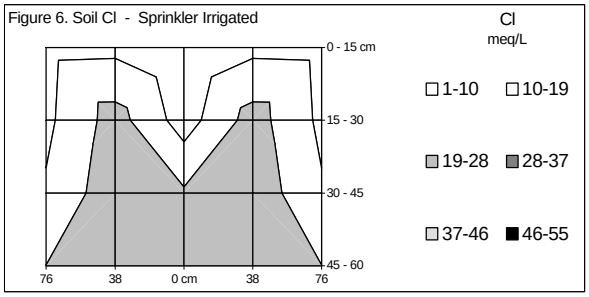
Figure 6. Soil Cl - Sprinkler Irrigated
Cl
meq/L
1-10
10-19
19-28
28-37
37-46
46-55
0 - 15 cm
15 - 30
30 - 45
45 - 60
76
38
0 cm
38
76

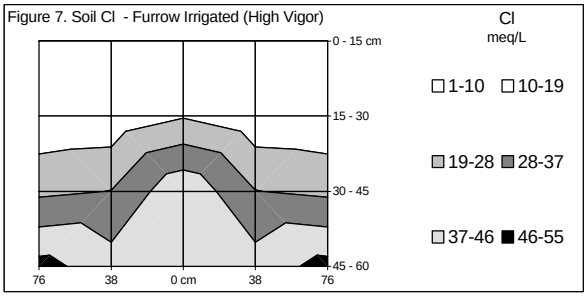
Figure 7. Soil Cl - Furrow Irrigated (High Vigor)
Cl
meq/L
1-10
10-19
19-28
28-37
37-46
46-55
0 - 15 cm
15 - 30
30 - 45
45 - 60
76
38
0 cm
38
76

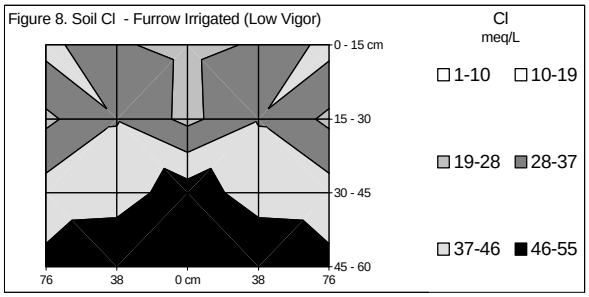
Figure 8. Soil Cl - Furrow Irrigated (Low Vigor)
Cl
meq/L
1-10
10-19
19-28
28-37
37-46
46-55
0 - 15 cm
15 - 30
30 - 45
45 - 60
76
38
0 cm
38
76

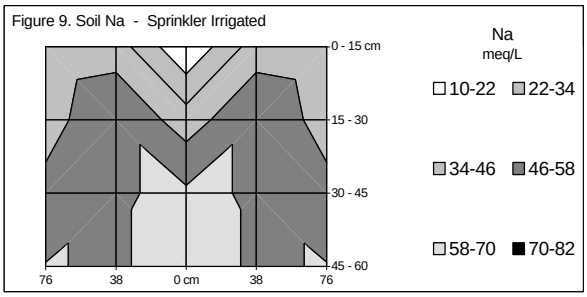
Figure 9. Soil Na - Sprinkler Irrigated
Na
meq/L
10-22
22-34
34-46
46-58
58-70
70-82
0 - 15 cm
15 - 30
30 - 45
45 - 60
76
38
0 cm
38
76

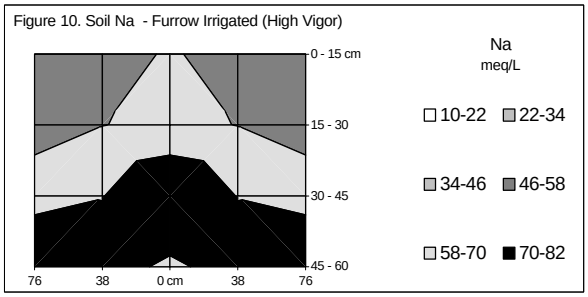
Figure 10. Soil Na - Furrow Irrigated (High Vigor)
Na
meq/L
10-22
22-34
34-46
46-58
58-70
70-82
0 - 15 cm
15 - 30
30 - 45
45 - 60
76
38
0 cm
38
76

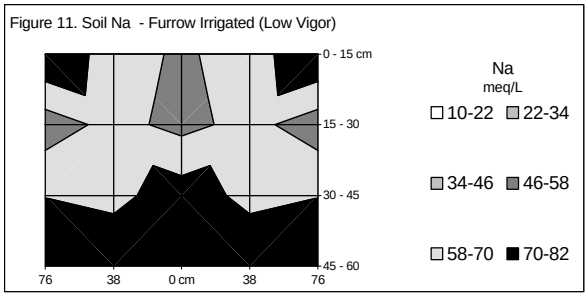
Figure 11. Soil Na - Furrow Irrigated (Low Vigor)
Na
meq/L
10-22
22-34
34-46
46-58
58-70
70-82
0 - 15 cm
15 - 30
30 - 45
45 - 60
76
38
0 cm
38
76

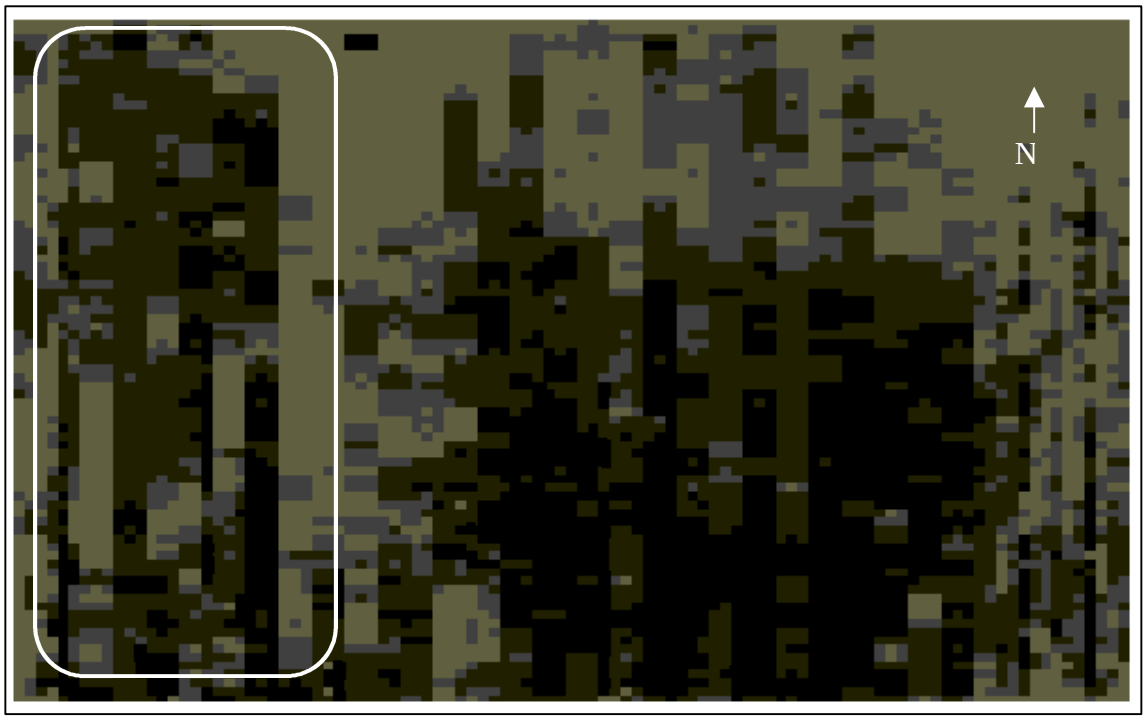

Figure 12. Yields measured throughout the field using a yield monitor. Rows run north to south and are 800 feet in length on 30 inch beds. The area within the white box was sprinkler irrigated, and the remainder of the field was furrow irrigated. Dark areas had the highest yields and lighter shaded areas were lower yielding.

Algal Community Assessment Under Different Nutrient and Grazing Intensity Regimes: Selenium Volatilization and Ecotoxic Risk

(PART OF A TEAM PROJECT ENTITLED "MITIGATING SELENIUM ECOTOXIC RISK BY COMBINING FOODCHAIN BREAKAGE WITH NATURAL REMEDIATION")

Project Investigators:

Eliska Rejmankova
Office: (530) 752-5433, E-mail: erejmankova@ucdavis.edu
Department of Environmental Science
University of California, Davis

Jaroslava Komarkova
E-mail: jarkakom@hbu.cas.cz
Hydrobiological Institute, Academy of Sciences of Czech Republic (AS CR)
Èeské Budìjovice, Czech Republic, CZ370 05

Ondrej Komarek,
E-mail: okomar@sci.muni.cz
Department of Zoology and Ecology, Masaryk University
Brno, Czech Republic, CZ-61137

Collaborators:

Dr. Teresa Fan , Department of Land, Air & Water Resources, University of California, Davis
Dr. Richard Higashi, Crocker Nuclear Laboratory, University of California, Davis

Research Staff:

Joy Futrell, Laboratory Assistant II

ABSTRACT

Previous research has noted that isolated cultures of microorganisms exhibit varying rates of selenium (Se) volatilization, which implies that Se volatilization depends on the taxonomic composition of microphyte communities (i.e., communities of green algae and cyanobacteria). Microphyte community composition is very important, as microphytes simultaneously act as the base of the foodchain and as the primary "fixers" of Se into organic forms. Our project was designed to assess effects of grazing by brine shrimp (*Artemia franciscana*) and other macroinvertebrates in combination with nutrient additions on microphyte community structure in TLDD and LHWD basins. We hypothesize that differences in grazing pressure by primary consumers affect microphyte community composition in individual basins. The main objective of this part of the multi-project Joint Research effort is to characterize the microphyte communities and evaluate the effects of grazing as well as nutrient input on the population dynamics of individual components of these microphyte communities.

During the first year of the project we conducted a microcosm experiment to study the changes in microphyte composition in response to various grazer (brine shrimp) densities. We have also conducted two field experiments in LTDD ponds. So far, microphyte composition from the microcosm experiments has been evaluated and the results of the field experiments are almost complete. This progress report will present the results of the microcosm experiment and a brief description of the field experiment. Data to confirm or reject the first hypothesis: H1: "Brine shrimp production increases with overall microphyte productivity" are still being evaluated. The results of the field experiment are in support of the second hypothesis: H2: "Overall microphyte primary production increases with addition of nutrients". For the third hypothesis: H3: "The microphyte species composition is affected more by grazing ("top down" effect), than by nutrients ("bottom up" effect)", we need to conduct more experiments. So far our results show that grazing by brine shrimp IS strongly selective. Cyanobacteria are grazed most heavily, followed by other groups, e.g., Flagelati. Green algae are grazed least.

KEYWORDS

Algae, cyanobacteria, brine shrimp, *Artemia franciscana*, feeding preferences, predation, hypersaline environment, fertilization response, Tulare Lake Drainage District (TLDD)

■ ■ ■ ■ ■

INTRODUCTION

Volatilization of Se from aerobic saline waters by microphytes is probably a widespread and global phenomenon (Amouroux and Donnard, 1996). In evaporation basins, the volatilization of Se by microphytes must be considered together with Se accumulation and potential ecotoxic risk, since the processes are linked. (Figure 1) Fan and Higashi have previously demonstrated in evaporation basins of the San Joaquin Valley that a substantial amount of Se (up to 70% of added Se) was removed from aerated culture media via volatilization by filamentous cyanobacteria isolated from TLDD waters (Fan et al., 1998). They have also shown that several other microphytes isolated from these basins behave similarly (Fan et al., 1997; Fan and Higashi, 1998; Fan and Higashi, 1999a). There are differences in rates of Se volatilization by isolated cultures, which implies that Se volatilization depends on the composition of microphyte communities (i.e., communities of green algae and cyanobacteria). The process of biovolatilization first requires "fixation" of Se by microphytes into their biomass. Fan et al. (Fan and Higashi, 1999a; Fan, 2000) have shown that the extent of bioaccumulation varies by microphyte species. These interspecific differences could cause the ecotoxic risk to vary by basin, a phenomenon that could be strategically exploited to reduce overall Se risk in evaporation basins. Fan (2000) documented the effect of this variation in evaporation pond biogeochemistry and provided data on some of the Se bioconcentration factors (BCF) of microphytes and invertebrates observed in TLDD and LHWD evaporation basins. Across a wide range of salinities and waterborne Se concentrations, the microphytes range approximately 10-fold in BCF, while the next trophic level, the invertebrates, range even wider. However, the microphytes and invertebrates BCFs are not related to either salinity or waterborne Se concentration; current evidence from these basins and elsewhere indicates that it is a function of the basin biogeochemistry (Fan et al., 1998; EPA Office

of Water, 1998). The biogeochemistry, in turn, is likely a function defined (in part) by the microphyte community composition, as they act simultaneously a the base of the foodchain and as primary "fixers" of Se into organic forms. (Figure 1)

In the summer of 2000 we surveyed the microphyte composition of TLDD and LHWD basins. This effort resulted in the identification and cataloging of dozens of species isolated from these basins. Based on these preliminary results we hypothesized that grazing pressure by brine shrimp cause changes in microphyte composition.

OBJECTIVES AND HYPOTHESES

Our current project is designed to assess effects of grazing by brine shrimp (*Artemia franciscana*) and other macroinvertebrates in combination with nutrient additions on microphyte community structure in TLDD and LHWD basins. The main objective of this part of the multi-project Joint Research effort is to characterize the microphyte communities and evaluate the effect of grazing as well as effect of nutrient input on the changes in population dynamics of individual components of these microphyte communities. Ultimately, we would like to modulate microphyte communities in two aspects: (1) create conditions that are most favorable for microphytes that contribute most to the volatilization process, and, at the same time (2) create conditions that would provide enough microphyte food for brine shrimp production.

This study uses both observations and experiments in the field to confirm or reject the following hypotheses:

H1: Brine shrimp production increases with overall microphyte productivity.

H2: Overall microphyte primary production increases with addition of nutrients.

H3: The microphyte species composition is affected more by grazing ("top down" effect), than by nutrients ("bottom up" effect).

The specific objectives are:

1. Monitor the microphyte composition and primary production (PP) indicators in basins;
2. Correlate the changes in microphyte composition and PP with water/nutrient chemistry data (projects of Gao/Dahlgren and Higashi/Flocchini) and with data on brine shrimp harvest;
3. Correlate the changes in the microphyte composition with 16S DNA and pigment analyses of the microphytes (project of Fan/Meeks). Correlate the changes in microphyte composition with Se volatilization and BCFs in the algae (project of Fan/Meeks). In the field experiment, assess responses of microphyte communities to factorial combinations of brine shrimp presence/absence, nitrogen, phosphorus, combined N and P, and chicken manure additions in terms of species composition and growth response (e.g. PP, chlorophyll a);
4. Relate these responses to Se volatilization (project of Fan/Meeks) and detritus chemistry (projects of Gao/Dahlgren and Higashi/Flocchini).
5. Correlate the microphyte composition with Se BCFs in the algae (project of Fan/Meeks).

METHODS

MICROCOSM EXPERIMENT 1

The algae assemblages were collected from several LTDD ponds and mixed to create a suspension representative of algae species as potential food source for *Artemia franciscana*. The water samples were filtered through a 50 µm net to screen out all invertebrates. Suspensions were cultivated in 200 ml of water in 400 ml beakers under ambient light and temperature conditions for 6 days. The first experiment included only a control and two treatments, each in two replicates. In treatment 1 we added 6 shrimp/beaker and in treatment 2 we added 12 shrimp/beaker. The biomass of algae was estimated as a number of cells per ml and expressed in mg/l according to Komarkova et al (2000). Samples for assessment of the microphyte composition were collected daily.

MICROCOSM EXPERIMENT 2

The second experiment was conducted in order to evaluate the feeding preferences of adult and larval brine shrimp. It was also designed to evaluate the timing of brine shrimp development under the experimental conditions.

Second experiment lasted five days and included three treatments and a control:

The treatments were:

O - Control (with no shrimp)

EGS - Eggs (added from the field collection)

AD - Adults (filtered each day to remove eggs and larvae)

ADE - Adults (newly laid eggs and hatched larvae kept in beakers)

Water salinity and volume were kept constant. pH was measured three times during the experiment. Light intensity was 100 W m^{-2}. Temperature ranged from 25 to 35^0C. Three ml water samples were taken daily from each beaker and fixed in Lugol solution and 4% formaldehyde for quantification and identification algal species. At final shrimp harvest, larval and egg abundance was assessed in all treatments.

Field Enclosure Experiments

Nutrient addition experiment was set up was within the C4 basin. Experimental treatments included brine shrimp presence/absence, additions of N, P, N&P, turkey manure, straw, and straw & manure, and a control with no additions. Three replicates were set up for each treatment. Enclosures were be made of clear plastic. Each enclosure was filled with filtered basin water and inoculated with the same microphyte inoculum existing in the basin pond. Treatments with brine shrimp received a shrimp density corresponding to typical densities experienced in that pond prior to harvest (data provided by Dr. Rofen). The enclosure experiments were run for two weeks with nutrients added twice. Phosphorus was added in form of K_2HPO_4 and N was added as KNO_3. The chicken manure addition corresponded to the amount that has been used by Novalek, Inc. for successful shrimp cultivation in the TLDD basins (data provided by Dr. Rofen).

Species composition of the microphyte assemblages was evaluated using a microscope at the beginning and at the end of the experiment. The microphyte biomass was estimated using chlorophyll *a* concentrations (Rejmánková & Komárková 2000). At the time of harvest, microphyte and brine shrimp samples were collected for tissue nutrient and Se analysis. Growth of brine shrimp under different treatments was assessed at the end of the experiment as total change in biomass.

Unexpected problems due to stormy weather on day 3 resulted in the loss of several replicates. Thus the results of this experiment should be considered only preliminary.

RESULTS AND DISCUSSION

MICROCOSM EXPERIMENT 1

In our microcosm experiment #1, brine shrimp grazing had a statistically significant effect on the algae population (Figure 1). The presence of brine shrimp was responsible for a significant reduction in algal biomass starting day 3 of the experiment. Figure 2 shows the changes in proportions of individual algal species biomass in the control over the course the experiment. The algal assembly in the control was influenced only by inter-specific competition and experimental conditions. The species in this experiment can be classified into three groups: 1) species whose biomass increased and achieved higher level than at the day zero, 2) species whose biomass did not change and, finally, 3) minority species that were not an important food source.

The structure and biomass of the algal population shifted with additions of shrimp. Grazing at both high and low intensity as shown in Fig. 3, decreases the biomass of all species except for genus *Oocystis.* This is in strong contrast to the control, which was dominated by Synechocystis *salina*. Apparently *S. salina* is a food source favored by *Artemia franciscana.* The next taxonomic groups to be grazed substantially were *Cylindrospermopsis* sp. (CPP – col), Cyanobacteria filaments (Cyano-fil), and to some degree *Anabaenopsis salina* (ABPSlSsal). The only species that were not grazed were both species of *Oocystis* genus; *Oocystis* cf *marsonii* and *Oocystis parva* + *composita*. We can conclude that predation pressure is advantageous for the *Oocystis* cf. *marsonii* under conditions of the first experiment.

Figures 5a-f show the proportion of the most important species in control and the two treatments. The individual species development in this experiment was as follows:

The increase in the biomass of *Oocystis* species (Figures 5a & b) in the two treatments as compared to control may be caused by the suppression of other algal species by brine shrimp. The relative increase of *Oocystis parva* + *composita* in the 2 treatments follows a pattern similar to the control. The green alga *Chlorella* sp.

(Figure 5c) showed a similar response, i.e., increase in biomass as a response to grazing pressure by brine shrimp. Cyanobacterial filaments group (Figure 5d) were a good feeding source for *Artemia franciscana* as were *Cylindrospermopsis* sp. CPP colonies (Figure 5e.) and Flagelates (Figure 5f). These were all significantly grazed by brine shrimp as evidenced by a sharp decrease in their relative biomass.

MICROCOSM EXPERIMENT 2

The goal of this second experiment was to determine the differences in selective grazing between larval and adult life stages of brine shrimp. The final brine-shrimp counts at harvest time have not yet been completed and will be presented in next year's report.

The algal assembly was grazed most heavily in Adults and Adults & Larvae treatments (Fig. 6). The biomass fluctuations seen in this figure were most probably caused by a behavior of the alga *Oocystis salina* during the course of this experiment (See Fig. 7). The substantial decrease in *Oocystis salina* biomass followed by its recovery after four days was apparently due to the stress caused by cultivation conditions.

The Eggs treatment (Figure 8) was not different from the control. On the contrary to the Eggs treatment, the Adult treatment showed a distinct decrease in the population of *Synechocystis salina* (Figure 9). The *Oocystis* biomass did not recover to the same level as in control, which indicates some level of grazing. No significant changes were seen in the *Picocystis salina* (PICSAL2) and *Prymnesium salina* (PRYMsal5) species. *Synechocystis salina,* the most abundant alga, was more extensively depleted than less abundant algal species at the end of experiment when the number of feeding animals increased in Adults/Eggs treatment (Figure 10). The individual species response to treatment conditions is summarized in Figure 11 a-f.

FIELD ENCLOSURE EXPERIMENT

As stated above, we are still in the process of evaluating the species composition of microphytes from this experiment. Data on chlorophyll concentration indicate changes in biomass of the whole algal community as a response to different treatments. The addition of nutrients, especially combined N&P, and manure caused significant increases in both chlorophyll a and pheophytin concentrations (Figures 12 and 13). The N&P treatment also shows a difference between presence and absence of brine shrimp. For information on Se content see report of Higashi (this Volume).

CONCLUSION

The microcosm experiments show the remarkable influence of *Artemia franciscana* grazing on different species of microphytes. Cyanobacteria were grazed most, followed by other groups, e.g., Flagelati. Green algae were grazed least in both experiments. An important factor influencing shrimp grazing was the abundance of individual algal species. More abundant species were grazed more intensively than less abundant species with the exception of green algae which aren't a very suitable food source for brine shrimp. The enclosure experiments showed the effect of fertilization on selenium volatilization (see Higashi, this volume). In the second year of the project we plan to conduct experiments to obtain more conclusive data on the strength of the effects of grazing by shrimp *vs.* nutrient addition.

■ ■ ■ ■ ■

REFERENCES CITED

Amouroux, D. and Donard, O.F.X. 1996. Maritime emission of selenium to the atmosphere in eastern Mediterranean seas. Geophys. Res. Lett. 23, 1777-1780.

EPA Office of Water. 1998. Report on the Peer Consultation Workshop on Selenium Aquatic Toxicity and Bioaccumulation, EPA-822-R-98-007, September 1998. Available at the website http://www.epa.gov/ost/selenium/report.html

Fan, T.W-M. 2000. Microphyte-mediated Se biogeochemistry and its role in bioremediation of Se ecotoxic consequences. In: UC Salinity/Drainage program annual report, 2000-01, in press.

Fan, T.W.-M. and R.M. Higashi. 1998. Biochemical fate of selenium in microphytes: Natural bioremediation by volatilization and sedimentation in aquatic environments. In: Environmental Chemistry of Selenium, W.T. Frankenberger and R.A. Engberg, eds., Marcel Dekker, Inc., New York, pp. 545-563.

Fan, T.W-M. and R.M. Higashi. 1999a. Microphyte-mediated Se biogeochemistry and its role in bioremediation of Se ecotoxic consequences. In: UC Salinity/Drainage program annual report, 1998-99, p.35-52.

Fan, T.W-M., A.N. Lane, and R.M. Higashi. 1997. Selenium biotransformations by a euryhaline microalga isolated from a saline evaporation pond. Environ. Sci. Technol. 31: 569-576.

Fan, T.W.-M., R.M. Higashi, and A.N. Lane. 1998. Biotransformations of Selenium Oxyanion by Filamentous Cyanophyte-Dominated Mat Cultured from Agricultural Drainage Waters", Environmental Science and Technology 32, 3185-3193

Rejmánková, E. & J. Komárková, 2000. A function of cyanobacterial mats in phosphorus -limited tropical wetlands. Hydrobiologia 431: 135-153.

■ ■ ■ ■ ■

Table 1. The list of abbreviation and whole names of algae species.

ABPSISsal6	**Anabaenopsis salina**
CPP-col	**Cylindrospermopsis sp.**
Cyano-fil	**Cyanobacterial fillaments**
Flagel	**Flagelates**
CHLORsal1	**Chlorella salina**
MYXBAK	**Myxobactron salinum**
NEPsal	**Nephrochlamys subsolitaria**
OOCMAsal10	**Oocystis cf.marsonii**
OOCPAR	**Oocystis parva+composita**
PRYMsal8	**Prymnesium salinum**
SYNCOsal2	**Synechococcus salina**
SYNCYsal4	**Synechocystis salina**

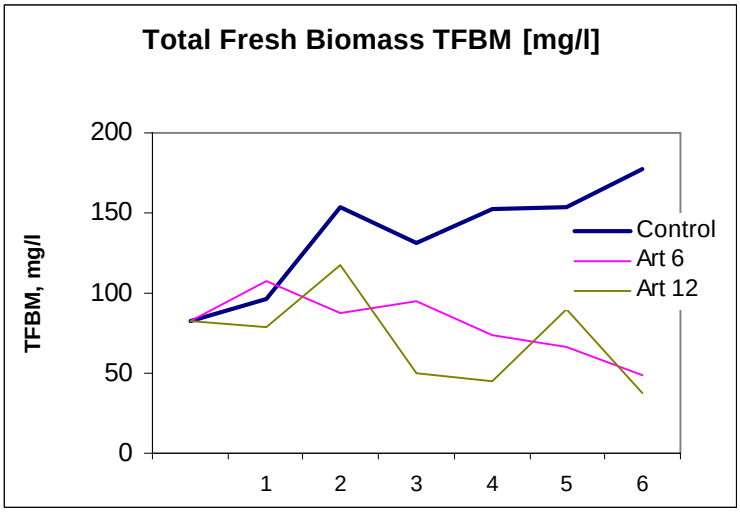

Figure 1. The total biomass of algal species in control and two treatments. (Art 6 = brine shrimp added, Art 12 = 12 brine shrimp added)

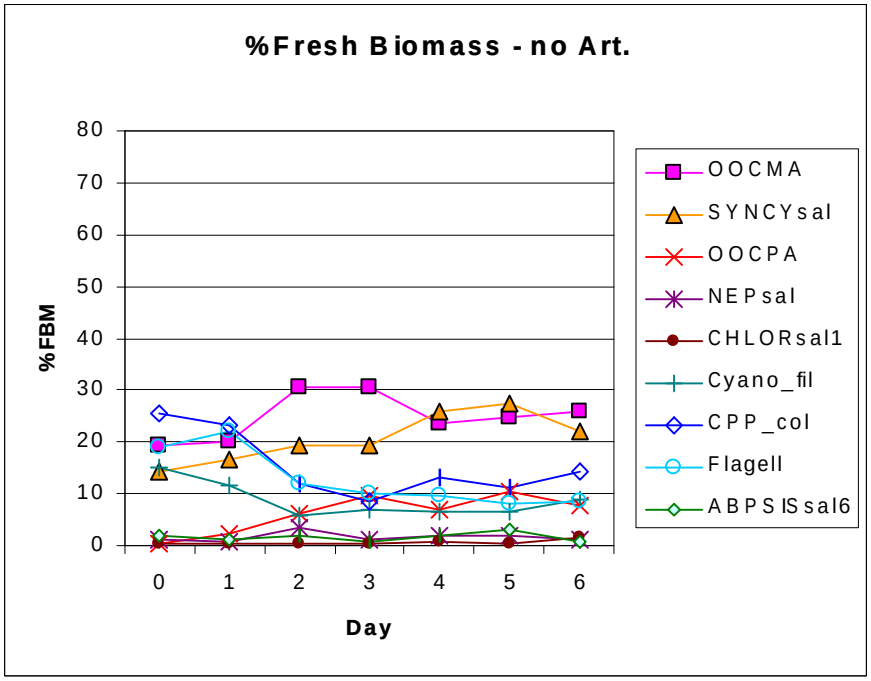

Figure 2. The control of the experiment with no predator pressure. Symbols in Table 1.

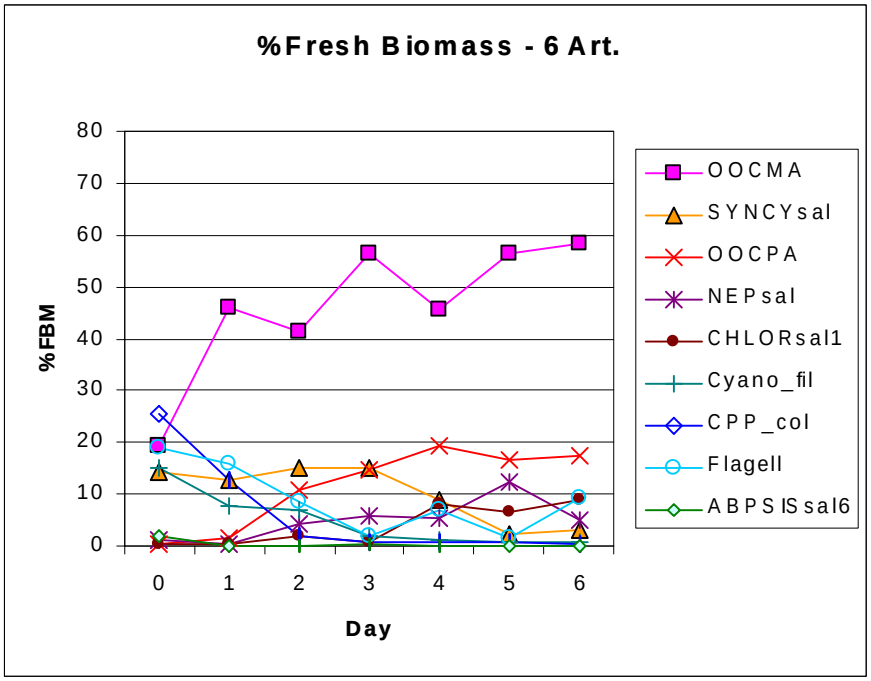

Figure 3: The biomass of the algae species under low grazing pressure (6 Artemia individuals in each beaker). Symbols in Table 1.

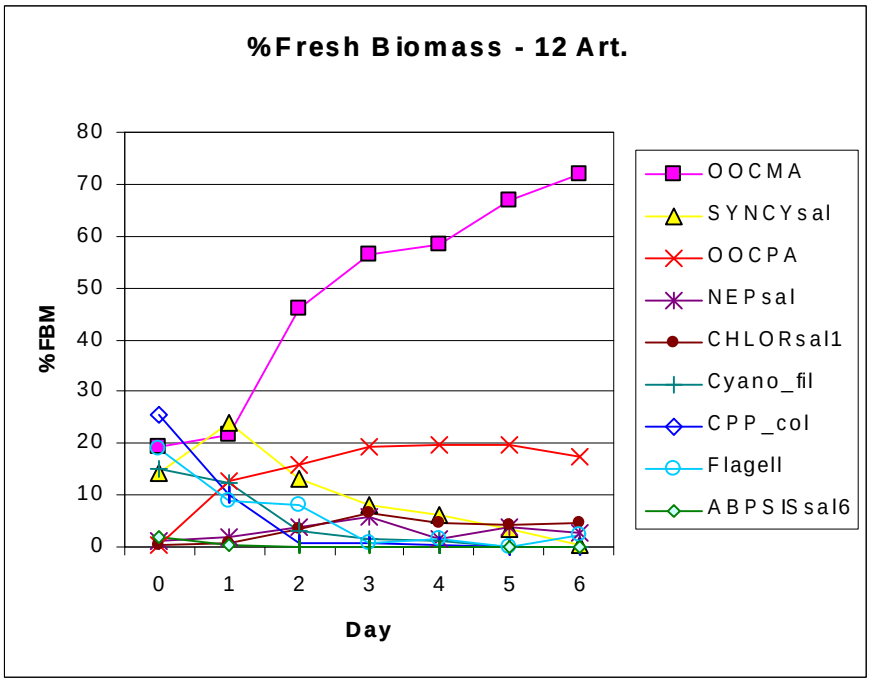

Figure 4: The experiment under high grazing pressure (12 individuals of *Artemia* in each beaker). Symbols in Table 1.

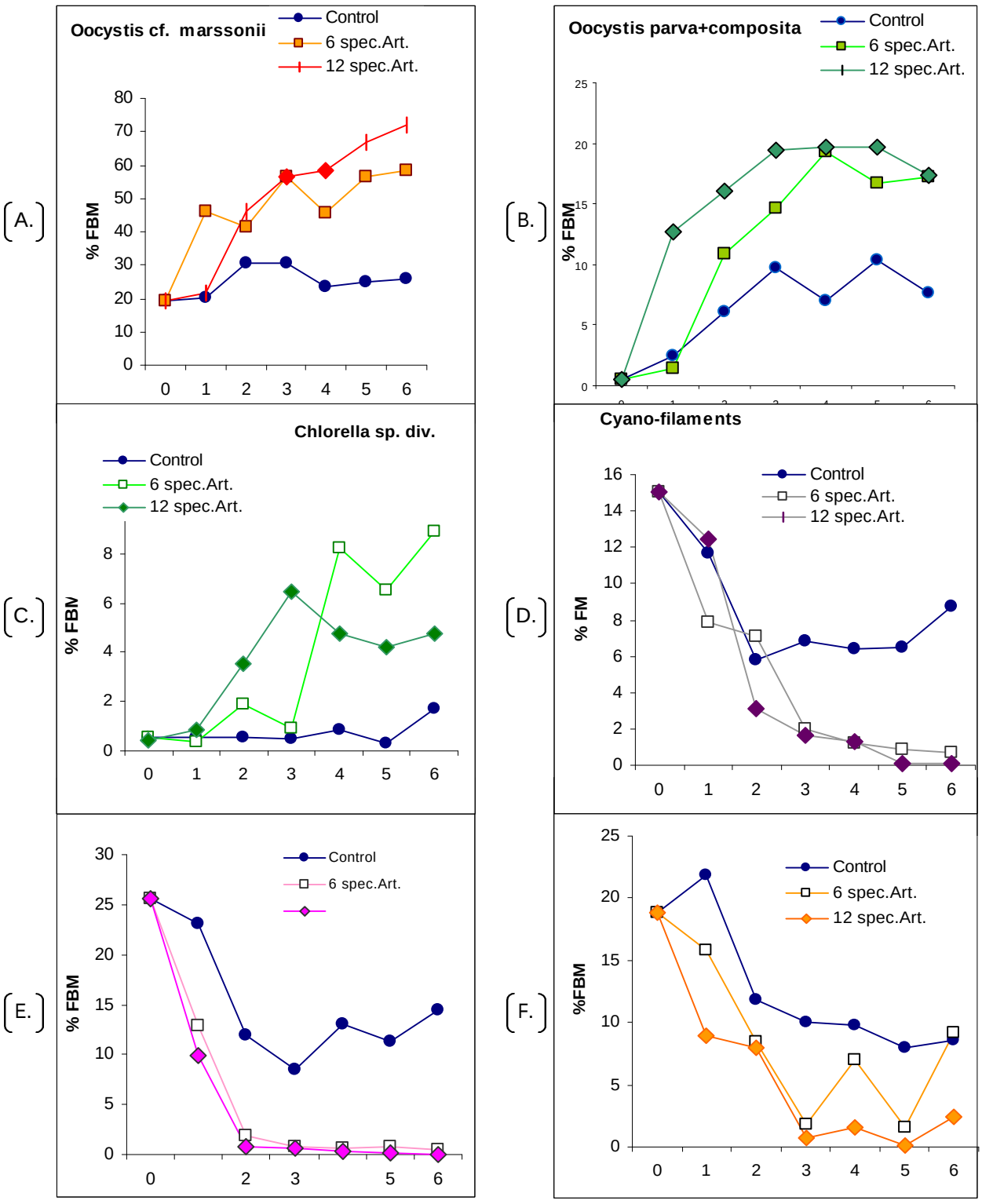

Figure 5. The relative percentage of fresh biomass of the *Oocystis* cf. *marsonii*, *Oocystis* parva + *composita*, *Chlorella* sp. div., Cyano—Filaments, *Cylindrospermopsis* sp. (CCP) and Flagelates in the control and two treatments.

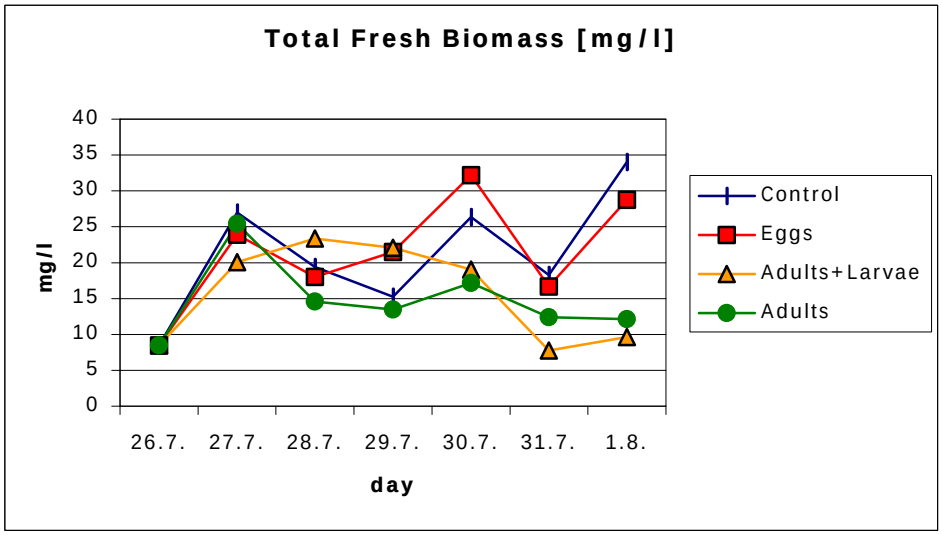

Figure 6. The timecourse of the Total Fresh Biomass of algae in control and the three treatments. Each point is the average of 5 replaction.

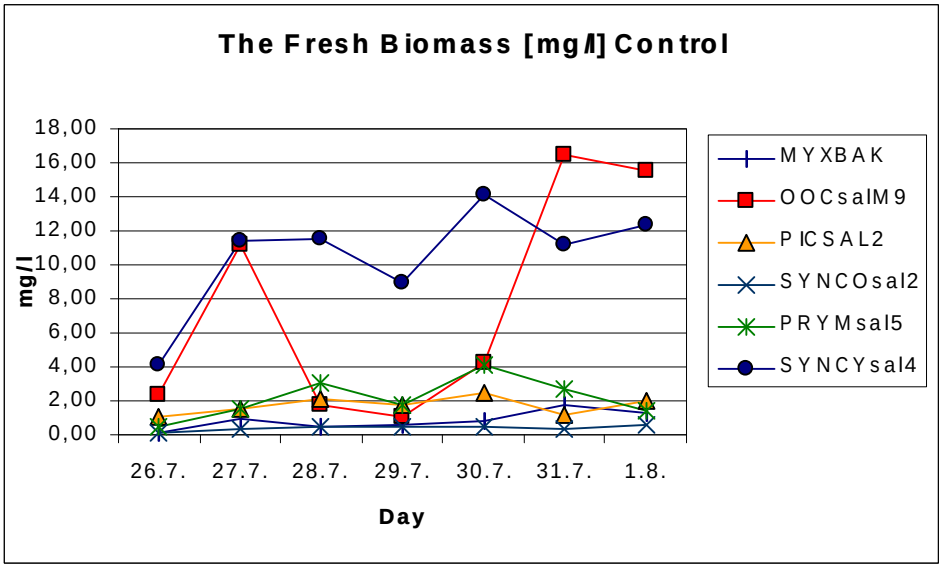

Figure 7. The fresh biomass of the algae species in control set of the experiment. Symbols in Table 1.

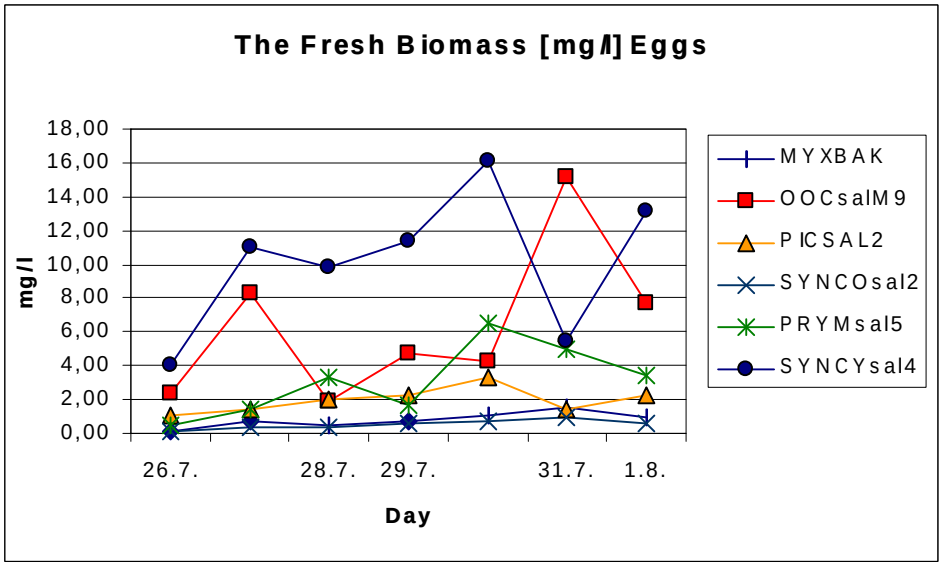

Figure 8. The biomass of individual species of algae in the treatment with eggs of *Artemia franciscana*. Symbols in Table 1.

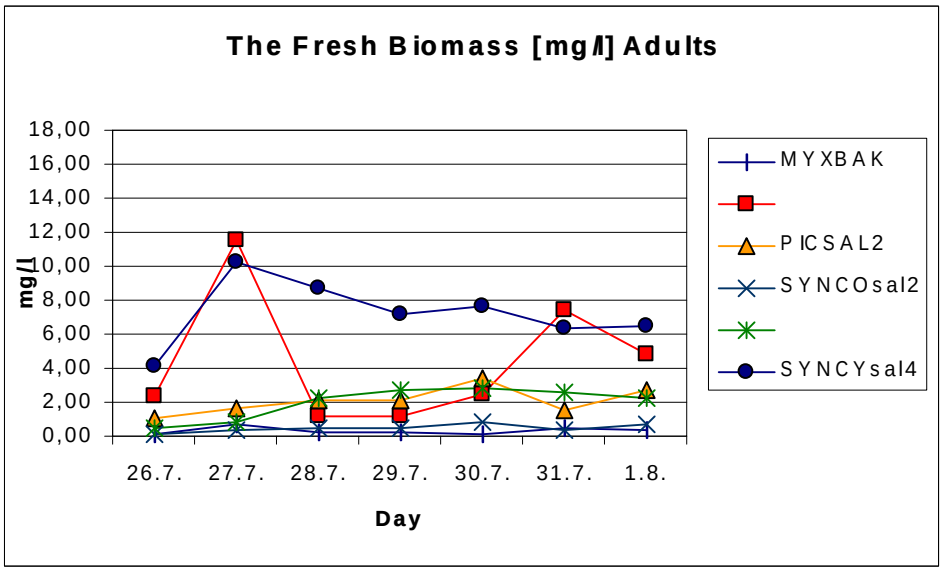

Figure 9. The fresh biomass of the individual algae species in the Adult *Artemia franciscana* treatment.

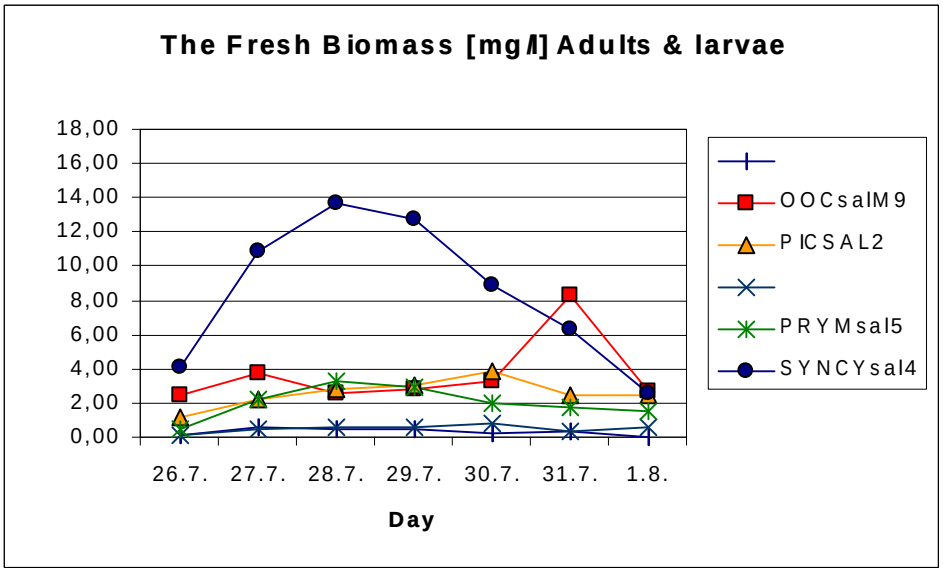

Figure 10. The fresh biomass of the individual aglae species in set of treatment with adults and larvae (rested eggs for hatching) of *Artemia franciscana*.

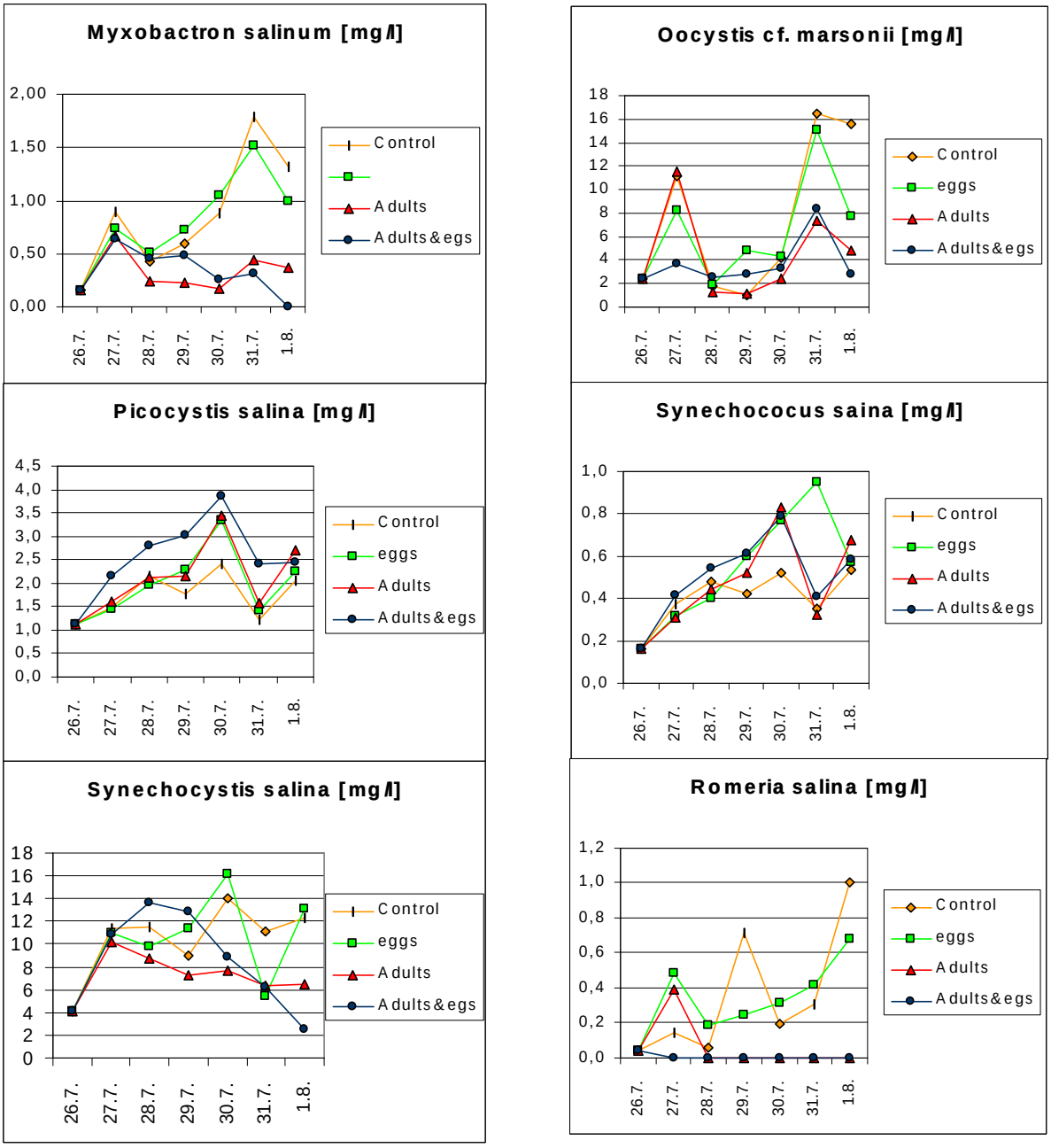

Figure 11. The fresh biomass of the *Myxobactron salinum*, *Oocystis* cf. *marsonii*, *Picocystis salina*, *Synechococcus salina*, *Synechocystis salina*, and *Romeria salina* at control and treatments.

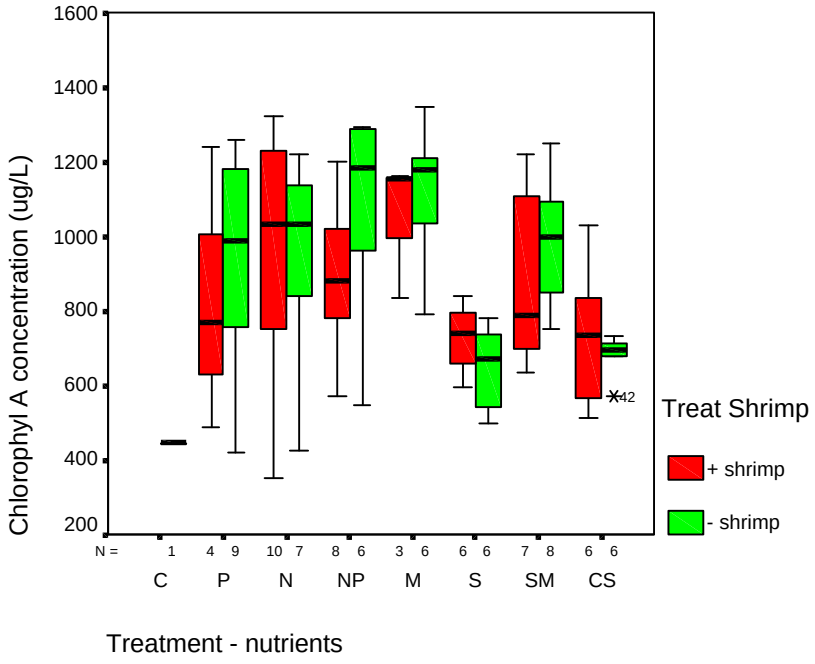

Figure 12. Chlorophyl a concentration under different treatments of enclosure experiment.

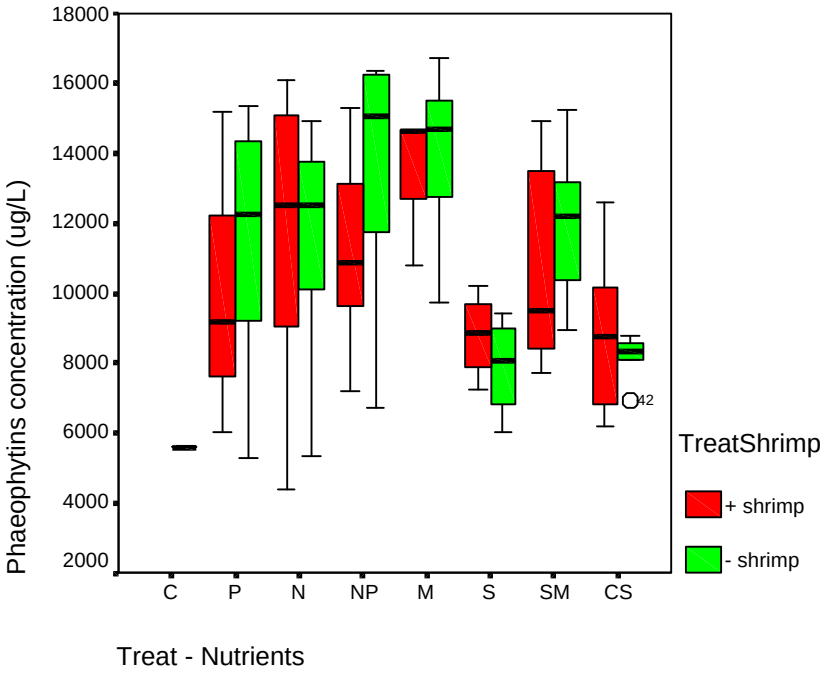

Figure 13. Phaeophytins concentration under different treatments of enclosure experiment.

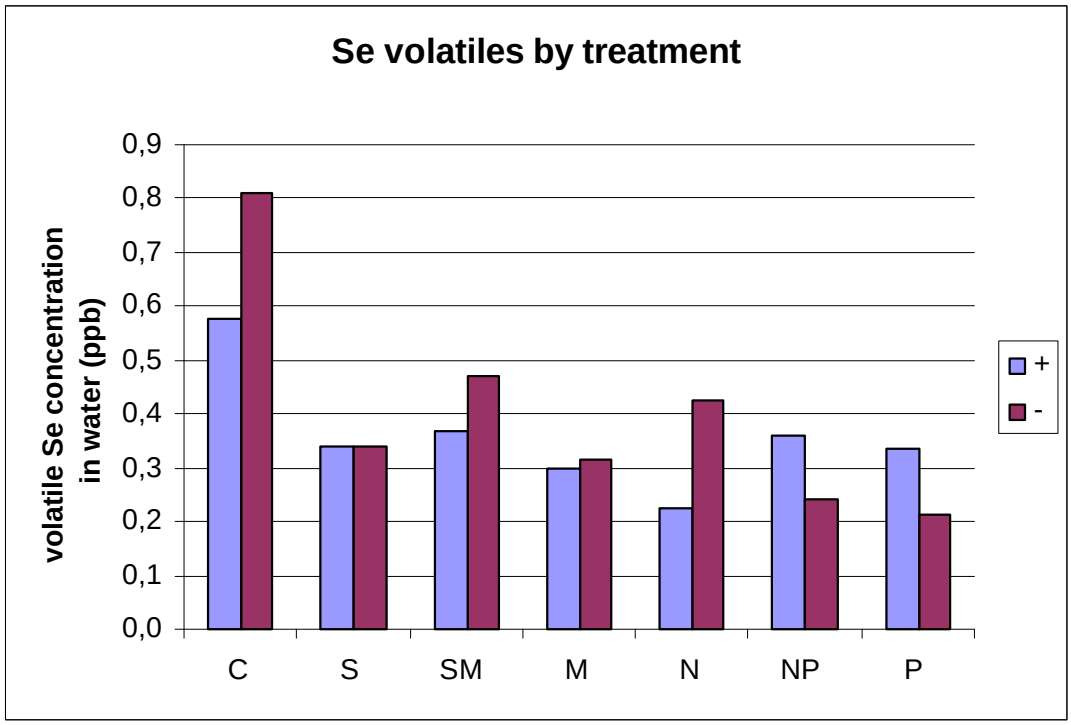

Figure 14. The Se in water in different treatments (T. Fan and R. Higashi).

An Economic Analysis of Alternative Methods to Control Salinity In the Western San Joaquin Valley

Project Investigator:

Kurt A. Schwabe
Office: (909) 787-2361, E-mail: kurt.schwabe@ucr.edu
Department of Environmental Sciences
University of California, Riverside

Co-Investigators:

Keith Knapp
E-mail: keith.knapp@ucr.edu
Department of Environmental Sciences
University of California, Riverside

Iddo Kan
E-mail: iddo.kan@ucr.edu
Department of Environmental Sciences
University of California, Riverside

ABSTRACT

Drainwater management strategies include source control, reuse, treatment, and evaporation ponds; questions of interest are efficient management, policy instruments, and sustainability. A high level of source control is indicated absent reuse due to the relatively high cost of evaporation ponds; this is accomplished largely through high uniformity/high cost irrigation systems. With reuse, the primary form of source control is reduction in land area devoted to freshwater production; the released land goes to reuse production. Reuse appears as an economically promising solution to the drainage problem. A high level of net returns is achieved while maintaining overall hydrologic balance in the system.

Economic efficiency and hydrologic balance may be attained through pricing or market schemes. With pricing, growers are charged for deep percolations flows, while reuse and evaporation pond operators are paid for extractions. With markets, permit supply is generated by extractions from the water table, while permit demand is generated by deep percolation. Competitive equilibrium exists, is efficient, and implies hydrologic balance. The analysis suggests that a high level of agricultural production may be possible for some period of time while still maintaining environmental quality.

KEYWORDS

Economics, irrigation, mathematical programming, regional management, reuse, salinity, salt-tolerant crops, San Joaquin Valley, source control, Westlands Water District

■ ■ ■ ■ ■

INTRODUCTION

Currently, irrigated agriculture in the western part of the San Joaquin Valley (SJV) is operating as a semi-closed basin; surface water is imported for irrigation but external drainage is either not allowed or is greatly restricted. Finding a solution to this drainage problem, a solution that maintains both agricultural productivity and environmental quality, requires consideration of a broad array of biophysical management options. These options will likely include some combination of source control, drain water reuse, and in-region disposal methods. Examples of source control options include more uniform irrigation systems and crop switching. Reusing the drainage water for crop production is another option, similar to source control, which can reduce waste emissions and conserve scarce freshwater supplies. Finally, in-region disposal methods include options such as evaporation ponds and solar evaporators. Identifying an efficient solution among these many different management combinations is a complex exercise that requires an understanding of both the relationships that exist between the options themselves and their impact on production and the environment.

This project analyzes the regional agricultural drainage problem. An empirical analysis is conducted for a region of the SJV that is currently heavily impacted by drainage problems. The results illustrate the importance of accounting for each of the major management options – source control, reuse, and in-region disposal – so as to accurately reflect the problem, substitution possibilities, and consequences confronting growers and policy makers. Our findings indicate that overlooking any of these options, and the substitution opportunities that exist among them has a substantial impact on the conclusions one can drawn about the relative attractiveness and efficiency of any particular policy scheme.

THE STUDY AREA AND DATA

The empirical analysis focuses on the Westlands Water District (WWD) within California's Central Valley. WWD consists of approximately 600,000 acres and is subject to an in-region drainage disposal requirement. A large portion of WWD confronts a high water table, the result of continued deep percolation flows from irrigation accumulating over time on top of the relatively impermeable Corcoran clay layer.

The modeling framework for this analysis uses a mathematical programming model that will evaluate the economic efficiency and profitability of various strategies confronting growers to reduce saline drainage water. In effect, the problem can be presented as one for which we have an objective of maximizing regional agricultural profits with specific constraints on land availability, surface water availability, groundwater availability, water table depth, and out-of-region discharges. Profits consist of the revenues generated from producing some combination of five crops less the costs of both producing the crops and disposing of the drainage water.

The model includes cotton, processing tomatoes, wheat, alfalfa, and lettuce as both freshwater crops and reuse water crops. Bermuda grass is an additional reuse crop. The irrigation systems and their respective Christensen Uniformity Coefficient (CUC) are furrow 0.5 mile (CUC=70), furrow 0.25 mile (CUC=75), linear move sprinklers (CUC=85), sprinkler (CUC=80), low-energy precise application system (CUC=90), and subsurface drip (CUC=90). Crop-water production functions are specified as

$$y = y_1(e - \underline{e}) + y_2(e - \underline{e})^2$$

$$e = \frac{\bar{e}}{1 + \acute{a}_1\left(c + \acute{a}_2 w^{\acute{a}_3}\right)^{\acute{a}_4}}$$

$$d = w - e$$

where e (ft/yr) denotes evapotranspiration, $\bar{e}$ (ft/yr) is the maximum evapotranspiration under non-stressed conditions, $\underline{e}$ (ft/yr) represents the minimum evapotranspiration level required for yield production, y is yield (ton/acre), and d (ft/y) is deep percolation flows. y's and a's are scalars, while w (ft/yr) and c (ds/m) are irrigation depth and salt concentration. This system is estimated for each crop-irrigation system combination. Data for yield, evapotranspiration, and deep-percolation flows given irrigation depth and salt concentration are generated using the Letey et al. (1985) plant-level model and assuming water is distributed over the field according to a lognormal distribution. Plant-level parameter values for the model are generally from Letey and Dinar (1986); distribution moments depend on irrigation system uniformity. The production function system was fit to the data using nonlinear regression analysis.

Non-water production costs and market prices for each cropping system are derived from UC Cooperative Extension Service (2000) crop budgets. The costs of irrigation include amortized capital costs along with maintenance and operating costs. Surface water costs are a weighted-average of water prices in WWD. Constraints are imposed to maintain acreages of individual crops within historical ranges observed in the 1990's. Evaporation pond construction and maintenance costs are $117.40/ac-yr and the evaporation rate is 5.32 ft/yr (Posnikoff and Knapp 1997). In-region disposal consists of evaporation ponds and their compensating habitat. Compensating habitat costs are estimated as $1,504/ac-yr.

EFFICIENT MANAGEMENT

The first column in Table 1 reports results with no constraints on net flows to the water table. This serves as a baseline for the hydrologic balance analysis and also to help verify the model. In effect, it represents the situation in WWD prior to 1985 when growers were allowed to discharge their drainage into nearby streams, rivers, or canals. As the results indicate, traditional irrigation systems are selected, there is no reuse, and deep percolation flows average slightly over 1 ft/yr. The historical average for deep percolation flows in this region is generally considered to be 1 ft/yr over the period time during which the current drainage problem developed.

The second column in Table 1 enforces the hydrologic balance constraint but with no reuse. This scenario mimics the WWD after the in-region disposal requirement but before the compensating habitat mandate imposed in 1995. The results suggest that efficient management entails both a substantial level of source control as well as in-region disposal of deep percolation flows to evaporation ponds. Total crop area declines to accommodate the evaporation ponds. Irrigation systems switch from traditional systems (furrow with ½ mile runs) to more uniform systems. Average deep percolation flows decline by almost 60% due to both improvements in irrigation efficiency as well as reductions in applied water. The pond area amounts to 7% of the regional area. While the results show that significant returns to land and management can be sustained while maintaining hydrologic balance, social net benefits decline by 17% compared to the unconstrained case.

In column three, the compensating habitat (CH) requirement is introduced with the intention to mimic regulations in the WWD post-1995. As shown, there is a dramatic shift to more uniform irrigation systems that contribute to a pronounced reduction in deep percolation flows by 12% as compared to the unconstrained case. Corresponding to the comparative statistics analysis (equation (25)), there is a reduction in surface water use, an increase in crop production area, and a 5% reduction in pond acreage, some of which was in turn used for the compensating habitat. While still positive, social net benefits decrease by nearly 37% as compared to column one.

The last column of Table 1 allows growers the choice of evaporation ponds (including compensating habitat) and/or reuse as a drainage disposal option. The results suggest that drainwater reuse offers great promise in maintaining agricultural production and hydrologic balance in the region. As shown, the area devoted to crop production with freshwater is reduced quite substantially to allow for reuse production. Compared to the baseline solution, reuse opportunities require little source control from growers. There is a 5% reduction only in the use of the less uniform irrigation systems and, surprisingly, deep percolation flows increase slightly.

While the details of the crop mix for freshwater crops is not shown, column three does illustrate that most of the drainwater reuse is applied to cotton. The constraint on total cotton acreage was binding at the upper bound of its observed historical levels, implying that additional acreage would lead to even larger gains. Cotton as a reuse crop is practical since it is both profitable and moderately salt tolerant (Mass and Hoffman 1977). In the presence of the reuse option, no evaporation ponds were chosen. Most noteworthy, though, is that with reuse the net returns to land and management are not only positive, implying that agriculture can be sustained in the region for some time, but also are only 5% below the unconstrained case.

POLICY

From a policy perspective, the common property nature of the drainage problem in the SJV seems suitable for some sort of collective action. One possibility is a pricing scheme. Under this scheme, growers are charged for deep percolation flows to the water table, while reusers and pond operators are compensated for extractions from the water table. Setting the charge at the correct level will induce hydrologic balance; this also implies revenue-neutrality. The last row in Table 1 reports the shadow values on drainage disposal, λ_d. These vary widely depending on the assumed conditions; however, the most realistic estimate at the present time would be that with reuse and its estimated drainage price of $19/ac-ft, a relatively modest amount. For crop production, this would imply a payment of $23/ac-yr given average deep percolation flows of 1.21/ft-yr. This would be the emission charge imposed by the regulator on deep percolation flows, and the payment to reuse and evaporation pond operators for extractions from the water table.

Another policy option is a marketable permit system. As in standard environmental economics, emissions to the water table need to be covered by a permit and the permits are freely tradable. The shadow values on drainage disposal, λ_d from Table 1, could serve as an initial estimate to initialize grower planning under a permit market. A novelty of the scheme here, however, is that permit supply is generated endogenously by operators extracting from the water table. Equilibrium in this market implies hydrologic balance. Under competitive conditions in both the permit and land markets, an efficient equilibrium will exist in the market. These results are driven, in part, by the profits from using reuse water on cotton, a profitable alternative that lowers the opportunity cost of foregoing freshwater crops.

CONCLUSIONS

A regional economic model is developed to evaluate and compare alternative management strategies confronting growers in the WWD with recognition of the current regional environmental restrictions associated with drainage water. Some level of source control is efficient since deep percolation flows generate disposal costs and/or environmental damages. Absent reuse, a very high level of source control is efficient due to the relatively high cost associated with evaporation ponds. This is accomplished largely through adoption of highly uniform/high-cost irrigation systems. With reuse allowed, the primary form of source control is reduction in land area devoted to freshwater production; the released land goes into reuse production.

Our empirical results suggest that reuse appears to be an extremely promising solution to the drainage problem. Maximizing regional net benefits while maintaining hydrologic balance seems best achieved with reuse and minimal source control thereby avoiding the expense and environmental implications associated with evaporation ponds. This strategy, though, requires a reduction in freshwater crop acreage for reuse production. Given the profitability of cotton as a reuse crop capable of enduring moderately high salt concentrations clearly reduces the opportunity costs of foregone freshwater crop

production. With reuse, potentially large net returns can be achieved while maintaining overall hydrologic balance in the system with the reuse strategy. These are promising results that may help better inform growers within the region who are confronting ever-increasing costs of disposal and policy makers searching for more efficient solutions that are both sustainable and environmentally friendly. This conclusion is conditioned in part on the existing salt concentration of the water table. Salt concentrations will likely vary between regions and evolve over time depending on the nature of the large-scale hydrologic regime. Furthermore, real-world outcomes will also depend on such elements as land quality, crop rotations, risk, grower knowledge, and a variety of other factors not considered here.

Whether agricultural production can be sustainable in a semi-closed basin while maintaining adequate levels of environmental quality is probably best answered with a dynamic analysis that is well beyond the scope of this study. The dynamics involve groundwater hydrology, including possible further increases in salt concentration, as well as possible buildup of human and physical capital, which might substitute in full or part for hydrologic degradation. The empirical analysis does suggest, though, that a high level of agricultural production may be possible for some period of time while still maintaining environmental quality.

■ ■ ■ ■ ■

REFERENCES

Letey, J., and A. Dinar. "Simulated Crop-Water Production Functions for Several Crops When Irrigated With Saline Waters." Hilgardia 54, no. 1 (1986):1-32.

Letey, J., A. Dinar, and K. C. Knapp. "Crop-Water Production Function Model for Saline Irrigation Waters." Soil Science Society of America Journal 49, no. 4 (1985):1005-1009.

Maas, E. V., and G. J. Hoffman. "Crop Salt Tolerance - Current Assessment." Journal of the Irrigation and Drainage Division, American Society of Civil Engineers 103 (1977):115-134.

Posnikoff, J. F., and K. C. Knapp. "Farm-Level Management of Deep Percolation Emissions in Irrigated Agriculture." Journal of the American Water Resources Association 33, no. 2 (1997):375-386.

University of California Cooperative Extension. Sample Costs to Produce Processing Tomatoes and Cotton (various reports). San Joaquin Valley. 2000.

PUBLICATIONS

Kan, I., K. A. Schwabe, and K. C. Knapp. "Microeconomics of Irrigation with Saline Water." Journal of Agricultural and Resource Economics 27, no. 1(2002): 16-39.

Table 1. Efficient Regional Drainwater Management

	Historical	No Reuse		Reuse
		No CH	CH	
Crop Production				
Area (acres)	0.83	0.762	0.789	0.514
Furrow 0.5 miles (%)	95			90
Furrow 0.25 miles (%)		75	22	
Linear move sprinklers (%)		20	73	
Drip (%)	5	5	5	10
Surface water (ft/yr)	3.23	2.44	1.99	3.17
Deep percolation (ft/yr)	1.17	0.48	0.14	1.21
Reuse				
Area (acres)	0	0	0	0.32
Crop / Irrigation system				Cotton / F4
				Wheat / F4
Ground water (ft/yr)				3.81
Deep percolation (ft/yr)				1.87
Land Disposal				
Evaporation pond (acres)	0	0.07	0.02	0
Compensation Habitat (acres)			0.02	
Region				
Social Net Benefits ($/yr)	311	258	196	294
Drainage shadow value ($/af)	0	80.68	393.86	18.69

F4 = furrow with 1/4 mile runs. Land areas and social net benefits are per regional acre. Irrigation system results are percent of the respective crop or reuse areas. Water variables are average depths over the cropped areas in the crop production and reuse sectors. CH = Compensating Habitat

Improving Water and Nutrient Management Practices on Dairies in the Southern San Joaquin Valley

Project Investigators:

Larry Schwankl
Office: (530) 752-1130, E-mail: *ljschwankl@ucdavis.edu*
Department of Land, Air, and Water Resources
University of California, Davis

Carol Frate
E-mail: cafrate@ucdavis.edu
University of California Cooperative Extension, Tulare Co.

Stuart Pettygrove
E-mail: gspettygrove@ucdavis.edu
University of California, Davis

Alison Eagle
E-mail: *ajeagle@ucdavis.edu*
University of California, Kearney Ag Center

ABSTRACT

Many of the dairies in the San Joaquin Valley use a water flush system to clean the manure from free-stall barns. This flush water is collected and held in large ponds until it can be mixed with freshwater and applied to cropland as part of flood irrigation practices. Due to the nutrients in the manure water, high irrigation and nutrient application efficiency and uniformity are important to minimize deep percolation of nitrates.

This two-year project is investigating (1) various management techniques (surge irrigation, furrow torpedoes, and reduction of field length) to improve furrow irrigation performance, and (2) controlling the timing of manure water additions during an irrigation set to improve the nutrient application efficiency and uniformity. Work has been completed on evaluating surge irrigation, furrow torpedo use, and reducing field lengths.

Surge irrigation use reduced the applied water during an irrigation event by 30–35%. Furrow torpedo use reduced the applied water by 15–25%. Reducing the field length (1250 ft. to 600 ft. in trial) was the most effective, reducing applied water by 40–50%.

Preliminary work has been done on controlling the timing of manure water additions during an irrigation set, with promising results. Work on this project objective is continuing.

KEYWORDS

dairy irrigation, dairy nutrient management, furrow irrigation, surge irrigation, furrow torpedo

■ ■ ■ ■ ■

INTRODUCTION

There are over 600 dairies in the southern San Joaquin Valley with a total animal population of well over a half-million cows. The fate of the dairy manure nutrients and concerns over groundwater contamination are major water quality and environmental issues in the San Joaquin Valley. Many of these dairies handle their manure with a combination of scraping and hauling of solid manure from corrals, and a water flush system of liquid manure of the free-stall barns and other dairy facilities. For a 1,000 cow dairy, it is estimated that 50,000 gallons of liquid manure water is generated daily. This manure water is stored in ponds until it is mixed with freshwater and applied to fields using furrow or border strip irrigation. The most common crop irrigated with manure water is corn silage but other crops such as cotton are also grown using manure water.

Operating furrow and border irrigation systems at high irrigation efficiency and high irrigation uniformity is a challenge. Irrigation efficiency is a measure of how much of the applied irrigation water is beneficially used. The primary beneficial use of irrigation is satisfying crop water needs. Inefficient irrigation uses are deep percolation (water draining below the crop's root zone) and tailwater runoff that is not reused. High irrigation efficiency indicates that most of the applied irrigation water goes to satisfy crop water needs. Irrigation uniformity is a measure of how evenly water is applied to a field. High irrigation uniformity means that all portions of a field receive nearly the same amount of water.

Irrigation efficiency of furrow and border irrigation systems is often low due to over-irrigation and poor irrigation system uniformity. Tailwater is seldom a problem in dairy manure water irrigation since no waters containing manure can leave the grower's property, and the standard practice is to not generate tailwater during irrigation. The major contributor to irrigation inefficiencies is deep percolation. Over-irrigation and poor irrigation efficiency is often the result of fields that are too long. A set amount of irrigation water is required to simply advance water to the end of the field. This is the minimum amount of applied water per irrigation event and this applied amount is often in excess of the water required to refill the crop's root zone; resulting in inefficient irrigation.

Poor irrigation uniformity of furrow irrigation systems (the predominant irrigation method on dairy field crops in the southern San Joaquin Valley) results in over-irrigation at the head of the field and potentially under-irrigation near the tail of the field. Over-irrigation, combined with irrigation non-uniformity, often results in significant deep percolation. Manure water additions to the irrigation water can therefore result in deep percolation of both water and nutrients.

PROJECT OBJECTIVES

1. Investigate and demonstrate the use of furrow torpedoes and surge irrigation to improve the irrigation water management of dairy manure water irrigation systems.

2. Investigate the effect of controlling the timing of manure water additions during irrigation events to improve manure water nutrient application uniformity and efficiency on dairies.
3. Extend the information developed in the project through field days and newsletters targeted at the dairies in the Southern San Joaquin Valley.

RESULTS

FURROW TORPEDOES

Furrow torpedoes are steel cylinders, often filled with concrete, which are dragged in the furrow to break up soil clods and smooth the soil surface. They can be effective in allowing water to advance across a field more quickly; resulting in improved irrigation uniformity and improved irrigation efficiency. Torpedo use is beneficial after field preparation or cultivation. They are not effective if there is no cultivation to disturb the furrow between irrigations.

The impact of torpedo use for manure water irrigations was evaluated by comparing 3 blocks of 25 torpedoed furrows each with a similar number of furrows (75) that were not torpedoed. All furrows were 1250 ft. long. For continuous flow irrigation, the amount of water required for irrigation was reduced from 12.9" to 9.4" –a 27% reduction (Table 1). For surge-irrigated fields (4 surge cycles), there also seemed to be an advantage to using torpedoes (Table 1) although Check 5 (surge irrigation / torpedoes) required more water for irrigation than did the non-torpedoed checks. There were field slope problems in Check 5, verified by surveying, and it was difficult to get water to the end of the field.

Torpedo use is not widespread in the San Joaquin Valley, primarily due to the difficulty and cost of their use. The torpedoes are dragged behind a tractor on a sled arrangement and it is often difficult to turn at the end of the field with the torpedoes attached. Some growers have solved this problem by having the sled and torpedoes connected so that they can be hydraulically lifted at the field ends. Because of these complications, furrows are usually torpedoed as a separate pass through the field– an added cost.

Alternatives to torpedoes are "packer wheels". Packer wheels are tires which are run in the furrows to break up soil clods, similar to the effect of torpedoes. The packer wheels can often be used in conjunction with other field preparation equipment and thus save making a separate pass through the field.

SURGE IRRIGATION

Surge irrigation is the on-off cycling of water during irrigation. This practice can improve irrigation uniformity by advancing water across the field while using less water. Research has shown an infiltration reduction on soil wetted by a previous surge cycle. This infiltration rate reduction is likely due to a sealing of the soil surface. Surge irrigation has not been previously investigated on manure water irrigated fields. Manure water contains a substantial amount of fine solids which may have a significant positive impact on surge irrigation performance.

Surge irrigation was evaluated by comparing 2 blocks of 25 furrows each, irrigated with continuous flow, with 4 blocks of 25 furrows each which were surge irrigated. Four surge cycles were used. Water was allowed to advance 1/4 of the way down the field (300') and then the water was transferred to another section of furrows. By the time the water was transferred back to the original section, water had infiltrated into the furrow. During the second surge, water was allowed to advance another 1/4 of the field (to 600'). Water was again transferred to another set of furrows. This continued for surges 3 (advance to 900') and surge 4 (advance to the end of the field–1250'.

Surge irrigation use was effective in reducing the amount of water required to irrigate the field. For furrows not torpedoed, applied water was reduced from 12.9" to 9.1" –a 30% decrease, and from 12.9" to 8.4" –a 35% decrease (Table 1). For torpedoed furrows, results were mixed with applied water on one section of furrows being reduced from 9.4" to 7.8" –a 17% decrease (Table 1). On another check of 25 furrows, the torpedoed furrows required more water (9.4" vs. 10.5" –a 12% increase, see Table 1). Again, note that Check 5 was the check with field slope problems.

A reduction in applied water of 17–35%, using surge irrigation is respectable. It is likely that the excess applied water would go to deep percolation that could leach nitrate. It would seem that surge irrigation would therefore be a natural practice for growers to adopt, but the

furrow irrigation systems on most dairies does not lend itself to surge irrigation.

Surge irrigation using freshwater is done using gated pipe and an automatic surge valve. Dairies seldom use gated pipe because the manure solids and trash (weeds, baling twine, etc.) in the water clog the discharge openings. Instead, dairies often use alfalfa valve(s) which discharge water into a block of furrows. An added complication is that the automatic surge valve has an internal, motorized, butterfly valve and this valve could easily become entangled with any trash in the water. To use surge irrigation on dairies now would require irrigators to manually open and close alfalfa valves–an increase in labor and management for irrigation.

REDUCTION IN FIELD LENGTH

The most effective change that can be made to improve irrigation and nutrient applications is to shorten the field length. San Joaquin Valley field lengths vary widely but a 1/4-mile field length is common. This is often too long a field to allow water applications to match crop water needs. As mentioned previously, the minimum irrigation application amount is determined by the amount of water needed to advance water to the end of the field. For example, if 6 inches of water is required to advance water to the end of the field but the crop water use since the last irrigation has been 4 inches, 2 inches of water would be lost to deep percolation. If nutrients are available to be leached, the excess water could be the vehicle for carrying them below the crop's root zone.

Shortening the field length allows a lesser irrigation amount to be applied during an irrigation set, allowing the irrigation amount to more closely match the water depleted from the crop's root zone and thereby increasing irrigation efficiency. Irrigation uniformity is also improved when shorter fields are used. The 1250 foot furrows were evaluated to see how much water would be required if field length was reduced to 600 feet (Table 2). Applied irrigation amounts could be reduced by 35–55% when field lengths were reduced from 1250 ft. to 600 ft.

Field length reduction has the greatest impact on irrigation performance, but it is also the most costly and inconvenient. To reduce a 1/4-mile length field to two 1/8-mile fields would require a new pipeline ($15,000–$20,000 for a 40-acre field), a new road (a capital cost and land lost from production), and possibly new tailwater collection facilities. Shorter field lengths are also a significant inconvenience for equipment movement through the field. This would impact field preparation, cultivation, pest and weed control, and harvest activities.

TIMING OF MANURE WATER APPLICATIONS

Preliminary work has been done on manipulating the timing of manure water additions during an irrigation set to improve nutrient application uniformity. This strategy hinges on infiltration characteristics varying during irrigation. The infiltration rate is high when water first comes in contact with a soil location and then decreases, often significantly, until a final, relatively constant, intake rate is reached. Due to the time required for water to advance across the field, water is in contact with the soil (intake opportunity time) at the head of the field for a significantly greater time than it is at the tail of the field. The result is greater infiltrated water at the head of the field than at the tail. The same is true of nutrient applications if manure water is added continuously to the irrigation water.

Adding manure water to an irrigation set after freshwater has advanced some distance down the field has the potential to improve nutrient application uniformity. The high intake period at the head of the field is avoided by delaying manure water additions, reducing the nutrient amount applied at the head of the field. At first analysis, it would seem that by delaying manure water additions, manure nutrients would never reach the tail end of the furrow. Again due to soil intake characteristics, manure nutrients move quickly down the furrow once they are added. For example, in one trial undertaken, in which a liquid sulfur fertilizer was used as a visual tracer, the injection of the sulfur was delayed until freshwater had reached the 750-foot mark along a 1000-foot furrow. By the time the advancing waterfront had reached 850 feet, the injected sulfur had caught up to the advancing freshwater front.

Field trials will be completed during the summer of 2002 and this nutrient management strategy will be further investigated.

■ ■ ■ ■ ■

Table 1. Effects of surge irrigation and furrow torpedoes on furrow irrigation performance.

Check No.	Torpedoed	Not Torpedoed	Continuous Flow	Surge Flow	Applied Water – in.
1		Yes	Yes		12.9
2		Yes		Yes	9.1
3		Yes		Yes	8.4
4	Yes			Yes	7.8
5	Yes			Yes	10.5
6	Yes		Yes		9.4

Table 2. Effect on irrigation performance of shortening field lengths.

Check No.	Irrigation Treatment	Field Length – ft.	Applied Water – in.
1	Not torpedoed / Continuous flow	1250	12.9
1	Not torpedoed / Continuous flow	600	7.1
2	Not torpedoed / Surge flow	1250	9.1
2	Not torpedoed / Surge flow	600	5.4
3	Not torpedoed / Surge flow	1250	8.4
3	Not torpedoed / Surge flow	600	5.2
4	Torpedoed / Surge flow	1250	7.8
4	Torpedoed / Surge flow	600	5.0
5	Torpedoed / Surge flow	1250	10.5
5	Torpedoed / Surge flow	600	4.8
6	Torpedoed / Continuous flow	1250	9.4
6	Torpedoed / Continuous flow	600	4.3

Mass Balance and Simulation Modeling for Se Remediation in TLDD Flow-Through Wetland Cells

Project Investigators:

Kenneth K. Tanji, Professor Emeritus
Office: (530) 752-6540, E-mail: kktanji@ucdavis.edu
Hydrology Program, Department of Land, Air and Water Resources
University of California, Davis

Suduan Gao
Office: (530) 752-5105, E-mail: sugao@ucdavis.edu
Hydrology Program, Department of Land, Air and Water Resources
University of California, Davis

Research Staff:

Alex T. Chow, Research Associate
Hydrology Program, Department of Land, Air and Water Resources
University of California, Davis

ABSTRACT

Prediction of selenium (Se) mass distribution and Se speciation in wetlands is desired for a comprehensive assessment of the capability of wetlands to remove Se from agricultural drainage waters prior to impound-ment in evaporation basins. A mathematical model was developed to describe Se transformations and transport in Tulare Lake Drainage District's wetland system. In the model, each wetland cell consists of ten internal compartments and Se can be transferred across the compartments by physical and chemical processes. Physical processes include water movement, litter drop and physical material breakdown. Chemical processes include Se reduction from Se(VI) to Se(IV), and further reduction to Se(0) and organic Se. In the chemical processes, Se transformation reaction was assumed to obey first-order kinetics and Arrhenius equation for temperature dependency. A total of 33 ordinary differential equations were written to describe all the processes within the internal compartments. A Fortran program with a numeric scheme using the 4th order Runge-Kutta method followed by the 4-step Adams-Bashforth-Moulton predictor-corrector method is written to solve the equations simultaneously. The model was successfully calibrated with results from Cell 4 (Smooth cordgrass) and validated with results from Cell 5 (Rabbitsfoot grass), Cell 6 (Saltgrass) and Cell 7 (Cattail). This model can demonstrate the seasonal variation of Se mass distribution and Se speciation in different compartments with considerations for water temperature. With the model, we also manipulated physical parameters such as water inflow rate, water depth or longitudinal length of a wetland and the results show decreasing the inflow rate, or increasing the water depth or increasing the longitudinal length of a wetland can increase the accumulation of Se in compartments of a wetland cell and reduce the total mass of Se in the outflow water. Such information will be useful for criteria for engineering design of constructed flow-through wetlands.

KEYWORDS

Se removal, Se transformations, Se speciation, Se reduction, engineering design criteria

■ ■ ■ ■ ■

INTRODUCTION

The TLDD flow-through wetland systems was established in 1996 by Tulare Lake Drainage District (TLDD), the UC Salinity/Drainage Program and the Department of Water Resources to determine the efficiency of wetland remediation for Se in saline irrigation drainage water prior to impoundment in evaporation basins. Reduction in Se concentration is desired to decrease the potential of Se toxicity to waterbirds attracted to evaporation basins. Ten, 15 m wide and 76 m long, unlined wetland cells with differing water depths (89 mm to 585 mm) and differing vegetations (Fig. 1) were operated from June 1996 to February 2001. Detailed information on the construction and the design of the wetland system is found in Terry (1997). Water inflow, obtained from a nearby tile drainage sump, was continuously monitored with a totalizing flow meter fitted with terminal plastic orifice pressure regulators, and outflow measured with a v-notch weir on weekly to twice a week schedule. After one year of freshwater irrigation the cells began receiving saline drainage waters. The sampling and in situ measurements began in May 1997, about 10 months after the wetland was initially vegetated, to February 2001 when the project was terminated. Total Se concentration in the inflow and outflow waters was determined weekly and water Se speciation was determined several times each year. A comprehensive sampling of the internal compartments of the cells was carried out in September 2000 (Gao et al., submitted).

In addition to the routine monitoring, various research teams have carried out their disciplinary investigations and are publishing their findings. Gao et al. (submitted) shows that for the ten cells an average 58.8% of the total inflow Se was retained in the cells and 35.5%, 3.6%, and 2.2% were outflow, seepage, and volatilization, respectively. Studies (Gao et al., 2000; Lin et al., submitted) indicate that the sediment was the major sink for the Se retained in the wetland and the reduction of Se (VI) to Se(IV), Se(0), and organic-Se, was mainly confined in the top 5 cm of surface sediments. Partitioning and speciation of selenium in plants (Terry, 2000; Lin et al., submitted) and different compartments within the wetland cells (Gao et al., submitted; Lin et al., submitted) were also examined. In addition, monthly volatilization rates in these constructed wetlands for different seasons were obtained (Terry 2000). With large data sets accumulated from

various disciplinary projects, there is a need for an overall assessment of the performance of the TLDD wetland cells. In this paper, we carry out Se mass balance and model simulations to better integrate the findings and make better use of those valuable dataset.

MODEL APPROACHES

The TLDD constructed wetland system is a continuous flow–through system. The system had been operated for 4.5 years and the results of field monitoring in September 2000 appear to indicate steady state has been approached (Tanji, 2001). To predict the fate of Se within the wetland cells and the efficiency of the remediation, both water and Se mass balance have to be considered together. In the model, each wetland cell consists of ten internal compartments and Se can be transferred across the compartments by physical and chemical processes. Physical processes include water movement, litter drop and physical material breakdown. Chemical processes include the Se reduction from Se(VI) to Se(IV), and further reduction to Se(0) and organic Se. In the chemical processes, the Se transformation reaction was assumed to obey first-order kinetics. In the model, Se transformations generally occur within the compartments and then transfer to other compartment by water flow.

COMPARTMENTS

Considering the wetland cell as the control volume, each wetland cell, as shown in Figs. 2 and 3, is divided into ten individual compartments: standing water (sw), detritus organic layer pore water (deorgw), detritus organic layer solid phase (deorgs), 0–5 cm surface sediment pore water (sed0w), 0-5 cm surface sediment solid phase (sed0s), 5-20 cm sediment pore water (sed5w), 5-20 cm sediment solid phase (sed5s), fallen litter (litter), plant and rhizosphere (plant), and volatile gas phase (gas).

The compartment sw is the free surface water within the wetland cell. Its volume can be calculated by multiplying a correction factor for substrate porosity, the length, the width, and the water depth. The substrate porosity for each plant in the TLDD wetland cells is shown in Table 1.

The compartments deorgw and deorgs are defined as the pore water phase and solid phase, respectively, of the detritus organic compartment. The detritus organic layer overlying the mineral sediments is a loose uncompacted layer, brownish in color and rich in fine decomposed organic materials. This layer is estimated to be about 1 cm in thickness in the wetland cells. Within this layer, a highly reduced environment exists and contains an important sink of Se (Gao et al. 2000). The density (ρ) of this layer was assigned 1.25 kg/m^3 as in typical organic materials and the pore volume (ϕ), 0.5.

Gao et al. (2000) showed that the highest total Se concentrations in the sediment were found in top 5 cm and concentrations dramatically decreased with depth exponentially. The model considers two mineral sediment layers, 0-5 cm (sed0) and 5- 20 cm (sed5) to account for the difference in Se accumulation. In each sediment layer, the model further divides each layer into pore water phase (w) and solid phase (s). Thus, the model has four compartments in sediment: 0-5 cm sediment pore water phase (sed0w), 0-5cm sediment solid phase (sed0s), 5-20cm sediment water phase (sed5w), and 5-20cm sediment solid phase (sed5s). The bulk density (ρ) and pore volume (ϕ) for these two sediment layers are assumed to be 1.9 kg/m^3 and 0.3, respectively.

The fallen litter compartment contains fresh to partially decomposed plant materials. Lin et al. (submitted)) showed that fallen littler is an important sink for the Se in the wetland cells. Fallen litter has a unique characteristic and it is different from either living plants or detritus materials. This compartment serves as a transition state from plant to organic detritus layer. The fallen litter is typically covered by a slimy layer rich in microbes. The density (ρ) was assumed to be the same as detritus organic layer.

Wetland plants are one of the most important compartments in the Se remediation because living plant can uptake Se and metabolizes it into plant tissue or volatilizes it into the atmosphere, and affects its fate in the environment. The decay products of plants intensify reduced conditions and reduce oxidized forms of Se. Also, plants extend from sediment layer, organic detritus layer, and standing water column and even extend above the water surface and this compartment cuts across or interconnects all other compartments. Indeed, the Se concentration in shoots and roots of plants are different (Lin et al., submitted). To simplify the model, one single plant compartment is assigned to include all components of living plant including the

rhizosphere. The plant coverage and plant biomass in each wetland cell were obtained from Lin et al. (submitted) and Terry (2000).

Se can be volatilized and lost to the atmosphere by biomethylation as dimethyl selenide and dimethylselnone (Chau et al., 1976; Cooke and Bruland, 1987). The chemical species of volatilized Se is not considered in the model. The gas compartment in the model is to account for the loss of Se due to volatilization by plants and microorganisms. This gas compartment is treated as outflow for the mass balance calculation.

WATER AND SE MASS BALANCE

Considering the wetland cell as the control volume and treating any fluxes cutting across the boundary of this control volume as inputs and outputs, the global mass balance of water can be seen in Fig. 2. By mass conservation and steady state assumption, $dV/dt = Qin + Qout + Qprecip + Qseep + Qet = 0$, where Qin is inflow rate, Qout is outflow rate, Qprecip is precipitation rate, Qseep is the rate of seepage loses and Qet is the evapotranspiration rate. Within the compartments of the control volume, mass conservation and steady state assumption also hold. The water flow among the compartments is labeled as q (Fig. 3). In most cases, water outflow from a given compartment becomes water inflow to the adjacent connected compartment. For the plant compartment, water input is uptake from sediment layers and then water output as evapotranspiration to the atmosphere.

We consider two types of Se transfer in the model, physical transfer and chemical transfer. For the physical transfer, Se is transferred from one compartment to another compartment by either water flow as seepage or uptake, or mass flow as fallen litter or physical material breakdown. This transfer does not involve any chemical reaction. For example, Se(VI) can be carried down from standing water into detritus and sediment layers by water flow as seepage. Also, organic Se can be transferred from plant into litter layer as fallen litter and then physical breakdown into standing water and detritus organic layer. The speciation of this physical transfer remains the same. For the chemical transfer, Se can be transformed from one species to other and its physical status can be changed. For example, soluble Se(VI) can be reduced to Se(IV) and finally reduced to insoluble elemental Se. Both physical and chemical transfers have to be considered within the compartment and within the control volume. A series of ordinary differential equations for the chemical reactions and physical mass balance are written to describe both processes. The formulations for the Se transformation within each compartment are discussed in the later section.

Model Formulation for Precipitation and Evapotranspiration

The rate of precipitation and evapotranspiration can be estimated by daily weather data from California Irrigation Management Information System (CIMIS), maintained by the California Department of Water Resources. The rate of rain falling into the wetland system can be obtained by multiplying the average daily precipitation rate for that month with the area of the wetland cell. For the rate of evapo-transpiration, Qet, can be obtained from Qet=ET*Kc*surface area, where ETo is the reference evaporation rate, and Kc is the crop coefficient. Crop coefficient is a dimensionless number and varies between 0.1 and 1.2. For free water body, Kc was assumed to be 1.2. Both the precipitation and the reference evapotranspiration rate were obtained from a nearby weather station at Stratford, CA. The time increment taken in the model is daily intervals but for precipitation and evapotranspiration an average daily value is used for the specified month.

Model Formulation for Seepage Loss

Seepage losses can be calculated by simple mass balance: Qseep = Qin + Qprecip – Qout – Qet. This closure approach was validated with observed seepage rates (Gao et al., submitted). With the calculated Qseep in the model, we use Darcy's Law to estimate apparent hydraulic conductivity in the TLDD wetland and effective hydraulic conductivity (Keff) in the modeling TLDD is 0.0354 m/day.

Model Formulation for Se Transformation

The pathways of Se transformation (i.e., Se(VI) reduced to Se(IV) and then further reduced to elemental Se or organic Se) in each compartment are basically the same, but with different reaction rates. Herbel et al. (submitted) suggested that the transformation of organic Se to elemental Se is the dominant transformation pathway but two pathways, Se(IV) to Se(0) and organic Se to Se(0), are considered in this model.

Figures 4 and 5 respectively illustrate Se transformation in pore water phase and solid phase of the detritus organic layer. As seen in Figure 3, there are three Se soluble species in the pore water phase, Se(VI), Se(IV) and organic Se, as indicated inside rectangular box. The superscript on the right hand side of the Se symbol indicates its chemical form or its oxidation state. The subscript indicates its presence in the specified compartment. For instance, Se^{VI}_{deorgw} represents Se(VI) in the organic detritus layer pore water phase. Also, the diagrams show Se species in other compartments, which are not marked with a rectangular box, indicating it is either an inflow or outflow as given by the arrows.

For each Se species, the dotted line indicates reaction transformation. In this model, all chemical reactions are assumed to obey first-order kinetics and a reaction constant, k, corresponding to its transformation is assigned above the dotted line. A number is assigned for each reaction in the compartment with the superscript and the subscript indicates its compartment. In addition, soluble Se can be carried into other compartments by water flow, q. The superscript on the right side of q indicates its original water compartment and the subscript indicate the type of water flow.

Figure 5 describes Se transformations in the organic detritus layer solid phase, deorgs. In addition to the three soluble species, an insoluble elemental Se is included. The soluble species in the solid phase compartment is assumed to be bound to mineral and humic materials that are not mobile. Also, the solid materials can be carried into standing water compartment and such mass transfer is denoted as Wdeorg-sw. For each species, a mass balance equation, in terms of rate change, to account for both reaction transformation and mass transfer, is written as shown in Figures 5 and 6. A total of 33 ordinary differential equations are written to account for all the chemical reactions and physical transfer within and among all 10 compartments.

Model Formulation for Temperature Effect

All reaction rate constants are based on 20°C reference temperature. The Arrhenius equation is used to consider effects of change in temperature on the reaction rate constant by $k(T) = k(20)\theta^{T-20}$, where k is the reaction rate constant in day^{-1}, T is the temperature in Celsius, and θ is a dimensionless constant. In the program, we set $\theta = 1.072$, which corresponds to a doubling of the rate for a temperature rise from 10°C to 20°C. The temperature used is water temperature that was monitored weekly and not air temperature.

MODEL PROGRAM

A Fortran program is written to solve the first-order system of ordinary differential equations numerically. The Fourth-order Runge-Kutta (R-K) method is used for starting the integration for the first three increments. Then, to carry out the final increments of integration, the routine switches to a more stable scheme, the Adams-Bashforth-Moulton (ABM) predictor-corrector method. The details of the mathematics of the numerical solution can be found in almost any numerical analysis textbook and was successfully used by Mehran and Tanji (1974) for simulating N transformations. In order to obtain a unique solution, initial values were assigned. We have used a time increment (step size) of 0.1 day, which gives stable solution.

To account for longitudinal changes in the wetland cells, and to evaluate the potential of different physical setting in the wetland cells, the model may be subdivided into sub-cells as shown in Figure 6. We have divided each wetland cell into five sub-cells, corresponding to the comprehensive sampling of September 2000. Indeed, each sub-cell functions as an individual control volume and the computer will solve the 33 ordinary equations with the ten compartments and provide an outflow flow as the input flow for the next sub-cell.

MODEL CALIBRATION, VALIDATION AND SENSITIVITY ANALYSIS

Most of the model parameters were obtained in previous field studies. Average monthly volatilization rates of Cell 1 to Cell 7 were provided by the research group of Norman Terry at UC Berkeley. The average plant biomass within each cell was obtained from Terry (2000). Se speciation within plants, fallen littler and organic detritus layer are obtained from Lin et al., (submitted) and Gao et al. (submitted). For all the soil parameters and Se speciation in standing water and mineral sediments compartments, the study from Gao et al. (submitted) were used. Not all the rate constants of Se transformation in the field study are available in the literature. Based on some rate constants from other studies (Arbestain and

Rodriguez Aros, 2002; White et al., 1994; Long et al., 1990), we have made a basic assumption that $k = 1\ day^{-1}$ for fast reactions, $0.01\ day^{-1}$ for moderately fast reactions and $0.001\ day^{-1}$ for slow reactions. Then, the Se transformation rates within each compartment are predicted by trial and error. The field data of Cell 4 (Smooth cordgrass) from Gao et al. (submitted) was used for model calibration and the final rate constants used in the model are listed in Table 2.

To validate the model, three sets of data from Gao et al. (submitted) are used. The first data set is the mass distribution within a cell and the second set is the Se speciation within each compartment. Cells 5, 6 and 7 are examined. The results are shown in Figs, 7, 8 and 9. The third set of data is the total Se mass in the surface water along the distance from the inlet of a wetland cell. Cells 4 and 5 are examined and the results are shown in Fig. 10. In the sensitivity analysis, attention is focused on the distribution of Se in different compartments per unit change of physical parameters of a wetland cell. This is the slope of each line in Figure 11. The slope of the outflow water is the greatest among other compartments when the physical dimensions of a cell or its inflow rate change. The total Se mass in outflow water can be interpreted as Se removal efficiency of a wetland and the analysis showed that it is sensitive to the physical settings of a wetland.

DISCUSSION

The performance of a wetland for remediation of Se-contaminated water and the fate of Se in a wetland depend on its biological and physical settings. With the simulation model, we can examine the physical parameters to obtain suitable physical settings for optimal Se removal efficiency and to predict Se distribution in a wetland. Considering the inflow rate in Cell 5 as an example, the field measurement showed that average flow rate is $31.4\ m^3day^{-1}$ and the total Se in outflow water is about 30% of total Se input after about 1200 days operation from May 1997 to September 2000. We simulated the wetland processes with different inflow rates, and the changes of Se distribution in some compartments are illustrated in Figure 11a. First we note that the total Se in the outflow water increases monotonously and Se accumulated in detritus layer and sediment layers decreases gradually with an increase in the rate of inflow water. More than 50% of total input Se passes through the wetland as outflow water if the inflow rate is more than $60\ m^3day^{-1}$ in Cell 5. Also, the model can predict the minimum rate of inflow water to avoid drying by evapotranspiration and seepage. For Cell 5, the minimum inflow rate is $22\ m^3day^{-1}$. Such low inflow rate can increase the mass accumulated in a wetland and reduce the outflow Se to 13%. At first glance, low inflow rate may have greater Se reduction. However, a decrease of the inflow rate decreases the volume of water to be treated. With the rate of $22\ m^3day^{-1}$, 26,400 m^3 of water can be treated in 1,200 days and 379 g Se are removed from the inflow water. In contrast, 72,000 m^3 of water can be treated in 1,200 days with $60\ m^3day^{-1}$ and 599 g Se are removed from the treated water.

The physical dimensions of a wetland can also affect the Se distribution in a wetland. We simulated the processes with different water depths and longitudinal lengths, and the results are shown in Figure 11b and 11c, respectively. Either the increase of water depth or longitudinal length of a wetland can reduce the total mass of Se in the outflow water and increase the accumulated mass of Se in the compartments of a wetland. With an increase of water depth from 0.01 m to 0.25 m, the total Se in the outflow water drops from 80% to 10%. With greater water depth, the hydraulic head of standing water increases and the seepage flow rate will also increase. The accumulate Se mass in seepage water can approach almost 10% with water depth at 0.25 m to 0.1% with water depth at 0.01 m. The increases of the seepage flow also allow more water passing through sediment layers and more Se can be adsorbed and accumulated in the sediment layers. With an increase of the longitudinal length, the total area of a wetland increases. The increase of area can increase the Se loss in volatilization and seepage.

Changing the physical setting actually changes the resident time of water in a wetland and it is one important control factor on the total mass and the concentration of Se in the outflow water. Resident time (t_R) of water in a wetland can be simply calculated by $t_R = V\varepsilon/Q$, where V is the volume of standing water, ε is the substrate porosity for plant volume correction, and Q is the inflow rate. By increasing the water depth or the length of a wetland, or decreasing the inflow rate, t_R will be increased. Consequently, the total mass of Se in the outflow water decreases. In general,

the Se in the outflow decreases with increases of t_R.

In addition to investigating the physical settings of wetland cell on the Se removal efficiency, the simulation model provides an insight to Se biogeochemistry within the wetland cell. Figures 12, 13 and 14 show the Se distribution in Cell 5 (Rabbitsfoot grass) and the variation of each Se species within each compartment. We first note that the dominant species are different in different compartments. As shown, Se(VI) is dominant in standing water, Se(IV) is dominant in detritus organic layer pore water, organic Se is dominant in sediment pore waters, and elemental Se is the major species in all the solid phases. Second, the seasonal climate or temperature effects play an important role on the Se speciation. All the rates of Se transformations reach their maximum in the hot summer and the reactions are slowest rates in the cold winter season. These seasonal changes can change the major Se speciation within each compartment and eventually affect the Se removal efficiency. For instance, in the standing water compartment, Se(VI) is the dominant species in winter, but Se(VI), Se(IV) and Se(org) are in equal amounts in summer. Also, according to the model, the detritus organic layer, sediment layer solid phases, fallen litter and plants can immobilize Se and accumulate it into these compartments. Most of the forms are in elemental Se except the plant compartment, in which Se(VI) is the major species. Among the compartments, the detritus layer solid phase is the important Se sink.

In the model calibration, rate constants of Se transformation were determined by trial and error and the results were summarized in Table 2. The rate constants of Se transformation ranged from 10^{-6} day^{-1} for Se(IV) to Se(VI) in the plant compartment, to 2.5 day^{-1} for Se(IV) to organic Se in detritus organic layer solid phase. Among the compartments, the detritus organic layer had the highest Se reaction rates in all the Se transformations, and most of the reaction is in the fast reaction regime ($k \geq 1$ day^{-1}). The reactions in the compartments of standing water, 0-5 cm sediment, and 5-20 cm sediment are in the moderately fast rate reaction regime ($k \approx 0.1$ day^{-1}). Most of the reactions in the compartments of fallen litter and plants had the lowest reaction rate constants, less than 10^{-3} day^{-1}. Previous studies showed that the Se rate coefficients ranged from 0.01 - 0.5 day^{-1}. For instance, White et al. (1994) showed that Se reduction coefficient is about 0.1 day^{-1} in groundwater systems; and Long et al. (1990) showed that it is about 0.01 to 0.1 day^{-1} in pond sediment. Losi and Frankenberger, Jr (1998) showed that the Se removal coefficient is 0.3 - 0.5 day^{-1} under laboratory conditions. Also, another computer modeling study (Camps Arbestain and Rodriguez Aros, 2002) indicated that $k = 0.13$ day^{-1} for Se(VI) to Se(IV) and $k = 0.52$ day^{-1} for Se(IV) to Se(0). In comparison to these, all the rate constants used in our model are in the reasonable range even though the rate constants in the detritus organic layer are in the higher end.

In designing the model, several assumptions have been made to simplify the calculations. These assumptions may limit the usage of the model. For example, the model assumed a plug flow reactor type and complete mixing or uniform distribution in each compartment. However, the water inlet is located in the center of a wetland as a point and the flow in the middle is higher than the edges. Also, a stagnant area may occur, in a wetland with greater width. Greater water depth also can create vertical stratification and the complete mixing assumption may not be valid. For the biological parameters, biomass, growth rate and death rate, and area coverage of plants are assumed constant in all seasons, and only the volatilization rate is based on monthly basis. Fortunately, the plant related compartments such as plant, fallen litter and volatilization are not major sinks for Se and each compartment only accumulated less than 5% of total input Se.

SUMMARY

A mathematical model was developed to predict the fate of Se in a remediation wetland system in Tulare Lake Drainage District at Corcoran, Central California. Based on mass balance and first order kinetics, 33 ordinary differential equations are proposed for modeling Se transformation and transport within the ten compartments of a wetland. A Fortran program based on 4th order Runge-Kutta method is written to solve the set of ordinary differential equations simultaneously. The model program are successfully calibrated and validated with field measurements. With this model, we can also examine the physical parameters of a wetland for design and predict the mass distribution of Se and the speciation in each compartment of a wetland cell.

■ ■ ■ ■ ■

REFERENCES

Arbestain, M. C., and A. R. Aros (2001). Modeling selenium transfer in straw amended soils. Soil Science 166(81): 539-547.

Chau, Y.K., P.T.S. Wong, B.A. Silverberg, P.L. Luxon, and G.A. Bengert (1976). Methylation of selenium in the aquatic environment. Science (Washington, DC) 192: 1130-1131.

Cooke, T.D., and K.W. Bruland (1987). Aquatic chemistry of selenium: Evidence of biomethylation. Environ. Sci. Technol. 21: 1214-1219.

Gao, S., K.K. Tanji, Z. Lin, N. Terry, and D.W. Peters (Submitted). Selenium removal and mass balance in a constructed flow -through wetland system.

Gao, S., K.K. Tanji, D.W. Peters, and M.J. Herbel (2000). Water selenium speciation and sediment fractionation in a California flow-through wetland system. J. of Environ. Qual. 29(41): 1275-1283.

Herbel, M. J., T.M. Johnson, K.K. Tanji, S. Gao, and T. D. Bullen (Submitted). Selenium stable isotope ratios in California agricultural drainage water management systems.

Lin, Z. N. T., S. Gao, K.K. Tanji, I.J. Pickering, P. Fox, H.S. Hussein (Submitted). Partitioning and speciation of selenium in 4-year old constructed wetlands treating agricultural tile-drainage water in central California.

Long, R. H., S.M. Benson, T.K. Tokunaga, and A. Yee (1990). Selenium immobilization in a pond bottom sediment at Kesterson Reservoir. J. of Environ. Qual. 19(1): 302-311.

Losi, M.E., and W.T. Frankenberger, Jr. (1994). Reduction of selenium oxanions by Enterobacter cloacae Strain SLD 1a-1. Environmental Chemistry of Selenium. W. T. Frankenberger, Jr. and R.A. Rngberg, R.A. ed. New York, Marcel Dekker, Inc: 514-544.

Mehran, M., and K.K. Tanji (1974). Computer modeling of nitrogen transformations in soils. J. of Environ. Qual. 3(41): 391-396.

Oremland, R. S. (1994). Biogeochemical transformations of selenium in anoxic environments. Selenium in the environment. W. T. Frankenberger, Jr. and S. Benson ed. New York, Marcel Dekker, Inc: 389-420.

Tanji, K., and S. Gao (2001). Selenium removal and mass balance in a constructed flow-through wetland system. p.105-132. *In* UC Salinity/Drainage Program Annual Report 2000-2001. University of California, Center for Water Resources.

Terry, N. (1997). Use of flow-through construction wetlands for the remediation of selenium in agricultural tiled-drainage water. p. 106-123. *In* UC Salinity/Drainage Program Annual Report 1999-2000. University of California, Center for Water Resources.

Terry, N. (2000). Use offlow-through constructed wetlands for the remediation of selenium in agricultural tiled-drainage water. p.192-227. *In* UC Salinity/Drainage Program Annual Report 1996-97. University of California, Center for Water Resources.

White, A. F., and N. M. Dubrovsky (1994). Chemical Oxidation-Reduction Controls on Selenium Mobility in Groundwater Systems. Selenium in the Environment. W.T. Frankenberger, Jr. and S. Benson. New York, Marcel Dekker, Inc: 185-221.

Zawislanski, P. T., and M. Zavarin (1996). Nature and rates of selenium transformations: A laboratory study of Kesterson reservoir soils. Soil Sci. Soc. Am. J. 60(1): 791-800.

Zhang, Y., and J.N. Moore (1996). Selenium fractionation and speciation in a wetland system. Environ. Sci. Technol. 30(1): 2613-2619.

APPENDIX - NOMENCLATURE

FLOW PARAMETERS

Qin	(m^3 day^{-1})	volumetric inflow rate into control volume
Qout	(m^3 day^{-1})	volumetric inflow rate out of control volume
Qseep	(m^3 day^{-1})	seepage rate out of control volume
Qet	(m^3 day^{-1})	evapotranspiration rate out of control volume
q_e	(m^3 day^{-1})	evaporation rate from standing water
q^{sed0}_{uptake}	(m^3 day^{-1})	water uptake by plants from compartment 0-5 cm sediment
q^{sed5}_{uptake}	(m^3 day^{-1})	water uptake by plants from compartment 5-20 cm sediment
q^{sw}_{seep}	(m^3 day^{-1})	seepage rate from compartment standing water
q^{deorg}_{seep}	(m^3 day^{-1})	seepage rate from compartment detritus organic layer
q^{sed0}_{seep}	(m^3 day^{-1})	seepage rate from compartment 0-5 cm sediment layer
q^{sed5}_{seep}	(m^3 day^{-1})	seepage rate from compartment 5-20 cm sediment layer
q_t	(m^3 day^{-1})	transpiration rate from plants
$W_{deorg-sw}$	(kg day^{-1})	mass transfer rate from detritus organic layer to standing water
$W_{litter-sw}$	(kg day^{-1})	mass transfer rate from fallen litter to standing water
$W_{litter-deorg}$	(kg day^{-1})	mass transfer rate from fallen litter to detritus organic layer
W_{plant}	(kg day^{-1})	mass transfer rate from plants to fallen litter

SELENIUM SPECIATION

Se^{VI}_{sw}	(mg m^{-3})	concentration of Se(VI) in standing water
Se^{IV}_{sw}	(mg m^{-3})	concentration of Se(IV) in standing water
Se^{org}_{sw}	(mg m^{-3})	concentration of organic Se in standing water
Se^{VI}_{deorgw}	(mg m^{-3})	concentration of Se(VI) in detritus organic layer pore water phase
Se^{IV}_{deorgw}	(mg m^{-3})	concentration of Se(IV) in detritus organic layer pore water phase
Se^{org}_{deorgw}	(mg m^{-3})	concentration of organic Se in detritus organic layer pore water
Se^{VI}_{deorgs}	(mg kg^{-1})	concentration of Se(VI) in detritus organic layer solid phase
Se^{IV}_{deorgs}	(mg kg^{-1})	concentration of Se(IV) in detritus organic layer solid phase
Se^{org}_{deorgs}	(mg kg^{-1})	concentration of organic Se in detritus organic layer solid phase
Se^{0}_{deorgs}	(mg kg^{-1})	concentration of elemental Se in detritus organic layer solid
Se^{VI}_{sed0w}	(mg m^{-3})	concentration of Se(VI) in 0-5 cm sediment pore water phase
Se^{IV}_{sed0w}	(mg m^{-3})	concentration of Se(IV) in 0-5 cm sediment pore water phase
Se^{org}_{sed0w}	(mg m^{-3})	concentration of organic Se in 0-5 cm sediment pore water phase
Se^{VI}_{sed0s}	(mg kg^{-1})	concentration of Se(VI) in 0-5 cm sediment layer solid phase
Se^{IV}_{sed0s}	(mg kg^{-1})	concentration of Se(IV) in 0-5 cm sediment layer solid phase
Se^{org}_{sed0s}	(mg kg^{-1})	concentration of organic Se in 0-5 cm sediment layer solid phase
Se^{0}_{sed0s}	(mg kg^{-1})	concentration of elemental Se in 0-5 cm sediment layer solid
Se^{VI}_{sed5w}	(mg m^{-3})	concentration of Se(VI) in 5-20 cm sediment pore water phase
Se^{IV}_{sed5w}	(mg m^{-3})	concentration of Se(IV) in 5-20 cm sediment pore water phase
Se^{org}_{sed5w}	(mg m^{-3})	concentration of organic Se in 5-20cm sediment pore water
Se^{VI}_{sed5s}	(mg kg^{-1})	concentration of Se(VI) in 5-20 cm sediment layer solid phase
Se^{IV}_{sed5s}	(mg kg^{-1})	concentration of Se(IV) in 5-20 cm sediment layer solid phase
Se^{org}_{sed5s}	(mg kg^{-1})	concentration of organic Se in 5-20 cm sediment layer solid phase
Se^{0}_{sed5s}	(mg kg^{-1})	concentration of elemental Se in 5-20 cm sediment layer solid

Se^{VI}_{litter}	(mg kg^{-1})	concentration of Se(VI) in fallen litter
Se^{IV}_{litter}	(mg kg^{-1})	concentration of Se(IV) in fallen litter
Se^{org}_{litter}	(mg kg^{-1})	concentration of organic Se in fallen litter
Se^{0}_{litter}	(mg kg^{-1})	concentration of elemental Se in fallen litter
Se^{VI}_{plant}	(mg kg^{-1})	concentration of Se(VI) in plant
Se^{IV}_{plant}	(mg kg^{-1})	concentration of Se(IV) in plant
Se^{org}_{plant}	(mg kg^{-1})	concentration of organic Se in plant
Se^{0}_{plant}	(mg kg^{-1})	concentration of elemental Se in plant
Se^{II}_{-gas}	(mg)	mass of volatilized Se

RATE CONSTANTS

k^{1}_{sw}	(day^{-1})	first order rate constant of Se(VI) in standing water to Se(IV) in
k^{2}_{sw}	(day^{-1})	first order rate constant of Se(VI) to Se(IV) in standing water
k^{3}_{sw}	(day^{-1})	first order rate constant of Se(IV) to organic Se in standing water
k^{4}_{sw}	(day^{-1})	first order rate constant of organic Se in standing water to
k^{1}_{deorg}	(day^{-1})	first order rate constant of Se(VI) from detritus layer pore water
k^{2}_{deorg}	(day^{-1})	first order rate constant of Se(VI) to Se(IV) in detritus layer pore
k^{3}_{deorg}	(day^{-1})	first order rate constant of Se(IV) in detritus layer pore water phase
k^{4}_{deorg}	(day^{-1})	first order rate constant of Se(IV) from detritus layer pore water
k^{5}_{deorg}	(day^{-1})	first order rate constant of Se(IV) to organic Se in detritus layer
k^{6}_{deorg}	(day^{-1})	first order rate constant of organic Se in detritus layer pore water
k^{7}_{deorg}	(day^{-1})	first order rate constant of organic Se from detritus layer pore
k^{8}_{deorg}	(day^{-1})	first order rate constant of elemental Se in detritus layer solid
k^{1}_{sed0}	(day^{-1})	first order rate constant of Se(VI) from 0-5 cm sediment layer pore
k^{2}_{sed0}	(day^{-1})	first order rate constant of Se(VI) to Se(IV) in 0-5 cm sediment layer
k^{3}_{sed0}	(day^{-1})	first order rate constant of Se(IV) in 0-5 cm sediment layer pore
k^{4}_{sed0}	(day^{-1})	first order rate constant of Se(IV) from 0-5 cm sediment layer pore
k^{5}_{sed0}	(day^{-1})	first order rate constant of Se(IV) to organic Se in 0-5 cm sediment
k^{6}_{sed0}	(day^{-1})	first order rate constant of organic Se in 0-5 cm sediment layer
k^{7}_{sed0}	(day^{-1})	first order rate constant of organic Se from 0-5 cm sediment layer
k^{1}_{sed5}	(day^{-1})	first order rate constant of Se(VI) from 5-20 cm sediment layer
k^{2}_{sed5}	(day^{-1})	first order rate constant of Se(VI) to Se(IV) in 5-20 cm sediment
k^{3}_{sed5}	(day^{-1})	first order rate constant of Se(IV) in 5-20 cm sediment layer pore
k^{4}_{sed5}	(day^{-1})	first order rate constant of Se(IV) from 5-20 cm sediment layer
k^{5}_{sed5}	(day^{-1})	first order rate constant of Se(IV) to organic Se in 5-20 cm
k^{6}_{sed5}	(day^{-1})	first order rate constant of organic Se in 5-20cm sediment layer
k^{7}_{sed5}	(day^{-1})	first order rate constant of organic Se from 5-20cm sediment layer
k^{1}_{litter}	(day^{-1})	first order rate constant of Se(VI) to Se(IV) in fallen litter
k^{2}_{litter}	(day^{-1})	first order rate constant of Se(VI) to elemental Se in fallen litter
k^{3}_{litter}	(day^{-1})	first order rate constant of elemental Se in fallen litter to Se(IV) in
k^{4}_{litter}	(day^{-1})	first order rate constant of Se(IV) to organic Se in fallen litter
k^{5}_{litter}	(day^{-1})	first order rate constant of organic Se to elemental Se in fallen
k^{1}_{plant}	(day^{-1})	first order rate constant of Se(VI) to Se(IV) in plant
k^{2}_{plant}	(day^{-1})	first order rate constant of Se(VI) to elemental Se in plant
k^{3}_{plant}	(day^{-1})	first order rate constant of Se(IV) to organic Se in plant

k^4_{plant}	(day^{-1})	first order rate constant of organic Se to elemental Se in plant
k^5_{plant}	(day^{-1})	first order rate constant of organic Se in plant to volatilized Se

WETLAND CELL PROPERTIES

M_{plant}	(kg)	total plant biomass in a wetland cell
M_{litter}	(kg)	total fallen litter mass in a wetland cell
M_{deorg}	(kg)	total dry mass of detritus organic layer in a wetland cell
M_{sed0}	(kg)	total dry mass of 0-5 cm sediment layer
M_{sed5}	(kg)	total dry mass of 5-20 cm sediment layer
V_{sw}	(m^3)	total water volume of standing water
V_{deorg}	(m^3)	total water volume in detritus organic layer
V_{sed0}	(m^3)	total water volume in 0-5 cm sediment layer
V_{sed5}	(m^3)	total water volume in 5-20 cm sediment layer
ETo	($mm\ day^{-1}$)	reference evapotranspiration rate
Kc	dimensionless	crop coefficient
ε	dimentionless	substrate porosity
L(i)	(m)	length of a wetland subcell i
W(i)	(m)	width of a wetland subcell i
D(i)	(m)	water depth of a wetland subcell i
A(i)	(m^2)	area of a wetland subcell i

Table 1. Vegetation parameters for different cells.

Cell	Plant Coverage Area	Substrate Porosity (ε)
1	97.2%	0.95
2	94.3%	0.95
3	100%	1.0
4	86.5%	0.95
5	99.5%	0.9
6	95.7%	0.9
7	99.5%	0.9
8	NA	0.99
9	NA	0.95
10	NA	0.9

Table 2. Rate constants used in the computer model.

Compartments	Rate Constant (day^{-1}) k1	k2	k3	k4	k5	k6	k7	k8
standing water (sw)	0.32	0.16	0.1	--	--	--	--	--
detritus organic layer (deorg)	0.001	1.5	0.35	0.15	2.5	1.5	1.5	10^{-4}
0-5 cm sediment (sed0)	0.001	1.3	0.08	0.06	0.8	0.8	0.08	--
5-20 cm sediment (sed5)	0.001	0.2	0.3	0.3	0.3	0.3	0.3	--
fallen litter (litter)	1	0.0015	0.004	0.018	0.004	--	--	--
plants (plant)	10^{-6}	0.0002	0.013	0.0025	--	--	--	--

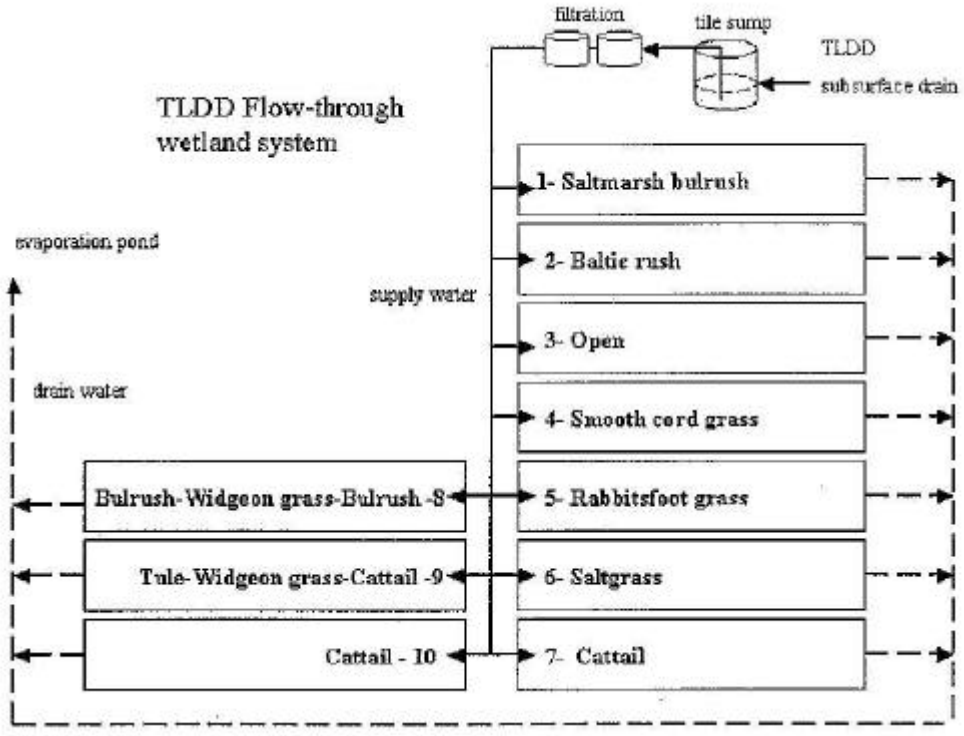

Figure 1. Schematic diagram of the layout of the TLDD flow-through wetland system.

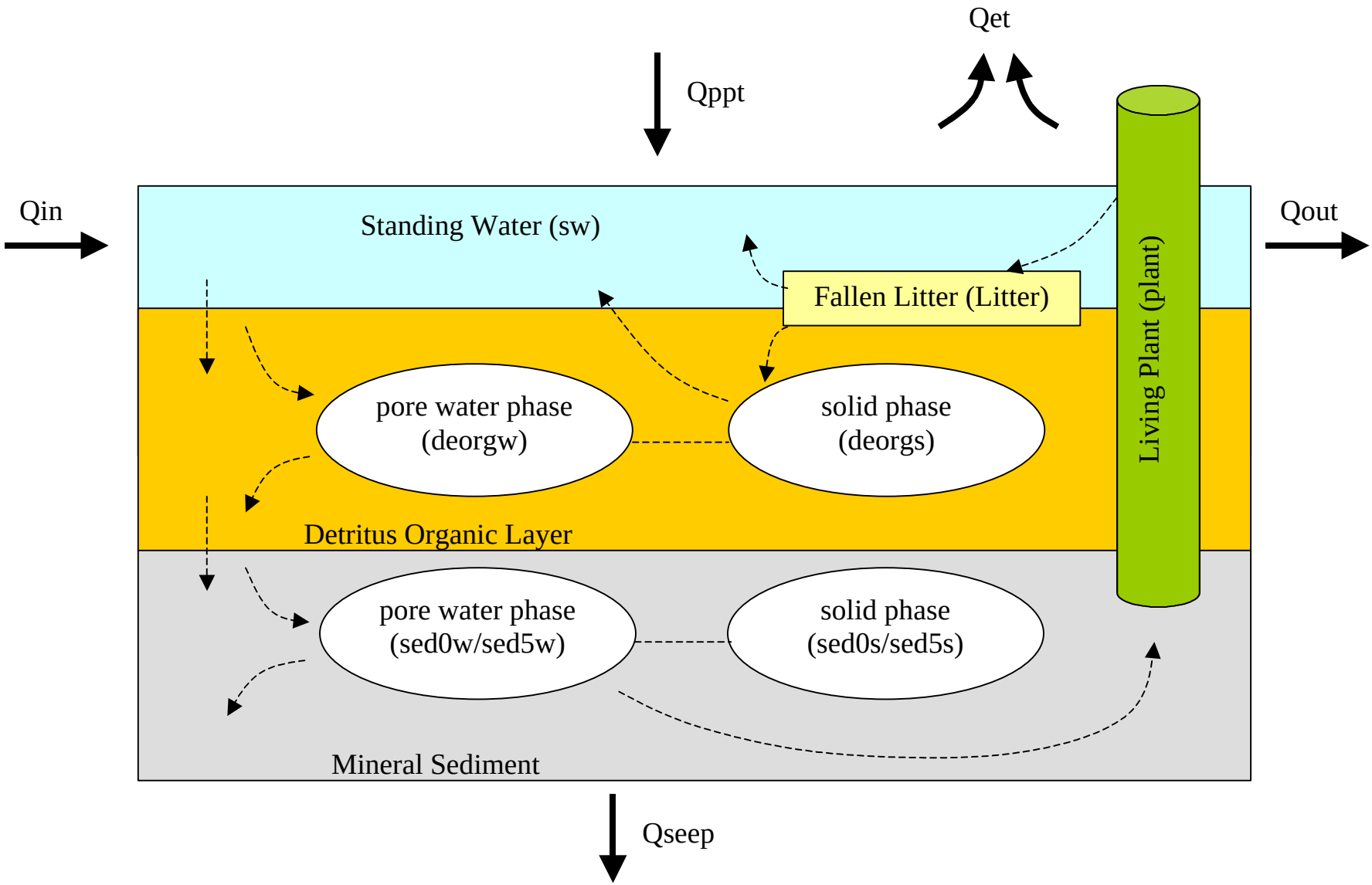

Figure 2. Conceptual model for water flows in a wetland cell. The words inside the brackets represents the abbreviates of corresponding compartments.

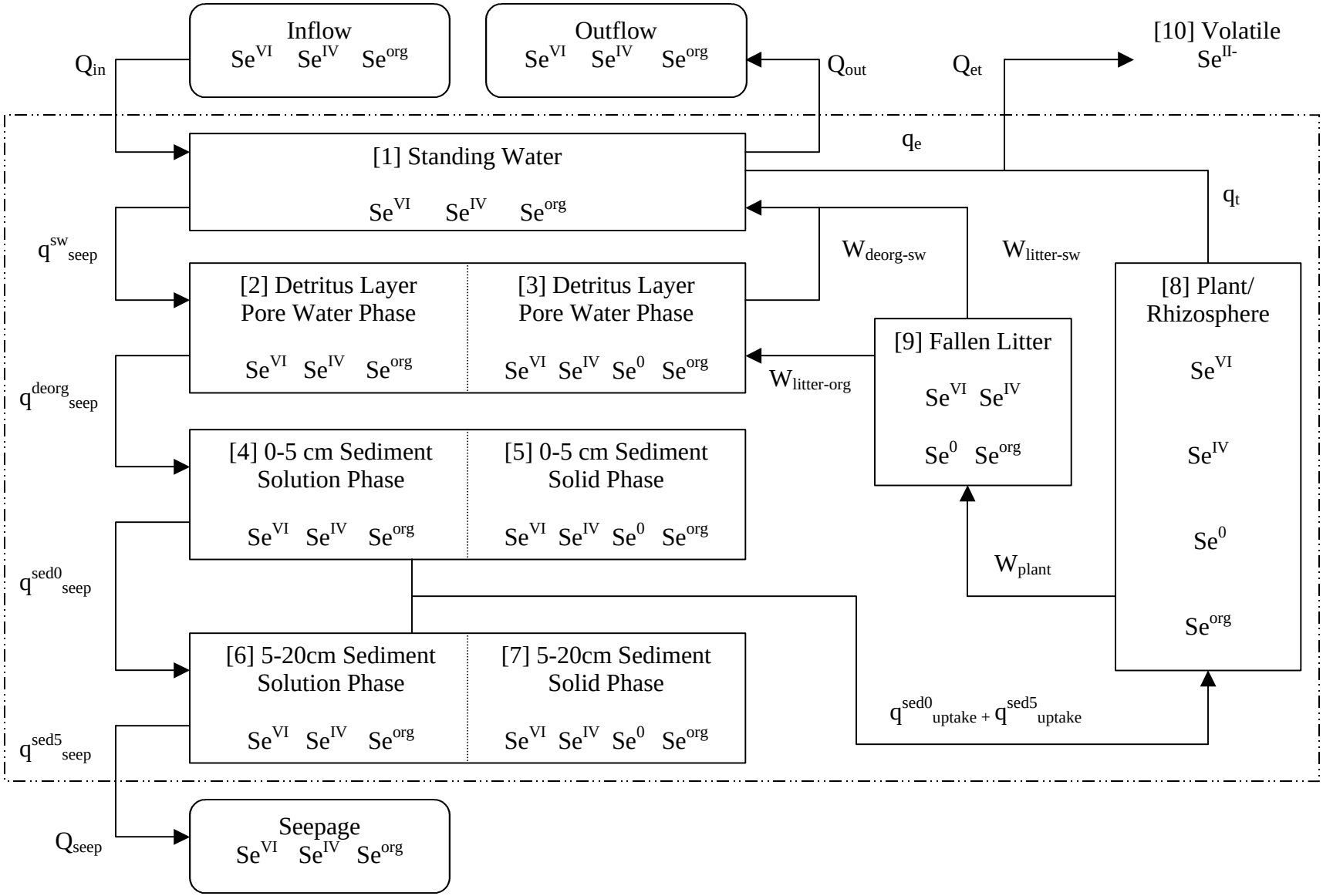

Figure 3. Ten compartments are considered in the model. Dashed line represents the control volume of a wetland cell.

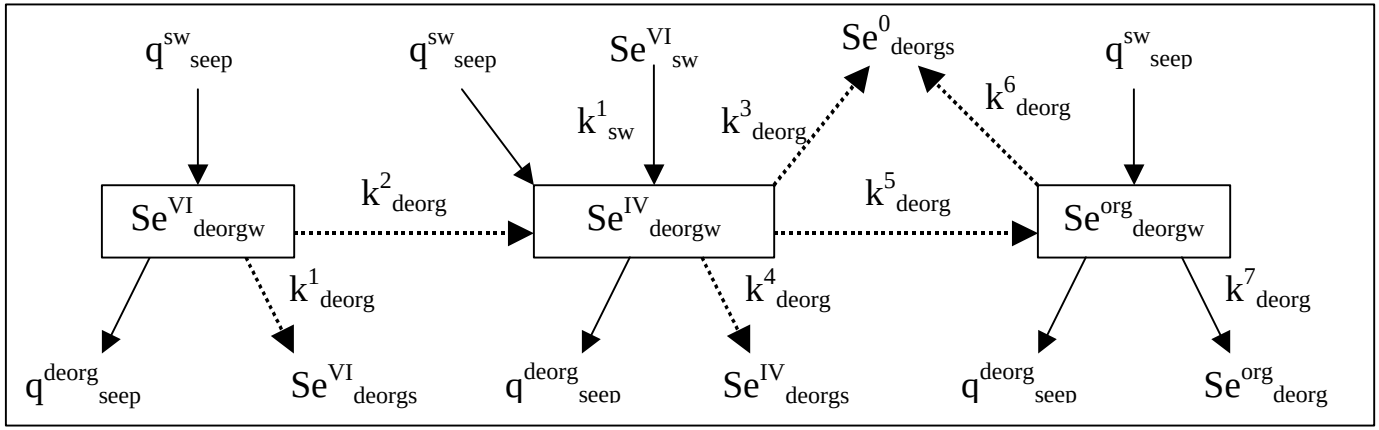

$$V_{deorg}\frac{dSe^{VI}_{deorgw}}{dt} = (q^{sw}_{seep}Se^{VI}_{sw} - q^{deorg}_{seep}Se^{VI}_{deorgw}) - k^{1}_{deorg}V_{deorg}Se^{VI}_{deorgw} - k^{2}_{deorg}V_{deorg}Se^{VI}_{deorgw}$$

$$V_{deorg}\frac{dSe^{IV}_{deorgw}}{dt} = (q^{sw}_{seep}Se^{IV}_{sw} - q^{deorg}_{seep}Se^{IV}_{deorgw}) + (k^{1}_{sw}V_{sw}Se^{VI}_{sw} + k^{2}_{deorg}V_{deorg}Se^{VI}_{deorgw} - k^{3}_{deorg}V_{deorg}Se^{IV}_{deorgw} - k^{4}_{deorg}V_{deorg}Se^{IV}_{deorgw} - k^{5}_{deorg}V_{deorg}Se^{IV}_{deorgw})$$

$$V_{deorg}\frac{dSe^{org}_{deorgw}}{dt} = (q^{sw}_{seep}Se^{org}_{sw} - q^{deorg}_{seep}Se^{org}_{deorgw}) + (k^{5}_{deorgw}V_{deorg}Se^{IV}_{deorgw} - k^{6}_{deorgw}V_{deorg}Se^{org}_{deorgw} - k^{7}_{deorgw}V_{deorg}Se^{org}_{deorgw})$$

Figure 4. Compartment 2: Organic detritus layer pore water phase. Solid line represents mass transfer and dashed line represents Se transformation.

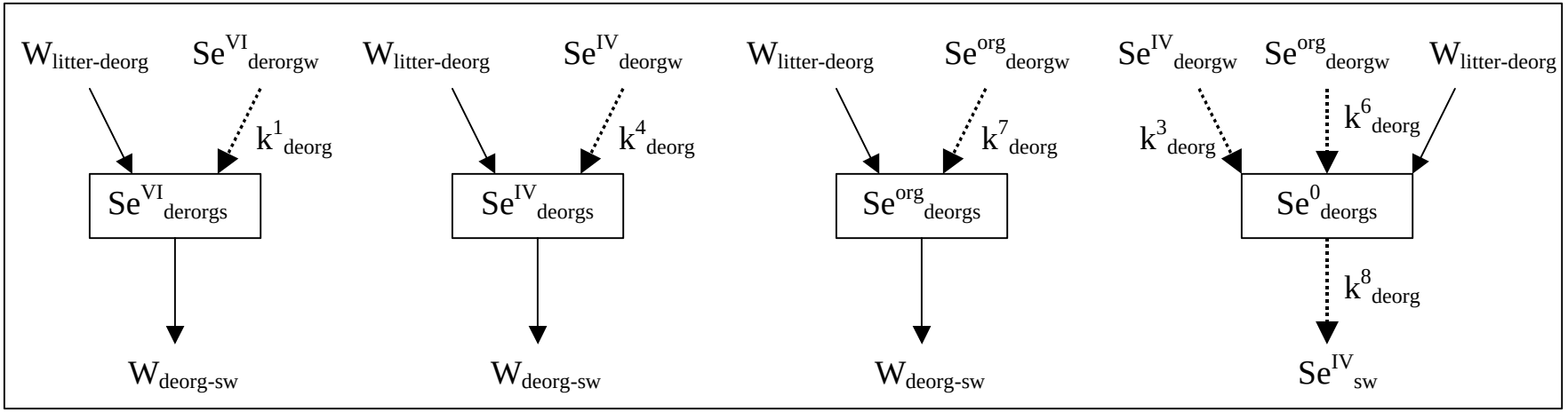

$$M_{deorg}\frac{dSe^{VI}_{deorgs}}{dt} = W_{litter-deorg}Se^{VI}_{litter} - W_{deorg-sw}Se^{VI}_{deorgs} + k^{1}_{deorg-sw}V_{deorg}Se^{VI}_{deorgw}$$

$$M_{deorg}\frac{dSe^{IV}_{deorgs}}{dt} = W_{litter-deorg}Se^{IV}_{litter} - W_{deorg-sw}Se^{IV}_{deorgs} + k^{4}_{deorg}V_{deorg}Se^{IV}_{deorgw}$$

$$M_{deorg}\frac{dSe^{org}_{deorgs}}{dt} = W_{litter-deorg}Se^{org}_{litter} - W_{deorg-sw}Se^{org}_{deorgs} + k^{7}_{deorg}V_{deorg}Se^{org}_{deorgw}$$

$$M_{deorg}\frac{dSe^{0}_{deorgs}}{dt} = W_{litter-deorg}Se^{0}_{litter} - W_{deorg-sw}Se^{0}_{deorgs} + k^{3}_{deorg}V_{deorg}Se^{IV}_{deorgw} + k^{6}_{deorg}V_{deorg}Se^{org}_{deorgw} - k^{8}_{deorg}M_{deorg}Se^{0}_{deorgs}$$

Figure 5. Compartment 3: Organic detritus layer solid phase. Solid line represents mass transfer and dashed line represents Se transformation.

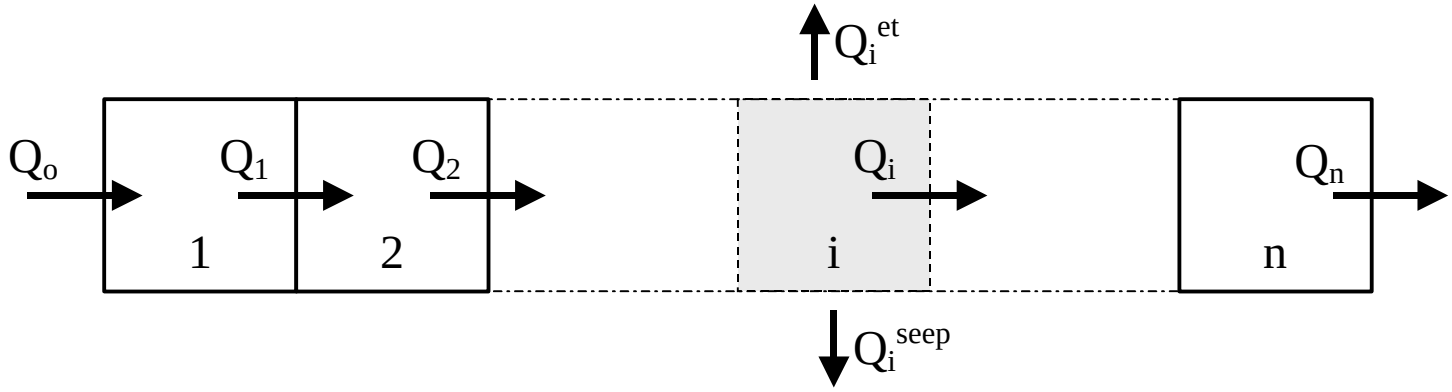

$$Q_i = Q_0 - \sum_{k=1}^{i} Q_k^{et} - \sum_{k=1}^{i} Q_k^{seep}$$

$$Q_i^{et} = ET_o \cdot Kc \cdot A_i$$

$$Q_i^{seep} = K_i^{eff} \cdot A_i \cdot \frac{D_i}{L_i}$$

$$tr_i = \frac{V_i \cdot e}{Q_i}$$

For each sub-cell i:

A_i : Area
D_i : Water Depth
ET_o : Reference Evapotranspiration Rate
Kc: Crop Coefficient
K_i^{eff} : Hydraulic Conductivity
L_i : Depth of Water Table
Q_i^{et} : Evapotranspiration
Q_i^{seep} : Seepage Loss
V_i : Volume of Water Body
tr_i: Resident Time
ε : Substrate Porosity

Figure 6. Schematic for water balance calculation in the model.

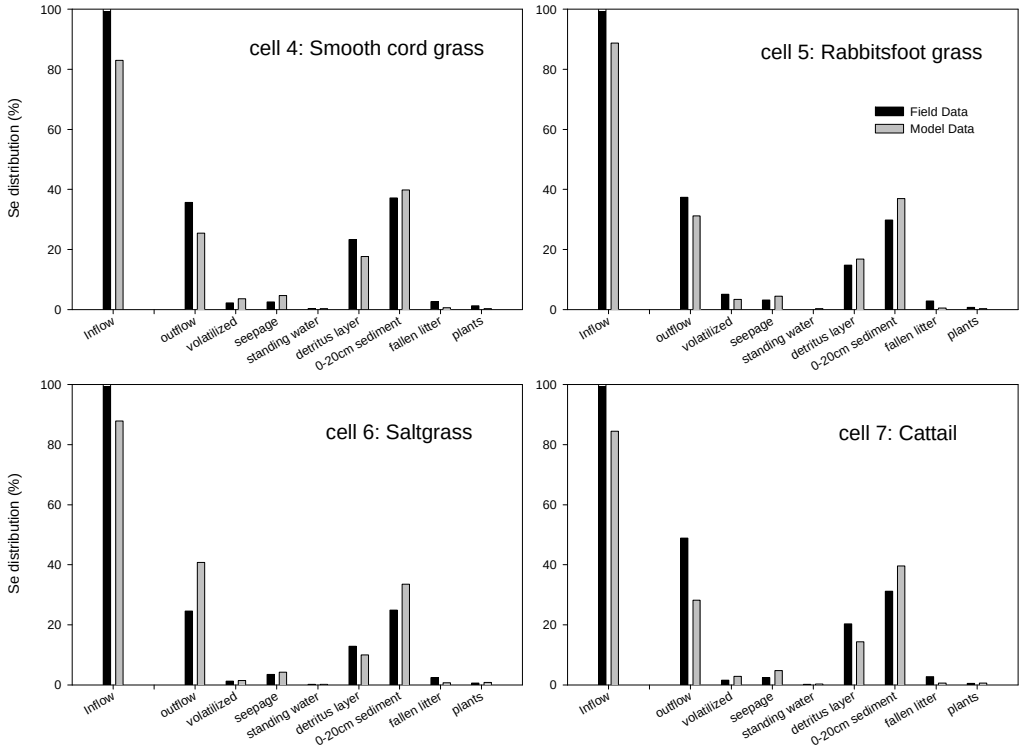

Figure 7. Model calibration and validation: Se mass distribution in different compartments

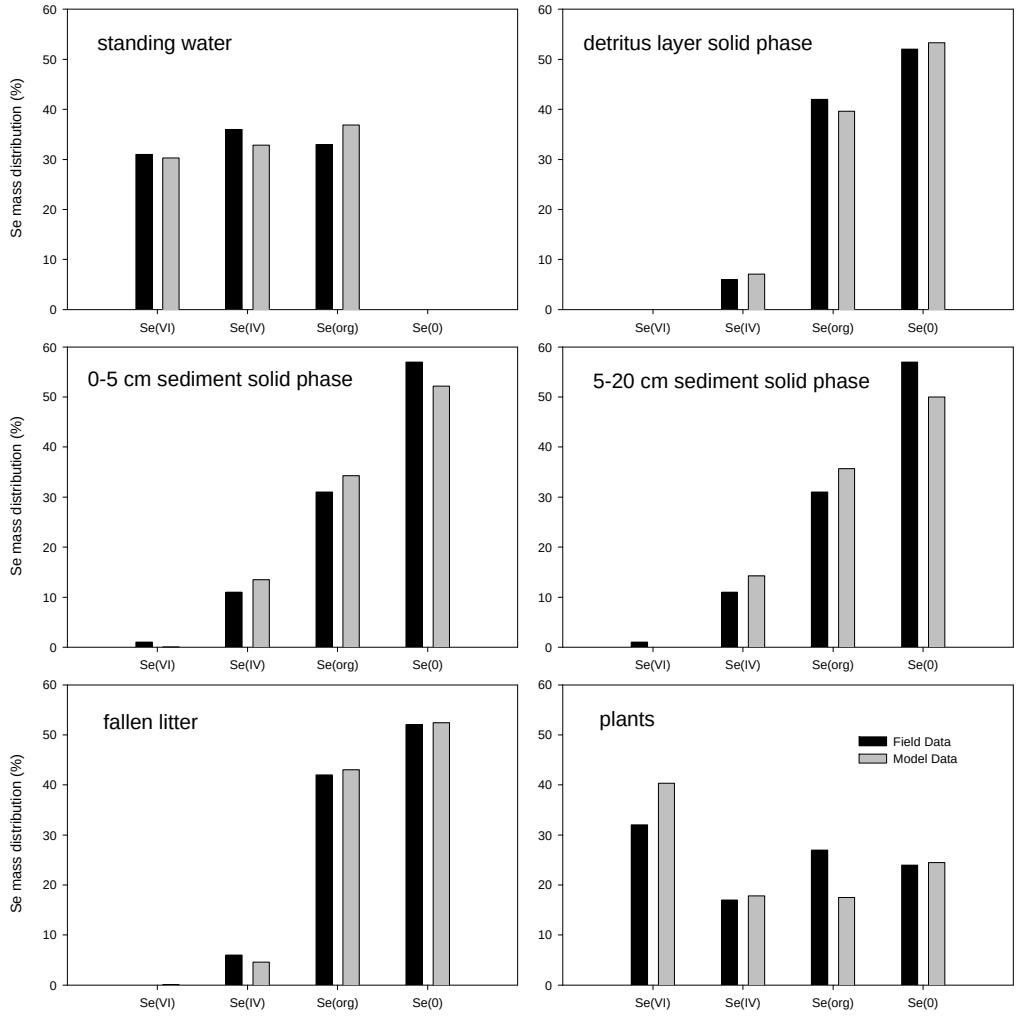

Figure 8. Model validation: Se speciation in different compartments in Cell 4 – Smooth cordgrass.

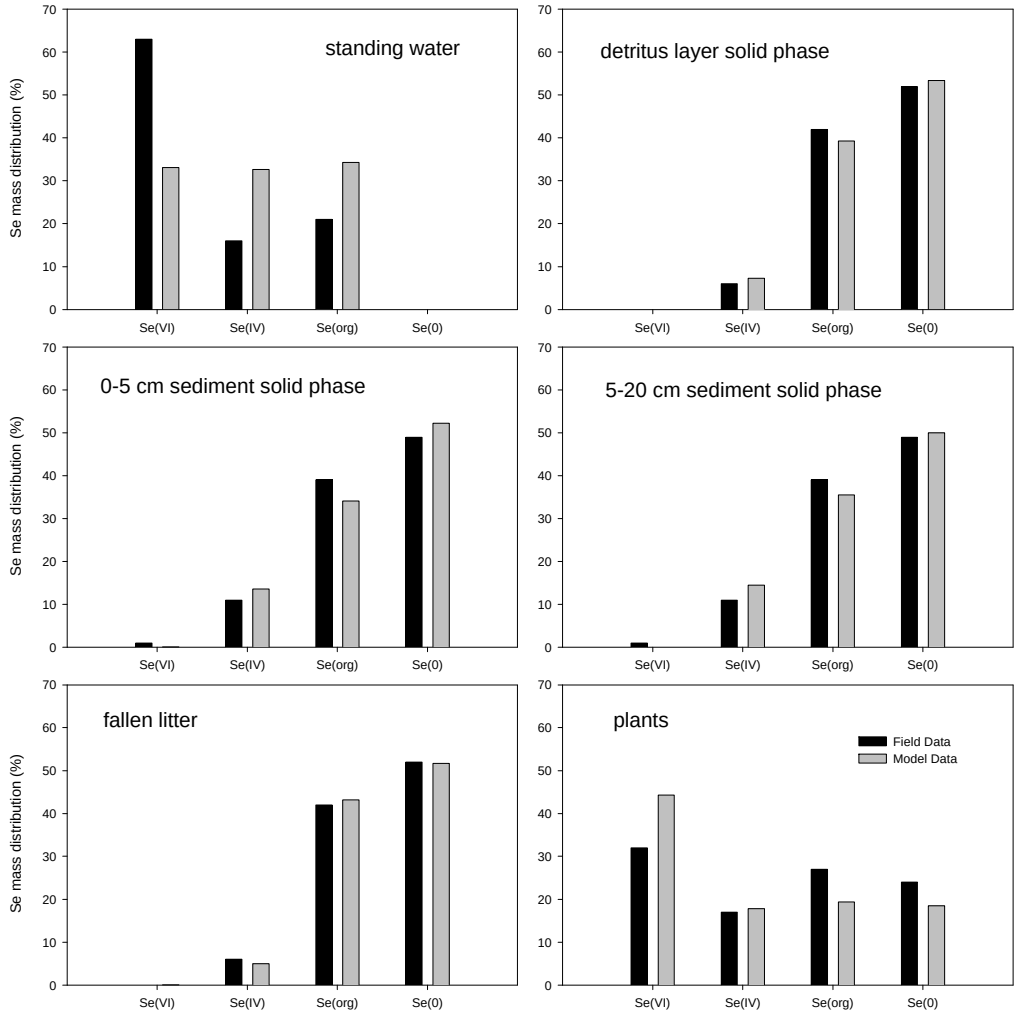

Figure 9. Model validation: Se speciation in different compartments in Cell 5 – Rabbitsfoot grass.

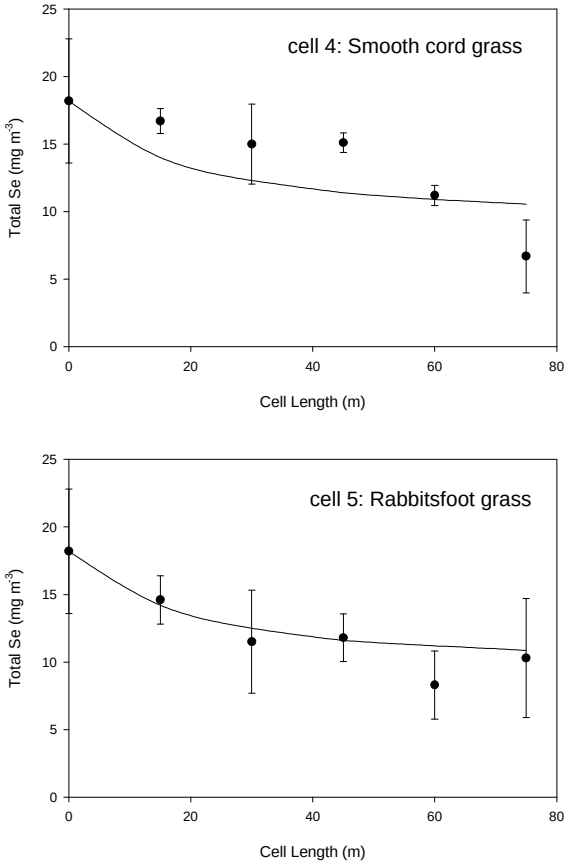

Figure 10. Model validation: Total Se mass in different cell length of Cell 4 (Smooth cordgrass) and Cell 5 (Rabbitsfoot grass).

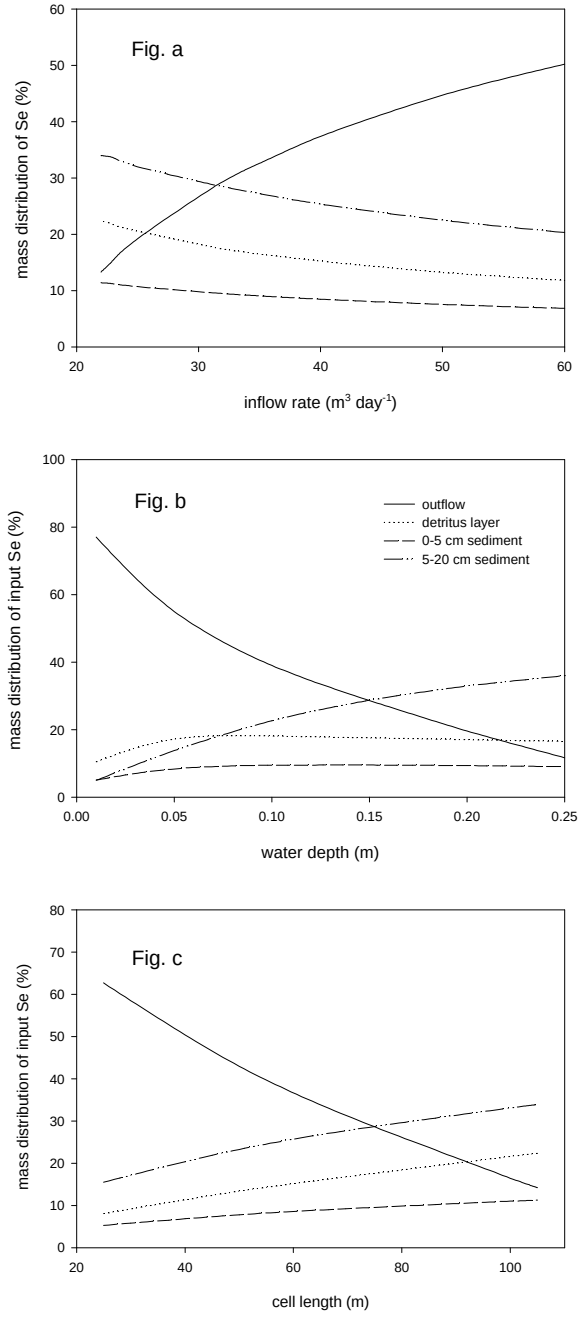

Figure 11. Model simulation predicts Se distribution with different physical setting of the wetland Cell 5 (Rabbitsfoot grass). Fig. 11a demonstrates the effects of the variation of inflow rate; Fig. 11b demonstrates the effects of the variation of water depth; Fig. 11c demonstrates the effects of the longitude length of a wetland cell. The compartments with less than 10% of total input Se are not shown.

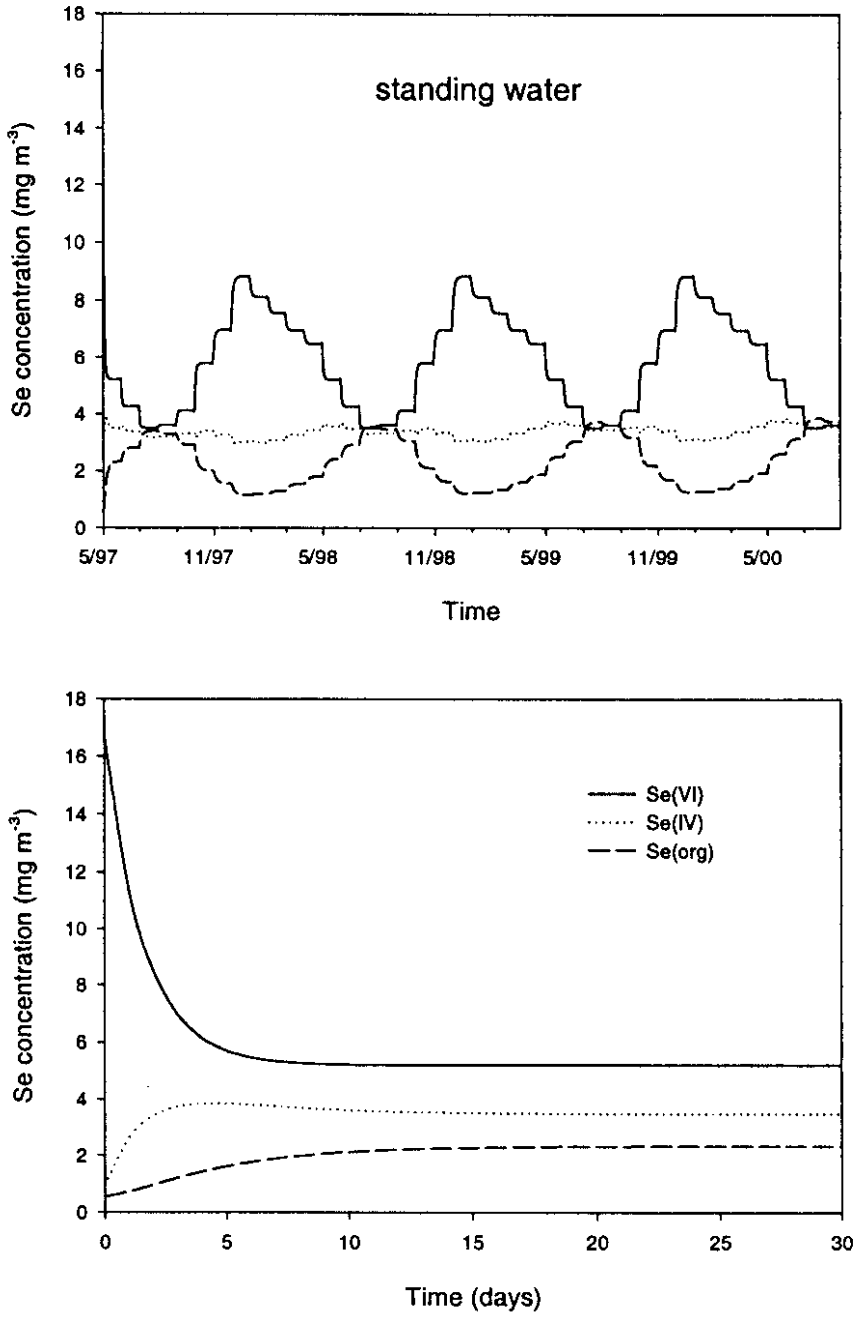

Figure 12. Se speciation in standing water of Cell 5 (Rabbitsfoot grass) for 1200 days and 30 days.

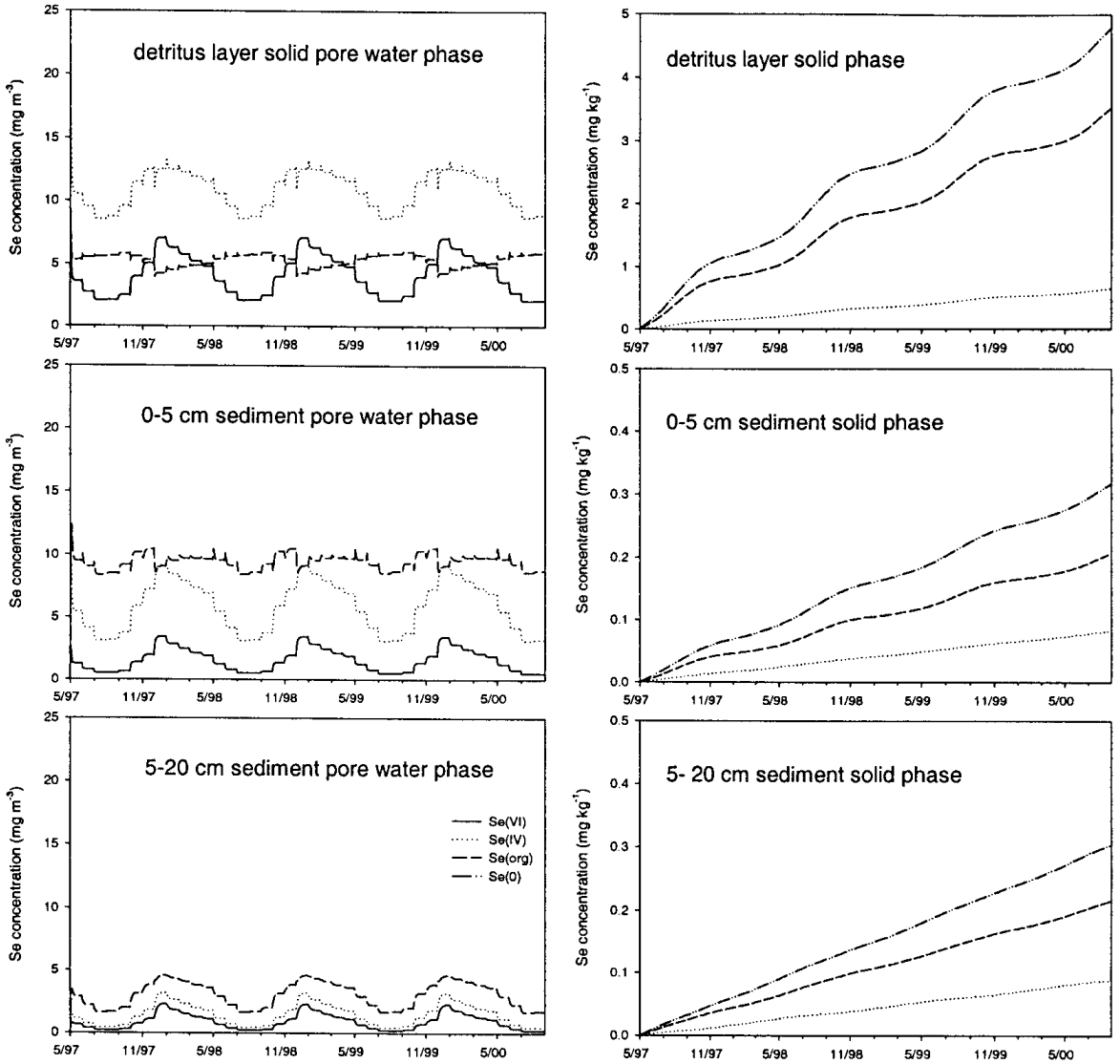

Figure 13. Se speciation in detritus organic layer and sediment layers of Cell 5 (Rabbitsfoot grass).

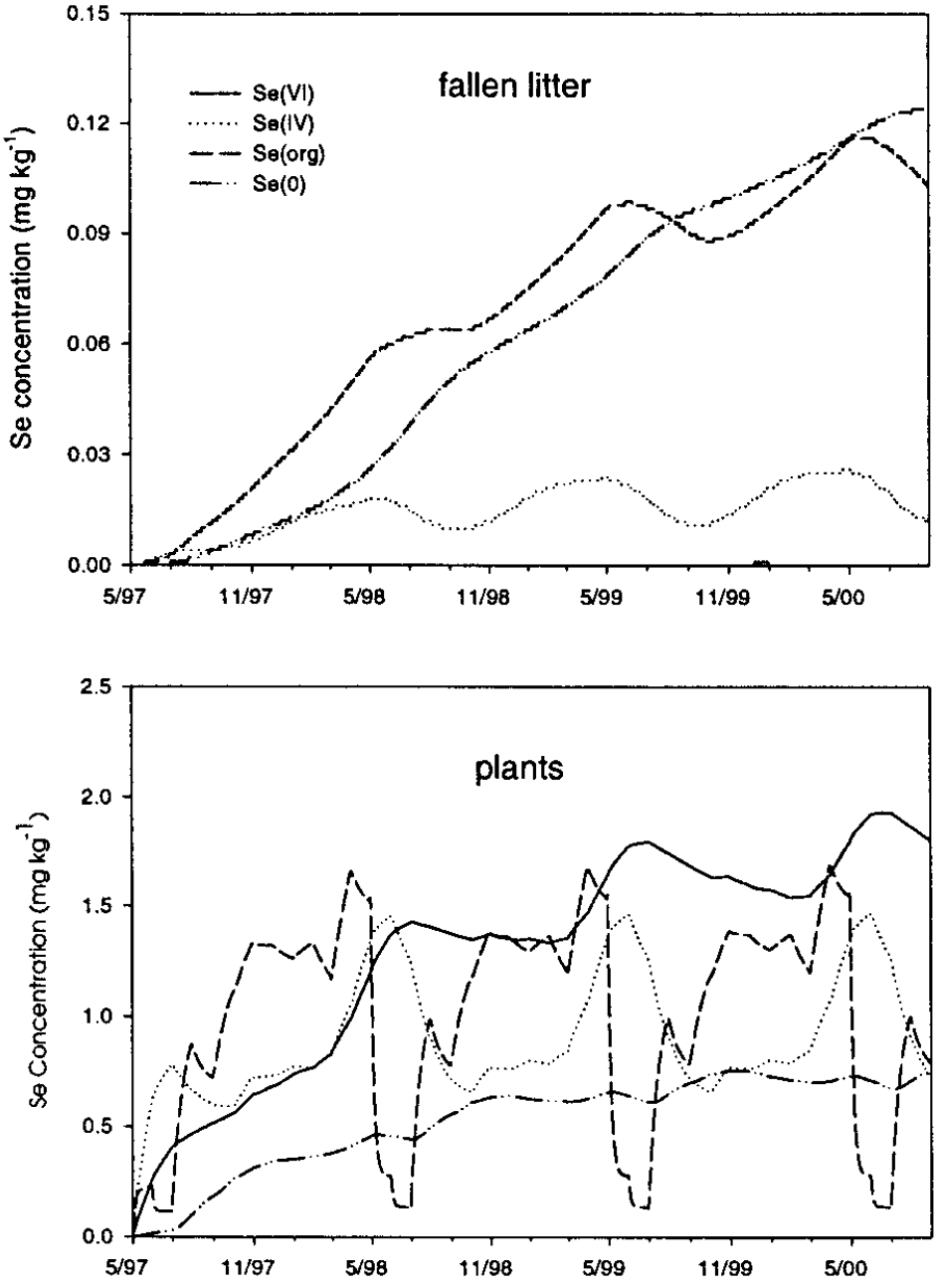

Figure 14. Se speciation in fallen litter and plants of Cell 5 (Rabbitsfoot grass).

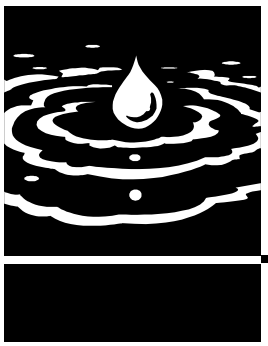

Significance of Selenium Volatilization in Wetlands Treating Se-laden Agricultural Drainage Water

Project Investigator:

Norman Terry
Office: (510) 642-3510, E-mail: nterry@nature.berkeley.edu
Department of Plant & Microbial Biology
University of California, Berkeley

Report Prepared by:

Z.-Q. Lin, D. LeDuc, H. Hussein, and N. Terry

ABSTRACT

Management of selenium (Se)-contaminated agricultural drainage water is one of the most important environmental issues in California. To evaluate the feasibility of utilizing constructed wetlands to remediate Se-laden drainage water and the role of biological volatilization in Se removal, 10 flow-through wetland cells were constructed in 1996 in Corcoran, California. The monthly-monitoring field study, which ran from May 1997 to December 1999, showed that vegetated wetlands were capable of significantly reducing Se from the inflow drainage water; an average 69.2% of the total Se mass in the inflow was removed. Most of the Se was retained in sediment, and <5% of the Se was accumulated in plant tissues. Selenium volatilization was highest in the rabbitfoot grass wetland cell, where 9.4% of the Se input was volatilized over a 2-year period. Volatilization is greater in spring and summer than in fall and winter. For example, in June 1998, 48% of the Se entering the rabbitfoot grass cell was volatilized, while in the summer months of 1999, 20 to 25% of the Se was removed from the cordgrass cell. Results from a rabbitfoot grass wetland microcosm experiment indicated that the presence of the volatilization chamber did not significantly affect the volatilization process. In addition to these results, the feasibility of using constructed wetland for Se remediation, ways of enhancing Se volatilization, and the importance of considering potential Se ecotoxicities are discussed.

KEYWORDS

selenium (Se), fate, volatilization, mass balance, constructed wetland, wetland microcosm

■ ■ ■ ■ ■

INTRODUCTION

Plants and microbes have the ability to take up inorganic forms of Se such as *selenate* and metabolize them to volatile forms consisting mainly of *dimethyl selenide* (DMSe), along with a small proportion of dimethyl diselenide (DMDSe) (Karlson and Frankenberger, 1988). This is referred to as "biological Se volatilization", which plays a significant role in the biogeochemical cycle of Se in aquatic ecosystems (Amouroux and Donard, 1996). From an environmental point of view, Se volatilization is a critically important pathway of Se removal for the following reasons: 1) DMSe has been shown to be ~500 times less toxic than the inorganic forms of Se to rats (McConnell and Portman, 1952; Wilber, 1980); 2) volatilization removes Se from the local ground ecosystem and diminishes the amount of Se available for entry into the food chain (Losi and Frankenberger, 1997; Zayed et al., 2000); and 3) volatile Se produced in the western part of San Joaquin Valley is most likely transported in the atmosphere out of the Valley to the surrounding mountainous regions and to other areas where soil Se is not excessive (Lin et al., 2000).

Despite the importance of volatilization in the remediation of Se-contaminated wastewaters, it remains to be resolved how significant a pathway volatilization is for Se removal by constructed wetlands. Cooke and Bruland (1987) estimated that about 30% of the Se removed from the drainage water in the Kesterson Ponds was released into the atmosphere through biological volatilization. Their estimate however, was not based on actual measurements of volatilization but on the amount of Se that remained unaccountable after other components in their mass balance were determined. Relatively few field studies have been made that actually attempt to measure Se volatilization under naturally occurring wetland conditions, and, in particular, there is little information on the spatial and temporal variation of Se volatilization in aquatic ecosystems (Frankenberger and Karlson, 1994; Hansen et al., 1998). Additionally, these earlier studies were made by measuring volatile Se production from portions of wetland enclosed with transparent collection chambers, a procedure also used in various forms by Biggar and Jayaweera (1993), Hansen et al. (1998), and Lin et al. (1999). The use of volatilization chambers to quantify rates of Se volatilization from an unenclosed field surface might result in a significant underestimation of volatilization rates. This is because volatile Se diffusing from the ground and plant surface might be removed by turbulent airflow more rapidly under normal field conditions than in the confines of a volatilization chamber. However, to our knowledge, there has been no attempt to evaluate such potential aerodynamic effects of the enclosed chamber system on the measurement of Se volatilization.

The goal of the present study was to determine the quantitative importance of Se removal by volatilization in the Corcoran treatment wetlands. The specific objectives were:

1) to quantify the extent to which Se is removed from the wetland through the volatilization pathway, compared with the other pathways of accumulation in sediments or in plant materials, 2) to explore the spatial and temporal variation of Se volatilization from specific wetland cells populated with different plant species, and 3) to evaluate the effects of physicochemical characteristics (pH, EC, DO, temperature, and sulfate concentration) of the surface water in wetlands on Se volatilization and Se removal by the flow-through wetlands. In addition, the accuracy of the collection chamber approach in the measurement of Se volatilization was evaluated by wetland microcosm experiments in which direct measurements of Se volatilization from enclosed microcosms was compared with volatilization rates (calculated by difference from Se mass balance) from unenclosed microcosms.

EXPERIMENTAL SECTION

FIELD STUDY

Flow-through Wetland

The flow-through wetland was constructed in 1996 at Corcoran, California. It consisted of 10 unlined wetland cells 15-m wide and 77-m long (Fig. 1). Cells 1 though 7 and Cell 10 had an even cell depth of 30 cm, while the remaining two cells were excavated with varying cell depths ranging from 30 to 60 cm. After the excavation, the 10 wetland cells were tilled and fertilized with 16-16-16 (N-P-K) type granular fertilizer (~450 g m^{-2}). The wetland cells were then flooded with clean irrigation water, followed by manual transplants of cattail (*Typha latifolia* L.), baltic rush (*Juncus balticus* Willd.), smooth cordgrass (*Spartina alternifolia* Loisel), saltgrass (*Distichlis spicata* (L.) Greene), tule (*Scirpus lacustris* L.), and widgeon grass (*Ruppia maritime* L.) into the cells at a plant spacing of 50 to 100 cm depending on the plant type. Saltmarsh bulrush (*Scirpus robustus* Pursh) and rabbitfoot grass (*Polypogon monspeliensis* (L.) Desf.) were vegetated from seeds. In seven of the 10 wetland cells, monotypic stands of individual wetland plant species were planted, two cells had combinations of plant species, and one cell was left unplanted as a control (Fig. 1).

Measurement of Se Volatilization

Rates of Se volatilization were determined monthly in triplicate in Cells 1 through 7 from September 1997 to August 1999. A detailed description of chamber design, calibration, and application was previously reported by Lin et al. (1999, 2002). Volatile Se in the air from the chamber was trapped using charcoal filters by pulling air at a flow rate of 0.85 m^3 h^{-1} from the chamber through the charcoal filters with a vacuum pump. Selenium volatilization measurements were conducted in each cell over 24 hours. A 24-hour sampling duration takes into account diurnal fluctuations of temperature or other environmental factors that influence the biological process of Se volatilization. The rate of Se volatilization obtained from a 24-hour measurement is comparable to the average rate derived from a 5-day continuous measurement (Lin et al., 2002).

At the end of the collection period, the charcoal filter holders were collected from the chambers and stored in a cooler at 4 °C. The Se-containing charcoal filters were extracted in alkaline peroxide solution as described earlier by Lin et al. (1999), and total Se concentrations in extraction solutions were determined by atomic absorption spectrophotometry (AAS) (Varian, SpectrAA-220FS, with UltrAA lamp and VGA-77 vapor generator) (Ward and Gray, 1996).

Sampling and In Situ Measurements

The sampling and *in situ* measurements began in May 1997, ~10 months after the wetland was initially vegetated, and were conducted monthly through December 1999. Water, sediment, and plant samples were collected from each wetland cell in triplicates. The water sampling (inlet, outlet, and in-cell) consisted of 500-ml samples, and the samples were acidified immediately after collection using trace metal grade concentrated HNO_3 (Byrnes, 1994). Sediments (0-15 cm depth) were collected with a sediment core sampler equipped with a replaceable butyrate liner (30 cm L x 2 cm D) according to the method described by Boulding (Boulding, 1994). Plant samples consisted of aboveground green shoot (leaf and stem), root/rhizome tissues, and standing and fallen litter.

In situ measurements of selected important physio-chemical properties of surface waters, including water pH, EC, DO, and temperature, were carried out in each wetland cell with a Corning Checkmate Modular Testing System. Each measurement was conducted in triplicates. The aboveground plant biomass was determined seasonally by the harvesting method over three

randomly selected 0.25 m^2 areas in each cell, while the underground root biomass was estimated by the ratio of shoot biomass to root biomass of the plant species.

Chemical Analysis of Total Se and Sulfate

Influent and effluent waters were acid-digested with HNO_3 and H_2O_2 according to EPA Method 3010A (US EPA, 1992). Wetland plant samples were dried at 60°C (Carlson et al., 1991) and ground in a Wiley Mill to pass a 0.43-mm mesh screen. Ground samples were wet-digested with HNO_3 and H_2O_2 (Bañuelos and Pflaum, 1990). Sediments removed from capped butyrate liners were cut into 5-cm profile sections, air-dried (Arthur et al., 1992), and ground to fine powder. Sediment samples were digested with HNO_3 and H_2O_2 according to EPA method 3050B (1996). Total Se concentrations in digested water, plant, and sediment samples were determined by AAS with hydride generation (Ward and Gray, 1996). The amount of Se loss during sample dehydration at a drying temperature of 60 °C was negligible (*i.e.*, <3% of the total Se accumulated in plant tissues)(Asher *et al.*, 1966). Total sulfate-sulfur in water was analyzed by ICP-AES (Thermo Jarrell Ash, Franklin, MA) (Wanty et al., 2001).

Partitioning of Se Mass Input

Expressing the total Se mass partitioned in various wetland compartments as a percentage of the total Se mass input into the wetland cell during a certain period of time ($\Delta T = T_{start} - T_{end}$) will help to formulate a Se mass balance model for the flow-through constructed wetlands. In this paper, the time period (ΔT) was defined from September 1997 (T_{start}) to August 1999 (T_{end}), during which the measurements of Se volatilization were conducted. The total Se mass input to or discharged from each wetland cell was calculated as the product of the Se concentration in the inflow or outflow water and the volume of the inflow or outflow water during the sampling month. The Se mass removal by volatilization was calculated as the product of the rate ($\mu g\ m^{-2}\ d^{-1}$) of Se volatilization determined for 24 hours and the number of days of the specific study month during which the measurement was made. The total Se mass in sediment was determined from the mass of sediment and the Se concentration in the sediment. The accumulation of Se in plant materials was obtained by the biomass and the Se concentration in the plant material.

Selenium Speciation by X-ray Absorption Spectroscopy (XAS)

Sediment and plant samples were frozen with dry ice immediately after collection from the wetlands. Plant shoots and roots were rinsed in deionized distilled water, frozen in liquid nitrogen, and then ground to a fine texture and stored at -80°C. XAS data collection was conducted at the Stanford Synchrotron Radiation Laboratory (SSRL) as described earlier (Lee et al., 2001).

Quantitative analysis was carried out using an edge-fitting method (Pickering et al., 1995) in which the normalized edge spectrum of a sample containing unknown Se species was fit to a linear combination of the spectra of standard Se compounds by using a least-squares minimization procedure. The fractional contribution of a standard spectrum to the fit was equivalent to the fractional abundance of Se in that chemical species in a sample. In the present work, spectra of 10 mM solutions of selenate, selenite and selenomethionine (SeMet), and solid red elemental Se measured in transmittance were chosen to be representative of potential Se species present (Pickering et al., 1999).

Statistical Analysis

This field study involved the collection of multiple samples from each experimental unit (i.e., wetland cell) sequentially every month during the 2.5-year study period. Since it was difficult to establish true replicates for each treatment due to the large scale of the wetland system, this field study was conducted with temporal pseudoreplication (Hurlbert, 1984). Repeated sampling on different sampling dates was taken to represent replicated treatments, and statistical significance tests were applied since different sampling and measurements were considered to be independent. In determining the difference between two wetland cells in a sampling month, the null hypothesis tested was that there was no difference between the two cells. Statistical analysis was performed using the Statistical Analysis System (SAS). Multiple comparisons among different seasonal means were conducted by PROC GLM with *Tukey* option, and correlation analysis was performed by PROC CORR (SAS, 1988).

GREENHOUSE STUDY

Wetland Microcosms and Se Treatments

Six wetland microcosms were constructed, each 0.76-m long, 0.76-m wide, and 0.2-m deep, with a surface area of 0.58 m^2 and a volume of 0.12 m^3. Each microcosm was filled with 84 kg of soil (15% water content) from the Corcoran wetland location and 7 kg peat moss (to increase the soil organic matter), which formed a final soil depth of 12-cm. The experimental soil contained a background Se concentration of ~0.3 mg kg^{-1}, mainly in the form of selenate.

Microcosms were maintained in a temperature-controlled greenhouse on the UC Berkeley campus. Each microcosm was vegetated from rabbitfoot grass seeds that were collected from Cell 5 of the Corcoran wetland. Microcosms consistently contained ~ 1-cm standing water above the topsoil after seed germination. After two months of plant growth, plant shoots were cut and left on the soil surface to increase the amount of organic material in the microcosms. A total of 510 mg Se was added to each microcosm, consisting of 170 mg of Se as selenate (Na_2SeO_4), selenite (Na_2SeO_3), and SeMet ($C_5H_{11}NO_2Se$). The mixed Se solution was applied to the soil surface five months after the establishment of the rabbitfoot grass microcosms. Three of the six microcosms were immediately enclosed with collection chambers for Se volatilization measurements. The other three microcosms remained open, and rotary fans were used to simulate wind turbulence occurring under field conditions. Wind speed was ~1.5 m s^{-1} above the unenclosed microcosms.

Selenium Mass Balance in Microcosms

The partitioning of Se in the microcosms enclosed with collection chambers included 1) Se mass accumulated in living plant tissues, 2) Se accumulation in plant litter, 3) Se retention in sediment, and 4) volatile Se emission from the microcosm system. In the microcosms without the collection chamber enclosure, the amount of volatile Se was derived from the total unaccountable Se mass from the Se mass balance.

Volatile Se was collected using the same open-flow sampling chamber system used in the field study. The sampling chamber was fitted to the top of each microcosm. The measurement of Se volatilization continued daily for 38 days. The water temperature inside the sampling chambers was 23.5 ± 2.7 °C during the study period. At the end of the microcosm experiment, rabbitfoot grass shoots and roots were collected from five randomly selected sampling areas in each microcosm; plant biomass was determined by harvesting all plants in each microcosm. Four sediment core (d = 5 cm) samples were collected from each microcosm at both the beginning and the end of the experiment. The sample preparation and chemical analysis of Se in plant and sediment were done in the manner described earlier for samples collected in the field.

RESULTS

TEMPORAL AND SPATIAL VARIATION OF SE VOLATILIZATION IN WETLANDS

Rates of Se volatilization were monitored over a 2-year period for each of seven wetland cells (Cells 1-7). The most important feature of the volatilization data was the significant temporal variation. This is illustrated in Fig. 2, with the changes shown for each of the three wetland cells that exhibited the highest overall rates of volatilization. The rates of Se volatilization were generally high in summer or spring months. In Cell 5, for instance, higher rates of 130.4 ± 10.1 and 274.4 ± 99.9 µg m^{-2} day^{-1} were attained in May and June of 1998, respectively, while Cell 3 attained a maximum value of 141.2 ± 9.2 µg m^{-2} day^{-1} in April of 1998. In the winter months however, rates were substantially lower, i.e., <5 µg m^{-2} day^{-1}.

To compare the levels of Se volatilization between different wetland cells, a relative comparison was made by averaging the rates of volatilization over the 2-year monitoring period for each wetland cell (Fig. 3). The highest average rates of volatilization were attained in Cell 5 (rabbitfoot grass), in which the average rate over the 2-year period was 32.8 ± 11.9 µg Se m^{-2} d^{-1}, with progressively lower rates in the order of Cells 3 (unvegetated), 4 (cordgrass), 2 (baltic rush), 7 (cattail), 6 (saltgrass), and 1 (saltmarsh bulrush). Furthermore, the in-cell spatial variation of Se volatilization among 5 randomly assigned sampling locations in each wetland cell was also determined from the coefficients of variation (i.e., $CV\ \% = s/X$, where s stands for the standard variation and X stands for the mean). The CVs generally ranged from ~30 to 50% with the least variation in the unvegetated wetland cell (~30%).

SIGNIFICANCE OF SE REMOVAL BY VOLATILIZATION IN WETLANDS

To determine the importance of volatilization as a pathway of Se removal, the mass of Se volatilized monthly from each wetland cell was calculated as a percentage of the monthly Se input to that cell over the 2-year period. The greatest amount of Se mass removed through volatilization was from Cell 5 (rabbitfoot grass) (Fig. 4); for example, in May and June of 1998, Se mass removal by volatilization in Cell 5 accounted for 35.1 and 47.6% of the monthly Se mass input, respectively. Significant amounts of Se were also removed from Cells 3 and 4 by volatilization (Fig. 4), with relatively smaller amounts from the remaining cells (monthly-data not shown). The total mass of Se removed by volatilization over the entire 2-year measurement period for each wetland cell was 9.4% of the Se input for Cell 5, 5.8% for Cell 3 (unvegetated), 4.5% for Cell 4 (cordgrass), 3.7% for Cell 2 (baltic rush), 2.6% for Cell 7 (cattail), 1.4% for Cell 6 (saltgrass), and 0.6% for Cell 1 (saltmarsh bulrush).

The mass balance of Se for the study period of September 1997 to August 1999 was calculated for the unvegetated cell (Cell 3) and the cordgrass cell (Cell 4) (Table 1). These two wetland cells were chosen for the following reasons: 1) the rates of Se volatilization were relatively high; 2) these two cells consistently had the best hydrological control of inflow and outflow rates and the least seepage compared to the other wetland cells; and 3) the comparison between Cell 3 and Cell 4 enabled us to identify the differences between vegetated and unvegetated wetland cells. Our data show that most of the Se mass input from inflow drainage water was retained in the surface layer of sediments (e.g., 35.4% of the total Se input in Cell 3 and 56% in Cell 4). Biological volatilization removed 5.8 and 4.5% of the Se mass input from Cells 3 and 4 to the atmosphere, respectively. About 1.2% of the Se mass input was accumulated in living plant tissues and litter materials in the cordgrass cell and ~0.3 to 0.5% in the standing water in the two wetland cells. Given that 59% and 31% of the total mass Se was discharged by outflow water from Cell 3 and Cell 4, respectively, the total Se mass recovery rate was 100.6% for the unvegetated wetland cell and 96.2% for the cordgrass cell (Table 1).

PHYSICOCHEMICAL CHARACTERISTICS OF WETLANDS AND THEIR EFFECTS ON SE REMOVAL BY VOLATILIZATION

Major physicochemical characteristics of the wetland cells that could potentially influence Se removal via volatilization, including pH, EC, DO, temperature, and the total sulfate concentration of the surface water, were monitored during the course of this study. Our monitoring results, compiled in Fig. 5, show that pH values in outflow water ranged from 8.2 to 9.1, which was significantly (P<0.05) greater than the average pH value of 7.7 in the inlet water. However, there was little change in pH of the surface water with time in any of the wetland cells. With regard to EC, the differences among the cells were not statistically significant (P<0.05), but in all cells it changed considerably with time, the highest values being measured in spring, while the lowest values were recorded in the fall of each year. With regard to variation of sulfate-sulfur in drainage water, Cell 3 (unvegetated) tended to have significantly (P<0.11) higher concentrations of sulfate in outflow water than Cell 6 (saltgrass), while no significant (P<0.05) differences in sulfate concentration were observed among other wetland cells (Fig. 7). Sulfate concentrations in inflow and outflow water generally varied from ~900 to 1100 mg L^{-1} during the study period, without showing an apparent pattern of seasonal variation. The water temperature tended to be high in the spring and summer months (~27 to 30 °C) and low in the fall and winter months (~10 to 15 °C), with Cells 5 and 3 attaining slightly higher average water temperature than most other wetland cells. Dissolved oxygen in surface water varied spatially and temporally (Fig. 5). High values of dissolved oxygen (~14 mg L^{-1}) were found in Cells 3, 8, and 9. Cells 6, 7, and 10, on the other hand, had much lower values of dissolved oxygen (~5 mg L^{-1}).

Selenium Se speciation analysis by X-ray absorption spectroscopy revealed that selenate entering the wetland cells in agricultural drainage water was reduced in sediment to a mixture of elemental Se (~45%), organic Se (~40%), and selenite (~15%) (Table 2). The Se speciation in the sediment from rabbitfoot grass rhizosphere differed substantially from that in the surface sediments in that the bulk (77%) of the Se retained was in organic forms.

Statistical analysis indicates that, among the monthly quantitative physiochemical variables above, changes in water temperature correlated most significantly with the rate of Se volatilization. The relationship between Se volatilization and water temperature can be represented by an exponential regression model of $Y=5.891 + 0.03 e^{0.226 X}$ ($R^2=0.21$, $P<0.0001$, where Y is the Se volatilization rate and X is water temperature).

VOLATILIZATION OF SE IN RABBITFOOT GRASS MICROCOSMS

The kinetics of Se volatilization in three chamber-enclosed microcosms was monitored continuously after the soil was treated with Se (Fig. 6). An average of 45.3±2.5 mg Se per microcosm was removed by volatilization over the 38-day experimental period. The volatilization rate was highest during the first week after the application of 510 mg of Se, and was relatively steady from day 10 to day 34. The overall average rate of Se volatilization was 2.4 ± 1.0 mg m^{-2} d^{-1}. The decrease in Se volatilization most likely resulted from decreasing availability of organic Se in the microcosms over time.

The partitioning of the total mass Se input (i.e., 510 mg Se applied to each microcosm) among the different compartments of the rabbitfoot grass microcosms was shown in Fig. 7. Most of the mass Se input in the microcosms (with or without chamber enclosure) remained in soil (~70% of the total Se input). About 12% of the Se input was accumulated in living plant tissues and ~7% in detrital material in microcosms. In the chamber-enclosed microcosms, biological volatilization removed 8.9% of the Se mass input, while 8.9% of the total Se mass input was missing from the microcosms that were not enclosed with volatilization chambers.

DISCUSSION

QUANTITATIVE IMPORTANCE OF VOLATILIZATION IN SE REMOVAL BY CONSTRUCTED WETLANDS

The results of the microcosm study support the view that the volatilization chamber method used in this field study did indeed provide accurate measurements of volatilization rates under field conditions. In the chamber-enclosed microcosms, the amount of Se removed by biological volatilization accounted for 8.9% of the Se mass input into the microcosm. In the unenclosed microcosms, 91.1% of the Se input into the microcosm went into the sediments and plant tissues, leaving 8.9% "unaccounted Se". Clearly the amount of Se volatilized could not have been greater than 8.9% of the total Se in the unenclosed microcosms, which was comparable to the amount volatilized in the chamber-enclosed microcosms. This indicates that the presence of the chamber did not significantly slow down the volatilization process in any way.

Selenium volatilization from Cells 3, 4, and 5 accounted for 5.8%, 4.5% and 9.4%, respectively, of the mass of Se flowing into each wetland cell over a 2-year period of study. This was somewhat less than at the San Francisco Bay wetland where Hansen et al. (1998) obtained values suggesting that up to 10 to 30% of the total Se mass removed by the wetland could have been volatilized. The higher volatilization rates observed at the San Francisco Bay wetland may have been due to the fact that measurements by Hansen et al. (1998) did not include the winter months when temperatures are lower and that the Chevron wetland received Se in the form of selenite which is volatilized at faster rates than selenate (Zayed et al., 1998), the predominant form of Se at Corcoran. In addition, high levels of sulfate in drainage water (Fig. 5) might also reduce, to a certain degree, the production of volatile Se at the Corcoran wetland (Zayed et al., 1992).

Rates of Se volatilization fluctuated substantially with time at the both Corcoran and the San Francisco Bay wetlands (Hansen et al., 1998). Rates of Se volatilization were higher in spring and early summer than in fall and winter in the Corcoran wetland. In June 1998 up to 48% of the Se entering the rabbitfoot grass wetland cell was volatilized, while volatilization in the cordgrass wetland cell accounted for 20-25% of the total Se input in the summer months of 1999 (Fig. 4). Rates may be higher in the spring and summer months because of the higher temperatures; our results show that the rate of Se volatilization was significantly (P <0.5) correlated with changes in water temperature in wetland cells (see also, Frankenberger and Karlson, 1994). This may be partly due to the fact that, for every 10º C increase in temperature, the vapor pressure of volatile Se (e.g., DMSe) increases 4-fold (Karlson et al., 1994); thus, a rise in water temperature will significantly increase the partition and transfer of volatile Se from water to air. Higher rates could also be associated with greater plant and microbial activity at higher temperatures, coupled

with greater supplies of organic carbon resulting from the death and decay of the previous year's plant growth (Lin et al., 2002).

FEASIBILITY OF USING CONSTRUCTED WETLANDS FOR REMOVING SE FROM DRAINAGE WATER

The total mass of Se removed by vegetated wetland cells at Corcoran was on average, about 70% of the inflow (Lin and Terry, 2000). Thus, this field study provides a clear proof of concept that constructed wetlands can remove substantial amounts of Se from agricultural drainage water. Vegetated wetland cells generally performed better in Se removal from drainage water than the unvegetated wetland cell, but there was little evidence that the type of species planted in the wetland cells significantly influenced the efficiency of Se removal (Tanji, 1999; Lin and Terry, 2000). Of the mass of Se loaded into the wetland cell, results from 2.5-years of monitoring show that by far the largest amounts of Se were retained in the top 0-5 cm layer of sediments; much less Se moved down through the profile to the 5-10 cm and 10-15 cm layers. Over the experimental period, a significant buildup (*e.g.*, a ~7-fold increase in Cell 3) of Se in the surface sediments was observed (Gao et al., 2000).

The efficiency of Se removal by treatment wetlands can undoubtedly be improved by increasing flow paths and residence times and other management techniques. However, the major problem of managing a treatment wetland may be in minimizing the exposure of wildlife to Se toxicity because the high accumulation of Se was observed in sediment and plant tissues. Potential Se ecotoxicity depends to a large extent on the chemical form of Se, rather than just on the concentration of total Se. Most of the Se in the drainage water entering the wetland cells was in the form of selenate, which is then reduced to other forms of Se including selenite, elemental Se, organic Se and dimethylselenide (Table 2). Elemental Se and dimethylselenide are relatively non-toxic, while selenite and organic forms of Se may be substantially more toxic. Selenium ecotoxicity may be minimized using various management techniques. For example, *Zon Guns* and bird scare flagging tape can be used to keep birds away from the contaminated wetland (Cervinka et al., 1999), according to the guidelines furnished by the California Department of Fish and Game and the US Fish and Wildlife Service. Another management approach is to provide an alternative wetland supplied with clean water as compensation habitat for birds to feed and reproduce, which has recently been successfully demonstrated at Tulare Lake Drainage District (TLDD) (Doug Davis, personal communication). Ultimately, it may be necessary to retire the wetland. Once the sediments and plant tissues accumulate Se to potentially toxic levels (Adriano et al., 2001), the wetland treatment system could be closed, drained, and converted to a moist treatment bed to promote biological volatilization of Se (Frankenberger and Karlson, 1994).

ENHANCING THE ROLE OF SE VOLATILIZATION IN SE REMOVAL

One way to substantially improve the feasibility of using constructed wetlands for the remediation of Se-contaminated agricultural drainage water is to increase the efficiency of Se volatilization from wetlands. As discussed in the Introduction, volatilization has the great benefit of removing Se from the local ecosystem, thereby minimizing its entry into the food chain. Even if the volatile Se is redeposited elsewhere, this may actually be beneficial in those places where Se is present in the environment in deficient supply with respect to animal nutrition. Volatilization may be enhanced in wetlands in a variety of ways, including the judicious use of plant species (Terry et al., 1992; Lin et al., 2002). The present research, as well as the study by Hansen et al. (1998) at the San Francisco Bay wetland, shows clearly that volatilization in wetlands populated with rabbitfoot grass yields high rates of volatilization.

One explanation for the high rates in Cell 5 is that rabbitfoot grass and its associated microbes facilitate a greater conversion of selenate to organic Se forms, which may be more rapidly metabolized to volatile compounds. Our speciation analysis showed that, in the rabbitfoot grass wetland cell, selenate (the dominant chemical form of Se) in the inflow was substantially reduced to organic Se forms; for example, 89±9% and 77±5% of the mass of Se accumulated in the root tissue of rabbitfoot grass, and in the sediment surrounding the root surface, were in the form of SeMet-like Se compounds, respectively (Table 2). Such organic Se forms may be more rapidly converted to volatile forms than inorganic forms (e.g., selenate or selenite). Zayed et al. (1998) found that the rate of volatilization by plants supplied with selenomethionine (SeMet) was 4-fold greater than those supplied with selenate, and ~2

times higher than those with selenite, while Frankenberger and Karlson (1994) obtained similar results with microbes. The hypothesis that rabbitfoot grass facilitates a greater reduction of selenate to organic forms is further supported by a previous study conducted by Gao et al. (2000) in the Corcoran wetland, which demonstrated that the percentage of waterborne Se present in organic forms was higher in the rabbitfoot grass wetland cell than any other cell. Therefore, approaches designed to increase levels of Se volatilization in wetlands may also include those that could enhance the biochemical reduction of selenate or selenite to organic forms of Se that are much more rapidly volatilized by microbes and plants. A further conversion of SeMet to SeMM may result in even more dramatic increases in Se volatilization, according to the Se assimilation pathway in plants (Terry et al., 2000). Such changes in the composition of organic Se forms have already been achieved through genetic engineering (Terry et al., 2000), and our laboratory is pursuing an active research program to develop transgenic plants that volatilize Se at enhanced rates.

By using wetland management approaches we may be able to enhance the ability of plants and microbes to volatilize Se from toxic organic Se compounds. One of the possible approaches to enhancing volatilization in wetlands is through manipulation of microbes and algae. The contribution of microbes and algae can be assessed by comparing rates of Se volatilization from unvegetated and vegetated wetland cells; for example, the unvegetated Cell 3 of the Corcoran wetland attained a mean rate of volatilization of 141±9 µg m^{-2} d^{-1}, which was the second highest of the 7 wetland cells measured. Hansen et al. (1998) obtained a high value of 170±30 µg m^{-2} d^{-1} in the unvegetated inlet channel of the San Francisco Bay wetland, compared to 150-180 µg m^{-2} d^{-1} in the vegetated areas. The other wetland management approaches designed to increase Se volatilization might include managing hydrological conditions (*e.g.*, drying or wetting cycling, Zhang and Moore, 1997), altering carbon availability to promote microbial activity (Frankenberger and Karlson, 1994), or "seeding" with microbes (Azaizeh et al., 1997) and microalgae. For instance, fertilization to the alfalfa-sediment system can substantially enhance the rate of Se volatilization, showing a 37% increase from 68 ± 8 to 111 ± 21µg m^{-2} d^{-1} (Lin and Terry, unpublished data). Future research needs to be directed to the development of applicable site management schemes for the enhancement of Se volatilization under field conditions.

■ ■ ■ ■ ■

REFERENCES

Adriano, D.C. *Trace Elements in Terrestrial Environments*, 2nd Edition. Springer: NY. 2001, p 736.

Amouroux, D. and Donard, O.F.X. 1996. Maritime emission of selenium to the atmosphere in eastern Mediterranean seas. Geophysical Research Letters. 23 (14): 1777-1780.

Arthur, M.A., G. Rubin, R.E. Schneider, and L.H. Weinstein. 1992. Uptake and accumulation of selenium by terrestrial plants growing on a coal fly ash landfill. Part I: corn. Environ. Toxicol. Chem. 11: 541-547.

Asher, C.J., C.S. Evans, and C.M. Johnson. 1967. Collection and partial characterization of volatile selenium compounds from *Medicago sativa* L. Aust. J. Biol. Sci. 20: 737-748.

Azaizeh, H.A., S. Gowthaman, and N. Terry. 1997. Microbial selenium volatilization in rhizosphere and bulk soils from a constructed wetland. J. Environ. Qual. 26: 666-672.

Bañuelos, G. and T. Pflaum. 1990. Determination of selenium in plant tissue with optimal digestion conditions. Commun. In Soil Sci. Plant Anal. 21: 1717-1726.

Biggar, J.W. and Jayaweera, G.R. 1993. Measurement of selenium volatilization in the field. Soil Sci. 155: 31-36.

Boulding, J.R. 1994. Description and sampling of contaminated soils. 2nd Ed. Lewis Pub., Boca Raton. 326 pp.

Byrnes, J.R. 1994. Field sampling methods for remedial investigations Lewis Pub., Boca Raton. 254 pp.

Carlson, C.L., D.C. Adriano, and P.M. Dixon. 1991. Effects of soil-applied selenium on the growth and selenium content of a forage species. J. Environ. Qaul. 20: 363-368.

Cervinka, V.; Diener, J.; Erickson, J.; Finch, C.; Martin, M.; Menezes, F.; Peters, D.; Shelton, J. *Integrated system for agricultural drainage management on irrigated farmland*. Bureau of Reclamation, U.S. Department of the Interior, Final research report, 4-FG-20-11920: 1999, 41 pp.

Cooke, T.D., and K.W. Bruland. 1987. Aquatic chemistry of selenium: evidence of biomethylation. Environ. Sci. Technol. 12: 1214-1219.

Frankenberger, W.T., Jr. and U. Karlson. 1994. Microbial volatilization of selenium from soil and sediments. pp. 369-387. In: W.T. Frankenberger, Jr. and S. Benson (eds.), Selenium in the Environments. Marcel Dekker, Inc., New York.

Gao, S. Tanji, K.K. Peters, D.W. and Herbel, M.J. 2000. Water selenium speciation and sediment fractionation in a California flow-through wetland system. J. Environ. Qual. 29: 1275-1283.

Hansen, D., P.J. Duda, A. Zayed, and N. Terry. 1998. Selenium removal by constructed wetlands: role of biological volatilization. Environ. Sci. Technol. 32: 591-597.

Hurlbert, S.H. 1984. Pseudoreplication and the design of ecological field experiments. Ecological Monographs. 54(2): 187-211.

Karlson, U., and W.T. Frankenberger. 1988. Determination of gaseous selenium-75 evolved from soil. Soil Sci. Soc. Am. J. 52: 678-681.

Karlson, U., W.T. Frankenberger, Jr., and W.F. Spencer. 1994. Physicochemical properties of dimethyl selenide and dimethyl diselenide. J. Chem. Eng. 39: 608-610.

Lee, A., Z.-Q. Lin, I.J. Pickering, and N. Terry. 2001. X-ray absorption spectroscopy study shows that the rapid selenium volatilizer, pickleweed (*Salicornia bigelovii* Torr.), reduces selenate to organic forms without the aid of microbes. Planta. 213: 977-980.

Lin, Z.Q. and Terry. 2000. Use of flow through constructed wetlands for the remediation of selenium in agricultural tile-drainage water. Final research report (96-7), the Center of Water Research, University of California, Riverside, California.

Lin, Z.-Q., D. Hansen, A. Zayed, and N. Terry. 1999. Biological selenium volatilization: method of measurement under field conditions. J. Environ. Qual. 28: 309-315.

Lin, Z.-Q., R.S. Schemenauer, V. Cervinka, A. Zayed, and N. Terry. 2000. Selenium volatilization from a soil-plant treatment system for the remediation of contaminated water and soil in the San Joaquin Valley. J. Environ. Qual. 29: 1-9.

Lin, Z.-Q., V. Cervinka, I.J. Pickering, A. Zayed, and N. Terry. 2002. Managing selenium-contaminated agricultural drainage water by the Integrated on-Farm Drainage Management system: role of selenium volatilization. *Water Research*. 12: 3149-3159

Losi, M.E. and W.T. Frankenberger, Jr. 1997. Bioremediation of selenium in soil and water. Soil Sci. 162(10): 692-702.

McConnell, K.P. and O.W.. Portman. 1952. Toxicity of dimethyl selenide in the rat and mouse. Proc.Soc. Exp. Biol. Med. 79: 230-231.

Pickering, I.J., G.E. Brown, Jr., and T.K. Tokunaga. 1995. Quantitative speciation of selenium in soils using x-ray absorption spectroscopy. Environ. Sci. Technol. 29: 2456-2459

Pickering, I.J., G.N. George, V. Van Fleet-Stalder, T.G. Chasteen, and R.C. Prince. 1999. X-ray absorption spectroscopy of selenium-containing amino acids. J. Bio. Inorg. Chem. 4: 791-794.

SAS Institute. 1988. SAS/STAT. User's Guide, Release 6.03. Edition. Statistical Analysis Systems Institute, Inc., Cary, NC, 1028 pp.

Tanji, K. 1999. TLDD flow-through wetland system: inflows and outflows of water and total Se as well as water Se speciation and sediment Se fractionation. pp. 227-252. UC Salinity/Drainage Program, annual report. University of California. Riverside.

Terry, N., C. Carlson, T.K. Raab, and A.M. Zayed. 1992. Rates of selenium volatilization among crop species. J. Environ. Qual. 21: 341-44.

Terry, N., A.M. Zayed, M.P. de Souza, and A.S. Tarun. 2000. Selenium in higher plants. Annu. Rev. Plant Mol. Biol. 51: 401-32.

US EPA. 1992. Acid digestion of aqueous samples and extracts for total metals for analysis by FLAA or ICP spectroscopy. In: Methods for Chemical Analysis of Water and Wastes. Method 3010A.

US EPA. 1996b. Acid digestion of sediments, sludges, and soils. 11pp. In: Methods for Chemical Analysis of Water and Wastes. Method 3050B.

Wanty1, R.B. Shanks III1, W.C. Lamothe1, P. Meier1, A. Lichte1, F. Briggs1, P.H. and Berger1, B.R. 2001. Results of chemical and stable isotopic analyses of water samples collected in the Patagonia mountains, southern Arizona. USGS, Open-File Report 01-463. 20 pp.

Ward, M. and A. Gray. 1996. Vapor generation Accessory VGA-77. Varian Australia Pty Ltd. Publication No. 85-101047-00.

Wilber, C.G. 1980. Toxicology of selenium: a review. Clinical Toxicol. 17: 171-230.

Zayed A, Lytle CM, Terry N. 1998. Accumulation and volatilization of different chemical species of selenium by plants. *Planta* 206: 284-92.

Zayed, A., E. Pilon-Smith, M. de Souza, Z.-Q. Lin, and N. Terry. 2000. Remediation of selenium-polluted soils and waters by phytovolatilization. pp. 63-86. In: N. Terry, G. Bañuelos (eds.), Phytoremediation of Metal-contaminated Water and Soils. CRC Press, Boca Raton, FL.

Zayed, A.M. and Terry, N. 1992. Selenium volatilization in broccoli as influenced by sulfate supply. J. Plant Physiology. 140: 646-652.

Zhang, Y.Q., and M.J. Moore. 1997. Environmental conditions controlling selenium volatilization from a wetland system. Environ. Sci. Technol. 31(2): 511-517.

■ ■ ■ ■ ■

TABLE 1. The partitioning of mass Se input among major pathways in Cell 3 (unvegetated) and Cell 4 (cordgrass) during a two-year study period from September 1997 to August 1999 during which volatilization measurements were made monthly[†]. The partitioning of mass Se in each compartment is presented as a percentage of the total Se mass input during the study period. N/A: not applicable.

	Unvegetated Cell	Cordgrass Cell
Total Se mass input (g Se per wetland cell)	361.6	396.0
Output from Wetland Cell (% of total input)		
Discharged by outflow water	58.9	31.1
Volatilized into the atmosphere	5.8	4.5
Remained in Wetland Cell (% of total input)		
Retained in top 10-cm sediment	35.4	55.9
Accumulated in plants and fallen litter [‡]	N/A	4.4
Contained in standing water [‡]	0.5	0.3

[†] A complete 2-year (24 months) time scale takes into account the seasonal variation in Se volatilization in the wetland cells. The amounts lost through vertical seepage were not taken into account because there were no significant changes in Se concentration in lower (below 15-cm deep) sediments, compared to their background levels (~0.25 mg kg^{-1}). Since there was no significant (P<0.05) increase in Se concentration at depths lower than 10 cm, the total Se mass accumulated in sediment was determined only for the top 10-cm of sediment for this partitioning study.

[‡] These values refer to the amounts of Se present in these compartments at the time of sampling, August 1999.

TABLE 2. Percentage contributions to the fit for Se K-edge spectra for surface sediments (0-2 cm depth) from unvegetated and rabbit-foot grass vegetated wetland cells and sediments from the root-zone of rabbitfoot grass. Data are presented with 3 times the estimated standard deviation and indicate the 99% confidence limit of the parameter in the fit.

	Se (VI)	Se (IV)	Se (0)	SeMet (-II)
Surface sediment, unvegetated	- [†]	16 ± 3	47 ± 5	37 ± 7
Surface sediment, rabbitfoot grass	-	13 ± 4	41 ± 6	46 ± 10
Root-zone sediment, rabbitfoot grass	-	23 ± 5	-	77 ± 5
Rabbitfoot grass shoot tissue	32 ± 2	17 ± 5	27 ± 7	24 ± 12
Rabbitfoot grass root tissue	-	11 ± 8	-	89 ± 9

[†] The contribution was not significant

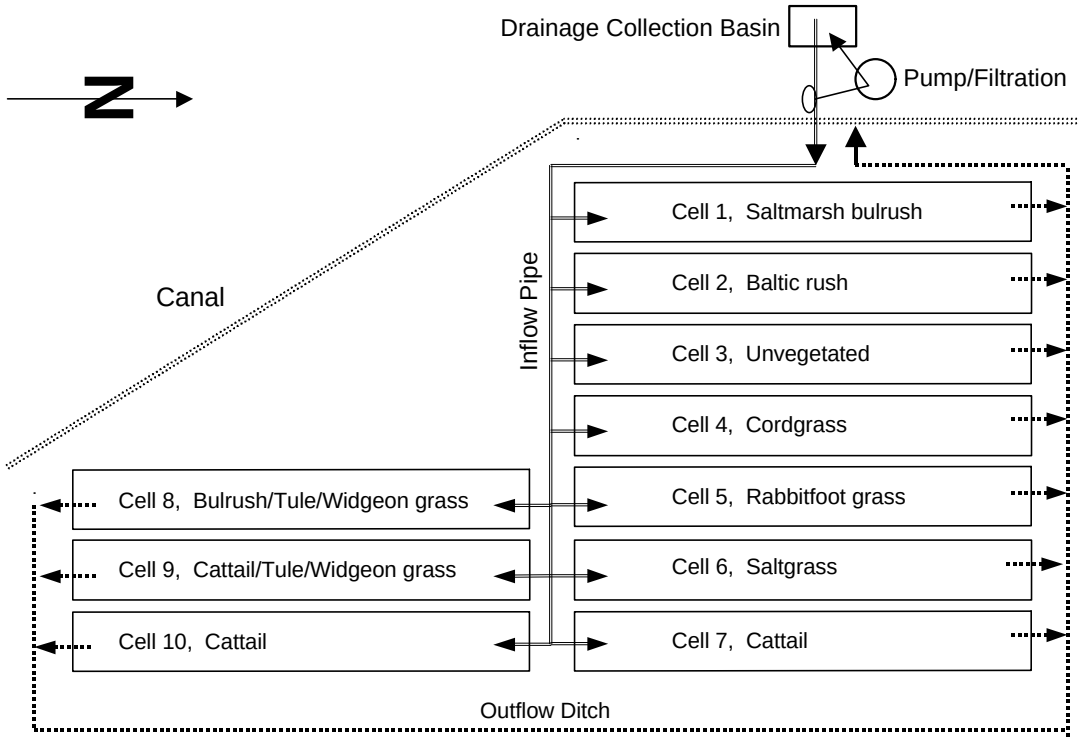

Figure 1. The field layout of 10 flow-through constructed wetland cells in Corcoran, California, built in May 1996 and terminated in February 2001.

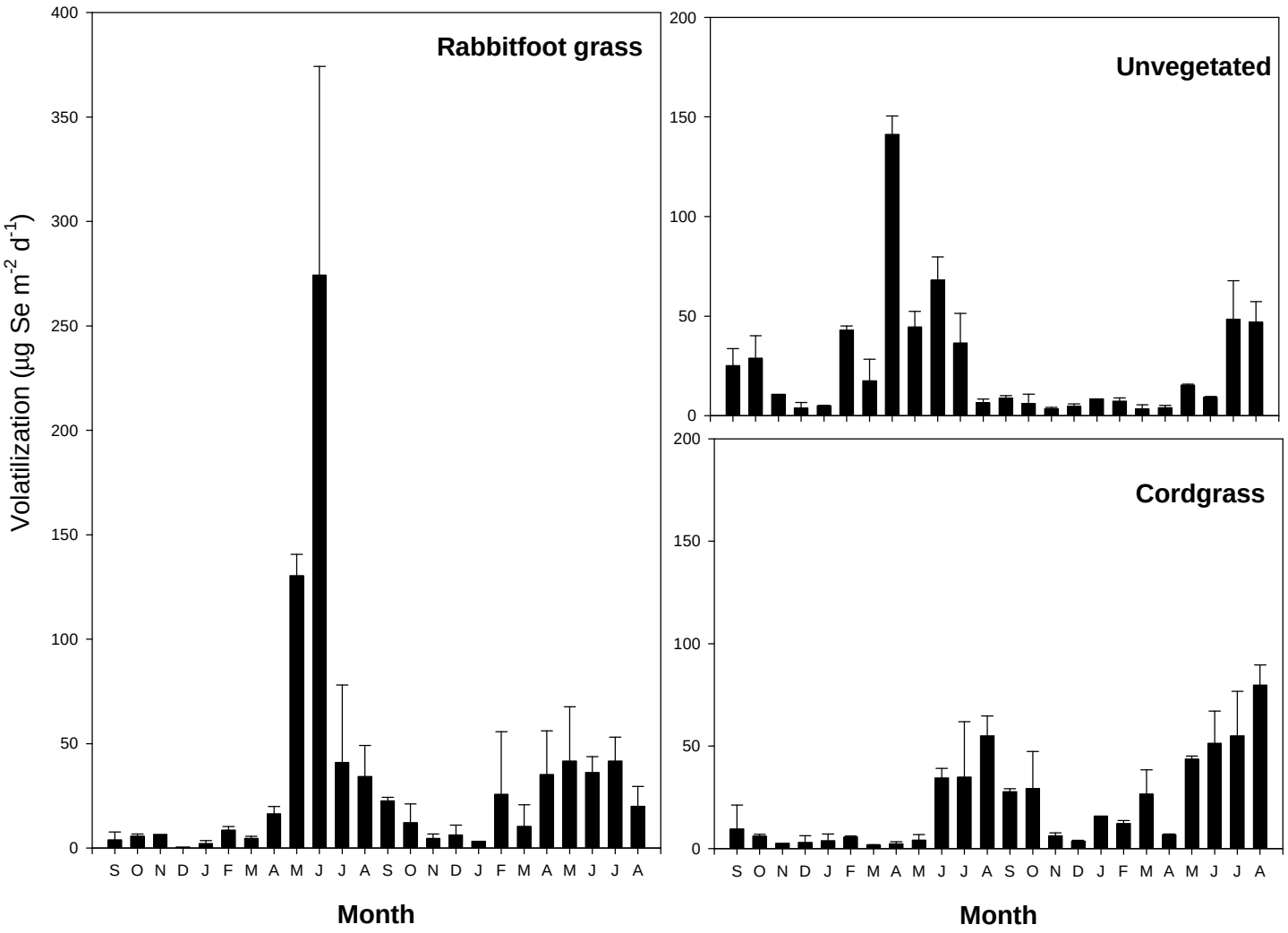

Figure 2. Temporal variation of Se volatilization in wetlands during the period of September 1997 to August 1999, illustrated by Cells 3 through 5. Data shown are means and standard deviation (n=3).

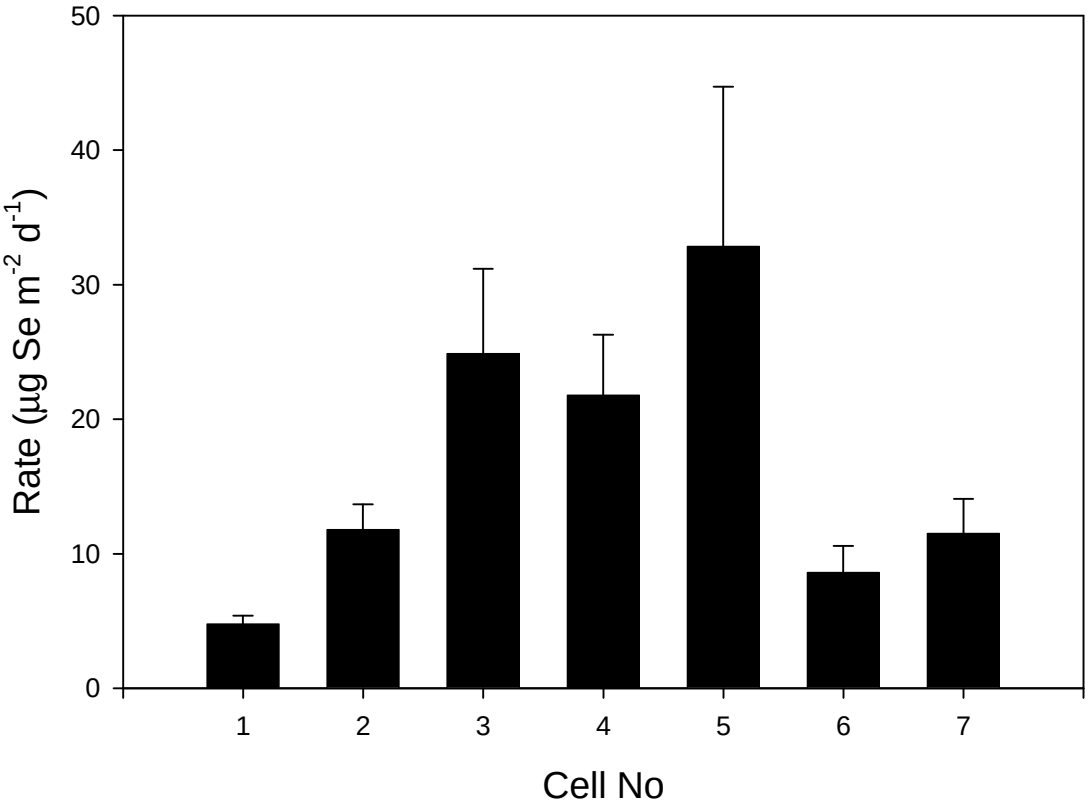

Figure 3. Rates of Se volatilization in different wetland cells. Data shown are means for the time period from May 1997 to August 1999 and associated one standard error (n=24).

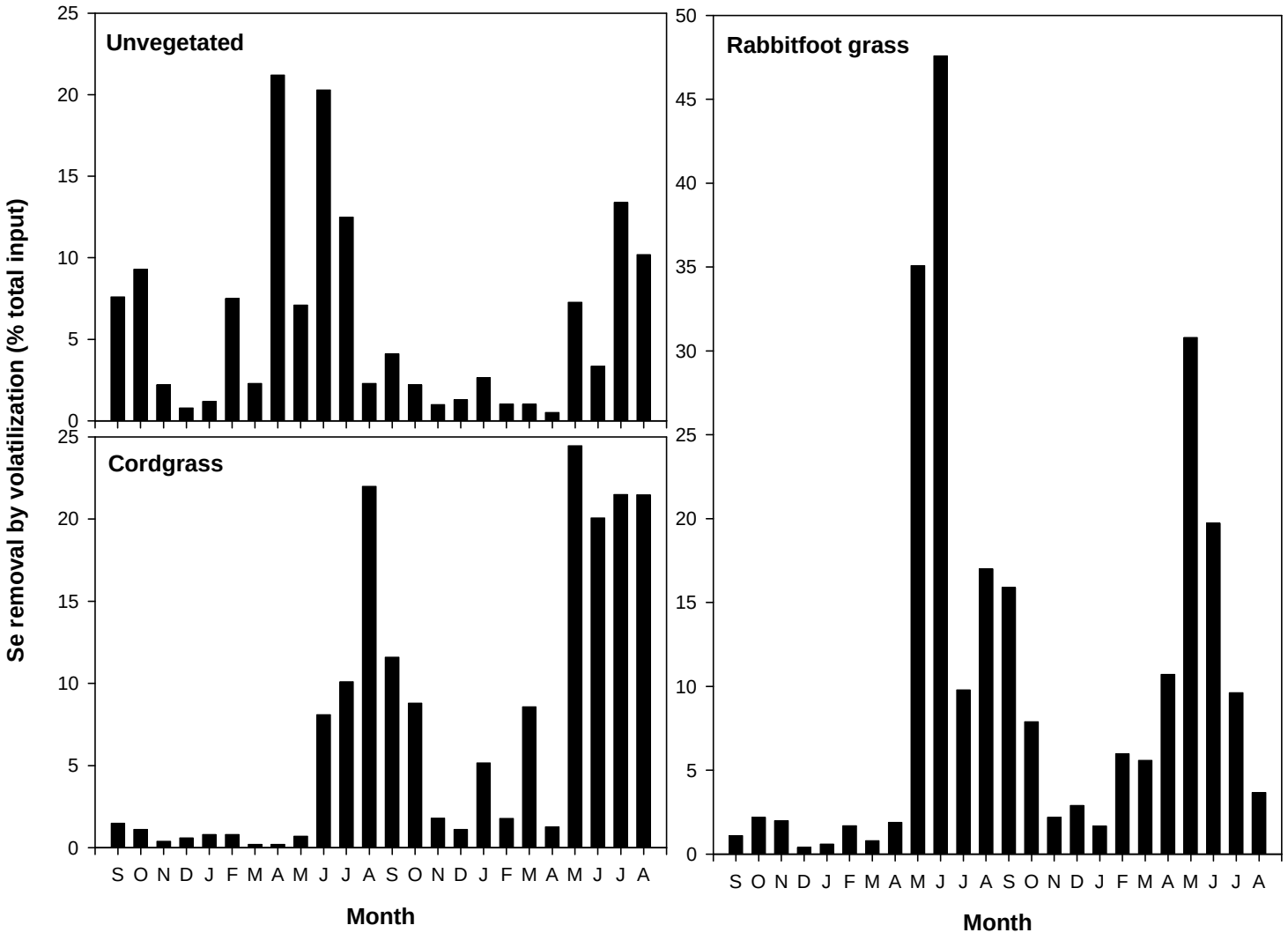

Figure 4. Selenium removal by volatilization from different wetland cells during a two-year study period. Data shown are presented as a percentage of the total Se mass input to each wetland cell.

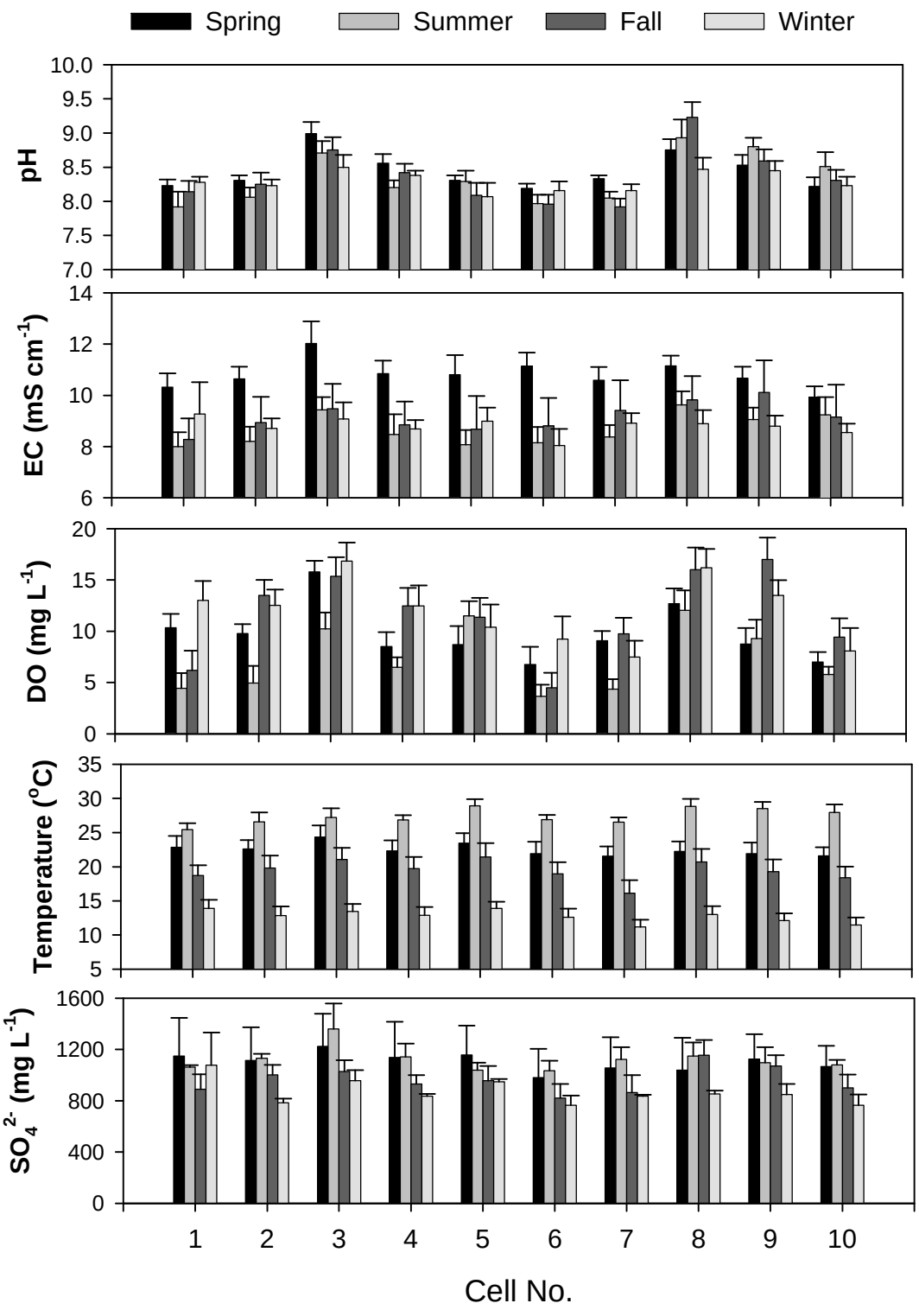

Figure 5. Seasonal variation of pH, EC, DO, temperature, and sulfate concentrations in surface water of each wetland cell. Data shown are means and one standard error (n=18).

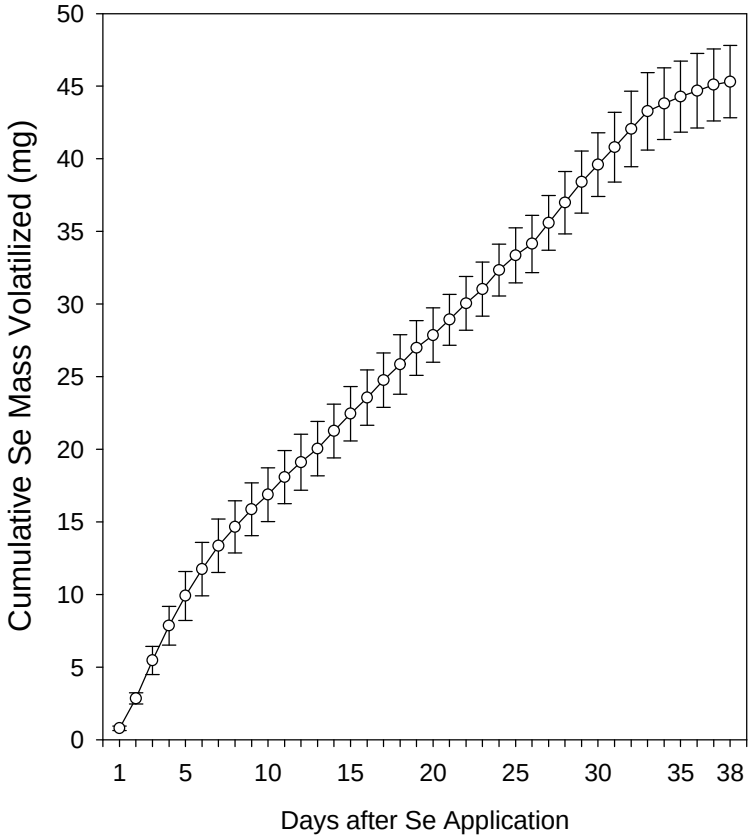

Figure 6. Cumulative Se mass volatilized from rabbitfoot grass microcosms enclosed with volatilization chambers. Data were averaged for three microcosms, with associated standard deviation.

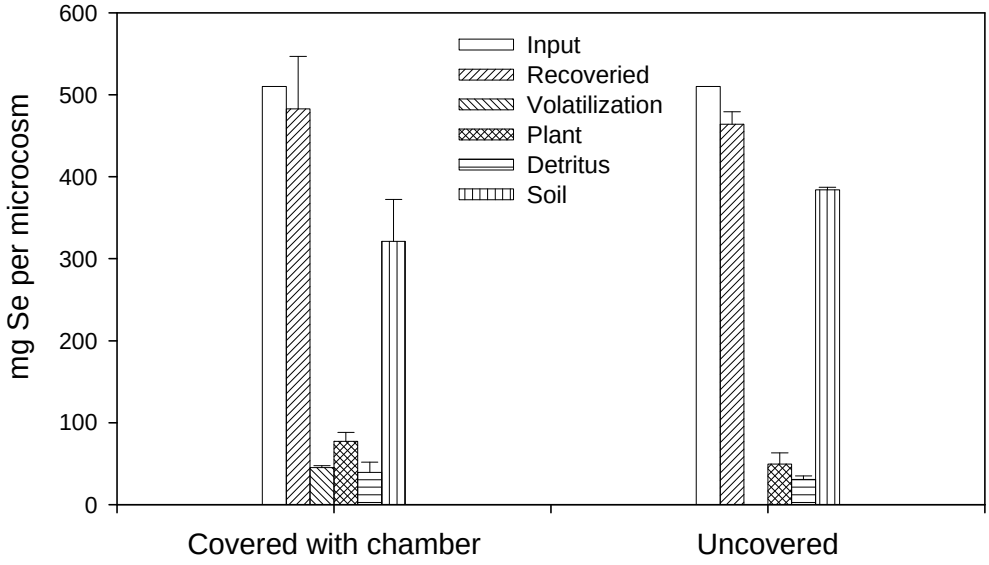

Figure 7. Partitioning of the total Se mass input in microcosms with rabbitfoot grass over a 38-day experimental period. Data are means and standard deviation (n=3).

Three-dimensional Unsaturated-Saturated Flow and Transport and Subsidence

Project Investigator:

Wesley W. Wallender
Office: (530) 752-0688, E-mail: wwwallender@ucdavis.edu
Departments of LAWR (Hydrology Program) and Biological and Agricultural Engineering,
University of California, Davis

Research Staff:

Purnendu N Singh, *PhD Student, 50% FTE*

ABSTRACT

Land subsidence due to groundwater extraction in the western San Joaquin Valley has been causing serous and costly damage. The use of surface irrigation water has reduced the subsidence but has caused the shallow water tables to rise resulting in inadequate drainage and accumulation of salts in the root zone. To manage drainage problems, one of the options is to increase groundwater pumping. Similarly it is expected that future deliveries of imported surface water for agriculture use may get reduced, resulting in increased groundwater pumping. The effect of groundwater pumping on land subsidence has been studied using one-dimensional consolidation theory of Terzaghi (1925). Larson, Basagaoglu, and Marino (2001) have used one dimensional Terzaghi theory for predicting optimal safe groundwater yield and land subsidence in the Los Banos-Kettleman City area. Biot's (1941) general theory of three-dimensional consolidation has been used by Burbey and Helm (1999) for modeling three-dimensional deformations in response to pumping of unconsolidated aquifers.

The existing use of theories of Terzaghi (1925) and Biot (1941) in subsidence modeling treats skeletal specific storage as a step function of the applied stress. They also do not consider the dependence of storage and aquifer properties on the nature and history of stress the aquifer is subjected to. The present modeling efforts of land subsidence also do not include the permanent effects of land subsidence on storage and hydraulic properties of the aquifer, which may be of vital importance in defining the subsequent behavior of the aquifer. Similarly the effects of land subsidence on solute transport characteristics of the aquifer are also not being considered.

This report highlights the need for a mathematical framework for using skeletal storage coefficient as a continuous function of the stress, and the need to develop relations coupling changes in land subsidence to permeability, hydraulic conductivity and dispersivity of the aquifer. The mathematical development can then be used to develop a three dimensional numerical model for simulating land subsidence and predict future behavior of the aquifer in terms of safe groundwater yield and land subsidence.

KEYWORDS

Subsidence, groundwater, inelastic compaction, San Joaquin Valley, California, three dimensional deformations, storage coefficients

■ ■ ■ ■ ■

BACKGROUND AND INTRODUCTION

California ranks as the largest agricultural revenue generating state in the nation, producing 11 percent of the total U.S. agricultural value. Irrigation has played a primary role in enabling the San Joaquin valley to become one of the world's most intensively farmed regions of the world. The irrigated agriculture was started in the valley with surface water flows of the Kings River and Kern River. After 1910, the development of groundwater resources started in the valley as nearly all the available surface water supply in San Joaquin Valley had been diverted and the only water left to be tapped was groundwater. Initially the development of groundwater resources involved the use of flowing wells, near the central part of the valley and shallow water aquifers. Around 1930, the development of the improved deep-well turbine pump together with rural electrification saw the use of groundwater on a large scale. Intensive agricultural activities in the San Joaquin valley saw accelerated groundwater extraction to meet the crop water demand. This situation continued until 1968 and irrigation water was supplied almost entirely by groundwater. The groundwater withdrawal rate increased with increases in the agricultural development of the valley over the years. For example, groundwater withdrawals for agricultural irrigation increased from four billion cubic meters in the early 1940s to 12 billion cubic meters in 1967 (Poland et al 1975). Because of this reliance on groundwater resources for irrigation needs, more water was pumped out of the aquifer than was recharged. This increased extraction of groundwater caused regional land subsidence. By 1970, when the last comprehensive survey of land subsidence was made, subsidence in excess of one foot had affected more than 5200 square miles of irrigable land-one half of the entire San Joaquin Valley (Poland et al, 1975). The maximum observed subsidence, near Mendota, was more than 28 feet.

In 1968, the construction of the California Aqueduct enabled delivery of surface water to some parts of the San Joaquin Valley. As a result

of the surface water supply, the use of groundwater declined substantially. Groundwater levels began a period of recovery and subsidence slowed or was arrested over a large part of the area. Water levels in the deep aquifer system recovered as much as 200 ft during the period 1967-1974 (Ireland et al, 1984). As a result, since the early 1970s land subsidence has in general slowed due to reductions in groundwater pumpage. In many areas, the land continued to subside even though the water levels were rebounding, suggesting a time delay in subsidence.

The two droughts in California in 1976-77 and 1987-91, resulted in diminished supply of surface water to the area. The farmers compensated this cutback in the supply of surface water by resorting to additional pumping. During the droughts, the increased pumping led to sharp declines in water levels and subsidence resumed. A relatively small amount of renewed pumping caused a rapid decline in water levels reflecting the permanent change in the characteristics of the aquifer as a consequence of the subsidence. The delivery of surface water has resulted in the increase in irrigation by about five fold in certain parts of the valley. Increased surface water application has resulted in increased recharge to the shallow aquifer system. As only 21 percent of the irrigated land in the northern regions of the valley can discharge drainage flows to the San Joaquin River while the remaining areas do not have any drainage outlets. The excess water applied to the crop goes to the shallow aquifer and this has caused the shallow water tables to rise. In most areas where the water table is less than 5 feet from the land surface, water is drawn upward and evaporates, leaving a deposit of salts on the surface and in the root zone which retards the growth of many crops. If the present trend continues and no comprehensive action is taken to solve drainage problems, the extent of the drainage problem area with the water table less than 5 feet from the ground surface may exceed 1,000,000 acres by the year of 2040 (SJV Drainage Program 1990). In the absence of comprehensive water and drainage management, these problems would lead to changes in farming practices and cause loss of farm income through conversion from salt-sensitive to salt tolerant crops. Eventually, the value of the land for irrigated agriculture would decline to a level that would force abandonment of the lands.

Since the major reason for continuous built up of the shallow water table is due to addition of irrigation recharge flow to the aquifer, it would logically follow that reductions in recharge from surface water would lessen the problem. The volume of net water added to shallow aquifer could be reduced either by increasing the irrigation efficiency or by reducing the use of surface water for irrigation. The required irrigation water then would have to be pumped from shallow or deep aquifers. Due to poor quality of water in the shallow aquifers, the deep aquifer is the choice for providing the additional irrigation water. It has been estimated that the effects of reducing recharge or increasing groundwater pumping on shallow water level or amount of drainage generated vary with the magnitude of the change relative to the average condition, but more than 40 percent of the area subject to bare soil evaporation could be reduced if pumping was increased by 0.5 foot per year in the model area of 551 square miles in the central part of the Western San Joaquin Valley (Belitz and Philips, 1992).

Groundwater pumping removes water from the aquifer and is therefore an effective alternative for reducing the shallow water table. But the use of the shallow aquifer is limited due to the poor water quality, and hence pumping from the confined aquifer is desirable from the water quality perspective. However there is always a danger of land subsidence if too much groundwater is extracted from the confined aquifer. The fact that a relatively small amount of renewed pumpage caused a rapid decline in water levels during the drought periods of 1976-77 and 1987-91 reflects the reduced groundwater storage capacity (lost pore space) caused by aquifers system compaction. It underscores the point that there are certain irreversible changes taking place in the aquifer characteristics due to land subsidence. The aquifer will behave differently at different times based on many factors including its past history and boundary conditions.

Prior to using the groundwater management option, it is necessary that the complex interacting factors involved in the mechanics of land subsidence due to groundwater pumping be defined and evaluated. Land subsidence, causes serious and costly environmental problems through changes in the water storage and flow as well as solute transport characteristics of the soil. It

is necessary to understand these changes to predict the future response of the aquifer.

MECHANICS OF LAND SUBSIDENCE

Water is released from the storage under conditions of decreasing head in the saturated zone from two mechanisms; the compression of the aquifer caused by increasing the effective stress and the expansion of water caused by decreasing pressure.

The specific storage, which is defined as the volume of water released from storage per unit volume of saturated solids due to unit increase in the pressure head [L^{-1}], is thus generally expressed as

$$S_s = \rho_w g_z (\alpha + n\beta) \qquad [1]$$

where , ρ_w is density of water [M/L^3], g_z is z component of the acceleration due to gravity [L/T^2], n is the porosity, α is compressibility of the soil matrix [LT^2/M] and β is the compressibility of water [LT^2/M].

The term $\rho_w g_z \alpha$ gives the volume of water released from a unit volume due to compression of the soil matrix caused by a unit change in pressure head and is controlled by the aquifer compressibility term α . This component of the specific storage is defined as the skeletal component (S_{sk}). The term $\rho_w g_c n\beta$ defines the volume of water released from a unit volume caused by expansion of water resulting from a unit change in pressure and is controlled by the water compressibility β . For most unconsolidated alluvial aquifer systems, the skeletal component of the specific storage is the dominant component in the specific storage of the aquifer system. This compression of the soil matrix caused by a change in pressure head as a result of groundwater withdrawal is identified as the crucial factor in land subsidence.

LAND SUBSIDENCE THEORIES

There are two basic theories, which have been used to explain and model the land subsidence. The first is the Terzaghi's principal of effective stress and the second one is the Biot's "general theory of three dimensional consolidations".

Terzaghi's Principal of Effective Stress

The concept of effective stress first proposed by Terzaghi in 1925 describes the relation between changes in water levels and pressure and deformation of the aquifer system (Terzaghi et al., 1996) in the vertical direction. This gives a one-dimensional analysis of the aquifer compaction.

At any arbitrary plane below the water table, the total stress (σ_T) is represented by the weight of the overlying soil and water. The upward force balancing this stress is represented by the pore fluid pressure (p) and the inter-granular or effective stress (σ_e)

$$\sigma_T = \sigma_e + p \qquad [2]$$

In the one-dimensional representation, the effective stress, total stress and pore fluid pressure are all expressed in units of force per unit area [FL^{-2}] in vertical direction. They may also be expressed as a height of column of water [L], by dividing quantities of force per unit area by the unit weight of water [F/L^3].

In the absence of any groundwater withdrawal from an undeveloped aquifer system, water levels are relatively stable though subject to seasonal and longer-term climatic variability. The recharge to the aquifer system is balanced by flow to streams and drains from the aquifer. In such a scenario, the weight of the overlying soil and water is balanced by the pore-fluid pressure and the inter-granular or effective stress. During development of groundwater resources, water levels decline causing changes in this balance of forces. Groundwater withdrawal from confined aquifers reduces fluid pressure (p). As the total stress (σ_T) remains nearly constant for a confined aquifer, a portion of the load shifts from the confined fluid to the skeleton of the aquifer system, increasing the effective stress (σ_e) and causing compression. Following the principle of effective stress, the compaction of a thick sequence of interbedded aquifers and aquitards can proceed only as rapidly as pore pressure throughout the sequence can move toward equilibrium with reduced pressure in the pumped aquifers.

The relationship between effective stress and the compression of the soil matrix is nonlinear. In this respect, the concept of elastic and inelastic compaction was introduced. Riley, 1969 and Helm 1975 postulated that elastic compaction or expansion of sediments is nearly proportional to change in effective stress. It has also been established through laboratory consolidation tests and field observations that when compressible fine grains sediments are stressed beyond a previous maximum stress, compaction is permanent. For defining the elastic and inelastic

compaction of the aquifer system, the skeletal component of specific storage is defined for two ranges of stress and is termed as elastic and inelastic component of specific storage. For a value of effective stress less than the previous maximum effective stress, s_e(max), the soil matrix is said to deform elastically. For any value of effective stress greater than the previous maximum stress s_e(max) the soil matrix deforms inelastically. Thus any compaction of the aquifer system is permanent, as the soil matrix cannot rebound to its original position even if the effective stress is reduced to its original value.

S_{sk} = S_{ske} (elastic specific storage)

$= a_{ke}\ r_w g_z$ for $s_e < s_e$(max) [3]

and

S_{sk} = S_{skv} (inelastic specific storage)

$= a_{kv}\ r_w g_z$ for $s_e > s_e$(max) [4]

where, S_{sk} is the skeletal component of the specific storage [L^{-1}], a_{ke} and a_{kv} are the elastic and inelastic components of the compressibility of soil matrix respectively [LT^2/M], r_w is the density of water [M/L^3] and g_z is acceleration due to gravity [L/T^2] in Z direction. For coarse-grained sediments, it is assumed that inelastic skeletal compressibility is negligible; therefore skeletal specific storage of the aquifer, S_{sk} can be approximated by the fully recoverable elastic component S_{ske}. Skeletal compressibility of fine-grained aquitards is higher by several orders of magnitude than skeletal compressibility of coarse-grained aquifers. Thus the compression of aquitards is usually the dominant component in the compression of an aquifer system.

In the context of confined aquifer systems, the change in effective stress is usually determined by measuring or evaluating changes in the hydraulic head

$$\Delta s_e = -\Delta h r_w g_z \qquad [5]$$

assuming there is no significant change in the density of fluid. So the previous maximum stress s_e(max) can generally be represented by the previous lowest groundwater level. For water levels higher than the pre-consolidated stress level aquifer system, the deformation to the soil matrix is elastic and the deformation is recoverable.

For groundwater level lower than the preconsolidation stress system, the pore structure is said to undergo a significant rearrangement of pore volume. This results into an inelastic reduction of pore volume which causes the land subsidence.

It has been reported (Leake and Prudic, 1992) that elastic compaction of sediments is nearly proportional to change in effective stress. Thus the relationship is expressed as

$$\Delta b = \frac{\Delta s_e}{g_w} S_{ske}\, b_o \qquad [6]$$

where,

Δb is change in thickness [L],

S_{ske} is skeletal component of elastic specific storage [L^{-1}],

g_w is the unit weight of water [FL^{-3}],

Δs_e is the change in effective stress [FL^{-2}] and

b_o is the thickness of the soil matrix [L].

For confined aquifers, the relation between change in head and change in thickness is

$$\Delta b = -\Delta h\ S_{ske}\, b_o. \qquad [7]$$

Approximate inelastic compaction is related to increase in effective stress with the same relation

$$\Delta b^* = \frac{\Delta s_e}{g_w} S_{skv}\, b_o \qquad [8]$$

where

Δb^* is approximate inelastic compaction[L], and

S_{skv} is the skeletal component of inelastic specific storage [L^{-1}].

For confined aquifers the expression is

$$\Delta b^* = -\Delta h\ S_{skv}\, b_o. \qquad [9]$$

Equation [2] defining the Terzaghi's principal of effective stress can also be derived using Newton's Second Law. To calculate the force exerted by the bottom boundary of a saturated porous media, begin with Newton's second law of motion

$$m\mathbf{a} = \sum \mathbf{F}$$

$$= \mathbf{F}_{net} = \int_A \mathbf{t}_{(n)}\, dA + \int_V r_s \mathbf{g} dV + \mathbf{S} \qquad [10]$$

where,

m is mass [M],

a is acceleration [L/T^2],

F is force [ML/T^2],

$\mathbf{F}_{net}$ is the net force,

$\mathbf{t}_{(n)}$ is the force on plane normal to unit vector **n,**

A is the area of solid,

ρ_s is the density of the solid,

g is the acceleration due to gravity,

V is the volume of the solid and

S is the force exerted by the bottom boundary on the solid.

For hydrostatic condition, **a** = 0 in which **0** is the null vector, not a scalar. Consider the upper surface A_2 and the lower surface A_1. The two regions are separated by a curve along which **k.n** = 0. Recall from eq. 2.2-8 (Whitaker, 1968) that $\mathbf{t}_{(n)} = -\mathbf{n}p$ where again p is pressure. Substitute into Newton's Second Law

$$0 = -\int_{A_2} \mathbf{n}_2 p|z = z_2 \, dA - \int_{A_1} \mathbf{n}_1 p|z = z_1 \, dA + \int_v \rho_s \mathbf{g} dV + \mathbf{S}$$

Take the dot product with unit vector **k**

$$\mathbf{k}.0 = -\int_{A_2} \mathbf{k}.\mathbf{n}_2 p|z = z_2 \, dA - \int_{A_1} \mathbf{k}.\mathbf{n}_1 p|z = z_1 \, dA + \int_v \mathbf{k}.\rho_s \mathbf{g} dV + \mathbf{k}.\mathbf{S}.$$

Change the variable of integration from the solid surface to the xy plane, noting that $\mathbf{k}.\mathbf{n}_2 dA = dA_{xy}$ for upper surface because the angle between **k** and $\mathbf{n}_2$ is $< \frac{p}{2}$,

$\mathbf{k}.\mathbf{n}_1 dA = -dA_{xy}$ for lower surface because the angle between **k** and $\mathbf{n}_2$ is $> \frac{p}{2}$ and

$\mathbf{k}.\mathbf{g} = -g_z$ because the angle between **k** and **g** is also $> \frac{p}{2}$,

$$0 = -\int_{A_{xy}} p\Big|_{z=z_2} dA_{xy} + \int_{A_{xy}} p\Big|_{z=z_1} dA_{xy} - \int_v \rho_s g_z dV + S_z.$$

Collect the pressure terms under a common integral

$$0 = \int_{A_{xy}} p\Big|_{z=z_1} - p\Big|_{z=z_2} dA_{xy} - \int_V \rho_s g_z dV + S_z.$$

Recalling eq 2.2 -17 (Whitaker, 1968), the pressure relation is given by

$p\Big|_{z=z} = -\rho_w g_z z + c$; in which ρ_w is water density, c is integration constant. Applying the boundary condition, $p = p_o$ at $z = L$ to give $c = p_o + \rho_w g_z L$ in which L is the free water surface elevation above the datum z = 0 and p_o is atmospheric pressure at the free water surface.

Thus $p\Big|_{z=z} = \rho_w g_z (L - z) + p_o$.

Substituting the above pressure relation,

$$0 = \int_{A_{xy}} \rho_w g_z (z_2 - z_1) dA_{xy} - \int_V \rho_s g_z dV + S_z$$

in which $\rho_w g_z$ and $\rho_s g_z$ are constants and the volume of the solid is both

$$V = \int_{A_{xy}} (z_2 - z_1) dA_{xy} \text{ and } V = \int_v dV.$$

Thus,

$0 = \rho_w g_z V - \rho_s g_z V + S_z$

and finally $S_z = g_z V (\rho_s - \rho_w)$. [11]

Thus effective stress σ_e of equation [2] is analogous to S_z in this development. The force component in the z direction is related to z component of the acceleration due to gravity, volume of the solid and the difference between water and solid.

Biot's theory of three-dimensional consolidation

The general three dimensional theory of consolidation was first formulated by Biot in 1941 and is also referred to as Biot's poroelastic theory. The key concept of poroelastic theory for an isotropic fluid filled porous medium is defined by the following two linear constitutive equations for the case of an isotropic applied stress field σ (Wang, 2000).

$$e = a_{11}\sigma + a_{12}p \quad [12]$$

$$\zeta = a_{21}\sigma + a_{22}p \quad [13]$$

in which $e = \frac{\partial V}{V}$, V is the bulk volume, ζ is the increment of fluid content, positive for fluid added and negative for fluid withdrawn from the control volume, σ is applied stress, positive for tensile and negative for compressive p is fluid pore pressure, which is positive if greater than atmospheric pressure [p_0] and a_{11}, a_{12}, a_{21} and a_{22} are poroelastic coefficients. Equation [12] implies that changes in applied stress and pore pressure

produce a fractional volume change, while equation [13] implies that changes in applied stress and pore pressure require fluid to be added to or removed from storage.

Poroelastic constants are defined as ratios of field variables while maintaining various constraints on the elementary control volume. Coefficients in the equations 5 and 6 are thus defined as

$a_{11} = \left.\frac{\partial e}{\partial s}\right|_{p=0} \equiv \frac{1}{K}$, which is compressibility of the material measured under drained condition and K is the drained bulk modulus;

$a_{12} = \left.\frac{\partial e}{\partial p}\right|_{s=0} \equiv \frac{1}{H}$, which is defined as poroelastic expansion coefficient;

$a_{21} = \left.\frac{\partial x}{\partial s}\right|_{p=0} \equiv \frac{1}{H_1} = \frac{1}{H}$; and

$a_{22} = \left.\frac{\partial x}{\partial p}\right|_{s=0} \equiv \frac{1}{R}$, which is a specific storage coefficient measured under conditions of constant applied stress. This development inherently assumes stress equilibrium and an elastic stress strain relationship. Land subsidence models need to be coupled with an appropriate groundwater flow models to yield useful results.

GROUNDWATER FLOW MODELS

There is a range of groundwater models having varying capabilities. Some of the commonly used models are presented next.

MODFLOW

It is a three-dimensional finite-difference groundwater model of the U.S Geological Survey (McDonald and Harbaugh, 1988), first introduced in 1984. The modular structure allows it to be adapted to particular conditions. Since its first development, many new versions have been introduced with added/improved functions. The latest version is MODFLOW-2000, which is capable of simulating steady and non-steady flow in an irregularly shaped flow system. The aquifer layers in the system can be confined, unconfined or a combination of both. It can simulate flow from external stresses, such as flow to wells, areal recharge, evapotranspiration, flow to drains, and flow through riverbeds. It is also possible to vary the hydraulic conductivities or transmissivities for any layer spatially, and the storage coefficient may be heterogeneous. MODFLOW is currently the most commonly used numerical groundwater flow model of U.S. Geological Survey for groundwater flow problems

MODFLOW SURFACT

MODFLOW SURFACT has been developed by Scientific Software group (Washington DC). It is a MODFLOW-based groundwater flow and contaminant transport model. The developers of the model have incorporated additional modules. It is capable of modeling saturated-unsaturated water flow (http://www.scisoftware.com/products/modflow_surfact_overview/modflow_surfact_overview.html). It is claimed to be a "seamless integration of flow and transport modules".

A team of researchers in our laboratory is currently working with this model on the project "Water and land management in irrigated ecosystem" also funded by the Task Force.

SWMS_3D

SWMS_3D is a three dimensional finite element groundwater flow and solute transport model developed by US Salinity Laboratory. The program is capable of simulating unsaturated-saturated water flow and solute transport, subject to root water uptake, drainage, and various fluxes at the soil atmosphere interface due to different irrigation practices. The program numerically solves the Richards' equation for saturated-unsaturated water flow and the convection-dispersion equation for solute transport. This model can handle irregular boundaries and local anisotropy.

SUBSIDENCE MODELING

In the early 1970s, Terzaghi's principle of effective stress coupled with Hubbert's force potential and Darcy's Law was used as the basis for one-dimensional subsidence modeling (Gambolati et al 1974; Helm, 1975, 1976). The first subsidence model to be used with a groundwater flow model was written by Meyer and Carr (1979). This model allowed for elastic– and inelastic-storage values to be used in a three-dimensional groundwater flow model. After the development of the three-dimensional MODFLOW groundwater flow model (McDonald and Harbaugh, 1988), it became the most widely used model to simulate groundwater flow. So a number of modular packages were developed to be used with MODFLOW to simulate land subsidence. Leake and Prudic (1991) developed a one dimensional subsidence program for MODFLOW called the

Interbed Storage Package (IBS1). In the IBS1 package, elastic- and inelastic- properties of compressible sediments are constants. The stress, which causes the compaction, is the head change. Delay in release of water from compressible Interbeds is ignored. This subsidence model is reported to be more versatile than the Meyer and Carr (1979) model and is used today as the standard for modeling subsidence in groundwater basins. Although this program does not contain the stress dependent parameter capabilities of the earlier Helm model, it allows for continuous calculation of subsidence due to pumping in the areal extent of the model grid. Leake (1990) added other capabilities to the original code by allowing the evaluation of delayed drainage from compressible interbeds within aquifer systems. This module is called the IBS2 package. Leake (1991) developed another Interbed Storage Package (IBS3) in which compaction is computed as a function of effective stress. Here, the elastic and in-elastic specific storage can vary with change in effective stress. Since all these "Interbed Storage" packages are based on one dimensional theory of effective stress, they can only be used for evaluating the vertical stress due to groundwater withdrawal: they can not simulate horizontal displacement.

Biot's fundamental expression of consolidation has been used by Hsieh, 1996 to develop a two dimensional axsymmetric finite-element displacement model referred to as HDM. However, the HDM model is not compatible with the MODFLOW group of groundwater flow models.

Biot's expression of consolidation is generally not compatible with MODFLOW. In the flow equations used in MODFLOW, the term specific storage is used, while in Biot's theory the term displacement of fluids is used. To make Biot's three-dimensional consolidation theory compatible with MODFLOW, an alternative formulation of poroelastic theory is used, which defines skeletal specific storage (S_s) for three dimensional problems as;

$$S_s = \frac{3\rho_w g_z}{3\lambda + 2G}$$

where, ρ_w is the density of water [M/L^3]

g_z is the z component of gravitational acceleration [L/T^2]

G is the shear modulus, and a Lame's constant [M/LT^2]

and λ is the other Lame's constant [M/LT^2].

Lame's constant λ is defined as

$$\lambda = \frac{2Gn}{1-2n}$$

where, n is the Poisson ratio.

This alternative formulation of Biot's three-dimensional consolidations is termed the Granular Displacement Model (GDM).

Burbey and Helm, 1999 used Granular Displacement Model (GDM) in conjunction with MODFLOW to simulate the displacement field of solids with unconsolidated aquifers in response to induced changes in water pressure. They used modifications to the assumptions of the Biot's theory. Biot's theory assumes that all deformation is purely elastic, but the observed behavior of compaction of aquifers suggests that there is a component of compaction that is non-recoverable and is thus inelastic in nature. To accurately simulate aquifer system compaction, it is thus necessary to incorporate the inelastic component of the deformation. They assumed that conversion from elastic to inelastic specific storage occurs when the previous maximum volume strain for a particular cell is exceeded. Burbey and Helm, 1999 have used elastic and inelastic specific storage and Poisson ratio as key parameters in their model. They compared the results from the GDM with the one dimensional subsidence model (IBS1) and HDM. They concluded, "under traction free conditions subsidence is a three dimensional problem and one dimensional subsidence model tend to focus excessive amounts of vertical deformation near the pumped well. The magnitude of vertical deformation in one dimensional subsidence models is exacerbated as the grid size becomes smaller in the vicinity of the pumping wells."

Larson, Basagaoglu and Marino, 2001 integrated numerical groundwater and land subsidence caused by groundwater overdraft in the Los-Banos Kettleman City area, California. They used MODFLOW as the groundwater flow model and Interbed Storage Package-1 (ISB1)(Leake and Prudic, 1991) as the land subsidence model. The ISB1 is a one dimensional land subsidence model using Terzaghi's theory of effective stress developed for use with MODFLOW. They used observed data from 1972-1998 to calibrate the program. The results of the simulation model have been used in evaluating the effect of land subsidence due to future

drought scenarios, based on different management alternatives.

AVAILABLE DATA SETS

The problems of land subsidence can be studied on two levels. On the pore scale, the land subsidence still needs to be formulated in terms of constitutive equations in terms of continuum mechanics. The terms like elastic and inelastic storage coefficients, permeability, and hydraulic conductivity should be explained in terms of time varying stress. Different sets of data would be required for this work which should mainly come from the study of compaction in soil mechanics

The second level of study is the regional scale. Observations and modeling of subsidence is found in literature for Los Banos-Kettleman City area, California. The following are some of the available data sets.

a. The geological survey professional paper 497-C, "Petrology of Sediments Underlying Area of Land Subsidence in Central California" (Meade, R., 1967) reports particle size distribution, spatial distribution of particle size, clay minerals and associated ions in the Los Banos-Kettleman City area.

b. The geological survey professional paper 497-A, "Physical and Hydrologic Properties of Water-Bearing Deposits in Subsiding areas in Central California" (Johnson. A I., Moston, R P., and Morris D.A., 1968) contains particle size distribution, permeability, specific gravity, dry unit weight, porosity, Atterberg limits, consolidation, acid solubility, and gypsum content. The results were based on the analysis of eight core holes drilled in different parts of the Los Banos-Kettleman City area in the western Fresno county, Tulare county and Santa Clara valley.

c. The geological survey professional paper 437-E, "Land Subsidence Due to Groundwater Withdrawal in the Los Banos- Kettleman City Area, California Part I. Changes in the hydrologic Environment conducive to subsidence" (Bull, W.B., and Miller, R., 1975) describes the extent, thickness, and hydraulic character of the deposits comprising the two principal aquifer systems and the confining clay that separates them.

d. A detailed ground and surface water flow model of the western San Joaquin Valley Called WESTSIM of the US bureau of Reclamation (USBR) is in the developmental stage. The WESTSIM model is expected to evaluate potential land subsidence that might occur in the future as a result of reduced surface water supplies and increased groundwater pumping. The U.S. Geological Survey has an open file report 01-35, Hydraulic and Mechanical Properties Affecting Ground-Water Flow and Aquifer System Compaction, San Joaquin Valley, California (Sneed, M.,2001), which summarizes the hydraulic and mechanical properties affecting groundwater flow and aquifer system compaction in the San Joaquin Valley. The data compiled in the report were taken from different published sources and include results of aquifer tests, stress-strain analysis of borehole extensometer observation, laboratory consolidation tests, and calibrated models of the aquifer system compaction. The report focuses on the skeletal specific storage values and the vertical conductivity of the aquitards.

e. Larson, K.J., Basagaoglu, H., and Marino, M.A., 2000 have used land subsidence results from six extensometers located at wells inside the study area. The six extensometers were installed by the US Geological Survey (USGS) and are now monitored by the San Joaquin District of the California DWR.

RESEARCH OBJECTIVES

Based on the status of the available land subsidence theories and the numerical methods employed to couple existing groundwater flow models like MODFLOW and numerical approaches for simulating land subsidence, the following issues related to land subsidence are highlighted.

a. Presently elastic and inelastic storage coefficients are treated as a step function of the stress. It is assumed that for stresses up to a certain preexisting value, elastic storage coefficient is to be used, while for stresses more than the preexisting value, the inelastic storage coefficient is to be used. We will determine if and how to include stress as a continuous function in the numerical formulations.

b. When the aquifer goes through a certain inelastic compaction, a rearrangement of the pore space takes place and the permeability of the soil is reduced permanently. Thus after

the aquifer goes through the permanent compaction, its aquifer properties like hydraulic conductivities and storage coefficient also changes permanently, and the subsequent behavior of the aquifer system is different than the previous behavior. We will investigate changes in the aquifer systems properties and how they affect its behavior.

c. Once the hydraulic conductivities of the aquifer system changes, the dispersivity coefficients are also changing thus permanently affecting the solute transport characteristics of the system. We will determine how these changes affect dispersivity of the aquifer.

■ ■ ■ ■ ■

REFERENCES

Belitz, K., Phillips, S.P., and Gronberg, J.M., 1992. Numerical Simulation of Ground-Water flow in the Central Part of the Western San Joaquin Valley, California, U.S. Geological Survey, Open-File Report 91-535, 71pp

Belitz, K., and Phillips, S.P., 1992. Simulation of Water –table response to management alternatives, central part of the western San Joaquin Valley, California, U.S. Geological Survey, Water –resources Investigation Report 91-4193

Bull, W.B., 1964. Alluvial fans and near surface subsidence in western Fresno County, California: U.S. Geological Survey Professional Paper 437-A, 71pp

Bull, W.B., and Miller, R.E., 1975. Land Subsidence due to groundwater withdrawal in the Los Banos –Kettleman City area, California, Part 1: Changes in the hydrologic environment conducive to subsidence. U S. Geological Survey Professional Paper 437-E, 71pp

Burbey, T.J., and Helm, D.C., 1999. Modeling three-dimensional deformation in response to pumping of unconsolidated aquifers, Environmental & Engineering Geoscience , Vol. 5, No. 2, pp 199-212

Domenico, P.A., and Schwartz, F.W., 1998. Physical and Chemicals Hydrogeology, John Wiley and Sons, Inc

Frind, E.O., and Rudolph, D.L., 1991. Hydraulic Response of Highly Compressible Aquitards during Consolidation, Water Resources Research, Vol. 22, No. 1, pp 17-30

Galloway, D., Jones, D.R., and Ingebritsen, S.E., Ed., 1999. Land Subsidence in the United States, U.S. Geological Survey, Circular 1182

Helm D.C., 1987. 3-dimensional consolidation theory in terms of the velocity of solids, Geotechnique 37, No 3, pp 369-392

Helm D.C., 1994. Horizontal Aquifer Movement in a Theis-Theim Confined Systems, Water Resources Research, Vol. 30, No. 4, pp 953-964

Ireland, R.L., 1986. Land Subsidence in the San Joaquin Valley, California, as of 1983: U.S. Geological Survey Water Resources Investigations Report 85-4196, 50 pp.

Johnson, A.I., Moston, R.P., and Morris, D.A., 1968. Physical and hydrologic properties of water-bearing deposits in subsiding areas in central California, U. S. Geological Survey Professional Paper-A, 71pp

Larson, K.J., Basagaoglu, H., and Marino, M.A., 2001. Prediction of optimal safe groundwater yield and land subsidence in the Los Banos-Kettleman city area, California, using a calibrated numerical simulation model, Journal of Hydrology 242 (2001), pp 79-102

Leake, S.A., 1992. Status of Computer programs for Simulating land subsidence with the modular finite-difference groundwater flow model, USGS subsidence Interest Group Conference, Edwards AFB, Antelope Valley, Nov 18-19, 1992

Leake, S.A., Leahy, P.P., and Navoy, A.S., 1994.Documentation of Computer Program to simulate Transient leakage from confining units using the modular finite-difference ground-water flow model, U.S Geological Survey, Open File report 94-59

Leake, S.A. and Prudic, D.E., 1991.Documentation of a Computer Program to simulate Aquifer-System compaction using the modular finite-difference ground-water flow model: U.S Geological Survey, Open File report 88-482

Li J. and Helm, D., 1998. Viscous drag, driving forces, and their reduction to Darcy's law, Water Resources Research, 34(7), pp 1675-1684

Lofgren, B. E., 1977. Changes in aquifer-system properties with ground-water depletion in Biennial Groundwater Conference, 11th, Fresno, California, September 15-16, Proceedings: Davis, California, water resources Center, 34pp.

Meade, R. H., 1967, Petrology of sediments underlying areas of land subsidence in central California: U.S. geological Survey Professional Paper 497-C, 83pp.

Poland, J.F., and working group, 1984. Mechanics of land subsidence due to fluid withdrawal; chapter 3 in Guidebook to studies of land subsidence due to groundwater withdrawal, UNESCO

Sneed, M., 2001, Hydraulic and Mechanical Properties Affecting Ground-Water Flow and Aquifer System Compaction, San Joaquin Valley, California, U.S. Geological Survey, Open File report 01-35

Terzaghi, K., Peck, R.B, and Mesri, G., 1996, Soil Mechanics in Engineering Practice, John Wiley and Sons

Wang, H.F., 2000, Theory of Linear Poroeasticity with application to geomechanics and hydrogeology, Princeton University Press

INDEX